Semiconductor Physics and Devices

Basic Principles

Third Edition

Donald A. Neamen
University of New Mexico

Boston Burr Ridge, IL Dubuque, IA Madison, WI New York San Francisco St. Louis
Bangkok Bogota Caracas Kuala Lumpur Lisbon London Madrid Mexico City
Milan Montreal New Delhi Santiago Seoul Singapore Sydney Taipei Toronto

VISIT…

LANZAROTE
Caliente.COM

McGraw-Hill Higher Education
A Division of The McGraw-Hill Companies

SEMICONDUCTOR PHYSICS AND DEVICES: BASIC PRINCIPLES
THIRD EDITION

Published by McGraw-Hill, a business unit of The McGraw-Hill Companies, Inc., 1221 Avenue of the Americas, New York, NY 10020. Copyright © 2003, 1997, 1992 by The McGraw-Hill Companies, Inc. All rights reserved. No part of this publication may be reproduced or distributed in any form or by any means, or stored in a database or retrieval system, without the prior written consent of The McGraw-Hill Companies, Inc., including, but not limited to, in any network or other electronic storage or transmission, or broadcast for distance learning.

Some ancillaries, including electronic and print components, may not be available to customers outside the United States.

This book is printed on acid-free paper.

International 1 2 3 4 5 6 7 8 9 0 DOC/DOC 0 9 8 7 6 5 4 3 2
Domestic 2 3 4 5 6 7 8 9 0 DOC/DOC 0 9 8 7 6 5 4 3

ISBN 0–07–232107–5
ISBN 0–07–119862–8 (ISE)

Publisher: *Elizabeth A. Jones*
Senior developmental editor: *Kelley Butcher*
Executive marketing manager: *John Wannemacher*
Project manager: *Joyce Waiters*
Production supervisor: *Sherry L. Kane*
Designer: *David W. Hash*
Cover designer: *Rokusek Design*
Cover image: *©Eyewire, Inc.*
Media project manager: *Sandra M. Schnee*
Media technology senior producer: *Phillip Meek*
Compositor: *Interactive Composition Corporation*
Typeface: *10/12 Times Roman*
Printer: *R. R. Donnelley/Crawfordsville, IN*

Library of Congress Cataloging-in-Publication Data

Neamen, Donald A.
Semiconductor physics and devices : basic principles / Donald A. Neamen. — 3rd ed.
p. cm.
Includes bibliographical references and index.
ISBN 0–07–232107–5 (acid-free paper)
I. Semiconductors. I. Title.

QC611 .N39 2003
537.6'22—dc21
2002019681
CIP

INTERNATIONAL EDITION ISBN 0–07–119862–8

Copyright © 2003. Exclusive rights by The McGraw-Hill Companies, Inc., for manufacture and export. This book cannot be re-exported from the country to which it is sold by McGraw-Hill. The International Edition is not available in North America.

www.mhhe.com

ABOUT THE AUTHOR

Donald A. Neamen is a professor emeritus in the Department of Electrical and Computer Engineering at the University of New Mexico where he taught for more than 25 years. He received his Ph.D. from the University of New Mexico and then became an electronics engineer at the Solid State Sciences Laboratory at Hanscom Air Force Base. In 1976, he joined the faculty in the EECE department at the University of New Mexico, where he specialized in teaching semiconductor physics and devices courses and electronic circuits courses. He is still a part-time instructor in the department.

In 1980, Professor Neamen received the Outstanding Teacher Award for the University of New Mexico. In 1983 and 1985, he was recognized as Outstanding Teacher in the College of Engineering by Tau Beta Pi. In 1990, and each year from 1994 through 2001, he received the Faculty Recognition Award, presented by graduating EECE students. He was also honored with the Teaching Excellence Award in the College of Engineering in 1994.

In addition to his teaching, Professor Neamen served as Associate Chair of the EECE department for several years and has also worked in industry with Martin Marietta, Sandia National Laboratories, and Raytheon Company. He has published many papers and is the author of *Electronic Circuit Analysis and Design*, 2nd edition.

CONTENTS IN BRIEF

Preface xi

Chapter 1 The Crystal Structure of Solids I

Chapter 2 Introduction to Quantum Mechanics 24

Chapter 3 Introduction to the Quantum Theory of Solids 56

Chapter 4 The Semiconductor in Equilibrium 103

Chapter 5 Carrier Transport Phenomena 154

Chapter 6 Nonequilibrium Excess Carriers in Semiconductors 189

Chapter 7 The pn Junction 238

Chapter 8 The pn Junction Diode 268

Chapter 9 Metal–Semiconductor and Semiconductor Heterojunctions 326

Chapter 10 The Bipolar Transistor 367

Chapter 11 Fundamentals of the Metal–Oxide–Semiconductor Field-Effect Transistor 449

Chapter 12 Metal–Oxide–SemiconductorField-Effect Transistor: Additional Concepts 523

Chapter 13 The Junction Field-Effect Transistor 570

Chapter 14 Optical Devices 617

Chapter 15 Semiconductor Power Devices 668

Appendix A Selected List of Symbols 703

Appendix B System of Units, Conversion Factors, and General Constants 711

Appendix C The Periodic Table 715

Appendix D The Error Function 717

Appendix E "Derivation" of Schrodinger's Wave Equation 719

Appendix F Unit of Energy—The Electron-Volt 721

Appendix G Answers to Selected Problems 723

Index 731

CONTENTS

Preface xi

CHAPTER 1
The Crystal Structure of Solids 1

Preview 1
1.1 Semiconductor Materials 1
1.2 Types of Solids 2
1.3 Space Lattices 3
1.3.1 Primitive and Unit Cell 3
1.3.2 Basic Crystal Structures 4
1.3.3 Crystal Planes and Miller Indices 5
1.3.4 The Diamond Structure 9
1.4 Atomic Bonding 11
***1.5** Imperfections and Impurities in Solids 13
1.5.1 Imperfections in Solids 13
1.5.2 Impurities in Solids 15
***1.6** Growth of Semiconductor Materials 16
1.6.1 Growth from a Melt 16
1.6.2 Epitaxial Growth 18
1.7 Summary 19
Problems 21

CHAPTER 2
Introduction to Quantum Mechanics 24

Preview 24
2.1 Principles of Quantum Mechanics 25
2.1.1 Energy Quanta 25
2.1.2 Wave–Particle Duality 26
2.1.3 The Uncertainty Principle 29
2.2 Schrodinger's Wave Equation 30
2.2.1 The Wave Equation 30
2.2.2 Physical Meaning of the Wave Function 32
2.2.3 Boundary Conditions 32
2.3 Applications of Schrodinger's Wave Equation 33
2.3.1 Electron in Free Space 33
2.3.2 The Infinite Potential Well 34
2.3.3 The Step Potential Function 38
2.3.4 The Potential Barrier 42
***2.4** Extensions of the Wave Theory to Atoms 45
2.4.1 The One-Electron Atom 45
2.4.2 The Periodic Table 48
2.5 Summary 50
Problems 51

CHAPTER 3
Introduction to the Quantum Theory of Solids *56*

Preview 56
3.1 Allowed and Forbidden Energy Bands 57
3.1.1 Formation of Energy Bands 57
**3.1.2 The Kronig–Penney Model 61*
3.1.3 The k-Space Diagram 66
3.2 Electrical Conduction in Solids 70
3.2.1 The Energy Band and the Bond Model 70
3.2.2 Drift Current 72
3.2.3 Electron Effective Mass 73
3.2.4 Concept of the Hole 76
3.2.5 Metals, Insulators, and Semiconductors 78
3.3 Extension to Three Dimensions 80
3.3.1 The k-Space Diagrams of Si and GaAs 81
3.3.2 Additional Effective Mass Concepts 82
3.4 Density of States Function 83
3.4.1 Mathematical Derivation 83
3.4.2 Extension to Semiconductors 86
3.5 Statistical Mechanics 88
3.5.1 Statistical Laws 88

3.5.2 *The Fermi–Dirac Probability Function 89*
3.5.3 *The Distribution Function and the Fermi Energy 91*
3.6 Summary 96
Problems 98

CHAPTER 4

The Semiconductor in Equilibrium 103

Preview 103
4.1 Charge Carriers in Semiconductors 104
- 4.1.1 *Equilibrium Distribution of Electrons and Holes 104*
- 4.1.2 *The n_0 and p_0 Equations 106*
- 4.1.3 *The Intrinsic Carrier Concentration 110*
- 4.1.4 *The Intrinsic Fermi-Level Position 113*

4.2 Dopant Atoms and Energy Levels 115
- 4.2.1 *Qualitative Description 115*
- 4.2.2 *Ionization Energy 117*
- 4.2.3 *Group III–V Semiconductors 119*

4.3 The Extrinsic Semiconductor 120
- 4.3.1 *Equilibrium Distribution of Electrons and Holes 121*
- 4.3.2 *The n_0p_0 Product 124*
- *4.3.3 *The Fermi–Dirac Integral 125*
- 4.3.4 *Degenerate and Nondegenerate Semiconductors 127*

4.4 Statistics of Donors and Acceptors 128
- 4.4.1 *Probability Function 128*
- 4.4.2 *Complete Ionization and Freeze-Out 129*

4.5 Charge Neutrality 132
- 4.5.1 *compensated Semiconductors 133*
- 4.5.2 *Equilibrium Electron and Hole Concentrations 133*

4.6 Position of Fermi Energy Level 139
- 4.6.1 *Mathematical Derivation 139*
- 4.6.2 *Variation of E_F with Doping Concentration and Temperature 142*
- 4.6.3 *Relevance of the Fermi Energy 144*

4.7 Summary 145
Problems 148

CHAPTER 5

Carrier Transport Phenomena 154

Preview 154
5.1 Carrier Drift 154
- 5.1.1 *Drift Current Density 155*
- 5.1.2 *Mobility Effects 157*
- 5.1.3 *Conductivity 162*
- 5.1.4 *Velocity Saturation 167*

5.2 Carrier Diffusion 169
- 5.2.1 *Diffusion Current Density 170*
- 5.2.2 *Total Current Density 173*

5.3 Graded Impurity Distribution 173
- 5.3.1 *Induced Electric Field 174*
- 5.3.2 *The Einstein Relation 176*

***5.4** The Hall Effect 177
5.5 Summary 180
Problems 182

CHAPTER 6

Nonequilibrium Excess Carriers in Semiconductors 189

Preview 189
6.1 Carrier Generation and Recombination 190
- 6.1.1 *The Semiconductor in Equilibrium 190*
- 6.1.2 *Excess Carrier Generation and Recombination 191*

6.2 Characteristics of Excess Carriers 194
- 6.2.1 *Continuity Equations 195*
- 6.2.2 *Time-Dependent Diffusion Equations 196*

6.3 Ambipolar Transport 197
- 6.3.1 *Derivation of the Ambipolar Transport Equation 198*
- 6.3.2 *Limits of Extrinsic Doping and Low Injection 200*
- 6.3.3 *Applications of the Ambipolar Transport Equation 203*
- 6.3.4 *Dielectric Relaxation Time Constant 211*
- *6.3.5 *Haynes–Shockley Experiment 213*

6.4 Quasi-Fermi Energy Levels 216

***6.5** Excess-Carrier Lifetime 218
- *6.5.1 Shockley–Read–Hall Theory of Recombination 219*
- *6.5.2 Limits of Extrinsic Doping and Low Injection 222*

***6.6** Surface Effects 224
- *6.6.1 Surface States 224*
- *6.6.2 Surface Recombination Velocity 226*

6.7 Summary 229

Problems 231

CHAPTER 7

The pn Junction 238

Preview 238

7.1 Basic Structure of the pn Junction 238

7.2 Zero Applied Bias 240
- *7.2.1 Built-in Potential Barrier 240*
- *7.2.2 Electric Field 242*
- *7.2.3 Space Charge Width 246*

7.3 Reverse Applied Bias 247
- *7.3.1 Space Charge Width and Electric Field 248*
- *7.3.2 Junction Capacitance 251*
- *7.3.3 One-Sided Junctions 253*

***7.4** Nonuniformly Doped Junctions 255
- *7.4.1 Linearly Graded Junction 255*
- *7.4.2 Hyperabrupt Junctions 258*

7.5 Summary 260

Problems 262

CHAPTER 8

The pn Junction Diode 268

Preview 268

8.1 pn Junction Current 269
- *8.1.1 Qualitative Description of Charge Flow in a pn Junction 269*
- *8.1.2 Ideal Current–Voltage Relationship 270*
- *8.1.3 Boundary Conditions 271*
- *8.1.4 Minority Carrier Distribution 275*
- *8.1.5 Ideal pn Junction Current 277*
- *8.1.6 Summary of Physics 281*
- *8.1.7 Temperature Effects 284*
- *8.1.8 The "Short" Diode 284*

8.2 Small-Signal Model of the pn Junction 286
- *8.2.1 Diffusion Resistance 286*
- *8.2.2 Small-Signal Admittance 288*
- *8.2.3 Equivalent Circuit 295*

8.3 Generation–Recombination Currents 297
- *8.3.1 Reverse-Bias Generation Current 297*
- *8.3.2 Forward-Bias Recombination Current 300*
- *8.3.3 Total Forward-Bias Current 303*

8.4 Junction Breakdown 305

***8.5** Charge Storage and Diode Transients 309
- *8.5.1 The Turn-off Transient 309*
- *8.5.2 The Turn-on Transient 312*

***8.6** The Tunnel Diode 313

8.7 Summary 316

Problems 318

CHAPTER 9

Metal–Semiconductor and Semiconductor Heterojunctions 326

Preview 326

9.1 The Schottky Barrier Diode 326
- *9.1.1 Qualitative Characteristics 327*
- *9.1.2 Ideal Junction Properties 329*
- *9.1.3 Nonideal Effects on the Barrier Height 333*
- *9.1.4 Current–Voltage Relationship 337*
- *9.1.5 Comparison of the Schottky Barrier Diode and the pn Junction Diode 341*

9.2 Metal–Semiconductor Ohmic Contacts 344
- *9.2.1 Ideal Nonrectifying Barriers 345*
- *9.2.2 Tunneling Barrier 346*
- *9.2.3 Specific Contact Resistance 348*

9.3 Heterojunctions 349
- *9.3.1 Heterojunction Materials 350*
- *9.3.2 Energy-Band Diagrams 350*
- *9.3.3 Two-Dimensional Electron Gas 351*
- **9.3.4 Equilibrium Electrostatics 354*
- **9.3.5 Current–Voltage Characteristics 359*

9.4 Summary 359

Problems 361

CHAPTER **10**

The Bipolar Transistor 367

Preview 367

10.1 The Bipolar Transistor Action 368

10.1.1 The Basic Principle of Operation 369

10.1.2 Simplified Transistor Current Relations 370

10.1.3 The Modes of Operation 374

10.1.4 Amplification with Bipolar Transistors 376

10.2 Minority Carrier Distribution 377

10.2.1 Forward-Active Mode 378

10.2.2 Other Modes of Operation 384

10.3 Low-Frequency Common-Base Current Gain 385

10.3.1 Contributing Factors 386

10.3.2 Mathematical Derivation of Current Gain Factors 388

10.3.3 Summary 392

10.3.4 Example Calculations of the Gain Factors 393

10.4 Nonideal Effects 397

10.4.1 Base Width Modulation 397

10.4.2 High Injection 401

10.4.3 Emitter Bandgap Narrowing 403

10.4.4 Current Crowding 405

10.4.5 Nonuniform Base Doping 406

10.4.6 Breakdown Voltage 408

10.5 Equivalent Circuit Models 413

10.5.1 Ebers–Moll Model 414

10.5.2 Gummel–Poon Model 416

10.5.3 Hybrid-Pi Model 418

10.6 Frequency Limitations 422

10.6.1 Time-Delay Factors 422

10.6.2 Transistor Cutoff Frequency 424

10.7 Large-Signal Switching 427

10.7.1 Switching Characteristics 427

10.7.2 The Schottky-Clamped Transistor 429

10.8 Other Bipolar Transistor Structures 430

10.8.1 Polysilicon Emitter BJT 430

10.8.2 Silicon–Germanium Base Transistor 431

10.8.3 Heterojunction Bipolar Transistors 434

10.9 Summary 435

Problems 438

CHAPTER **11**

Fundamentals of the Metal–Oxide–Semiconductor Field-Effect Transistor 449

Preview 449

11.1 The Two-Terminal MOS Structure 450

11.1.1 Energy-Band Diagrams 450

11.1.2 Depletion Layer Thickness 455

11.1.3 Work Function Differences 458

11.1.4 Flat-Band Voltage 462

11.1.5 Threshold Voltage 465

11.1.6 Charge Distribution 471

11.2 Capacitance–Voltage Characteristics 474

11.2.1 Ideal C-V Characteristics 474

11.2.2 Frequency Effects 479

11.2.3 Fixed Oxide and Interface Charge Effects 480

11.3 The Basic MOSFET Operation 483

11.3.1 MOSFET Structures 483

11.3.2 Current–Voltage Relationship—Concepts 486

11.3.3 Current–Voltage Relationship—Mathematical Derivation 490

11.3.4 Transconductance 498

11.3.5 Substrate Bias Effects 499

11.4 Frequency Limitations 502

11.4.1 Small-Signal Equivalent Circuit 502

11.4.2 Frequency Limitation Factors and Cutoff Frequency 504

11.5 The CMOS Technology 507

11.6 Summary 509

Problems 513

CHAPTER **12**

Metal–Oxide–Semiconductor Field-Effect Transistor: Additional Concepts *523*

Preview 523

12.1 Nonideal Effects 524

12.1.1 Subthreshold Conduction 524

12.1.2 Channel Length Modulation 526
12.1.3 Mobility Variation 530
12.1.4 Velocity Saturation 532
12.1.5 Ballistic Transport 534
12.2 MOSFET Scaling 534
12.2.1 Constant-Field Scaling 534
12.2.2 Threshold Voltage—First Approximations 535
12.2.3 Generalized Scaling 536
12.3 Threshold Voltage Modifications 537
12.3.1 Short-Channel Effects 537
12.3.2 Narrow-Channel Effects 541
12.4 Additional Electrical Characteristics 543
12.4.1 Breakdown Voltage 544
**12.4.2 The Lightly Doped Drain Transistor 550*
12.4.3 Threshold Adjustment by Ion Implantation 551
***12.5** Radiation and Hot-Electron Effects 554
12.5.1 Radiation-Induced Oxide Charge 555
12.5.2 Radiation-Induced Interface States 558
12.5.3 Hot-Electron Charging Effects 560
12.6 Summary 561
Problems 563

CHAPTER 13
The Junction Field-Effect Transistor *570*

Preview 570
13.1 JFET Concepts 571
13.1.1 Basic pn JFET Operation 571
13.1.2 Basic MESFET Operation 575
13.2 The Device Characteristics 577
13.2.1 Internal Pinchoff Voltage, Pinchoff Voltage, and Drain-to-Source Saturation Voltage 577
13.2.2 Ideal DC Current-Voltage Relationship—Depletion Mode JFET 582
13.2.3 Transconductance 587
13.2.4 The MESFET 588
***13.3** Nonideal Effects 593
13.3.1 Channel Length Modulation 594
13.3.2 Velocitj Saturation Efects 596
13.3.3 Subthreshold and Gate Current Effects 596
***13.4** Equivalent Circuit and Frequency Limitations 598
13.4.1 Small-Signal Equivalent Circuit 598
13.4.2 Frequency Limitation Factors and Cutoff Frequency 600
***13.5** High Electron Mobility Transistor 602
13.5.1 Quantum Well Structures 603
13.5.2 Transistor Performance 604
13.6 Summary 609
Problems 611

CHAPTER 14
Optical Devices 617

Preview 617
14.1 Optical Absorption 618
14.1.1 Photon Absorption Coefficient 618
14.1.2 Electron–Hole Pair Generation Rate 621
14.2 Solar Cells 623
14.2.1 The pn Junction Solar Cell 623
14.2.2 Conversion Ejjiciency and Solar Concentration 626
14.2.3 Nonuniform Absorption Efects 628
14.2.4 The Heterojunction Solar Cell 628
14.2.5 Amorphous Silicon Solar Cells 630
14.3 Photodetectors 631
14.3.1 Photoconductor 632
14.3.2 Photodiode 634
14.3.3 PIN Photodiode 639
14.3.4 Avalanche Photodiode 640
14.3.5 Phototransistor 641
14.4 Photoluminescence and Electroluminescence 642
14.4.1 Basic Transitions 643
14.4.2 Luminescent Efficiency 645
14.4.3 Materials 645
14.5 Light Emitting Diodes 647
14.5.1 Generation of Light 648

PREFACE

PHILOSOPHY AND GOALS

The purpose of the third edition of this book is to provide a basis for understanding the characteristics, operation, and limitations of semiconductor devices. In order to gain this understanding, it is essential to have a thorough knowledge of the physics of the semiconductor material. The goal of this book is to bring together quantum mechanics, the quantum theory of solids, semiconductor material physics. and semiconductor device physics. All of these components are vital to the understanding of both the operation of present day devices and any future development in the field.

The amount of physics presented in this text is greater than what is covered in many introductory semiconductor device books. Although this coverage is more extensive, the author has found that once the basic introductory and material physics have been thoroughly covered. the physics of the semiconductor device follows quite naturally and can he covered fairly quickly and efficiently. The emphasis on the underlying physics will also be a benefit in understanding and perhaps in developing new semiconductor devices.

Since the objective of this text is to provide an introduction to the theory of semiconductor devices, there is a great deal of advanced theory that is not considered. In addition. fabrication processes are not described in detail. There are a few references and general discussions about processing techniques such as diffusion and ion implantation, but only where the results of this processing have direct impact on device characteristics.

PREREQUISITES

This book is intended for junior and senior undergraduates. The prerequisites for understanding the material are college mathematics. up to and including differential equations, and college physics, including an introduction to modern physics and electrostatics. Prior completion of an introductory course in electronic circuits is helpful, but not essential.

ORGANIZATION

The text begins with the introductory physics, moves on to the semiconductor material physics, and then covers the physics of semiconductor devices. Chapter 1 presents an introduction to the crystal structure of solids, leading to the ideal single-crystal semiconductor material. Chapters 2 and **3** introduce quantum mechanics and the quantum theory of solids, which together provide the necessary basic physics.

Chapters 4 through6 cover the semiconductor material physics. Chapter4 presents the physics of the semiconductor in thermal equilibrium; Chapter 5 treats the transport phenomena of the charge carriers in a semiconductor. The nonequilibrium excess carrier characteristics are then developed in Chapter 6. Understanding the behavior of excess carriers in a semiconductor is vital to the goal of understanding the device physics.

The physics of the basic semiconductor devices is developed in Chapters 7 through 13. Chapter 7 treats the electrostatics of the basic pn junction. and Chapter 8 covers the current-voltage characteristics of the pn junction. Metal-semiconductor junctions, both rectifying and nonrectifying, and semiconductor heterojunctions are considered in Chapter 9, while Chapter 10 treats the bipolar transistor. The physics of the metal-oxide-semiconductor field-effect transistor is presented in Chapters 11 and 12. and Chapter 13 covers the junction field-effect transistor. Once the physics of the pn junction is developed, the chapters dealing with the three basic transistors may be covered in any order—these chapters are written so as not to depend on one another. Chapter 14 considers optical devices and finally Chapter 15 covers power semiconductor devices.

USE OF THE BOOK

The text is intended for a one-semester course at the junior or senior level. As with most textbooks, there is more material than can be conveniently covered in one semester; this allows each instructor some flexibility in designing the course to his/her own specific needs. Two possible orders of presentation are discussed later in a separate section in this preface. However, the text is not an encyclopedia. Sections in each chapter that can be skipped without loss of continuity are identified by an asterisk in both the table of contents and in the chapter itself. These sections, although important to the development of semiconductor device physics, can be postponed to a later time.

The material in the text has been used extensively in a course that is required for junior-level electrical engineering students at the University of New Mexico. Slightly less than half of the semester is devoted to the first six chapters; the remainder of the semester is devoted to the pn junction, the bipolar transistor. and the metal-oxide-semiconductor field-effect transistor. A few other special topics may be briefly considered near the end of the semester.

Although the bipolar transistor is discussed in Chapter 10 before the MOSFET or JFET, each chapter dealing with one of the three basic types of transistors is written to stand alone. Any one of the transistor types may be covered first.

NOTES TO THE READER

This book introduces the physics of semiconductor materials and devices. Although many electrical engineering students are more comfortable building electronic circuits or writing computer programs than studying the underlying principles of semiconductor devices, the material presented here is vital to an understanding of the limitations of electronic devices, such as the microprocessor.

Mathematics is used extensively throughout the book. This may at times seem tedious, but the end result is an understanding that will not otherwise occur. Although some of the mathematical models used to describe physical processes may seem abstract, they have withstood the test of time in their ability to describe and predict these physical processes.

The reader is encouraged to continually refer to the preview sections so that the objective of the chapter and the purposes of each topic can be kept in mind. This constant review is especially important in the first five chapters, dealing with basic physics.

The reader must keep in mind that, although some sections may be skipped without loss of continuity, many instructors will choose to cover these topics. The fact that sections are marked with an asterisk does not minimize the importance of these subjects.

It is also important that the reader keep in mind that there may be questions still unanswered at the end of a course. Although the author dislikes the phrase. "it can be shown that.. .," there are some concepts used here that rely on derivations beyond the scope of the text. This book is intended as an introduction to the subject. Those questions remaining unanswered at the end of the course, the reader is encouraged to keep "in a desk drawer." Then, during the next course in this area of concentration, the reader can take out these questions and search for the answers.

ORDER OF PRESENTATION

Each instructor has a personal preference for the order in which the course material is presented. Listed below are two possible scenarios. The first case, called the classical approach, covers the bipolar transistor before the MOS transistor. However, because the MOS transistor topic is left until the end of the semester. time constraints may shortchange the amount of class time devoted to this important topic.

The second method of presentation listed, called the nonclassical approach, discusses the MOS transistor before the bipolar transistor. Two advantages to this approach are that the MOS transistor will not get shortchanged in terms of time devoted to the topic and, since a "real device" is discussed earlier in the semester, the reader may have more motivation to continue studying this course material. A possible disadvantage to this approach is that the reader may be somewhat intimidated by jumping from Chapter 7 to Chapter I I. However. the material in Chapters 1 I and I? is written so that this jump can be made.

Unfortunately, because of time constraints, every topic in every chapter cannot be covered in a one-semester course. The remaining topics must be left for a second-semester course or for further study by the reader.

Classical **approach**

Chapter 1	Crystal structure
Chapters 2, 3	Selected topics from quantum mechanics and theory of solids
Chapter 4	Semiconductor physics
Chapter 5	Transport phenomena
Chapter 6	Selected topics from nonequilibrium characteristics
Chapters 7, 8	The pn junction and diode
Chapter 9	A brief discussion of the Schottky diode
Chapter 10	The bipolar transistor
Chapters 11, 12	The MOS transistor

Nonclassical approach	
Chapter 1	Crystal structure
Chapters 2, 3	Selected topics from quantum mechanics and theory of solids
Chapter 4	Semiconductor physics
Chapter 5	Transport phenomena
Chapter 7	The pn junction
Chapters 11, 12	The MOS transistor
Chapter 6	Selected topics from nonequilibrium characteristics
Chapter 8	The pn junction diode
Chapter 9	A brief discussion of the Schottky diode
Chapter 10	The bipolar transistor

FEATURES OF THE THIRD EDITION

- ***Preview section:*** A preview section introduces each chapter. This preview links the chapter to previous chapters and states the chapter's goals, i.e., what the reader should gain from the chapter.
- ***Examples:*** An extensive number of worked examples are used throughout the text to reinforce the theoretical concepts being developed. These examples contain all the details of the analysis or design, so the reader does not have to fill in missing steps.
- ***Test your understanding:*** Exercise or drill problems are included throughout each chapter. These problems are generally placed immediately after an example problem, rather than at the end of a long section. so that readers can immediately test their understanding of the material just covered. Answers are given for each drill problem so readers do not have to search for an answer at the end of the book. These exercise problems will reinforce readers' grasp of the material before they move on to the next section.
- ***Summary section:*** A summary section, in bullet form, follows the text of each chapter. This section summarizes the overall results derived in the chapter and reviews the basic concepts developed.
- ***Glossary of important terms:*** A glossary of important terms follows the Summary section of each chapter. This section defines and summarizes the most important terms discussed in the chapter.
- ***Checkpoint:*** A checkpoint section follows the Glossary section. This section states the goals that should have been met and states the abilities the reader should have gained. The Checkpoints will help assess progress before moving on to the next chapter.
- ***Review questions:*** A list of review questions is included at the end of each chapter. These questions serve as a self-test to help the reader determine how well the concepts developed in the chapter have been mastered.
- ***End-of-chapter problems*** A large number of problems are given at the end of each chapter, organized according to the subject of each section in the chapter

body. A larger number of problems have been included than in the second edition. Design-oriented or open-ended problems are included at the end in a Summary and Review section.

- *Computer simulation:* Computer simulation problems are included in many end-of-chapter problems. Computer simulation has not been directly incorporated into the text. However, a website has been established that considers computer simulation using MATLAB. This website contains computer simulations of material considered in most chapters. These computer simulations enhance the theoretical material presented. There also are exercise or drill problems that a reader may consider.
- ***Reading list:*** A reading list finishes up each chapter. The references, that are at an advanced level compared with that of this text, are indicated by an asterisk.
- ***Answers to selected problems:*** Answers to selected problems are given in the last appendix. Knowing the answer to a problem is an aid and a reinforcement in problem solving.

ICONS

Computer Simulations

Design Problems and Examples

SUPPLEMENTS

This book is supported by the following supplements:

- Solutions Manual available to instructors in paper form and on the website.
- Power Point slides of important figures are available on the website.
- Computer simulations are available on the website.

ACKNOWLEDGMENTS

I am indebted to the many students I have had over the years who have helped in the evolution of the third edition as well as the first and second editions of this text. I am grateful for their enthusiasm and constructive criticism. The University of New Mexico has my appreciation for providing an atmosphere conducive to writing this book.

I want to thank the many people at McGraw-Hill, for their tremendous support. A special thanks to Kelley Butcher, senior developmental editor. Her attention to details and her enthusiasm throughout the project are especially recognized and appreciated. I also appreciate the efforts of Joyce Watters, project manager, who guided the work through its final phase toward publication.

The following reviewers deserve thanks for their constructive criticism and suggestions for the third edition of this text.

Thomas Mantei, *University of Cincinnati*
Cheng Hsiao Wu, *University of Missouri—Rolla*
Kamtoshi Najita, *University of Hawaii at Manoa*
John Naber, *University of Louisville*
Gerald Oleszek, *University of Colorado—Colorado Springs*
Marc Cahay, *University of Cincinnati*

The following reviewers deserve thanks for their constructive criticism and suggestions for the second edition:

Jon M. Meese, *University of Missouri—Columbia*
Jacob *B*. Khurgin, *Johns Hopkins University*
Hong Koo Kim, *University of Pittsburgh*
Gerald M. Oleszek, *University of Colorado — Colorado Springs*
Ronald J. Roedel, *Arizona Stare University*
Leon McCaughan, *University of Wisconsin*
A. Anil Kumar, *Prairie View A & M University*

Since the third edition is an outgrowth of the first edition of the text, the following reviewers of the first edition deserve my continued thanks for their thorough reviews and valuable suggestions:

Timothy J. Drummond, *Sandia Laboratories*
J. *L*. Davidson, *Vanderbilt University*
Robert Jackson, *University* of *Massachusetts—Amherst*
C. H. *Wu*, *University of Missouri—Rolla*
D. K. Reinhard, *Michigan State University*
Len Trombetta, *University of Houston*
Dan Moore, *Virginia Polytechnic Institute and State University*
Bruce *P*. Johnson, *University ofNevada — Reno*
William Wilson, *Rice University*
Dennis Polla, *university of Minnesota*
G. *E*. Stillman, *University of Illinois—Urbana-Champaign*
Richard C. Jaeger, *Auburn University*
Anand Kulkarni, *Michigan Technological University*
Ronald *D*. Schrimpf, *University of Arizona*

I appreciate the many fine and thorough reviews — your suggestions have made this a better book.

Donald A. Neamen

PROLOGUE

Semiconductors and the Integrated Circuit

PREVIEW

We often hear that we are living in the information age. Large amounts of information can be obtained via the Internet, for example, and can also be obtained quickly over long distances via satellite communication systems. The development of the transistor and the integrated circuit (IC) has lead to these remarkable capabilities. The IC permeates almost every facet of our daily lives, including such things as the compact disk player, the fax machine, laser scanners at the grocery store, and the cellular telephone. One of the most dramatic examples of IC technology is the digital computer—a relatively small laptop computer today has more computing capability than the equipment used to send a man to the moon a few years ago. The semiconductor electronics field continues to be a fast-changing one. with thousands of technical papers published each year. ■

HISTORY

The semiconductor device has a fairly long history, although the greatest explosion of IC technology has occured during the last two or three decades.[1] The metal–semiconductor contact dates back to the early work of Rraun in 1874, who discovered the asymmetric nature of electrical conduction between metal contacts and semiconductors, such as copper, iron, and lead sulfide. These devices were used as detectors in early experiments on radio. In 1906, Pickard took out a patent for a point contact detector using silicon and, in 1907. Pierce published rectification characteristics of diodes made by sputtering metals onto a variety of semiconductors.

---

[1] This brief introduction is intended to give a flavor of the history of the semiconductor device and integrated circuit. Thousands of engineers and scientists have made significant contributions to the development of semiconductor electronics-the few events and names mentioned here are not meant to imply that these are the only significant events or people involved in the semiconductor history.

By 1935. selenium rectifiers and silicon point contact diodes were available for use as radio detectors. With the development of radar. the need for detector diodes and mixers increased. Methods of achieving high-purity silicon and germanium were developed during this time. A significant advance in our understanding of the metal–semiconductor contacr was aided by developments in the semiconductor physics. Perhaps most important during this period was Bethe's thermionic-emission theory in 1942, according to which the current is determined by the process of emission of electrons into the metal rather than by drift or diffusion.

Another big breakthrough came in December 1947 when the first transistor was constructed and tested at Bell Telephone Laboratories by William Shockley, John Bardeen, and Walter Brattain. This tirst transistor was a point contacr device and used polycrystalline germanium. The transistor effect was soon demonstrated in silicon as well. **A** significant improvement occurred at the end of 1949 when single-crystal material was used rather than rhe polycrystalline material. The single crystal yields uniform and improved properties throughout the whole semiconductor material.

The next significant step in the development of the transistor was the use of the diffusion process to form the necessary junctions. This process allowed better control of the transistor characteristics and yielded higher-frequency devices. The diffused mesa transistor was commercially available in germanium in 1957 and in silicon in 1958. The diffusion process also allowed many transistors to be fabricated on a single silicon slice. so the cost of these devices decreased.

THE INTEGRATED CIRCUIT (IC)

Up to this point, each component in an electronic circuit had ro he individually connected by wires. In September 1958. Jack Kilby of Texas Instruments demonstrated the first integrated circuit, which was fabricated in germanium. At about the same time, Robert Noyce of Fairchild Semiconductor introduced the integrated circuit in silicon using a planar technology. The tirst circuit used bipolar transistors. Practical MOS transistors were then developed in the mid-'60s. The MOS technologies, especially CMOS, have become a major focus for IC design and development. Silicon is the main semiconductor material. Gallium arsenide and other compound semiconductors are used for special applications requiring very high frequency devices and for optical devices.

Since that first IC, circuit design has become more sophisticated, and the integrated circuit more complex. A single silicon chip may be on the order of 1 square centimeter and contain over a million transistors. Some ICs may have more than a hundred terminals, while an individual transistor has only three. An IC can contain the arithmetic, logic. and memory functions on a single semiconductor chip—the primary example of this type of IC is the microprocessor. Intense research on silicon processing and increased automation in design and manufacturing have led to lower costs and higher fabrication yields.

FABRICATION

The integrated circuit is a direct result of the development of various processing techniques needed to fabricate the transistor and interconnect lines on the single chip. The total collection of these processes for making an IC is called a *technology*. The following few paragraphs provide an introduction to a few of these processes. This introduction is intended to provide the reader with some of the basic terminology used in processing.

Thermal Oxidation A major reason for the success of silicon ICs is the fact that an excellent native oxide, SiO_2, can be formed on the surface of silicon. This oxide is used as a gate insulator in the MOSFET and is also used as an insulator, known as the field oxide, between devices. Metal interconnect lines that connect various devices can be placed on top of the field oxide. Most other semiconductors do not form native oxides that are of sufficient quality to be used in device fabrication.

Silicon will oxidize at room temperature in air forming a thin native oxide of approximately 25 A thick. However, most oxidations are done at elevated temperatures since the basic process requires that oxygen diffuse through the existing oxide to the silicon surface where a reaction can occur A schematic of the oxidation process is shown in Figure 0.1. Oxygen diffuses across a stagnant gas layer directly adjacent to the oxide surface and then diffuses through the existing oxide layer to the silicon surface where the reaction between O_2 and Si forms SiO_2. Because of this reaction, silicon is actually consumed from the surface of the silicon. The amount of silicon consumed is approximately 44 percent of the thickness of the final oxide.

Photomasks and Photolithography The actual circuitry on each chip is created through the use of photomasks and photolithography. The photomask is a physical representation of a device or a portion of a device. Opaque regions on the mask are made of an ultraviolet-light-absorbing material. A photosensitive layer, called photoresist, is first spread over the surface of the semiconductor. The photoresist is an

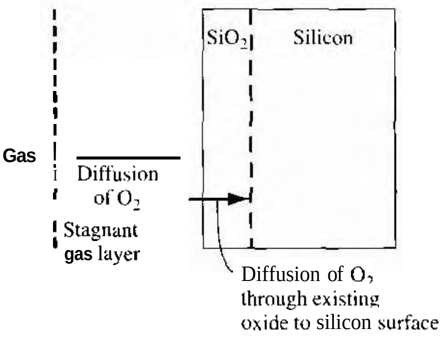
SiO$_2$
Silicon
Gas
Diffusion of O$_2$
Stagnant gas layer
Diffusion of O$_2$ through existing oxide to silicon surface

Figure 0.1 | Schematic of the oxidation process.

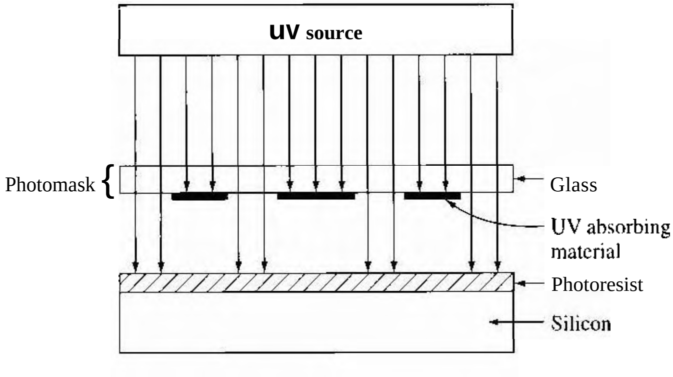

Figure 0.2 | Schematic showing the use of a photomask

organic polymer that undergoes chemical change when exposed to ultraviolet light. The photoresist is exposed to ultraviolet light through the photomask as indicated in Figure 0.2. The photoresist is then developed in a chemical solution. The developer is used to remove the unwanted portions of the photoresist and generate the appropriate patterns on the silicon. The photomasks and photolithography process is critical in that it determines how small the devices can be made. Instead of using ultraviolet light, electrons and x-rays can also be used to expose the photoresist.

Etching After the photoresist pattern is formed, the remaining photoresist can be used as a mask, so that the material not covered by the photoresist can be etched. Plasma etching is now the standard process used in IC fabrication. Typically. an etch gas such as chlorofluorocarbons are injected into a low-pressure chamber. A plasma is created by applying a radio-frequency voltage between cathode and anode terminals. The silicon wafer is placed on the cathode. Positively charged ions in the plasma are accelerated toward the cathode and bombard the wafer normal to the surface. The actual chemical and physical reaction at the surface is complex. but the net result is that silicon can be etched anisotropically in very selected regions of the wafer. If photoresist is applied on the surface of silicon dioxide. then the silicon dioxide can also be etched in a similar way.

Diffusion A thermal process that is used extensively in IC fabrication is diffusion. Diffusion is the process by which specific types of "impurity" atoms can be introduced into the silicon material. This doping process changes the conductivity type of the silicon so that pn junctions can be formed. (The pn junction is a basic building block of semiconductor devices.) Silicon wafers are oxidized to form a layer of silicon dioxide and windows are opened in the oxide in selected areas using photolithography and etching as just described.

The wafers are then placed in a high-temperature furnace (about 1100 C) and dopant atoms such as boron or phosphorus are introduced. The dopant atoms gradually diffuse or move into the silicon due to a density gradient. Since the diffusion process requires a gradient in the concentration of atoms, the final concentration of diffused atoms is nonlinear. as shown in Figure 0.3. When the wafer is removed from the furnace and the wafer temperature return:, to room temperature, the diffusion coefficient of the dopant atoms is essentially zero so that the dopant atoms are then fixed in the silicon material.

Ion Implantation A fabrication process that is an alternative to high-temperature diffusion is ion implantation. A beam of dopant ions is accelerated to a high energy and is directed at the surface of a semiconductor. As the ions enter the silicon, they collide with silicon atoms and lose energy and finally come to rest at some depth within the crystal. Since the collision process is statistical in nature, there is a distribution in the depth of penetration of the dopant ions. Figure 0.4 shows such an example of the implantation of boron into silicon at a particular energy.

Two advantages of the ion implantation process compared to diffusion are (1) the ion implantation process is a low temperature process and (2) very well defined doping layers can be achieved. Photoresist layers or layers of oxide can he used to block the penetration of dopant atoms so that ion implantation can occur in very selected regions of the silicon.

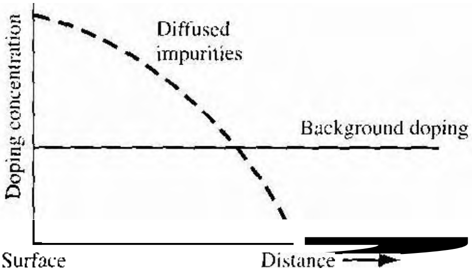

Figure 0.3 | Final concentration of diffused impurities into the surface of a semiconductor.

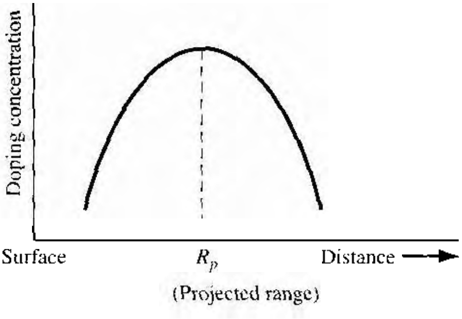

Figure 0.4 | Final concentration of ion-implanted boron into silicon.

One disadvantage of ion implantation is that the silicon crystal is damaged by the penetrating dopant atoms because of collisions between the incident dopant atoms and the host silicon atoms. However, most of the damage can be removed by thermal annealing the silicon at an elevated temperature. The thermal annealing temperature, however, is normally much less that the diffusion process temperature.

Metallization, Bonding, and Packaging After the semiconductor devices have been fabricated by the processing steps discussed. they need to be connected to each other to form the circuit. Metal films are generally deposited by a vapor deposition technique and the actual interconnect lines are formed using photolithography and etching. In general, a protective layer of silicon nitride is finally deposited over the entire chip.

The individual integrated circuit chips are separated by scribing and breaking the wafer. The integrated circuit chip is then mounted in a package. Lead bonders are finally used to attach gold or aluminum wires between the chip and package terminals.

Summary: Simplified Fabrication of a pn Junction Figure 0.5 shows the basic steps in forming a pn junction. These steps involve some of the processing described in the previous paragraphs.

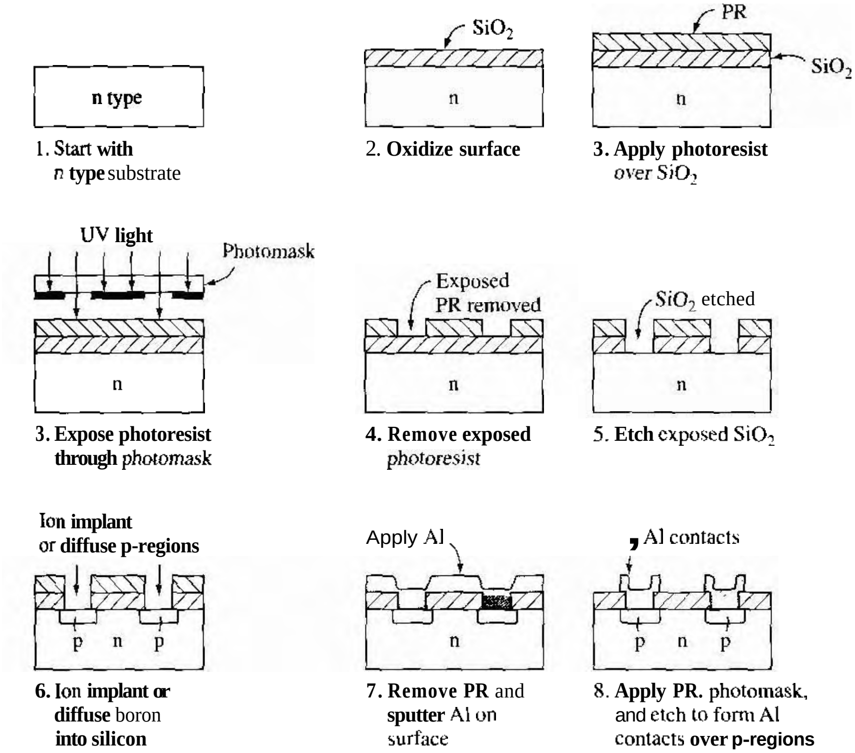

1. Start with *n* type substrate

2. Oxidize surface

3. Apply photoresist over SiO$_2$

3. Expose photoresist through photomask

4. Remove exposed photoresist

5. Etch exposed SiO$_2$

6. Ion implant or diffuse boron into silicon

7. Remove PR and sputter Al on surface

8. Apply PR. photomask, and etch to form Al contacts over p-regions

Figure 0.5 | The basic steps in forming a pn junction.

CHAPTER 1

The Crystal Structure of Solids

PREVIEW

This text deals with the electrical properties and characteristics of semiconductor materials and devices. The electrical properties of solids are therefore of primary interest. The semiconductor is in general a single-crystal material. The electrical properties of a single-crystal material are determined not only by the chemical composition but also by the arrangement of atoms in the solid; this being true, a brief study of the crystal structure of solids is warranted. The formation, or growth, of the single-crystal material is an important part of semiconductor technology. A short discussion of several growth techniques is included in this chapter to provide the reader with some of the terminology that describes semiconductor device structures. This introductory chapter provides the necessary background in single-crystal materials and crystal growth for the basic understanding of the electrical properties of semiconductor materials and devices. ■

1.1 | SEMICONDUCTOR MATERIALS

Semiconductors are a group of materials having conductivities between those of metals and insulators. Two general classifications of semiconductors are the elemental semiconductor materials, found in group IV of the periodic table, and the compound semiconductor materials, most of which are formed from special combinations of group III and group V elements. Table 1.1 shows a portion of the periodic table in which the more common semiconductors are found and Table 1.2 lists a few of the semiconductor materials. (Semiconductors can also be formed from combinations of group II and group VI elements. but in general these will not be considered in this text.)

The elemental materials, those that are composed of single species of atoms, are silicon and germanium. Silicon is by far the most common semiconductor used in integrated circuits and will be emphasized to a great extent.

Table **1.1** | A portion of the periodic table

III	IV	V
B	C	
Al	Si	P
Ga	Ge	As
In		Sb

Table 1.2 | A list of some semiconductor materials

Elemental semiconductors	
Si	Silicon
Ge	Germanium
Compound semiconductors	
AlP	Aluminum phosphide
AlAs	Aluminum arsenide
GaP	Gallium phosphide
GaAs	Gallium arsenide
InP	Indium phosphide

The two-element, or *binary*, compounds such as gallium arsenide or gallium phosphide are formed by combining one group III and one group V element. Gallium arsenide is one of the more common of the compound semiconductors. Its good optical properties make it useful in optical devices. GaAs is also used in specialized applications in which, for example, high speed is required.

We can also form a three-element, or *ternary*, compound semiconductor. An example is $Al_xGa_{1-x}As$, in which the subscript x indicates the fraction of the lower atomic number element component. More complex semiconductors can also be formed that provide flexibility when choosing material properties.

1.2 | TYPES OF SOLIDS

Amorphous, polycrystalline, and single crystal are the three general types of solids. Each type is characterized by the size of an ordered region within the material. An ordered region is a spatial volume in which atoms or molecules have a regular geometric arrangement or periodicity. Amorphous materials have order only within a few atomic or molecular dimensions, while polycrystalline materials have a high degree

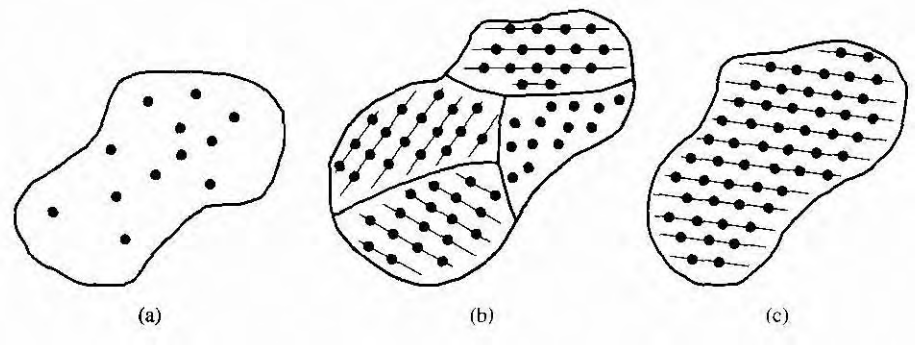

Figure **1.1** | Schematics of three general types of crystals: (a) amorphous, (b) polycrystalline, (c) single crystal.

of order over many atomic or molecular dimensions. These ordered regions. or single-crystal regions, vary in size and orientation with respect to one another. The single-crystal regions are called grains and are separated from one another by grain boundaries. Single-crystal materials, ideally, have a high degree of order, or regular geometric periodicity, throughout the entire volume of the material. The advantage of a single-crystal material is that. in general, its electrical properties are superior to those of a nonsingle-crystal material, since grain boundaries tend to degrade the electrical characteristics. Two-dimensional representations of amorphous, polycrystalline, and single-crystal materials are shown in Figure 1.1.

1.3 | SPACE LATTICES

Our primary concern will be the single crystal with its regular geometric periodicity in the atomic arrangement. A representative unit, or group of atoms, is repeated at regular intervals in each of the three dimensions to form the single crystal. The periodic arrangement of atoms in the crystal is called the *lattice.*

1.3.1 Primitive and Unit Cell

We can represent a particular atomic array by a dot that is called a *lattice point.* Figure 1.2 shows an infinite two-dimensional array of lattice points. The simplest means of repeating an atomic array is by translation. Each lattice point in Figure 1.2 can be translated a distance a_1 in one direction and a distance b_1 in a second noncolinear direction to generate the two-dimensional lattice. A third noncolinear translation will produce the three-dimensional lattice. The translation directions need not be perpendicular.

Since the three-dimensional lattice is a periodic repetition of a group of atoms, we do not need to consider the entire lattice, but only a fundamental unit that is being repeated. *A unit cell* is a small volume of the crystal that can be used to reproduce the entire crystal. A unit cell is not a unique entity. Figure 1.3 shows several possible unit cells in a two-dimensional lattice.

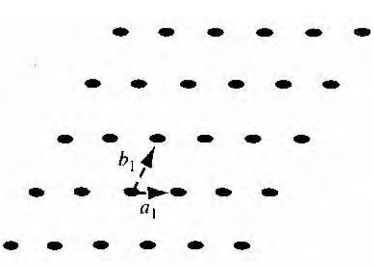

Figure 1.2 | Two-dimensional representation of a single-crystal lattice.

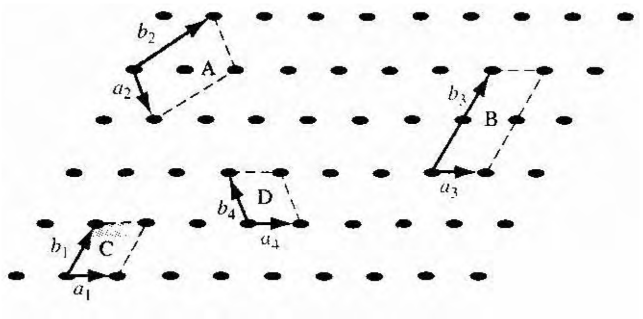

Figure 1.3 | Two-dimensional representation of a single-crystal lattice showing various possible unit cells.

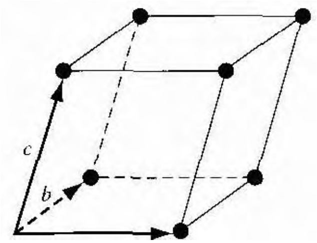

Figure 1.4 | A generalized primitive unit cell.

The unit cell A can be translated in directions a_2 and b_2, the unit cell B can be translated in directions a_3 and b_3, and the entire two-dimensional lattice can be constructed by the translations of either of these unit cells. The unit cells C and D in Figure 1.3 can also be used to construct the entire lattice by using the appropriate translations. This discussion of two-dimensional unit cells can easily be extended to three dimensions to describe a real single-crystal material.

A primitive cell is the smallest unit cell that can be repeated to form the lattice. In many cases, it is more convenient to use a unit cell that is not a primitive cell. Unit cells may be chosen that have orthogonal sides, for example, whereas the sides of a primitive cell may be nonorthogonal.

A generalized three-dimensional unit cell is shown in Figure 1.4. The relationship between this cell and the lattice is characterized by three vectors $\bar{a}$, 6, and ?, which need not be perpendicular and which may or may not be equal in length. Every equivalent lattice point in the three-dimensional crystal can be found using the vector

$$\bar{r} = p\bar{a} + q\bar{b} + s\bar{c} \tag{1.1}$$

where p, q, and s are integers. Since the location of the origin is arbitrary, we will let p, q, and s be positive integers for simplicity.

1.3.2 Basic Crystal Structures

Before we discuss the semiconductor crystal, let us consider three crystal structures and determine some of the basic characteristics of these crystals. Figure 1.5 shows the simple cubic, body-centered cubic, and face-centered cubic structures. For these simple structures, we may choose unit cells such that the general vectors $\bar{a}$, 6, and $\bar{c}$ are perpendicular to each other and the lengths are equal. The ***simple cubic*** (sc) structure has an atom located at each corner: the ***body-centered cubic*** (bcc) structure has an additional atom at the center of the cube; and the ***face-centered cubic*** (fcc) structure has additional atoms on each face plane.

By knowing the crystal structure of a material and its lattice dimensions, we can determine several characteristics of the crystal. For example, we can determine the volume density of atoms.

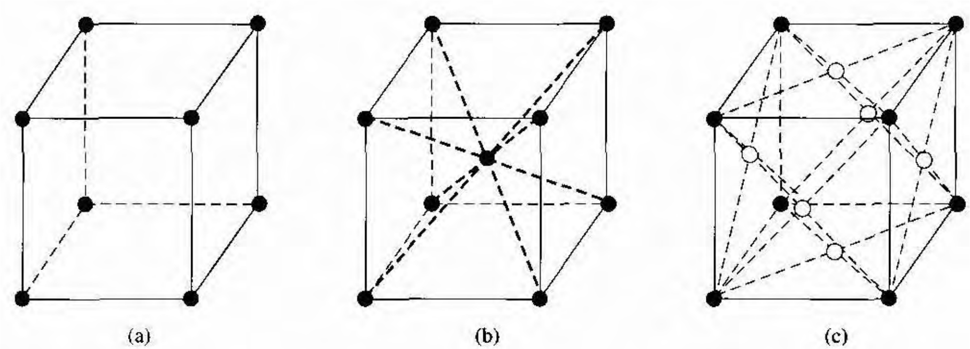

Figure 1.5 | Three lattice types: (a) simple cubic. (b) body-centered cubic. (c) face-centered cubic.

Objective | **EXAMPLE 1.1**

To find the volume density of atoms in a crystal.

Consider a single-crystal material that is a body-centered cubic with a lattice constant $a = 5\ \text{Å} = 5 \times 10^{-8}$ cm. A corner atom is shared by eight unit cells which meet at each corner so that each corner atom effectively contributes one-eighth of its volume to each unit cell. The eight corner atoms then contribute an equivalent of one atom to the unit cell. If we add the body-centered atom to the corner atoms, each unit cell contains an equivalent of two atoms.

■ **Solution**

The volume density of atoms is then found as

$$\text{Density} = \frac{2\ \text{atoms}}{(5 \times 10^{-8})^3} = 1.6 \times 10^{22}\ \text{atoms per cm}^3$$

■ **Comment**

The volume density of atoms just calculated represents the order of magnitude of density for most materials. The actual density is a function of the crystal type and crystal structure since the packing density—number of atoms per unit cell—depends on crystal structure.

TEST **YOUR** UNDERSTANDING

E1.1 The lattice constant of a face-centered-cubic structure is 4.75 Å. Determine the volume density of atoms. (Ans. $3.73 \times 10^{22}\ \text{cm}^{-3}$)

E1.2 The volume density of atoms for a simple cubic lattice is $3 \times 10^{22}\ \text{cm}^{-3}$. Assume that the atoms are hard spheres with each atom touching its nearest neighbor. Determine the lattice constant and the radium of the atom. (Ans. $a_0 = 3.22$ Å, $r = 1.61$ Å)

1.3.3 Crystal Planes and Miller Indices

Since real crystals are not infinitely large, they eventually terminate at a surface. Semiconductor devices are fabricated at or near a surface, so the surface properties may influence the device characteristics. We would like to be able to describe these surfaces in terms of the lattice. Surfaces, or planes through the crystal, can be described by first considering the intercepts of the plane along the $\bar{a}$, $\bar{b}$, and $\bar{c}$ axes used to describe the lattice.

EXAMPLE 1.2

Objective

To describe the plane shown in Figure 1.6. (The lattice points in Figure 1.6 are shown along the $\bar{a}$, $\bar{b}$, and? axes only.)

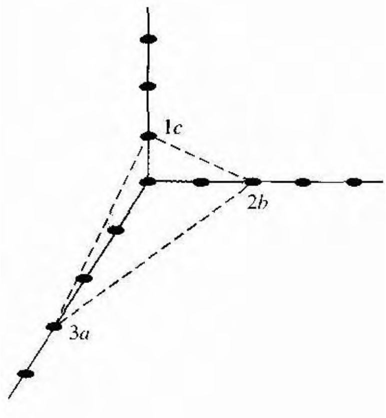

Figure **1.6** | A representative crystal lattice plane.

Solution

From Equation (1.1), the intercepts of the plane correspond to $p = 3$, $q = 2$, and $s = 1$. Now write the reciprocals of the intercepts, which gives

$$\left(\frac{1}{3}, \frac{1}{2}, \frac{1}{1}\right)$$

Multiply by the lowest common denominator, which in this case is 6, to obtain (2, 3, 6). The plane in Figure 1.6 is then referred to as the (236) plane. The integers are referred to as the Miller indices. We will refer to a general plane as the (hkl) plane.

■ Comment

We can show that the same three Miller indices are obtained for any plane that is parallel to the one shown in Figure 1.6. Any parallel plane is entirely equivalent to any other

---

Three planes that are commonly considered in a cubic crystal are shown in Figure 1.7. The plane in Figure 1.7a is parallel to the $\bar{b}$ and $\bar{c}$ axes so the intercepts are given as $p = 1$, $q = \infty$, and $s = \infty$. Taking the reciprocal, we obtain the Miller indices as (1, 0, 0), so the plane shown in Figure 1.7a is referred to as the (100) plane. Again, any plane parallel to the one shown in Figure 1.7a and separated by an integral

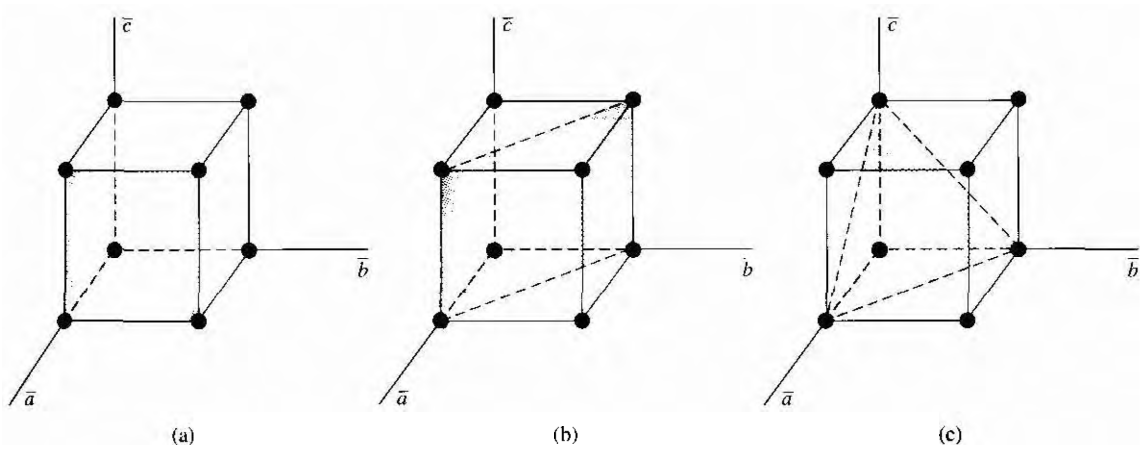

Figure 1.7 | Three lattice planes: (a) (100) plane. (b) (110) plane. (c) (111) plane.

number of lattice constants is equivalent and is referred to as the (100) plane. One advantage to taking the reciprocal of the intercepts to obtain the Miller indices is that the use of infinity is avoided when describing a plane that is parallel to an axis. If we were to describe a plane passing through the origin of our system, we would obtain infinity as one or more of the Miller indices after taking the reciprocal of the intercepts. However, the location of the origin of our system is entirely arbitrary and so, by translating the origin to another equivalent lattice point. we can avoid the use of infinity in the set of Miller indices.

For the simple cubic structure, the body-centered cubic. and the face-centered cubic, there is a high degree of symmetry. The axes can be rotated by 90" in each of the three dimensions and each lattice point can again be described by Equation (1.1) as

$$\bar{r} = p\bar{a} + q\bar{b} + s\bar{c} \tag{1.1}$$

Each face plane of the cubic structure shown in Figure 1.7a is entirely equivalent. These planes are grouped together and are referred to as the {100} set of planes.

We may also consider the planes shown in Figures 1.7b and 1.7c. The intercepts of the plane shown in Figure 1.7b are $p = 1$, $q = 1$, and $s = \infty$. The Miller indices are found by taking the reciprocal of these intercepts and, as a result, this plane is referred to as the (110) plane. In a similar way, the plane shown in Figure 1.7c is referred to as the (111) plane.

One characteristic of a crystal that can be determined is the distance between nearest equivalent parallel planes. Another characteristic is the surface concentration of atoms, number per square centimeter (#/cm^2), that are cut by a particular plane. Again, a single-crystal semiconductor is not infinitely large and must terminate at some surface. The surface density of atoms may be important, for example, in determining how another material, such as an insulator, will "fit" on the surface of a semiconductor material.

EXAMPLE 1.3

Objective

To calculate the surface density of atoms on a particular plane in a crystal.

Consider the body-centered cubic structure and the (110) plane shown in Figure 1.8a. Assume the atoms can be represented as hard spheres with the closest atoms touching each other. Assume the lattice constant is $a_1 = 5$ Å. Figure 1.8b shows how the atoms are cut by the (110) plane.

The atom at each corner is shared by four similar equivalent lattice planes, so each corner atom effectively contributes one-fourth of its area to this lattice plane as indicated in the figure. The four corner atoms then effectively contribute one atom to this lattice plane. The atom in the center is completely enclosed in the lattice plane. There is no other equivalent plane that cuts the center atom and the corner atoms, so the entire center atom is included in the number of atoms in the crystal plane. The lattice plane in Figure 1.8b, then, contains two atoms.

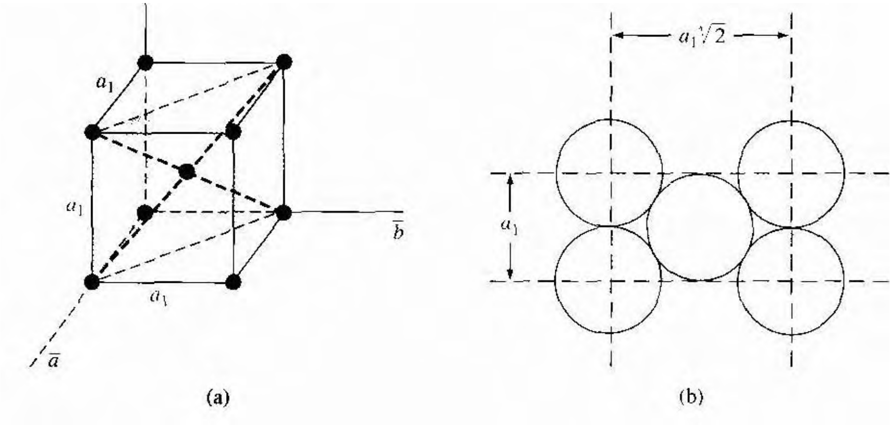

Figure 1.8 | (a) The (110) plane in a body-centered cubic and (b) the atoms cut by the (110) plane in a body-centered cubic.

■ Solution

We find the surface density by dividing the number of lattice atoms by the surface area, or in this case

$$\text{Surface density} = \frac{2\text{ atoms}}{(a_1)(a_1\sqrt{2})} = \frac{2}{(5\times 10^{-8})^2(\sqrt{2})}$$

which is

$$5.66 \times 10^{14}\ \text{atoms/cm}^2$$

■ Comment

The surface density of atoms is a function of the particular crystal plane in the lattice and generally varies from one crystal plane to another

TEST YOUR UNDERSTANDING

E1.3 Determine the distance between nearest (110) planes in a simple cubic lattice with a lattice constant of $a_0 = 4.83$ Å. (Ans. 3.42 Å)

E1.4 The lattice constant of a face-centered-cubic structure is 4.75 Å. Calculate the surface density of atoms for (*a*) a (100) plane and (*b*) a (110) plane.
[Ans. (a) 8.86×10^{14} cm^{-2}, (b) 6.27×10^{14} cm^{-2}]

In addition to describing crystal planes in a lattice, we may want to describe a particular direction in the crystal. The direction can be expressed as a set of three integers which are the components of a vector in that direction. For example, the body diagonal in a simple cubic lattice is composed of vector components 1, 1, 1. The body diagonal is then described as the [111] direction. The brackets are used to designate direction as distinct from the parentheses used for the crystal planes. The three basic directions and the associated crystal planes for the simple cubic structure are shown in Figure 1.9. Note that in the simple cubic lattices, the [*hkl*] direction is perpendicular to the (*hkl*) plane. This perpendicularity may not be true in noncubic lattices.

1.3.4 The Diamond Structure

As already stated, silicon is the most common semiconductor material. Silicon is referred to as a group IV element and has a diamond crystal structure. Germanium is also a group IV element and has the same diamond structure. A unit cell of the diamond structure, shown in Figure 1.10, is more complicated than the simple cubic structures that we have considered up to this point.

We may begin to understand the diamond lattice by considering the tetrahedral structure shown in Figure 1.11. This structure is basically a body-centered cubic with

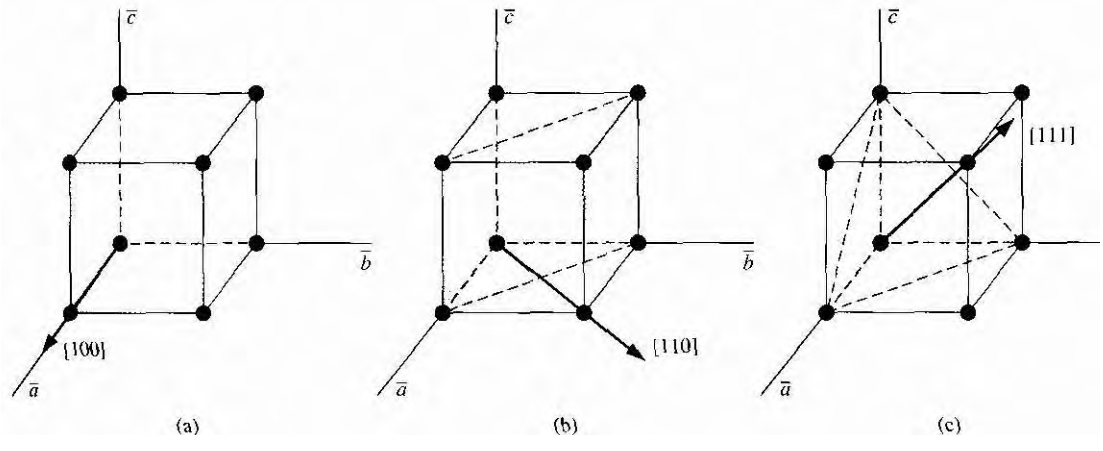

(a) (b) (c)

Figure 1.9 | Three lattice directions and planes: (a) (100) plane and [100] direction, (b) (110) plane and [110] direction, (c) (111) plane and [111] direction.

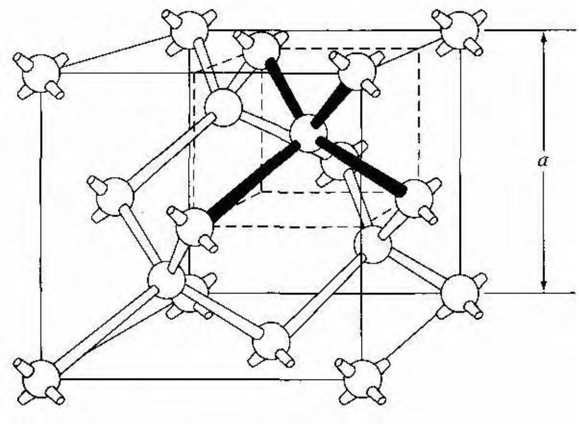

Figure 1.10 | The diamond structure.

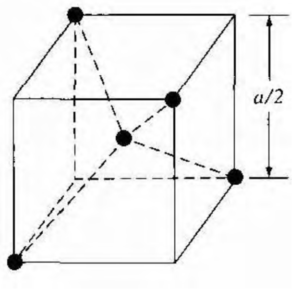

Figure 1.11 | The tetrahedral structure of closest neighbors in the diamond lattice.

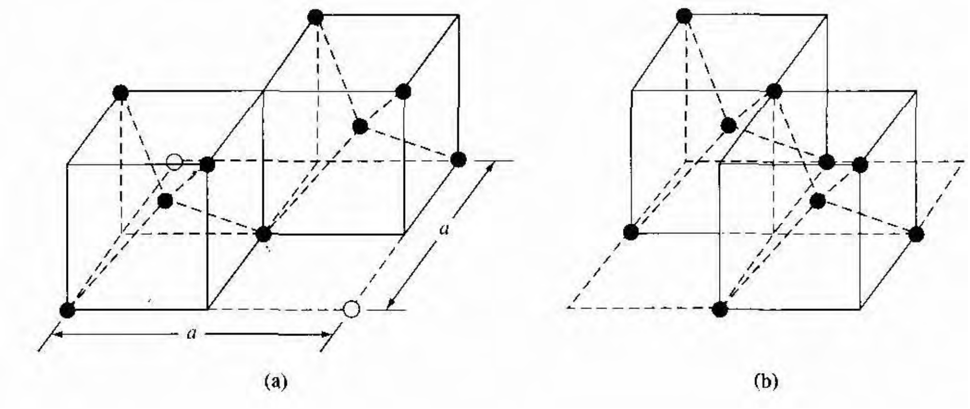

(a)

(b)

Figure 1.12 | Portions of the diamond lattice: (a) bottom half and (b) top half

four of the comer atoms missing. Every atom in the tetrahedral structure has four nearest neighbors and it is this structure which is the basic building block of the diamond lattice.

There are several ways to visualize the diamond structure. One way to gain a further understanding of the diamond lattice is by considering Figure 1.12. Figure 1.12a shows two body-centercd cubic, or tetrahedral, structures diagonally adjacent to each other. The shaded circles represent atoms in the lattice that are generated when the structure is translated to the right or left, one lattice constant, a. Figure 1.12b represents the top half of the diamond structure. The top half again consists of two tetrahedral structures joined diagonally, but which are at 90" with respect to the bottom-half diagonal. An important characteristic of the diamond lattice is that any atom within the diamond structure will have four nearest neighboring atoms. We will note this characteristic again in our discussion of atomic bonding in the next section.

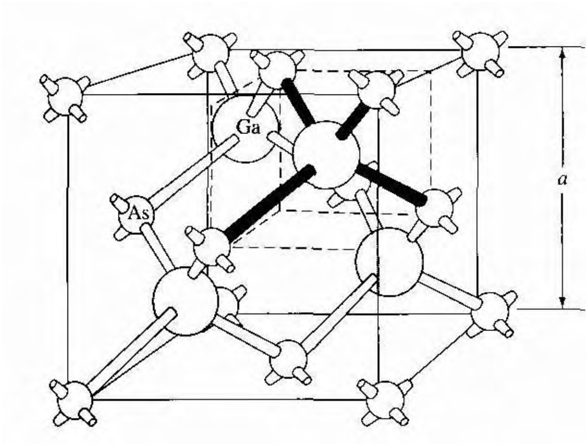

Figure 1.13 | The zincblende (sphalerite) lattice of GaAs.

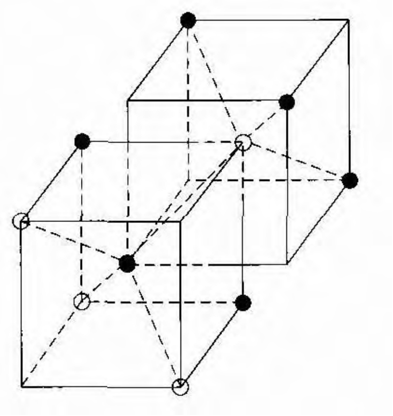

Figure 1.14 | The tetrahedral structure of closest neighbors in the zincblende lattice

The diamond structure refers to the particular lattice in which all atoms are of the same species, such as silicon or germanium. The rincblende (sphalerite) structure differs from the diamond structure only in that there are two different types of atoms in the lattice. Compound semiconductors, such as gallium arsenide, have the zincblende structure shown in Figure 1.13. The important feature of both the diamond and the zincblende structures is that the atoms are joined together to form a tetrahedron. Figure 1.14 shows the basic tetrahedral structure of GaAs in which each Ga atom has four nearest As neighbors and each As atom has four nearest Ga neighbors. This figure also begins to show the interpenetration of two sublattices that can be used to generate the diamond or zincblende lattice.

TEST YOUR UNDERSTANDING

E1.5 *The* lattice constant of silicon is 5.43 Å. Calculate the volume density of silicon atoms. (Ans. 5 × 10^{22} cm^{-3})

1.4 | ATOMIC BONDING

We have been considering various single-crystal structures. The question arises as to why one particular crystal structure is favored over another for a particular assembly of atoms. A fundamental law of nature is that the total energy of a system in thermal equilibrium tends to reach a minimum value. The interaction that occurs between atoms to form a solid and to reach the minimum total energy depends on the type of atom or atoms involved. The type of bond, or interaction, between atoms, then, depends on the particular atom or atoms in the crystal. If there is not a strong bond between atoms, they will not "stick together" to create a solid.

The interaction between atoms can be described by quantum mechanics. Although an introduction to quantum mechanics is presented in the next chapter, the quantum-mechanical description of the atomic bonding interaction is still beyond the scope of this text. We can nevertheless obtain a qualitative understanding of how various atoms interact by considering the valence, or outermost, electrons of an atom.

The atoms at the two extremes of the periodic table (excepting the inert elements) tend to lose or gain valence electrons, thus forming ions. These ions then essentially have complete outer energy shells. The elements in group I of the periodic table tend to lose their one electron and become positively charged. while the elements in group VII tend to gain an electron and become negatively charged. These oppositely charged ions then experience a coulomb attraction and form a bond referred to as an ***ionic bond.*** If the ions were to get too close, a repulsive force would become dominant, so an equilibrium distance results between these two ions. In a crystal, negatively charged ions tend to be surrounded by positively charged ions and positively charged ions tend to he surrounded by negatively charged ions, so a periodic array of the atoms is formed to create the lattice. A classic example of ionic bonding is sodium chloride.

The interaction of atoms tends to form closed valence shells such as we see in ionic bonding. Another atomic bond that tends to achieve closed-valence energy shells is ***covalent bonding,*** an example of which is found in the hydrogen molecule. A hydrogen atom has one electron and needs one more electron to complete the lowest energy shell. A schematic of two noninteracting hydrogen atoms, and the hydrogen molecule with the covalent bonding, are shown in Figure 1.15. Covalent bonding results in electrons being shared between atoms, so that in effect the valence energy shell of each atom is full.

Atoms in group IV of the periodic table, such as silicon and germanium, also tend to form covalent bonds. Each of these elements has four valence electrons and needs four more electrons to complete the valence energy shell. If a silicon atom, for example, has four nearest neighbors, with each neighbor atom contributing one valence electron to be shared. then the center atom will in effect have eight electrons in its outer shell. Figure 1.16a schematically shows live noninteracting silicon atoms with the four valence electrons around each atom. A two-dimensional representation

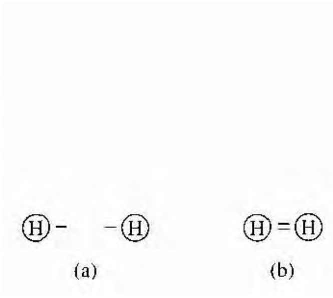

Figure 1.15 | Representation of (a) hydrogen valence electrons and (b) covalent bonding in a hydrogen molecule.

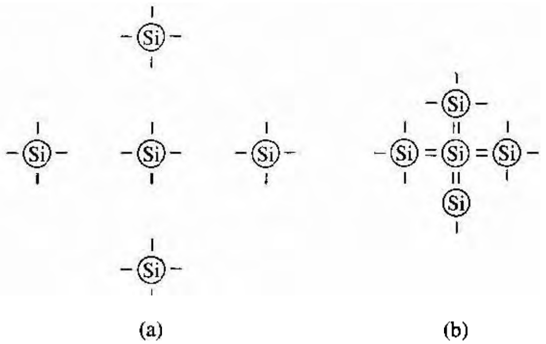

Figure 1.16 | Representation of (a) silicon valence electrons and (b) covalent bonding in the silicon crystal.

of the covalent bonding in silicon is shown in Figure 1.16b. The center atom has eight shared valence electrons.

A significant difference between the covalent bonding of hydrogen and of silicon is that, when the hydrogen molecule is formed, it has no additional electrons to form additional covalent bonds, while the outer silicon atoms always have valence electrons available for additional covalent bonding. The silicon array may then be formed into an infinite crystal, with each silicon atom having four nearest neighbors and eight shared electrons. The four nearest neighbors in silicon forming the covalent bond correspond to the tetrahedral structure and the diamond lattice, which were shown in Figures 1.11 and 1.10, respectively. Atomic bonding and crystal structure are obviously directly related.

The third major atomic bonding scheme is referred to as *metallic bonding*. Group I elements have one valence electron. If two sodium atoms ($Z = 11$), for example. are brought into close proximity, the valence electrons interact in a way similar to that in covalent bonding. When a third sodium atom is brought into close proximity with the first two, the valence electrons can also interact and continue to form a bond. Solid sodium has a body-centered cubic structure, so each atom has eight nearest neighbors with each atom sharing many valence electrons. We may think of the positive metallic ions as being surrounded by a sea of negative electrons, the solid being held together by the electrostatic forces. This description gives a qualitative picture of the metallic bond.

A fourth type of atomic bond. called the *Van der Waals* bond, is the weakest of the chemical bonds. A hydrogen fluoride (HF) molecule, for example, is formed by an ionic bond. The effective center of the positive charge of the molecule is not the same as the effective center of the negative charge. This nonsymmetry in the charge distribution results in a small electric dipole that can interact with the dipoles of other HF molecules. With these weak interactions, solids formed by the Van der Waals bonds have a relatively low melting temperature — in fact, most of these materials are in gaseous form at room temperature.

*1.5 | IMPERFECTIONS AND IMPURITIES IN SOLIDS

Up to this point, we have been considering an ideal single-crystal structure. In a real crystal, the lattice is not perfect, hut contains imperfections or defects; that is, the perfect geometric periodicity is disrupted in some manner. Imperfections tend to alter the electrical properties of a material and, in some cases, electrical parameters can be dominated by these defects or impurities.

1.5.1 Imperfections in Solids

One type of imperfection that all crystals have in common is atomic thermal vibration. Aperfect single crystal contains atoms at particular lattice sites, the atoms separated from each other by a distance we have assumed to be constant. The atoms in a

---

*Indicates sections that can bc skipped without loss of continuity.

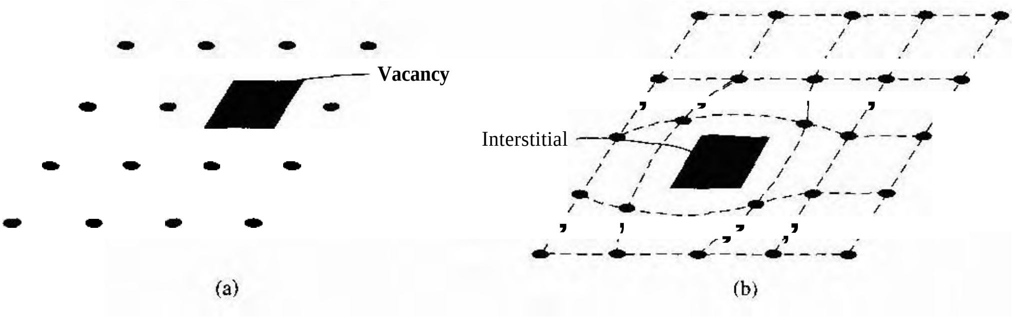

(a)

(b)

Figure 1.17 | Two-dimensional representation of a single-crystal lattice showing (a) a vacancy defect and (b) an interstitial defect.

crystal, however, have a certain thermal energy, which is a function of temperature. The thermal energy causes the atoms to vibrate in a random manner about an equilibrium lattice point. This random thermal motion causes the distance between atoms to randomly fluctuate, slightly disrupting the perfect geometric arrangement of atoms. This imperfection, called lattice vibrations, affects some electrical parameters, as we will see later in our discussion of semiconductor material characteristics.

Another type of defect is called a *point defect.* There are several of this type that we need to consider. Again, in an ideal single-crystal lattice, the atoms are arranged in a perfect periodic arrangement. However, in a real crystal, an atom may be missing from a particular lattice site. This defect is referred to as a *vacancy;* it is schematically shown in Figure 1.17a. In another situation, an atom may be located between lattice sites. This defect is referred to as an *interstitial* and is schematically shown in Figure 1.17b. In the case of vacancy and interstitial defects, not only is the perfect geometric arrangement of atoms broken, but also the ideal chemical bonding between atoms is disrupted, which tends to change the electrical properties of the material. A vacancy and interstitial may be in close enough proximity lo exhibit an interaction between the two point defects. This vacancy-interstitial defect, also known as a Frenkel defect, produces different effects than the simple vacancy or interstitial.

The point defects involve single atoms or single-atom locations. In forming single-crystal materials, more complex defects may occur. A line defect. for example, occurs when an entire row of atoms is missing from its normal lattice site. This defect is referred to as a line *dislocation* and is shown in Figure 1.18. As with a point defect, a line dislocation disrupts both the normal geometric periodicity of the lattice and the ideal atomic bonds in the crystal. This dislocation can also alter the electrical properties of the material, usually in a more unpredictable manner than the simple point defects.

Other complex dislocations can also occur in it crystal lattice. However. this introductory discussion is intended only to present a few of the basic types of defect, and to show that a real crystal is not necessarily a perfect lattice structure. The effect of these imperfections on the electrical properties of a semiconductor will be considered in later chapters.

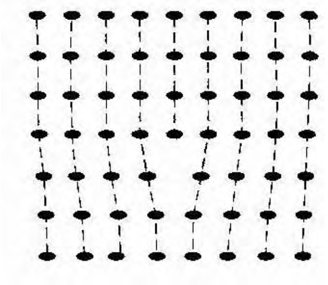

Figure 1.18 | A two-dimensional representation of a line dislocation.

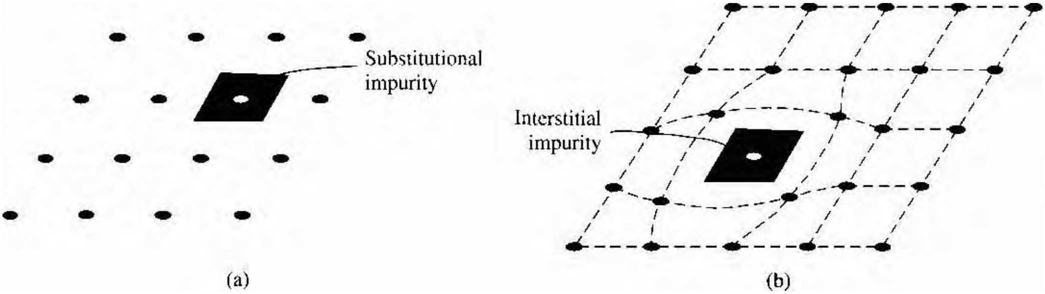

Figure 1.19 | Two-dimensional representation of a single-crystal lattice showing (a) a substitutional impurity and (b) an intersitital impurity.

1.5.2 Impurities in Solids

Foreign atoms, or impurity atoms, may be present in a crystal lattice. Impurity atoms may be located at normal lattice sites, in which case they are called *substitutional* impurities. Impurity atoms may also be located between normal sites, in which case they are called *interstitial* impurities. Both these impurities are lattice defects and are schematically shown in Figure 1.19. Some impurities, such as oxygen in silicon, tend to he essentially inert; however, other impurities, such as gold or phosphorus in silicon, can drastically alter the electrical properties of the material.

In Chapter 4 we will see that, by adding controlled amounts of particular impurity atoms, the electrical characteristics of a semiconductor material can be favorably altered. The technique of adding impurity atoms to a semiconductor material in order to change its conductivity is called *doping*. There are two general methods of doping: impurity diffusion and ion implantation.

The actual diffusion process depends to some extent on the material but, in general, impurity diffusion occurs when a semiconductor crystal is placed in a high-temperature (= 1000°C) gaseous atmosphere containing the desired impurity atom. At this high temperature, many of the crystal atoms can randomly move in and out of their single-crystal lattice sites. Vacancies may be created by this random motion so that impurity atoms can move through the lattice by hopping from one vacancy to another. Impurity diffusion is the process by which impurity particles move from a region of high concentration near the surface, to a region of lower concentration within the crystal. When the temperature decreases, the impurity atoms become permanently frozen into the substitutional lattice sites. Diffusion of various impurities into selected regions of a semiconductor allows us to fabricate complex electronic circuits in a single semiconductor crystal.

Ion implantation generally takes place at a lower temperature than diffusion. A beam of impurity ions is accelerated to kinetic energies in the range of 50 keV or greater and then directed to the surface of the semiconductor. The high-energy impurity ions enter the crystal and come to rest at some average depth from the surface. One advantage of ion implantation is that controlled numbers of impurity atoms can be introduced into specific regions of the crystal. A disadvantage of this technique is that the incident impurity atoms collide with the crystal atoms. causing lattice-displacement damage. However, most of the lattice damage can he removed by thermal annealing, in which the temperature of the crystal is raised for a short time. Thermal annealing is a required step after implantation.

*1.6 | GROWTH OF SEMICONDUCTOR MATERIALS

The success in fabricating very large scale integrated (VLSI) circuits is a result, to a large extent, of the development of and improvement in the formation or growth of pure single-crystal semiconductor materials. Semiconductors are some of the purest materials. Silicon, for example, has concentrations of most impurities of less than 1 part in 10 billion. The high purity requirement means that extreme care is necessary in the growth and the treatment of the material at each step of the fabrication process. The mechanics and kinetics of crystal growth are extremely complex and will be described in only very general terms in this text. However, a general knowledge of the growth techniques and terminology is valuable.

1.6.1 Growth from a Melt

A common technique for growing single-crystal materials is called the ***Czochralski method.*** In this technique, a small piece of single-crystal material, known as a ***seed,*** is brought into contact with the surface of the same material in liquid phase, and then slowly pulled from the melt. As the seed is slowly pulled, solidification occurs along the plane between the solid–liquid interface. Usually the crystal is also rotated slowly as it is being pulled, to provide a slight stirring action to the melt, resulting in a more uniform temperature. Controlled amounts of specific impurity atoms, such as boron or phosphorus, may be added to the melt so that the grown semiconductor crystal is intentionally doped with the impurity atom. Figure 1.20 shows a schematic of the Czochralski growth process and a silicon ingot or boule grown by this process.

---

*Indicates sections that can be skipped without loss of continuity

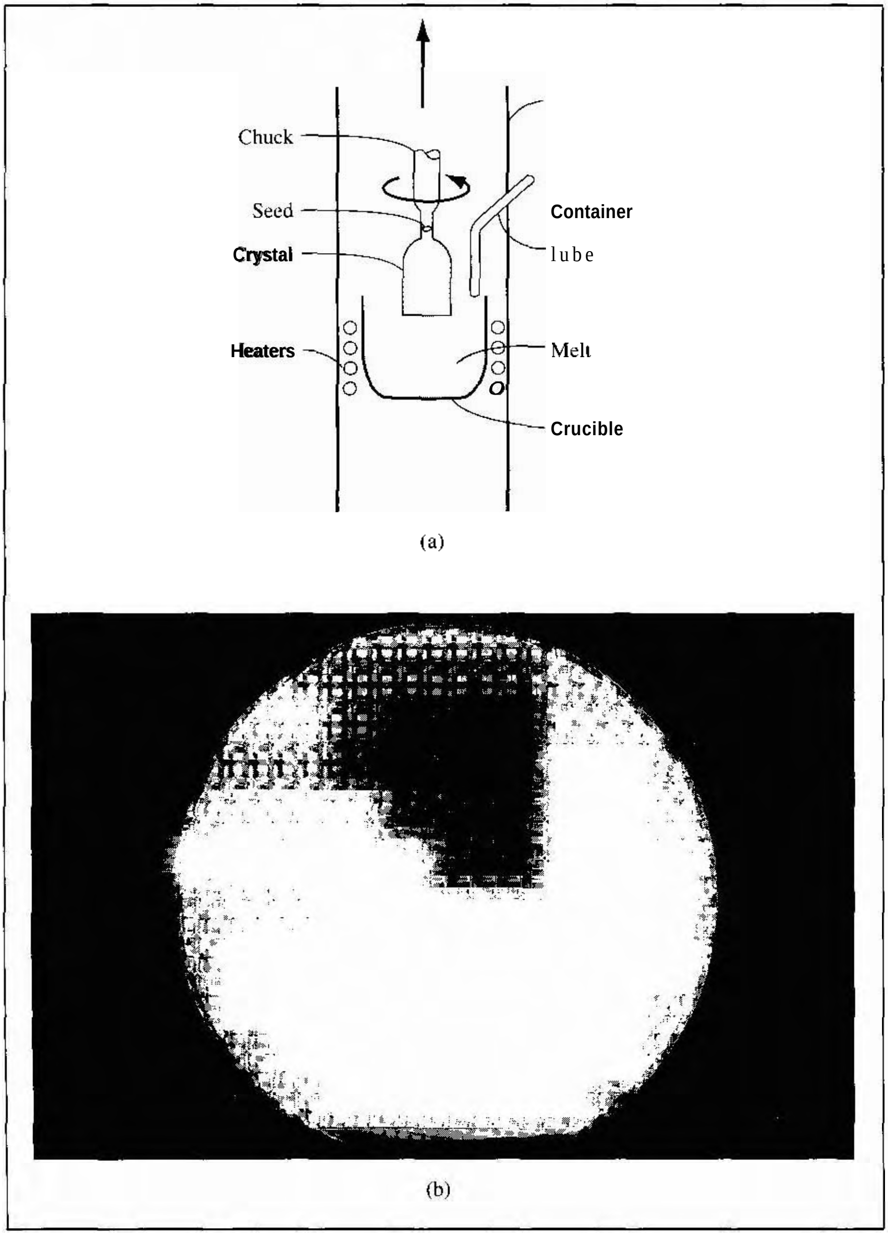
Chuck
Seed
Crystal
Heaters
Container
Tube
Melt
Crucible
(a)
(b)

Figure 1.20 | **(a)** Model of a crystal puller and (b) photograph of a silicon wafer with an array of integrated circuits. The circuits are tested on the wafer then sawed apart into chips that are mounted into packages. (Photo courtesy of Intel Corporation.)

Some impurities may be present in the ingot that are undesirable. Zone refining is a common technique for purifying material. A high-temperature coil. or r-f induction coil, is slowly passed along the length of the boule. The temperature induced by the coil is high enough so that a thin layer of liquid is formed. At the solid–liquid interface, there is a distribution of impurities between the two phases. The parameter that describes this distribution is called the ***segregation coefficient:*** the ratio of the concentration of impurities in the solid to the concentration in the liquid. If the segregation coefficient is 0.1, for example, the concentration of impurities in the liquid is a factor of 10 greater than that in the solid. As the liquid zone moves through the material. the impurities are driven along with the liquid. After several passes of the r-f coil, most impurities are at the end of the bar, which can then be cut off. The moving molten zone, or the zone-refining technique, can result in considerable purification.

After the semiconductor is grown, the boule is mechanically trimmed to the proper diameter and a flat is ground over the entire length of the boule to denote the crystal orientation. The flat is perpendicular to the [110] direction or indicates the (110) plane. (See Figure 1.20b.) This then allows the individual chips to be fabricated along given crystal planes so that the chips can be sawed apart more easily. The boule is then sliced into wafers. The wafer must be thick enough to mechanically support itself. A mechanical two-sided lapping operation produces a flat wafer of uniform thickness. Since the lapping procedure can leave a surface damaged and contaminated by the mechanical operation, the surface must be removed by chemical etching. The final step is polishing. This provides a smooth surface on which devices may be fabricated or further growth processes may be carried out. This final semiconductor wafer is called the substrate material.

1.6.2 Epitaxial Growth

A common and versatile growth technique that is used extensively in device and integrated circuit fabrication is epitaxial growth. ***Epitaxial growth*** is a process whereby a thin, single-crystal layer of material is grown on the surface of a single-crystal substrate. In the epitaxial process, the single-crystal substrate acts as the seed, although the process takes place far below the melting temperature. When an epitaxial layer is grown on a substrate of the same material, the process is termed ***homoepitaxy.*** Growing silicon on a silicon substrate is one example of a homoepitaxy process. At present, a great deal of work is being done with ***heteroepitaxy.*** In a heteroepitaxy process, although the substrate and epitaxial materials are not the same, the two crystal structures should be very similar if single-crystal growth is to be obtained and if a large number of defects are to be avoided at the epitaxial–substrate interface. Growing epitaxial layers of the ternary alloy AlGaAs on a GaAs substrate is one example of a heteroepitaxy process.

One epitaxial growth technique that has been used extensively is called ***chemical vapor-phase deposition (CVD).*** Silicon epitaxial layers, for example, are grown on silicon substrates by the controlled deposition of silicon atoms onto the surface from a chemical vapor containing silicon. In one method, silicon tetrachloride reacts with hydrogen at the surface of a heated substrate. The silicon atoms are released in the reaction and can he deposited onto the substrate, while the other chemical reactant, HCI, is in gaseous form and is swept out of the reactor. A sharp demarcation between the impurity doping in the substrate and in the epitaxial layer can be achieved using the CVD process. This technique allows great flexibility in the fabrication of semiconductor devices.

***Liquid-phase** epitaxy* is another epitaxial growth technique. **A** compound of the semiconductor with another element may have a melting temperature lower than that of the semiconductor itself. The semiconductor substrate is held in the liquid compound and, since the temperature of the melt is lower than the melting temperature of the substrate, the substrate does not melt. As the solution is slowly cooled, a single-crystal semiconductor layer grows on the seed crystal. This technique, which occurs at a lower temperature than the Czochralski method, is useful in growing group III–V compound semiconductors.

A versatile technique for growing epitaxial layers is the *molecular beam epitaxy* (MBE) process. A substrate is held in vacuum at a temperature normally in the range of 400 to 800°C, a relatively low temperature compared with many semiconductor-processing steps. Semiconductor and dopant atoms are then evaporated onto the surface of the substrate. In this technique, the doping can he precisely controlled resulting in very complex doping profiles. Complex ternary compounds, such as AlGaAs, can be grown on substrates, such as GaAs, where abrupt changes in the crystal composition are desired. Many layers of various types of epitaxial compositions can be grown on a substrate in this manner. These structures are extremely beneficial in optical devices such as laser diodes.

1.7 | SUMMARY

- A few of the most common semiconductor (materials were listed. Silicon is the most common semiconductor material.
- The properties of semiconductors and other materials are determined to a large extent by the single-crystal lattice structure. The unit cell is a small volume of the crystal that is used to reproduce the entire crystal. Three basic unit cells **are** the simple cubic. body-centered cubic. and face-centered cubic.
- Silicon has the diamond crystal structure. Atoms are formed in a tetrahedral configuration with four nearest neighbor atoms. The binary semiconductors have a zincblende lattice, that is basically the came as the diamond lattice.
- Miller indices are used to describe planer in a crystal lattice. These planes may be used to describe the surface of a semiconductor material. The Miller indices are also used to describe directions in a crystal.
- Imperfections do exist in semiconductor materials. A few of these imperfections are vacancies, substitutional impurities, and interstitial impurities. Small amounts of controlled substitutional impurities can favorably alter semiconductor properties as we will see in later chapters.
- A brief description of semiconductor growth methods was given. Bulk growth produces the starting semiconductor material or substrate. Epitaxial growth can be used to control the surface properties of a semiconductor Most semiconductor devices are fabricated in the epitaxial layer.

GLOSSARY OF IMPORTANT TERMS

binary semiconductor A two-element compound semiconductor, such as gallium arsenide (GaAs).

covalent bonding The bonding between atoms in which valence electrons are shared.

diamond lattice The atomic crystal structure of silicon, for example, in which each atom has four nearest neighhors in a tetrahedral configuration.

doping The process of adding specific types of atoms to a semiconductor to favorably alter the electrical characteristics.

elemental semiconductor A semiconductor composed of **a** single species of atom, such as silicon or germanium.

epitaxial layer A thin, single-crystal layer of material formed on the surface of a substrate.

ion implantation One particular process of doping a semiconductor.

lattice The periodic arrangement of atoms in a crystal.

Miller indices The set of integers used to describe a crystal plane.

primitive cell The smallest unit cell that can be repeated to form a lattice.

substrate A semiconductor wafer or other material used as the starling material for further semiconductor processing. such as epitaxial growth or diffusion.

ternary semiconductor A three-element compound semiconductor. such as aluminum gallium arsenide (AlGaAs).

unit cell A small volume of a crystal that can be used to reproduce the entire crystal.

zincblende lattice A lattice structure identical to the diamond lattice except that there arc two types of atoms instead of one.

CHECKPOINT

After studying this chapter, the reader should hare the ability to:

- Determine the volume density of atoms for various lattice structures.
- Determine the Miller indices of a crystal-lattice plane.
- Sketch a lattice plane riven the Miller indices.
- Determine the surface density of atoms on a given crystal-lattice plane.
- Understand and describe various defects in a single-crystal lattice.

REVIEW QUESTIONS

1. List two elemental semiconductor materials and two compound semiconductor materials.
2. Sketch three lattice structures: (*a*) simple cubic, (*b*) body-centered cubic, and (*c*) face-centered cubic.
3. Describe the procedure for finding the volume density of atoms in a crystal.
4. Describe the procedure for obtaining the Miller indices that describe a plane in a crystal.
5. What is meant by a substitutional impurity in a crystal? What is meant by an interstitial impurity'?

PROBLEMS

Section 1.3 Space Lattices

1.1 Determine the number of atoms per unit cell in **a** (*a*) face-centered cubic, (b) body-centered cubic, and (*c*) diamond lattice.

1.2 (a) The lattice constant of GaAs is 5.65 Å. Determine the number of Ga atoms and As atoms per cm^3. *(h)* Determine the volume density of germanium atoms in a germanium semiconductor. The lattice constant of germanium is 5.65 Å.

Assume that each atom is a hard sphere with the surface of each atom in contact with the surface of its nearest neighbor. Determine the percentage of total unit cell volume that is occupied in *(a)* a simple cubic lattice, (b) a face-centered cubic lattice, (c) a body-centered cubic lattice, and (d) **a** diamond lattice.

A material, with a volume of I cm', is composed of an fcc lattice with a lattice constant of 2.5 *mm*. The "atoms" in this material are actually coffee beans. Assume the coffee beans are hard spheres with each bean touching its nearest neighbor. Determine the volume of coffee after the coffee beans have been ground. (Assume 100 percent packing density of the ground coffee.)

1.5 If the lattice constant of silicon is 5.41 Å, calculate (a) the distance from the center of one silicon atom to the center of its nearest neighbor, *(h)* the number density of silicon atoms (#per cm^3), and (*c*) the mass density (grams per cm^3) of silicon.

1.6 A crystal is composed of two elements, A and B. The basic crystal structure is a body-centered cubic with elements A at each of the corners and element B in the center. The effective radius of element A is 1.02 Å. Assume the elements arc hard spheres with the surface of each A-type atom in contact with the surface of its nearest A-type neighbor. Calculate (a) the maximum radius of the B-type atom that will fit into this structure, and *(b)* the volume density (#/cm^3) of both the A-type atoms and the B-type atoms.

The crystal structure of sodium chloride (NaCl) is a simple cubic with the Na and Cl atoms alternating positions. Each Na atom is then surrounded by six Cl atoms and likewise each Cl atom is surrounded by six Na atoms. (a) Sketch the atoms in a (100) plane. (b) Assume the atoms arc hard spheres with nearest neighbors touching. The effective radius of Na is 1.0 Å and the effective radius of Cl is 1.8 Å. Determine the lattice constant. (c) Calculate the volume density of Na and Cl atoms. (d) Calculate the mass density of NaCl.

(*a*) **A** material is composed of two types of atoms. Atom A has an effective radius of 2.2 Å and atom B has an effective radius of 1.8 Å. The lattice is a bcc with atoms A at the comers and atom B in the center. Determine the lattice constant and the volume densities of A atoms and B atoms. (b) Repeat part (a) with atoms B at the corners and atom A in the center *(c)* What comparison can be made of the materials in pans (*a*) and (*b*)?

Consider the materials described in Problem 1.8 in pans (a) and (b). For each case, calculate the surface density of A atoms and B atoms in the (110) plane. What comparison can be made of the two materials?

1.10 ***(a)*** The crystal structure of a particular material consists of a single atom in the center of a cube. The lattice constant is a, and the diameter of the atom is a_0. Determine the volume density of atoms and the surface density of atoms in the (110) plane.
(b) Compare the results of part (a) to the results for the case of the simple cubic structure shown in Figure 1.5a with the same lattice constant.

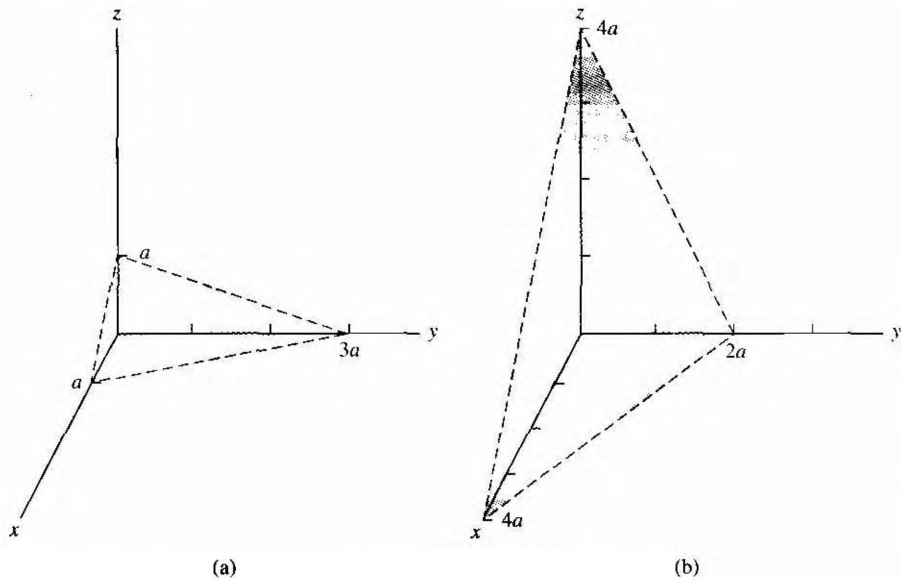

Figure 1.21 | Figure for Problem 1.12.

1.11 Consider a three-dimensional cubic lattice with a lattice constant equal loo. (a) Sketch the following planes: (*i*) (100), (*ii*) (110), (iii) (310), and ***(iv)*** (230). (*b*) Sketch the following directions: (i) [100], (ii) [110], (*iii*) [310], and (iv) [230].

1.12 For a simple cubic lattice, determine the Miller indices for the planes shown in Figure 1.21.

1.13 The lattice constant of a simple cubic cell is *5.63* Å. Calculate the distance between the nearest parallel (*a*) (100), (*b*) (110), and (*c*) (111) planes.

1.14 The lattice constant of a single crystal is 4.50 Å. Calculate the surface density of atoms (# per cm^2) on the following planes: (*i*) (100), (ii) (110), (*iii*) (111) for each of the following lattice structures: (*a*) simple cubic, (h) body-centered cubic, and (*c*) face-centered cubic.

1.15 Determine the surface density of atoms for silicon on the (a) (100) plane, (*b*) (110) plane, and (*c*) (111) plane.

1.16 Consider a face-centered cubic lattice. Assume the atoms are hard spheres with the surfaces of the nearest neighbors touching. Assume the radius of the atom is 2.25 Å. (*a*) Calculate the volume density of atoms in the crystal. (*b*) Calculate the distance between nearest (110) planes. (c) Calculate the surface density of atoms on the (I10) plane.

Section 1.4 Atomic Bonding

1.17 Calculate the density of valence electrons in silicon

1.18 The structure of GaAs is the zincblende lattice. The lattice constant is 5.65 Å. Calculate the density of valence electrons in GaAs.

Section 1.5 Imperfections and Impurities in Solids

1.19 (a) If 2 x 10^{16} boron atoms per cm' are added to silicon as a substitutional impurity, determine what percentage of the silicon atoms are displaced in the single crystal lattice. *(b)* Repeat pall *(a)* for 10^{15} boron atoms per cm^3.

1.20 (a) Phosphorus atoms, at a concentration of 5 x 10^{16} cm^{-3}, are added to a pure sample of silicon. Assume the phosphorus atoms are distributed homogeneously throughout the silicon. What is the fraction by weight of phosphorus'? *(b)* If boron atoms, at a concentration of 10^{18} cm^{-3}, are added to the material in part (a), determine the fraction by weight of boron.

1.21 If 2 x 10^{15} gold atoms per cm^3 are added to silicon as a substitutional impurity and are distributed uniformly throughout the semiconductor, determine the distance between gold atoms in terms of the silicon lattice constant. (Assume the gold atoms are distributed in a rectangular or cubic array.)

READING LIST

1. Azaroff. L.V., and J. J. Brophy. Electronic *Processes* in *Materials*. New York: McGraw-Hill, 1963.
2. Campbell, S. A. The Science *and Engineering* of Microelectronic *Fabrication.* New York: Oxford University Press, 1996.
3. Kittel, C. *Introduction* to Solid Stare *Physics*, 7th ed. Berlin: Springer-Verlag, 1993.

*4. Li, S. S. Semiconductor Physical Electronics. New York: Plenum Press, 1993.

5. McKelvey, J. P. Solid State Physics for *Engineering and Materials* Science. Malabar, FL: Krieger, 1993.
6. Pierret, R. F. Semiconductor *Device* Fundamentals. Reading, MA: Addison-Wesley, 1996.
7. Runyan, W. R., and K. E. Bean. *Semiconductor Integrated* Circuit Processing and Technology Reading, MA: Addison-Wesley, 1990.
8. Singh, J. *Semiconductor Devices:* Basic *Principles.* New York: John Wiley and Sons, 2001.
9. Streetman, B. G., and S. Banerjee. *Solid* State Electronic *Devices*, 5th ed. Upper Saddle River, NJ: Prentice Hall, 2000.
10. Sze, S. M. VLSI *Technology.* New York: McGraw-Hill, 1983.

*11. Wolfe, C. M., N. Holonyak. Jr., and G. E. Stillman. Physical Properties *of Semiconductors.* Englewood Cliffs. NJ: Prentice Hall, 1989.

---

*Indicates references that are at an advanced level compared to this text.

CHAPTER 2

Introduction to Quantum Mechanics

PREVIEW

The goal of this text is to help readers understand the operation and characteristics of semiconductor devices. Ideally, we would like to begin discussing these devices immediately. However, in order to understand the current–voltage characteristics, we need some knowledge of the electron behavior in a crystal when the electron is subjected to various potential functions.

The motion of large objects, such as planets and satellites, can be predicted to a high degree of accuracy using classical theoretical physics based on Newton's laws of motion. But certain experimental results, involving electrons and high-frequency electromagnetic waves, appear to he inconsistent with classical physics. However, these experimental results can be predicted by the principles of quantum mechanics. The quantum mechanical wave theory is the basis for the theory of semiconductor physics.

We are ultimately interested in semiconductor materials whose electrical properties arc directly related to the behavior of electrons in the crystal lattice. The behavior and characteristics of these electrons can be described by the formulation of quantum mechanics called wave mechanics. The essential elements of this wave mechanics, using Schrodinger's wave equation, are presented in this chapter.

The goal of this chapter is to provide a brief introduction to quantum mechanics so that readers gain an understanding of and become comfortable with the analysis techniques. This introductory material forms the basis of semiconductor physics..

2.1 | PRINCIPLES OF QUANTUM MECHANICS

Before we delve into the mathematics of quantum mechanics. there are three principles we need to consider: the principle of energy quanta, the wave–particle duality principle, and the uncertainty principle.

2.1.1 Energy Quanta

One experiment that demonstrates an inconsistency between experimental results and the classical theory of light is called the photoelectric effect. If monochromatic light is incident on a clean surface of a material, then under certain conditions, electrons (photoelectrons) are emitted from the surface. According to classical physics. if the intensity of the light is large enough, the work function of the material will be overcome and an electron will be emitted from the surface independent of the incident frequency. This result is not observed. The observed effect is that, at a constant incident intensity, the maximum kinetic energy of the photoelectron varies linearly with frequency with a limiting frequency $\nu = \nu_0$, below which no photoelectron is produced. This result is shown in Figure 2.1. If the incident intensity varies at a constant frequency, the rate of photoelectron emission changes, but the maximum kinetic energy remains the same.

Planck postulated in 1900 that thermal radiation is emitted from a heated surface in discrete packets of energy called *quanta*. The energy of these quanta is given by $E = h\nu$, where ν is the frequency of the radiation and h is a constant now known as Planck's constant ($h = 6.625 \times 10^{-34}$ J-s). Then in 1905, Einstein interpreted the photoelectric results by suggesting that the energy in a light wave is also contained in discrete packets or bundles. The particle-like packet of energy is called a photon, whose energy is also given by $E = h\nu$. A photon with sufficient energy, then, can knock an electron from the surface of the material. The minimum energy required to remove an electron is called the work function of the material

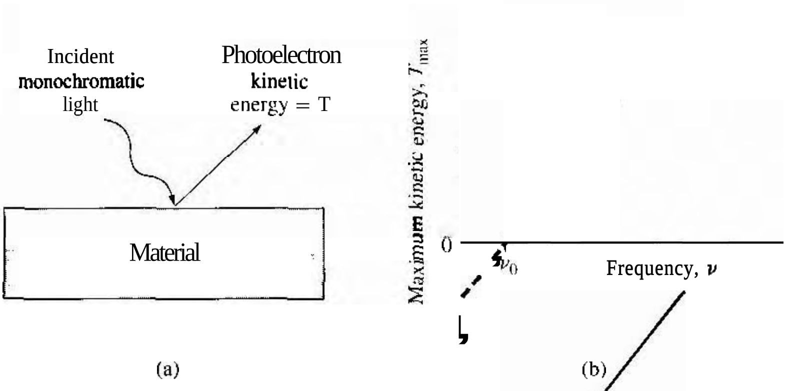
Incident monochromatic light
Photoelectron kinetic energy = T
Material
Maximum kinetic energy, T_{max}
0
ν_0
Frequency, ν
(a)
(b)

Figure 2.1 | (a) The photoelectric effect and (b) the maximum kinetic energy of the photoelectron as a function of incident frequency.

and any excess photon energy goes into the kinetic energy of the photoelectron. This result was confirmed experimentally as demonstrated in Figure 2.1. The photoelectric effect shows the discrete nature of the photon and demonstrates the particle-like behavior of the photon.

The maximum kinetic energy of the photoelectron can be written as

$$T_{\max} = \frac{1}{2}mv^2 = h\nu - h\nu_0 \quad (\nu \geq \nu_0) \tag{2.1}$$

where $h\nu$ is the incident photon energy and $h\nu_0$ is the minimum energy, or work function, required to remove an electron from the surface.

EXAMPLE 2.1

Objective

To calculate the photon energy corresponding to a particular wavelength.

Consider an x-ray with a wavelength of $\lambda = 0.708 \times 10^{-8}$ cm.

■ **Solution**

The energy is

$$E = h\nu = \frac{hc}{\lambda} = \frac{(6.625 \times 10^{-34})(3 \times 10^{10})}{0.708 \times 10^{-8}} = 2.81 \times 10^{-15} \text{ J}$$

This value of energy may be given in the more common unit of electron-volt (see Appendix F). We have

$$E = \frac{2.81 \times 10^{-15}}{1.6 \times 10^{-19}} = 1.75 \times 10^4 \text{ eV}$$

■ **Comment**

The reciprocal relation between photon energy and wavelength is demonstrated: A large m-ergy corresponds to a short wavelength.

2.1.2 Wave–Particle Duality

We have seen in the last section that light waves, in the photoelectric effect, behave as if they are particles. The particle-like behavior of electromagnetic waves was also instrumental in the explanation of the Compton effect. In this experiment. an x-ray beam was incident on a solid. A portion of the x-ray beam was deflected and the frequency of the deflected wave had shifted compared to the incident wave. The observed change in frequency and the deflected angle corresponded exactly to the expected results of a "billiard ball" collision between an x-ray quanta, or photon, and an electron in which both energy and momentum are conserved.

In 1924. de Broglie postulated the existence of matter waves. He suggested that since waves exhibit particle-like behavior, then panicles should he expected to show wave-like properties. The hypothesis of de Broglie was the existence of a *wave–particle duality principle*. The momentum of a photon is given by

$$p = \frac{h}{\lambda} \tag{2.2}$$

where A is the wavelength of the light wave. Then, de Broglie hypothesized that the wavelength of a particle can be expressed as

$$\lambda = \frac{h}{p} \tag{2.3}$$

wherep is the momentum of the particle and A is known as the *de Broglie wavelength* of the matter wave.

The wave nature of electrons has been tested in several ways. In one experiment by Davisson and Germer in 1927, electrons from a heated filament were accelerated at normal incidence onto a single crystal of nickel. A detector measured the scattered electrons as a function of angle. Figure 2.2 shows the experimental setup and Figure 2.3 shows the results. The existence of a peak in the density of scattered electrons can be explained as a constructive interference of waves scattered by the periodic atoms in the planes of the nickel crystal. The angular distribution is very similar to an interference pattern produced by light diffracted from a grating.

In order to gain some appreciation of the frequencies and wavelengths involved in the wave-particle duality principle. Figure 2.4 shows the electromagnetic frequency spectrum. We see that a wavelength of 72.7 A obtained in the next example is in the ultraviolet range. Typically, we will be considering wavelengths in the

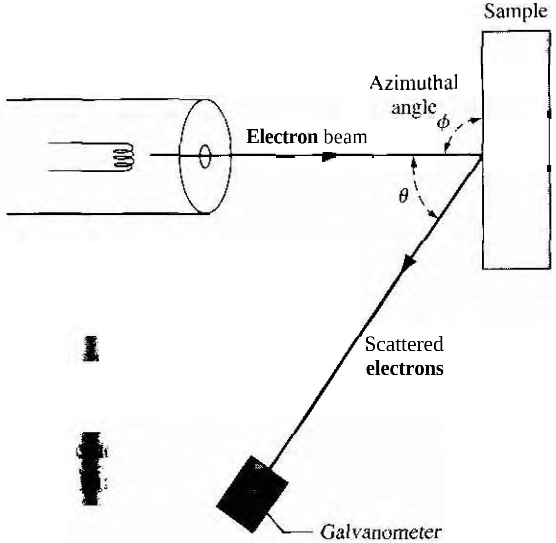

Figure **2.2** | Experimental arrangement of the Davisson–Germer experiment.

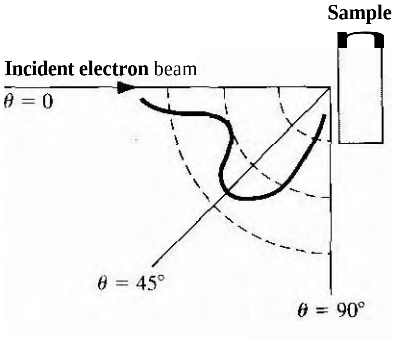

Figure **2.3** | Scattered electron flux as a function **of** scattering angle for the Davisson–Germer experiment.

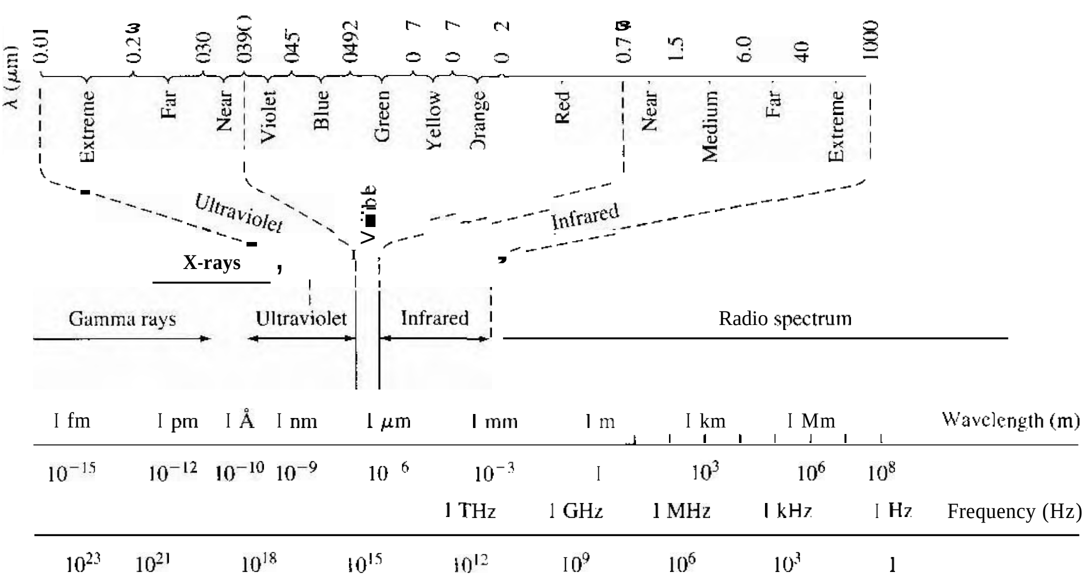
λ (μm)
0.01
0.23
0.30
0.390
0.455
0.492
0.7
0.7
0.2
0.770
1.5
6.0
40
1000
Extreme
Far
Near
Violet
Blue
Green
Yellow
Orange
Red
Near
Medium
Far
Extreme
Ultraviolet
Visible
Infrared
X-rays
Gamma rays
Ultraviolet
Infrared
Radio spectrum
1 fm
1 pm
1 Å
1 nm
1 μm
1 mm
1 m
1 km
1 Mm
Wavelength (m)
10^-15
10^-12
10^-10
10^-9
10^-6
10^-3
1
10^3
10^6
10^8
1 THz
1 GHz
1 MHz
1 kHz
1 Hz
Frequency (Hz)
10^23
10^21
10^18
10^15
10^12
10^9
10^6
10^3
1

Figure 2.4 | The electromagnetic frequency spectrum

ultraviolet and visible range. These wavelengths are very short compared to the usual radio spectrum range.

EXAMPLE 2.2

Objective

To calculate the de Broglie wavelength of a particle.

Consider an electron traveling at a velocity of 10^7 cm/sec $= 10^5$ m/s.

■ Solution

The momentum is given by

$$p = mv = (9.11 \times 10^{-31})(10^5) = 9.11 \times 10^{-26}$$

Then, the de Broglie wavelength is

$$\lambda = \frac{h}{p} = \frac{6.625 \times 10^{-34}}{9.11 \times 10^{-26}} = 7.27 \times 10^{-9} \text{ m}$$

or

$$\lambda = 72.7 \text{ Å}$$

■ Comment

This calculation shows the order of magnitude of the de Broglie wavelength for a "typical" electron.

In some cases electromagnetic waves behave as if they are particles (photons) and sometimes particles behave as if they are waves. This wave–particle duality principle of quantum mechanics applies primarily to small particles such as electrons, but it has also been shown to apply to protons and neutrons. For very large particles, we can show that the relevant equations reduce to those of classical mechanics. The wave–particle duality principle is the basis on which we will use wave theory to describe the motion and behavior of electrons in a crystal.

TEST YOUR UNDERSTANDING

E2.1 Determine the energy of a photon having wavelengths of (a) A = 10.000 A and *(b)* $\lambda = 10$ Å. [Ans. (*a*) 1.99×10^{-19} J or 1.24 eV; (*b*) 1.99×10^{-16} J or 1.24×10^{3} eV]

E2.2 (a) Find the momentum and energy of a particle with mass of 5×10^{-31} kg and a de Broglie wavelength of 180 Å. (*b*) An electron has a kinetic energy of 20 meV. Determine the de Broglie wavelength. [Ans. (*a*) $p = 3.68 \times 10^{-26}$ kg-m/s, $E = 1.35 \times 10^{-21}$ J or 8.46×10^{-3} eV, (*b*) $p = 7.64 \times 10^{-26}$ kg-m/s, $\lambda = 86.7$ Å]

2.1.3 The Uncertainty Principle

The Heisenberg uncertainty principle, given in 1927, also applies primarily to very small particles, and states that we cannot describe with absolute accuracy the behavior of these subatomic particles. The uncertainty principle describes a fundamental relationship between conjugate variables, including position and momentum and also energy and time.

The first statement of the uncertainty principle is that it is impossible to simultaneously describe with absolute accuracy the position and momentum of a particle. If the uncertainty in the momentum is Δp and the uncertainty in the postion is Δx, then the uncertainty principle is stated as[1]

$$\Delta p \, \Delta x \geq \hbar \tag{2.4}$$

where $\hbar$ is defined as $\hbar = h/2\pi = 1.054 \times 10^{-34}$ J-s and is called a modified Planck's constant. This statement may be generalized to include angular position and angular momentum.

The second statement of the uncertainty principle is that it is impossible to simultaneously describe with absolute accuracy the energy of a particle and the instant of time the particle has this energy. Again, if the uncertainty in the energy is given by ΔE and the uncertainty in the time is given by Δt, then the uncertainty principle is stated as

$$\Delta E \, \Delta t \geq \hbar \tag{2.5}$$

One way to visualize the uncertainty principle is to consider the simultaneous measurement of position and momentum, and the simultaneous measurement of energy and time. The uncertainty principle implies that these simultaneous measurements are in error to a certain extent. However, the modified Planck's constant $\hbar$ is very small; the uncertainty principle is only significant for subatomic particles. We must keep in mind nevertheless that the uncertainty principle is a fundamental statement and does not deal only with measurements.

---

[1] In some texts, the uncertainty principle is stated as $\Delta p \, \Delta x \geq \hbar/2$. We are interested here in the order of magnitude and will not be concerned with small differences.

One consequence of the uncertainty principle is that we cannot. for example. determine the exact position of an electron. We will, instead, determine the *probability* of finding an electron at a particular position. In later chapters, we will develop a *probability density function* that will allow us to determine the probability that an electron has a particular energy. So in describing electron behavior, we will he dealing with probability functions.

TEST YOUR UNDERSTANDING

E2.3 The uncertainty in position of an electron is 12 Å. Determine the minimum uncertainty in momentum and also the corresponding uncertainly in kinetic energy. (Ans. $\Delta p = 8.79 \times 10^{-26}$ kg-m/s, $\Delta E = 0.0265$ eV)

E2.4 An electron's energy is measured with an uncertainty of 1.2 eV. What is the minimum uncertainty in time over which the energy is measured'? (Ans. $\Delta t = 5.49 \times 10^{-16}$ s)

2.2 | SCHRODINGER'S WAVE EQUATION

The various experimental results involving electromagnetic waves and particles. which could not be explained by classical laws of physics, showed that a revised formulation of mechanics was required. Schrodinger, in 1926. provided a formulation called *wave mechanics,* which incorporated the principles of quanta introduced by Planck, and the wave–particle duality principle introduced by de Broglie. Based on the wave–particle duality principle. we will describe the motion of electrons in a crystal by wave theory. This wave theory is described by Schrodinger's wave equation.

2.2.1 The Wave Equation

The one-dimensional, nonrelativistic Schrodinger's wave equation is given by

$$\frac{-\hbar^2}{2m} \cdot \frac{\partial^2 \Psi(x,t)}{\partial x^2} + V(x)\Psi(x,t) = j\hbar\frac{\partial \Psi(x,t)}{\partial t} \qquad (2.6)$$

where $\Psi(x,t)$ is the wave function, $V(x)$ is the potential function assumed to he independent of time, m is the mass of the particle, and j is the imaginary constant $\sqrt{-1}$. There are theoretical arguments that justify the form of Schrodinger's wave equation. hut the equation is a basic postulate of quantum mechanics. The wave function $\Psi(x,t)$ will be used to describe the behavior of the system and, mathematically, $\Psi(x,t)$ can be a complex quantity.

We may determine the time-dependent portion of the wave function and the position-dependent, or time-independent, portion of the wave function by using the technique of separation of variables. Assume that the wave function can he written in the form

$$\Psi(x,t) = \psi(x)\phi(t) \tag{2.7}$$

where $\psi(x)$ is a function of the position x only and $\phi(t)$ is a function of time t only. Substituting this form of the solution into Schrodinger's wave equation, we obtain

$$\frac{-\hbar^2}{2m}\phi(t)\frac{\partial^2\psi(x)}{\partial x^2} + V(x)\psi(x)\phi(t) = j\hbar\psi(x)\frac{\partial\phi(t)}{\partial t} \tag{2.8}$$

If we divide by the total wave function. Equation (2.8) becomes

$$\frac{-\hbar^2}{2m}\frac{1}{\psi(x)}\frac{\partial^2\psi(x)}{\partial x^2} + V(x) = j\hbar\cdot\frac{1}{\phi(t)}\cdot\frac{\partial\phi(t)}{\partial t} \tag{2.9}$$

Since the left side of Equation **(2.9)** is a function of position x only and the right side of the equation is a function of time t only, each side of this equation must he equal to a constant. We will denote this separation of variables constant by η.

The time-dependent portion of Equation (2.9) is then written as

$$\eta = j\hbar\cdot\frac{1}{\phi(t)}\cdot\frac{\partial\phi(t)}{\partial t} \tag{2.10}$$

where again the parameter η is called a separation constant. The solution of Equation (2.10) can be written in the form

$$\phi(t) = e^{-j(E/\hbar)t} \tag{2.11}$$

The form of this solution is the classical exponential form of a sinusoidal wave where $\eta/\hbar$ is the radian frequency w. We have that $E = h\nu$ or $E = h\omega/2\pi$. Then $\omega = \eta/\hbar = E/\hbar$ so that the separation constant is equal to the total energy E of the particle.

The time-independent portion of Schrodinger's wave equation can now he written from Equation (2.9) as

$$\frac{-\hbar^2}{2m}\cdot\frac{1}{\psi(x)}\cdot\frac{\partial^2\psi(x)}{\partial x^2} + V(x) = E \tag{2.12}$$

where the separation constant is the total energy E of the particle. Equation (2.12) may he written as

$$\boxed{\frac{\partial^2\psi(x)}{\partial x^2} + \frac{2m}{\hbar^2}(E - V(x))\psi(x) = 0} \tag{2.13}$$

where again m is the mass of the particle, $V(x)$ is the potential experienced by the particle, and E is the total energy of the particle. This time-independent Schrodinger's wave equation can also be justified on the basis of the classical wave equation as shown in Appendix E. The pseudo-derivation in the appendix is a simple approach but shows the plausibility of the time-independent Schrodinger's equation.

2.2.2 Physical Meaning of the Wave Function

We are ultimately trying to use the wave function $\Psi(x, t)$ to describe the behavior of an electron in a crystal. The function $\Psi(x, t)$ is a wave function. so it is reasonable to ask what the relation is between the function and the electron. The total wave function is the product of the position-dependent, or time-independent, function and the time-dependent function. We have from Equation (2.7) that

$$\boxed{\Psi(x, t) = \psi(x)\phi(t) = \psi(x)e^{-j(E/\hbar)t}} \tag{2.14}$$

Since the total wave function $\Psi(x, t)$ is a complex function. it cannot by itself represent a real physical quantity.

Max Born postulated in 1926 that the function $|\Psi(x, t)|^2\,dx$ is the probability of finding the particle between x and $x + dx$ at a given time, or that $|\Psi(x, t)|^2$ is a probability density function. We have that

$$|\Psi(x, t)|^2 = \Psi(x, t) \cdot \Psi^*(x, t) \tag{2.15}$$

where $\Psi^*(x, t)$ is the complex conjugate function. Therefore

$$\Psi^*(x, t) = \psi^*(x) \cdot e^{+j(E/\hbar)t}$$

Then the product of the total wave function and its complex conjugate is given by

$$\Psi(x, t)\Psi^*(x, t) = \left[\psi(x)e^{-j(E/\hbar)t}\right]\left[\psi^*(x)e^{+j(E/\hbar)t}\right] = \psi(x)\psi^*(x) \tag{2.16}$$

Therefore, we have that

$$|\Psi(x, t)|^2 = \psi(x)\psi^*(x) = |\psi(x)|^2 \tag{2.17}$$

is the probability density function and is independent of time. One major difference between classical and quantum mechanics is that in classical mechanics, the position of a particle or body can be determined precisely, whereas in quantum mechanics, the position of aparticlr is found in terms o f a probability. We will determine the probability density function for several examples, and, since this property is independent of time. we will, in general, only be concerned with the time-independent wave function.

2.2.3 Boundary Conditions

Since the function $|\Psi(x, t)|^2$ represents the probability density function, then for a single particle. we must have that

$$\boxed{\int_{-\infty}^{\infty} |\psi(x)|^2\,dx = 1} \tag{2.18}$$

The probability of finding the particle somewhere is certain. Equation (2.18) allows us to normalize the wave function and is one boundary condition that is used to determine some wave function coefficients.

The remaining boundary conditions imposed on the wave function and its derivative are postulates. However. we may state the boundary conditions and present arguments that justify why they must be imposed. The wave function and its first derivative must have the following properties if the total energy E and the potential $V(x)$ are finite everywhere.

Condition 1. $\psi(x)$ must be finite, single-valued, and continuous.

Condition 2. $\partial\psi(x)/\partial x$ must be finite, single-valued, and continuous.

Since $|\psi(x)|^2$ is a probability density, then $\psi(x)$ must be finite and single-valued. If the probability density were to become infinite at some point in space, then the probability of finding the particle at this position would be certain and the uncertainty principle would be violated. If the total energy E and the potential $V(x)$ are finite everywhere, then from Equation (2.13), the second derivative must be finite, which implies that the first derivative must be continuous. The first derivative is related to the particle momentum, which must be finite and single-valued. Finally, a finite first derivative implies that the function itself must he continuous. In some of the specific examples that we will consider, the potential function will become infinite in particular regions of space. For these cases. the first derivative will not necessarily be continuous, but the remaining boundary conditions will still hold.

2.3 I APPLICATIONS OF SCHRODINGER'S WAVE EQUATION

We will now apply Schrodinger's wave equation in several examples using various potential functions. These examples will demonstrate the techniques used in the solution of Schrodinger's differential equation and the results of these examples will provide an indication of the electron behavior under these various potentials. We will utilize the resulting concepts later in the discussion of semiconductor properties.

2.3.1 Electron in Free Space

As a first example of applying the Schrodinger's wave equation, consider the motion of an electron in free space. If there is no force acting on the particle, then the potential function $V(x)$ will be constant and we must have $E > V(x)$. Assume, for simplicity, that the potential function $V(x) = 0$ for all x. Then, the time-independent wave equation can he written from Equation (2.13) as

$$\frac{\partial^2\psi(x)}{\partial x^2} + \frac{2mE}{\hbar^2}\psi(x) = 0 \tag{2.19}$$

The solution to this differential equation can be written in the form

$$\psi(x) = A\exp\left[\frac{jx\sqrt{2mE}}{\hbar}\right] + B\exp\left[\frac{-jx\sqrt{2mE}}{\hbar}\right] \tag{2.20}$$

Recall that the time-dependent portion of the solution is

$$\psi(t) = e^{-j(E/\hbar)t} \tag{2.21}$$

Then the total solution for the wave function is given by

$$\Psi(x,t) = A\exp\left[\frac{j}{\hbar}(x\sqrt{2mE} - Et)\right] + B\exp\left[\frac{-j}{\hbar}(x\sqrt{2mE} + Et)\right] \tag{2.22}$$

This wave function solution is a traveling wave, which means that a particle moving in free space is represented by a traveling wave. The first term, with the coefficient A. is a wave traveling in the $+x$ direction, while the second term, with the coefficient B. is a wave traveling in the x direction. The value of these coefficients will be determined from boundary conditions. We will again see the traveling-wave solution for an electron in a crystal or semiconductor material.

Assume, for a moment, that we have a particle traveling in the $+x$ direction. which will be described by the $+x$ traveling wave. The coefficient $B = 0$. We can write the traveling-wave solution in the form

$$\Psi(x,t) = A\exp[j(kx - \omega t)] \tag{2.23}$$

where k is a wave number and is

$$k = \frac{2\pi}{\lambda} \tag{2.24}$$

The parameter A is the wavelength and, comparing Equation (2.23) with Equation (2.22), the wavelength is given by

$$\lambda = \frac{h}{\sqrt{2mE}} \tag{2.25}$$

From de Broglie's wave–particle duality principle, the wavelength is also given by

$$\lambda = \frac{h}{p} \tag{2.26}$$

A free particle with a well-defined energy will also have a well-defined wavelength and momentum.

The probability density function is $\Psi(x,t)\Psi^*(x,t) = AA^*$, which is a constant independent of position. A free particle with a well-defined momentum can be found anywhere with equal probability. This result is in agreement with the Heisenberg uncertainty principle in that a precise momentum implies an undefined position.

A localized free particle is defined by a wave packet, formed by a superposition of wave functions with different momentum or k values. We will not consider the wave packet here.

2.3.2 The Infinite Potential Well

The problem of a particle in the infinite potential well is a classic example of a bound particle. The potential $V(x)$ as a function of position for this problem is shown in

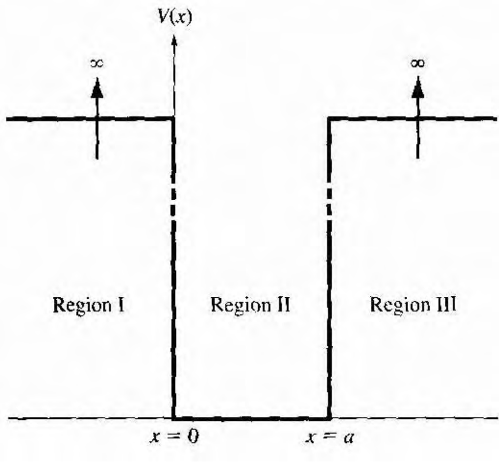

Figure 2.5 | Potential function of the infinite potential well.

Figure 2.5. The particle is assumed to exist in region II so the particle is contained within a finite region of space. The time-independent Schrodinger's wave equation is again given by Equation *(2.13)* as

$$\frac{\partial^2 \psi(x)}{\partial x^2} + \frac{2m}{\hbar^2}(E - V(x))\psi(x) = 0 \tag{2.13}$$

where E is the total energy of the particle. If E is finite, the wave function must be zero, or $\psi(x) = 0$, in both regions I and III. A particle cannot penetrate these infinite potential barriers, so the probability of finding the particle in regions I and III is zero.

The time-independent Schrodinger's wave equation in region II, where $V = 0$. becomes

$$\frac{\partial^2 \psi(x)}{\partial x^2} + \frac{2mE}{\hbar^2}\psi(x) = 0 \tag{2.27}$$

A particular form of solution to this equation is given by

$$\psi(x) = A_1 \cos Kx + A_2 \sin Kx \tag{2.28}$$

where

$$K = \sqrt{\frac{2mE}{\hbar^2}} \tag{2.29}$$

One boundary condition is that the wave function $\psi(x)$ must be continuous so that

$$\psi(x = 0) = \psi(x = a) = 0 \tag{2.30}$$

Applying the boundary condition at $x = 0$, we must have that $A_1 = 0$. At $x = a$, we have

$$\psi(x = a) = 0 = A_2 \sin Ka \tag{2.31}$$

This equation is valid if $Ka = n\pi$, where the parameter n is a positive integer, or $n = 1, 2, 3, \ldots$. The parameter n is referred to as a quantum number. We can write

$$K = \frac{n\pi}{a} \tag{2.32}$$

Negative values of n simply introduce a negative sign in the wave function and yield redundant solutions for the probability density function. We cannot physically distinguish any difference between $+n$ and $-n$ solutions. Because of this redundancy, negative values of n are not considered.

The coefficient A_2 can be found from the normalization boundary condition that was given by Equation (2.18) as $\int_{-\infty}^{\infty} \psi(x)\psi^*(x)\,dx = 1$. If we assume that the wave function solution $\psi(x)$ is a real function, then $\psi(x) = \psi^*(x)$. Substituting the wave function into Equation (2.18), we have

$$\int_0^a A_2^2 \sin^2 Kx\,dx = 1 \tag{2.33}$$

Evaluating this integral gives[2]

$$A_2 = \sqrt{\frac{2}{a}} \tag{2.34}$$

Finally, the time-independent wave solution is given by

$$\psi(x) = \sqrt{\frac{2}{a}} \sin\left(\frac{n\pi x}{a}\right) \qquad \text{where } n = 1, 2, 3, \ldots \tag{2.35}$$

This solution represents the electron in the infinite potential well and is a standing wave solution. The free electron was represented by a traveling wave, and now the bound particle is represented by a standing wave.

The parameter K in the wave solution was defined by Equations (2.29) and (2.32). Equating these two expressions for K, we obtain

$$\frac{2mE}{\hbar^2} = \frac{n^2\pi^2}{a^2} \tag{2.36}$$

---

[2] A more thorough analysis shows that $|A_2|^2 = 2/a$, so solutions for the coefficient A_2 include $+\sqrt{2/a}$, $-\sqrt{2/a}$, $+j\sqrt{2/a}$, $-j\sqrt{2/a}$, or any complex number whose magnitude is $\sqrt{2/a}$. Since the wave function itself has no physical meaning, the choice of which coefficient to use is immaterial: They all produce the same probability density function.

The total energy can then be written as

$$\boxed{E = E_n = \frac{\hbar^2 n^2 \pi^2}{2ma^2}} \qquad \text{where } n = 1, 2, 3, \ldots \tag{2.37}$$

For the particle in the infinite potential well. the wave function is now given by

$$\psi(x) = \sqrt{\frac{2}{a}} \sin Kx \tag{2.38}$$

where the constant K must have discrete values, implying that the total energy of the particle can only have discrete values. This result *means* that the energy *of the* particle is quantized. That is, *the energy of the particle can only have particular discrete values.* The quantization of the particle energy is contrary to results from classical physics, which would allow the particle to have continuous energy values. The discrete energies lead to quantum states that will be considered in more detail in this and later chapters. The quantization of the energy of a bound particle is an extremely important result.

Objective **EXAMPLE 2.3**

To calculate the first three energy levels of an electron in an infinite potential well

Consider an electron in an infinite potential well of width 5 Å.

■ **Solution**

From Equation **(2.37)** we have

$$E_n = \frac{(\hbar^2 n^2 \pi^2)}{2ma^2} = \frac{n^2(1.054 \times 10^{-34})^2 \pi^2}{2(9.11 \times 10^{-31})(5 \times 10^{-10})^2} = n^2(2.41 \times 10^{-19})\ \text{J}$$

or

$$E_n = \frac{n^2(2.41 \times 10^{-19})}{1.6 \times 10^{-19}} = n^2(1.51)\ \text{eV}$$

Then.

$$E_1 = 1.51\ \text{eV}, \quad E_2 = 6.04\ \text{eV}, \quad E_3 = 13.59\ \text{eV}$$

■ **Comment**

This calculation shows the order of magnitude of the energy levels of a bound electron.

Figure 2.6a shows the first four allowed energies for the particle in the infinite potential well, and Figures 2.6b and 2.6c show the corresponding wave functions and probability functions. We may note that as the energy increases, the probability of finding the particle at any given value of x becomes more uniform.

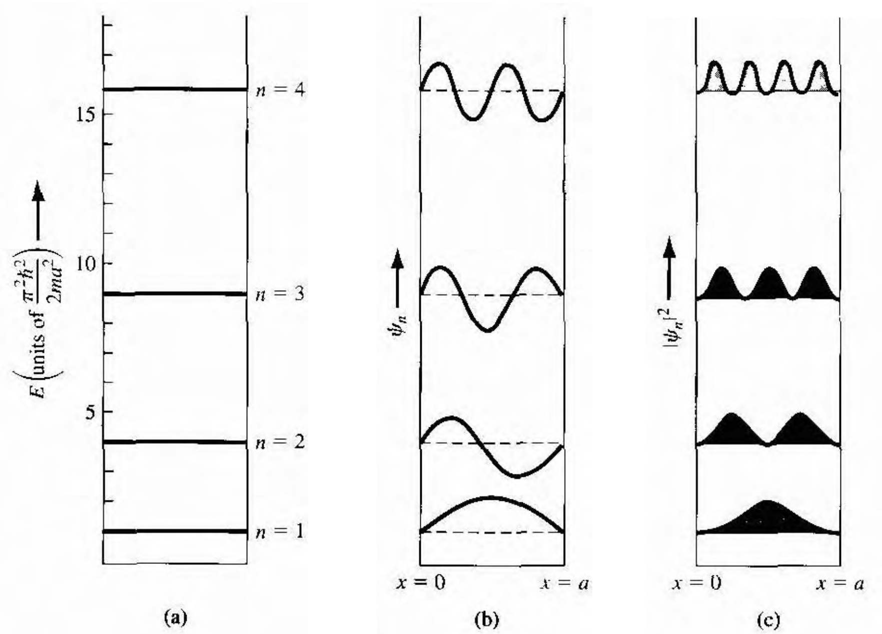

Figure 2.6 | Particle in an infinite potential well: (a) Four lowest discrete energy levels. (b) Corresponding wave functions. (c) Corresponding probability functions. *(From Pierret [9].)*

TEST YOUR UNDERSTANDING

E2.5 The width of the infinite potential well in Example 2.3 is doubled to 10 Å. Calculate the first three energy levels in terms of electron volts for an electron. (Ans. 0.376 eV, 1.50 eV, 3.38 eV)

E2.6 The lowest energy of a particle in an infinite potential well with a width of 100 Å is 0.025 eV. What is the mass of the particle? (Ans. 1.37×10^{-31} kg)

2.3.3 The Step Potential Function

Consider now a step potential function as shown in Figure 2.7. In the previous section, we considered a particle being confined between two potential barriers. In this example, we will assume that a flux of particles is incident on the potential barrier. We will assume that the particles are traveling in the $+x$ direction and that they originated at $x = -\infty$. A particularly interesting result is obtained for the case when the total energy of the particle is less than the barrier height, or $E < V_0$.

We again need to consider the time-independent wave equation in each of the two regions. This general equation was given in Equation (2.13) as $\partial^2\psi(x)/\partial x^2 + 2m/\hbar^2(E - V(x))\psi(x) = 0$. The wave equation in region I, in which $V = 0$, is

$$\frac{\partial^2\psi_1(x)}{\partial x^2} + \frac{2mE}{\hbar^2}\psi_1(x) = 0 \tag{2.39}$$

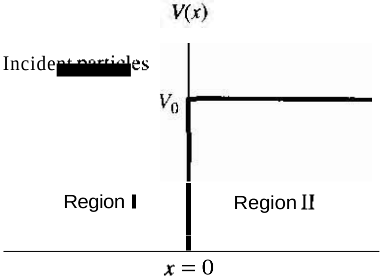

Figure 2.7 I The step potential function.

The general solution to this equation can be written in the form

$$\psi_1(x) = A_1 e^{jK_1 x} + B_1 e^{-jK_1 x} \quad (x \le 0) \tag{2.40}$$

where the constant K_1 is

$$K_1 = \sqrt{\frac{2mE}{\hbar^2}} \tag{2.41}$$

The first **term** in Equation (2.40) is a traveling wave in the $+x$ direction that represents the incident wave, and the second term is a traveling wave in the $-x$ direction that represents a reflected wave. As in the case of a free particle, the incident and reflected particles are represented by traveling waves.

For the incident wave, $A_1 \cdot$ A; is the probability density function of the incident panicles. If we multiply this probability density function by the incident velocity, then $v_i \cdot A_1 \cdot A_1^*$ is the flux of incident particles in units of #/cm^2-s. Likewise, the quantity $v_r \cdot B_1 \cdot B_1^*$ is the Hux of the reflected particles, where v_r is the velocity of the reflected wave. (The parameters v_i and v_r in these terms are actually the magnitudes of the velocity only.)

In region II, the potential is $V = V_0$. If we assume that $E < V_0$, then the differential equation describing the wave function in region 11 can be written as

$$\frac{\partial^2 \psi_2(x)}{\partial x^2} - \frac{2m}{\hbar^2}(V_0 - E)\psi_2(x) = 0 \tag{2.42}$$

The general solution may then be written in the form

$$\psi_2(x) = A_2 e^{-K_2 x} + B_2 e^{+K_2 x} \quad (x \ge 0) \tag{2.43}$$

where

$$K_2 = \sqrt{\frac{2m(V_0 - E)}{\hbar^2}} \tag{2.44}$$

One **boundary** condition is that the wave function $\psi_2(x)$ must remain finite, which means that the coefficient $B_2 = 0$. The wave function is now given by

$$\psi_2(x) = A_2 e^{-K_2 x} \quad (x \ge 0) \tag{2.45}$$

The wave function at $x = 0$ must be continuous so that

$$\psi_1(0) = \psi_2(0) \tag{2.46}$$

Then from Equations (2.40), (2.45), and (2.46), we obtain

$$A_1 + B_1 = A_2 \tag{2.47}$$

Since the potential function is everywhere finite, the first derivative of the wave function must also be continuous so that

$$\left.\frac{\partial \psi_1}{\partial x}\right|_{x=0} = \left.\frac{\partial \psi_2}{\partial x}\right|_{x=0} \tag{2.48}$$

Using Equations (2.40), (2.45), and (2.48), we obtain

$$jK_1A_1 - jK_1B_1 = -K_2A_2 \tag{2.49}$$

We can solve Equations (2.47) and (2.49) to determine the coefficients B_1 and A_2 in terms of the incident wave coefficient A_1. The results are

$$B_1 = \frac{-(K_2^2 + 2jK_1K_2 - K_1^2)A_1}{(K_2^2 + K_1^2)} \tag{2.50a}$$

and

$$A_2 = \frac{2K_1(K_1 - jK_2)A_1}{(K_2^2 + K_1^2)} \tag{2.50b}$$

The reflected probability density function is given by

$$B_1 \cdot B_1^* = \frac{(K_2^2 - K_1^2 + 2jK_1K_2)(K_2^2 - K_1^2 - 2jK_1K_2)A_1 \cdot A_1^*}{(K_2^2 + K_1^2)^2} \tag{2.51}$$

We can define a reflection coefficient, R, as the ratio of the reflected flux to the incident flux, which is written as

$$R = \frac{v_r \cdot B_1 \cdot B_1^*}{v_1 \cdot A_1 \cdot A_1^*} \tag{2.52}$$

where v_i and v_r are the incident and reflected velocities. respectively. of the particles. In region I, $V = 0$ so that $E = T$, where T is the kinetic energy of the particle. The kinetic energy is given by

$$T = \frac{1}{2}mv^2 \tag{2.53}$$

so that the constant K_1, from Equation (2.41), may be written as

$$K_1 = \sqrt{\frac{2m}{\hbar^2}\left(\frac{1}{2}mv^2\right)} = \sqrt{m^2\frac{v^2}{\hbar^2}} = \frac{mv}{\hbar} \tag{2.54}$$

The incident velocity can then be written as

$$v_i = \frac{\hbar}{m} \cdot K_1 \tag{2.55}$$

Since the reflected particle also exists in region I, the reflected velocity (magnitude) is given by

$$v_r = \frac{\hbar}{m} \cdot K_1 \tag{2.56}$$

The incident and reflected velocities (magnitudes) are equal. The reflection coefficient is then

$$R = \frac{v_r \cdot B_1 \cdot B_1^*}{v_i \cdot A_1 \cdot A_1^*} = \frac{B_1 \cdot B_1^*}{A_1 \cdot A_1^*} \tag{2.57}$$

Substituting the expression from Equation (2.51) into Equation (2.57), we obtain

$$R = \frac{B_1 \cdot B_1^*}{A_1 \cdot A_1^*} = \frac{\left(K_2^2 - K_1^2\right)^2 + 4K_1^2K_2^2}{\left(K_2^2 + K_1^2\right)^2} = 1.0 \tag{2.58}$$

The result of $R = 1$ implies that all of the particles incident on the potential barrier for $E < V_0$ are eventually reflected. Particles are not absorbed or transmitted through the potential barrier. This result is entirely consistent with classical physics and one might ask why we should consider this problem in terms of quantum mechanics. The interesting result is in terms of what happens in region II.

The wave solution in region II was given by Equation (2.45) as $\psi_2(x) = A_2e^{-K_2x}$. The coefficient A_2 from Equation (2.47) is $A_2 = A_1 + B_1$, which we derived from the boundary conditions. For the case of $E < V_0$, the coefficient A_2 is not zero. If A_2 is not zero, then the probability density function $\psi_2(x) \cdot \psi_2^*(x)$ of the particle being found in region II is not equal to zero. ***This result implies that there is a finite probability that the incident particle will penetrate the potential barrier and exist in region II. The probability of a particle penetrating the potential barrier is another difference between classical and quantum mechanics: The quantum mechanical penetration is classically not allowed.*** Although there is a finite probability that the particle may penetrate the barrier, since the reflection coefficient in region I is unity, the particle in region II must eventually turn around and move back into region I.

EXAMPLE 2.4

Objective

To calculate the penetration depth of a panicle impinging on a potential barrier.

Consider an incident electron that is traveling at a velocity of 1×10^5 m/s in region I.

Solution

With $V(x) = 0$, the total energy is also equal to the kinetic energy so that

$$E = T = \frac{1}{2}mv^2 = 4.56 \times 10^{-21}\,\text{J} = 2.85 \times 10^{-2}\,\text{eV}$$

Now, assume that the potential barrier at $x = 0$ is twice as large as the total energy of the incident particle, or that $V_0 = 2E$. The wave function solution in region II is $\psi_2(x) = A_2 e^{-K_2 x}$, where the constant K_2 is given by $K_2 = \sqrt{2m(V_0 - E)/\hbar^2}$.

In this example, we want to determine the distance $x = d$ at which the wave function magnitude has decayed to e^{-1} of its value at $x = 0$. Then, for this case, we have $K_2 d = 1$ or

$$1 = d\sqrt{\frac{2m(2E - E)}{\hbar^2}} = d\sqrt{\frac{2mE}{\hbar^2}}$$

The distance is then given by

$$d = \sqrt{\frac{\hbar^2}{2mE}} = \frac{1.054 \times 10^{-34}}{\sqrt{2(9.11 \times 10^{-31})(4.56 \times 10^{-21})}} = 11.6 \times 10^{-10} \text{ m}$$

or

$$d = 11.6 \text{ Å}$$

■ Comment

This penetration distance corresponds to approximately two lattice constants of silicon. The numbers used in this example are rather arbitrary. We used a distance at which the wave function decayed to e ^{1} of its initial value. We could have arbitrarily used e^{-2}, for example, but the results give an indication of the magnitude of penetration depth.

The case when the total energy of a particle, which is incident on the potential barrier, is greater than the barrier height, or $E > V_0$, is left as an exercise at the end of the chapter.

TEST YOUR UNDERSTANDING

E2.7 The probability of finding a particle at a distance d in region II compared to that at $x = 0$ is given by $\exp(-2K_2 d)$. Consider an electron traveling in region I at a velocity of 10' m/s incident on a potential barrier whose height is **3** times the kinetic energy of the electron. Find the probability of finding the electron at a distance d compared to $x = 0$ where d is (*a*) 10 Å and (*b*) 100 Å into the potential barrier.
[Ans. (*a*) 8.72 percent, (*b*) 2.53×10^{-9} percent]

2.3.4 The Potential Barrier

We now want to consider the potential barrier function, which is shown in Figure 2.8. The more interesting problem, again, is in the case when the total energy of an incident particle is $E < V_0$. Again assume that we have a flux of incident particles originating on the negative x axis traveling in the $+x$ direction. As before, we need to solve Schrodinger's time-independent wave equation in each of the three regions. The

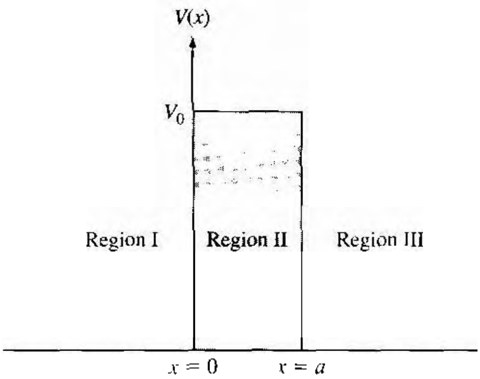

Figure **2.8** | The potential barrier function.

solutions of the wave equation in regions I, II, and III are given, respectively, as

$$\psi_1(x) = A_1 e^{jK_1x} + B_1 e^{-jK_1x} \tag{2.59a}$$

$$\psi_2(x) = A_2 e^{K_2x} + B_2 e^{-K_2x} \tag{2.59b}$$

$$\psi_3(x) = A_3 e^{jK_1x} + B_3 e^{-jK_1x} \tag{2.59c}$$

where

$$K_1 = \sqrt{\frac{2mE}{\hbar^2}} \tag{2.60a}$$

and

$$K_2 = \sqrt{\frac{2m}{\hbar^2}(V_0 - E)} \tag{2.60b}$$

The coefficient B_3 in Equation (2.59c) represents a negative traveling wave in region III. However, once a particle gets into region III, there are no potential changes to cause a reflection; therefore, the coefficient B_3 must be zero. We must keep both exponential terms in Equation (2.59b) since the potential barrier width is finite; that is, neither term will become unbounded. We have four boundary relations for the boundaries at $x = 0$ and $x = a$ corresponding to the wave function and its first derivative being continuous. We can solve for the four coefficients B_1, A_2, B_2, and A_3 in terms of A_1. The wave solutions in the three regions are shown in Figure 2.9.

One particular parameter of interest is the transmission coefficient, in this case defined as the ratio of the transmitted flux in region III to the incident flux in region I. Then the transmission coefficient T is

$$T = \frac{v_t \cdot A_3 \cdot A_3^*}{v_i \cdot A_1 \cdot A_i^*} = \frac{A_3 \cdot A_3^*}{A_1 \cdot A_1^*} \tag{2.61}$$

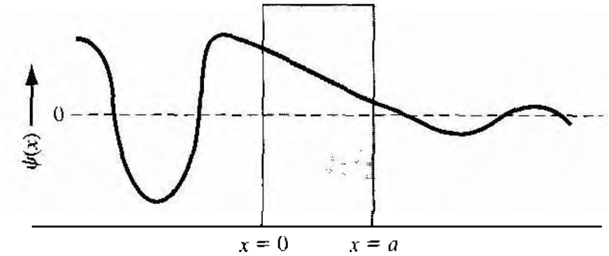

Figure 2.9 | The wave functions through the potential barrier.

where v_t and v_i are the velocities of the transmitted and incident particles, respectively. Since the potential $V = 0$ in both regions I and III, the incident and transmitted velocities are equal. The transmission coefficient may be determined by solving the boundary condition equations. For the special case when $E \ll V_0$, we find that

$$\boxed{T \approx 16\left(\frac{E}{V_0}\right)\left(1 - \frac{E}{V_0}\right)\exp\left(-2K_2 a\right)} \tag{2.62}$$

Equation (2.62) implies that there is a finite probability that a particle impinging a potential barrier will penetrate the barrier and will appear in region III. This phenomenon is called tunneling ***and it, too, contradicts classical mechanics.*** We will see later how this quantum mechanical tunneling phenomenon can be applied to semiconductor device characteristics, such as in the tunnel diode.

EXAMPLE 2.5

Objective

To calculate the probability of an electron tunneling through a potential barrier.

Consider an electron with an energy of 2 eV impinging on a potential barrier with $V_0 = 20$ eV and a width of 3 Å.

■ Solution

Equation (2.62) is the tunneling probability. The factor K_2 is

$$K_2 = \sqrt{\frac{2m(V_0 - E)}{\hbar^2}} = \sqrt{\frac{2(9.11 \times 10^{-31})(20 - 2)(1.6 \times 10^{-19})}{(1.054 \times 10^{-34})^2}}$$

or

$$K_2 = 2.17 \times 10^{10}\ \mathrm{m}^{-1}$$

Then

$$T = 16(0.1)(1 - 0.1)\exp\left[-2(2.17 \times 10^{10})(3 \times 10^{-10})\right]$$

and finally

$$T = 3.17 \times 10^{-6}$$

Comment

The tunneling probability may appear to be a small value, but the value is not zero. If a large number of particles impinge on a potential barrier, a significant number can penetrate the barrier.

TEST YOUR UNDERSTANDING

E2.8 Estimate the tunneling probability of an electron tunneling through a rectangular barrier with a barrier height of $V_0 = 1$ eV and a barrier width of 15 Å. The electron energy is 0.20 eV. (Ans. $T = 2.76 \times 10^{-6}$)

E2.9 For a rectangular potential barrier with a height of $V_0 = 2$ eV and an electron with an energy of 0.25 eV, plot the tunneling probability versus barrier width over the range $2 \leq a \leq 20$ Å. Use a log scale for the tunneling probability.

E2.10 A certain semiconductor device requires a tunneling probability of $T = 10^{-5}$ for an electron tunneling through a rectangular barrier with a barrier height of $V_0 = 0.4$ eV. The electron energy is 0.04 eV. Determine the maximum barrier width. (Ans. $a = 19.3$ Å)

Additional applications of Schrodinger's wave equation with various one-dimensional potential functions are found in problems at the end of the chapter. Several of these potential functions represent quantum well structures that are found in modern semiconductor devices.

*2.4 | EXTENSIONS OF THE WAVE THEORY TO ATOMS

So far in this chapter. we have considered several one-dimensional potential energy functions and solved Schrodinger's time-independent wave equation to obtain the probability function of finding a particle at various positions. Consider now the one-electron, or hydrogen, atom potential function. We will only briefly consider the mathematical details and wave function solutions, but the results are extremely interesting and important.

2.4.1 The One-Electron Atom

The nucleus is a heavy, positively charged proton and the electron is a light. negatively charged particle that, in the classical Bohr theory, is revolving around the nucleus. The potential function is due to the coulomb attraction between the proton and electron and is given by

$$V(r) = \frac{-e^2}{4\pi\epsilon_0 r} \tag{2.63}$$

where e is the magnitude of the electronic charge and ϵ_0 is the permittivity of free space. This potential function, although spherically symmetric, leads to a three-dimensional problem in spherical coordinates.

---

*Indicates sections that can be skipped without loss of continuity.

We may generalize the time-independent Schrodinger's wave equation to three dimensions by writing

$$\nabla^2\psi(r,\theta,\phi)+\frac{2m_0}{\hbar^2}(E-V(r))\psi(r,\theta,\phi)=0 \tag{2.64}$$

where V^2 is the **Laplacian** operator and must be written in spherical coordinates for this case. The parameter m_0 is the rest mass of the electron.' In spherical coordinates, Schrodinger's wave equation may be written as

$$\frac{1}{r^2}\cdot\frac{\partial}{\partial r}\left(r^2\frac{\partial\psi}{\partial r}\right)+\frac{1}{r^2\sin^2\theta}\cdot\frac{\partial^2\psi}{\partial\phi^2}+\frac{1}{r^2\sin\theta}\cdot\frac{\partial}{\partial\theta}\left(\sin\theta\cdot\frac{\partial\psi}{\partial\theta}\right)$$
$$+\frac{2m_0}{\hbar^2}(E-V(r))\psi=0 \tag{2.65}$$

The solution to Equation (2.65) can be determined by the **separation-of-variables** technique. We will assume that the solution to the time-independent wave equation can be written in the form

$$\psi(r,\theta,\phi)=R(r)\cdot\Theta(\theta)\cdot\Phi(\phi) \tag{2.66}$$

where ***R*. O,** and Φ, are functions only of r, H, and ϕ, respectively. Substituting this form of solution into Equation (2.65), we will obtain

$$\frac{\sin^2\theta}{R}\cdot\frac{\partial}{\partial r}\left(r^2\frac{\partial R}{\partial r}\right)+\frac{1}{\Phi}\cdot\frac{\partial^2\Phi}{\partial\phi^2}+\frac{\sin\theta}{\Theta}\cdot\frac{\partial}{\partial\theta}\left(\sin\theta\cdot\frac{\partial\Theta}{\partial\theta}\right)$$
$$+r^2\sin^2\theta\cdot\frac{2m_0}{\hbar^2}(E-V)=0 \tag{2.67}$$

We may note that the second term in Equation (2.67) is a function of ϕ only, while all the other terms are functions of either r or θ. We may then write that

$$\frac{1}{\Phi}\cdot\frac{\partial^2\Phi}{\partial\phi^2}=-m^2 \tag{2.68}$$

where m is a separation of variables constant? The solution to Equation (2.68) is of the form

$$\Phi=e^{jm\phi} \tag{2.69}$$

Since the wave function must be single-valued. we impose the condition that m is an integer, or

$$m=0,\pm1,\pm2,\pm3,\ldots \tag{2.70}$$

'The mass should be the rest mass of the two-particle system, but since the proton mass is much greater than the electron mass, the equivalent mass reduces to that of the electron.

[4] Where m means the separation-of-variables constant developed historically. That meaning will be retained here even though there may be some confusion with the electron mass. In general, the mass parameter will be used in conjunction with a subscript.

Incorporating the separation-of-variables constant we can further separate the variables Band r and generate two additional separation-of-variables constants 1 and n. The separation-of-variables constants n, l, and m are known as *quantum* ***numbers*** and are related by

$$\begin{aligned} n &= 1, 2, 3, \ldots \\ l &= n-1, n-2, n-3, \ldots, 0 \\ |m| &= l, l-1, \ldots, 0 \end{aligned} \tag{2.71}$$

Each set of quantum numbers corresponds to a quantum state which the electron may occupy.

The electron energy may be written in the form

$$\boxed{E_n = \frac{-m_0 e^4}{(4\pi\epsilon_0)^2 2\hbar^2 n^2}} \tag{2.72}$$

where n is the principal quantum number. The negative energy indicates that the electron is bound to the nucleus and we again see that the energy of the bound electron is quantized. If the energy were to become positive, then the electron would no longer he a bound panicle and the total energy would no longer be quantized. Since the parametern in Equation (2.72) is an integer, the total energy of the electron can take on only discrete values. The quantized energy is again a result of the particle being bound in a finite region of space.

TEST YOUR UNDERSTANDING

E2.11 Calculate the lowest energy (in electron volts) of an electron in a hydrogen atom. (Ans. $E_1 = -13.6$ eV)

The solution of the wave equation may be designated by ψ_{nlm}, where n, I, and mare again the various quantum numbers. For the lowest energy state, $n =$ I. 1 $=$ 0, and $m = 0$, and the wave function is given by

$$\psi_{100} = \frac{1}{\sqrt{\pi}} \cdot \left(\frac{1}{a_0}\right)^{3/2} e^{-r/a_0} \tag{2.73}$$

This function is spherically symmetric, and the parameter a_0 is given by

$$a_0 = \frac{4\pi\epsilon_0\hbar^2}{m_0 e^2} = 0.529\ \text{Å} \tag{2.74}$$

and is equal to the Bohr radius.

The radial probability density function, or the probability of finding the electron at a particular distance from the nucleus, is proportional to the product $\psi_{100} \cdot \psi_{100}^*$ and also to the differential volume of the shell around the nucleus. The probability

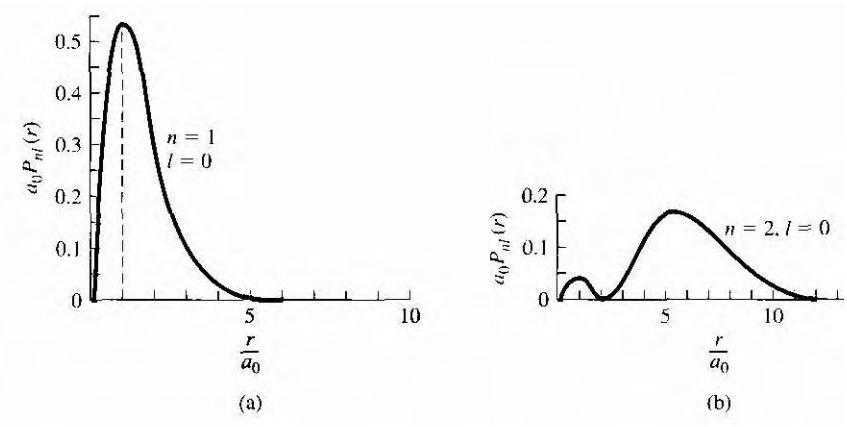

Figure 2.10 | The radial probability density function for the one-electron atom in the (a) lowest energy state and (b) next-higher energy slate.
(From Eisberg and Resnick [4].)

density function for the lowest energy state is plotted in Figure 2.10a. The most probable distance from the nucleus is at $r = a_0$, which is the same as the Bohr theory. Considering this spherically symmetric probability function, we may now begin to conceive the concept of an electron cloud, or energy shell, surrounding the nucleus rather than a discrete particle orbiting around the nucleus.

The radial probability density function for the next higher, spherically symmetric wave function, corresponding to $n = 2, l = 0$. and $m = 0$, is shown in Figure 2.10b. This figure shows the idea of the next-higher energy shell of the electron. The second energy shell is at a greater radius from the nucleus than the first energy shell. As indicated in the figure, though, there is still a small probability that the electron will exist at the smaller radius. For the case of $n = 2$ and $I = I$. there are three possible states corresponding to the three allowed values of the quantum numberm. These wave functions are no longer spherically symmetric.

Although we have not gone into a great deal of mathematical detail for the one-electron atom, three results are important for the further analysis of semiconductor materials. The first is the solution of Schrodinger's wave equation, which again yields electron probability functions, as it did for the simpler potential functions. In developing the physics of semiconductor materials in later chapters, we will also be considering electron probability functions. The second result is the quantization of allowed energy levels for the hound electron. The third is the concept of quantum numbers and quantum states, which evolved from the separation-of-variables technique. We will consider this concept again in the next section and in later chapters when we deal with the semiconductor material physics.

2.4.2 The Periodic Table

The initial portion of the periodic table of elements may he determined by using the results of the one-electron atom plus two additional concepts. The tirst concept needed is that of *electron spin*. The electron has an intrinsic angular momentum, or spin, which is quantized and may take on one of two possible values. The spin is designated by a quantum number s, which has a value of $s = +\frac{1}{2}$ or $s = -\frac{1}{2}$. We now have four basic quantum numbers: n, l, m, and s.

The second concept needed is the *Pauli exclusion principle*. The Pauli exclusion principle states that, in any given system (an atom, molecule, or crystal), no two electrons may occupy the same quantum state. In an atom, the exclusion principle means that no two electrons may have the same set of quantum numbers. We will see that the exclusion principle is also an important factor in determining the distribution of electrons among available energy states in a crystal.

Table 2.1 shows the first few elements of the periodic table. For the first element, hydrogen, we have one electron in the lowest energy state corresponding to $n = 1$. From Equation (2.71) both quantum numbers l and m must be zero. However, the electron can take on either spin factor $+\frac{1}{2}$ or $-\frac{1}{2}$. For helium, two electrons may exist in the lowest energy state. For this case, $l = m = 0$, so now both electron spin states are occupied and the lowest energy shell is full. The chemical activity of an element is determined primarily by the valence, or outermost, electrons. Since the valence energy shell of helium is full, helium does not react with other elements and is an inert element.

The third element, lithium, has three electrons. The third electron must go into the second energy shell corresponding to $n = 2$. When $n = 2$, the quantum number l may be 0 or 1, and when $l = 1$, the quantum number m may be -1, 0, or $+1$. In each case, the electron spin factor may be $+\frac{1}{2}$ or $-\frac{1}{2}$. For $n = 2$, then, there are eight possible quantum states. Neon has ten electrons. Two electrons are in the $n = 1$ energy shell and eight electrons are in the $n = 2$ energy shell. The second energy shell is now full, which means that neon is also an inert element.

From the solution of Schrodinger's wave equation for the one electron atom, plus the concepts of electron spin and the Pauli exclusion principle, we can begin to build up the periodic table of elements. As the atomic numbers of the elements increase, electrons will begin to interact with each other, so that the buildup of the periodic table will deviate somewhat from the simple method.

Table 2.1 | Initial portion of the periodic table

Element	Notation	n	l	m	s
Hydrogen	$1s^1$	1	0	0	$+\frac{1}{2}$ or $-\frac{1}{2}$
Helium	$1s^2$	1	0	0	$+\frac{1}{2}$ and $-\frac{1}{2}$
Lithium	$1s^2 2s^1$	2	0	0	$+\frac{1}{2}$ or $-\frac{1}{2}$
Beryllium	$1s^2 2s^2$	2	0	0	$+\frac{1}{2}$ and $-\frac{1}{2}$
Boron	$1s^2 2s^2 2p^1$	2	1		$m = 0, -1, +1$ $s = +\frac{1}{2}, -\frac{1}{2}$
Carbon	$1s^2 2s^2 2p^2$	2	1		
Nitrogen	$1s^2 2s^2 2p^3$	2	1		
Oxygen	$1s^2 2s^2 2p^4$	2	1		
Fluorine	$1s^2 2s^2 2p^5$	2	1		
Neon	$1s^2 2s^2 2p^6$	2	1		

2.5 | SUMMARY

- We considered some of the basic concepts of quantum mechanics, which can be used to describe the behavior of electrons under various potential functions. The understanding of electron behavior is crucial in understanding semiconductor physics.
- The wave–particle duality principle is an important element in quantum mechanics. Particles can have wave-like behavior and waves can have particle-like behavior.
- Schrodinger's wave equation forms the basis for describing and predicting the behavior of electrons.
- Man Born postulated that $|\psi(x)|^2$ is a probability density function.
- A result of applying Schrodinger's wave equation to a bound panicle is that the energy of the bound particle is *quantized*.
- A result of applying Schrodinger's wave equation to an electron incident on a potential barrier is that there is a tinite probability of *tunneling*.
- The basic structure of the periodic table is predicted by applying Schrodinger's wave equation to the one-electron atom.

GLOSSARY OF IMPORTANT TERMS

de Bruglie wavelength The wavelength of a particle given as the ratio of Planck's constant to momentum.

Heisenberg uncertainty principle The principle that states that we cannot describe with absolute accuracy the relationship between sets of conjugate variables that describe the behavior of particles, such as momentum and position.

Pauli exclusion principle The principle that states that no two electrons can occupy the same quantum state.

photon The particle-like packet of electromagnetic energy.

quanta The particle-like packet of thermal radiation.

quantized energies The allowed discrete energy levels that bound panicles may occupy.

quantum numbers A set of numbers that describes the quantum state of a particle, such as an electron in an atom.

quantum state A particular state of an electron that may he described, for example, by a set of quantum numbers.

tunneling The quantum mechanical phenomenon by which a particle may penetrate through a thin potential barrier.

wave–particle duality The characteristic by which electromagnetic waves sometimes exhibit particle-like behavior and particles sometimes exhibit wave-like behavior.

CHECKPOINT

After studying this chapter, the reader should have the ability to:

- Discuss the principle of energy quanta, the wave–particle duality principle, and the uncertainty principle.
- Apply Schrodinger's wave equation and boundary conditions to problems with various potential functions.
- Determine quantized energy levels of bound particles.

  Determine the approximate tunneling probability of a particle incident on a potential barrier.

REVIEW QUESTIONS

1. State the wave–particle duality principle and state the relationship between momentum and wavelength.
2. What is the physical meaning of Schrodinger's wave function?
3. What is meant by a probability density function?
4. List the boundary conditions for solutions to Schrodinger's wave equation.
5. What is meant by quantized energy levels?
6. Describe the concept of tunneling.
7. List the quantum numbers of the one-electron atom and discuss how they were developed

PROBLEMS

2.1 The classical wave equation for a two-wire transmission line is given by $\partial^2 V(x,t)/\partial x^2 = LC \cdot \partial^2 V(x,t)/\partial t^2$. One possible solution is given by $V(x,t) = (\sin Kx) \cdot (\sin \omega t)$ where $K = n\pi/a$ and $\omega = K/\sqrt{LC}$. Sketch, on the same graph, the function $V(x,t)$ as a function of x for $0 \le x \le a$ and $n = 1$ when (i) $\omega t = 0$, (*ii*) $\omega t = \pi/2$, (iii) $\omega t = \pi$, (iv) $\omega t = 3\pi/2$, and (v) $\omega t = 2\pi$.

2.2 The function $V(x,t) = \cos(2\pi x/\lambda - \omega t)$ is also a solution to the classical wave equation. Sketch on the same graph the function $V(x,t)$ as a function of x for $0 \le x \le 3\lambda$ when: (*i*) $\omega t = 0$, (*ii*) $\omega t = 0.25\pi$, (*iii*) $\omega t = 0.5\pi$, (iv) $\omega t = 0.75\pi$, and (v) $\omega t = \pi$.

2.3 Repeat Problem 2.2 for the function $V(x,t) = \cos(2\pi x/\lambda + \omega t)$.

2.4 Determine the phase velocities of the traveling waves described in Problems 2.2 and **2.3.**

Section 2.1 Principles of Quantum Mechanics

2.5 The work function of a material refers to the minimum energy required to remove an electron from the material. Assume that the work function of gold is 4.90 eV and that of cesium is 1.90 eV. Calculate the maximum wavelength of light for the photoelectric emission of electrons for gold and cesium.

2.6 Calculate the de Broglie wavelength, $\lambda = h/p$, for: (*a*) An electron with kinetic energy of (i) 1.0 eV, and (ii) 100 eV. (*b*) A proton with kinetic energy of 1.0 eV. (*c*) A singly ionized tungsten atom with kinetic energy of 1.0 eV. (*d*) A 2000-kg truck traveling at 20 m/s.

2.7 According to classical physics, the average energy of an electron in an electron gas at thermal equilibrium is $3kT/2$. Determine, for $T = 300$ K, the average electron energy (in eV), average electron momentum, and the de Broglie wavelength.

***2.8** An electron and a photon have the same energy. At what value of energy (in eV) will the wavelength of the photon be 10 times that of the electron?

2.9 (*a*) An electron is moving with a velocity of 2×10^6 cm/s. Determine the electron energy (in eV), momentum, and de Broglie wavelength (in Å). (*b*) The de Broglie wavelength of an electron is 125 Å. Determine the electron energy (in eV), momentum, and velocity.

2.10 It is desired to produce x-ray radiation with a wavelength of 1 Å. (*a*) Through what potential voltage difference must the electron be accelerated in vacuum so that it can, upon colliding with a target. generate such a photon'! (Assume that all of the electron's energy is transferred to the photon.) (*b*) What is the de Broglie wavelength of the electron in part (*a*) just before it hits the target'!

2.11 When the uncertainty principle is considered, it is not possible to locate a photon in space more precisely than about one wavelength. Consider a photon with wavelength $\lambda = 1\ \mu m$. What is the uncertainty in the photon's (*a*) momentum and (*b*) energy?

2.12 The uncertainty in position is 12 Å for a particle of mass 5×10^{-29} kg. Determine the minimum uncertainty in (a) the momentum of the panicle and (*b*) the kinetic energy of the particle.

2.13 Repeat Problem 2.12 for a particle of mass 5×10^{-26} kg.

2.14 An automobile has a mass of 1500 kg. What is the uncertainty in the velocity (in miles per hour) when its center of mass is located with an uncertainty no greater than I cm'!

2.15 (*a*) The uncertainty in the position of an electron is no greater than I Å. Determine the minimum uncertainty in its momentum. (*b*) The electron's energy is measured with an uncertainty no greater than 1 eV. Determine the minimum uncertainty in the time aver which the measurement is made.

Section 2.2 Schrodinger's Wave Equation

2.16 Assume that $\Psi_1(x, t)$ and $\Psi_2(x, t)$ are solutions of the one-dimensional time-dependent Schrodinger's wave equation. (*n*) Show that $\Psi_1 +$ *> is a solution. (*b*) Is $\Psi_1 \cdot \Psi_2$ a solution of the Schrodinger's equation in general'! Why or why not?

2.17 Considerthe wave function $\Psi(x, t) = A(\sin \pi x)e^{-j\omega t}$ for -1 5 $x \le +1$. Determine **A** so that $\int_{-1}^{1} |\Psi(x, t)|^2\, dx = 1$

2.18 Consider the wave function $\Psi(x, t) = A(\sin n\pi x)e^{-j\omega t}$ for $0 \le x \le 1$. Determine A so that $\int_0^1 |\Psi(x, t)|^2\, dx = 1$

2.19 The solution to Schrodinger's wave equation for a particular situation is given by $\psi(x) = \sqrt{2/a_0} \cdot e^{-x/a_0}$. Determine the probability of finding the particle between the following limits: (*a*) $0 \le x \le a_0/4$, (*b*) $a_0/4 \le x \le a_0/2$, and (*c*) $0 \le x \le a_0$.

Section 2.3 Applications of Schrodinger's Wave Equation

2.20 An electron in free space is described by a plane wave given by $\Psi(x, t) = Ae^{j(kx-\omega t)}$ where $k = 1.5 \times 10^9\ m^{-1}$ **and** $\omega = 1.5 \times 10^{13}$ rad/s. (*a*) Determine the phase velocity of the plane wave. (b) Calculate the wavelength, momentum, and kinetic energy (in eV) of the electron.

2.21 An electron is traveling in the negative *x* direction with a kinetic energy of 0.015 eV. Write the equation of a plane wave that describes thic particle.

2.22 An electron is hound in a one-dimensional infinite potential well with a width of 100 Å. Determine the electron energy levels for $n = 1, 2, 3$.

2.23 A one-dimensional infinite potential well with a width of 12 A contains an electron. (a) Calculate the first two energy levels that the electron may occupy. (*b*) If an electron drops from the second energy level to the first, what is the wavelength of a photon that might be emitted"

2.24 Consider a panicle with mass of 10 mg in an infinite potential well 1.0 cm wide. (*a*) If the energy of the particle is 10 mJ, calculate the value of *n* for that state. (*b*) What is

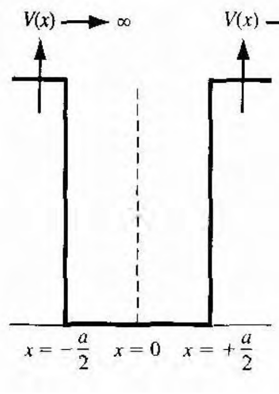

Figure 2.11 | Potential function for Problem 2.26.

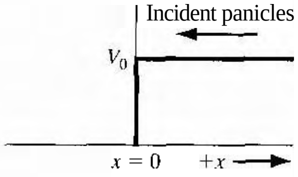

Figure 2.12 | Potential function for Problem 2.30

the kinetic energy of the $(n + 1)$ state? (*c*) Would quantum effects be observable for this particle?

2.25 Calculate the lowest energy level for a neutron in a nucleus, by treating it as if it were in an infinite potential well of width equal to 10^{-14} m. Compare this with the lowest energy level for an electron in the same infinite potential well.

2.26 Consider the particle in the infinite potential well as shown in Figure 2.11. Derive and sketch the wave functions corresponding to the four lowest energy levels. (Do not normalize the wave functions.)

***2.27** Consider a three-dimensional infinite potential well. The potential function is given by $V(x) = 0$ for $0 < x < a, 0 < y < a, 0 < z < a$, and $V(x) = \infty$ elsewhere. Start with Schrodinger's wave equation, use the separation of variables technique, and show that the energy is quantized and is given by

$$E_{n_x n_y n_z} = \frac{\hbar^2 \pi^2}{2ma^2}\left(n_x^2 + n_y^2 + n_z^2\right)$$

where $n_x = 1, 2, 3, \ldots, n_y = 1, 2, 3, \ldots, n_z = 1, 2, 3, \ldots$.

'2.28 Consider a **free** electron bound within a two-dimensional infinite potential well defined by $V = 0$ for $0 < x < 25$ Å, $0 < y < 50$ Å, and $V = \infty$ elsewhere. Determine the expression for the allowed electron energies.

Describe any similarities and any differences to the results of the one-dimensional infinite potential well.

2.29 Consider a proton in a one-dimensional inhnite potential well shown in Figure 2.5. (a) Derive the expression for the allowed energy states of the proton. (*b*) Calculate the energy difference (in units of eV) between the lowest possible energy and the next higher energy state fur (i) $a = 4$ Å, and (*ii*) $a = 0.5$ cm.

2.30 For the step potential function shown in Figure 2.12, assume that $E > V_0$ and that particles are incident from the $+x$ direction traveling in the $-x$ direction. (*a*) Write the wave solutions for each region. (*b*) Derive expressions for the transmission and reflection coefficients.

2.31 Consider the penetration of a step potential function of height 2.4 eV by an electron whose energy is 2.1 eV. Determine the relative probability of finding the electron at the distance (*a*) 12 Å beyond the barrier, and (*h*)48 Å beyond the barrier, compared to the probability of finding the incident panicle at the barrier edge.

2.32 Evaluate the transmission coefficient for an electron of energy 2.2 eV impinging on a potential barrier of height 6.0 eV and thickness 10^{-10} m. Repeat the calculation for a barrier thickness of 10^{-9} m. Assume that Equation (2.62) is valid.

2.33 (*a*) Estimate the tunneling probability of a particle with **an** effective mass of $0.067\,m_0$ (an electron in gallium arsenide), where m_0 is the mass of an electron, tunneling through a rectangular potential barrier of height $V_0 = 0.8$ eV and width 15 Å. The panicle kinetic energy is 0.20 eV. (*b*) Repeat pan (*a*)if the effective mass of the panicle is $1.08\,m_0$ (an electron in silicon).

2.34 A proton attempts to penetrate a rectangular potential barrier of height 10 MeV and thickness 10^{14} m. The panicle has a total energy of 3 MeV. Calculate the probability that the particle will penetrate the potential barrier. Assume that Equation (2.62) is valid.

***2.35** **An** electron with energy E is incident on a rectangular potential barrier as shown in Figure 2.8. The potential harrier is of width a and height $V_0 \gg E$. (*a*) Write the form of the wave function in each of the three regions. (b) For this geometry, determine what coefficient in the wave function solutions is zero. (r)Derive the expression for the transmission coefficient for the electron (tunneling probability). (d) Sketch the wave function for the electron in each region.

***2.36** **A** potential function is shown in Figure 2.13 with incident particles coming from $-\infty$ with a total energy $E > V_2$. The constants k are defined as

$$k_1 = \sqrt{\frac{2mE}{\hbar^2}} \qquad k_2 = \sqrt{\frac{2m}{\hbar^2}(E - V_1)} \qquad k_3 = \sqrt{\frac{2m}{\hbar^2}(E - V_2)}$$

Assume a special case for which $k_2 a = 2n\pi$, $n = 1, 2, 3, \ldots$. Derive the expression, in terms of the conslants, k_1, k_2, and k_3, for the transmission coefficient. The transmission coefficient is defined as the ratio of the flux of particles in region **III** to the incident flux in region I.

***2.37** Consider the one-dimensional potential function shown in Figure 2.14. Assume the total energy of an electron is $E < V_0$. (a)Write the wave solutions that apply in each

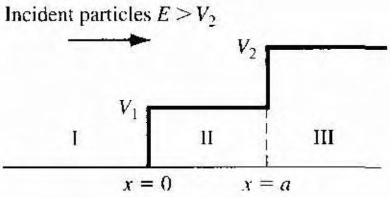

Figure 2.13 | Potential function for Problem 2.36.

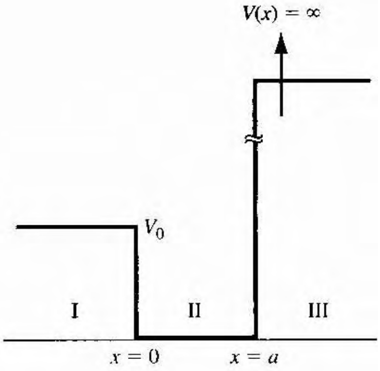

Figure 2.14 | Potential function for Problem 2.37.

region. (*b*) Write the set of equations that result from applying the boundary conditions. (*c*) Show explicitly why, or why not. the energy levels of the electron are quantized.

Section 2.4 Extensions of the Wave Theory to Atoms

2.38 Calculate the energy of the electron in the hydrogen atom (in units of eV) for the first four allowed energy levels.

2.39 Show that the most probable value of the radius r for the 1s electron in a hydrogen atom is equal to the Bohr radius ***a,.***

2.40 Show that the wave function for ψ_{100} given by Equation (2.73) is a solution to the differential equation given by Equation (2.64).

2.41 What property do H. Li, Na, and K have in common?

READING LIST

1.** Datta, S. *Quantum Phenomena*. Vol. 8 of ***Modular Series** on Solid State **Devices. Reading. ***Mass.:*** Addison–Wesley, 1989.

2.** deCogan, D. ***Solid State Devices: A Quantum Physics Approach. New York: Springer-Verlag, 1987.

3. Eisberg, R. M. *Fundamentals **of** Modern **Physics.*** New York: Wilcy, 1961

4. Eisberg, R., and R. Resnick. ***Qunntum** Physics of Atoms, **Molecules, Solids, Nuclei, arid Particles.*** New York: Wiley, 1974.

5. Kano, K. *Semiconductor **Devices.*** Upper Saddle River, NJ: Prentice Hall, 1998.

6. Kittel, C. *Introduction to **Solid State Physics,*** 7th ed. Berlin: Springer-Verlag, 1993.

7. McKelvey, J. P. ***Solid** State **Physics for** Engineering and Materials **Science.*** Malabar, FL.: Krieger Publishing, 1993.

8. Pauling, L., and E. B. Wilson. *Introduction to Quantum Mechanics.* New York: McGraw-Hill, 1935.

9. Pierret, R. F. *Semiconductor Device **Fundamentals**.* Reading, MA. Addison-Wesley Publishing Co., 1996.

10. Pohl, H. A. ***Qunntum Mechunics for Science** and Engineering.* Englewood Cliffs, N.J.: Prentice Hall, 1967.

11. Schiff, L. I. *Quantum Mechanics.* New York: McGraw-Hill, 1955.

12. Shur, M. ***Inrroduction** to **Electronic** Devices.* New York: John Wiley and Sons, 1996.

CHAPTER 3

Introduction to the Quantum Theory of Solids

PREVIEW

In the last chapter, we applied quantum mechanics and Schrodinger's wave equation to determine the behavior of electrons in the presence of various potential functions. We found that one important characteristic of an electron bound to an atom or bound within a finite space is that the electron can take on only discrete values of energy; that is, the energies are quantized. We also discussed the Pauli exclusion principle, which stated that only one electron is allowed to occupy any given quantum state. In this chapter, we will generalize these concepts to the electron in a crystal lattice.

One of our goals is to determine the electrical properties of a semiconductor material, which we will then use to develop the current-voltage characteristics of semiconductor devices. Toward this end, we have two tasks in this chapter: to determine the properties of electrons in a crystal lattice, and to determine the statistical characteristics of the very large number of electrons in a crystal.

To start, we will expand the concept of discrete allowed electron energies that occur in a single atom to a band of allowed electron energies in a single-crystal solid. First we will qualitatively discuss the feasibility of the allowed energy bands in a crystal and then we will develop a more rigorous mathematical derivation of this theory using Schrodinger's wave equation. This energy band theory is a basic principle of semiconductor material physics and can also be used to explain differences in electrical characteristics between metals, insulators, and semiconductors.

Since current in a solid is due to the net *flow* of charge, it is important to determine the response of an electron in the crystal to an applied external force, such as an electric field. The movement of an electron in a lattice is different than that of an electron in free space. We will develop a concept allowing us to relate the quantum mechanical behavior of electrons in a crystal to classical Newtonian mechanics. This analysis leads to a parameter called the electron effective mass. As part of this development, we will find that we can define a new particle in a semiconductor called a *hole*. The motion of both electrons and holes gives rise to currents in a semiconductor.

Because the number of electrons in a semiconductor is very large, it is impossible to follow the motion of each individual particle. We will develop the statistical behavior of electrons in a crystal, noting that the Pauli exclusion principle is an important factor in determining the statistical law the electrons must follow. The resulting probability function will determine the distribution of electrons among the available energy states. The energy band theory and the probability function will be used extensively in the next chapter, when we develop the theory of the semiconductor in equilibrium. ■

3.1 | ALLOWED AND FORBIDDEN ENERGY BANDS

In the last chapter, we treated the one-electron, or hydrogen, atom. That analysis showed that the energy of the bound electron is quantized: Only discrete values of electron energy are allowed. The radial probability density for the electron was also determined. This function gives the probability of finding the electron at a particular distance from the nucleus and shows that the electron is not localized at a given radius. We can extrapolate these single-atom results to a crystal and qualitatively derive the concepts of allowed and forbidden energy bands. We can then apply quantum mechanics and Schrodinger's wave equation to the problem of an electron in a single crystal. We find that the electronic energy states occur in hands of allowed states that are separated by forbidden energy bands.

3.1.1 Formation of Energy Bands

Figure 3.1a shows the radial probability density function for the lowest electron energy state of the single, noninteracting hydrogen atom, and Figure 3.1b shows the same probability curves for two atoms that are in close proximity to each other. The wave functions of the two atom electrons overlap, which means that the two electrons

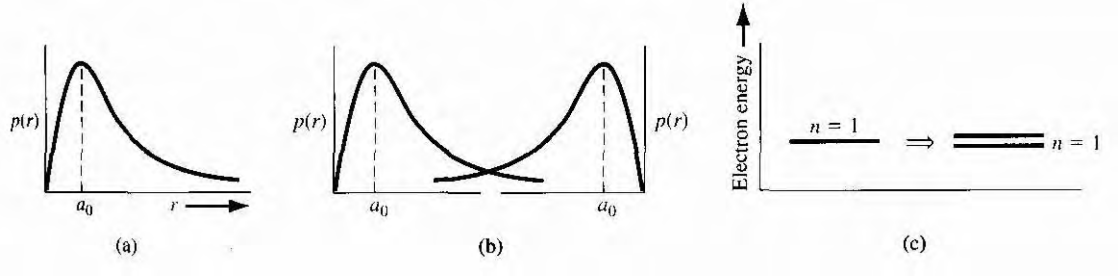

Figure 3.1 | (a) Probability density function of an isolated hydrogen atom. (b) Overlapping probability density functions of two adjacent hydrogen atoms. (c) The splitting of the $n = 1$ state.

will interact. This interaction or perturbation results in the discrete quantized energy level splitting into two discrete energy levels, schematically shown in Figure 3.1c. The splitting of the discrete state into two states is consistent with the Pauli exclusion principle.

A simple analogy of the splitting of energy levels by interacting particles is the following. Two identical race cars and drivers are far apart on a race track. There is no interaction between the cars, so they both must provide the same power to achieve a given speed. However, if one car pulls up close behind the other car, there is an interaction called ***draft.*** The second car will be pulled to an extent by the lead car. The lead car will therefore require more power to achieve the same speed, since it is pulling the second car and the second car will require less power since it is being pulled by the lead car. So there is a "splitting" of power (energy) of the two interacting race cars. (Keep in mind not to take analogies too literally.)

Now, if we somehow start with a regular periodic arrangement of hydrogen-type atoms that are initially very far apart, and begin pushing the atoms together, the initial quantized energy level will split into a band of discrete energy levels. This effect is shown schematically in Figure 3.2, where the parameter r_0 represents the equilibrium interatomic distance in the crystal. At the equilibrium interatomic distance, there is a band of allowed energies, but within the allowed band, the energies are at discrete levels. The Pauli exclusion principle states that the joining of atoms to form a system (crystal) does not alter the total number of quantum states regardless of size. However, since no two electrons can have the same quantum number. the discrete energy must split into a band of energies in order that each electron can occupy a distinct quantum state.

We have seen previously that, at any energy level, the number of allowed quantum states is relatively small. In order to accommodate all of the electrons in a crystal, then, we must have many energy levels within the allowed band. As an example, suppose that we have a system with 10^{19} one-electron atoms and also suppose that, at the equilibrium interatomic distance, the width of the allowed energy band is 1 eV. For simplicity, we assume that each electron in the system occupies a different energy level and, if the discrete energy states are equidistant, then the energy levels are separated by 10^{-19} eV. This energy difference is extremely small, so that for all practical purposes, we have a quasi-continuous energy distribution through the allowed

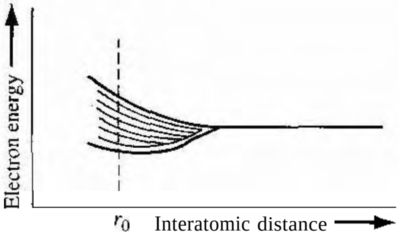

Figure 3.2 | The splitting of an energy state into a band of allowed energies.

energy band. The fact that 10^{-19} eV is a very small difference between two energy states can be seen from the following example.

EXAMPLE 3.1

Objective

To calculate the change in kinetic energy of an electron when the velocity changes by a small value.

Consider an electron traveling at a velocity of 10^7 cm/s. Assume the velocity increases by a value of 1 cm/s. The increase in kinetic energy is given by

$$\Delta E = \frac{1}{2}mv_2^2 - \frac{1}{2}mv_1^2 = \frac{1}{2}m\left(v_2^2 - v_1^2\right)$$

Let $v_2 = v_1 + \Delta v$. Then

$$v_2^2 = (v_1 + A'')' = v_1^2 + 2v_1\Delta v + (\Delta v)^2$$

But $\Delta v \ll v_1$, so we have that

$$\Delta E \approx \frac{1}{2}m(2v_1\Delta v) = mv_1\Delta v$$

Solution

Substituting the number into this equation, we obtain

$$\Delta E = (9.11 \times 10^{-3})(10^5)(0.01) = 9.11 \times 10^{-28}\ \mathrm{J}$$

which may be converted to units of electron volts as

$$\Delta E = \frac{9.11 \times 10^{-28}}{1.6 \times 10^{-19}} = 5.7 \times 10^{-9}\ \mathrm{eV}$$

Comment

A change in velocity of I cm/s compared with 10^7 cm/s results in a change in energy of 5.7×10^{-9} eV, which is orders of magnitude larger than the change in energy of 10^{-19} eV between energy states in the allowed energy hand. This example serves to demonstrate that a difference in adjacent energy states of 10^{-19} eV is indeed very small, so that the discrete energies within an allowed band may be treated as a quasi-continuous distribution.

Consider again a regular periodic arrangement of atoms, in which each atom now contains more then one electron. Suppose the atom in this imaginary crystal contains electrons up through the $n = 3$ energy level. If the atoms are initially very far apart, the electrons in adjacent atoms will not interact and will occupy the discrete energy levels. If these atoms are brought closer together, the outermost electrons in the $n = 3$ energy shell will begin to interact initially, so that this discrete energy level will split into a band of allowed energies. If the atoms continue to move closer together, the electrons in the $n = 2$ shell may begin to interact and will also split into a band of allowed energies. Finally, if the atoms become sufficiently close together, the innermost electrons in then = I level may interact. so that this energy level may also split into a band of allowed energies. The splitting of these discrete energy levels is

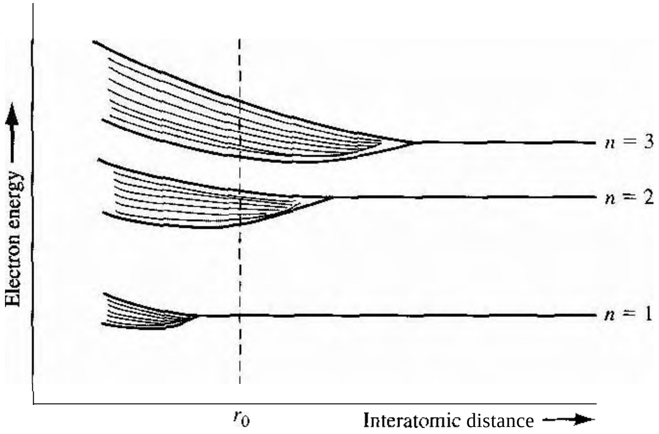
Electron energy
$n = 3$
$n = 2$
$n = 1$
r_0
Interatomic distance

Figure 3.3 | Schematic showing the splitting of three energy states into allowed bands of energies.

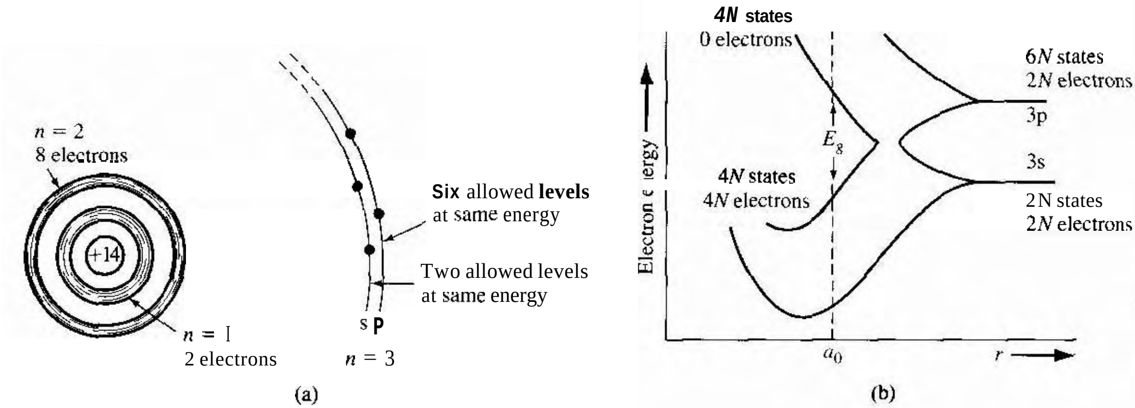
$n = 2$
8 electrons
+14
$n = 1$
2 electrons
Six allowed levels at same energy
Two allowed levels at same energy
s p
$n = 3$
(a)
4N states
0 electrons
6N states
2N electrons
3p
3s
E_g
4N states
4N electrons
2N states
2N electrons
Electron energy
a_0
r
(b)

Figure 3.4 | (a) Schematic of an isolated silicon atom. (b) The splitting of the 3s and 3p states of silicon into the allowed and forbidden energy bands.
(From Shockley [5].)

qualitatively shown in Figure 3.3. If the equilibrium interatomic distance is r_0, then we have bands of allowed energies that the electrons may occupy separated by bands of forbidden energies. This energy-band splitting and the formation of allowed and forbidden bands is the energy-band theory of single-crystal materials.

The actual hand splitting in a crystal is much more complicated than indicated in Figure 3.3. A schematic representation of an isolated silicon atom is shown in Figure 3.4a. Ten of the fourteen silicon atom electrons occupy deep-lying energy levels close to the nucleus. The four remaining valence electrons are relatively weakly bound and are the electrons involved in chemical reactions. Figure 3.4b shows the hand splitting of silicon. We need only consider the $n = 3$ level for the valence electrons, since the first two energy shells are completely full and are tightly bound to the nucleus. The

3s state corresponds to n = 3 and l = 0 and contains two quantum states per atom. This state will contain two electrons at T = 0 K. The 3p state corresponds to n = 3 and l = 1 and contains six quantum states per atom. This state will contain the remaining two electrons in the individual silicon atom.

As the interatomic distance decreases, the 3s and 3p states interact and overlap. At the equilibrium interatomic distance, the bands have again split. hut now four quantum states per atom are in the lower band and four quantum states per atom are in the upper band. At absolute zero degrees, electrons are in the lowest energy state, so that all states in the lower band (the valence band) will he full and all states in the upper band (the conduction band) will be empty. The bandgap energy E_g between the top of the valence band and the bottom of the conduction hand is the width of the forbidden energy band.

We havediscussed qualitatively how and why bands of allowed and forbidden energies are formed in a crystal. The formation of these energy bands is directly related to the electrical characteristics of the crystal, as we will see later in our discussion.

*3.1.2 The Kronig–Penney Model

In the previous section, we discussed qualitatively the spitting of allowed electron energies as atoms are hrought together to form a crystal. The concept of allowed and forbidden energy bands can bc developed more rigorously by considering quantum mechanics and Schrodinger's wave equation. It may be easy for the reader to "get lost" in the following derivation, but the result forms the basis for the energy-band theory of semiconductors.

The potential function of a single, noninteracting, one-electron atom is shown in Figure 3.5a. Also indicated on the figure are the discrete energy levels allowed for theelectron. Figure 3.5b shows the same type of potential function for the case when several atoms are in close proximity arranged in a one-dimensional array. The potential functions of adjacent atoms overlap, and the net potential function for this case is shown in Figure 3.5c. It is this potential function we would need to use in Schrodinger's wave equation to model a one-dimensional single-crystal material.

The solution to Schrodinger's wave equation, for this one-dimensional single-crystal lattice, is made more tractable by considering a simpler potential function. Figure 3.6 is the one-dimensional Kronig–Penney model of the periodic potential function, which is used to represent a one-dimensional single-crystal lattice. We need to solve Schrodinger's wave equation in each region. As with previous quantum mechanical problems, the more interesting solution occurs for the case when $E < V_0$, which corresponds to a particle being bound within the crystal. The electrons are contained in the potential wells, but we have the possibility of tunneling between wells. The Kronig–Penney model is an idealized periodic potential representing a one-dimensional single crystal. but the results will illustrate many of the important featuresof the quantum behavior of electrons in a periodic lattice.

To obtain the solution to Schrodinger's wave equation, we make use of a mathematical theorem by Bloch. The theorem states that all one-electron wave functions,

---

*Indicates sections that can he skipped without loss of continuity

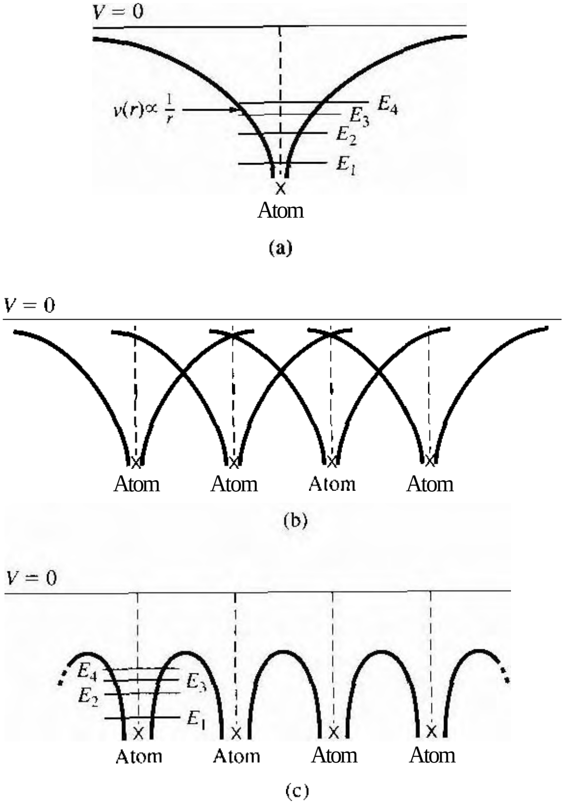
V = 0
v(r) ∝ 1/r
E4
E3
E2
E1
Atom
(a)
V = 0
Atom
Atom
Atom
Atom
(b)
V = 0
E4
E2
E3
E1
Atom
Atom
Atom
Atom
(c)

Figure 3.5 | (a) Potential function of a single isolated atom. (b) Overlapping potential functions of adjacent atoms. (c) Net potential function of a one-dimensional single crystal.

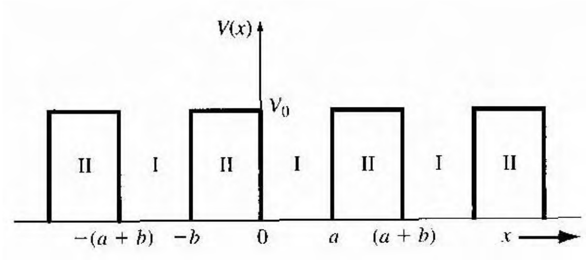
V(x)
V0
II
I
II
I
II
I
II
−(a + b)
−b
0
a
(a + b)
x

Figure 3.6 | The one-dimensional periodic potential function of the Kronig–Penney model.

for problems involving periodically varying potential energy functions, must be of the form

$$\psi(x) = u(x)e^{jkx} \tag{3.1}$$

The parameter k is called a constant of motion and will be considered in more detail as we develop the theory. The function $u(x)$ is a periodic function with period $(a\ \mathbf{t}\ b)$.

We stated in Chapter 2 that the total solution to the wave equation is the product of the time-independent solution and the time-dependent solution, or

$$\Psi(x,t) = \psi(x)\phi(t) = u(x)e^{jkx} \cdot e^{-j(E/\hbar)t} \tag{3.2}$$

which may be written as

$$\Psi(x,t) = u(x)e^{j(kx-(E/\hbar)t)} \tag{3.3}$$

This traveling-wave solution represents the motion of an electron in a single-crystal material. The amplitude of the traveling wave is a periodic function and the parameter k is also referred to as a wave number.

We can now begin to determine a relation between the parameter k, the total energy E, and the potential V_0. If we consider region I in Figure 3.6 $(0 < x < a)$ in which $V(x) = 0$, take the second derivative of Equation (3.1), and substitute this result into the time-independent Schrodinger's wave equation given by Equation (2.13). we obtain the relation

$$\frac{d^2u_1(x)}{dx^2} + 2jk\frac{du_1(x)}{dx} - (k' - \alpha^2)u_1(x) = 0 \tag{3.4}$$

The function $u_1(x)$ is the amplitude of the wave function in region I and the parameter a is defined as

$$\alpha^2 = \frac{2mE}{\hbar^2} \tag{3.5}$$

Consider now a specific region II, $-b < x < 0$, in which $V(x) = V_0$, and apply Schrodinger's wave equation. We obtain the relation

$$\frac{d^2u_2(x)}{dx^2} + 2jk\frac{du_2(x)}{dx} - \left(k^2 - \alpha^2 + \frac{2mV_0}{\hbar^2}\right)u_2(x) = 0 \tag{3.6}$$

where $u_2(x)$ is the amplitude of the wave function in region II. We may define

$$\frac{2m}{\hbar^2}(E - V_0) = \alpha^2 - \frac{2mV_0}{\hbar^2} = \beta^2 \tag{3.7}$$

so that Equation (3.6) may be written as

$$\frac{d^2u_2(x)}{dx^2} + 2jk\frac{du_2(x)}{dx} (k^2 - \beta^2)u_2(x) = 0 \tag{3.8}$$

Note that from Equation (3.7). if $E > V_0$, the parameter β is real, whereas if $E < V_0$, then β is imaginary.

The solution to Equation (3.4), for region I, is of the form

$$u_1(x) = Ae^{j(\alpha-k)x} + Be^{-j(\alpha+k)x} \qquad \text{for } (0 < x < a) \tag{3.9}$$

and the solution to Equation (3.8), for region II, is of the form

$$u_2(x) = Ce^{j(\beta-k)x} + De^{-j(\beta+k)x} \qquad \text{for } (-b < x < 0) \tag{3.10}$$

Since the potential function $V(x)$ is everywhere finite, both the wave function $\psi(x)$ and its first derivative $\partial\psi(x)/\partial x$ must be continuous. This continuity condition implies that the wave amplitude function $u(x)$ and its first derivative $\partial u(x)/\partial x$ must also be continuous.

If we consider the boundary at $x = 0$ and apply the continuity condition to the wave amplitude, we have

$$u_1(0) = u_2(0) \tag{3.11}$$

Substituting Equations (3.9) and (3.10) into Equation (3.11), we obtain

$$A + B - C - D = 0 \tag{3.12}$$

Now applying the condition that

$$\left.\frac{du_1}{dx}\right|_{x=0} = \left.\frac{du_2}{dx}\right|_{x=0} \tag{3.13}$$

we obtain

$$(\alpha - k)A - (\alpha + k)B - (\beta - k)C + (\beta + k)D = 0 \tag{3.14}$$

We have considered region I as $0 < x < a$ and region II as $-b < x < 0$. The periodicity and the continuity condition mean that the function u_1, as a $\rightarrow a$, is equal to the function u_2, as $x \rightarrow -b$. This condition may be written as

$$u_1(a) = u_2(-b) \tag{3.15}$$

Applying the solutions for $u_1(x)$ and $u_2(x)$ to the boundary condition in Equation (3.15) yields

$$Ae^{j(\alpha-k)a} + Be^{-j(\alpha+k)a} \quad Ce^{-j(\beta-k)b} - De^{j(\beta+k)b} = 0 \tag{3.16}$$

The last boundary condition is

$$\left.\frac{du_1}{dx}\right|_{x=a} = \left.\frac{du_2}{dx}\right|_{x=-b} \tag{3.17}$$

which gives

$$\begin{aligned} &(\alpha - k)Ae^{j(\alpha-k)a} - (\alpha + k)Be^{-j(\alpha+k)a} - (\beta - k)Ce^{-j(\beta-k)b} \\ &\quad + (\beta + k)De^{j(\beta+k)b} = 0 \end{aligned} \tag{3.18}$$

We now have four homogeneous equations, Equations (3.12), (3.14), (3.16), and (3.18), with four unknowns as a result of applying the four boundary conditions. In a set of simultaneous, linear, homogeneous equations, there is a nontrivial solution if, and only if, the determinant of the coefficients is zero. In our case, the coefficients in question are the coefficients of the parameters A, B, C, and D.

The evaluation of this determinant is extremely laborious and will not he considered in detail. The result is

$$\frac{-(\alpha^2+\beta^2)}{2\alpha\beta}(\sin\alpha a)(\sin\beta b)+(\cos\alpha a)(\cos\beta b)=\cos k(a+b) \qquad (3.19)$$

Equation (3.19) relates the parameter k to the total energy E (through the parameter a) and the potential function V_0 (through the parameter β).

As we mentioned, the more interesting solutions occur for $E < V_0$, which applies lo theelectron bound within the crystal. From Equation (3.7), the parameter β is then an imaginary quantity. We may define

$$\beta = j\gamma \qquad (3.20)$$

where y is areal quantity. Equation (3.19) can he written in terms of γ as

$$\frac{\gamma^2-\alpha^2}{2\alpha\gamma}(\sin\alpha a)(\sinh\gamma b)+(\cos\alpha a)(\cosh\gamma b)=\cos k(a+b) \qquad (3.21)$$

Equation (3.21) does not lend itself to an analytical solution, but must be solved using numerical or graphical techniques to obtain the relation between k, E. and V_0. The solution of Schrodinger's wave equation for a single bound particle resulted in discrete allowed energies. The solution of Equation (3.21) will result in a band of allowed energies.

To obtain an equation that is more susceptible to a graphical solution and thus will illustrate the nature of the results, let the potential barrier width b → 0 and the barrier height $V_0 \to \infty$, but such that the product bV_0 remains finite. Equation (3.21) then reduces to

$$\left(\frac{mV_0ba}{\hbar^2}\right)\frac{\sin\alpha a}{\alpha a}+\cos\alpha a=\cos ka \qquad (3.22)$$

We may define a parameter P' as

$$P'=\frac{mV_0ba}{\hbar^2} \qquad (3.23)$$

Then, finally, we have the relation

$$P'\frac{\sin ao}{\alpha a}+\cos\alpha a=\cos ku \qquad (3.24)$$

Equation (3.24) *again* gives the relation *between* the *parameter* k, total energy E *(through* the parameter a*)*, *and* the potential barrier bV_0. We may note that Equation (3.24)*is* not a *solution of Schrodinger's wave* equation but *gives* the *conditions* for which Schrodinger's wave equation ***will** have* a solution. If we assume the crystal is infinitely large, then k in Equation (3.24) can assume a continuum of values and must be real.

3.1.3 The k-Space Diagram

To begin to understand the nature of the solution, initially consider the special case for which $V_0 = 0$. In this case P' = 0, which corresponds to a free particle since there are no potential barriers. From Equation (3.24). we have that

$$\cos aa = \cos ka \tag{3.25}$$

or

$$\alpha = k \tag{3.26}$$

Since the potential is equal to zero, the total energy E is equal to the kinetic energy, so that, from Equation (3.5), Equation (3.26) may be written as

$$\alpha = \sqrt{\frac{2mE}{\hbar^2}} = \sqrt{\frac{2m\left(\frac{1}{2}mv^2\right)}{\hbar^2}} = \frac{p}{\mathrm{h}} = k \tag{3.27}$$

where p is the particle momentum. The constant of the motion parameter k is related to the particle momentum for the free electron. The parameter k is also referred to as a wave number.

We can also relate the energy and momentum as

$$E = \frac{p^2}{2m} = \frac{k^2\hbar^2}{2m} \tag{3.28}$$

Figure 3.7 shows the parabolic relation of Equation (3.28) between the energy E and momentum p for the free particle. Since the momentum and wave number are linearly related, Figure 3.7 is also the E versus k curve for the free panicle.

We now want to consider the relation between E and k from Equation (3.24) for the particle in the single-crystal lattice. As the parameter P' increases, the particle becomes more tightly bound to the potential well or atom. We may define the left side of Equation (3.24) to be a function f (αa), so that

$$\mathrm{f}\,(\alpha a) = P'\frac{\sin \alpha a}{\alpha a} + \cos \alpha a \tag{3.29}$$

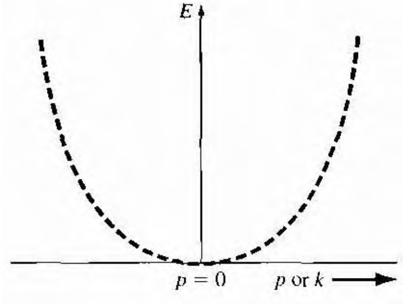

Figure 3.7 | The parabolic E versus k curve for the free electron.

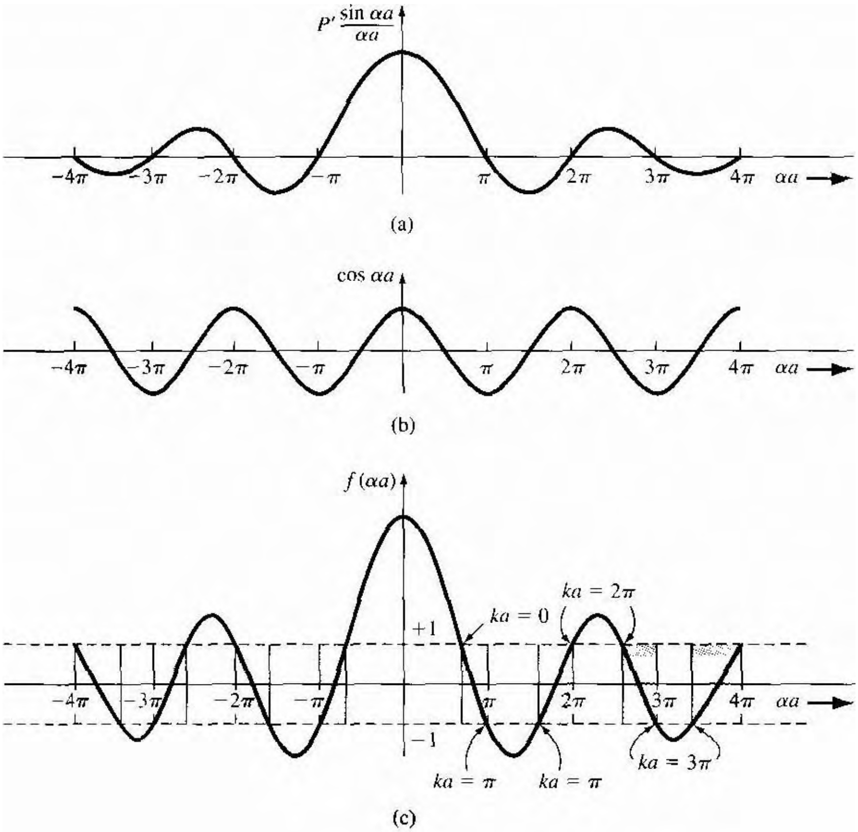

Figure 3.8 | A plot of (a) the first term in Equation (3.29), (b) the second term in Equation (3.29), and (c) the entire $f(\alpha a)$ function. The shaded areas show the allowed values of (αa) corresponding to real values of k.

Figure 3.8a is a plot of the first term of Equation (3.29) versus αa. Figure 3.8b shows a plot of the cos αa term and Figure 3.8c is the sum of the two terms, or $f(\alpha a)$.

Now from Equation (3.24). we also have that

$$f(\alpha a) = \cos ka \tag{3.30}$$

For Equation (3.30) to be valid, the allowed values of the $f(\alpha a)$ function must be bounded between +1 and −1. Figure 3.8c shows the allowed values of $f(\alpha a)$ and the allowed values of αa in the shaded areas. Also shown on the figure are the values of ka from the right side of Equation (3.30) which correspond to the allowed values of $f(\alpha a)$.

The parameter α is related to the total energy E of the particle through Equation (3.5), which is $\alpha^2 = 2mE/\hbar^2$. A plot of the energy E of the particle as a function of the wave number k can be generated from Figure 3.8c. Figure 3.9 shows this plot and shows the concept of allowed energy bands for the particle propagating in the

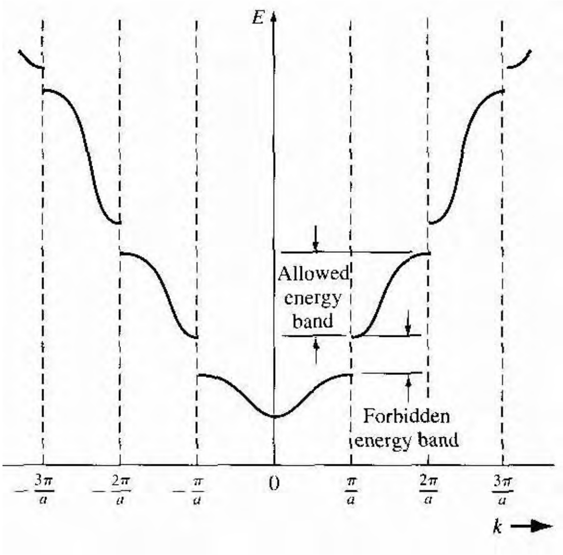

Figure 3.9 | The E versus k diagram generated from Figure 3.8. The allowed energy bands and forbidden energy bandgaps are indicated.

crystal lattice. Since the energy E has discontinuities, we also have the concept of forbidden energies for the particles in the crystal.

EXAMPLE 3.2

Objective

To determine the lowest allowed energy bandwidth.

Assume that the coefficient $P' = 10$ and that the potential width $a = 5$ Å

8 Solution

To find the lowest allowed energy bandwidth. we need to find the difference in αa values as ka changes from 0 to π (see Figure 3.8c). For $ka = 0$, Equation (3.29) becomes

$$1 = 10\frac{\sin \alpha a}{\alpha a} + \cos \alpha a$$

By trial and error, we find $\alpha a = 2.628$ rad. We see that for $ka = \pi$, $\alpha a = \pi$.

For $\alpha a = \pi$, we have

$$\sqrt{\frac{2mE_2}{\hbar^2}} \cdot a = \pi$$

or

$$E_2 = \frac{\pi^2\hbar^2}{2ma^2} = \frac{\pi^2(1.054 \times 10^{-34})^2}{2(9.11 \times 10^{-31})(5 \times 10^{-10})^2} = 2.407 \times 10^{-19}\ \text{J} = 1.50\ \text{eV}$$

For $\alpha a = 2.628$. we find that $E_1 = 1.68 \times 10^{-19}$ J $= 1.053$ eV. The allowed energy bandwidth is then

$$\Delta E = E_2 - E_1 = 1.50 - 1.053 = 0.447\ \text{eV}$$

■ Comment

We see from Figure 3.8c that. as the energy increases, the widths of the allowed bands increase from this Kronig–Penney model.

TEST YOUR UNDERSTANDING

E3.1 Using the parameters given in Example 3.2, determine the width (in eV) of the forbidden energy band that exists at $ka = \pi$ (see Figure 3.8c). (Ans. $\Delta E = 2.79$ eV)

Consider again the right side of Equation (3.24), which is the function cos ka. The cosine function is periodic so that

$$\cos ka = \cos(ka + 2n\pi) = \cos(ka - 2n\pi) \tag{3.31}$$

where n is a positive integer. We may consider Figure 3.9 and displace portions of the curve by 2π. Mathematically, Equation (3.24) is still satisfied. Figure 3.10 shows how various segments of the curve can be displaced by the 2π factor. Figure **3.11** shows the case in which the entire E versus k plot is contained within $-\pi/a < k < \pi/a$. This plot is referred to as a reduced k-space diagram, or a reduced-zero representation.

We noted in Equation (3.27) that for a free electron, the particle momentum and the wave number k are related by $p = \hbar k$. Given the similarity between the free

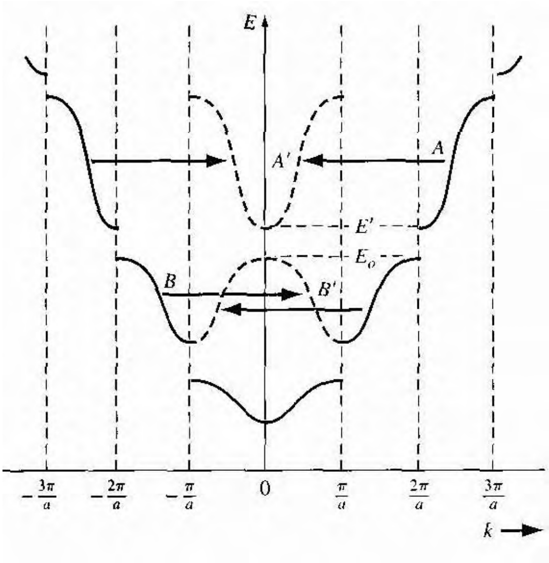

Figure 3.10 | The E versus k diagram showing 2π displacements of several sections of allowed energy bands.

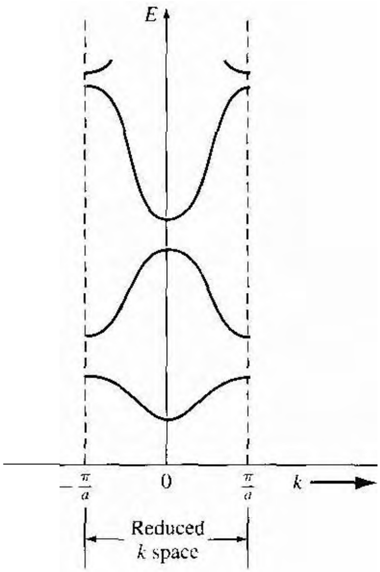

Figure **3.11** | The E versus k diagram in the reduced-zone representation.

electron solution and the results of the single crystal shown in Figure 3.9, the parameter $\hbar k$ in a single crystal is referred to as the *crystal momentum*. This parameter is not the actual momentum of the electron in the crystal, but is a constant of the motion that includes the crystal interaction.

We have been considering the Kronig–Penney model, which is a one-dimensional periodic potential function used to model a single-crystal lattice. The principle result of this analysis, sofa,: is that electrons in the crystal occupy certain allowed energy bands and are excluded from the forbidden energy bands. For real three-dimensional single-crystal materials, a similar energy-band theory exists. We will obtain additional electron properties from the Kronig–Penney model in the next sections.

3.2 | ELECTRICAL CONDUCTION IN SOLIDS

Again, we are eventually interested in determining the current–voltage characteristics of semiconductor devices. We will need to consider electrical conduction in solids as it relates to the band theory we have just developed. Let us begin by considering the motion of electrons in the various allowed energy hands.

3.2.1 The Energy Band and the Bond Model

In Chapter 1, we discussed the covalent bonding of silicon. Figure 3.12 shows a two-dimensional representation of the covalent bonding in a single-crystal silicon lattice. This figure represents silicon at T = 0 K in which each silicon atom is surrounded by eight valence electrons that are in their lowest energy state and are directly involved in the covalent bonding. Figure 3.4b represented the splitting of the discrete silicon energy states into bands of allowed energies as the silicon crystal is formed. At T = 0 K, the 4N states in the lower band, the valence band, are tilled with the valence electrons. All of the valence electrons schematically shown in Figure 3.12 are in the valence band. The upper energy band, the conduction band, is completely empty at T = 0 K.

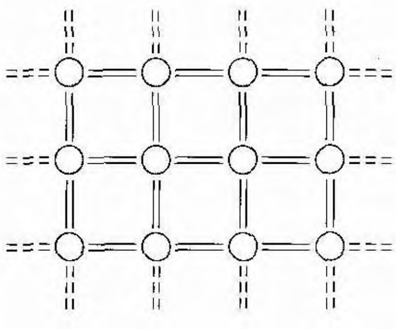

Figure 3.12 | Two-dimensional representation of the covalent bonding in a semiconductor at T = 0 K.

As the temperature increases above 0 K, a few valence band electrons may gain enough thermal energy to break the covalent bond and jump into the conduction band. Figure 3.13a shows a two-dimensional representation of this bond-breaking effect and Figure 3.13b, a simple line representation of the energy-band model, shows the same effect.

The semiconductor is neutrally charged. This means that, as the negatively charged electron breaks away from its covalent bonding position, a positively charged "empty state" is created in the original covalent bonding position in the valence band. As the temperature further increases, more covalent bonds are broken, more electrons jump to the conduction band, and more positive "empty states" are created in the valence band.

We can also relate this bond breaking to the E versus k energy bands. Figure 3.14a shows the E versus k diagram of the conduction and valence bands at

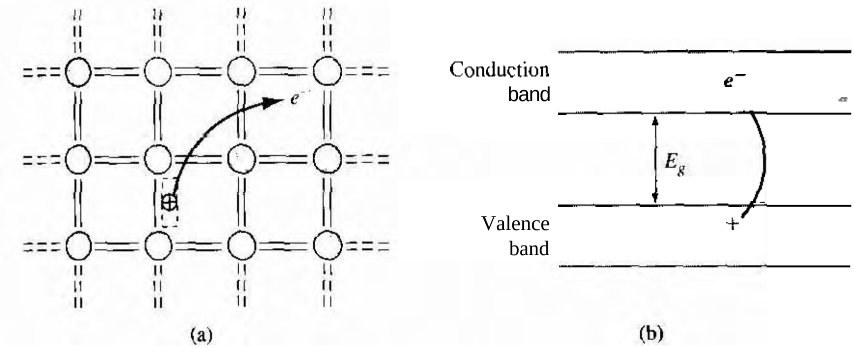

Figure 3.13 | (a) Two-dimensional representation of the breaking of a covalent bond. (b) Corresponding line representation of the energy band and the generation of a negative and positive charge with the breaking of a covalent bond.

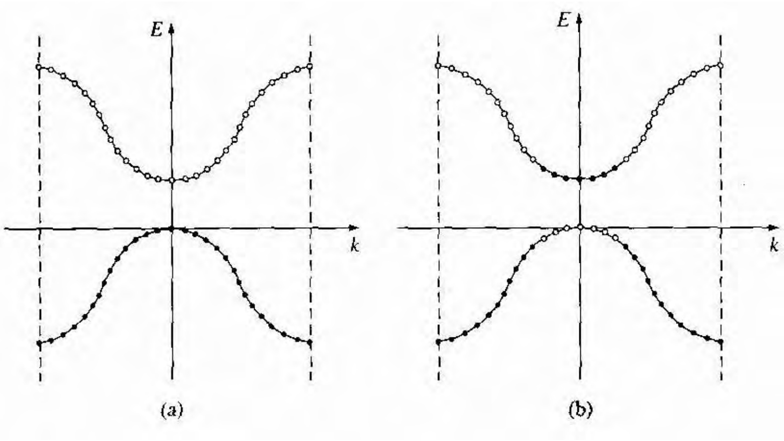

Figure 3.14 | The E versus k diagram of the conduction and valence bands of a semiconductor at (a) $T = 0$ K and (b) $T > 0$ K.

$T = 0$ K. The energy states in the valence band are completely full and the states in the conduction band are empty. Figure 3.14b shows these same bands for $T > 0$ K, in which some electrons have gained enough energy to jump to the conduction band and have left empty states in the valence band. We are assuming at this point that no external forces are applied so the electron and "empty state" distributions are symmetrical with k.

3.2.2 Drift Current

Current is due to the net flow of charge. If we had a collection of positively charged ions with a volume density N (cm^{-3}) and an average drift velocity v_d (cm/s), then the drift current density would be

$$J = qNv_d \qquad \text{A/cm}^2 \tag{3.32}$$

If, instead of considering the average drift velocity, we considered the individual ion velocities, then we could write the drift current density as

$$J = q\sum_{i=1}^{N} v_i \tag{3.33}$$

where v_i is the velocity of the **ith** ion. The summation in Equation (3.33) is taken over a unit volume so that the current density **J** is still in units of A/cm^2.

Since electrons are charged particles, a net drift of electrons in the conduction band will give rise to a current. The electron distribution in the conduction band, as shown in Figure 3.14b, is an even function of ***k*** when no external force is applied. Recall that ***k*** for a free electron is related to momentum so that, since there are as many electrons with a $+|k|$ value as there are with a $-|k|$ value, the net drift current density due to these electrons is zero. This result is certainly expected since there is no externally applied force.

If a force is applied to a particle and the particle moves, it must gain energy. This effect is expressed as

$$dE = F\,dx = Fv\,dt \tag{3.34}$$

where F is the applied force, dx is the differential distance the particle moves, v is the velocity, and dE is the increase in energy. If an external force is applied to the electrons in the conduction band, there are empty energy states into which the electrons can move: therefore, because of the external force, electrons can gain energy and a net momentum. The electron distribution in the conduction band may look like that shown in Figure 3.15, which implies that the electrons have gained a net momentum.

We may write the drift current density due to the motion of electrons as

$$J = -e\sum_{i=1}^{n} v_i \tag{3.35}$$

where e is the magnitude of the electronic charge and n is the number of electrons per unit volume in the conduction band. Again, the summation is taken over a unit

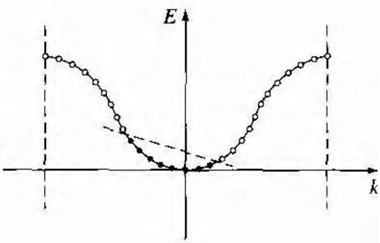

Figure 3.15 | The asymmetric distribution of electrons in the E versus k diagram when an external force is applied.

volume so the current density is A/cm^2. We may note from Equation (3.35) that the current is directly related to the electron velocity; that is, the current is related to how well the electron can move in the crystal.

3.2.3 Electron Effective Mass

The movement of an electron in a lattice will, in general, be different from that of an electron in free space. In addition to an externally applied force, there are internal forces in the crystal due to positively charged ions or protons and negatively charged electrons, which will influence the motion of electrons in the lattice. We can write

$$F_{\text{total}} = F_{\text{ext}} + F_{\text{int}} = ma \tag{3.36}$$

where F_{total}, F_{ext}, and F_{int} are the total force, the externally applied force, and the internal forces, respectively, acting on a particle in a crystal. The parameter a is the acceleration and m is the rest mass of the particle.

Since it is difficult to take into account all of the internal forces, we will write the equation

$$F_{\text{ext}} = m^*a \tag{1.37}$$

where the acceleration a is now directly related to the external force. The parameter ***m**.** called the ***effective mass,*** takes into account the panicle mass and also takes into account the effect of the internal forces.

To use an analogy for the effective mass concept, consider the difference in motion between a glass marble in a container filled with water and in a container filled with oil. In general, the marble will drop through the water at a faster rate than through the oil. The external force in this example is the gravitational force and the internal forces are related to the viscosity of the liquids. Because of the difference in motion of the marble in these two cases, the mass of the marble would appear to be different in water than in oil. (As with any analogy, we must be careful not to be too literal.)

We can also relate the effective mass of an electron in a crystal to the E versus k curves, such as was shown in Figure 3.11. In a semiconductor material, we will be dealing with allowed energy bands that are almost empty of electrons and other energy bands that are almost full of electrons.

To begin, consider the case of a free electron whose E versus k curve was shown in Figure 3.7. Recalling Equation (1.28). the energy and momentum are related by $E = p^2/2m = \hbar^2 k^2/2m$, where m is the mass of the electron. The momentum and wave number k are related by $p = Rk$. If we take the derivative of Equation (3.28) with respect to k, we obtain

$$\frac{dE}{dk} = \frac{\hbar^2 k}{m} = \frac{\hbar p}{m} \tag{3.38}$$

Relating momentum to velocity, Equation (3.38) can be written as

$$\frac{1}{\hbar}\frac{dE}{dk} = \frac{p}{m} = v \tag{3.39}$$

where v is the velocity of the particle. The first derivative of E with respect to k is related to the velocity of the panicle.

If we now take the second derivative of E with respect to k, we have

$$\frac{d^2 E}{dk^2} = \frac{\hbar^2}{m} \tag{3.40}$$

We may rewrite Equation (3.40) as

$$\boxed{\frac{1}{\hbar^2}\frac{d^2 E}{dk^2} = \frac{1}{m}} \tag{3.41}$$

The second derivative of E with respect to k is inversely proportional to the mass of the particle. For the case of a free electron, the mass is a constant (nonrelativistic effect), so the second derivative function is a constant. We may also note from Figure 3.7 that d^2E/dk^2 is a positive quantity, which implies that the mass of the electron is also a positive quantily.

If we apply an electric field to the free electron and use Newton's classical equation of motion, we can write

$$F = ma = -e\mathrm{E} \tag{3.42}$$

where a is the acceleration, E is the applied electric field, and e is the magnitude of the electronic charge. Solving for the acceleration, we have

$$a = \frac{-e\mathrm{E}}{m} \tag{3.43}$$

The motion of the free electron is in the opposite direction to the applied electric field because of the negative charge.

We may now apply the results to the electron in the bottom of an allowed energy band. Consider the allowed energy band in Figure 3.16a. The energy near the bottom of this energy band may be approximated by a parabola, just as that of a free particle. We may write

$$E - E_c = C_1(k)^2 \tag{3.44}$$

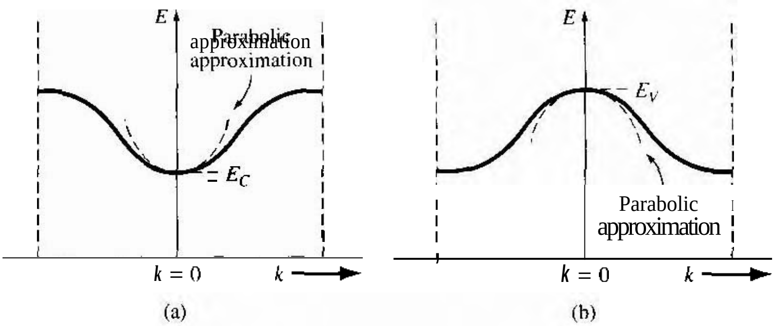

(a) (b)

Figure 3.16 | (a) The conduction band in reduced k space, and the parabolic approximation. (b) The valence band in reduced k space, and the parabolic approximation.

The energy E_c is the energy at the bottom of the band. Since $E > E_c$, the parameter C_1 is a positive quantity.

Taking the second derivative of E with respect to k from Equation (3.44), we obtain

$$\frac{d^2E}{dk^2} = 2C_1 \tag{3.45}$$

We may put Equation (3.45) in the form

$$\frac{1}{\hbar^2}\frac{d^2E}{dk^2} = \frac{2C_1}{\hbar^2} \tag{3.46}$$

Comparing Equation (3.46) with Equation (3.41), we may equate $\hbar^2/2C_1$ to the mass of the particle. However, the curvature of the curve in Figure 3.16a will not, in general, be the same as the curvature of the free-particle curve. We may write

$$\frac{1}{\hbar^2}\frac{d^2E}{dk^2} = \frac{2C_1}{\hbar^2} = \frac{1}{m^*} \tag{3.47}$$

where m^* is called the effective mass. Since $C_1 > 0$, we have that $m^* > 0$ also.

The effective mass is a parameter that relates the quantum mechanical results to the classical force equations. In most instances, the electron in the bottom of the conduction band can be thought of as a classical particle whose motion can be modeled by Newtonian mechanics, provided that the internal forces and quantum mechanical properties are taken into account through the effective mass. If we apply an electric field to the electron in the bottom of the allowed energy band, we may write the acceleration as

$$a = \frac{-e\mathrm{E}}{m_n^*} \tag{3.48}$$

where m_n^* is the effective mass of the electron. The effective mass m_n^* of the electron near the bottom of the conduction band is a constant.

3.2.4 Concept of the Hole

In considering the two-dimensional representation of the covalent bonding shown in Figure 3.13a, a positively charged "empty state" was created when a valence electron was elevated into the conduction band. For $T > 0$ K, all valence electrons may gain thermal energy; if a valence electron gains a small amount of thermal energy, it may hop into the empty state. The movement of a valence electron into the empty state is equivalent to the movement of the positively charged empty state itself. Figure 3.17 shows the movement of valence electrons in the crystal alternately filling one empty state and creating a new empty state, a motion equivalent to a positive charge moving in the valence band. The crystal now has a second equally important charge carrier that can give rise to a current. This charge carrier is called a ***hole*** and, as we will see, can also be thought of as a classical particle whose motion can be modeled using Newtonian mechanics.

The drift current density due to electrons in the valence band, such as shown in Figure 3.14b, can be written as

$$J = -e \sum_{i\,(\text{filled})} v_i \tag{3.49}$$

where the summation extends over all filled states. This summation is inconvenient since it extends over a nearly full valence band and takes into account a very large number of states. We may rewrite Equation (3.49) in the form

$$J = -e \sum_{i\,(\text{total})} v_i + e \sum_{i\,(\text{empty})} v_i \tag{3.50}$$

If we consider a band that is totally full, all available states are occupied by electrons. The individual electrons can be thought of as moving with a velocity as given by Equation (3.39):

$$v(E) = \left(\frac{1}{\hbar}\right)\left(\frac{dE}{dk}\right) \tag{3.39}$$

The band is symmetric in k and each state is occupied so that, for every electron with a velocity $|v|$, there is a corresponding electron with a velocity $-|v|$. Since the band is full, the distribution of electrons with respect to k cannot he changed with an externally applied force. The net drift current density generated from a completely full

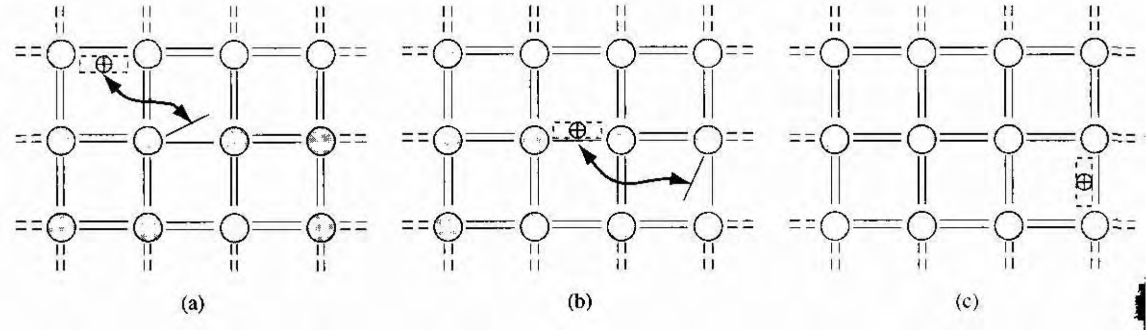

(a) (b) (c)

Figure 3.17 | Visualization of the movement of a hole in a semiconductor.

band, then, is zero, or

$$-e \sum_{i\,(\text{total})} v_i \equiv 0 \tag{3.51}$$

We can now write the drift current density from Equation (3.50) for an almost full band as

$$J = +e \sum_{i\,(\text{empty})} v_i \tag{3.52}$$

where the v_i in the summation is the

$$v(E) = \left(\frac{1}{\hbar}\right)\left(\frac{dE}{dk}\right)$$

associated with the empty state. Equation (3.52) is entirely equivalent to placing a positively charged particle in the empty states and assuming all other states in the band are empty, or neutrally charged. This concept is shown in Figure 3.18. Figure 3.18a shows the valence band with the conventional electron-filled states and empty states, while Figure 3.18b shows the new concept of positive charges occupying the original empty states. This concept is consistent with the discussion of the positively charged "empty state" in the valence band as shown in Figure 3.17.

The v_i in the summation of Equation (3.52) is related to how well this positively charged particle moves in the semiconductor. Now consider an electron near the top of the allowed energy band shown in Figure 3.16b. The energy near the top of the allowed energy band may again be approximated by a parabola so that we may write

$$(E - E_v) = -C_2(k)^2 \tag{3.53}$$

The energy E_v is the energy at the top of the energy band. Since $E < E_v$ for electrons in this band, then the parameter C_2 must be a positive quantity.

Taking the second derivative of E with respect to k from Equation (3.53). we obtain

$$\frac{d^2E}{dk^2} = -2C_2 \tag{3.54}$$

We may rearrange this equation so that

$$\frac{1}{\hbar^2}\frac{d^2E}{dk^2} = \frac{-2C_2}{\hbar^2} \tag{3.55}$$

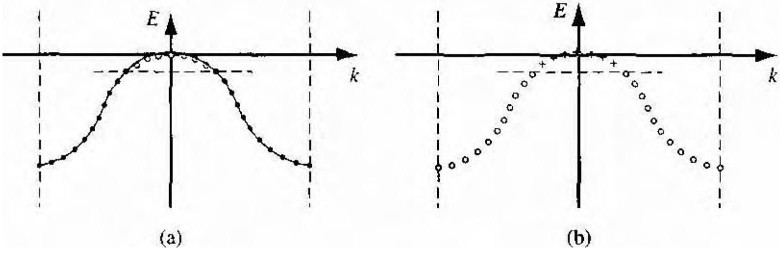

(a) (b)

Figure 3.18 | (a) Valence band with conventional electron-filled states and empty states. (b) Concept of positive charges occupying the original empty states.

Comparing Equation (3.55) with Equation (3.41), we may write

$$\frac{1}{\hbar^2}\frac{d^2E}{dk^2} = \frac{-2C_2}{h^2} = \frac{1}{m^*} \tag{3.56}$$

where m* is again an effective mass. We have argued that C_2 is a positive quantity, which now implies that m^* is a negative quantity. An electron moving near the topo an allowed energy hand behaves as if it has a negative mass.

We must keep in mind that the effective mass parameter is used to relate quantum mechanics and classical mechanics. The attempt to relate these two theories leads to this strange result of a negative effective mass. However, we must recall that solutions to Schrodinger's wave equation also led to results that contradicted classical mechanics. The negative effective mass is another such example.

In discussing the concept of effective mass in the last section, we used an analogy of marbles moving through two liquids. Now consider placing an ice cube in the center of a container filled with water: the ice cube will move upward toward the surface in a direction opposite to the gravitational force. The ice cube appears to have a negative effective mass since its acceleration is opposite to the external force. The effective mass parameter takes into account all internal forces acting on the particle.

If we again consider an electron near the top of an allowed energy band and use Newton's force equation for an applied electric field, we will have

$$F = m^*a = -e\mathrm{E} \tag{3.57}$$

However, m^* is now a negative quantity, so we may write

$$a = \frac{-e\mathrm{E}}{-|m^*|} = \frac{+e\mathrm{E}}{|m^*|} \tag{3.58}$$

An electron moving near the top of an allowed energy band moves in the same direction as the applied electric field.

The net motion of electrons in a nearly full hand can he described by considering just the empty states, provided that a positive electronic charge is associated with each state and that the negative of m* from Equation (3.56) is associated with each state. We now can model this band as having particles with a positive electronic charge and a positive effective mass. The density of these panicles in the valence band is the same as the density of empty electronic energy states. This new panicle is the *hole*. The hole, then, has a positive effective mass denoted by m_p^* and a positive electronic charge, so it will move in the same direction as an applied field.

3.2.5 Metals, Insulators, and Semiconductors

Each crystal has its own energy-band structure. We noted that the splitting of the energy states in silicon, for example, to form the valence and conduction bands, was complex. Complex band splitting occurs in other crystals, leading to large variations in band structures between various solids and to a wide range of electrical characteristics observed in these various materials. We can qualitatively begin to understand some basic differences in electrical characteristics caused by variations in band structure by considering some simplified energy bands.

There are several possible energy-band conditions to consider. Figure 3.19a shows an allowed energy band that is completely empty of electrons. If an electric field is applied, there are no particles to move, so there will be no current. Figure 3.19b shows another allowed energy band whose energy states are completely full of electrons. We argued in the previous section that a completely full energy band will also not give rise to a current. A material that has energy bands either completely empty or completely full is an insulator. The resistivity of an insulator is very large or, conversely, the conductivity of an insulator is very small. There are essentially no charged particles that can contribute to a drift current. Figure 3.19c shows a simplified energy-band diagram of an insulator. The bandgap energy E_g of an insulator is usually on the order of 3.5 to 6 eV or larger, so that at room temperature, there are essentially no electrons in the conduction band and the valence band remains completely full. There are very few thermally generated electrons and holes in an insulator.

Figure 3.20a shows an energy band with relatively few electrons near the bottom of the band. Now, if an electric field is applied, the electrons can gain energy, move to

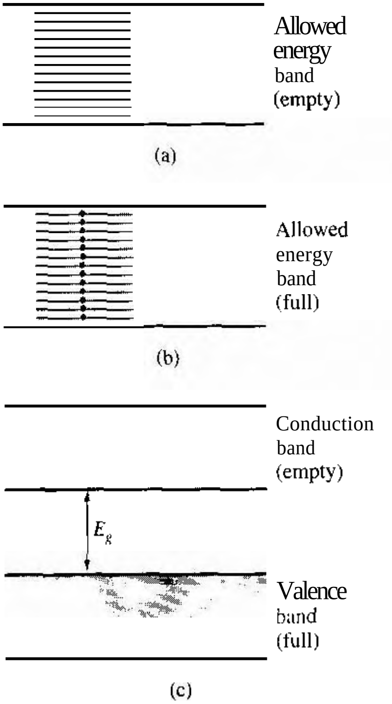
Allowed
energy
band
(empty)
(a)
Allowed
energy
band
(full)
(b)
Conduction
band
(empty)
E_g
Valence
band
(full)
(c)

Figure 3.19 | Allowed energy bands showing (a) an empty band, (b) a completely full band, and (c) the bandgap energy between the two allowed bands.

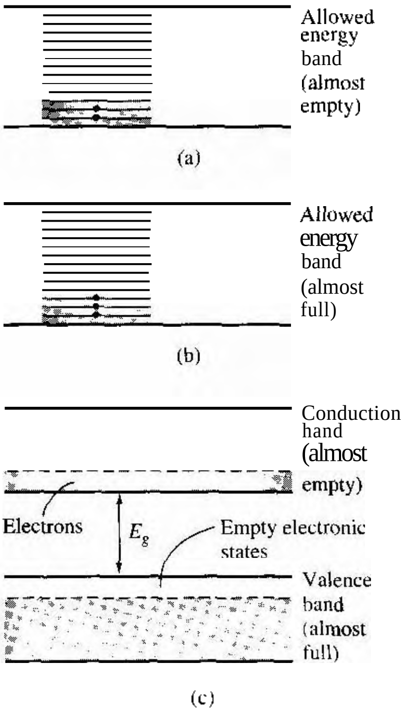
Allowed
energy
band
(almost
empty)
(a)
Allowed
energy
band
(almost
full)
(b)
Conduction
band
(almost
empty)
Electrons
E_g
Empty electronic
states
Valence
band
(almost
full)
(c)

Figure 3.20 | Allowed energy bands showing (a) an almost empty band, (b) an almost full band, and (c) the bandgap energy between the two allowed bands.

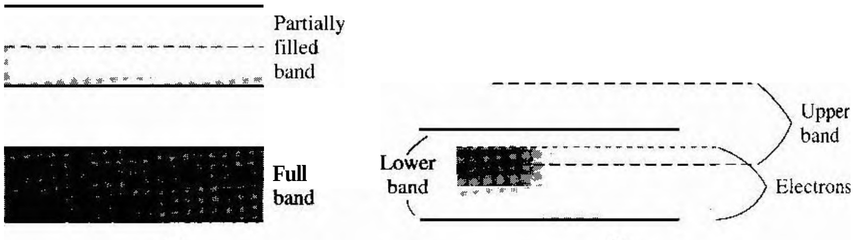

(a) (b)

Figure 3.21 | Two possible energy bands of a metal showing (a) a partially filled band and (b) overlapping allowed energy bands.

higher energy states, and move through the crystal. The net flow of charge is a current. Figure 3.20b shows an allowed energy band that is almost full of electrons. which means that we can consider the holes in this band. If an electric field is applied, the holes can move and give rise to a current. Figure 3.20c shows the simplified energy-band diagram for this case. The bandgap energy may be on the order of 1 eV. This energy-band diagram represents a semiconductor for $T > 0$ K. The resistivity of a semiconductor, as we will see in the next chapter, can be controlled and varied over many orders of magnitude.

The characteristics of a metal include a very low resistivity. The energy-band diagram for a metal may be in one of two forms. Figure 3.21a shows the case of a partially full band in which there are many electrons available for conduction, so that the material can exhibit a large electrical conductivity. Figure 3.21b shows another possible energy-band diagram of a metal. The band splitting into allowed and forbidden energy bands is a complex phenomenon and Figure 3.21b shows a case in which the conduction and valence bands overlap at the equilibrium interatomic distance. As in the case shown in Figure 3.21a, there are large numbers of electrons as well as large numbers of empty energy states into which the electrons can move, so this material can also exhibit a very high electrical conductivity.

3.3 | EXTENSION TO THREE DIMENSIONS

The basic concept of allowed and forbidden energy bands and the basic concept of effective mass have been developed in the last sections. In this section, we will extend these concepts to three dimensions and to real crystals. We will qualitatively consider particular characteristics of the three-dimensional crystal in terms of the E versus k plots, bandgap energy, and effective mass. We must emphasize that we will only briefly touch on the basic three-dimensional concepts; therefore, many details will not be considered.

One problem encountered in extending the potential function to a three-dimensional crystal is that the distance between atoms varies as the direction through the crystal changes. Figure 3.22 shows a face-centered cubic structure with the [100] and [110] directions indicated. Electrons traveling in different directions encounter different potential patterns and therefore different k-space boundaries. The E versus k diagrams are in general a function of the k-space direction in a crystal.

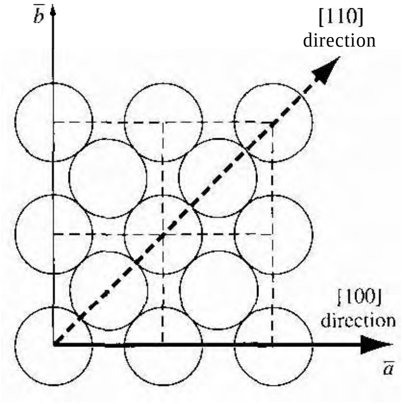

Figure **3.22** | The (100) plane of a face-centered cubic crystal showing the [100] and [110] directions.

3.3.1 The k-Space Diagrams of Si and GaAs

Figure 3.23 shows an E versus k diagram of gallium arsenide and of silicon. These simplified diagrams show the basic properties considered in this text, but do not show many of the details more appropriate for advanced-level courses.

Note that in place of the usual positive and negative k axes, we now show two different crystal directions. The E versus k diagram for the one-dimensional model

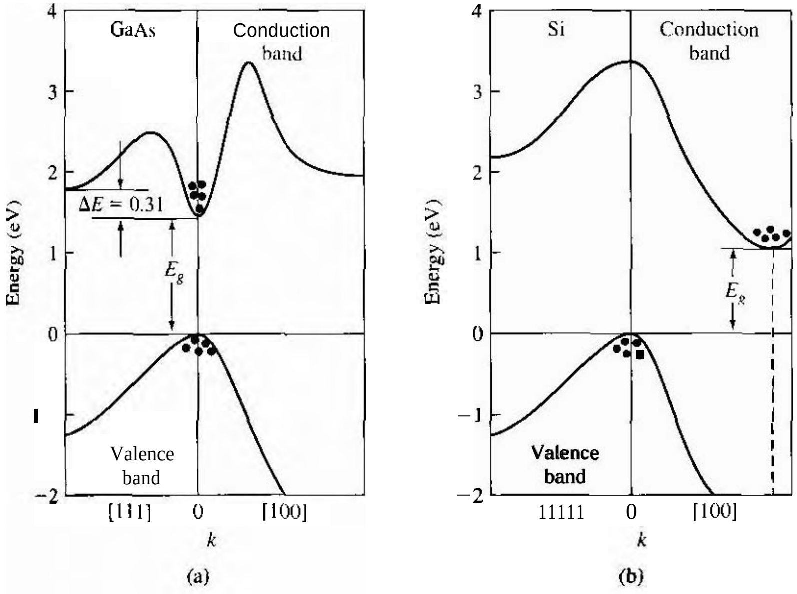

Figure **3.23** | Energy band structures of (a) GaAs and (b) Si

(From Sze [11].)

was symmetric in k so that no new information is obtained by displaying the negative axis. It is normal practice to plot the [100] direction along the normal $+k$ axis and to plot the [111] portion of the diagram so the $+k$ points to the left. In the case of diamond or zincblende lattices, the maxima in the valence band energy and minima in the conduction band energy occur at k = 0 or along one of these two direction*.

Figure 3.23a shows the E versus k diagram for GaAs. The valence band maximum and the conduction hand minimum both occur at k = 0. The electrons in the conduction band tend to settle at the minimum conduction band energy which is at k = 0. Similarly, holes in the valence band tend to congregate at the uppermost valence band energy. In GaAs, the minimum conduction band energy and maximum valence band energy occur at the same k value. A semiconductor with this property is said to be a *direct* bandgap semiconductor; transitions between the two allowed bands can take place with no change in crystal momentum. This direct nature has significant effect on the optical properties of the material. GaAs and other direct bandgap materials are ideally suited for use in semiconductor lasers and other optical devices.

The E versus k diagram for silicon is shown in Figure 3.23b. The maximum in the valence band energy occurs at k = 0 as before. The minimum in the conduction band energy occurs not at k = 0, hut along the [100] direction. The difference between the minimum conduction band energy and the maximum valence band energy is still defined as the bandgap energy E_g. A semiconductor whose maximum valence band energy and minimum conduction band energy do not occur at the same k value is called an *indirect* bandgap semiconductor. When electrons make a transition between the conduction and valence bands, we must invoke the law of conservation of momentum. A transition in an indirect bandgap material must necessarily include an interaction with the crystal so that crystal momentum is conserved.

Germanium is also an indirect bandgap material, whose valence band maximum occurs at k = 0 and whose conduction band minimum occurs along the [111] direction. GaAs is a direct bandgap semiconductor, but other compound semiconductors, such as GaP and AlAs, have indirect bandgaps.

3.3.2 Additional Effective Mass Concepts

The curvature of the E versus k diagrams near the minimum of the conduction band energy is related to the effective mass of the electron. We may note from Figure 3.2 that the curvature of the conduction band at its minimum value for GaAs is large than that of silicon, so the effective mass of an electron in the conduction hand o GaAs will be smaller than that in silicon.

For the one-dimensional E versus k diagram, the eftective mass was defined by Equation (3.41) as $1/m^* = 1/\hbar^2 \cdot d^2E/dk^2$. A complication occurs in the effecti mass concept in a real crystal. A three-dimensional crystal can be described by t k vectors. The curvature of the E versus kdiagram at the conduction band minimum m not be the same in the three k directions. We will not consider the details of the vari effective mass parameters here. In later sections and chapters, the effective mass parameters used in calculations will be a kind of statistical average that is adequate for most device calculations.

3.4 | DENSITY OF STATES FUNCTION

As we have stated. we eventually wish to describe the current-voltage characteristics of semiconductor devices. Since current is due to the flow of charge. an important step in the process is to determine the number of electrons and holes in the semiconductor that will he available for conduction. The number of carriers that can contribute to the conduction process is a function of the number of available energy or quantum states since, by the Pauli exclusion principle, only one electron can occupy a given quantum state. When we discussed the splitting of energy levels into bands of allowed and forbidden energies, we indicated that the band of allowed energies was actually made up of discrete energy levels. We must determine the density of these allowed energy states as a function of energy in order to calculate the electron and hole concentrations.

3.4.1 *Mathematical* Derivation

To determine the density of allowed quantum states as a function of energy, we need to consider an appropriate mathematical model. Electrons are allowed to move relatively freely in the conduction band of a semiconductor, but are confined to the crystal. As a first step, we will consider a free electron confined to a three-dimensional infinite potential well, where the potential well represents the crystal. The potential of the infinite potential well is defined as

$$\begin{aligned} V(x, y, z) &= 0 \qquad &&\text{for } 0 < x < a \\ & &&0 < y < a \\ & &&0 < z < a \\ V(x, y, z) &= \infty &&\text{elsewhere} \end{aligned} \tag{3.59}$$

where the crystal is assumed to be a cube with length a. Schrodinger's wave equation in three dimensions can be solved using the separation of variables technique. Extrapolating the results from the one-dimensional infinite potential well, we can show (see Problem 3.21) that

$$\frac{2mE}{\hbar^2} = k^2 = k_x^2 + k_y^2 + k_z^2 = \left(n_x^2 + n_y^2 + n_z^2\right)\left(\frac{\pi^2}{a^2}\right) \tag{3.60}$$

where n_x, n_y, and n_z are positive integers. (Negative values of n_x, n_y, and n_z yield the same wave function, except for the sign, as the positive integer values, resulting in the same probability function and energy, so the negative integers do not represent a different quantum state.)

We can schematically plot the allowed quantum states in k space. Figure 3.24a shows a two-dimensional plot as a function of k_x and k_y. Each point represents an allowed quantum state corresponding to various integral values of n_x and n_y. Positive and negative values of k_x, k_y, or k_z have the same energy and represent the same

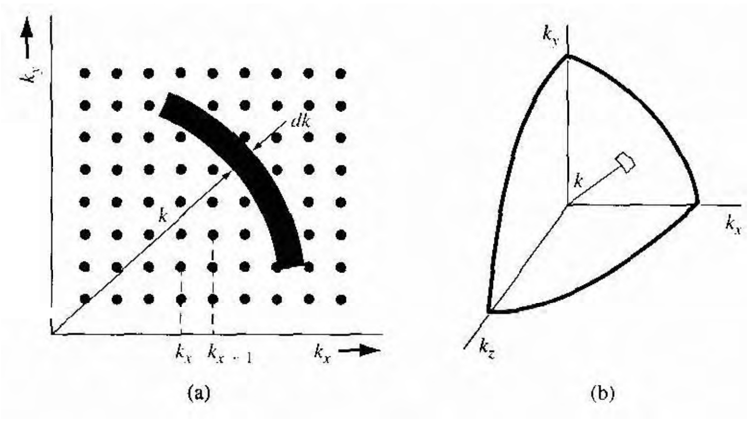

Figure 3.24 | (a) A two-dimensional array of allowed quantum states in k space. (b) The positive one-eighth of the spherical k space.

energy state. Since negative values of k_x, k_y, or k_z do not represent additional quantum states, the density of quantum states will be determined by considering only the positive one-eighth of the spherical k space as shown in Figure 3.24b.

The distance between two quantum states in the k_x direction, for example, is given by

$$k_{x+1} - k_x = (n_x + 1)\left(\frac{\pi}{a}\right) - n_x\left(\frac{\pi}{a}\right) = \frac{\pi}{a} \tag{3.61}$$

Generalizing this result to three dimensions, the volume V_k of a single quantum state is

$$V_k = \left(\frac{\pi}{a}\right)^3 \tag{3.62}$$

We can now determine the density of quantum states in k space. **A** differential volume in k space is shown in Figure 3.24b and is given by $4\pi k^2\,dk$, so the differential density of quantum states in k space can be written as

$$g_T(k)\,dk = 2\left(\frac{1}{8}\right)\frac{4\pi k^2\,dk}{\left(\dfrac{\pi}{a}\right)^3} \tag{3.63}$$

The first factor, 2, takes into account the two spin states allowed for each quantum state; the next factor, $\frac{1}{8}$, takes into account that we are considering only the quantum states for positive values of k_x, k_y, and k_z. The factor $4\pi k^2\,dk$ is again the differential volume and the factor $(\pi/a)^3$ is the volume of one quantum state. Equation (3.63) may be simplified to

$$g_T(k)\,dk = \frac{\pi k^2\,dk}{\pi^3}\cdot a^3 \tag{3.64}$$

Equation (3.64) gives the density of quantum states as a function of momentum, through the parameter k. We can now determine the density of quantum states as a function of energy E. For a free electron, the parameters E and k are related by

$$k^2 = \frac{2mE}{\hbar^2} \tag{3.65a}$$

or

$$k = \frac{1}{\hbar}\sqrt{2mE} \tag{3.65b}$$

The differential dk is

$$dk = \frac{1}{\hbar}\sqrt{\frac{m}{2E}}\,dE \tag{3.66}$$

Then, substituting the expressions for k^2 and dk into Equation (3.64). the number of energy states between E and E $+ dE$ is given by

$$g_T(E)\,dE = \frac{\pi a^3}{\pi^3}\left(\frac{2mE}{\hbar^2}\right)\cdot\frac{1}{\hbar}\sqrt{\frac{m}{2E}}\,dE \tag{3.67}$$

Since $\hbar = h/2\pi$, Equation (3.67) becomes

$$g_T(E)\,dE = \frac{4\pi a^3}{h^3}\cdot(2m)^{3/2}\cdot\sqrt{E}\,dE \tag{3.68}$$

Equation (3.68) gives the total number of quantum states between the energy E and E t dE in the crystal space volume of u^3. If we divide by the volume a^3, then we will obtain the density of quantum states per unit volume of the crystal. Equation (3.68) then becomes

$$g(E) = \frac{4\pi(2m)^{3/2}}{h^3}\sqrt{E} \tag{3.69}$$

The density of quantum states is a function of energy E. As the energy of this free electron becomes small, the number of available quantum states decreases. This density function is really a double density, in that the units are given in terms of states per unit energy per unit volume.

Objective

EXAMPLE 3.3

To calculate the density of states per unit volume over a particular energy range.

Consider the density of states for a free electron given by Equation (3.69). Calculate the density of states per unit volume with energies between 0 and 1 eV.

■ Solution

The volume density of quantum states, from Equation (3.69), is

$$\blacksquare = \int_0^{1\text{ eV}} g(E)\,dE = \frac{4\pi(2m)^{3/2}}{h^3}\cdot\int_0^{1\text{ eV}}\sqrt{E}\,dE$$

or

$$N = \frac{4\pi(2m)^{3/2}}{h^3}\cdot\frac{2}{3}\cdot E^{3/2}$$

The density of states is now

$$N = \frac{4\pi[2(9.11\times 10^{\ 31})]^{3/2}}{(6.625\times 10^{-34})^3}\cdot\frac{2}{3}\cdot(1.6\times 10^{-19})^{3/2} = 4.5\times 10^{27}\text{ m}^{-3}$$

or

$$N = 4.5\times 10^{21}\text{ states/cm}^3$$

■ Comment

The density of quantum states is typically a large number. An effective density of states in a semiconductor, as we will see in the following sections and in the next chapter, is also a large number, but is usually less than the density of atoms in the semiconductor crystal.

3.4.2 Extension to Semiconductors

In the last section, we derived a general expression for the density of allowed electron quantum states using the model of a free electron with mass m bounded in a three-dimensional infinite potential well. We can extend this same general model to a semiconductor to determine the density of quantum states in the conduction band and the density of quantum states in the valence band. Electrons and holes are confined within the semiconductor crystal so we will again use the basic model of the infinite potential well.

The parabolic relationship between energy and momentum of a free electron was given in Equation (3.28) as $E = p^2/2m = \hbar^2k^2/2m$. Figure 3.16a showed the conduction energy band in the reduced k space. The E versus k curve near $k = 0$ at the bottom of the conduction band can be approximated as a parabola, so we may write

$$E = E_c + \frac{\hbar^2k^2}{2m_n^*} \qquad (3.7$$

where E_c is the bottom edge of the conduction band and m_n^* is the electron effecti mass. Equation (3.70) may be rewritten to give

$$E - E_c = \frac{\hbar^2k^2}{2m;} \qquad (3.71$$

The general form of the E versus k relation for an electron in the bottom of a conduction band is the same as the free electron, except the mass is replaced by the effective mass. We can then think of the electron in the bottom of the conduction band as being a "free" electron with its own particular mass. The right side of Equation (3.71) is of the same form a the right side of Equation (3.28), which was used in the derivation of the density of states function. Because of this similarity, which yields the "free" conduction electron model, we may generalize the free electron results of Equation *(3.69)* and write the density of allowed electronic energy states in the conduction band as

$$\boxed{g_c(E) = \frac{4\pi(2m_n^*)^{3/2}}{h^3}\sqrt{E - E_c}} \tag{3.72}$$

Equation *(3.72)* is valid for $E \geq E_c$. **As** the energy of the electron in the conduction band decreases, the number of available quantum states also decreases.

The density of quantum states in the valence band can be obtained by using the same infinite potential well model, since the hole is also confined in the semiconductor crystal and can be treated as a "free" particle. The effective mass of the hole is m_p^*. Figure 3.16b showed the valence energy band in the reduced k space. We may also approximate the E versus k curve near $k = 0$ by a parabola for a "free" hole, so that

$$E = E_v - \frac{\hbar^2 k^2}{2m_p^*} \tag{3.73}$$

Equation *(3.73)* may be rewritten to give

$$E_v - E = \frac{\hbar^2 k^2}{2m_p^*} \tag{3.74}$$

Again, the right side of Equation *(3.74)* is of the same form used in the general derivation of the density of states function. We may then generalize the density of states function from Equation *(3.69)* to apply to the valence band, so that

$$\boxed{g_v(E) = \frac{4\pi(2m_p^*)^{3/2}}{h^3}\sqrt{E_v - E}} \tag{3.75}$$

Equation *(3.75)* is valid for $E \leq E_v$.

We have argued that quantum states do not exist within the forbidden energy band, so $g(E) = 0$ for $E_v < E < E_c$. Figure 3.25 shows the plot of the density of quantum states as a function of energy. If the electron and hole effective masses were equal, then the functions $g_c(E)$ and $g_v(E)$ would be symmetrical about the energy midway between E_c and E_v, or the midgap energy. E_{midgap}.

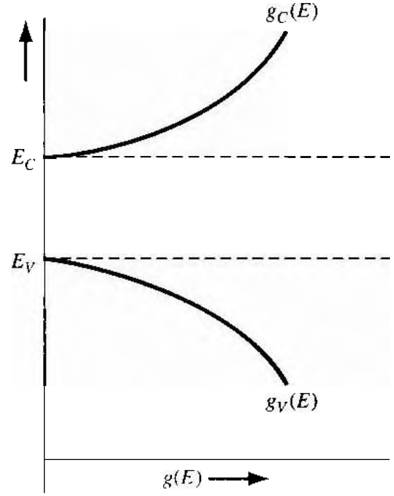

Figure 3.25 | The density of energy states in the conduction band and the density of energy states in the valence band as a function of energy.

TEST YOUR UNDERSTANDING

E3.2 Determine the total number of energy states in silicon between E_c and $E_c + kT$ at $T = 300$ K. (Ans. $2.12 \times 10^{19}\ \text{cm}^{-3}$)

E3.3 Determine the total number of energy states in silicon between E_v and $E_v - kT$ at $T = 300$ K. (Ans. $7.92 \times 10^{18}\ \text{cm}^{-3}$)

3.5 | STATISTICAL MECHANICS

In dealing with large numbers of particles, we are interested only in the statistical behavior of the group as a whole rather than in the behavior of each individual particle. For example, gas within a container will exert an average pressure on the walls of the vessel. The pressure is actually due to the collisions of the individual gas molecules with the walls, but we do not follow each individual molecule as it collides with the wall. Likewise in a crystal, the electrical characteristics will be determined by the statistical behavior of a large number of electrons.

3.5.1 Statistical Laws

In determining the statistical behavior of particles, we must consider the laws that the particles obey. There are three distribution laws determining the distribution of particles among available energy states.

One distribution law is the Maxwell–Boltzmann probability function. In this case, the panicles are considered to be distinguishable by being numbered, for example, from I to N. with no limit to the number of particles allowed in each energy state. The behavior of gas molecules in a container at fairly low pressure is an example of this distribution.

A second distribution law is the Bose–Einstein function. The panicles in this case are indistinguishable and, again, there is no limit to the number of particles permitted in each quantum state. The behavior of photons, or black body radiation, is an example of this law.

The third distribution law is the Fermi–Dirac probability function. In this case, the particles are again indistinguishable, but now only one particle is permitted in each quantum state. Electrons in a crystal obey this law. In each case, the particles are assumed to be noninteracting.

3.5.2 The Fermi–Dirac Probability Function

Figure 3.26 shows the ith energy level with g_i quantum states. A maximum of one particle is allowed in each quantum state by the Pauli exclusion principle. There are g_i ways of choosing where to place the first panicle, $(g_i - 1)$ ways of choosing where to place the second particle, $(g_i - 2)$ ways of choosing where to place the third particle, and so on. Then the total number of ways of arranging N_i particles in the *i*th energy level (where $N_i \leq g_i$) is

$$(g_i)(g_i - 1)\cdots(g_i - (N_i - 1)) = \frac{g_i!}{(g_i - N_i)!} \tag{3.76}$$

This expression includes all permutations of the N, particles among themselves.

However, since the particles are indistinguishable, the $N_i!$ number of permutations that the particles have among themselves in any given arrangement do not count as separate arrangements. The interchange of any two electrons. for example, does not produce a new arrangement. Therefore, the actual number of independent ways of realizing a distribution of N_i particles in the ith level is

$$W_i = \frac{g_i!}{N_i!(g_i - N_i)!} \tag{3.77}$$

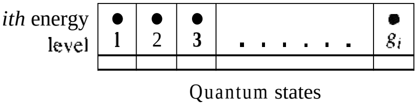

Figure 3.261 The *ith* energy level wrth g_i quantum states.

EXAMPLE 3.4

Objective

To determine the possible number of ways of realizing a particular distribution.

Let $g_i = N_i = 10$. Then $(g_i - N_i)! = 1$.

■ Solution

Equation (3.77) becomes

$$\frac{g_i!}{N_i!(g_i - N_i)!} = \frac{10!}{10!} = 1$$

■ Comment

If we have 10 particles to be arranged in 10 quantum states, there is only one possible arrangement. Each quantum state contains one particle.

EXAMPLE 3.5

Objective

To again determine the possible number of ways of realizing a particular distribution.

Let $g_i = 10$ and $N_i = 9$. In this case $g_i - N_i = 1$ so that $(g_i - N_i)! = 1$.

■ Solution

Equation (3.77) becomes

$$\frac{g_i!}{N_i!(g_i - N_i)!} = \frac{10!}{(9!)(1)} = \frac{(10)(9!)}{9!} = 10$$

■ Comment

In this case, if we have 10 quantum states and 9 particles. there is one empty quantum state. There are 10 possible arrangements, or positions, for the one empty state.

Equation (3.77) gives the number of independent ways of realizing a distribution of N_i particles in the ith level. The total number of ways of arranging $(N_1, N_2, N_3, \ldots, N_n)$ indistinguishable particles among n energy levels is the product of all distributions, or

$$W = \prod_{i=1}^{n} \frac{g_i!}{N_i!(g_i - N_i)!} \tag{3.78}$$

The parameter W is the total number of ways in which N electrons can be arranged in this system, where $N = \sum_{i=1}^{n} N_i$ is the total number of electrons in the system. We want to find the most probable distribution, which means that we want to find the maximum W. The maximum W is found by varying N_i among the E_i levels, which varies the distribution, but at the same time, we will keep the total number of particles and total energy constant.

We may write the most probable distribution function as

$$\boxed{\frac{N(E)}{g(E)} = f_F(E) = \frac{1}{1 + \exp\left(\dfrac{E - E_F}{kT}\right)}} \tag{3.79}$$

where E_F is called the Fermi energy. The number density $N(E)$ is the number of particles per unit volume per unit energy and the function $g(E)$ is the number of quantum states per unit volume per unit energy. The function $f_F(E)$ is called the **Fermi–Dirac** distribution or probability function and gives the probability that a quantum state at the energy E will be occupied by an electron. Another interpretation of the distribution function is that $f_F(E)$ is the ratio of filled to total quantum states at any energy E.

3.5.3 The Distribution Function and the Fermi Energy

To begin to understand the meaning of the distribution function and the Fermi energy, we can plot the distribution function versus energy. Initially, let T = 0 K and consider the case when E $< E_F$. The exponential term in Equation (1.79) becomes $\exp[(E - E_F)/kT] \to \exp(-\infty) = 0$. The resulting distribution function is $f_F(E < E_F) = 1$. Again let T = 0 K and consider the case when $E > E_F$. The exponential term in the distribution function becomes $\exp[(E - E_F)/kT] \to \exp(+\infty) \to +\infty$. The resulting Fermi–Dirac distribution function now becomes $f_F(E > E_F) = 0$.

The Fermi–Dirac distribution function for T = 0 K is plotted in Figure 3.27. This result shows that, for T = 0 K, the electrons are in their lowest possible energy states. The probability of a quantum state being occupied is unity for $E < E_F$ and the probability of a state being occupied is zero for $E > E_F$. All electrons have energies below the Fermi energy at T = 0 K.

Figure 3.28 shows discrete energy levels of a particular system as well as the number of available quantum states at each energy. If we assume, for this case, that

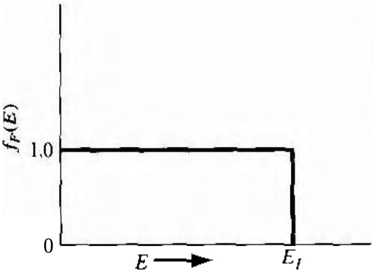

Figure 3.27 | The Fermi probability function versus energy for T = 0 K.

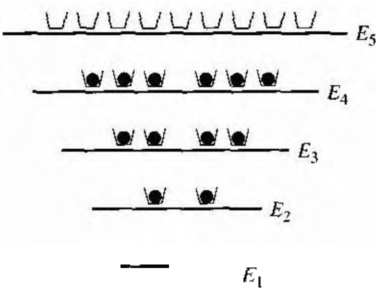

Figure 3.28 | Discrete energy states and quantum states for a particular system at T = 0 K.

the system contains 13 electrons. then Figure 3.28 shows how these electrons are distributed among the various quantum states at T = 0 K. The electrons will be in the lowest possible energy state, so the probability of a quantum state being occupied in energy levels E_1 through E_4 is unity, and the probability of a quantum state being occupied in energy level E_5 is zero. The Fermi energy, for this case, must be above E_4 but less than E_5. The Fermi energy determines the statistical distribution of electrons and does not have to correspond to an allowed energy level.

Now consider a case in which the density of quantum states $g(E)$ is a continuous function of energy as shown in Figure 3.29. If we have N_0 electrons in this system, then the distribution of these electrons among the quantum states at T = 0 K is shown by the dashed line. The electrons are in the lowest possible energy state so that all states below E_F are filled and all states above E_F are empty. If $g(E)$ and N_0 are known for this particular system, then the Fermi energy E_F can be determined.

Consider the situation when the temperature increases above T = 0 K. Electrons gain a certain amount of thermal energy so that some electrons can jump to higher energy levels, which means that the distribution of electrons among the available energy states will change. Figure 3.30 shows the same discrete energy levels and quantum states as in Figure 3.28. The distribution of electrons among the quantum states has changed from the $T = 0$ K case. Two electrons from the E_4 level have gained enough energy to jump to E_5, and one electron from E_3 has jumped to E_4. As the temperature changes, the distribution of electrons versus energy changes.

The change in the electron distribution among energy levels for T > 0 K can be seen by plotting the Fermi–Dirac distribution function. If we let $E = E_F$ and T > 0K, then Equation (3.79) becomes

$$f_F(E = E_F) = \frac{1}{1+\exp(0)} = \frac{1}{1+1} = \frac{1}{2}$$

The probability of a state being occupied at $E = E_F$ is $\frac{1}{2}$. Figure 3.31 shows the Fermi–Dirac distribution function plotted for several temperatures, assuming the Fermi energy is independent of temperature.

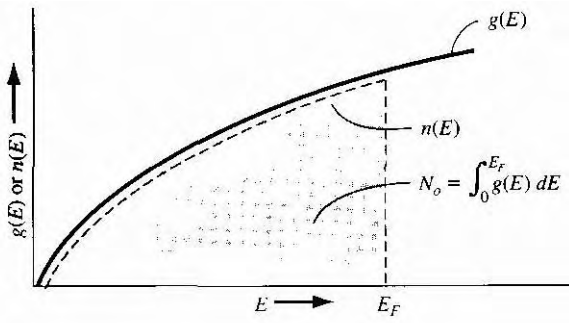

Figure 3.29 | Density of quantum states and electrons in a continuous energy system at T = 0 K.

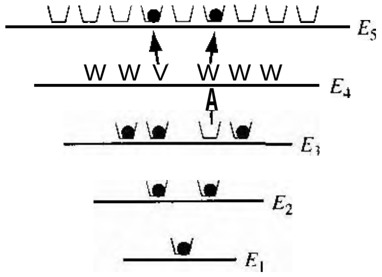

Figure 3.30 | Discrete energy states and quantum states for the same system shown in Figure 3.28 for T > 0 K.

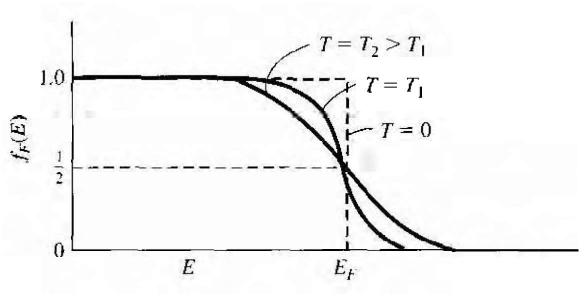

Figure 3.31 | The Fermi probability function versus energy for different temperatures.

We can see that for temperatures above absolute zero, there is a nonzero probability that some energy states above E_F will be occupied by electrons and some energy states below E_F will be empty. This result again means that some electrons have jumped to higher energy levels with increasing thermal energy.

Objective | EXAMPLE 3.6

To calculate the probability that an energy state above E_F is occupied by an electron.

Let T = 300 K. Determine the probability that an energy level 3kT above the Fermi energy is occupied by an electron.

■ Solution

From Equation (3.79), we can write

$$f_F(E) = \frac{1}{1 + \exp\left(\frac{E - E_F}{kT}\right)} = \frac{1}{1 + \exp\left(\frac{3kT}{kT}\right)}$$

which becomes

$$f_F(E) = \frac{1}{1 + 20.09} = 0.0474 = 4.74\%$$

■ Comment

At energies above E_F, the probability of a state being occupied by an electron can become significantly less than unity. or the ratio of electrons to available quantum states can be quite small.

TEST YOUR UNDERSTANDING

E3.4 Assume the Fermi energy level is 0.30 eV below the conduction band energy.
(*a*) Determine the probability of a state being occupied by an electron at E_c.
(*b*) Repeat part (*a*) for an energy state at $E_c + kT$. Assume T = 300 K.
[Ans. (*a*) 9.32×10^{-6}, (*b*) 3.43×10^{-6}]

E3.5 Assume the Fermi energy level is 0.35 eV above the valence band energy. (*a*) Determine the probability of a state being empty of an electron at E_V. (*b*) Repeat part (*a*) for an energy state at $E_V - kT$. Assume $T = 300$ K.
[Ans. (*a*) 1.35×10^{-6}, (*b*) 4.98×10^{-7}]

We can see from Figure 3.31 that the probability of an energy above E_F being occupied increases as the temperature increases and the probability of a state below E_F being empty increases as the temperature increases.

EXAMPLE 3.7

Objective

To determine the temperature at which there is a 1 percent probability that an energy state is empty.

Assume that the Fermi energy level for a particular material is 6.25 eV and that the electrons in this material follow the Fermi–Dirac distribution function. Calculate the temperature at which there is a 1 percent probability that a state 0.30 eV below the Fermi energy level will not contain an electron.

■ Solution

The probability that a state is empty is

$$1 - f_F(E) = 1 - \frac{1}{1 + \exp\left(\dfrac{E - E_F}{kT}\right)}$$

Then

$$0.01 = 1 - \frac{1}{1 + \exp\left(\dfrac{5.95 - 6.25}{kT}\right)}$$

Solving for kT, we find $kT = 0.06529$ eV, so that the temperature is $T = 756$ K

■ Comment

The Fermi probability function is a strong function of temperature

---

TEST YOUR UNDERSTANDING

E3.6 Repeat Exercise E3.4 for $T = 400$ K. [Ans. (*a*) 1.69×10^{-4}, (*b*) 6.20×10^{-5}]

E3.7 Repeat Exercise E3.5 for $T = 400$ K. [Ans. (*a*) 3.96×10^{-5}, (*b*) 1.46×10^{-5}]

We may note that the probability of a state a distance dE above E_F being occupied is the same as the probability of a state a distance dE below E_F being empty. The function $f_F(E)$ is symmetrical with the function $1 - f_F(E)$ about the Fermi energy, E_F. This symmetry effect is shown in Figure 3.32 and will be used in the next chapter.

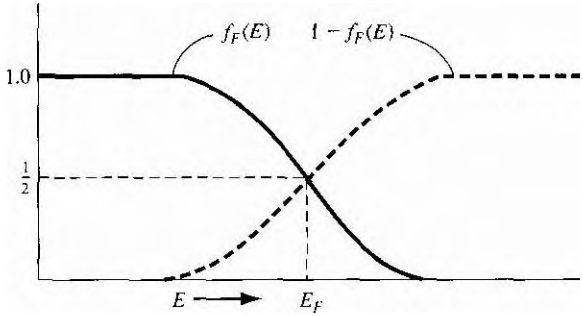

Figure 3.32 | The probability of a state being occupied. $f_F(E)$, and the probability of a state being empty, $1 - f_F(E)$

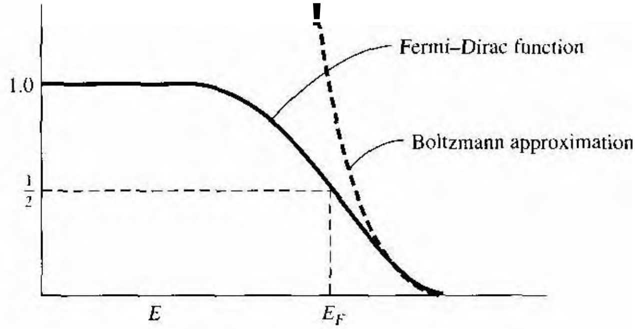

Figure 3.33 | The Fermi–Dirac probability function and the Maxwell–Boltzmann approximation.

Consider the case when $E - E_F \gg kT$, where the exponential term in the denominator of Equation (3.79) is much greater than unity. We may neglect the 1 in the denominator, so the Fermi–Dirac distribution function becomes

$$\boxed{f_F(E) \approx \exp\left[\frac{-(E - E_F)}{kT}\right]} \tag{3.80}$$

Equation (3.80) is known as the Maxwell–Boltzmann approximation, or simply the Boltzmann approximation. to the Fermi–Dirac distribution function. Figure 3.33 shows the Fermi–Dirac probability function and the Boltzmann approximation. This figure gives an indication of the range of energies over which the approximation is valid.

EXAMPLE 3.8

Objective

To determine the energy at which the Boltzmann approximation may be considered valid.

Calculate the energy, in terms of kT and E_F, at which the difference between the Boltzmann approximation and the Fermi–Dirac function is 5 percent of the Fermi function.

Solution

We can write

$$\frac{\exp\left[\dfrac{-(E-E_F)}{kT}\right]-\dfrac{1}{1+\exp\left(\dfrac{E-E_F}{kT}\right)}}{\dfrac{1}{1+\exp\left(\dfrac{E-E_F}{kT}\right)}}=0.05$$

If we multiply both numerator and denominator by the 1 + exp ( ) function, we have

$$\exp\left[\frac{-(E-E_F)}{kT}\right]\left\{1+\exp\left[\frac{E-E_F}{kT}\right]\right\}-1=0.05$$

which becomes

$$\exp\left[\frac{-(E-E_F)}{kT}\right]=0.05$$

$$(E-E_F)=kT\,ln\left(\frac{1}{0.05}\right)\approx 3kT$$

Comment

As seen in this example and in Figure 3.33. the $E - E_F \gg kT$ notation is somewhat misleading. The Maxwell–Boltzmann and Fermi–Dirac functions are within 5 percent of each other when $E - E_F \approx 3kT$.

The actual Boltzmann approximation is valid when $\exp[(E-E_F)/kT] \gg 1$ However, it is still common practice to use the $E - E_F \gg kT$ notation when applying the Boltzmann approximation. We will use this Boltzmann approximation in our discussion of semiconductors in the next chapter.

3.6 | SUMMARY

- Discrete allowed electron energies split into a band of allowed energies as atoms are brought together to form a crystal.
- The concept of allowed and forbidden energy bands was developed more rigorously by considering quantum mechanics and Schrodinger's wave equation using the Kronig–Penney model representing the potential function of a single crystal material. This result forms the basis of the energy band theory of semiconductors.
- The concept of effective mass was developed. Effective mass relates the motion of a particle in a crystal to an externally applied force and takes into account the effect of the crystal lattice on the motion of the particle.
- Two charged particles exist in a semiconductor An electron is a negatively charged panicle with a positive effective mass existing at the bottom of an allowed energy band. A hole is a positively charged particle with a positive effective mass existing at the top of an allowed energy band.

- The E versus k diagram of silicon and gallium arsenide were given and the concept of direct and indirect bandgap semiconductors was discussed.
- Energies within an allowed energy band are actually at discrete levels and each contains a finite number of quantum states. The density per unit energy of quantum states was determined by using the three-dimensional infinite potential well as a model.
- In dealing with large numbers of electrons and holes, we must consider the statistical behavior of these particles. The Fermi–Dirac probability function was developed. which gives the probability of a quantum state at an energy E of being occupied by an electron. The Fermi energy was defined.

GLOSSARY OF IMPORTANT TERMS

allowed energy band A band or range of energy levels that an electron in a crystal is allowed to occupy based on quantum mechanics.

density of states function The density of available quantum states as a function of energy, given in units of number per unit energy per unit volume.

electron effective mass The parameter that relates the acceleration of an electron in the conduction band of a crystal to an external force: a parameter that takes into account the effect of internal forces in the crystal.

Fermi–Dirac probability function The function describing the statistical distribution of electrons among available energy states and the probability that an allowed energy state is occupied by an electron.

fermi energy In the simplest definition, the energy below which all states are filled with electrons and above which all states are empty at $T = 0$ K.

forbidden energy band A band or range of energy levels that an electron in a crystal is not allowed to occupy based on quantum mechanics.

hole The positively charged "particle" associated with an empty state in the top of the valence band.

hole effective mass The parameter that relates the acceleration of a hole in the valence band of a crystal to an applied external force (a positive quantity); a parameter that takes into account the effect of internal forces in a crystal.

k-space diagram The plot of electron energy in a crystal versus k, where k is the momentum-related constant of the motion that incorporates the crystal interaction.

Kronig–Penney model The mathematical model of a periodic potential function representing a one-dimensional single-crystal lattice by a series of periodic step functions.

Maxwell–Boltzmann approximation The condition in which the energy is several kT above the Fermi energy or several kT below the Fermi energy so that the Fermi–Dirac probability function can be approximated by a simple exponential function.

Pauli exclusion principle The principle which states that no two electrons can occupy the same quantum state.

CHECKPOINT

After studying this chapter, the reader should have the ability to:

- Discuss the concept of allowed and forbidden energy bands in a single crystal both qualitatively and more rigorously from the results of using the Kronig–Penney model

- Discuss the splitting of energy bands in silicon.
- State the definition of effective mass from the E versus k diagram and discuss its meaning in terms of the movement of a particle in a crystal.
- Discuss the concept of a hole.
- Qualitatively, in terms of energy hands, discuss the difference between a metal, insulator, and semiconductor
- Discuss the effective density of states function.
- Understand the meaning of the Fermi–Dirac distribution function and the Fenni energy.

REVIEW QUESTIONS

1. What is the Kronig–Penney model'?
2. State two results of using the Kronig–Penney model with Schrodinger's wave equation.
3. What is effective mass?
4. What is a direct bandgap semiconductor? What is an indirect bandgap semiconductor?
5. What is the meaning of the density of states function'!
6. What was the mathematical model used in deriving the density of states function?
7. In general, what is the relation between density of states and energy?
8. What is the meaning of the Fermi–Dirac probability function?
9. What is the Fermi energy?

PROBLEMS

Section 3.1 Allowed and Forbidden Energy Bands

3.1 Consider Figure 3.4b, which shows the energy-band splitting of silicon. If the equilibrium lattice spacing were to change by a small amount. discuss how you would expect the electrical properties of silicon to change. Determine at what point the material would behave like an insulator or like a metal.

3.2 Show that Equations (3.4) and (3.6) are derived from Schrodinger's wave equation. using the form of solution given by Equation (3.3).

3.3 Show that Equations (3.9) and (3.10) are solutions of the differential equations given by Equations (3.4) and (3.8), respectively.

3.4 Show that Equations (3.12), (3.14), (3.16), and (3.18) result from the boundary conditions in the Kronig–Penney model.

3.5 Plot the function $f(\alpha a) = 9\sin\alpha a/\alpha a + $ cosaa for $0 \le \alpha a \le 6\pi$. Also, given the function f(aa) = cosku, indicate the allowed values of αa which will satisfy this equation

3.6 Repeat Problem 3.5 for the function

$$f(\alpha a) = 6\sin\alpha a/\alpha a + \cos\alpha a = \cos ka$$

3.7 Using Equation (3.24), show that $dE/dk = 0$ at $k = n\pi/a$, where $n = 0, 1, 2, \ldots$.

3.8 Using the parameters in Problem 3.5 and letting $a = 5$ A, determine the width (in eV) of the forbidden energy bands that exist at (*a*) $ka = \pi$. **(b)** $ka = 2\pi$, (*c*) $ka = 3\pi$. and (d) $ka = 4$n. Refer to Figure 3.8c.

3.9 Using the parameters in Problem 3.5 and letting $a = 5$ Å, determine the width (in eV) of the allowed energy bands that exist for (*a*) $0 < ka < \pi$, (h) $\pi < ka < 2\pi$, (*c*) $2\pi < ko < 3\pi$, and (*d*) $3\pi < ka < 4\pi$.

3.10 Repeat Problem 3.8 using the parameters in Problem **3.6.**

3.11 Repeat Problem 3.9 using the parameters in Problem **3.6.**

3.12 The bandgap energy in a semiconductor is usually a slight function of temperature In some cases. the bandgap energy versus temperature can be modeled by

$$E_g = E_g(0) - \frac{\alpha T^2}{(\beta + T)}$$

where $E_g(0)$ is the value of the bandgap energy at $T = 0$ K. For silicon. the parameter values are $E_g(0) = 1.170$ eV, $\alpha = 4.73 \times 10^{-4}$ eV/K and $\beta = 636$ K. Plot E_g versus Tover the range $0 \leq T \leq 600$ K. In particular, note the value at $T = 300$ K.

Section 3.2 Electrical Conduction in Solids

3.13 Two possible conduction bands are shown in the *E* ***versus*** k diagram given in Figure 3.34. State which hand will result in the heavier electron effective mass; state why.

3.14 Two possible valence bands are shown in the *E* versus ***k*** diagram given in Figure 3.35. State which band will result in the heavier hole effective mass; state why.

3.15 The E versus ***k*** diagram for a panicular allowed energy band is shown in Figure 3.36. Determine (*a*) the sign of the effective mass and (h) the direction of velocity for a particle at each of the four positions shown.

3.16 Figure 3.37 shows the parabolic *E* versus ***k*** relationship in the conduction band for an electron in two particular semiconductor materials. Determine the effective mass (in units of the free electron mass) of the two electrons.

3.17 Figure 3.38 shows the parabolic *E* versus ***k*** relationship in the valence band for a hole in two particular semiconductor materials. Determine the effective mass (in units of the free electron mass) of the two holes.

3.18 The forbidden energy band of GaAs is 1.42 eV. (*a*) Determine the minimum frequency of an incident photon that can interact with a valence electron and elevate the electron to the conduction band. (b) What is the corresponding wavelength?

3.19 The *E* versus *k* diagrams for a free electron (curve A) and for an electron in a semiconductor (curve B) are shown in Figure 3.39. Sketch (a) dE/dk versus ***k*** and

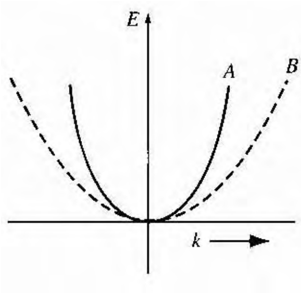

Figure 3.34 | Conduction bands for Problem 3.13.

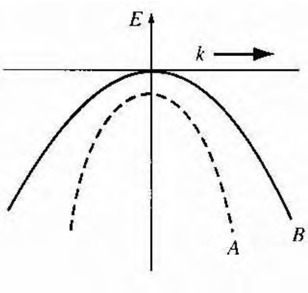

Figure 3.35 | Valence bands for Problem 3.14.

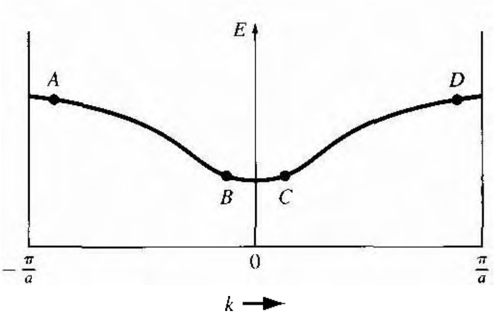

Figure 3.36 | Figure for Problem 3.15

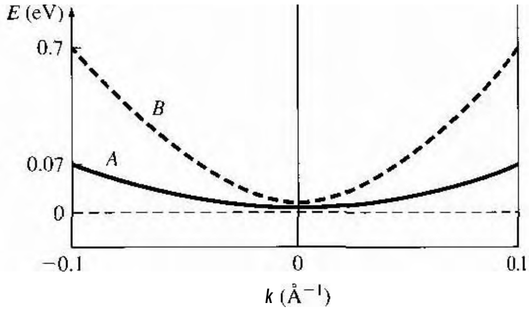

Figure 3.37 | Figure for Problem 3.16.

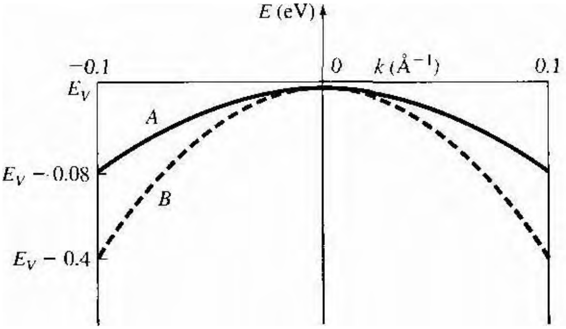

Figure 3.38 | Figure for Problem 3.17.

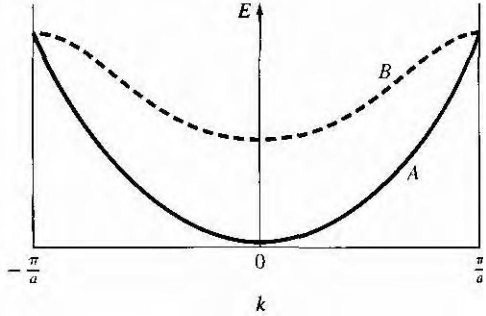

Figure 3.39 | Figure for Problem 3.19.

(b) d^2E/dk^2 versus k for each curve. (c) What conclusion can you make concerning a comparison in effective masses for the two cases?

Section 3.3 Extension to Three Dimensions

3.20 The energy band diagram for silicon is shown in Figure 3.23b. The minimum energy in the conduction band is in the [100] direction. The energy in this one-dimensional direction near the minimum value can be approximated by

$$E = E_0 - E_1 \cos \alpha (k - k_0)$$

where k_0 is the value of k at the minimum energy. Determine the effective mass of the particle at $k = k_0$ in terms of the equation parameters.

Section 3.4 Density of States Function

3.21 Starting with the three-dimensional infinite potential well function given by Equation (3.59) and using the separation of variables technique, derive Equation (3.60).

3.22 Show that Equation (3.69) can be derived from Equation (3.64).

3.23 Determine the total number of energy states in GaAs between E_c and $E_c + kT$ at $T = 300$ K.

3.24 Determine the total number of energy states in GaAs between E_c and $E_t - kT$ at $T = 300$ K.

3.25 (*a*) Plot the density of states in the conduction band for silicon over the range $E_c \leq E \leq E_c + 0.2$ eV. (*b*) Repeat pan (a) for the density of states in the valence band over the range $E_v - 0.2\,\text{eV} \leq \text{E} \leq E,$.

3.26 Find the ratio of the effective density of states in the conduction band at E,. $+ kT$ to theeffective density of states in the valence band at $E_v - kT$.

Section 3.5 Statistical Mechanics

3.27 Plot the Fermi–Dirac probability function, given by Equation (3.79), over the range $-0.2 \leq (E - E_F)$ **I** 0.2 eV for (a) $T = 200$ K, (*b*) $T = 300$ K, and (*c*) T = 400 K.

3.28 Repeat Example 3.4 for the case when g, = 10 and $N_i = 8$.

3.29 **(a)** If E_F = E, , find the probability of a state being occupied at E = $E_c + kT$. (*b*) If $E_F = E_v$, find the probability of a state being empty at E = $E_v - kT$.

3.30 Determine the probability that an energy level is occupied by an electron if the state is above the Fermi level by (*a*) kT, (*b*) $5kT$, and (*c*) $10kT$.

3.31 Determine the probability that an energy level is empty of an electron if the state is below the Fermi level by (*a*)kT, (b) $5kT$, and (*c*)$10kT$.

3.32 The Fermi energy in silicon is 0.25 eV below the conduction band energy E_c. (*a*) Plot the probability of a state being occupied by an electron over the range $E_c \leq$ E 5 $E_t + 2kT$. Assume $T = 300$ K. (*b*) Repeat part (*a*) for T = 400 K.

333 Four electrons exist in a one-dimensional infinite potential well of width a = 10 Å. Assuming the free electron mass, what is the Fermi energy at $T = 0$ K.

334 **(a) Five** electrons exist in a three-dimensional infinite potential well with all three widths equal to $a = 10$ Å. Assuming the free electron mass. what is the Fermi energy at T = 0 K. (*b*) Repeat pan (*a*) for 13 electrons.

3.35 Show that the probability of an energy state being occupied A E above the Fermi energy is the same as the probability of a state being empty A E below the Fermi level.

3.36 **(a)** Determine for what energy above E_F (in terms of kT) the Fermi–Dirac probability function is within I percent of the Boltzmann approximation. (*b*) Give the value of the probability function at this energy.

3.37 The Fermi energy level for a particular material at $T = 300$ K is 6.25 eV. The electrons in this material follow the Fermi–Dirac distribution function. (*a*) Find the probability of an energy level at 6.50 eV being occupied by an electron. (*b*) Repeat pan (a) if the temperature is increased to $T = 950$ K. (Assume that E_F is a constant.) (*c*) Calculate the temperature at which there is a 1 percent probability that a state 0.30 eV below the Fermi level will be empty of an electron.

3.38 The Fermi energy for copper at $T = 300$ K is 7.0 eV. The electrons in copper follow the Fermi–Dirac distribution function. (a) Find the probability of an energy level at 7.15 eV being occupied by an electron. (*b*) Repeat part (*a*) for $T = 1000$ K. (Assume that E_F is a constant.) (c) Repeat part (*a*) for E = 6.85 eV and $T = 300$ K. (*d*) Determine the probability of the energy state at E = E_F being occupied at $T = 300$ K and at T = 1000 K.

3.39 Consider the energy levels shown in Figure 3.40. Let $T = 300$ K. (*a*) If $E_1 - E_F =$ 0.30 eV, determine the probability that an energy state at E = E_1 is occupied by an electron and the probability that an energy state at $E = E_2$ is empty. (*b*) Repeat pan (a) if $E_F - E_2 = 0.40$ eV.

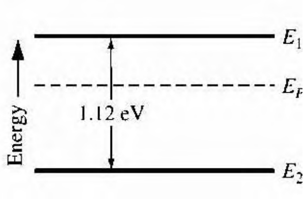

Figure 3.40 | Energy levels for Problem 3.39.

3.40 Repeat problem 3.39 for the case when $E_1 - E_2 = 1.42$ eV.

3.41 Determine the derivative with respect to energy of the Fermi–Dirac distribution function. Plot the derivative with respect to energy for (*a*) $T = 0$ K, (*b*) $T = 300$ K, and (*c*) $T = 500$ K.

3.42 Assume the Fermi energy level is exactly in the center of the bandgap energy of a semiconductor at $T = 300$ K. (*a*) Calculate the probability that an energy state in the bottom of the conduction band is occupied by an electron for Si, Ge. and GaAs. (*b*) Calculate the probability that an energy state in the top of the valence hand is empty for Si, Ge, and GaAs.

3.43 Calculate the temperature at which there is a 10– [illegible] robability that an energy state 0.55 eV above the Fermi energy level is occupied by an electron.

3.44 Calculate the energy range (in eV) between $f_F(E) = 0.95$ and $f_F(E) = 0.05$ for $E_F = 7.0$ eV and for (*a*) $T = 300$ K and (b) $T = 500$ K.

READING LIST

1. Kano, K. *Semiconductor Devices.* Upper Saddle River. NJ: Prentice Hall, 1998.
2. Kittel, C. *Introduction to Solid State Physics,* 7th ed. Berlin: Springer-Verlag, 1993.
3. McKelvey, J. P *Solid State Physics for Engineering and Materials Science.* Malabar, FL.: Krieger, 1993.
4. Pierret, R. F. *Semiconducror Device Fundamentals.* Reading, MA: Addison-Wesley. 1996.

*5. Shockley, W. *Electrons and Holes in Semiconductors.* New York: D. Van Nostrand, 1950.

6. Shur, M. *Introduction to Electronic Devices.* New York: John Wiley and Sons, 1996.

*7. Shur, M. *Physics of Semiconductor Devices.* Englewood Cliffs. NJ: Prentice Hall, 1990.

8. Singh, J. *Semiconductor Devices: An Introduction.* New York: McGraw-Hill, 1994.
9. Singh, J. *Semiconductor Devices: Basic Principles.* New York: John Wiley and Sons, 2001.
10. Streetman, B. G., and S. Banerjee. *Solid State Electronic Devices,* 5th ed. Upper Saddle River, NJ: Prentice-Hall, 2000.
11. Sze, S. M. *Semiconductor Devices: Physics and Technology,* 2nd ed. New York: John Wiley and Sons, 2001

*12. Wang, S. *Fundamentals of Semiconductor Theory and Device Physics.* Englewood Cliffs, NJ: Prentice Hall, 1988.

CHAPTER 4

The Semiconductor in Equilibrium

PREVIEW

So far, we have been considering a general crystal and applying to it the concepts of quantum mechanics in order to determine a few of the characteristics of electrons in a single-crystal lattice. In this chapter, we will apply these concepts specifically to a semiconductor material. In particular, we will use the density of quantum states in the conduction band and the density of quantum states in the valence band along with the Fermi–Dirac probability function to determine the concentration of electrons and holes in the conduction and valence bands, respectively. We will also apply the concept of the Fermi energy to the semiconductor material.

This chapter deals with the semiconductor in equilibrium. Equilibrium, or thermal equilibrium, implies that no external forces such as voltages, electric fields. magnetic fields, or temperature gradients are acting on the semiconductor. All properties of the semiconductor will be independent of time in this case. Equilibrium is our starting point for developing the physics of the semiconductor. We will then be able to determine the characteristics that result when deviations from equilibrium occur, such as when a voltage is applied to a semiconductor device.

We will initially consider the properties of an intrinsic semiconductor, that is, a pure crystal with no impurity atoms or defects. We will see that the electrical properties of a semiconductor can be altered in desirable ways by adding controlled amounts of specific impurity atoms. called *dopant atoms,* to the crystal. Depending upon the type of dopant atom added, the dominant charge carrier in the semiconductor will be either electrons in the conduction band or holes in the valence band. Adding dopant atoms changes the distribution of electrons among the available energy states, so the Fermi energy becomes a function of the type and concentration of impurity atoms.

Finally, as part of this discussion, we will attempt to add more insight into the significance of the Fermi energy. ■

4.1 | CHARGE CARRIERS IN SEMICONDUCTORS

Current is the rate at which charge flows. In a semiconductor. two types of charge carrier, the electron and the hole, can contribute to a current. Since the current in a semiconductor is determined largely by the number of electrons in the conduction band and the number of holes in the valence hand, an important characteristic of the semiconductor is the density of these charge carriers. The density of electrons and holes is related to the density of states function and the Fermi distribution function, both of which we have considered. Aqualitative discussion of these relationships will be followed by a more rigorous mathematical derivation of the thermal-equilibrium concentration of electrons and holes.

4.1.1 Equilibrium Distribution of Electrons and Holes

The distribution (with respect to energy) of electrons in the conduction band is given by the density of allowed quantum states times the probability that a state is occupied by an electron. This statement is written in equation form as

$$n(E) = g_c(E) f_F(E) \tag{4.1}$$

where $f_F(E)$ is the Fermi–Dirac probability function and $g_c(E)$ is the density of quantum states in the conduction band. The total electron concentration per unit volume in the conduction band is then found by integrating Equation (4.1) over the entire conduction-band energy.

Similarly, the distribution (with respect to energy) of holes in the valence bend is the density of allowed quantum states in the valence hand multiplied by the probability that a state is nor occupied by an electron. We may express this as

$$p(E) = g_v(E)[1 - f_F(E)] \tag{4.2}$$

The total hole concentration per unit volume is found by integrating this function over the entire valcncc-band energy.

To find the thermal-equilibrium electron and hole concentrations, we need to determine the position of the Fermi energy E_F with respect to the bottom of the conduction-band energy E_c and the top of the valence-band energy E_v. To address this question, we will initially consider an intrinsic semiconductor. An ideal intrinsic semiconductor is a pure semiconductor with no impurity atoms and no lattice defects in the crystal (e.g., pure silicon). We have argued in the previous chapter that, for an intrinsic semiconductor at T = 0 K, all energy states in the valence band are filled with electrons and all energy states in the conduction band are empty of electrons. The Fermi energy must, therefore, be somewhere between E_c and E,.. (The Fermi energy does not need to correspond to an allowed energy.)

As the temperature begins to increase above 0 K, the valence electrons will gain thermal energy. A few electrons in the valence band may gain sufficient energy to jump to the conduction band. As an electron jumps from the valence band to the conduction band, an empty state, or hole, is created in the valence band. In an intrinsic semiconductor, then, electrons and holes are created in pairs by the thermal energy so

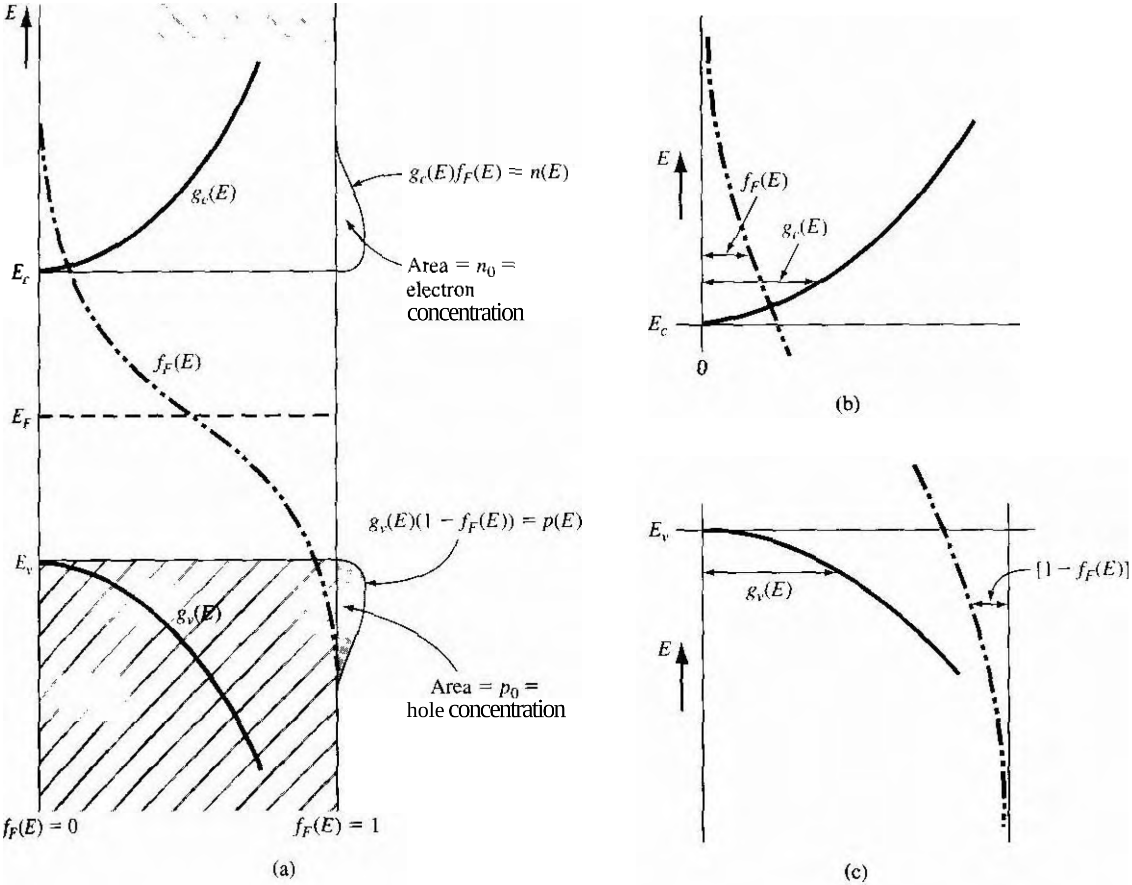
E
E_c
$g_c(E)$
$g_c(E)f_F(E) = n(E)$
Area = n_0 = electron concentration
$f_F(E)$
E_F
$g_v(E)(1 - f_F(E)) = p(E)$
E_v
$g_v(E)$
Area = p_0 = hole concentration
$f_F(E) = 0$
$f_F(E) = 1$
(a)
E
$f_F(E)$
$g_c(E)$
E_c
0
(b)
E_v
$[1 - f_F(E)]$
$g_v(E)$
E
(c)

Figure 4.1 | (a) Density of states functions, Fermi–Dirac probability function, and areas representing electron and hole concentrations for the case when E_F is near the midgap energy; (b) expanded view near the conduction band energy; and (c) expanded view near the valence band energy.

that the number of electrons in the conduction band is equal to the number of holes in the valence band.

Figure 4.1a shows a plot of the density of states function in the conduction band $g_c(E)$, the density of states function in the valence band $g_v(E)$, and the Fermi–Dirac probability function for $T > 0$ K when E_F is approximately halfway between E_c and E_v. If we assume, for the moment, that the electron and hole effective masses are *equal,* then $g_c(E)$ and $g_v(E)$ are symmetrical functions about the midgap energy (the energy midway between E_c and E_v). We noted previously that the function $f_F(E)$ for $E > E_F$ is symmetrical to the function $1 - f_F(E)$ for $E < E_F$ about the energy $E = E_F$. This also means that the function $f_F(E)$ for $E = E_F + dE$ is equal to the function $1 - f_F(E)$ for $E = E_F - dE$.

Figure 4.1b is an expanded view of the plot in Figure 4.1a showing $f_F(E)$ and $g_c(E)$ above the conduction band energy E_c. The product of $g_c(E)$ and $f_F(E)$ is the distribution of electrons $n(E)$ in the conduction band given by Equation (4.1). This product is plotted in Figure 4.1a. Figure 4.1c is an expanded view of the plot in Figure 4.1a showing $[1 - f_F(E)]$ and $g_v(E)$ below the valence band energy E_v. The product of $g_v(E)$ and $[1 - f_F(E)]$ is the distribution of holes $p(E)$ in the valence band given by Equation (4.2). This product is also plotted in Figure 4.1a. The area under these curves are then the total density of electrons in the conduction band and the total density of holes in the valence band. From this we see that if $g_c(E)$ and $g_v(E)$ are symmetrical, the Fermi energy must be at the midgap energy in order to obtain equal electron and hole concentrations. If the effective masses of the electron and hole are not exactly equal, then the effective density of states functions $g_c(E)$ and $g_v(E)$ will not be exactly symmetrical about the midgap energy. The Fermi level for the intrinsic semiconductor will then shift slightly from the midgap energy in order to obtain equal electron and hole concentrations.

4.1.2 The n_0 and p_0 Equations

We have argued that the Fermi energy for an intrinsic semiconductor is near midgap In deriving the equations for the thermal-equilibrium concentration of electrons n_0 and the thermal-equilibrium concentration of holes p_0, we will not be quite so restrictive. We will see later that, in particular situations, the Fermi energy can deviate from this midgap energy. We will assume initially, however, that the Fermi level remains within the bandgap energy.

The equation for the thermal-equilibrium concentration of electrons may be found by integrating Equation (4.1) over the conduction band energy, or

$$n_0 = \int g_c(E) f_F(E)\, dE \tag{4.3}$$

The lower limit of integration is E_c and the upper limit of integration should be the top of the allowed conduction band energy. However, since the Fermi probability function rapidly approaches zero with increasing energy as indicated in Figure 4.1a we can take the upper limit of integration to be infinity.

We are assuming that the Fermi energy is within the forbidden-energy bandgap For electrons in the conduction band, we have $E > E_c$. If $(E_c - E_F) \gg kT$, then $(E - E_F) \gg kT$, so that the Fermi probability function reduces to the Boltzmann approximation,[1] which is

$$f_F(E) = \frac{1}{1 + \exp\dfrac{(E - E_F)}{kT}} \approx \exp\frac{[-(E - E_F)]}{kT} \tag{4.4}$$

---

[1] The Maxwell–Boltzmann and Fermi–Dirac distribution functions are within 5 percent of each other when $E - E_F \approx 3kT$ (see Figure 3.33). The $\gg$ notation is then somewhat misleading to indicate when the Boltzmann approximation is valid, although it is commonly used.

Applying the Boltzmann approximation to Equation (4.3), the thermal-equilibrium density of electrons in the conduction band is found from

$$n_0 = \int_{E_c}^{\infty} \frac{4\pi(2m_n^*)^{3/2}}{h^3} \quad E - E_c \exp\left[\frac{-(E-E_F)}{kT}\right] dE \tag{4.5}$$

The integral of Equation *(4.5)* may be solved more easily by making a change of variable. If we let

$$\eta = \frac{E - E_c}{kT} \tag{4.6}$$

then Equation *(4.5)* becomes

$$n_0 = \frac{4\pi(2m_n^*kT)^{3/2}}{h^3} \exp\left[\frac{-(E_c - E_F)}{kT}\right] \int_0^{\infty} \eta^{1/2} \exp(-\eta)\, d\eta \tag{4.7}$$

The integral is the gamma function, with a value of

$$\int_0^{\infty} \eta^{1/2} \exp(-\eta)\, d\eta = \frac{1}{2}\sqrt{\pi} \tag{4.8}$$

Then Equation *(4.7)* becomes

$$n_0 = 2\left(\frac{2\pi m_n^* kT}{h^2}\right)^{3/2} \exp\left[\frac{-(E_c - E_F)}{kT}\right] \tag{4.9}$$

We may define a parameter N_c as

$$N_c = 2\left(\frac{2\pi m_n^* kT}{h^2}\right)^{3/2} \tag{4.10}$$

so that the thermal-equilibrium electron concentration in the conduction band can be written as

$$\boxed{n_0 = N_c \exp\left[\frac{-(E_c - E_F)}{kT}\right]} \tag{4.11}$$

The parameter N_c is called the *effective density of states function in the conduction band*. If we were to assume that $m_n^* = m_0$, then the value of the effective density of states function at T = 300 K is $N_c = 2.5 \times 10^{19}$ cm^{-3}, which is the order of magnitude of N_c for most semiconductors. If the effective mass of the electron is larger or smaller than m_0, then the value of the effective density of states function changes accordingly, but is still of the same order of magnitude.

EXAMPLE 4.1

Objective

Calculate the probability that a state in the conduction band is occupied by an electron and calculate the thermal equilibrium electron concentration in silicon at $T = 100$ K.

Assume the Fermi energy is 0.25 eV below the conduction band. The value of N_c for silicon at T = 100 K is $N_c = 2.8 \times 10^{19}$ cm^{-3}.

■ Solution

The probability that an energy state at $E = E_c$ is occupied by an electron is given by

$$f_F(E_c) = \frac{1}{1 + \exp\left(\frac{E_c - E_F}{kT}\right)} \approx \exp\left[\frac{-(E_c - E_F)}{kT}\right]$$

or

$$f_F(E_c) = \exp\left(\frac{-0.25}{0.0259}\right) = 6.43 \times 10^{-5}$$

The electron concentration is given by

$$n_0 = N_c \exp\left[\frac{-(E_c -}{kT}\right] = (2.8 \times 10^{19}) \exp\left(\frac{-0.25}{0.0259}\right)$$

or

$$n_0 = 1.8 \times 10^{15}\ \text{cm}^{-3}$$

■ Comment

The probability of a state being occupied can be quite small, but the fact that there are a larg number of states means that the electron concentration is a reasonable value.

The thermal-equilibrium concentration of holes in the valence band is found b integrating Equation (4.2) over the valence band energy, or

$$p_0 = \int g_v(E)[1 - f_F(E)]\, dE \qquad (4.12$$

We may note that

$$1 - f_F(E) = \frac{1}{1 + \exp\left(\frac{E_F - E}{kT}\right)} \qquad (4.13a)$$

For energy states in the valence band, $E < E_v$. If $(E_F - E_v) \gg kT$ (the Fermi function is still assumed to be within the bandgap), then we have a slightly different form of the Boltzmann approximation. Equation (4.13a) may be written as

$$1 - f_F(E) = \frac{1}{1 + \exp\left(\frac{E_F - E}{kT}\right)} \approx \exp\left[\frac{-(E_F - E)}{kT}\right] \qquad (4.13b$$

Applying the Boltzmann approximation of Equation (4.13b) to Equation (4.12), we find the thermal-equilibrium concentration of holes in the valence band is

$$p_0 = \int_{-\infty}^{E_v} \frac{4\pi(2m_p^*)^{3/2}}{h^3} \sqrt{E_v - E}\, \exp\left[\frac{-(E_F - E)}{kT}\right] dE \qquad (4.14)$$

where the lower limit of integration is taken as minus infinity instead of the bottom of the valence band. The exponential term decays fast enough so that this approximation is valid.

Equation (4.14) may be solved more easily by again making a change of variable. If we let

$$\eta' = \frac{E_v - E}{kT} \tag{4.15}$$

then Equation (4.14) becomes

$$p_0 = \frac{-4\pi(2m_p^*kT)^{3/2}}{h^3}\exp\left[\frac{-(E_F - E_v)}{kT}\right]\int_{+\infty}^{0}(\eta')^{1/2}\exp(-\eta')\,d\eta' \tag{4.16}$$

where the negative sign comes from the differential $dE = -kT\,d\eta'$. Note that the lower limit of η' becomes $+\infty$ when $E = -\infty$. If we change the order of integration, we introduce another minus sign. From Equation (4.8). Equation (4.16) becomes

$$p_0 = 2\left(\frac{2\pi m_p^*kT}{h^2}\right)^{3/2}\exp\left[\frac{-(E_F - E_v)}{kT}\right] \tag{4.17}$$

We may define a parameter N_v as

$$N_v = 2\left(\frac{2\pi m_p^*kT}{h^2}\right)^{3/2} \tag{4.18}$$

which is called the *effective density of states function in the valence band*. The thermal-equilibrium concentration of holes in the valence band may now be written as

$$\boxed{p_0 = N_v \exp\left[\frac{-(E_F - E_v)}{kT}\right]} \tag{4.19}$$

The magnitude of N_v is also on the order of 10^{19} cm^{-3} at T = 300 K for most semiconductors.

Objective **EXAMPLE 4.2**

Calculate the thermal equilibrium hole concentration in silicon at T = 400 K.

Assume that the Fermi energy is 0.27 eV above the valence band energy. The value of N_v for silicon at T = 300 K is $N_v = 1.04 \times 10^{19}$ cm^{-3}.

■ Solution

The parameter values at T = 400 K are found as:

$$N_v = (1.04 \times 10^{19})\left(\frac{400}{300}\right)^{3/2} = 1.60 \times 10^{19}\,\text{cm}^{-3}$$

$$kT = (0.0259)\left(\frac{400}{300}\right) = 0.03453\ \text{eV}$$

The hole concentration is then

$$p_0 = N_v \exp\left[\frac{-(E_F - E_v)}{kT}\right] = (1.60 \times 10^{19}) \exp\left(\frac{-0.27}{0.03453}\right)$$

or

$$p_0 = 6.43 \times 10^{15} \text{ cm}^{-3}$$

■ **Comment**

The parameter values at any temperature can easily be found by using the 300 K values and the temperature dependence.

The effective density of states functions, N_c and N_v, are constant for a given semiconductor material at a fixed temperature. Table 4.1 gives the values of the density of states function and of the effective masses for silicon, gallium arsenide, and germanium. Note that the value of N_c for gallium arsenide is smaller than the typical 10^{19} cm^{-3} value. This difference is due to the small electron effective mass in gallium arsenide.

The thermal equilibrium concentrations of electrons in the conduction band and of holes in the valence band are directly related to the effective density of states constants and to the Fermi energy level,

TEST YOUR UNDERSTANDING

E4.1 Calculate the thermal equilibrium electron and hole concentration in silicon at T = 300 K for the case when the Fermi energy level is 0.22 eV below the conduction band energy E_c. The value of E_g is given in Appendix B.4.
(Ans. $n_0 = 5.73 \times 10^{15}$ cm^{-3}, $p_0 = 8.43 \times 10^{3}$ cm^{-3})

E4.2 Determine the thermal equilibrium electron and hole concentration in GaAs at T = 300 K for the case when the Fermi energy level is 0.30 eV above the valence band energy E_v. The value of E_g is given in Appendix B.4.
(Ans. $n_0 = 0.0779$ cm^{-3}, $p_0 = 6.53 \times 10^{13}$ cm^{-3})

4.1.3 The Intrinsic Carrier Concentration

For an intrinsic semiconductor, the concentration of electrons in the conduction band is equal to the concentration of holes in the valence band. We may denote n_i and p_i

Table 4.1 | Effective density of states function and effective mass values

	N_c (cm^{-3})	N_v (cm^{-3})	m_n^*/m_0	m_p^*/m_0
Silicon	2.8×10^{19}	1.04×10^{19}	1.08	0.56
Gallium arsenide	4.7×10^{17}	7.0×10^{18}	0.067	0.48
Germanium	1.04×10^{19}	6.0×10^{18}	0.55	0.37

as the electron and hole concentrations, respectively, in the intrinsic semiconductor. These parameters are usually referred to as the intrinsic electron concentration and intrinsic hole concentration. However, $n_i = p_i$, so normally we simply use the parameter n_i as the intrinsic carrier concentration, which refers to either the intrinsic electron or hole concentration.

The Fermi energy level for the intrinsic semiconductor is called the intrinsic Fermi energy, or $E_F = E_{Fi}$. If we apply Equations (4.11) and (4.19) to the intrinsic semiconductor, then we can write

$$n_0 = n_i = N_c \exp\left[\frac{-(E_c - E_{Fi})}{kT}\right] \tag{4.20}$$

$$p_0 = p_i = n_i = N_v \exp\left[\frac{-(E_{Fi} - E_v)}{kT}\right] \tag{4.21}$$

If we take the product of Equation.; (4.20) and (4.21). we obtain

$$n_i^2 = N_c N_v \exp\left[\frac{-(E_c - E_{Fi})}{kT}\right] \cdot \exp\left[\frac{-(E_{Fi} - E_v)}{kT}\right] \tag{4.22}$$

$$\boxed{n_i^2 = N_c N_v \exp\left[\frac{-(E_c - E_v)}{kT}\right] = N_c N_v \exp\left[\frac{-E_g}{kT}\right]} \tag{4.23}$$

where E_g is the bandgap energy. For a given semiconductor material at a constant temperature, the value of n, is a constant, and independent of the Fermi energy.

The intrinsic carrier concentration for silicon at T = 300 K may be calculated by using the effective density of states function values from Table 4.1. The value of n_i calculated from Equation (4.23) for $E_g = 1.12$ eV is $n_i = 6.95 \times 10^9$ cm^{-3}. The commonly accepted value' of n_i for silicon at T = 300 K is approximately 1.5×10^{10} cm^{-3}. This discrepancy may arise from several sources. First, the values of the effective masses are determined at a low temperature where the cyclotron resonance experiments are performed. Since the effective mass is an experimentally determined parameter, and since the effective mass is a measure of how well a particle moves in a crystal, this parameter may be a slight function of temperature. Next, the density of states function for a semiconductor was obtained by generalizing the model of an electron in a three-dimensional infinite potential well. This theoretical function may also not agree exactly with experiment. However, the difference between the theoretical value and the experimental value of *n,* is approximately a factor

---

[2] Various references may list slightly different values of the intrinsic silicon concentration at room temperature. In general, they are all between 1 × 10^{10} and 1.5 × 10^{10} cm^{-3}. This difference is, in most carer, not significant.

Table 4.2 | Commonly accepted values of n_i at $T = 300$ K

Silicon	$n_i = 1.5 \times 10^{10}\ \text{cm}^{-3}$
Gallium arsenide	$n_i = 1.8 \times 10^{6}\ \text{cm}^{-3}$
Germanium	$n_i = 2.4 \times 10^{13}\ \text{cm}^{-3}$

of 2, which, in many cases, is not significant. Table 4.2 lists the commonly accepted values of n_i for silicon, gallium arsenide, and germanium at $T = 300$ K.

The intrinsic carrier concentration is a very strong function ot temperature.

EXAMPLE 4.3

Objective

To calculate the intrinsic carrier concentration in gallium arsenide at $T = 300$ K and at $T = 450$ K.

The values of N_c and N_v at 300 K for gallium arsenide are $4.7 \times 10^{17}\ \text{cm}^{-3}$ and $7.0 \times 10^{18}\ \text{cm}^{-3}$, respectively. Both N_c and N_v vary as $T^{3/2}$. Assume the bandgap energy of gallium arsenide is 1.42 eV and does not vary with temperature over this range. The value of kT at 450 K is

$$kT = (0.0259)\left(\frac{450}{300}\right) = 0.03885\ \text{eV}$$

Solution

Using Equation (4.23). we find for $T = 300$ K

$$n_i^2 = (4.7 \times 10^{17})(7.0 \times 10^{18})\exp\left(\frac{-1.42}{0.0259}\right) = 5.09 \times 10^{12}$$

so that

$$n_i = 2.26 \times 10^{6}\ \text{cm}^{-3}$$

At $T = 450$ K, we find

$$n_i^2 = (4.7 \times 10^{17})(7.0 \times 10^{18})\left(\frac{450}{300}\right)^3 \exp\left(\frac{-1.42}{0.03885}\right) = 1.48 \times 10^{21}$$

so that

$$n_i = 3.85 \times 10^{10}\ \text{cm}^{-3}$$

Comment

We may note from this example that the intrinsic carrier concentration increased by over 4 orders of magnitude as the temperature increased by 150°C.

Figure 4.2 is a plot of n_i from Equation (4.23) for silicon, gallium arsenide, and germanium as a function of temperature. As seen in the figure, the value of n_i for these semiconductors may easily vary over several orders of magnitude as the temperature changes over a reasonable range.

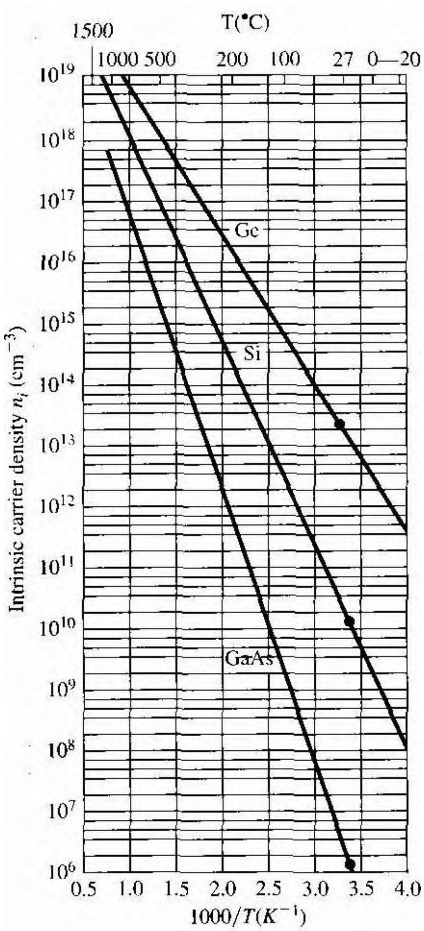

Figure 4.2 | The intrinsic carrier concentration of Ce, Si, and GaAs as a function of temperature.
(From Sze [13].)

TEST YOUR UNDERSTANDING

E4.3 Find the intrinsic carrier concentration in silicon at (*a*) $T = 200$ K and (*b*) $T = 400$ K. [Ans. (*a*) 7.68×10^{4} cm^{-3}, (*b*) 2.38×10^{12} cm^{-3}]

E4.4 Repeat **E4.3** for GaAs. [Ans. (*a*) 1.38 cm^{-3}, (*b*) 3.28×10^{9} cm^{-3}]

E4.5 Repeat **E4.3** for Ge. [Ans. (*a*) 2.16×10^{10} cm^{-3}, (*b*) 8.6×10^{14} cm^{-3}]

4.1.4 The Intrinsic Fermi-Level Position

We have qualitatively argued that the Fermi energy level is located near the center of the forbidden bandgap for the intrinsic semiconductor. We can specifically calculate the intrinsic Fermi-level position. Since the electron and hole concentrations are equal, setting Equations (4.20) and (4.21) equal to each other, we have

$$N_c \exp\left[\frac{-(E_c - E_{Fi})}{kT}\right] = N_v \exp\left[\frac{-(E_{Fi} - E_v)}{kT}\right] \tag{4.24}$$

If we take the natural log of both sides of this equation and solve for E_{Fi}, we obtain

$$E_{Fi} = \frac{1}{2}(E_c + E_v) + \frac{1}{2} kT \ln\left(\frac{N_v}{N_c}\right) \tag{4.25}$$

From the definitions for N_c and N_v given by Equations (4.10) and (4.18), respectively, Equation (4.25) may be written as

$$E_{Fi} = \frac{1}{2}(E_c + E_v) + \frac{3}{4} kT \ln\left(\frac{m_p^*}{m_n^*}\right) \tag{4.26a}$$

The first term, $\frac{1}{2}(E_c + E_v)$, is the energy exactly midway between E_c and E_v, or the midgap energy. We can define

$$\frac{1}{2}(E_c + E_v) = E_{\text{midgap}}$$

so that

$$\boxed{E_{Fi} - E_{\text{midgap}} = \frac{3}{4} kT \ln\left(\frac{m_p^*}{m_n^*}\right)} \tag{4.26b}$$

If the electron and hole effective masses are equal so that $m_p^* = m_n^*$, then the intrinsic Fermi level is exactly in the center of the bandgap. If $m_p^* > m_n^*$, the intrinsic Fermi level is slightly above the center, and if $m_p^* < m_n^*$, it is slightly below the center of the bandgap. The density of states function is directly related to the carrier effective mass: thus a larger effective mass means a larger density of states function. The intrinsic Fermi level must shift away from the band with the larger density of states in order to maintain equal numbers of electrons and holes.

EXAMPLE 4.4

Objective

To calculate the position of the intrinsic Fermi level with respect to the center of the bandgap in silicon at $T = 300$ K.

The density of states effective carrier masses in silicon are $m_n^* = 1.08m_0$ and $m_p^* = 0.56m_0$.

■ Solution

The intrinsic Fermi level with respect to the center of the bandgap is

$$E_{Fi} - E_{\text{midgap}} = \frac{3}{4} kT \ln\left(\frac{m_p^*}{m_n^*}\right) = \frac{3}{4}(0.0259) \ln\left(\frac{0.56}{1.08}\right)$$

or

$$E_{Fi} - E_{\text{midgap}} = -0.0128 \text{ eV} = -12.8 \text{ meV}$$

■ Comment

The intrinsic Fermi level in silicon is 12.8 meV below the midgap energy. If we compare 12.8 meV to 560 meV, which is one-half of the bandgap energy of silicon, we can, in many applications, simply approximate the intrinsic Fermi level to be in the center of the bandgap.

TEST YOUR UNDERSTANDING

E4.6 Determine the position of the intrinsic Fermi level with respect to the center of the bandgap in GaAs at T = 300 K. (Ans. −38.2 meV)

4.2 | DOPANT ATOMS AND ENERGY LEVELS

The intrinsic semiconductor may be an interesting material, but the real power of semiconductors is realized by adding small, controlled amounts of specific dopant, or impurity, atoms. This doping process, described briefly in Chapter I, can greatly alter the electrical characteristics of the semiconductor. The doped semiconductor, called an ***extrinsic*** material, is the primary reason we can fabricate the various semiconductor devices that we will consider in later chapters.

4.2.1 Qualitative Description

In Chapter **3,** we discussed the covalent bonding of silicon and considered the simple two-dimensional representation of the single-crystal silicon lattice as shown in Figure 4.3. Now consider adding a group V element, such as phosphorus, as a substitutional impurity. The group V element has five valence electrons. Four of these will contribute to the covalent bonding with the silicon atoms, leaving the fifth more loosely hound to the phosphorus atom. This effect is schematically shown in Figure 4.4. We refer to the fifth valence electron as a donor electron.

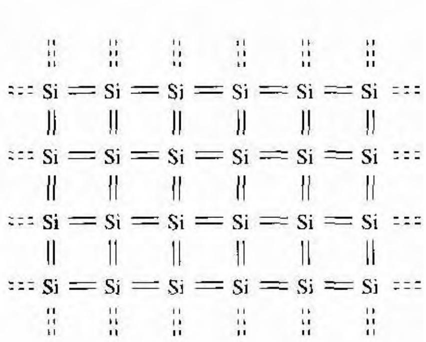

Figure 4.3 | Two-dimensional representation of the intrinsic silicon lattice.

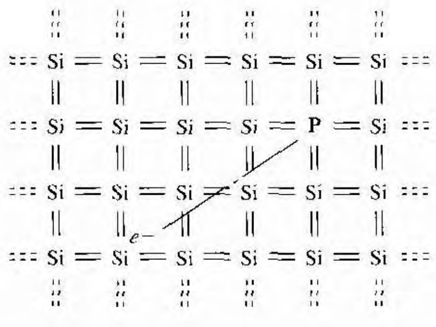

Figure 4.4 | Two-dirnsnsional representation of the silicon lattice doped with a phosphorus atom.

The phosphorus atom without the donor electron is positively charged. At very low temperatures, the donor electron is bound to the phosphorus atom. However, by intuition, it should seem clear that the energy required to elevate the donor electron into the conduction band is considerably less than that for the electrons involved in the covalent bonding. Figure 4.5 shows the energy-hand diagram that we would expect. The energy level, E_d, is the energy state of the donor electron.

If a small amount of energy, such as thermal energy, is added to the donor electron, it can be elevated into the conduction band, leaving behind a positively charged phosphorus ion. The electron in the conduction band can now move through the crystal generating a current, while the positively charged ion is fixed in the crystal. This type of impurity atom donates an electron to the conduction band and so is called a ***donor** impurity atom.* The donor impurity atoms add electrons to the conduction band without creating holes in the valence band. The resulting material is referred to as an *n-type* semiconductor (*n* for the negatively charged electron).

Now consider adding a group III element, such as boron, as a substitutional impurity to silicon. The group III element has three valence electrons, which are all taken up in the covalent bonding. As shown in Figure 4.6a, one covalent bonding position appears to he empty. If an electron were to occupy this "empty" position, its

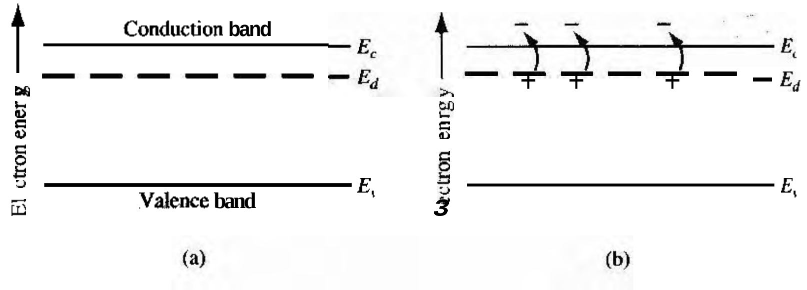

Figure 4.5 | The energy-hand diagram showing (a) the discrete donor energy state and (b) the effect of a donor state being ionized.

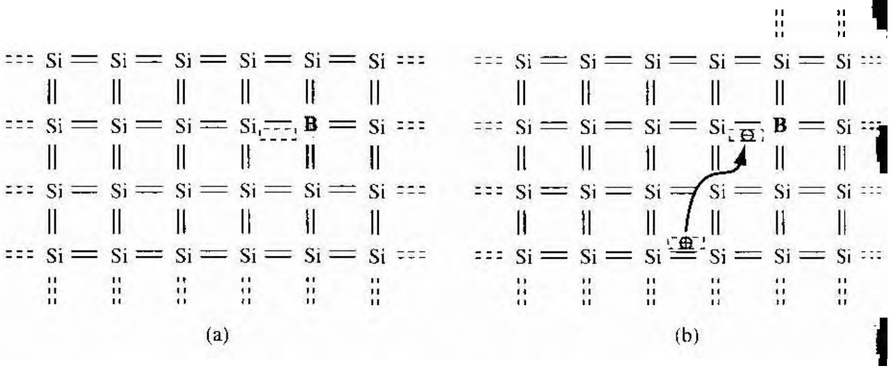

Figure 4.6 | Two-dimensional representation of a silicon lattice (a) doped with a boron atom and (b) showing the ionization of the boron atom resulting in a hole.

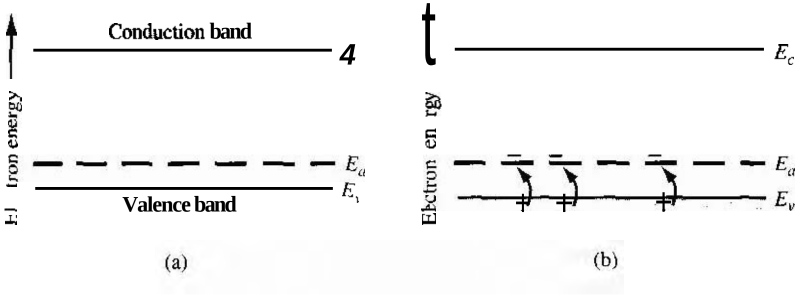

Figure 4.7 | The energy-band diagram showing (a) the discrete acceptor energy state and (b) the effect of an acceptor state being ionized.

energy would have to be greater than that of the valence electrons, since the net charge state of the boron atom would now be negative. However, the electron occupying this "empty" position does not have sufficient energy to be in the conduction band, so its energy is far smaller than the conduction-band energy. Figure 4.6b shows how valence electrons may gain a small amount of thermal energy and move about in the crystal. The "empty" position associated with the boron atom becomes occupied, and other valence electron positions become vacated. These other vacated electron positions can be thought of as holes in the semiconductor material.

Figure 4.7 shows the expected energy state of the "empty" position and also the formation of a hole in the valence band. The hole can move through the crystal generating a current, while the negatively charged boron atom is fixed in the crystal. The group III atom accepts an electron from the valence band and so is referred to as an *acceptor impurity atom*. The acceptor atom can generate holes in the valence band without generating electrons in the conduction band. This type of semiconductor material is referred to as a *p-type* material (p for the positively charged hole).

The pure single-crystal semiconductor material is called an intrinsic material. Adding controlled amounts of dopant atoms, either donors or acceptors, creates a material called an *extrinsic semiconductor*. An extrinsic semiconductor will have either a preponderance of electrons (n type) or a preponderance of holes (p type).

42.2 Ionization Energy

We can calculate the approximate distance of the donor electron from the donor impurity ion, and also the approximate energy required to elevate the donor electron into the conduction band. This energy is referred to as the ionization energy. We will use the Bohr model of the atom for these calculations. The justification for using this model is that the most probable distance of an electron from the nucleus in a hydrogen atom, determined from quantum mechanics, is the same as the Bohr radius. The energy levels in the hydrogen atom determined from quantum mechanics are also the same as obtained from the Bohr theory.

In the case of the donor impurity atom, we may visualize the donor electron orbiting the donor ion, which is embedded in the semiconductor material. We will need to use the permittivity of the semiconductor material in the calculations rather than

the permittivity of free space as is used in the case of the hydrogen atom. We will al
use the effective mass of the electron in the calculations.

The analysis begins by setting the coulomb force of attraction between the ele
tron and ion equal to the centripetal force of the orbiting electron. This condition w
give a steady orbit. We have

$$\frac{e^2}{4\pi\epsilon r_n^2} = \frac{m^* v^2}{r,,}$$

where v is the magnitude of the velocity and r_n is the radius of the orbit. If we assu
the angular momentum is also quantized, then we can write

$$m^* r_n v = n\hbar \qquad \text{(4.2}$$

where n is a positive integer. Solving for v from Equation (4.28), substituting in
Equation (4.27), and solving for the radius, we obtain

$$r_n = \frac{n^2\hbar^2 4\pi\epsilon}{m^* e^2}$$

The assumption of the angular momentum being quantized leads to the radius al
being quantized.

The Bohr radius is defined as

$$a_0 = \frac{4\pi\epsilon_0\hbar^2}{m_0 e^2} = 0.53\ \text{Å}$$

We can normalize the radius of the donor orbital to that of the Bohr radius, which giv

$$\frac{r_n}{a_0} = n^2\epsilon_r\left(\frac{m_0}{m^*}\right)$$

where ϵ_r is the relative dielectric constant of the semiconductor material, m_0 is I
rest mass of an electron, and m^* is the conductivity effective mass of the electron
the semiconductor.

If we consider the lowest energy state in which n = 1, and if we consider silic
in which $\epsilon_r = 11.7$ and the conductivity effective mass is $m^*/m_0 = 0.26$. then'
have that

$$\frac{r_1}{a_0} = 45$$

or $r_1 = 23.9$ ~This radius corresponds to approximately four lattice constants
silicon. Recall that one unit cell in silicon effectively contains eight atoms, so the
dius of the orbiting donor electron encompasses many silicon atoms. The donor ele
tron is not tightly bound to the donor atom.

The total energy of the orbiting electron is given by

$$E = T + V \qquad \text{(4.3}$$

where T is the kinetic energy and V is the potential energy of the electron. The kinetic energy is

$$T = \frac{1}{2}m^*v^2 \tag{4.34}$$

Using the velocity v from Equation (4.28) and the radius r,, from Equation (4.29), the kinetic energy becomes

$$T = \frac{m^*e^4}{2(n\hbar)^2(4\pi\epsilon)^2} \tag{4.35}$$

The potential energy is

$$V = \frac{-e^2}{4\pi\epsilon r_n} = \frac{-m^*e^4}{(n\hbar)^2(4\pi\epsilon)^2} \tag{4.36}$$

The total energy is the sum of the kinetic and potential energies, so that

$$E = T + V = \frac{-m^*e^4}{2(n\hbar)^2(4\pi\epsilon)^2} \tag{4.37}$$

For the hydrogen atom, $m^* = m_0$ and $\epsilon = \epsilon_0$. The ionization energy of the hydrogen atom in the lowest energy state is then $E = -13.6$ eV. If we consider silicon, the ionization energy is $E = -25.8$ meV, much less than the bandgap energy of silicon. This energy is the approximate ionization energy of the donor atom, or the energy required to elevate the donor electron into the conduction band.

For ordinary donor impurities such as phosphorus or arsenic in silicon or germanium, this hydrogenic model works quite well and gives some indication of the magnitudes of the ionization energies involved. Table 4.3 lists the actual experimentally measured ionization energies for a few impurities in silicon and germanium. Germanium and silicon have different relative dielectric constants and effective masses; thus we expect the ionization energies to differ.

4.2.3 Group III–V Semiconductors

In the previous sections, we have been discussing the donor and acceptor impurities in a group IV semiconductor, such as silicon. The situation in the group III–V

Table 4.3 | Impurity ionization energies in silicon and germanium

	Ionization energy (eV)	
Impurity	**Si**	***Ge***
Donors		
Phosphorus	0.045	0.012
Arsenic	0.05	0.0127
Acceptors		
Boron	0.045	0.0104
Aluminum	0.06	0.0102

Table 4.4 | Impurity ionization energies in gallium arsenide

Impurity	Ionization energy (eV)
Donors	
Selenium	0.0059
Tellurium	0.0058
Silicon	0.0058
Germanium	0.0061
Acceptors	
Beryllium	0.028
Zinc	0.0307
Cadmium	0.0347
Silicon	0.0345
Germanium	0.0404

compound semiconductors, such as gallium arsenide, is more complicated. Group I elements, such as beryllium, zinc, and cadmium, can enter the lattice as subst tional impurities, replacing the group III gallium element to become acceptor impurities. Similarly, group VI elements, such as selenium and tellurium, can enter the lattice substitutionally, replacing the group V arsenic element to become donor impurities. The corresponding ionization energies for these impurities are smaller than for the impurities in silicon. The ionization energies for the donors in gallium arsenide are also smaller than the ionization energies for the acceptors, because of the smaller effective mass of the electron compared to that of the hole.

Group IV elements, such as silicon and germanium, can also be impurity atoms in gallium arsenide. If a silicon atom replaces a gallium atom, the silicon impurity will act as a donor. but if the silicon atom replaces an arsenic atom. then the silicon impurity will act as an acceptor. The same is true for germanium as an impurity atom. Such impurities are called ***amphoreric.*** Experimentally in gallium arsenide, it is found that germanium is predominantly an acceptor and silicon is predominantly a donor. Table 4.4 lists the ionization energies for the various impurity atoms in gallium arsenide.

TEST YOUR UNDERSTANDING

E4.7 Calculate the radius (normalized to a Bohr radius) of a donor electron in its lowest energy state in GaAs. (Ans. 195.5)

4.3 | THE EXTRINSIC SEMICONDUCTOR

We defined an intrinsic semiconductor as a material with no impurity atoms prese in the crystal. An ***extrinsic*** *semiconductor* is defined as a semiconductor in whic controlled amounts of specific dopant or impurity atoms have been added so that th thermal-equilibrium electron and hole concentrations are different from the intrins carrier concentration. One type of carrier will predominate in an extrinsic semiconductor.

4.3.1 Equilibrium Distribution of Electrons and Holes

Adding donor or acceptor impurity atoms to a semiconductor will change the distribution of electrons and holes in the material. Since the Fermi energy is related to the distribution function, the Fermi energy will change as dopant atoms are added. If the Fermi energy changes from near the midgap value, the density of electrons in the conduction band and the density of holes in the valence band will change. These effects are shown in Figures 4.8 and 4.9. Figure 4.8 shows the case for $E_F > E_{Fi}$ and Figure 4.9 shows the case for $E_F < E_{Fi}$. When $E_F > E_{Fi}$, the electron concentration is larger than the hole concentration, and when $E_F < E_{Fi}$, the hole concentration

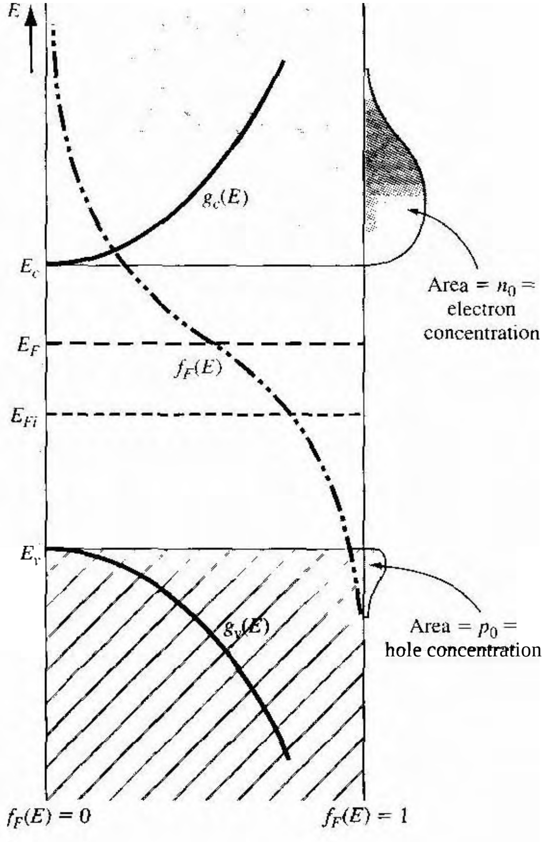

Figure 4.8 | Density of states functions. Fermi–Dirac probability function, and areas representing electron and hole concentrations for the case when E_F is **above** the intrinsic Fermi energy.

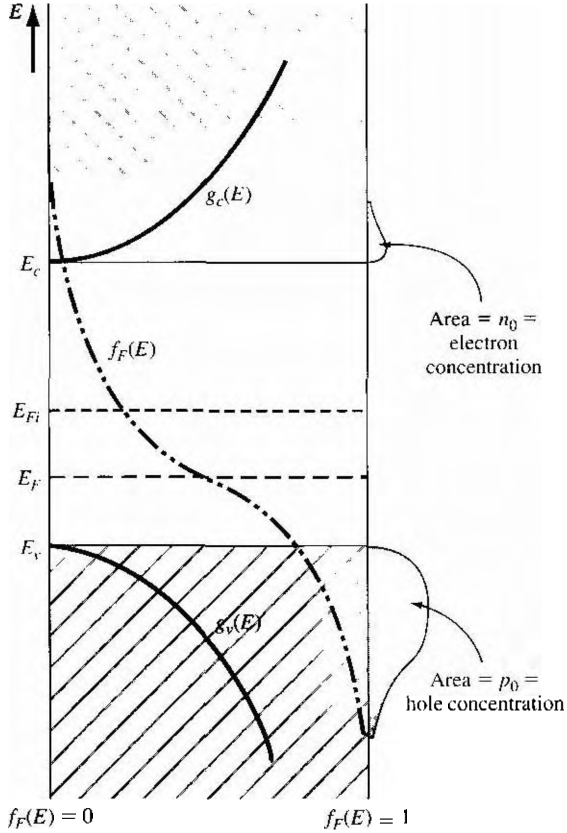

Figure 4.9 | Density of states functions, Fermi–Dirac probability function, and areas representing electron and hole concentrations for the case when E_I is below the intrinsic Fermi energy.

is larger than the electron concentration. When the density of electrons is greater than the density of holes, the semiconductor is n type; donor impurity atoms have been added. When the density of holes is greater than the density of electrons, the semiconductor is p type; acceptor impurity atoms have been added. The Fermi energy level in a semiconductor changes as the electron and hole concentrations change and, again, the Fermi energy changes as donor or acceptor impurities are added. The change in the Fermi level as a function of impurity concentrations will be considered in Section 4.6.

The expressions previously derived for the thermal-equilibrium concentration of electrons and holes, given by Equations (4.11) and (4.19) are general equations for n_0 and p_0 in terms of the Fermi energy. These equations are again given as

$$n_0 = N_c \exp\left[\frac{-(E_c - E_F)}{kT}\right]$$

and

$$p_0 = N,\exp\left[\frac{-(E_F - E_v)}{kT}\right]$$

As we just discussed, the Fermi energy may vary through the bandgap energy, which will then change the values of n_0 and p_0.

Objective **EXAMPLE 4.5**

To calculate the thermal equilibrium concentrations of electrons and holes for a given Fermi energy.

Consider silicon at T = 300 K so that N, = 2.8 x 10^{19} cm^{-3} and N, = 1.04 × 10^{19} cm^{-3}. Assume that the Fermi energy is 0.25 eV below the conduction hand. If we assume that the bandgap energy of silicon is 1.12 eV, then the Fermi energy will be 0.87 eV above the valence band.

■ **Solution**

Using Equation (4.11), we have

$$n_0 = (2.8 \times 10^{19})\exp\left(\frac{-0.25}{0.0259}\right) = 1.8 \times 10^{15}\ \text{cm}^{-3}$$

From Equation (4.19), we can write

$$p_0 = (1.04 \times 10^{19})\exp\left(\frac{-0.87}{0.0259}\right) = 2.7 \times 10^{4}\ \text{cm}^{-3}$$

■ **Comment**

The change in the Fermi level is actually a function of the donor or acceptor impurity concentrations that are added to the semiconductor. However, this example shows that electron and hole concentrations change by orders of magnitude from the intrinsic carrier concentration as the Fermi energy changes by a few tenths of an electron-volt.

In this example, since *no* > p_0, the semiconductor is n type. In an n-type semiconductor, electrons are referred to as the majority carrier and holes as the minority carrier. By comparing the relative values of n_0 and p_0 in the example, it is easy to see how this designation came about. Similarly, in a p-type semiconductor where p_0 > *no*, holes are the majority carrier and electrons are the minority carrier.

We may derive another form of the equations for the thermal-equilibrium concentrations of electrons and holes. If we add and subtract an intrinsic Fermi energy in the exponent of Equation (4.11), we can write

$$n_0 = N_c\exp\left[\frac{-(E_c - E_{Fi}) + (E_F - E_{Fi})}{kT}\right] \tag{4.38a}$$

or

$$n_0 = N_c\exp\left[\frac{-(E_c - E_{Fi})}{kT}\right]\exp\left[\frac{(E_F - E_{Fi})}{kT}\right] \tag{4.38b}$$

The intrinsic carrier concentration is given by Equation (4.20) as

$$n_i = N_c \exp\left[\frac{-(E_c - E_{Fi})}{kT}\right]$$

so that the thermal-equilibrium electron concentration can be written as

$$\boxed{n_0 = n_i \exp\left[\frac{E_F - E_{Fi}}{kT}\right]} \tag{4.39}$$

Similarly, if we add and subtract an intrinsic Fermi energy in the exponent of Equation (4.19), we will obtain

$$\boxed{p_0 = n_i \exp\left[\frac{-(E_F - E_{Fi})}{kT}\right]} \tag{4.40}$$

As we will see, the Fermi level changes when donors and acceptors are added, but Equations (4.39) and (4.40) show that, as the Fermi level changes from the intrinsic Fermi level, n_0 and p_0 change from their value. If $E_F > E_{Fi}$, then we will have $n_0 > n_i$ and $p_0 < n_i$. One characteristic of an n-type semiconductor is that $E_F > E_{Fi}$ so that $n_0 > p_0$. Similarly, in a p-type semiconductor, $E_F < E_{Fi}$ so that $p_0 > n_i$ and $n_0 < n_i$; thus $p_0 > n_0$.

We can see the functional dependence of n_0 and p_0 with E_F in Figures 4.8 and 4.9. As E_F moves above or below E_{Fi}, the overlapping probability function with the density of states functions in the conduction band and valence band changes. As E_F moves above E_{Fi}, the probability function in the conduction band increases, while the probability, $1 - f_F(E)$, of an empty state (hole) in the valence band decreases. As E_F moves below E_{Fi}, the opposite occurs.

4.3.2 The n_0p_0 Product

We may take the product of the general expressions for n_0 and p_0 as given in Equations (4.11) and (4.19), respectively. The result is

$$n_0p_0 = N_cN_v \exp\left[\frac{-(E_c - E_F)}{kT}\right] \exp\left[\frac{-(E_F - E_v)}{kT}\right] \tag{4.41}$$

which may be written as

$$n_0p_0 = N_cN_v \exp\left[\frac{-E_g}{kT}\right] \tag{4.42}$$

As Equation (4.42) was derived for a general value of Fermi energy, the values of n_0 and p_0 are not necessarily equal. However, Equation (4.42) is exactly the same as Equation (4.23), which we derived for the case of an intrinsic semiconductor. We then have that, for the semiconductor in thermal equilibrium,

$$\boxed{n_0 p_0 = n_i^2} \tag{4.43}$$

Equation (4.43) states that the product of n_0 and p_0 is always a constant for a given semiconductor material at a given temperature. Although this equation seems very simple, it is one of the fundamental principles of semiconductors in thermal equilibrium. The significance of this relation will become more apparent in the chapters that follow. It is important to keep in mind that Equation (4.43) was derived using the Boltrmann approximation. If the Boltzmann approximation is not valid, then likewise, Equation (4.43) is not valid.

An extrinsic semiconductor in thermal equilibrium does not, strictly speaking, contain an intrinsic carrier concentration, although some thermally generated carriers are present. The intrinsic electron and hole carrier concentrations are modified by the donor or acceptor impurities. However, we may think of the intrinsic concentration n_i in Equation (4.41) simply as a parameter of the semiconductor material.

*4.3.3 The Fermi–Dirac Integral

In the derivation of the Equations (4.11) and (4.19) for the thermal equilibrium electron and hole concentrations, we assumed that the Boltzmann approximation was valid. If the Boltrmann approximation does not hold. the thermal equilibrium electron concentration is written from Equation (4.3) as

$$n_0 = \frac{4\pi}{h^3}(2m_n^*)^{3/2} \int_{E_c}^{\infty} \frac{(E - E_c)^{1/2}\, dE}{1 + \exp\left(\dfrac{E - E_F}{kT}\right)} \tag{4.44}$$

If we again make a change of variable and let

$$\eta = \frac{E - E_c}{kT} \tag{4.45a}$$

and also define

$$\eta_F = \frac{E_F - E_c}{kT} \tag{4.45b}$$

then we can rewrite Equation (4.44) as

$$n_0 = 4\pi \left(\frac{2m_n^* kT}{h^2}\right)^{3/2} \int_0^{\infty} \frac{\eta^{1/2}\, d\eta}{1 + \exp(\eta - \eta_F)} \tag{4.46}$$

The integral is defined as

$$F_{1/2}(\eta_F) = \int_0^{\infty} \frac{\eta^{1/2}\, d\eta}{1 + \exp(\eta - \eta_F)} \tag{4.47}$$

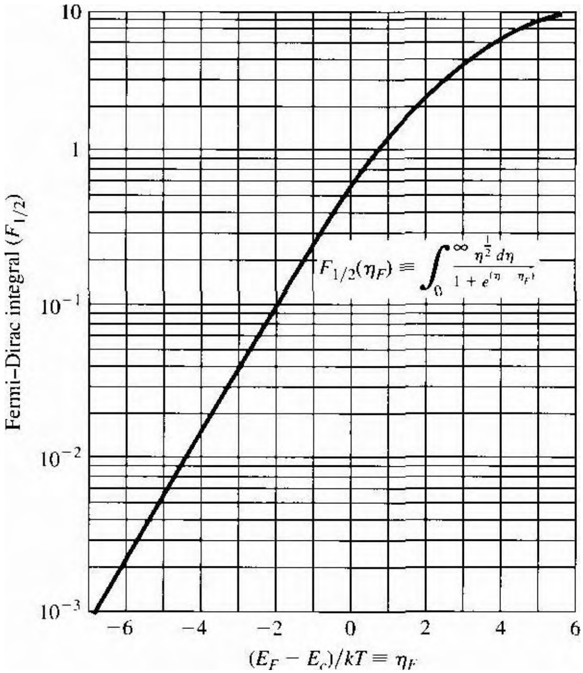

Figure 4.10 | The Fermi–Dirac integral $F_{1/2}$ as a function of the Fermi energy.
(From Sze [13].)

This function, called the Fermi–Dirac integral, is a tabulated function of the variabl η_F. Figure 4.10 is a plot of the Fermi–Dirac integral. Note that if $\eta_F > 0$, the $E_F > E_c$; thus the Fermi energy is actually in the conduction band.

EXAMPLE 4.6

Objective

To calculate the electron concentration using the Fermi–Dirac integral.

Let $\eta_F = 2$ so that the Fermi energy is above the conduction band by approximatel 52 meV at T = 300 K.

■ Solution

Equation (4.46) can be written as

$$n_0 = \frac{2}{\sqrt{\pi}} N_c F_{1/2}(\eta_F)$$

For silicon at 300 K, $N_c = 2.8 \times 10^{19}$ cm^{-3} and, from Figure 4.10, the Fermi–Dirac integr has a value of $F_{1/2}(2) = 2.3$. Then

$$n_0 = \frac{2}{\sqrt{\pi}}(2.8 \times 10^{19})(2.3) = 7.27 \times 10^{19} \text{ cm}^{-3}$$

Comment

Note that if we had used Equation (4.11). the thermal equilibrium value of n_0 would be $n_0 = 2.08 \times 10^{20}$ cm^{-3}, which is incorrect since the Boltzmann approximation is not valid for this case.

We may use the same general method to calculate the thermal equilibrium concentration of holes. We obtain

$$p_0 = 4\pi \left(\frac{2m_p^* kT}{h^2}\right)^{3/2} \int_0^\infty \frac{(\eta')^{1/2}\, d\eta'}{1 + \exp(\eta' - \eta'_F)} \tag{4.48}$$

where

$$\eta' = \frac{E_v - E}{kT} \tag{4.49a}$$

$$\eta'_F = \frac{E_v - E_F}{kT} \tag{4.49b}$$

The integral in Equation (4.48) is the same Fermi–Dirac integral defined by Equation (4.47), although the variables have slightly different definitions. We may note that if $\eta'_F > 0$, then the Fermi level is in the valence band.

TEST YOUR UNDERSTANDING

E4.8 Calculate the thermal equilibrium electron concentration in silicon for the case when $E_F =$ E, and $T = 300$ K. (Ans. 1.9×10^{19} cm^{-3})

4.3.4 Degenerate and Nondegenerate Semiconductors

In our discussion of adding dopant atoms to a semiconductor, we have implicitly assumed that the concentration of dopant atoms added is small when compared to the density of host or semiconductor atoms. The small number of impurity atoms are spread far enough apart so that there is no interaction between donor electrons, for example, in an n-type material. We have assumed that the impurities introduce discrete, noninteracting donor energy states in the n-type semiconductor and discrete. noninteracting acceptor states in the p-type semiconductor. These types of semiconductors are referred to as nondegenerate semiconductors.

If the impurity concentration increases, the distance between the impurity atoms decreases and a point will be reached when donor electrons, for example, will begin to interact with each other When this occurs, the single discrete donor energy will split into a band of energies. As the donor concentration further increases, the band of donor states widens and may overlap the bottom of the conduction band. This overlap occurs when the donor concentration becomes comparable with the effective density of states. When the concentration of electrons in the conduction band exceeds

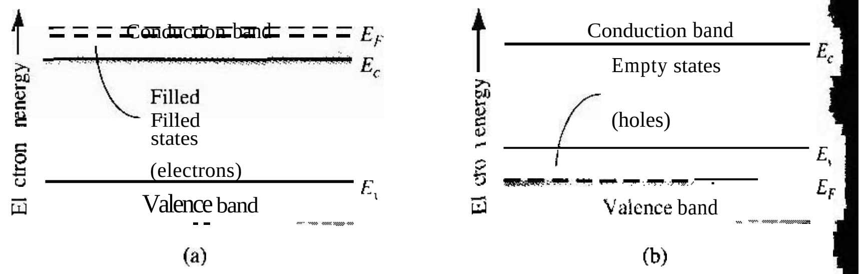

Figure 4.11 | Simplified energy-band diagrams for degenerately doped (a) n-type and (b) p-type semiconductors.

the density of states N_c, the Fermi energy lies within the conduction band. This typ of semiconductor is called a degenerate n-type semiconductor.

In a similar way, as the acceptor doping concentration increases in a p-typ semiconductor, the discrete acceptor energy states will split into a band of energie and may overlap the top of the valence band. The Fermi energy will lie in the valenc band when the concentration of holes exceeds the density of states N_v. This type o semiconductor is called a degenerate p-type semiconductor.

Schematic models of the energy-band diagrams for a degenerate n-type and degenerate p-type semiconductor are shown in Figure 4.11. The energy states below E_F are mostly filled with electrons and the energy states above E_F are mostly empty. I the degenerate n-type semiconductor, the states between E_F and E_c are mostly fille with electrons; thus, the electron concentration in the conduction band is very large Similarly, in the degenerate p-type semiconductor, the energy states between E_v an E_F are mostly empty; thus, the hole concentration in the valence band is very large

4.4 | STATISTICS OF DONORS AND ACCEPTORS

In the last chapter, we discussed the Fermi–Dirac distribution function, which gives the probability that a particular energy state will be occupied by an electron. We need to reconsider this function and apply the probability statistics to the donor and acceptor energy states.

4.4.1 Probability Function

One postulate used in the derivation of the Fermi–Dirac probability function was the Pauli exclusion principle, which states that only one particle is permitted in eac quantum state. The Pauli exclusion principle also applies to the donor and accepto states.

Suppose we have N_i electrons and g_i quantum states, where the subscript i indicates the ith energy level. There are g_i ways of choosing where to put the first particle. Each donor level has two possible spin orientations for the donor electron; thus each donor level has two quantum states. The insertion of an electron into one quantum state, however, precludes putting an electron into the second quantum state. B adding one electron, the vacancy requirement of the atom is satisfied, and the addition of a second electron in the donor level is not possible. The distribution function of donor electrons in the donor energy states is then slightly different than the Fermi–Dirac function.

The probability function of electrons occupying the donor state is

$$n_d = \frac{N_d}{1 + \dfrac{1}{2}\exp\left(\dfrac{E_d - E_F}{kT}\right)} \tag{4.50}$$

where n_d is the density of electrons occupying the donor level and E_d is the energy of the donor level. The factor $\frac{1}{2}$ in this equation is a direct result of the spin factor just mentioned. The $\frac{1}{2}$ factor is sometimes written as $1/g$, where g is called a degeneracy factor.

Equation (4.50) can also be written in the form

$$n_d = N_d - N_d^+ \tag{4.51}$$

where N_d^+ is the concentration of ionized donors. In many applications, we will be interested more in the concentration of ionized donors than in the concentration of electrons remaining in the donor states.

If we do the same type of analysis for acceptor atoms, we obtain the expression

$$p_a = \frac{N_a}{1 + \dfrac{1}{g}\exp\left(\dfrac{E_F - E_a}{kT}\right)} = N_a - N_a^- \tag{4.52}$$

where N_a is the concentration of acceptor atoms. E_a is the acceptor energy level, p_a is the concentration of holes in the acceptor states, and N_a^- is the concentration of ionized acceptors. A hole in an acceptor state corresponds to an acceptor atom that is neutrally charged and still has an "empty" bonding position as we discussed in Section 4.2.1. The parameter g is, again, a degeneracy factor. The ground state degeneracy factor g is normally taken as four for the acceptor level in silicon and gallium arsenide because of the detailed band structure.

4.4.2 Complete Ionization and Freeze-Out

The probability function for electrons in the donor energy state was just given by Equation (4.50). If we assume that $(E_d - E_F) \gg kT$, then

$$n_d \approx \frac{N_d}{\dfrac{1}{2}\exp\left(\dfrac{E_d - E_F}{kT}\right)} = 2N_d \exp\left[\frac{-(E_d - E_F)}{kT}\right] \tag{4.53}$$

If $(E_d - E_F) \gg kT$, then the Boltzmann approximation is also valid for the electrons in the conduction band so that. from Equation (4.11),

$$n_0 = N_c \exp\left[\frac{-(E_c - E_F)}{kT}\right]$$

We can determine the relative number of electrons in the donor state compa with the total number of electrons; therefore we can consider the ratio of electrons the donor state to the total number of electrons in the conduction band plus do state. Using the expressions of Equations (4.53) and (4.11), we write

$$\frac{n_d}{n_d+n_0}=\frac{2N_d\exp\left[\dfrac{-(E_d-E_F)}{kT}\right]}{2N_d\exp\left[\dfrac{-(E_d-E_F)}{kT}\right]+N_c\exp\left[\dfrac{-(E_c-E_F)}{kT}\right]}\qquad\text{(4.5}$$

The Fermi energy cancels out of this expression. Dividing by the numerator term, obtain

$$\frac{n_d}{n_d+n_0}=\frac{1}{1+\dfrac{N_c}{2N_d}\exp\left[\dfrac{-(E_c-E_d)}{kT}\right]}\qquad\text{(4.5}$$

The factor (E_c-E_d) is just the ionization energy of the donor electrons.

EXAMPLE 4.7

Objective

To determine the fraction of total electrons still in the donor states at T = 300 K.

Consider phosphorus doping in silicon, for T = 300 K, at a concentration of N_d 10^{16} cm^{-3}.

■ Solution

Using Equation (4.55), we find

$$\frac{n_d}{n_0+n_d}=\frac{1}{1+\dfrac{2.8\times10^{19}}{2(10^{16})}\exp\left(\dfrac{-0.045}{0.0259}\right)}=0.0041=0.41\%$$

■ Comment

This example shows that there are very few electrons in the donor state compared with th conduction band. Essentially all of the electrons from the donor states are in the conductio band and. since only about 0.4 percent of the donor states contain electrons, the donor state are said to be completely ionized.

At room temperature, then, the donor states are essentially completely ionize and, for a typical doping of 10^{16} cm^{-3}, almost all donor impurity atoms have donate an electron to the conduction band.

At room temperature, there is also essentially *complete ionization* of the acceptor atoms. This means that each acceptor atom has accepted an electron from the valence band so that p_a is zero. At typical acceptor doping concentrations, a hole is created in the valence band for each acceptor atom. This ionization effect and the creation of electrons and holes in the conduction band and valence band, respectively, are shown in Figure 4.12.

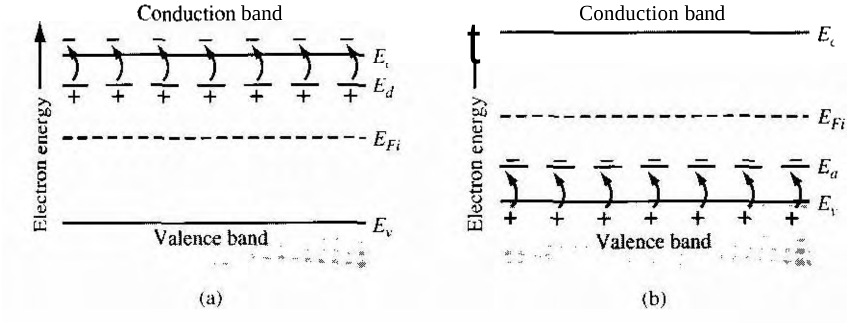
Conduction band
E_c
E_d
E_{Fi}
E_v
Valence band
Electron energy
(a)
Conduction band
E_c
E_{Fi}
E_a
E_v
Valence band
Electron energy
(b)

Figure 4.12 | Energy-hand diagrams showing complete ionization of (a) donor states and (b) acceptor states.

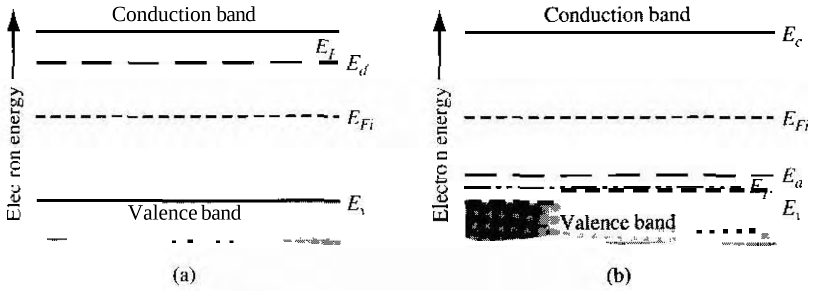
Conduction band
E_F
E_d
E_{Fi}
E_v
Valence band
Electron energy
(a)
Conduction band
E_c
E_{Fi}
E_a
E_F
E_v
Valence band
Electron energy
(b)

Figure 4.13 | Energy-band diagram at $T = 0$ K for (a) n-type and (b) p-type semiconductors.

The opposite of complete ionization occurs at $T = 0$ ***K*.** At absolute zero degrees, all electrons are in their lowest possible energy state; that is, for an n-type semiconductor, each donor state must contain an electron, therefore $n_d = N_d$ or $N_d^+ = 0$. We must have, then, from Equation (4.50) that exp $[(E_d - E_F)/kT] = 0$. Since T = 0 K, this will occur for exp $(-\infty) = 0$, which means that $E_F > E_d$. The Fermi energy level must he above the donor energy level at absolute zero. In the case of a p-type semiconductor at absolute zero temperature, the impurity atoms will not contain any electrons, so that the Fermi energy level must be below the acceptor energy state. The distribution of electrons among the various energy states, and hence the Fermi energy, is a function of temperature.

A detailed analysis, not given in this text, shows that at $T = 0$ ***K*,** the Fermi energy is halfway between E, and E_d for the n-type material and halfway between E_a and E_v for the p-type material. Figure 4.13 shows these effects. No electrons from the donor state are thermally elevated into the conduction band; this effect is called freeze-our. Similarly, when no electrons from the valance band are elevated into the acceptor states, the effect is also called freeze-out.

Between $T = 0$ K, freeze-out, and $T = 300$ K, complete ionization, we hav partial ionization of donor or acceptor atoms.

EXAMPLE 4.8

Objective

To determine the temperature at which 90 percent of acceptor atoms are ionized.

Consider p-type silicon doped with boron at a concentration of $N_a = 10^{16}$ cm^{-3}.

■ Solution

Find the ratio of holes in the acceptor state to the total number of holes in the valence band pl acceptor state. Taking into account the Boltzmann approximation and assuming the degeneracy factor is $g = 4$, we write

$$\frac{p_a}{p_0 + p_a} = \frac{1}{1 + \dfrac{N_v}{4N_a} \cdot \exp\left[\dfrac{-(E_a - E_v)}{kT}\right]}$$

For 90 percent ionization,

$$\frac{p_a}{p_0 + p_a} = 0.10 = \frac{1}{1 + \dfrac{(1.04 \times 10^{19})\left(\dfrac{T}{300}\right)^{3/2}}{4(10^{16})} \cdot \exp\left[\dfrac{-0.045}{0.0259\left(\dfrac{T}{300}\right)}\right]}$$

Using trial and error, we find that $T = 193$ K.

■ Comment

This example shows that at approximately 100°C below room temperature, we still hav 90 percent of the acceptor atoms ionized; in other words, 90 percent of the acceptor atom have "donated" a hole to the valence band.

TEST YOUR UNDERSTANDING

E4.9 Determine the fraction of total holes still in the acceptor states in silicon at $T = 300$ K for a boron impurity concentration of $N_a = 10^{17}$ cm^{-3}. (Ans. 0.179)

E4.10 Consider silicon with a phosphorus impurity concentration of $N_d = 5 \times 10^{15}$ cm^{-3}. Plot the percent of ionized impurity atoms versus temperature over the range $100 \le T \le 400$ K.

4.5 | CHARGE NEUTRALITY

In thermal equilibrium, the semiconductor crystal is electrically neutral. The electrons are distributed among the various energy states, creating negative and positiv charges, but the net charge density is zero. This charge-neutrality condition is used t determine the thermal-equilibrium electron and hole concentrations as a function o the impurity doping concentration. We will define a compensated semiconductor and then determine the electron and hole concentrations as a function of the donor and acceptor concentrations.

4.5.1 compensated Semiconductors

A compensated semiconductor is one that contains both donor and acceptor impurity atoms in the same region. A compensated semiconductor can he formed, for example, by diffusing acceptor impurities into an n-type material, or by diffusing donor impurities into a p-type material. An n-type compensated semiconductor occurs when $N_d > N_a$, and a p-type compensated semiconductor occurs when $N_a > N_d$. If $N_a = N_d$, we have a completely compensated semiconductor that has. as we will show, the characteristics of an intrinsic material. Compensated semiconductors are created quite naturally during device fabrication as we will see later.

4.5.2 Equilibrium Electron and Hole Concentrations

Figure 4.14 shows the energy-hand diagram of a semiconductor when both donor and acceptor impurity atoms are added to the same region to form a compensated

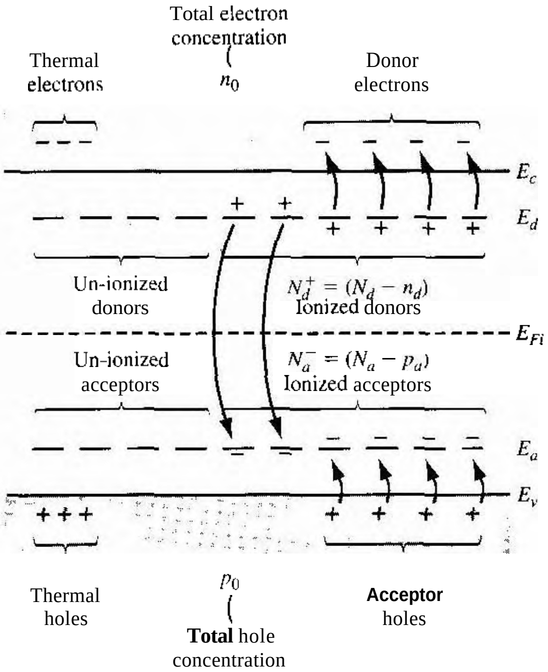
Total electron concentration
n_0
Thermal electrons
Donor electrons
E_c
E_d
Un-ionized donors
$N_d^+ = (N_d - n_d)$ Ionized donors
E_{Fi}
Un-ionized acceptors
$N_a^- = (N_a - p_a)$ Ionized acceptors
E_a
E_v
Thermal holes
p_0
Total hole concentration
Acceptor holes

Figure 4.14 | Energy-band diagram of a campenrated semiconductor showing ionized and un-ionized donors and acceptors.

semiconductor. The figure shows how the electrons and holes can be distributed among the various states.

The charge neutrality condition is expressed by equating the density of negative charges to the density of positive charges. We then have

$$n_0 + N_a^- = p_0 + N_d^+ \tag{4.56}$$

or

$$n_0 + (N_a - p_a) = p_0 + (N_d - n_d) \tag{4.57}$$

where n_0 and p_0 are the thermal-equilibrium concentrations of electrons and holes the conduction band and valence band, respectively. The parameter n_d is the conce tration of electrons in the donor energy states, so $N_d^+ = N_d - n_d$ is the concentrati of positively charged donor states. Similarly, **p**, is the concentration of holes in t acceptor states, so N_a^- = N,, − **p**, is the concentration of negatively charged acceptor states. We have expressions for n_0, p_0, n_d, and p_a in terms of the Fermi energy and temperature.

If we assume complete ionization, n_d and p_a are both zero, and Equation (4.57) becomes

$$n_0 + N_a = p_0 + N_d \tag{4.58}$$

If we express p_0 as n_i^2/n_0, then Equation (4.58) can be written as

$$n_0 + N_a = \frac{n_i^2}{n_0} + N_d \tag{4.59a}$$

which in turn can be written as

$$n_0^2 - (N_d - N_a)n_0 - n_i^2 = 0 \tag{4.59b}$$

The electron concentration n_0 can be determined using the quadratic formula, or

$$\boxed{n_0 = \frac{(N_d - N_a)}{2} + \sqrt{\left(\frac{N_d - N_a}{2}\right)^2 + n_i^2}} \tag{4.60}$$

The positive sign in the quadratic formula must be used, since, in the limit of an intrinsic semiconductor when $N_a = N_d = 0$. the electron concentration must he a positive quantity, or $n_0 = n_i$.

Equation (4.60) is used to calculate the electron concentration in an n-type semiconductor, or when $N_d > N_a$. Although Equation (4.60) was derived for a compensated semiconductor, the equation is also valid for $N_a = 0$.

EXAMPLE 4.9

Objective

To determine the thermal equilibrium electron and hole concentrations fur a given doping concentration.

Consider **an** n-type silicon semiconductor at T = 300 K in which $N_d = 10^{16}$ cm ^{3} and $N_a = 0$. The intrinsic carrier concentration is assumed to be n_i = 1.5 x 10^{10} cm^{-3}

Solution

From Equation (4.60), the majority carrier electron concentration is

$$n_0 = \frac{10^{16}}{2} + \sqrt{\left(\frac{10^{16}}{2}\right)^2 + (1.5 \times 10^{10})^2} \approx 10^{16}\ \text{cm}^{-3}$$

The minority carrier hole concentration is found as

$$p_0 = \frac{n_i^2}{n_0} = \frac{(1.5 \times 10^{10})^2}{1 \times 10^{16}} = 2.25 \times 10^4\ \text{cm}^{-3}$$

Comment

In this example, $N_d \gg n_i$, so that the thermal-equilibrium majority carrier electron concentration is essentially equal to the donor impurity concentration. The thermal-equilibrium majority and minority carrier concentrations can differ by many orders of magnitude.

We have argued in our discussion and we may note from the results of Example 4.9 that the concentration of electrons in the conduction band increases above the intrinsic carrier concentration as we add donor impurity atoms. *At* the same time, the minority carrier hole concentration decreases below the intrinsic carrier concentration as we add donor atoms. We must keep in mind that as we add donor impurity atoms and the corresponding donor electrons, there is a redistribution of electrons among available energy states. Figure 4.15 shows a schematic of this physical redistribution. A few of the donor electrons will fall into the empty states in the valence

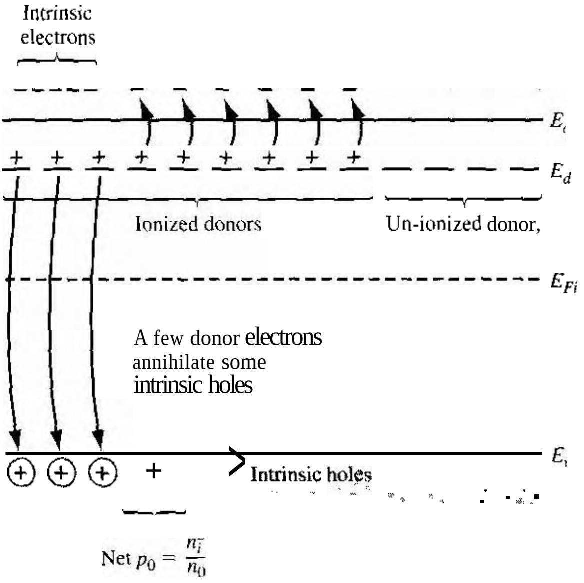
Intrinsic electrons
E_c
E_d
Ionized donors
Un-ionized donor,
E_{Fi}
A few donor electrons annihilate some intrinsic holes
E_v
Intrinsic holes
Net $p_0 = \frac{n_i^2}{n_0}$

Figure 4.15 | Energy-band diagram showing the redistribution of electrons when donors are added.

band and, in doing so, will annihilate some of the intrinsic holes. The minority carrier hole concentration will therefore decrease as we have seen in Example 4.9. At the same time, because of this redistribution, the net electron concentration in the conduction band is *not* simply equal to the donor concentration plus the intrinsic electron concentration.

EXAMPLE 4.10

Objective

To calculate the thermal-equilibrium electron and hole concentrations in a germanium sample for a given doping density.

Consider a germanium sample at $T = 300$ K in which $N_d = 5 \times 10^{13}$ cm^{-3} and $N_a =$

Assume that $n_i = 2.4 \times 10^{13}$ cm^{-3}.

■ Solution

Again, from Equation (4.60), the majority carrier electron concentration is

$$n_0 = \frac{5 \times 10^{13}}{2} + \sqrt{\left(\frac{5 \times 10^{13}}{2}\right)^2 + (2.4 \times 10^{13})^2} = 5.97 \times 10^{13} \text{ cm}^{-3}$$

The minority carrier hole concentration is

$$p_0 = \frac{n_i^2}{n_0} = \frac{(2.4 \times 10^{13})^2}{5.97 \times 10^{13}} = 9.65 \times 10^{12} \text{ cm}^{-3}$$

Comment

If the donor impurity concentration is not too different in magnitude from the intrinsic carrier concentration, then the thermal-equilibrium majority carrier electron concentration is influenced by the intrinsic concentration.

We have seen that the intrinsic carrier concentration n_i is a very strong function of temperature. As the temperature increases, additional electron-hole pairs are thermally generated so that the n_i^2 term in Equation (4.60) may begin to dominate. The semiconductor will eventually lose its extrinsic characteristics. Figure 4.16 shows the electron concentration versus temperature in silicon doped with 5×10^{14} donors per cm^3. As the temperature increases, we can see where the intrinsic concentration begins to dominate. Also shown is the partial ionization, or the onset of freeze-out, at the low temperature.

If we reconsider Equation (4.58) and express n_0 as n_i^2/p_0, then we have

$$\frac{n_i^2}{p_0} + N_a = p_0 + N_d \tag{4.61a}$$

which we can write as

$$p_0^2 - (N_a - N_d)p_0 - n_i^2 = 0 \tag{4.61b}$$

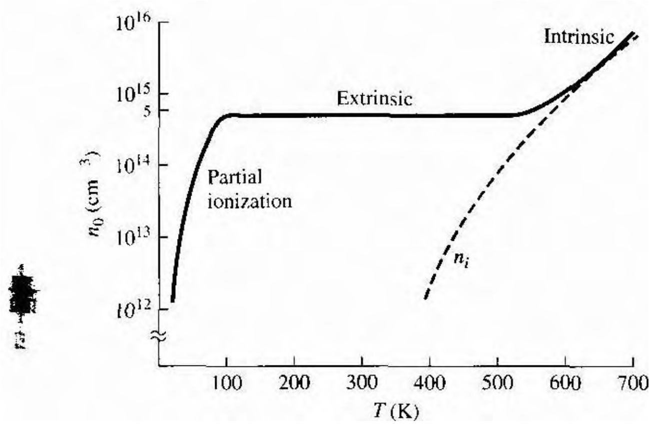

Figure 4.16 | Electron concentration versus temperature showing the ***three*** regions: partial ionization, extrinsic, and intrinsic.

Using the quadratic formula, the hole concentration is given by

$$\boxed{p_0 = \frac{N_a - N_d}{2} + \sqrt{\left(\frac{N_a - N_d}{2}\right)^2 + n_i^2}} \tag{4.62}$$

where the positive sign, again, must be used. Equation (4.62) is used to calculate the thermal-equilibrium majority carrier hole concentration in a p-type semiconductor, or when $N_a > N_d$. This equation also applies for $N_d = 0$.

Objective | EXAMPLE 4.11

To calculate the thermal-equilibrium electron and hole concentrations in a compensated p-type semiconductor.

Consider a silicon semiconductor at $T = 300$ K in which $N_a = 10^{16}$ cm^{-3} and $N_d = 3 \times 10^{15}$ cm^{-3}. Assume $n_i = 1.5 \times 10^{10}$ cm^{-3}.

■ Solution

Since $N_a > N_d$, the compensated semiconductor is p-type and the thermal-equilibrium majority carrier hole concentration is given by Equation (4.62) as

$$p_0 = \frac{10^{16} - 3 \times 10^{15}}{2} + \sqrt{\left(\frac{10^{16} - 3 \times 10^{15}}{2}\right)^2 + (1.5 \times 10^{10})^2}$$

so that

$$p_0 \approx 7 \times 10^{15} \text{ cm}^{-3}$$

The minority carrier electron concentration is

$$n_0 = \frac{n_i^2}{p_0} = \frac{(1.5 \times 10^{10})^2}{7 \times 10^{15}} = 3\ 21 \times 10^4 \text{ cm}^{-3}$$

■ Comment

If we assume complete ionization and if $(N_a - N_d) \gg$ n,, then the majority carrier hole co centration is, to a very good approximation, just the difference between the acceptor and dono concentrations.

We may note that, for a compensated p-type semiconductor, the minority carrie electron concentration is determined from

$$n_0 = \frac{n_i^2}{p_0} = \frac{n_i^2}{(N_a - N_d)}$$

DESIGN EXAMPLE 4.12

Objective

To determine the required impurity doping concentration in a semiconductor material.

A silicon device with n-type material is to be operated at T = 550 K. At this temperatur the intrinsic carrier concentration must contribute no more than 5 percent of the total electro concentration. Determine the minimum donor concentration required to meet this specificatio

■ Solution

At T = 550 K, the intrinsic carrier concentration is found from Equation (4.23) as

$$n_i^2 = N_c N_v \exp\left(\frac{-E_g}{kT}\right) = (2.8 \times 10^{19})(1.04 \times 10^{19})\left(\frac{550}{300}\right)^3 \exp\left[\frac{-1.12}{0.0259}\left(\frac{300}{550}\right)\right]$$

or

$$n_i^2 = 1.02 \times 10^{29}$$

so that

$$n_i = 3.20 \times 10^{14} \text{ cm}^{-3}$$

For the intrinsic carrier concentration to contribute no more than 5 percent of the total electro concentration, we set $n_0 = 1.05 N_d$.

From Equation (4.60), we have

$$n_0 = \frac{N_d}{2} + \sqrt{\left(\frac{N_d}{2}\right)^2 + n_i^2}$$

or

$$1.05 N_d = \frac{N_d}{2} + \sqrt{\left(\frac{N_d}{2}\right)^2 + (3.20 \times 10^{14})^2}$$

which yields

$$N_d = 1.39 \times 10^{15}\ \mathrm{cm}^{-3}$$

Comment

If the temperature remains less than $T = 550$ K, then the intrinsic carrier concentration will contribute less than 5 percent of the total electron concentration for this donor impurity concentration.

Equations (4.60) and (4.62) are used to calculate the majority carrier electron concentration in an n-type semiconductor and majority carrier hole concentration in a p-type semiconductor, respectively. The minority carrier hole concentration in an n-type semiconductor could, theoretically, be calculated from Equation (4.62). However, we would be subtracting two numbers on the order of $10^{16}\ \mathrm{cm}^{-3}$, for example, to obtain a number on the order of $10^{4}\ \mathrm{cm}^{-3}$, which from a practical point of view is not possible. The minority carrier concentrations are calculated from $n_0 p_0 = n_i^2$ once the majority carrier concentration has been determined.

TEST YOUR UNDERSTANDING

E4.11 Consider a compensated GaAs semiconductor at T = 300 K doped at $N_d = 5 \times 10^{15}\ \mathrm{cm}^{-3}$ and N,, $= 2 \times 10^{16}\ \mathrm{cm}^{-3}$. Calculate the thermal equilibrium electron and hole concentrations. (Ans. $p_0 = 1.5 \times 10^{16}\ \mathrm{cm}^{-3}$, $n_0 = 2.16 \times 10^{-4}\ \mathrm{cm}^{-3}$)

E4.12 Silicon is doped at $N_d = 10^{15}\ \mathrm{cm}^{-3}$ and $N_a = 0$. (n) Plot the concentration of electrons versus temperature over the range $300 \le T \le 600$ K. (b) Calculate the temperature at which the electron concentration is equal to $1.1 \times 10^{15}\ \mathrm{cm}^{-3}$. (Ans. $T \approx 552$ K)

4.6 | POSITION OF FERMI ENERGY LEVEL

We discussed qualitatively in Section 4.3.1 how the electron and hole concentrations change as the Fermi energy level moves through the bandgap energy. Then, in Section 4.5, we calculated the electron and hole concentrations as a function of donor and acceptor impurity concentrations. We can now determine the position of the Fermi energy level as a function of the doping concentrations and as a function of temperature. The relevance of the Fermi energy level will be further discussed after the mathematical derivations.

4.6.1 Mathematical Derivation

The position of the Fermi energy level within the bandgap can be determined by using the equations already developed for the thermal-equilibrium electron and hole concentrations. If we assume the Boltzmann approximation to be valid, then from Equation (4.11) we have $n_0 = N_c \exp[-(E_c - E_F)/kT]$. We can solve for $E_c - E_F$

from this equation and obtain

$$\boxed{E_c - E_F = kT \ln\left(\frac{N_c}{n_0}\right)} \qquad \text{(4.6}$$

where n_0 is given by Equation (4.60). If we consider an n-type semiconductor which $N_d \gg n_i$, then $n_0 \approx N_d$, so that

$$E_c - E_F = kT \ln\left(\frac{N_c}{N_d}\right) \qquad (4.64)$$

The distance between the bottom of the conduction band and the Fermi energy is a logarithmic function of the donor concentration. As the donor concentration increases, the Fermi level moves closer to the conduction band. Conversely, if the Fermi level moves closer to the conduction band, then the electron concentration in the conduction band is increasing. We may note that if we have a compensated semiconductor, then the N_d term in Equation (4.64) is simply replaced by $N_d - N_a$, or the net effective donor concentration.

DESIGN EXAMPLE 4.13

Objective

To determine the required donor impurity concentration to obtain a specified Fermi energy.

Silicon at T = 300 K contains an acceptor impurity concentration of $N_a = 10^{16}$ cm^{-3}. Determine the concentration of donor impurity atoms that must be added so that the silicon is n type and the Fermi energy is 0.20 eV below the conduction band edge.

■ Solution

From Equation (4.64). we have

$$E_c - E_F = kT \ln\left(\frac{N_c}{N_d - N_a}\right)$$

which can be rewritten as

$$N_d - N, = N_c \exp\left[\frac{-(E_c - E_F)}{kT}\right]$$

Then

$$N_d - N, = 2.8 \times 10^{19} \exp\left[\frac{-0.20}{0.0259}\right] = 1.24 \times 10^{16} \text{ cm}^{-3}$$

or

$$N_d = 1.24 \times 10^{16} + N_a = 2.24 \times 10^{16} \text{ cm}^{-3}$$

■ Comment

A compensated semiconductor can be fabricated to provide a specific Fermi energy level.

We may develop a slightly different expression for the position of the Fermi level. We had from Equation (4.39) that $n_0 = n_i \exp[(E_F - E_{Fi})/kT]$. We can solve for $E_F - E_{Fi}$ as

$$\boxed{E_F - E_{Fi} = kT \ln\left(\frac{n_0}{n_i}\right)} \tag{4.65}$$

Equation (4.65) can be used specifically for an n-type semiconductor, where n_0 is given by Equation (4.60), to find the difference between the Fermi level and the intrinsic Fermi level as a function of the donor concentration. We may note that, if the net effective donor concentration is zero, that is, $N_d - N_a = 0$, then $n_0 = n$, and $E_F = E_{Fi}$. A completely compensated semiconductor has the characteristics of an intrinsic material in terms of carrier concentration and Fermi level position.

We can derive the same types of equations for a p-type semiconductor. From Equation (4.19), we have $p_0 = N_v \exp[-(E_F - E_v)/kT]$, so that

$$\boxed{E_F - E_v = kT \ln\left(\frac{N_v}{p_0}\right)} \tag{4.66}$$

If we assume that $N_a \gg n_i$, then Equation (4.66) can be written as

$$E_F - E_v = kT \ln\left(\frac{N_v}{N_a}\right) \tag{4.67}$$

The distance between the Fermi level and the top of the valence-band energy for a p-type semiconductor is a logarithmic function of the acceptor concentration: as the acceptor concentration increases, the Fermi level moves closer to the valence band. Equation (4.67) still assumes that the Boltzmann approximation is valid. Again. if we have a compensated p-type semiconductor, then the N_a term in Equation (4.67) is replaced by $N_a - N_d$, or the net effective acceptor concentration.

We can also derive an expression for the relationship between the Fermi level and the intrinsic Fermi level in terms of the hole concentration. We have from Equation (4.40) that $p_0 = n_i \exp[-(E_F - E_{Fi})/kT]$, which yields

$$\boxed{E_{Fi} - E_F = kT \ln\left(\frac{p_0}{n_i}\right)} \tag{4.68}$$

Equation (4.68) can be used to find the difference between the intrinsic Fermi level and the Fermi energy in terms of the acceptor concentration. The hole concentration p_0 in Equation (4.68) is given by Equation (4.62).

We may again note from Equation (4.65) that, for an n-type semiconductor, $n_0 > n_i$ and $E_F > E_{Fi}$. The Fermi level for an n-type semiconductor is above E_{Fi}. For a p-type semiconductor, $p_0 > n_i$, and from Equation (4.68) we see that

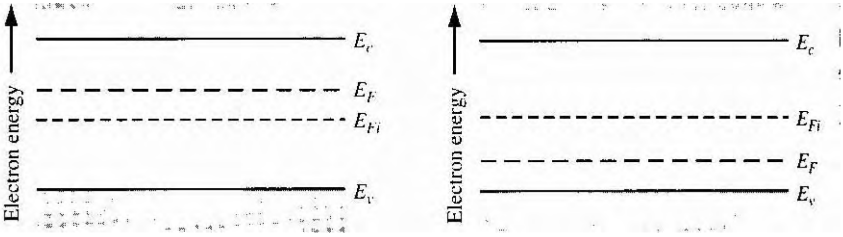

(a) (b)

Figure 4.17 | Position of Fermi level for an (a) n-type ($N_d > N_a$) and (b) p-type ($N_d > N_a$) semiconductor.

$E_{Fi} > E_F$. The Fermi level for a p-type semiconductor is below E_{Fi}. These result are shown in Figure 4.17.

4.6.2 Variation of E_F with Doping Concentration and Temperature

We may plot the position of the Fermi energy level as a function of the doping concentration. Figure 4.18 shows the Fermi energy level as a function of donor concentration (n type) and as a function of acceptor concentration (p type) for silicon a T = 300 K. As the doping levels increase, the Fermi energy level moves closer to the conduction band for the n-type material and closer to the valence band for the p-typ material. Keep in mind that the equations for the Fermi energy level that we have derived assume that the Boltzmann approximation is valid.

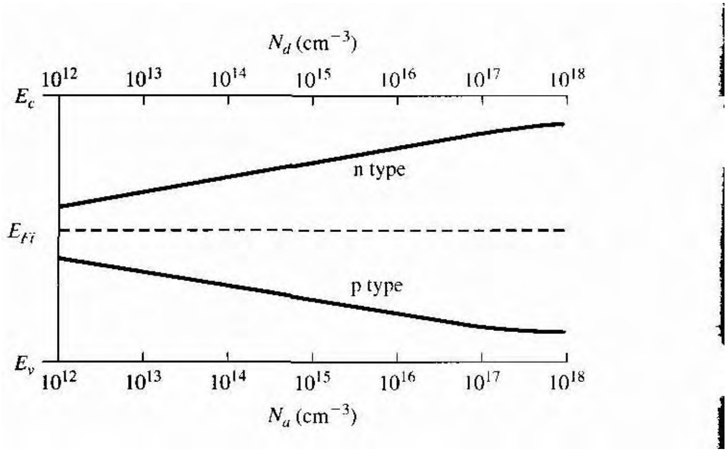

Figure 4.18 | Position of Fermi level as a function of donor concentration (n type) and acceptor concentration (p type).

EXAMPLE 4.14

Objective

To determine the Fermi-level position and the maximum doping at which the Boltzmann approximation is still valid.

Consider p-type silicon, at T = 300 K, doped with boron. We may assume that the limit of the Boltzmann approximation occurs when $E_F - E_a = 3kT$. (See Section 4.1.2.)

■ Solution

From Table 4.3, we find the ionization energy is $E_a - E_v = 0.045$ eV for boron in silicon. If we assume that $E_{Fi} \approx E_{\text{midgap}}$, then from Equation (4.68), the position of the Fermi level at the maximum doping is given by

$$E_{Fi} - E_F = \frac{E_g}{2} - (E_a - E_v) - (E_F - E_a) = kT \ln\left(\frac{N_a}{n_i}\right)$$

or

$$0.56 - 0.045 - 3(0.0259) = 0.437 = (0.0259) \ln\left(\frac{N_a}{n_i}\right)$$

We can then solve for the doping as

$$N_a = n_i \exp\left(\frac{0.437}{0.0259}\right) = 3.2 \times 10^{17}\ \text{cm}^{-3}$$

■ Comment

If the acceptor (or donor) concentration in silicon is greater than approximately 3×10^{17} cm^{-3}, then the Boltzmann approximation of the distribution function becomes less valid and the equations for the Fermi-level position are no longer quite as accurate.

TEST YOUR UNDERSTANDING

E4.13 Determine the position of the Fermi level with respect to the valence band energy in p type GaAs at T = 300 K. The doping concentrations are $N_a = 5 \times 10^{16}$ cm^{-3} and $N_d = 4 \times 10^{15}$ cm^{-3}. (Ans. $E_F - E_v = 0.130$ eV)

E4.14 Calculate the position of the Fermi energy level in n-type silicon at $T = 300$ K with respect to the intrinsic Fermi energy level. The doping concentrations are $N_d = 2 \times 10^{17}$ cm^{-3} and $N_a = 3 \times 10^{16}$ cm^{-3}. (Ans. $E_F - E_{Fi} = 0.421$ eV)

The intrinsic carrier concentration n_i, in Equations (4.65) and (4.68), is a strong function of temperature, so that E_F is a function of temperature also. Figure 4.19 shows the variation of the Fermi energy level in silicon with temperature for several donor and acceptor concentrations. As the temperature increases, n_i increases, and E_F moves closer to the intrinsic Fermi level. At high temperature, the semiconductor material begins to lose its extrinsic characteristics and begins to behave more like an intrinsic semiconductor. At the very low temperature, freeze-out occurs; the Boltzmann approximation is no longer valid and the equations we derived for the

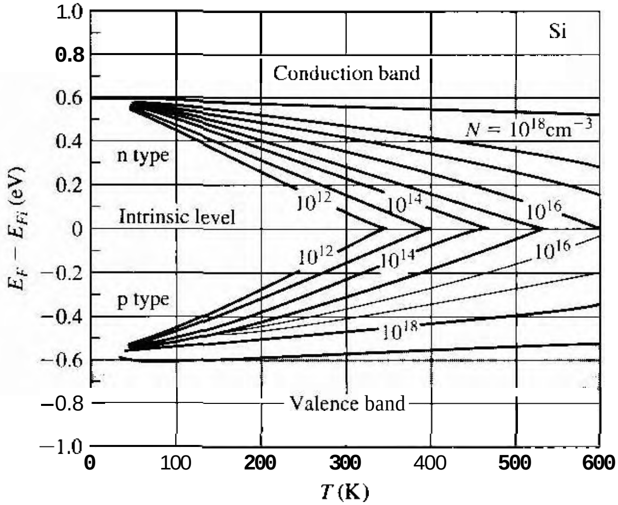

Figure 4.19 | Position of Fermi level as a function of temperature for various doping concentrations.
(From *Sze [13]*.)

Fermi-level position no longer apply. At the low temperature where freeze-out occurs, the Fermi level goes above E_d for the n-type material and below E_a for the p-type material. At absolute zero degrees, all energy states below E_F are full and all energy states above E_F are empty.

4.6.3 Relevance of the Fermi Energy

We have been calculating the position of the Fermi energy level as a function of doping concentrations and temperature. This analysis may seem somewhat arbitrary and fictitious. However, these relations do become significant later in our discussion of pn junctions and the other semiconductor devices we consider. An important point is that, in thermal equilibrium, the Fermi energy level is a constant throughout a system. We will not prove this statement, but we can intuitively see its validity by considering the following example.

Suppose we have a particular material, A, whose electrons are distributed in the energy states of an allowed band as shown in Figure 4.20a. Most of the energy states below E_{FA} contain electrons and most of the energy states above E_{FA} are empty of electrons. Consider another material, B, whose electrons are distributed in the energy states of an allowed band as shown in Figure 4.20b. The energy states below E_{FB} are mostly full and the energy states above E_{FB} are mostly empty. If these two materials are brought into intimate contact, the electrons in the entire system will tend to seek the lowest possible energy. Electrons from material A will flow into the lower energy states of material B, as indicated in Figure 4.20c, until thermal equilibrium is reached. Thermal equilibrium occurs when the distribution of electrons, as

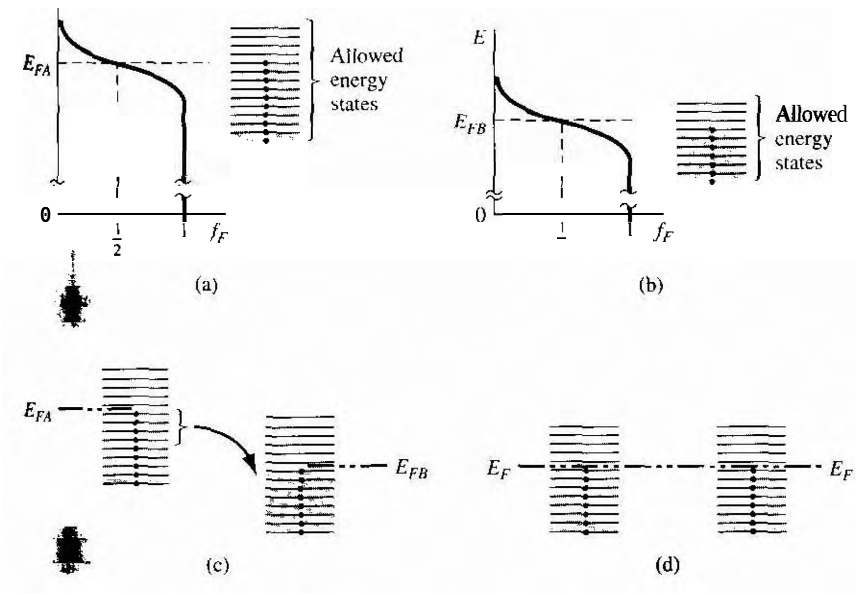

Figure 4.20 | The Fermi energy of (a) material A in thermal equilibrium, (b) material B in thermal equilibrium, (c) materials A and B at the instant they are placed in contact, and (d) materials A and B in contact at thermal equilibrium.

a function of energy, is the same in the two materials. This equilibrium state occurs when the Fermi energy is the same in the two materials as shown in Figure 4.20d. The Fermi energy, important in the physics of the semiconductor, also provides a good pictorial representation of the characteristics of the semiconductor materials and devices.

4.7 | SUMMARY

- The concentration of electrons in the conduction band is the integral over the conduction band energy of the product of the density of states function in the conduction band and the Fermi–Dirac probability function.
- The concentration of holes in the valence band is the integral over the valence band energy of the product of the density of states function in the valence band and the probability of a state being empty, which is $[1 - f_F(E)]$.
- Using the Maxwell–Boltzmann approximation, the thermal equilibrium concentration of electrons in the conduction band is given by

$$n_0 = N_c \exp\left[\frac{-(E_c - E_F)}{kT}\right]$$

where N_c is the effective density of states in the conduction band

- Using the Maxwell–Boltzmann approximation, the thermal equilibrium concentration of holes in the valence band is given by

  $$p_0 = N_v \exp\left[\frac{-(E_F - E_v)}{kT}\right]$$

  where N_v is the effective density of states in the valence band

  The intrinsic carrier concentration is found from

  $$n_i^2 = N_c N_v \exp\left[\frac{-E_g}{kT}\right]$$

- The concept of doping the semiconductor with donor (group V elements) impurities and acceptor (group III elements) impurities to form n-type and p-type extrinsic semiconductors was discussed.

  The fundamental relationship of $n_0 p_0 = n_i^2$ was derived.

  Using the concepts of complete ionization and charge neutrality, equations for the electron and hole concentrations as a function of impurity doping concentrations were derived.

  The position of the Fermi energy level as a function of impurity doping concentrations was derived.

  The relevance of the Fermi energy was discussed. The Fermi energy is a constant throughout a semiconductor that is in thermal equilibrium.

GLOSSARY OF IMPORTANT TERMS

acceptor atoms Impurity atoms added to a semiconductor to create a p-type material

charge carrier The electron and/or hole that moves inside the semiconductor and gives rise to electrical currents.

compensated semiconductor A semiconductor that contains both donors and acceptors i the same semiconductor region.

complete ionization The condition when all donor atoms are positively charged by givi up their donor electrons and all acceptor atoms are negatively charged by accepting electron

degenerate semiconductor A semiconductor whose electron concentration or hole conce tration is greater than the effective density of states, so that the Fermi level is in the condu tion band (n type) or in the valence band (p type).

donor atoms Impurity atoms added to a semiconductor to create an n-type material.

effective density of states The parameter N_c, which results from integrating the densty quantum states $g_c(E)$ times the Fermi function $f_F(E)$ over the conduction-band energy, a the parameter N_v, which results from integrating the density of quantum states $g_v(E)$ tim $[1 - f_F(E)]$ over the valence-band energy.

extrinsic semiconductor A semiconductor in which controlled amounts of donors and acceptors have been added so that the electron and hole concentrations change from th i trinsic carrier concentration and a preponderance of either electrons (n type) or holes (p typ is created.

freeze-out The condition that occurs in a semiconductor when the temperature is lower and the donors and acceptors become neutrally charged. The electron and hole concentratic become very small.

intrinsic carrier concentration n_i The electron concentration in the conduction hand and the hole concentration in the valence band (equal values) in an intrinsic semiconductor.

intrinsic Fermi level E_{Fi} The position of the Fermi level in an intrinsic semiconductor.

intrinsic semiconductor A pure semiconductor material with no impurity atoms and no lattice defects in the crystal.

nondegenerate semiconductor A semiconductor in which a relatively small number of donors and/or acceptors have been added so that discrete, noninteracting donor states and/or discrete, noninteracting acceptor states are introduced.

CHECKPOINT

After studying this chapter. the reader should have the ability to:

- Derive the equations for the thermal equilibrium concentrations of electrons and holes in terms of the Fermi energy.
- Derive the equation for the intrinsic carrier concentration.
- State the value of the intrinsic carrier concentration for silicon at $T = 300$ K.
- Derive the expression for the intrinsic Fermi level.
- Describe the effect of adding donor and acceptor impurity atoms to a semiconductor.
- Understand the concept of complete ionization.
- Understand the derivation of the fundamental relationship $n_0 p_0 = n_i^2$
- Describe the meaning of degenerate and nondegenerate semiconductors.
- Discuss the concept of charge neutrality.
- Derive the equations for n_0 and p_0 in terms of impurity doping concentrations.
- Discuss the variation of the Fermi energy with doping concentration and temperature.

REVIEW QUESTIONS

1. Write the equation for $n(E)$ as a function of the density of states and the Fermi probability function. Repeat for the function $p(E)$.
2. In deriving the equation for n_0 in terms of the Fermi function. the upper limit of the integral should be the energy at the top of the conduction hand. Justify using infinity instead.
3. Assuming the Boltzmann approximation applies, write the equations for n_0 and p_0 in terms of the Fermi energy.
4. What is the value of the intrinsic carrier concentration in silicon at $T = 300$ K?
5. Under what condition would the intrinsic Fermi level be at the midgap energy?
6. What is a donor impurity'! What is an acceptor impurity?
7. What is meant by complete ionization? What is meant by freeze-out?
8. What is the product of n_0 and p_0 equal to?
9. Write the equation for charge neutrality for the condition of complete ionization.
10. Sketch a graph of n_0 versus temperature for an n-type material.
11. Sketch graphs of the Fermi energy versus donor impurity concentration and versus temperature.

PROBLEMS

Section 4.1 Charge Carriers in Semiconductors

4.1 Calculate the intrinsic carrier concentration, n,. at T = 200. 400. and 600 K for (*a*) silicon, (*b*) germanium, and (*c*) gallium arsenide.

4.2 The intrinsic carrier concentration in silicon is to be no greater than $n_i = 1 \times 10^{12}$ cm^{-3}. Assume $E_g = 1.12$ eV. Determine the maximum temperature allowedfc the silicon.

4.3 Plot the intrinsic carrier concentration, n_i, for a temperature range of $200 \le T \le 600$ K for (*a*)silicon, (b) germanium, and (*c*) gallium arsenide. (Use a log scale for n_i.)

4.4 In a particular semiconductor material, the effective density of states functions are given hy $N_c = N_{c0}(T)^{3/2}$ and $N_v = N_{v0}(T)^{3/2}$ where N_{c0} and N_{v0} are consrants independent of temperature. The experimentally determined intrinsic carrier concentrations as a function of temperature are given in Table 4.5. Determine the product $N_{c0}N_{v0}$ and the bandgap energy E_g. (Assume E_g is independent of temperature.)

4.5 (*a*) The magnitude of the product $g_C(E)f_F(E)$ in the conduction band is a function energy as shown in Figure 4.1. Assume the Boltrmann approximation is valid. Determine the energy with respect to E_c at which the maximum occurs. (*b*) Repeat pan (*a* for the magnitude of the product $g_V(E)$ [I − $f_F(E)$] in the valence band.

4.6 Assume the Boltzmann approximation in a semiconductor is valid. Determine the ratio of $n(E) = g_C(E)f_F(E)$ at $E = E_c + 4kT$ to that at $E = E_c + kT/2$.

4.7 Assume that E, − $E_F = 0.20$ eV in silicon. Plot $n(E) = g_C(E)f_F(E)$ over the ran $E_c \le E \le E_c + 0.10$ eV for (*a*) $T = 200$ K and (*b*) $T = 400$ K.

4.8 Two semiconductor materials have exactly the same properties except that material has a bandgap energy of 1.0 eV and material B has a bandgap energy of 1.2 eV. Determine the ratio of n_i of material A to that of material B for $T = 300$ K.

4.9 (*a*) Consider silicon at $T = 300$ K. Plot the thermal equilibrium electron concentration n_0 (on a log scale) over the energy range $0.2 \le E_c - E_F \le 0.4$ eV. (*b*) Repeat part (*a*) lor the hole concentration over the range $0.2 \le E_F -$ E, ≤ 0.4 eV.

4.10 Given the effective messes of electrons and holes in silicon. germanium. and galliu arsenide, calculate the position of the intrinsic Fermi energy level with respect to th center of the bandgap for each semiconductor at $T = 300$ K.

4.11 (a)The carrier effective masses in a semiconductor are $m_n^* = 0.62m_0$ and $m_p^* = 1.4m$ Determine the oosition of the intrinsic Fermi level with resnect to the center of the bandgap at T = 300 K. ***(b)***Repeat pan (*a*) if $m_n^* = 1.10m_0$ and $m_p^* = 0.25m_0$.

Table 4.5 | Intrinsic concentration as a function of temperature

T (K)	n_i (cm^{-3})
200	1.82×10^{2}
300	5.83×10^{7}
400	3.74×10^{10}
500	1.95×10^{12}

4.12 Calculate E_{Fi} with respect to the center of the bandgap in silicon for $T = 200$, 400, and 600 K.

4.13 Plot the intrinsic Fermi energy E_{Fi} with respect to the center of the bandgap in silicon for $200 \le T \le 600$ K.

4.14 If the density of states function in the conduction band of a particular semiconductor is a constant equal to K, derive the expression for the thermal-equilibrium concentration of electrons in the conduction band, assuming Fermi–Dirac statistics and assuming the Boltzmann approximation is valid.

4.15 Repeat Problem 4.14 if the density of states function is given by $g_c(E) = C_1(E - E_c)$ for $E \ge E_c$ where C_1 is a constant.

Section 4.2 Dopant Atoms and Energy Levels

4.16 Calculate the ionization energy and radius of the donor electron in germanium using the Bohr theory. (Use the density of states effective mass as a first approximation.)

4.17 Repeat Problem 4.16 for gallium arsenide.

Section 4.3 The Extrinsic Semiconductor

4.18 The electron concentration in silicon at $T = 300$ K is $n_0 = 5 \times 10^4$ cm^{-3}. *(a)* Determine p_0. Is this n- or p-type material? *(b)* Determine the position of the Fermi level with respect to the intrinsic Fermi level.

4.19 Determine the values of n_0 and p_0 for silicon at $T = 300$ K if the Fermi energy is 0.22 eV above the valence band energy.

4.20 *(a)* If $E_c - E_F = 0.25$ eV in gallium arsenide at $T = 400$ K, calculate the values of n_0 and p_0. (b) Assuming the value of n_0 from part (a) remains constant, determine $E_c - E_F$ and p_0 at $T = 300$ K.

4.21 The value of p_0 in silicon at $T = 300$ K is 10^{15} cm^{-3}. Determine (a) $E_c - E_F$ and *(b)* n_0.

4.22 *(a)* Consider silicon at $T = 300$ K. Determine p_0 if $E_{Fi} - E_F = 0.35$ eV. *(b)* Assuming that p_0 from part *(a)* remains constant, determine the value of $E_{Fi} - E_F$ when $T = 400$ K. *(c)* Find the value of n_0 in both parts **(a)** and (b).

4.23 Repeat problem 4.22 for GaAs.

***4.24** Assume that $E_F = E_c$ at $T = 300$ K in silicon. Determine p_0.

***4.25** Consider silicon at $T = 300$ K, which has $n_0 = 5 \times 10^{19}$ cm^{-3}. Determine $E_c - E_F$.

Section 4.4 Statistics of Donors and Acceptors

***4.26** The electron and hole concentrations as a function of energy in the conduction band and valence band peak at a particular energy as shown in Figure 4.8. Consider silicon and assume $E_c - E_F = 0.20$ eV. Determine the energy, relative to the band edges, at which the concentrations peak.

***4.27** For the Boltzmann approximation to be valid for a semiconductor, the Fermi level must be at least 3kT below the donor level in an n-type material and at least 3kT above the acceptor level in a p-type material. If $T = 300$ K, determine the maximum electron concentration in an n-type semiconductor and the maximum hole concentration in a p-type semiconductor for the **Boltzmann** approximation to be valid in (*a*) silicon and (b) gallium arsenide.

4.28 Plot the ratio of un-ionized donor atoms to the total electron concentration versus temperature for silicon over the range $50 \leq T \leq 200$ K.

Section 4.5 Charge Neutrality

4.29 Consider a germanium semiconductor at T = 300 K. Calculate the thermal equilibrium concentrations of n_0 and p_0 for $(a) N_a = 10^{13}$ c m ^{3}. $N_d = 0$, and $(b)\ N_d = 5 \times 10^{15}$ cm^{-3}, $N_a = 0$.

***4.30** The Fermi level in n-type silicon at $T = 300$ K is 245 meV below the conduction band and 200 meV below the donor level. Determine the probability of finding an electron (*a*) in the donor level and (*b*) in a state in the conduction band kT above the conduction band edge.

4.31 Determine the equilibrium electron and hole concentrations in silicon for the following conditions:

(a) $T = 300$ K, $N_d = 2 \times 10^{15}$ cm^{-3}, $N_a = 0$

(b) $T = 300$ K. $N_d = 0$, N„ $= 10^{16}$ cm^{-3}

(*c*) T = 300 K. $N_d = N_a = 10^{15}$ cm^{-3}

(*d*) $T = 400$ K. $N_d = 0$. N„ $= 10^{14}$ cm^{-3}

(*e*) 7 = 500 K. $N_d = 10^{14}$ cm^{-3}. $N_a = 0$

4.32 Repeat problem 4.31 for GaAs.

4.33 Assume that silicon. germanium, and gallium arsenide each have dopant concentrations of $N_d =$ I x 10^{13} cm^{-3} and N, = 2.5 x 10^{13} cm^{-3} at T = 300 K. For eachof the three materials (*a*) Is this material n type or p type'?(*b*) Calculate n_0 and p_0.

4.34 A sample of silicon at T = 450 K is doped with boron at a concentration of 1.5 x 10^{15} cm ^{3} and with arsenic at a concentration of 8 **x** 10^{14} cm^{-3}. (*a*) Is the material n or p type? (*b*) Determine the electron and hole concentrations. (*c*) Calculate the total ionized impurity concentration.

4.35 The thermal equilibrium hole concentration in silicon at $T = 300$ K is $p_0 = 2 \times 10^5$ cm^{-3}. Determine the thermal equilibrium electron concentration. Is the material n type or p type?

4.36 In a sample of GaAs at $T = 200$ K, we have experimentally determined that $n_0 = 5p$ and that $N_a = 0$. Calculate n_0, p_0, and N_d.

4.37 Consider a sample of silicon doped at $N_d = 0$ and $N_a = 10^{14}$ cm^{-3}. Plot the majorit carrier concentration versus temperature over thr range $200 \leq T \leq 500$ K.

4.38 The temperature of a sample of silicon is T = 300 K and the acceptor doping conceo tration is N„ = 0. Plat the minority carrier concentratiun (on a log–log plot) versus N over the range $10^{15} \leq N_d \leq 10^{18}$ cm^{-3}.

4.39 Repeat problem **4.38** for GaAs.

4.40 A particular semiconductor material is doped at $N_d = 2 \times 10^{13}$ cm^{-3}. $N_a = 0$, and the intrinsic carrier concentration is $n_i = 2 \times 10^{13}$ cm^{-3}. Assume complete ionizatio Determine the thermal equilibrium majority and minority carrier concenuations.

4.41 ***(a)*** Silicon at $T = 300$ K is uniformly doped with arsenic atoms at a concentrationof 2 x 10^{16} cm^{-3} and boron atoms at a concentration of 1 x 10^{16} cm ^{3}. Determine the thermal equilibrium concentrations of majority and minority carriers. (b) Repeat part (a) if the impurity concentrations are 2 x 10^{15} cm^{-3} phosphorus atoms and 3 x 10^{16} cm^{-3} boron atoms.

4.42 In silicon at T = 300 K. we have experimentally found that n_0 = 4.5 x 10' cm^{-3} and N_d = 5 x 10'' cm^{-3}. *(a)* Is the material n type or p type? *(b)* Determine the majority and minority carrier concentrations. *(c)* What types and concentrations of impurity atoms exist in the material?

Section 4.6 Position of Fermi Energy Level

4.43 Consider germanium with an acceptor concentration of $N_a = 10^{15}$ cm^{-3} and a donor concentration of $N_d = 0$. Consider temperatures of T = 200,400. and 600 K. Calculate the position of the Fermi energy with respect to the intrinsic Fermi level at these temperatures.

4.44 Consider germanium at T = 300 K with donor concentrations of $N_d = 10^{14}$, 10^{16}, and 10^{18} cm^{-3}. Let $N_a = 0$. Calculate the position of the Fermi energy level with respect to the intrinsic Fermi level for these doping concentrations.

4.45 A GaAs device is doped with a donor concentration of 3 x 10^{15} cm^{-3}. For the device to operate properly. the intrinsic carrier concentration must remain less than 5 percent of the total electron concentration. What is the maximum temperature that the device may operate?

4.46 Consider germanium with an acceptor concentration of $N_a = 10^{15}$ cm^{-3} and a donor concentration of $N_d = 0$. Plot the position of the Fermi energy with respect to the intrinsic Fermi level as a function of temperature over the range $200 \le T \le 600$ K.

4.47 Consider silicon at T = 300 K with $N_a = 0$. Plot the position of the Fermi energy level with respect to the intrinsic Fermi level as a function of the donor doping concentration over the range $10^{14} \le N_d$ S 10^{18} cm^{-3}

4.48 For a particular semiconductor, $E_g = 1.50$ eV, $m_p^* = 10m_n^*$, $T = 300$ K, and n_i = I x 10^5 cm^{-3}. *(a)* Determine the position of the intrinsic Fermi energy level with respect to the center of the bandgap. *(b)* Impurity atoms are added so that the Fermi energy level is 0.45 eV below the center of the bandgap. *(i)* Are acceptor or donor atoms added? *(ii)* What is the concentration of impurity atoms added?

4.49 Silicon at T = 300 K contains acceptor atoms at a concentration of N_a = 5 x 10^{15} cm^{-3}. Donor atoms are added forming an n-type compensated semiconductor such that the Fermi level is 0.215 eV below the conduction band edge. What concentration of donor atoms are added?

4.50 Silicon at $T = 300$ K is doped with acceptor atoms at a concentration of N_a = 7 x 10^{15} cm^{-3}. (a) Determine E_F − E,. *(b)* Calculate the concentration of additional acceptor atoms that must be added to move the Fermi level a distance kT closer to the valence-band edge.

4.51 (a) Determine the position of the Fermi level with respect to the intrinsic Fermi level in silicon at T = 300 K that is doped with phosphorus atoms at a concentration of 10^{15} cm^{-3}. *(h)* Repeat part *(a)* if the silicon is doped with boron atoms at a concentration of 10^{15} cm^{-3}. *(c)* Calculate the electron concentration in the silicon for parts *(a)* and *(b)*.

4.52 Gallium arsenide at T = 300 K contains acceptor impurity atoms at a density of 10^{15} cm^{-3}. Additional impurity atoms are to be added so that the Fermi level is 0.45 eV below the intrinsic level. Determine the concentration and type (donor or acceptor) of impurity atoms to be added.

4.53 Determine the Fermi energy level with respect to the intrinsic Fermi level for each condition given in Problem 4.31

4.54 Find the Fermi energy level with respect to the valence band energy for **the conditi** given in Problem 4.32.

4.55 Calculate the position of the Fermi energy level with respect to the intrinsic Fermi fo the conditions given in Problem 4.42.

Summary and Review

3

4.56 A special semiconductor material is to he "designed." The semiconductor is to be n-type and doped with 1×10^{15} cm^{-3} donor atoms. Assume complete ionization and assume $N_a = 0$. The effective density of states functions are given by N, $= N_v =$ 1.5×10^{19} cm^{-3} and are independent of temperature. A particular semiconductor device fabricated with this material requires the electron concentration to he no greater than 1.01×10^{15} cm^{-3} at $T = 400$ K. What is the minimum value of the bandgap energy'!

4.57 Silicon atoms, at a concentration of 10^{10} c m ^{3}, are added to gallium arsenide. Assum that the silicon atoms act as fully ionized dopant atoms and that 5 percent of the c on-centration added replace gallium atoms and 95 percent replace arsenic atoms. Let $T = 300$ K. *(a)* Determine the donor and acceptor concmtrations. *(h)* Calculate the electron and hole concentrations and the position of the Fcrmi level with respect to ***E,,*** .

4.58 Defects in a semiconductor material introduce allowed energy states within the forbidden bandgap. Assume that a particular defect in silicon introduces two discrete lev els: a donor level 0.25 eV above the top of the valence band, and an acceptor level 0.65 eV above the top of the valence band. The charge state of each defect is a function of the position of the Fermi level. ***(a)*** Sketch the charge density of each defect as the Fermi level moves from ***E,*** to ***E,***. Which defect level dominates in heavily doped n-type material'? In heavily doped p-type material? *(h)* Determine the electron and hole concentrations and the location of the Fermi level in *(i)* an n-type sample doped at $N_d = 10^{17}$ cm^{-3} and ***(ii)*** in a p-type sample doped at $N_a = 10^{17}$ cm^{-3}. *(c)* Determine the Fermi level position if no dopant atoms are added. Is the material n-type, p-type, or intrinsic?

READING LIST

1.** Hess, K. *Advanced Theory* ***of Semiconductor *Devices*. Englewood Cliffs, NJ: Prentice Hall, 1988.

2. Kano, K. *Semiconductor* ***Devices.*** Upper Saddle River, NJ: Prentice Hall, 1998.

3.** Li, S. S. ***Semiconductor Physical *Electronics.* New York: Plenum Press. 1993.

4. McKelvey, J. P. *Solid* ***State*** *Physics for* ***Engineering*** *and Materials Science.* Malabar, FL.: Krieger Publishing, 1993.

5. Navon, D. H. *Semiconductor Microdevices and* ***Materials.*** New York: Halt, Rinehart &Winston. 1986.

6. Pierret, R. F. *Semiconductor* ***Device*** *Fundamentals.* Reading. ***MA:*** Addison-Wesley, 1996.

7. Shur, M. ***Introduction to*** *Electronic Devices.* New York: John Wiley and Sons, 1996.

***8.** Shur, M. *Physics of Semiconductor Devices.* Englewood Cliffs, NJ: Prentice Hall. 1990.

9. Singh, J. *Semiconductor Devices: An Introduction.* New York: McGraw-Hill, 1994.

10. Singh, J. *Semiconductor Devices: Basic Principles.* New York: John Wiley and Sons, 2001.

***11.** Smith, R. A. *Semiconductors.* 2nd ed. New York; Cambridge University Press, 1978.

12. Streetman, B. G., and S. Banerjee. *Solid State Electronic Devices.* 5th ed. Upper Saddle River, NJ: Prentice Hall, 2000.

13. Sze, S. M. *Physics of Semiconductor Devices.* 2nd ed. New York: Wiley, 1981.

***14.** Wang, S. *Fundamentals of Semiconductor Theory and Device Physics.* Englewood Cliffs, NJ: Prentice Hall, 1989.

***15.** Wolfe, C. M., N. Holonyak, Jr, and G. E. Stillman. *Physical Properties of Semiconductors.* Englewood Cliffs, NJ: Prentice Hall. 1989.

16. Yang, E. S. *Microelectronic Devices.* New York: McGraw-Hill, 1988.

CHAPTER 5

Carrier Transport Phenomena

PREVIEW

In the previous chapter, we considered the semiconductor in equilibrium and determined electron and hole concentrations in the conduction and valence bands, respectively. A knowledge of the densities of these charged particles is important toward an understanding of the electrical properties of a semiconductor material. The net flow of the electrons and holes in a semiconductor will generate currents. The process by which these charged particles move is called ***transport.*** In this chapter we will consider the two basic transport mechanisms in a semiconductor crystal: drift—the movement of charge due to electric fields, and diffusion—the flow of charge due to density gradients. We should mention, in passing, that temperature gradients in a semiconductor can also lead to carrier movement. However, as the semiconductor device size becomes smaller, this effect can usually be ignored. The carrier transport phenomena are the foundation for finally determining the current-voltage characteristics of semiconductor devices. We will implicitly assume in this chapter that, though there will be a net flow of electrons and holes due to the transport processes, thermal equilibrium will not be substantially disturbed. Nonequilibrium processes will be considered in the next chapter. ■

5.1 | CARRIER DRIFT

An electric field applied to a semiconductor will produce a force on electrons and holes so that they will experience a net acceleration and net movement, provided there are available energy states in the conduction and valence bands. This net movement of charge due to an electric field is called *drift.* The net drift of charge gives rise to a ***drift current.***

5.1.1 Drift Current Density

If we have a positive volume charge density ρ moving at an average drift velocity v_d, the drift current density is given by

$$J_{drf} = \rho v_d \tag{5.1}$$

where J is in units of C/cm^2-s or amps/cm^2. If the volume charge density is due to positively charged holes, then

$$J_{p|drf} = (ep)v_{dp} \tag{5.2}$$

where $J_{p|drf}$ is the drift current density due to holes and v_{dp} is the average drift velocity of the holes.

The equation of motion of a positively charged hole in the presence of an electric field is

$$F = m_p^* a = e\text{E} \tag{5.3}$$

where e is the magnitude of the electronic charge, a is the acceleration, E is the electric field, and m_p^* is the effective mass of the hole. If the electric field is constant, then we expect the velocity to increase linearly with time. However, charged particles in a semiconductor are involved in collisions with ionized impurity atoms and with thermally vibrating lattice atoms. These collisions, or scattering events, alter the velocity characteristics of the particle.

As the hole accelerates in a crystal due to the electric field, the velocity increases. When the charged particle collides with an atom in the crystal, for example, the panicle loses most, or all, of its energy. The particle will again begin to accelerate and gain energy until it is again involved in a scattering process. This continues over and over again. Throughout this process, the particle will gain an average drift velocity which, for low electric fields, is directly proportional to the electric field. We may then write

$$v_{dp} = \mu_p \text{E} \tag{5.4}$$

where μ_p is the proportionality factor and is called the *hole mobility*. The mobility is an important parameter of the semiconductor since it describes how well a particle will move due to an electric tield. The unit of mobility is usually expressed in terms of cm^2/V-s.

By combining Equations *(5.2)* and (5.4). we may write the drift current density due to holes as

$$J_{p|drf} = (ep)v_{dp} = e\mu_p p\text{E} \tag{5.5}$$

The drift current due to holes is in the same direction as the applied electric field.

The same discussion of drift applies to electrons. We may write

$$J_{n|drf} = \rho v_{dn} = (-en)v_{dn} \tag{5.6}$$

where $J_{n|drf}$ is the drift current density due to electrons and v_{dn} is the average drift velocity of electrons. The net charge density of electrons is negative.

Table 5.1 | Typical mobility values at $T = 300$ K and low doping concentrations

	μ_n (cm^2/V-s)	μ_p (cm^2/V-s)
Silicon	1350	480
Gallium arsenide	8500	400
Germanium	3900	1900

The average drift velocity of an electron is also proportional to the electric fiel for small fields. However, since the electron is negatively charged, the net motion o the electron is opposite to the electric field direction. We can then write

$$\upsilon_{dn} = -\mu_n \mathrm{E} \qquad (5$$

where μ_n is the *electron mobility* and is a positive quantity. Equation (5.6) may no be written as

$$J_{n|drf} = (-en)(-\mu_n \mathrm{E}) = e\mu_n n \mathrm{E} \qquad (5.8$$

The conventional drift current due to electrons is also in the same direction as th applied electric field even though the electron movement is in the opposite directio

Electron and hole mobilities are functions of temperature and doping concentra tions, as we will see in the next section. Table 5.1 shows some typical mobility val ues at T = 300 K for low doping concentrations.

Since both electrons and holes contribute to the drift current, the total *drift curren density* is the sum of the individual electron and hole drift current densities, so we ma write

$$\boxed{J_{drf} = e(\mu_n n + \mu_p p)\mathrm{E}} \qquad (5.$$

EXAMPLE 5.1

Objective

To calculate the drift current density in a semiconductor for a given electric field.

Consider a gallium arsenide sample at $T = 300$ K with doping concentrations of $N_a =$ and $N_d = 10^{16}$ cm^{-3}. Assume complete ionization and assume electron and hole mobiliti given in Table 5.1. Calculate the drift current density if the applied electric field is E = 10 V/c

■ Solution

Since $N_d > N_a$, the semiconductor is n type and the majority carrier electron concentratio from Chapter 4 is given by

$$n = \frac{N_d - N_a}{2} + \sqrt{\left(\frac{N_d - N_a}{2}\right)^2 + n_i^2} \approx 10^{16} \text{ cm}^{-3}$$

The minority carrier hole concentration is

$$p = \frac{n_i^2}{n} = \frac{(1.8 \times 10^6)^2}{10^{16}} = 3.24 \times 10^{-4} \text{ cm}^{-3}$$

For this extrinsic n-type semiconductor, the drift current density is

$$J_{drf} = e(\mu_n n + \mu_p p)\mathrm{E} \approx e\mu_n N_d \mathrm{E}$$

Then

$$J_{drf} = (1.6 \times 10^{-19})(8500)(10^{16})(10) = 136 \text{ A/cm}^2$$

■ **Comment**

Significant drift current densities can be obtained in a semiconductor applying relatively small electric fields. We may note from this example that the drift current will usually be due primarily to the majority carrier in an extrinsic semiconductor.

TEST YOUR UNDERSTANDING

E5.1 Consider a sample of silicon at T = 300 K doped at an impurity concentration of $N_d = 10^{15}$ cm^{-3} and $N_a = 10^{14}$ cm^{-3}. Assume electron and hole mobilities given in Table 5.1. Calculate the drift current density if the applied electric field is E = 35 V/cm. (Ans. 6.80 A/cm^2)

E5.2 A drift current density of $J_{drf} = 120$ A/cm^2 is required in a particular semiconductor device using p-type silicon with an applied electric field of E = 20 V/cm. Determine the required impurity doping concentration to achieve this specification. Assume electron and hole mobilities given in Table 5.1. (Ans. $p_0 = N_a = 7.81 \times 10^{16}$ cm^{-3})

5.1.2 Mobility Effects

In the last section, we defined mobility, which relates the average drift velocity of a carrier to the electric field. Electron and hole mobilities are important semiconductor parameters in the characterization of carrier drift, as seen in Equation (5.9).

Equation (5.3) related the acceleration of a hole to a force such as an electric field. We may write this equation as

$$F = m_p^* \frac{dv}{dt} = e\mathrm{E} \tag{5.10}$$

where v is the velocity of the particle due to the electric field and does not include the random thermal velocity. If we assume that the effective mass and electric field are constants, then we may integrate Equation (5.10) and obtain

$$v = \frac{e\mathrm{E}t}{m_p^*} \tag{5.11}$$

where we have assumed the initial drift velocity to be zero.

Figure 5.1a shows a schematic model of the random thermal velocity and motion of a hole in a semiconductor with zero electric field. There is a mean time between collisions which may be denoted by τ_{cp}. If a small electric field (E-field) is

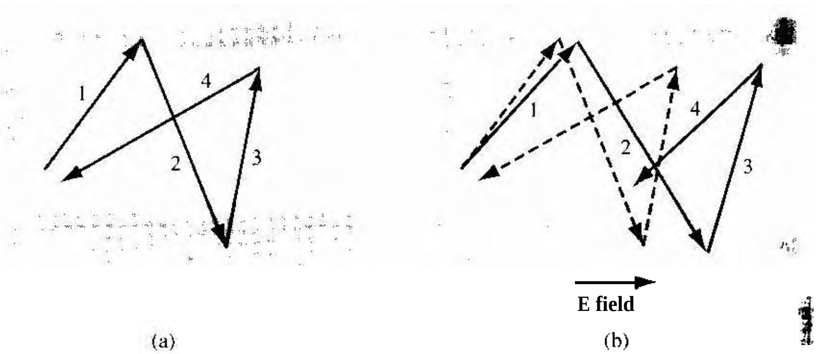

(a) (b)

Figure 5.1 | Typical random behavior of a hole in a semiconductor (a) without an electric field and (b) with an electric field.

applied as indicated in Figure 5.1b, there will be a net drift of the hole in the direction of the E-field, and the net drift velocity will be a small perturbation on the random thermal velocity, so the time between collisions will not be altered appreciably. If we use the mean time between collisions τ_{cp} in place of the time t in Equation (5.11), then the mean peak velocity just prior to a collision or scattering event is

$$v_{d|\text{peak}} = \left(\frac{e\tau_{cp}}{m_p^*}\right)\mathrm{E} \tag{5.12a}$$

The average drift velocity is one half the **peak** value so that we can write

$$\langle v_d \rangle = \frac{1}{2}\left(\frac{e\tau_{cp}}{m_p^*}\right)\mathrm{E} \tag{5.12b}$$

However, the collision process is not as simple as this model, but is statistical in nature. In a more accurate model including the effect of a statistical distribution, the factor $\frac{1}{2}$ in Equation (5.12b) does not appear. The hole mobility is then given by

$$\mu_p = \frac{v_{dp}}{\mathrm{E}} = \frac{e\tau_{cp}}{m_p^*}$$

The same analysis applies to electrons; thus we can write the electron mobility as

$$\mu_n = \frac{e\tau_{cn}}{m_n^*} \tag{5.14}$$

where τ_{cn} is the mean time between collisions for an electron.

There are two collision or scattering mechanisms that dominate in a semiconductor and affect the carrier mobility: phonon or lattice scattering, and ionized impurity scattering.

The atoms in a semiconductor crystal have a certain amount of thermal energy at temperatures above absolute zero that causes the atoms to randomly vibrate about their lattice position within the crystal. The lattice vibrations cause a disruption in the perfect periodic potential function. A perfect periodic potential in a solid allows electrons to move unimpeded, or with no scattering, through the crystal. But the thermal vibrations cause a disruption of the potential function, resulting in an interaction between the electrons or holes and the vibrating lattice atoms. This *lattice scattering* is also referred to as *phonon scattering.*

Since lattice scattering is related to the thermal motion of atoms, the rate at which the scattering occurs is a function of temperature. If we denote μ_L as the mobility that would be observed if only lattice scattering existed, then the scattering theory states that to first order

$$\mu_L \propto T^{-3/2} \tag{5.15}$$

Mobility that is due to lattice scattering increases as the temperature decreases. Intuitively, we expect the lattice vibrations to decrease as the temperature decreases, which implies that the probability of a scattering event also decreases, thus increasing mobility.

Figure 5.2 shows the temperature dependence of electron and hole mobilities in silicon. In lightly doped semiconductors, lattice scattering dominates and the carrier mobility decreases with temperature as we have discussed. The temperature dependence of mobility is proportional to T^{-n}. The inserts in the figure show that the parameter n is not equal to ; as the first-order scattering theory predicted. However, mobility does increase as the temperature decreases.

The second interaction mechanism affecting carrier mobility is called *ionized impurity scattering.* We have seen that impurity atoms are added to the semiconductor to control or alter its characteristics. These impurities are ionized at room temperature so that a coulomb interaction exists between the electrons or holes and the ionized impurities. This coulomb interaction produces scattering or collisions and also alters the velocity characteristics of the charge canier. If we denote μ_I as the mobility that would be observed if only ionized impurity scattering existed, then to first order we have

$$\mu_I \propto \frac{T^{+3/2}}{N_I} \tag{5.16}$$

where $N_I = N_d^+ + N_a^-$ is the total ionized impurity concentration in the semiconductor. If temperature increases, the random thermal velocity of a carrier increases, reducing the time the carrier spends in the vicinity of the ionized impurity center. The less time spent in the vicinity of a coulomb force, the smaller the scattering effect and the larger the expected value of μ_I. If the number of ionized impurity centers increases, then the probability of a carrier encountering an ionized impurity center increases, implying a smaller value of μ_I.

Figure 5.3 is a plot of electron and hole mobilities in germanium, silicon, and gallium arsenide at T = 300 K as a function of impurity concentration. More accurately, these curves are of mobility versus ionized impurity concentration N_I. As the impurity concentration increases, the number of impurity scattering centers increases, thus reducing mobility.

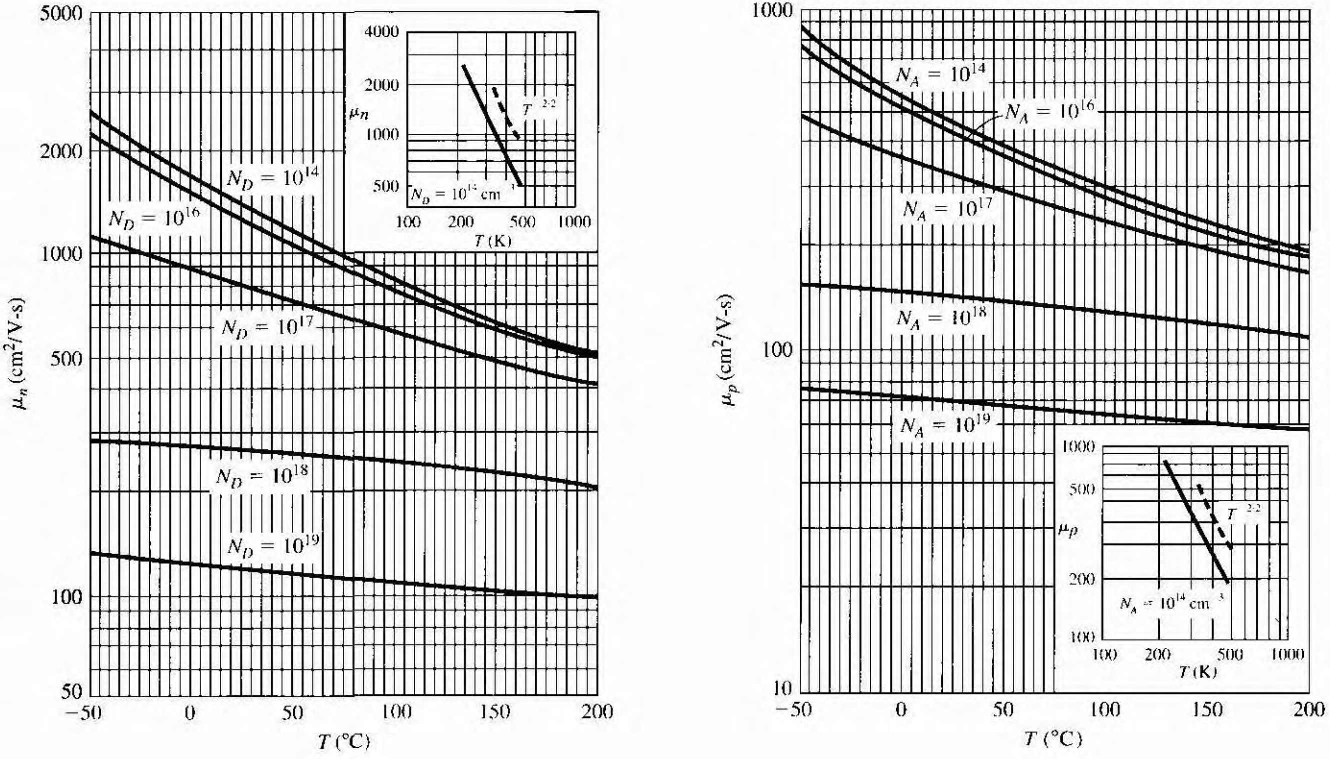

(a)

(b)

Figure 5.2 | (a) Electron and (b) hole mobilities in silicon versus temperature for various doping concentrations. Inserts show temperature dependence for "almost" intrinsic silicon.

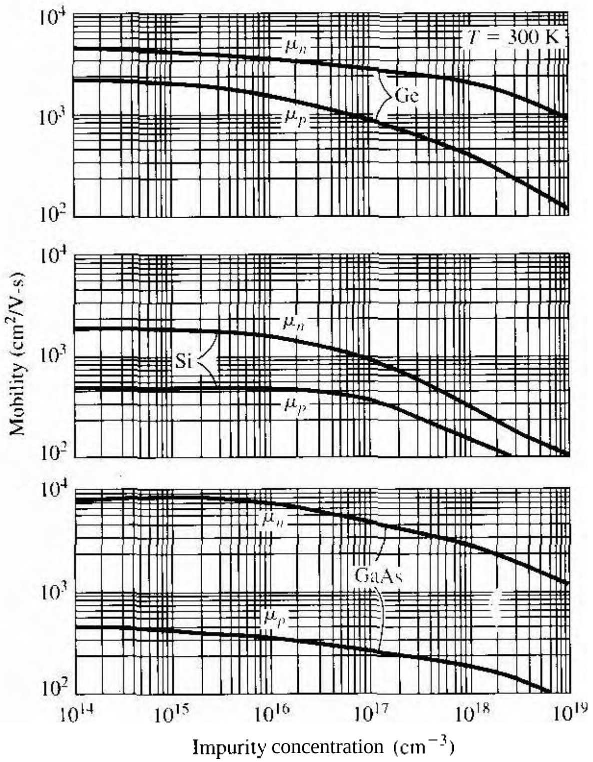

Figure 5.3 | Electron and hole mobilities versus impurity concentrations for germanium, silicon, and gallium arsenide at T = 300 K.
(From Sze [12].)

TEST YOUR UNDERSTANDING

E5.3 ***(a)*** Using Figure *5.2*, find the electron mobility for *(i)* $N_d = 10^{17}$ cm^{-3}, $T = 150$°C and ***(ii)*** $N_d = 10^{16}$ cm^{-3}, $T = 0$°C. *(b)* Find the hole mobilities for *(i)* $N_a = 10^{16}$ cm^{-3}, $T = 50$°C; and *(ii)* $N_a = 10^{17}$ cm^{-3}, $T = 150$°C.
[Ans. *(a) (i)* 500 cm^2/V-s, *(ii)* ~1500 cm^2/V-s; *(b) (i)* ~380 cm^2/V-s, *(ii)* ~200 cm^2/V-s]

E5.4 Using Figure 5.3, determine the electron and hole mobilities in ***(a)*** silicon for $N_d = 10^{15}$ cm^{-3}, $N_a = 0$; *(b)* silicon for $N_d = 10^{17}$ cm^{-3}, $N_a = 5 \times 10^{16}$ cm^{-3}; (c) silicon for $N_d = 10^{16}$ cm^{-3}, $N_a = 10^{17}$ cm^{-3}; and *(d)* GaAs for $N_d = N_a = 10^{17}$ cm^{-3}.
[Ans. *(a)* $\mu_n \approx 1350$, $\mu_p = 480$; *(b)* $\mu_n \approx 700$, $\mu_p \approx 300$; *(c)* $\mu_n \approx 800$, $\mu_p \approx 310$; *(d)* $\mu_n \approx 4500$, $\mu_p \approx 220$ cm^2/V-s]

If τ_L is the mean time between collisions due to lattice scattering, then dt/τ_L is the probability of a lattice scattering event occurring in a differential time dt. Likewise, if τ_I is the mean time between collisions due to ionized impurity scattering, then dt/τ_I is the probability of an ionized impurity scattering event occurring in th differential time **dt.** If these two scattering processes are independent, then the tota probability of a scattering event occurring in the differential time **dt** is the sum of th individual events, or

$$\frac{dt}{\tau} = \frac{dt}{\text{TI}} + \frac{dt}{\tau_L}$$ (5.1

where r is the mean time between any scattering event.

Comparing Equation (5.17) with the definitions of mobility given by Equa tion (5.13) or (5.14), we can write

$$\boxed{\frac{1}{\mu} = \frac{1}{\mu_I} + \frac{1}{\mu_L}}$$

where μ_I is the mobility due to the ionized impurity scattering process and μ_L is th mobility due to the lattice scattering process. The parameter μ is the net mobilit With two or more independent scattering mechanisms, the inverse mobilities add which means that the net mobility decreases.

5.1.3 Conductivity

The drift current density, given by Equation (5.9), may be written as

$$J_{drf} = e(\mu_n n + \mu_p p)\mathrm{E} = \sigma \mathrm{E}$$ (5.19

where σ is the **conductivity** of the semiconductor material. The conductivity is give in units of $(\Omega\text{-cm})^{-1}$ and is a function of the electron and hole concentrations and mobilities. We have just seen that the mobilities are functions of impurity concentration, conductivity, then is a somewhat complicated function of impurity concentration.

The reciprocal of conductivity is **resistivity,** which is denoted by ρ and is give in units of ohm-cm. We can write the formula for resistivity as

$$\boxed{\rho = \frac{1}{\sigma} = \frac{1}{e(\mu_n n + \mu_p p)}}$$ (5.2

Figure 5.4 is a plot of resistivity as a function of impurity concentration in silico germanium, gallium arsenide, and gallium phosphide at T = 300 K. Obviously, th curves are not linear functions of N_d or N_a because of mobility effects.

If we have a bar of semiconductor material as shown in Figure 5.5 with a voltage applied that produces a current I, then we can write

$$J = \frac{I}{A}$$ (5.21a

and

$$\mathrm{E} = \frac{V}{L}$$ (5.21b

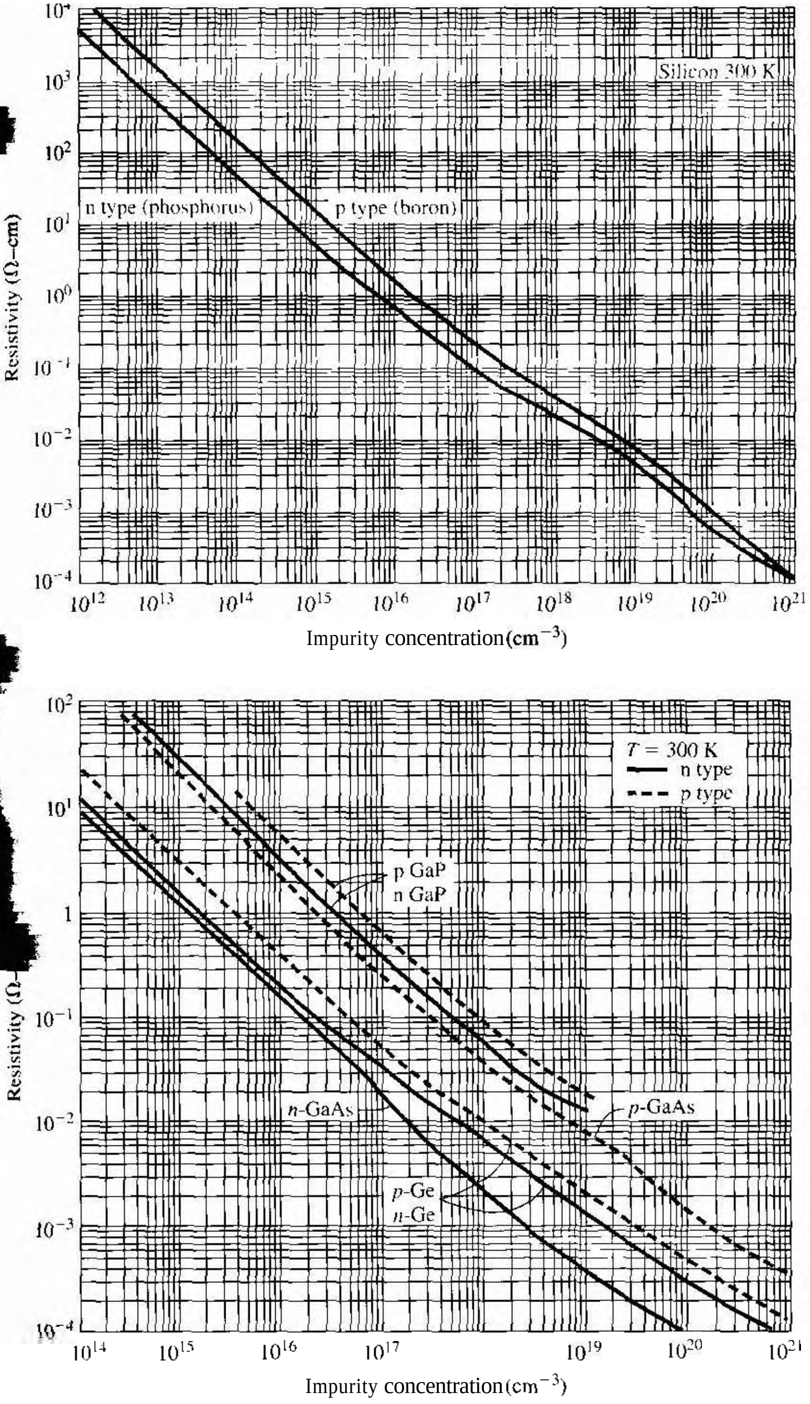

Figure 5.4 | Resistivity versus impurity concentration at $T = 300$ K in (a) silicon and (b) germanium, gallium arsenide, and gallium phosphide.
(From Sze [12].)

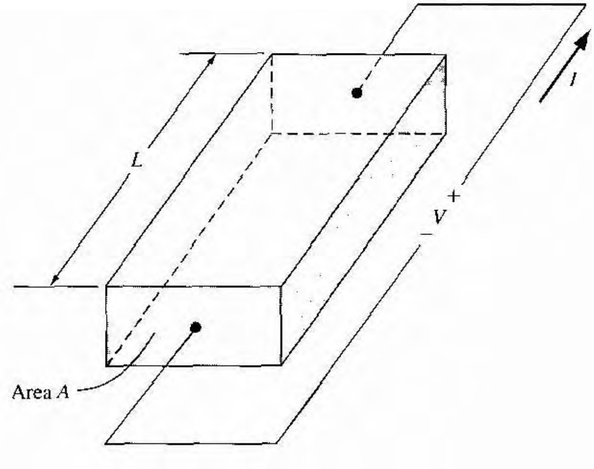

Figure 5.5 | Bar of semiconductor material as a resistor.

We can now rewrite Equation (5.19) as

$$\frac{I}{A} = \sigma\left(\frac{V}{L}\right) \tag*{(5.22}$$

or

$$V = \left(\frac{L}{\sigma A}\right) I = \left(\frac{\rho L}{A}\right) I = IR \tag*{(5.22}$$

Equation (5.22b) is Ohm's law for a semiconductor. The resistance is a function of resistivity, or conductivity, as well as the geometry of the semiconductor.

If we consider. for example, a p-type semiconductor with an acceptor doping $N_a (N_d = 0)$ in which $N_a \gg n_i$, and if we assume that the electron and hole mobilities are of the same order of magnitude, then the conductivity becomes

$$\sigma = e(\mu_n n + \mu_p p) \approx e\mu_p p \tag*{(5.23)}$$

If we also assume complete ionization, then Equation (5.23) becomes

$$\sigma \approx e\mu_p N_a \approx \frac{1}{\rho} \tag*{(5.24)}$$

The conductivity and resistivity of an extrinsic semiconductor are a function primarily of the majority carrier parameters.

We may plot the carrier concentration and conductivity of a semiconductor as a function of temperature for a particular doping concentration. Figure 5.6 shows the electron concentration and conductivity of silicon as a function of inverse temperature for the case when $N_d = 10^{15}$ cm^{-3}. In the midtemperature range, or extrinsic range, as shown, we have complete ionization—the electron concentration remains essentially constant. However, the mobility is a function of temperature so the conductivity

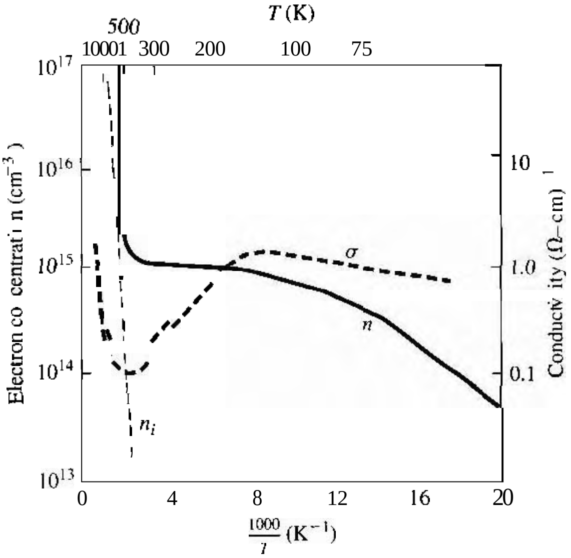

Figure 5.6 | Electron concentration and conductivity versus inverse temperature for silicon.
(After Sze [12].)

varies with temperature in this range. At higher temperatures, the intrinsic carrier concentration increases and begins to dominate the electron concentration as well as the conductivity. In the lower temperature range, freeze-out begins to occur; the electron concentration and conductivity decrease with decreasing temperature.

Objective

EXAMPLE 5.2

To determine the doping concentration and majority carrier mobility given the type and conductivity of a compensated semiconductor

Consider compensated n-type silicon at T = 300 K, with a conductivity of $\sigma = 16\,(\Omega\text{-cm})^{-1}$ and an acceptor doping concentration of 10^{17} cm^{-3}. Determine the donor concentration and the electron mobility.

■ Solution

For n-type silicon at $T = 300$ K, we can assume complete ionization; therefore the conductivity, assuming $N_d - N_a \gg n_i$, is given by

$$\sigma \approx e\mu_n n = e\mu_n(N_d - N_a)$$

We have that

$$16 = (1.6 \times 10^{-19})\mu_n(N_d - 10^{17})$$

Since mobility is a function of the ionized impurity concentration. we can use Figure 5.3 along with trial and error to determine μ_n and N_d. For example, if we choose $N_d = 2 \times 10^{17}$, then

$N_I = N_d^+ + N_a^- = 3 \times 10^{17}$ so that $\mu_n \approx 510$ cm²/V-s which gives $\sigma = 8.16\ (\Omega\text{-cm})^-$ If we choose $N_d = 5 \times 10^{17}$, then $N_I =$ h $\times 10^{17}$ so that $\mu_n \approx 325$ cm²/V-s, which giv $\sigma = 20.8\ (\Omega\text{-cm})^{-1}$. The doping is bounded between these two values. Further trial ander yields

$$N_d \approx 3.5 \times 10^{17}\ \text{cm}^{-3}$$

and

$$\mu_n \approx 400\ \text{cm}^2/\text{V-s}$$

which gives

$$\sigma \approx 16\ (\Omega\text{-cm})^{-1}$$

■ Comment

We can see from this example that, in high-conductivity semiconductor material, mobility is strong function of carrier concentration.

DESIGN EXAMPLE 5.3

Objective

To design a semiconductor resistor with a specified resistance to handle a given current densit

A silicon semiconductor at T = 300 K is initially doped with donors at a concentration $N_d = 5 \times 10^{15}$ cm^{-3}. Acceptors are to be added to form a compensated p-type material. Th resistor is to have a resistance of 10 kΩ and handle a current density of 50 A/cm² when 5 V applied.

Solution

For 5 V applied to a 10-kΩ resistor, the total current is

$$I = \frac{V}{R} = \frac{5}{10} = 0.5\ \text{mA}$$

If the current density is limited to 50 A/cm², then the cross-sectional area is

$$A = \frac{I}{J} = \frac{0.5 \times 10^{-3}}{50} = 10^{-5}\ \text{cm}^2$$

If we, somewhat arbitrarily at this point, limit the electric field to E = 100 V/cm, then th length of the resistor is

$$L = \frac{V}{\text{E}} = \frac{5}{100} = 5 \times 10^{-2}\ \text{cm}$$

From Equation (5.22b), the conductivity of the semiconductor is

$$\sigma = \frac{L}{RA} = \frac{5 \times 10^{-2}}{(10^4)(10^{-5})} = 0.50\ (\Omega\text{-cm})^{-1}$$

The conductivity of a compensated p-type semiconductor is

$$\sigma \approx e\mu_p p = e\mu_p(N_a - N_d)$$

where the mobility is a function of the total ionized impurity concentration $N_a + N_d$.

Using trial and error, if $N_a = 1.25 \times 10^{16}$ cm^{-3}, then $N_a + N_d = 1.75 \times 10^{16}$ cm^{-3}, and the hole mobility, from Figure 5.3, is approximately $\mu_p = 410$ cm^2/V-s. The conductivity is then

$$\sigma = e\mu_p(N_a - N_d) = (1.6 \times 10^{-19})(410)(1.25 \times 10^{16} - 5 \times 10^{15}) = 0.492$$

which is very close to the value we need

■ Comment

Since the mobility is related to the total ionized impurity concentration, the determination of the impurity concentration to achieve a particular conductivity is not straightforward.

TEST YOUR UNDERSTANDING

E5.5 Silicon at T = 300 K is doped with impurity concentrations of $N_d = 5 \times 10^{16}$ cm^{-3} and $N_a = 2 \times 10^{16}$ cm^{-3}. (a) What are the electron and hole mobilities? (*b*) Determine the conductivity and resistivity of the material.
[Ans. (*a*) $\mu_n = 1000$ cm^2/V-s, $\mu_p = 350$ cm^2/V-s; (*b*) $\sigma = 4.8$ $(\Omega\text{-cm})^{-1}$, $\rho = 0.208$ Ω-cm]

E5.6 For a particular silicon semiconductor device at T = 300 K, the required material is n type with a resistivity of 0.10 Ω-cm. (*a*) Determine the required impurity doping concentration and (b) the resulting electron mobility.
[Ans. (*a*) From Figure 5.4, $N_d \approx 9 \times 10^{16}$ cm^{-3}, (*b*) $\mu_n \approx 695$ cm^2/V-s]

E5.7 A bar of p-type silicon, such as shown in Figure 5.5, has a cross-sectional area of $A = 10^{-6}$ cm^2 and a length of $L = 1.2 \times 10^{-3}$ cm. For an applied voltage of 5 V, a current of 2 mA is required. What is the required (*a*) resistance, (*b*) resistivity of the silicon, and (*c*) impurity doping concentration?
[Ans. (*a*) 2.5 kΩ, (*b*) 2.08 Ω-cm, (*c*) $N_a \approx 7 \times 10^{15}$ cm^{-3}]

For an intrinsic material, the conductivity can be written as

$$\sigma_i = e(\mu_n + \mu_p)n_i \tag{5.25}$$

The concentrations of electrons and holes are equal in an intrinsic semiconductor, so the intrinsic conductivity includes both the electron and hole mohility. Since, in general, the electron and hole mobilities are not equal, the intrinsic conductivity is not the minimum value possible at a given temperature.

5.1.4 Velocity Saturation

So far in our discussion of drift velocity, we have assumed that mobility is not a function of electric field, meaning that the drift velocity will increase linearly with applied electric field. The total velocity of a particle is the sum of the random thermal velocity and drift velocity. At T = 300 K, the average random thermal energy is given by

$$\tfrac{1}{2}mv_{th}^2 = \tfrac{3}{2}kT = \tfrac{3}{2}(0.0259) = 0.03885 \text{ eV} \tag{5.26}$$

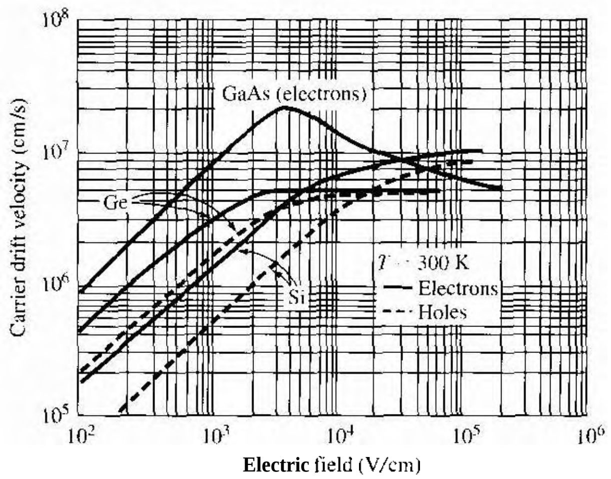

Figure 5.7 | Carrier drift velocity versus electric field for high-purity silicon. germanium, and gallium arsenide. *(From Sze [12].)*

This energy translates into a mean thermal velocity of approximately 10^7 cm/s for an electron in silicon. If we assume an electron mobility of $\mu_n = 1350$ cm^2/V-s in low-doped silicon, a drift velocity of 10^5 cm/s, or 1 percent of the thermal velocity, is achieved if the applied electric field is approximately 75 V/cm. This applied electric field does not appreciably alter the energy of the electron.

Figure 5.7 is a plot of average drift velocity as a function of applied electric field for electrons and holes in silicon, gallium arsenide, and germanium. At low electric fields, where there is a linear variation of velocity with electric field, the slope of the drift velocity versus electric field curve is the mobility. The behavior of the drift velocity of carriers at high electric fields deviates substantially from the linear relationship observed at low fields. The drift velocity of electrons in silicon, for example. saturates at approximately 10^7 cm/s at an electric field of approximately 30 kV/cm. If the drift velocity of a charge carrier saturates, then the drift current density also saturates and becomes independent of the applied electric field.

The drift velocity versus electric field characteristic of gallium arsenide is more complicated than for silicon or germanium. At low fields, the slope of the drift velocity versus E-field is constant and is the low-field electron mobility, which is approximately 8500 cm^2/V-s for gallium arsenide. The low-field electron mobility in gallium arsenide is much larger than in silicon. As the field increases, the electron drift velocity in gallium arsenide reaches a peak and then decreases. A differential mobility is the slope of the v_d versus E curve at a particular point on the curve and the negative slope of the drift velocity versus electric field represents a negative differential mobility. The negative differential mobility produces a negative differential resistance; this characteristic is used in the design of oscillators.

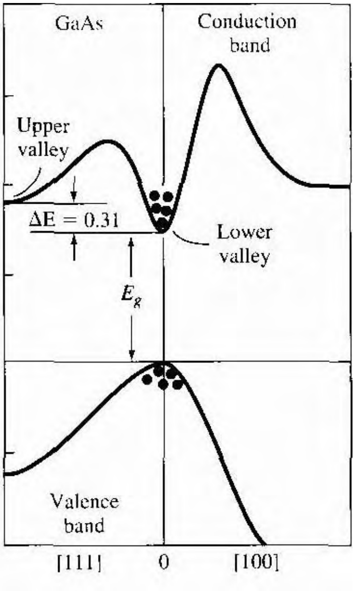

Figure 5.8 | Energy-band structure for gallium arsenide showing the upper valley and lower valley in the conduction band.
(From Sze [13].)

The negative differential mobility can be understood by considering the E versus k diagram for gallium arsenide, which is shown again in Figure 5.8. The density of states effective mass of the electron in the lower valley is $m_n^* = 0.067m_0$. The small effective mass leads to a large mobility. As the E-field increases. the energy of the electron increases and the electron can be scattered into the upper valley, where the density of states effective mass is $0.55m_0$. The larger effective mass in the upper valley yields a smaller mobility. This intervalley transfer mechanism results in a decreasing average drift velocity of electrons with electric field, or the negative differential mobility characteristic.

5.2 | CARRIER DIFFUSION

There is a second mechanism, in addition to drift, that can induce a current in a semiconductor. We may consider a classic physics example in which a container, as shown in Figure 5.9, is divided into two parts by a membrane. The left side contains gas molecules at a particular temperature and the right side is initially empty. The gas molecules are in continual random thermal motion so that, when the membrane is broken, the gas molecules flow into the right side of the container. *Diffusion* is the process whereby particles flow from a region of high concentration toward a region of low

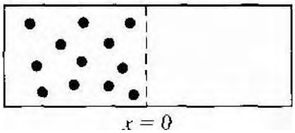

Figure 5.9 | Container divided by a membrane with gas molecules on one side.

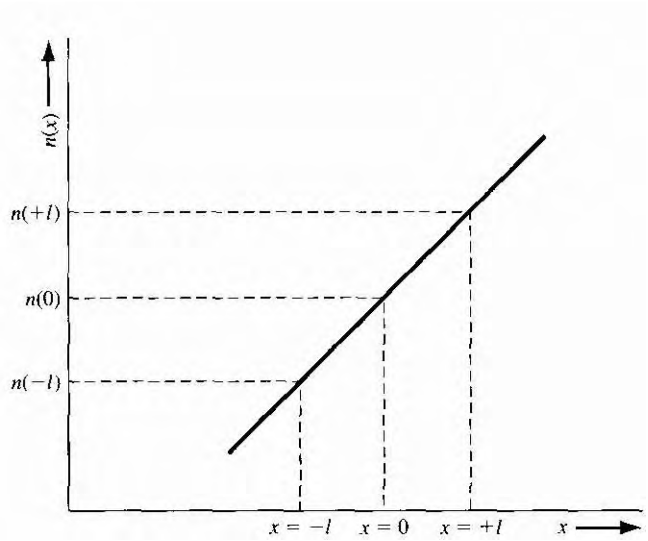

Figure 5.10 | Electron concentration versus distance.

concentration. If the gas molecules were electrically charged, the net flow of cha would result in a *diffusion current.*

5.2.1 Diffusion Current Density

To begin to understand the diffusion process in a semiconductor, we will consider simplified analysis. Assume that an electron concentration varies in one dimension shown in Figure 5.10. The temperature is assumed to be uniform so that the averag thermal velocity of electrons is independent of x. To calculate the current, we will d termine the net Row of electrons per unit time per unit area crossing the planed $x = 0$. If the distance l shown in Figure 5.10 is the mean-free path of an electron, th is, the average distance an electron travels between collisions (I $= v_{th}\tau_{cn}$), then the average, electrons moving to the right at $x = -l$ and electrons moving to the at $x = +l$ will cross the $x = 0$ plane. One half of the electrons at $x = -l$ will be tra eling to the right at any instant of time and one half of the electrons at $x = +l$ will b traveling to the left at any given time. The net rate of electron flow, F,,, in the +

direction at $x = 0$ is given by

$$F_n = \tfrac{1}{2}n(-l)v_{th} - \tfrac{1}{2}n(+l)v_{th} = \tfrac{1}{2}v_{th}[n(-l) - n(+l)] \tag{5.27}$$

If we expand the electron concentration in a Taylor series about $x = 0$ keeping only the first two terms, then we can write Equation (5.27) as

$$F_n = \frac{1}{2}v_{th}\left\{\left[n(0) - l\,\frac{dn}{dx}\right] - \left[n(0) + l\,\frac{dn}{dx}\right]\right\} \tag{5.28}$$

which becomes

$$F_n = -v_{th}l\,\frac{dn}{dx} \tag{5.29}$$

Each electron has a charge $(-e)$, so the current is

$$J = -eF_n = +ev_{th}l\,\frac{dn}{dx} \tag{5.30}$$

The current described by Equation *(5.30)* is the electron diffusion current and is proportional to the spatial derivative, or density gradient, of the electron concentration.

The diffusion of electrons from a region of high concentration to a region of low concentration produces a flux of electrons flowing in the negative x direction for this example. Since electrons have a negative charge, the conventional current direction is in the positive x direction. Figure 5.11a shows these one-dimensional flux and current directions. We may write the electron diffusion current density for this one-dimensional case. in the form

$$\boxed{J_{nx|dif} = eD_n\,\frac{dn}{dx}} \tag{5.31}$$

where D_n is called the ***electron diffusion coefficient,*** has units of cm^2/s, and is a positive quantity. If the electron density gradient becomes negative, the electron diffusion current density will be in the negative x direction.

Figure 5.11b shows an example of a hole concentration as a function of distance in a semiconductor. The diffusion of holes, from a region of high concentration to a region of low concentration, produces a flux of holes in the negative x direction. Since holes are positively charged particles, the conventional diffusion current density is also in the negative x direction. The hole diffusion current density is proportional to the hole density gradient and to the electronic charge, so we may write

$$\boxed{J_{px|dif} = -eD_p\,\frac{dp}{dx}}$$

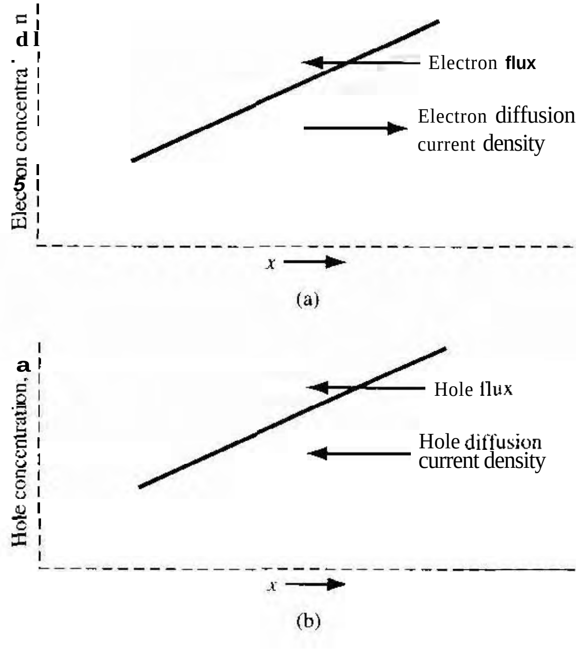
Electron concentration, n
Electron flux
Electron diffusion current density
x
(a)
Hole concentration, p
Hole flux
Hole diffusion current density
x
(b)

Figure 5.11 | (a) Diffusion of electrons due to a density gradient. (b) Diffusion of holes due to a density gradient.

for the one-dimensional case. The parameter D_p is called the ***hole diffusion coe cient***, has units of cm^2/s, and is a positive quantity. If the hole density gradient comes negative, the hole diffusion current density will be in the positive x directi

EXAMPLE 5.4

Objective

To calculate the diffusion current density given a density gradient.

Assume that, in an n-type gallium arsenide semiconductor at $T = 300$ K, the electr concentration varies linearly from 1×10^{18} to 7×10^{17} cm^{-3} over a distance of 0.10 cm. Ca culate the diffusion current density if the electron diffusion coefficient is $D_n = 225$ cm^2/s

■ Solution

The diffusion current density is given by

$$J_{n|dif} = eD_n \frac{dn}{dx} \approx eD_n \frac{\Delta n}{\Delta x}$$

$$= (1.6 \times 10^{-19})(225)\left(\frac{1 \times 10^{18} - 7 \times 10^{17}}{0.10}\right) = 108 \text{ A/cm}^2$$

■ Comment

A significant diffusion current density can be generated in a semiconductor material with o a modest density gradient.

TEST YOUR UNDERSTANDING

E5.8 The electron concentration in silicon is given by $n(x) = 10^{15} e^{-(x/L_n)}$ cm^{-3} $(x \geq 0)$ where $L_n = 10^{-4}$ cm. The electron diffusion coefficient is $D_n = 25$ cm^2/s. Determine the electron diffusion current density at (*a*) $x = 0$, (*b*) $x = 10^{-4}$ cm, and (*c*) $x \to \infty$.
[Ans. (*a*) −40 A/cm^2, (*b*) −14.7 A/cm^2, (*c*) 0]

E5.9 The hole concentration in silicon varies linearly from $x = 0$ to $x = 0.01$ cm. The hole diffusion coefficient is $D_p = 10$ cm^2/s, the hole diffusion current density is 20 A/cm^2, and the hole concentration at $x = 0$ is $p = 4 \times 10^{17}$ cm^{-3}. What is the value of the hole concentration at $x = 0.01$ cm? (Ans. 2.75×10^{17} cm^{-3})

E5.10 The hole concentration in silicon is given by $p(x) = 2 \times 10^{15} e^{-(x/L_p)}$ cm^{-3} $(x \geq 0)$. The hole diffusion coefficient is $D_p = 10$ cm^2/s. The value of the diffusion current density at $x = 0$ is $J_{\text{dif}} = +6.4$ A/cm^2. What is the value of L_p?
(Ans. $L_p = 5 \times 10^{-4}$ cm)

5.2.2 Total Current Density

We now have four possible independent current mechanisms in a semiconductor. These components are electron drift and diffusion currents and hole drift and diffusion currents. The total current density is the sum of these four components, or, for the one-dimensional case,

$$J = en\mu_n E_x + ep\mu_p E_x + eD_n \frac{dn}{dx} - eD_p \frac{dp}{dx} \tag{5.33}$$

This equation may be generalized to three dimensions as

$$J = en\mu_n E + ep\mu_p E + eD_n \nabla n - eD_p \nabla p \tag{5.34}$$

The electron mobility gives an indication of how well an electron moves in a semiconductor as a result of the force of an electric field. The electron diffusion coefficient gives an indication of how well an electron moves in a semiconductor as a result of a density gradient. The electron mobility and diffusion coefticient are not independent parameters. Similarly. the hole mobility and diffusion coefficient are not independent parameters. The relationship between mobility and the diffusion coefficient will be developed in the next section.

The expression for the total current in a semiconductor contains four terms. Fortunately in most situations, we will only need to consider one term at any one time at a particular point in a semiconductor.

5.3 | GRADED IMPURITY DISTRIBUTION

In most cases so far, we have assumed that the semiconductor is uniformly doped. In many semiconductor devices, however, there may be regions that are nonuniformly doped. We will investigate how a nonuniformly doped semiconductor reaches thermal

equilibrium and, from this analysis, we will derive the Einstein relation, which re
mobility and the diffusion coefficient.

5.3.1 Induced Electric Field

Consider a semiconductor that is nonuniformly doped with donor impurity atoms. the semiconductor is in thermal equilibrium, the Fermi energy level is co through the crystal so the energy-band diagram may qualitatively look like th shown in Figure 5.12. The doping concentration decreases as x increases in this cas There will be a diffusion of majority carrier electrons from the region of high con centration to the region of low concentration, which is in the $+x$ direction. The flo of negative electrons leaves behind positively charged donor ions. The separation o positive and negative charge induces an electric field that is in a direction to oppos the diffusion process. When equilibrium is reached, the mobile carrier concentratio is not exactly equal to the fixed impurity concentration and the induced electric fiel prevents any further separation of charge. In most cases of interest, the space charg induced by this diffusion process is a small fraction of the impurity concentration thus the mobile carrier concentration is not too different from the impurity dopa density.

The electric potential ϕ is related to electron potential energy by the char $(-e)$, so we can write

$$\phi = +\frac{1}{e}(E_F - E_{Fi})$$ (5

The electric field for the one-dimensional situation is defined as

$$\mathrm{E}_x = -\frac{d\phi}{dx} = \frac{1}{e}\frac{dE_{Fi}}{dx}$$ (5

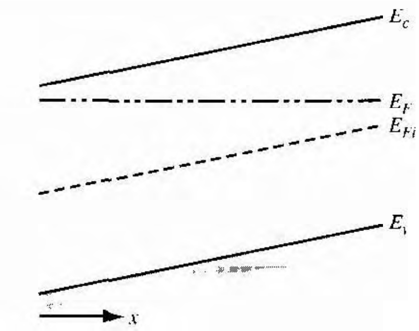

Figure 5.12 | Energy-band diagram for a semiconductor in thermal equilibrium with a nonuniform **donor** impurity concentration

If the intrinsic Fermi level changes as a function of distance through a semiconductor in thermal equilibrium, an electric field exists in the semiconductor.

If we assume a quasi-neutrality condition in which the electron concentration is almost equal to the donor impurity concentration, then we can still write

$$n_0 = n_i \exp\left[\frac{E_F - E_{Fi}}{kT}\right] \approx N_d(x) \tag{5.37}$$

Solving for $E_F - E_{Fi}$, we obtain

$$E_F - E_{Fi} = kT \ln\left(\frac{N_d(x)}{n_i}\right) \tag{5.38}$$

The Fermi level is constant for thermal equilibrium so when we take the derivative with respect to x we obtain

$$-\frac{dE_{Fi}}{dx} = \frac{kT}{N_d(x)} \frac{dN_d(x)}{dx} \tag{5.39}$$

The electric field can then be written, combining Equations (5.39) and (5.36), as

$$\mathrm{E}_x = -\left(\frac{kT}{e}\right) \frac{1}{N_d(x)} \frac{dN_d(x)}{dx} \tag{5.40}$$

Since we have an electric field, there will be a potential difference through the semiconductor due to the nonuniform doping.

EXAMPLE 5.5

Objective

To determine the induced electric field in a semiconductor in thermal equilibrium, given a linear variation in doping concentration.

Assume that the donor concentration in an n-type semiconductor at $T = 300$ K is given by

$$N_d(x) = 10^{16} - 10^{19}x \qquad (\text{cm}^{-3})$$

where x is given in cm and ranges between $0 \le x \le 1\ \mu\text{m}$.

■ **Solution**

Taking the derivative of the donor concentration, we have

$$\frac{dN_d(x)}{dx} = -10^{19} \qquad (\text{cm}^{-4})$$

The electric field is given by Equation (5.40), so we have

$$\mathrm{E}_x = \frac{-(0.0259)(-10^{19})}{(10^{16} - 10^{19}x)}$$

At $x = 0$, for example, we find

$$\mathrm{E}_x = 25.9 \text{ V/cm}$$

■ **Comment**

We may recall from our previous discussion of drift current that fairly small electric fields c produce significant drift current densities, so that an induced electric field from nonuni doping can significantly influence semiconductor device characteristics.

5.3.2 The Einstein Relation

If we consider the nonuniformly doped semiconductor represented by the ener band diagram shown in Figure 5.12 and assume there are no electrical connections that the semiconductor is in thermal equilibrium, then the individual electron a hole currents must be zero. We can write

$$J_n = 0 = en\mu_n \mathrm{E}_x + eD_n \frac{dn}{dx} \qquad (5.$$

If we assume quasi-neutrality so that n $\approx N_d(x)$, then we can rewrite Equ tion (5.41) as

$$J_n = 0 = e\mu_n N_d(x)\mathrm{E}_x + eD_n \frac{dN_d(x)}{dx} \qquad (5.4$$

Substituting the expression for the electric field from Equation (5.40) into Eq tion (5.42), we obtain

$$0 = -e\mu_n N_d(x)\left(\frac{kT}{e}\right)\frac{1}{N_d(x)}\frac{dN_d(x)}{dx} + eD_n\frac{dN_d(x)}{dx} \qquad (5.4$$

Equation (5.43) is valid for the condition

$$\frac{D_n}{\mu_n} = \frac{kT}{e} \qquad (5.44$$

The hole current must also be zero in the semiconductor. From this conditi we can show that

$$\frac{D_p}{\mu_p} = \frac{kT}{e} \qquad (5.44$$

Combining Equations (5.44a) and (5.44b) gives

$$\boxed{\frac{D_n}{\mu_n} = \frac{D_p}{\mu_p} = \frac{kT}{e}} \qquad (5.$$

The diffusion coefficient and mobility are not independent parameters. This rela between the mobility and diffusion coefficient, given by Equation (5.45), is know the *Einstein relation.*

Table 5.2 | Typical mobility and diffusion coefficient values at T = 300 K (μ = cm^2/V-s and D = cm^2/s)

	μ_m	D_n	a	D_p
Silicon	1350	35	480	12.4
Gallium arsenide	8500	220	400	10.4
Germanium	3900	101	1900	49.2

EXAMPLE 5.6

Objective

To determine the diffusion coefficient given the carrier mobility. Assume that the mobility of a particular carrier is 1000 cm^2/V-s at T = 300 K.

■ Solution

Using the Einstein relation. we have that

$$D = \left(\frac{kT}{e}\right)\mu = (0.0259)(1000) = 25.9\ \text{cm}^2/\text{s}$$

■ Comment

Although this example is fairly simple and straightforward. it is important to keep in mind the relative orders of magnitude of the mobility and diffusion coefficient. The diffurion coefficient is approximately 40 times smaller than the mobility at room temperature.

Table 5.2 shows the diffusion coefficient values at T = 300 K corresponding to the mobilities listed in Table 5.1 for silicon. gallium arsenide. and germanium.

The relation between the mobility and diffusion coefficient given by Equation (5.45) contains temperature. It is important to keep in mind that the major temperature effects are a result of lattice scattering and ionized impurity scattering processes, as discussed in Section 5.1.2. As the mobilities are strong functions of temperature because of the scattering processes, the diffusion coefficients are also strong functions of temperature. The specific temperature dependence given in Equation (5.45) is a small fraction of the real temperature characteristic.

*5.4 | THE HALL EFFECT

The Hall effect is a consequence of the forces that are exerted on moving charges by electric and magnetic fields. The Hall effect is used to distinguish whether a semiconductor is n type or p type[t] and to measure the majority carrier concentration and majority carrier mobility. The Hall effect device, as discussed in this section, is used to experimentally measure semiconductor parameters. However, it is also used extensively in engineering applications as a magnetic probe and in other circuit applications.

---

[t] We will assume an extrinsic semiconductor material in which the majority carrier concentration is much larger than the minority carrier concentration.

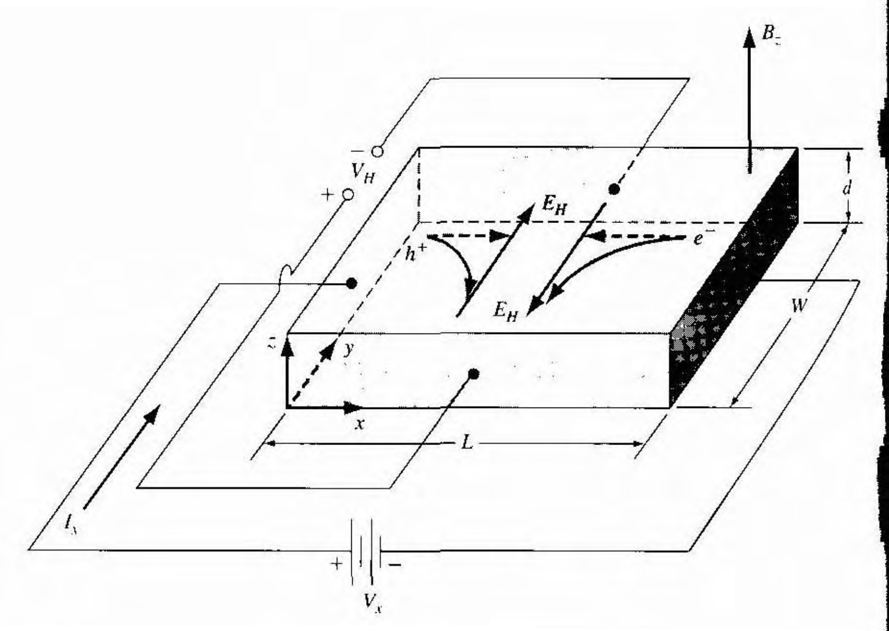

Figure 5.13 | *Geometry for measuring the Hall effect*

The force on a particle having a charge q and moving in a magnetic field is given by

$$F = qv \times B \tag{5.46}$$

where the cross product is taken between velocity and magnetic field so that the force vector is perpendicular to both the velocity and magnetic field.

Figure 5.13 illustrates the Hall effect. A semiconductor with a current I_x placed in a magnetic field perpendicular to the current. In this case, the magnetic field is in the z direction. Electrons and holes flowing in the semiconductor will experience a force as indicated in the figure. The force on both electrons and holes is in the $(-y)$ direction. In a p-type semiconductor ($p_0 > n_0$), there will be a buildup of positive charge on the $y = 0$ surface of the semiconductor and. in an n-type semiconductor ($n_0 > p_0$), there will be a buildup of negative charge on the $y = 0$ surface. This net charge induces an electric field in the y-direction as shown in the figure. In steady state, the magnetic field force will be exactly balanced by the induced electric field force. This balance may be written as

$$F = q[\mathrm{E} + v \times B] = 0 \tag{5.47a}$$

which becomes

$$q\mathrm{E}_y = qv_x B_z \tag{5.47b}$$

The induced electric field in the y-direction is called the *Hall field.* The Hall field produces a voltage across the semiconductor which is called the *Hall voltage.* We can write

$$V_H = +\mathrm{E}_H W \tag{5.48}$$

The hole mobility is then given by

$$\mu_p = \frac{I_x L}{e p V_x W d} \quad (5$$

Similarly for an n-type semiconductor, the low-field electron mobility is determi from

$$\mu_n = \frac{I_x L}{e n V_x W d}$$

EXAMPLE 5.7

Objective

To determine the majority carrier concentration and mobility. given Hall effect parameter

Consider the geometry shown in Figure 5.13. Let L = 10^{-1} cm, W = 10^{-2} cm, d = 10^{-3} cm. Also assume that I_x = 1.0 mA, $V_x = 12.5$ V, $B_z = 500$ gauss $= 5 \times 10^{-2}$ t and $V_H = -6.25$ mV.

■ Solution

A negative Hall voltage for this geometry implies that we have an n-type semicondu Using Equation (5.54). we can calculate the electron concentration as

$$n = \frac{-(10^{-3})(5\times 10^{-2})}{(1.6\times 10^{-19})(10^{-5})(-6.25\times 10^{-3})} = 5\times 10^{21}\ \mathrm{m}^{-3} = 5\times 10^{15}\ \mathrm{cm}^{-3}$$

The electron mobility is then determined from Equation (5.58) as

$$\mu_n = \frac{(10^{-3})(10^{-3})}{(1.6\times 10^{-19})(5\times 10^{21})(12.5)(10^{-4})(10^{-5})} = 0.10\ \mathrm{m}^2/\mathrm{V\text{-}s}$$

or

$$\mu_n = 1000\ \mathrm{cm}^2/\mathrm{V\text{-}s}$$

■ Comment

It is important to note that the MKS units must be used consistently in the Hall effect equat to yield correct results.

5.5 | SUMMARY

- The two basic transport mechanisms are drift, due to an applied electric field. and diffusion. due to a density gradient.

  Carriers reach an average drift velocity in the presence of an applied electric field, d to scattering events. Two scattering processes within a semiconductor are lattice scattering and impurity scattering.
- The average drift velocity is a linear function of the applied electric field for small values of electric field, but the drift velocity reaches a saturation limit that is on the order of 10^7 cm/s at high electric fields.

- Carrier mobility is the ratio of the average drift velocity and applied elechic field. The electron and hole mobilities are functions of temperature and of the ionized impurity concentration.
- The drift current density is the product of conductivity and electric field (a form of Ohm's law). Conductivity is a function of the carrier concentrations and mobilities. Resistivity is the inverse of conductivity
- The diffusion current density is proportional to the carrier diffusion coefficient and the carrier density gradient.
- The diffusion coefficient and mohilitv are related through the Einstein relation.
- The Hall effect is a consequence of a charged carrier moving in the presence of perpendicular electric and magnetic fields. The charged carrier is deflected. inducing a Hall voltage. The polarity of the Hall voltage is a function of the semiconductor conductivity type. The majority carrier concentration and mobility can he determined from the Hall voltage.

GLOSSARY OF IMPORTANT TERMS

conductivity **A** material parameter related to carrier drift; quantitatively, the ratio of drift current density to electric field.

diffusion The process whereby particles flow from a region of high concentration to a region of low concentration.

diffusion coefficient The parameter relating particle flux to the particle density gradient.

diffusion **current** The current that results from the diffusion of charged particle?.

drift The process wherehy charged particles move while under the influence of an electric field.

drift current The current that results from the drift of charged particles.

drift velocity The average velocity of charged particles in the presence of an electric field.

Einstein **relation** The relation between the mobility and the diffusion coefficient.

Hall voltage The voltage induced across a semiconductor in a Hall effect measurement.

ionized impurity scattering The interaction between a charged carrier and an ionized impurity center.

latticescattering The interaction between a charged carrier and a thermally vibrating lattice atom.

mobility The parameter relating carrier drift velocity and electric field.

resistivity The reciprocal of conductivity; a material parameter that is a measure of the resistance to current.

velocity saturation The saturation of carrier drift velocity with increasing electric field.

CHECKPOINT

After studying this chapter, the reader should have the ability to:

- Discuss carrier drift current density.
- Explain why carriers reach an average drift velocity in the presence of an applied electric field.
- Discuss the mechanisms of lattice scattering and impurity scattering.

- Define mobility and discuss the temperature and ionized impurity concentration dependence on mobility.
- Define conductivity and resistivity.
- Discuss velocity saturation.
- Discuss carrier diffusion current density.
- State the Einstein relation.
- Describe the Hall effect.

REVIEW QUESTIONS

1. Write the equation for the total drift current density.
2. Define carrier mobility. What is the unit of mobility'?
3. Explain the temperature dependence of mobility. Why is the carrier mobility a functi of the ionized impurity concentrations?
4. Define conductivity. Define resistivity. What are the units of conductivity and resistiv
5. Sketch the drift velocity of electrons in silicon versus electric field. Repeat for GaAs
6. Write the equations for the diffusion current densities of electrons and holes.
7. What is the Einstein relation?
8. Describe the Hall effect.
9. Explain why the polarity of the Hall voltage changes depending on the conductivity (n type or p type) of the semiconductor.

PROBLEMS

(*Note;* Use the semiconductor parameters given in Appendix B if the parameters are specifically given in a problem.)

Section 5.1 Carrier Drift

5.1 Consider a homogeneous gallium arsenide semiconductor at T = 300 K with N_d 10^{16} cm^{-3} and $N_a = 0$. (*a*) Calculate the thermal-equilibrium values of electron a hole concentrations. (*b*) For an applied E-field of 10 V/cm, calculate the drift curr density. (*c*) Repeat parts (*a*) and (*b*) if $N_d = 0$ and $N_a = 10^{16}$ cm^{-3}.

5.2 A silicon crystal having a cross-sectional area of 0.001 cm^2 and a length of 10^{-3} c connected at its ends to a 10-V battery. At T = 300 K, we wanr a current of 100 m in the silicon. Calculate: (*a*) the required resistance R. (*b*) the required conductivit (*c*) the density of donor atoms to be added to achieve this conductivity. and id) the concentration of acceptor atoms to be added to form a compensated p-type materi with the conductivity given from part (*b*) if the initial concentration of donor atom $N_d = 10^{15}$ cm^{-3}.

5.3 (*a*) A silicon semiconductor is in the shape of a rectangular har with a cross-sectio area of 100 μm^2, a length of 0.1 cm, and is doped with 5 × 10^{16} cm^{-3} arsenic ator The temperature is T = 300 K. Determine the current if 5 V is applied across the length. (*b*) Repeat part (*a*) if the length is reduced to 0.01 cm. (*c*) Calculate the average drift velocity of electrons in parts (*a*) and (*b*).

5.4 (*a*) A GaAs semiconductor resistor is doped with acceptor impurities at a concentra tion of $N_a = 10^{17}$ cm^{-3}. The cross-sectional area is 85 μm^2. The current in the resistor is to be I = 20 mA with 10 V applied. Determine the required length of the device. (b) Repeat part (a) for silicon.

5.5 (a) Three volts is applied across a 1-cm-long semiconductor bar. The average electron drift velocity is 10^4 cm/s. Find the electron mobility. (*b*) If the electron mobility in part (a) were 800 cm²/V-s, what is the average electron drift velocity?

5.6 Use the velocity-field relations for silicon and gallium arsenide shown in Figure 5.7 to determine the transit time of electrons through a 1-μm distance in these materials for an electric field of (a) 1 kV/cm and (*b*) 50 kV/cm.

5.7 A perfectly compensated semiconductor is one in which the donor and acceptor impurity concentrations are exactly equal. Assuming complete ionization, determine the conductivity of silicon at T = 300 K in which the impurity concentrations are (a) $N_a = N_d = 10^{14}$ cm^{-3} and (*b*) $N_a = N_d = 10^{18}$ cm^{-3}.

5.8 (*a*) In a p-type gallium arsenide semiconductor, the conductivity is $\sigma = 5$ (Ω-cm)$^{-1}$ at T = 300 K. Calculate the thermal-equilibrium values of the electron and hole concentrations. (b) Repeat part (*a*) for n-type silicon if the resistivity is $\rho = 8$ Ω-cm.

5.9 In a particular semiconductor material, $\mu_n = 1000$ cm²/V-s, $\mu_p = 600$ cm²/V-s, and $N_C = N_V = 10^{19}$ cm^{-3}. These parameters are independent of temperature. The measured conductivity of the intrinsic material is $\sigma = 10^{-6}$ (Ω-cm)$^{-1}$ at $T = 300$ K. Find the conductivity at $T = 500$ K.

5.10 (*a*) Calculate the resistivity at T = 300 K of intrinsic (*i*) silicon, (*ii*) germanium, and (iii) gallium arsenide. (*b*) If rectangular semiconductor bars are fabricated using the materials in part (a), determine the resistance of each bar if its cross-sectional area is 85 μm^2 and length is 200 μm.

5.11 An n-type silicon sample has a resistivity of 5 Ω-cm at T = 300 K. (a) What is the donor impurity concentration? (*b*) What is the expected resistivity at (*i*) T = 200 K and (ii) T = 400 K.

5.12 Consider silicon doped at impurity concentrations of $N_d = 2 \times 10^{16}$ cm^{-3} and $N_a = 0$. An empirical expression relating electron drift velocity to electric field is given by

$$v_d = \frac{\mu_{n0}E}{\sqrt{1 + \left(\frac{\mu_{n0}E}{v_{sat}}\right)^2}}$$

where $\mu_{n0} = 1350$ cm²/V-s, $v_{sat} = 1.8 \times 10^7$ cm/s, and E is given in V/cm. Plot electron drift current density (magnitude) versus electric field (log–log scale) over the range $0 \le E \le 10^6$ V/cm.

5.13 Consider silicon at $T = 300$ K. Assume the electron mobility is $\mu_n = 1350$ cm²/V-s. The kinetic energy of an electron in the conduction band is $(1/2)m_n^* v_d^2$, where m_n^* is the effective mass and v_d is the drift velocity Determine the kinetic energy of an electron in the conduction band if the applied electric field is (*a*) 10 V/cm and (*b*) 1 kV/cm.

5.14 Consider a semiconductor that is uniformly doped with $N_d = 10^{14}$ cm^{-3} and $N_a = 0$, with an applied electric field of E = 100 V/cm. Assume that $\mu_n = 1000$ cm²/V-s and $\mu_p = 0$. Also assume the following parameters:

$$N_c = 2 \times 10^{19}(T/300)^{3/2} \text{ cm}^{-3}$$

$$N_v = 1 \times 10^{19}(T/300)^{3/2} \text{ cm}^{-3}$$

$$E_g = 1.10 \text{ eV}$$

(a) Calculate the electric-current density at $T = 300$ K. (b) At what temperature wil this current increase by 5 percent? (Assume the mobilities are independent of temperature.)

5.15 A semiconductor material has electron and hole mobilities μ_n and μ_p, respective When the conductivity is considered as a function of the hole concentration p_0, (a) show that the minimum value of conductivity, $\sigma_{\min}$, can be written as

$$\sigma_{\min} = \frac{2\sigma_i (\mu_n \mu_p)^{1/2}}{(\mu_n + \mu_p)}$$

where σ_i is the intrinsic conductivity, and (b) show that the corresponding hole concentration is $p_0 = n_i(\mu_n/\mu_p)^{1/2}$.

5.16 A particular intrinsic semiconductor has a resistivity of 50 Ω-cm at $T = 300$ K and 5 Ω-cm at $T = 330$ K. Neglecting the change in mobility with temperature, determ the bandgap energy of the semiconductor

5.17 Three scattering mechanisms are present in a particular semiconductor material. If only the first scattering mechanism were present, the mobility would be $\mu_1 = 2000$ cm^2/V-s, if only the second mechanism were present, the mobility would be $\mu_2 = 1500$ cm^2/V-s, and if only the third mechanism were present, the mobility wo be $\mu_3 = 500$ cm^2/V-s. What is the net mobility?

5.18 Assume that the mobility of electrons in silicon at T = 300 K is $\mu_n = 1300$ cm^2/V Also assume that the mobility is limited by lattice scattering and varies as $T^{-3/2}$. Determine the electron mobility at (a) $T = 200$ K and (b) $T = 400$ K.

5.19 Two scattering mechanisms exist in a semiconductor. If only the first mechanism w present, the mobility would be 250 cm^2/V-s. If only the second mechanism wer p sent, the mobility would be 500 cm^2/V-s. Determine the mobility when both scatte mechanisms exist at the same time.

5.20 The effective density of states functions in silicon can be written in the form

$$N_c = 2.8 \times 10^{19} \left(\frac{T}{300}\right)^{3/2} \qquad N_v = 1.04 \times 10^{19} \left(\frac{T}{300}\right)^{3/2}$$

Assume the mobilities are given by

$$\mu_n = 1350 \left(\frac{T}{300}\right)^{-3/2} \qquad \mu_p = 480 \left(\frac{T}{300}\right)^{-3/2}$$

Assume the bandgap energy is $E_g = 1.12$ eV and independent of temperature. Pl the intrinsic conductivity as a function of T over the range $200 \le T \le 600$ K

5.21 (a) Assume that the electron mobility in an n-type semiconductor is given by

$$\mu_n = \frac{1350}{\left(1 + \dfrac{N_d}{5 \times 10^{16}}\right)^{1/2}} \text{ cm}^2/\text{V-s}$$

where N_d is the donor concentration in cm^{-3}. Assuming complete ionization. plot t conductivity as a function of N_d over the range $10^{15} \le N_d \le 10^{18}$ cm^{-3}. (b) Com the results of part (a) to that if the mobility were assumed to be a constant equal to

1350 cm^2/V-s. (*c*) If an electric field of $E = 10$ V/cm is applied to the semiconductor, plot the electron drift current density of pans (*a*) and (*b*)

Section 5.2 Carrier Diffusion

5.22 Consider a sample of silicon at T = 300 K. Assume that the electron concentration varies linearly with distance, as shown in Figure 5.14. The diffusion current density is found to be $J_n = 0.19$ A/cm^2. If the electron diffusion coefficient is $D_n = 25$ cm^2/s, determine the electron concentration at $x = 0$.

5.23 The electron concentration in silicon decreases linearly from 10^{16} cm^{-3} to 10^{15} cm^{-3} over a distance of 0.10 cm. The cross-sectional area of the sample is 0.05 cm^2. The electron diffusion coefficient is 25 cm^2/s. Calculate the electron diffusion current.

5.24 The electron concentration in a sample of n-type silicon varies linearly from 10^{17} cm^{-3} at x = 0 to 6×10^{16} cm^{-3} at $x = 4$ μm. There is no applied electric field. The electron current density is experimentally measured to be -400 A/cm^2. What is the electron diffusion coefficient?

5.25 The hole concentration in p type GaAs is given by $p = 10^{16}(1 - x/L)$ cm^{-3} for $0 \leq x \leq L$ where $L = 10$ μm. The hole diffusion coefficient is 10 cm^2/s. Calculate the hole diffusion current density at (*a*) x = 0, (*b*) x = 5 μm, and (*c*) $x = 10$ μm.

5.26 The hole concentration is given by $p = 10^{15} \exp(-x/L_p)$ cm^{-3} for $x \geq 0$ and the electron concentration is given by $5 \times 10^{14} \exp(+x/L_n)$ cm^{-3} for $x \leq 0$. The values of L_p and L_n are 5×10^{-4} cm and 10^{-3} cm, respectively. The hole and electron diffusion coefficients are 10 cm^2/s and 25 cm^2/s, respectively. The total current density is defined as the sum of the hole diffusion current density at $x = 0$ and the electron diffusion current density at $x = 0$. Calculate the total current density.

5.27 The hole concentration in germanium at T = 300 K varies as

$$p(x) = 10^{15} \exp\left(\frac{-x}{22.5}\right) \text{cm}^{-3}$$

where x is measured in μm. If the hole diffusion coefficient is $D_p = 48$ cm^2/s, determine the hole diffusion current density as a function of x.

5.28 The electron concentration in silicon at T = 300 K is given by

$$n(x) = 10^{16} \exp\left(\frac{-x}{18}\right) \text{cm}^{-3}$$

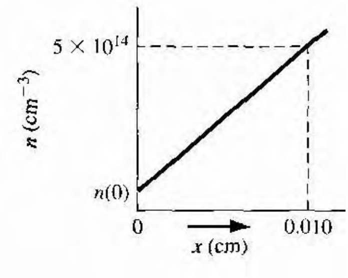

Figure 5.14 | Figure for Problem 5.22.

where x is measured in μm and is limited to $0 \le x \le 25\ \mu$m. The electron diffusio coefticient is $D_n = 25$ cm'ls and the electron mobility is $\mu_n = 960$ cm^2/V-s. The to electron current density through the semiconductor is constant and equal to $J_n = -40$ Alcm^2. The electron current has both diffusion and drift current components. Determine the electric field as a function of x which must exist in the semiconducto

5.29 The total current in a semiconductor is constant and is composed of electron drift current and hole diffusion current. The electron concentration is constant and is equ to 10^{16} cm^{-3}. The hole concentration is given by

$$p(x) = 10^{15} \exp\left(\frac{-x}{L}\right) \text{cm}^{-3} \qquad (x \ge 0)$$

where L $= 12\ \mu$m. The hole diffusion coefficient is $D_p = 12$ cm^2/s and the electro mobility is $\mu_n = 1000$ cm^2/V-s. The total current density is $J = 4.8$ A/cm^2. Calcula ***(a)*** the hole diffusion current density versus x, (b) the electron current density versu x, and ***(r)*** the electric field versus x.

***5.30** A constant electric field, E $= 12$ V/cm, exists in the $+x$ direction of an n-type galli arsenide semiconductor for $0 \le x \le 50\ \mu$m. The total current density is a constant and is $J = 100$ A/cm^2. **At** $x = 0$, the drift and diffusion currents are equal. Let T $= 300$ K and $\mu_n = 8000$ cm^2/V-s. *(a)* Determine the expression for the electron concentration $n(x)$. *(b)* Calculate the electron concentration at $x = 0$ and at $x = 50\ \mu$m. (c) Calculate the drift and diffusion current densities at $x = 50\ \mu$m.

5.31** In n-type silicon, the Fermi energy level varies linearly with distance over a shon range. At $x = 0$, $E_F - E_{Fi} = 0.4$ eV and, at $x = 10^{-3}$ cm, $E_F - E_{Fi} = 0.15$ eV. ***(a) Write the expression for the electron concentration over the distance. (b) If the electron diffusion coefficient is D,, $= 25$ cm^2/s, calculate the electron diffusion current density at $(i)\ x = 0$ and $(ii)\ x = 5 \times 10^{-4}$ cm.

***5.32** (a) The electron concentration in **a** semiconductor is given by $n = 10^{16}(1 - x/L)$ cm for $0 \le x \le$ L. where L $= 10\ \mu$m. The electron mobility and diffusion coefficient $\mu_n = 1000$ cm^2/V-s and D,, $= 25.9$ cm^2/s. An electric field is applied such that the total electron current density is a constant over the given range of x and is J,, $= -80$ A/cm^2. Determine the required electric field versus distance function. *(b)* Rep part *(a)* if J,, $= -20$ A/cm^2.

Section 5.3 Graded Impurity Distribution

5.33 Consider a semiconductor in thermal equilibrium (no current). Assume that the donor concenvation varies exponentially as

$$N_d(x) = N_{d0} \exp(-ax)$$

over the range $0 \le x \le 1/\alpha$ where N_{d0} is **a** constant. ***(a)*** Calculate the electric field as a function of x for $0 \le x \le 1/\alpha$. (b) Calculate the potential difference between $x = 0$ and $x = 1/\alpha$.

5.34 Using the data in Example 5.5, calculate the potential difference between $x = 0$ and $x = 1\ \mu$m.

5.35 Determine a doping profile in a semiconductor at T $= 300$ K that will induce an electric field of I **k**V/cm over a length of 0.2 μm.

***5.36** In GaAs, the donor impurity concentration varies as $N_{d0}\exp(-x/L)$ for $0 \leq x \leq L$, where $L = 0.1\ \mu$m and $N_{d0} = 5 \times 10^{16}$ cm^{-3}. Assume $\mu_n = 6000$ cm^2/V-s and $T = 300$ K. (o) Derive the expression for the electron diffusion current density versus distance over the given range of x. (*b*) Determine the induced electric field that generates a drift current density that compensates the diffusion current density.

5.37 ***(a)*** Consider the electron mobility in silicon for $N_d = 10^{17}$ cm^{-3} from Figure 5.2a. Calculate and plot the electron diffusion coefficient versus temperature over the range $-50 \leq T \leq 200$°C. (*b*) Repeat pan (a) if the electron diffusion coefficient is given by $D_n = (0.0259)\mu_n$ for all temperatures. What conclusion can be made about the temperature dependence of the diffusion coefficient?

5.38 (*a*) Assume that the mobility of a carrier at $T = 300$ K is $\mu = 925$ cm^2/V-s. Calculate the carrier diffusion coefficient. ***(b)*** Assume that the diffusion coefficient of a carrier at $T = 300$ K is $D = 28.3$ cm^2/s. Calculate the carrier mobility.

Section 5.4 The Hall Effect

(*Note:* Refer to Figure 5.13 fur the geometry of the Hall effect.)

5.39 A sample of silicon is doped with 10^{16} baron atoms per cm'. The Hall sample has the same geometrical dimensions given in Example 5.7. The current is $I_x = 1$ mA with $B_z = 350$ gauss $= 3.5 \times 10^{-2}$ tesla. Determine (*a*) the Hall voltage and ***(b)*** the Hall held.

5.40 Germanium is doped with 5×10^{15} donor atoms per cm^3 at $T = 300$ K. The dimensions of the Hall device are $d = 5 \times 10^{-3}$ cm, $W = 2 \times 10^{-2}$ cm, and $L = 10^{-1}$ cm. The current is $I_x = 250\ \mu$A, the applied voltage is $V_x = 100$ mV, and the magnetic flux density is $B_z = 500$ gauss $= 5 \times 10^{-2}$ tesla. Calculate: (a) the Hall voltage, ***(b)*** the Hall field. and (*c*) the carrier mobility

5.41 A silicon Hall device at $T = 300$ K has the following geometry: $d = 10^{-3}$ cm, $W = 10^{-2}$ cm, and $L = 10^{-1}$ cm. The following parameters are measured: $I_x = 0.75$ mA, $V_x = 15$ V, $V_H = +5.8$ mV, and $B_z = 1000$ gauss $= 10^{-1}$ tesla. Determine (*a*) the conductivity type, (*b*) the majority carrier concentration, and ***(c)*** the majority carrier mobility.

5.42 Consider silicon at $T = 300$ K. A Hall effect device is fabricated with the following geometry: $d = 5 \times 10^{-3}$ cm, $W = 5 \times 10^{-2}$ cm, and $L = 0.50$ cm. The electrical parameters measured are: $I_x = 0.50$ mA, $V_x = 1.25$ V, and $B_z = 650$ gauss $= 6.5 \times 10^{-2}$ tesla. The Hall field is $E_H = -16.5$ mV/cm. Determine (*a*) the Hall voltage, (*b*) the conductivity type, (*c*) the majority carrier concentration, and (d) the majority carrier mobility.

5.43 Consider a gallium arsenide sample at $T = 300$ K. A Hall effect device has been fabricated with the following geometry: $d = 0.01$ cm, $W = 0.05$ cm. and $L = 0.5$ cm The electrical parameters are: $I_x = 2.5$ mA, $V_x = 2.2$ V, and $B_z = 2.5 \times 10^{-2}$ tesla. The Hall voltage is $V_H = -4.5$ mV. Find: (a) the conductivity type, ***(h)*** the majority carrier concentration, (*c*) the mobility, and (d) the resistivity.

Summary and Review

5.44 An n-type silicon semiconductor resistor is to be designed so that it carries a current of 5 mA with an applied voltage of 5 V. (a) If $N_d = 3 \times 10^{14}$ cm^{-3} and $N_a = 0$, design a resistor lo meet the required specifications. (b) If $N_d = 3 \times 10^{16}$ cm^{-3} and

$N_a = 2.5 \times 10^{16}$ cm', redesign the resistor. (*c*) Discuss the relative lengths of the two designs compared to the doping concentration. Is there a linear relationship'!

5.45 In fabricating a Hall effect device, the two points at which the Hall voltage is measured may not be lined up exactly perpendicular to the current ***I,*** (see Figure 5.13). Discuss the effect this misalignment will have on the Hall voltage. Show that a valid Hall voltage can be obtained from two measurements: first with the magnetic field in the $+z$ direction, and then in the $-z$ direction.

5.46 Another technique for determining the conductivity type of a semiconductor is called the hot probe method. It consists of two probes and an ammeter that indicates the direction of current. One probe is heated and the other is at room temperature. No voltage is applied, but a current will exist when the probes touch the semiconductor Explain the operation of this hot probe technique and sketch a diagram indicating the direction of current for p- and n-type semiconductor samples.

READING LIST

1.** Bube, R. H. ***Electrons in Solids: An Introductory Survey. 3rd ed. San Diego, CA: Academic Press, 1992.

2. Kano, K. ***Semiconductor Devices.*** Upper Saddle River, NJ: Prentice Hall, 1998.

3.** Lundstrom, M. ***Fundamentals of Carrier Transport. Vol. ***X*** of ***Modular Series on Solid State Devices.*** Reading, MA: Addison-Wesley, 1990.

4. Muller, R. S., and T. I. Kamins. ***Device Electronics for Integrated Circuits.*** 2nd ed. New York: Wiley, 1986.

5. Navon, D. H. ***Semiconductor Microdevices and Materials.*** New ***York:*** Holt, Rinehart & Winston, 1986.

6. Pierret, R. F. ***Semiconductor Device Fundamentals.*** Reading, MA: Addison-Wesley Publishing Co., 1996.

7. Shur, M. ***Introduction to Electronic Devices.*** New York: John Wiley and Sons, 1996.

8.** Shur, M. ***Physics of Semiconducror Devices. Englewood Cliffs, NJ: Prentice Hall, 1990.

9. Singh, J. ***Semiconductor Devices: An Introduction.*** New York: McGraw-Hill, 1994.

10. Singh, J. ***Semiconductor Devices: Basic Principles.*** New York: John Wiley and Sons. 2001.

11. Streetman, B. G., and S. Banerjee. ***Solid State Electronic Devices.*** 5th ed. Upper Saddle River, NJ: Prentice Hall, 2000.

12. Sre, S. M. ***Physics of Semiconducror Devices.*** 2nd ed. New York: John Wiley and Sons. 1981.

13. Sze, S. M. ***Semiconducror Devices: Physics and Technology*** 2nd ed. New York: John Wiley and Sons, 2001.

14.** van der Ziel, A. ***Solid State Physical Electronics. 2nd ed. Englewood Cliffs, NJ: Prentice Hall, 1968.

15. Wang, S. ***Fundamentals of Semiconductor Theory and Device Physics.*** Englewood Cliffs, NJ: Prentice Hall, 1989.

16. Yang, E. S. ***Microelectronic Devices.*** New York: McGraw-Hill. 1988.

CHAPTER

6

Nonequilibrium Excess Carriers in Semiconductors

PREVIEW

Our discussion of the physics of semiconductors in Chapter 4 was based on thermal equilibrium. When a voltage is applied or a current exists in a semiconductor device, the semiconductor is operating under nonequilibrium conditions. In our discussion of current transport in Chapter 5, we did not address nonequilibrium conditions but implicitly assumed that equilibrium was not significantly disturbed. Excess electrons in the conduction band and excess holes in the valence band may exist in addition to the thermal-equilibrium concentrations if an external excitation is applied to the semiconductor. In this chapter, we will discuss the behavior of nonequilibrium electron and hole concentrations as functions of time and space coordinates.

Excess electrons and excess holes do not move independently of each other. They diffuse, drift, and recombine with the same effective diffusion coefficient, drift mobility, and lifetime. This phenomenon is called ambipolar transport. We will develop the ambipolar transport equation which describes the behavior of the excess electrons and holes. The behavior of excess carriers is fundamental to the operation of semiconductor devices. Several examples of the generation of excess carriers will be explored to illustrate the characteristics of the ambipolar transport phenomenon.

The Fermi energy was previously defined for a semiconductor in thermal equilibrium. The creation of excess electrons and holes means that the semiconductor is no longer in thermal equilibrium. We can define two new parameters that apply to the nonequilibrium semiconductor: the quasi-Fermi energy for electrons and the quasi-Fermi energy for holes.

Semiconductor devices are generally fabricated at or near a surface. We will study the effect of these surfaces on the characteristics of excess electrons and holes. These effects can significantly influence the semiconductor device properties. ■

6.1 | CARRIER GENERATION AND RECOMBINATION

In this chapter, we discuss carrier generation and recombination, which we can define as follows: ***generation*** is the process whereby electrons and holes are created, and ***recombination*** is the process whereby electron? and holes are annihilated.

Any deviation from thermal equilibrium will tend to change the electron and hole concentrations in a semiconductor. A sudden increase in temperature, for example, will increase the rate at which electrons and holes are thermally generated so that their concentrations will change with time until new equilibriuin values are reached. An external excitation, such as light (a flux of photons), can also generate electrons and holes, creating a nonequilibrium condition. To understand the generation and recombination processes, we will first consider direct band-to-band generation and recombination, and then, later, the effect of allowed electronic energy states within the bandgap, referred to as traps or recombination centers.

6.1.1 The Semiconductor in Equilibrium

We have determined the thermal-equilibrium concentration of electrons and holes in the conduction and valence bands, respectively. In thermal equilibrium, these concentrations are independent of time. However, electrons are continually being thermally excited from the valence band into the conduction band by the random nature of the thermal process. At the same time, electrons moving randomly through the crystal in the conduction band may come in close proximity to holes and "fall" into the empty states in the valence band. This recombination process annihilates both the electron and hole. Since the net carrier concentrations are independent of time in thermal equilibrium, the rate at which electrons and holes are generated and the rate at which they recombine must be equal. The generation and recombination processes are schematically shown in Figure 6.1.

Let G_{n0} and G_{p0} be the thermal-generation rates of electrons and holes, respectively, given in units of #/cm^3-s. For the direct band-to-band generation. the electrons and holes are created in pairs, so we must have that

$$G_{n0} = G_{p0} \tag{6.1}$$

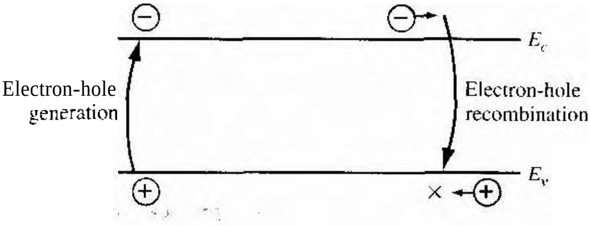

Figure 6.1 | Electrun-hole generation and recombination

Let R_{n0} and R_{p0} be the recombination rates of electrons and holes, respectively, for a semiconductor in thermal equilibrium, again given in units of #/cm^3-s. In direct band-to-band recombination, electrons and holes recombine in pairs, so that

$$R_{n0} = R_{p0} \tag{6.2}$$

In thermal equilibrium, the concentrations of electrons and holes are independent of time; therefore, the generation and recombination rates are equal, so we have

$$G_{n0} = G_{p0} = R_{n0} = R_{p0} \tag{6.3}$$

6.1.2 Excess Carrier Generation and Recombination

Additional notation is introduced in this chapter. Table 6.1 lists some of the more pertinent symbols used throughout the chapter. Other symbols will be defined as we advance through the chapter.

Electrons in the valence band may be excited into the conduction band when, for example, high-energy photons are incident on a semiconductor. When this happens, not only is an electron created in the conduction band, but a hole is created in the valence band; thus an electron-hole pair is generated. The additional electrons and holes created are called ***excess electrons*** and ***excess holes.***

The excess electrons and holes are generated by an external force at a particular rate. Let g'_n be the generation rate of excess electrons and g'_p be that of excess holes. These generation rates also have units of #/cm^3-s. For the direct band-to-band generation, the excess electrons and holes are also created in pairs, so we must have

$$g'_n = g'_p \tag{6.4}$$

When excess electrons and holes are created, the concentration of electrons in the conduction band and of holes in the valence band increase above their thermal-equilibrium value. We may write

$$n = n_0 + \delta n \tag{6.5a}$$

and

$$p = p_0 + \delta p \tag{6.5b}$$

Table 6.1 | Relevant notation used in Chapter 6

Symbol	Definition
n_0, p_0	Thermal equilibrium electron and hole concentrations (independent of time and also usually position).
n, p	Total electron and hole concentrations (may be functions of time and/or position).
$\delta n = n - n_0$ $\delta p = p - p_0$	Excess electron and hole concentrations (may be functions of time and/or position).
g'_n, g'_p	Excess electron and hole generation rates.
R'_n, R'_p	Excess electron and hole recombination rates.
τ_{n0}, τ_{p0}	Excess minority carrier electron and hole lifetimes.

where n_0 and p_0 are the thermal-equilibrium concentrations, and δn and δp are the excess electron and hole concentrations. Figure 6.2 shows the excess electron-hole generation process and the resulting carrier concentrations. The external force has perturbed the equilibrium condition so that the semiconductor is no longer in thermal equilibrium. We may note from Equations (6.5a) and (6.5b) that, in a nonequilibrium condition, $np \neq n_0 p_0 = n_i^2$.

A steady-state generation of excess electrons and holes will not cause a continual buildup of the carrier concentrations. As in the case of thermal equilibrium, an electron in the conduction band may "fall down" into the valence band, leading to the process of excess electron-hole recombination. Figure 6.3 shows this process. The recombination rate for excess electrons is denoted by R'_n and for excess holes by R'_p. Both parameters have units of #/cm^3-s. The excess electrons and holes recombine in pairs, so the recombination rates must be equal. We can then write

$$R'_n = R'_p \tag{6.6}$$

In the direct band-to-band recombination that we are considering, the recombination occurs spontaneously: thus, the probability of an electron and hole recombining is constant with time. The rate at which electrons recombine must be proportional

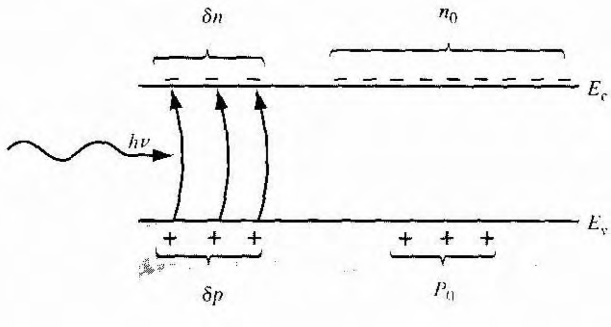

Figure 6.2 | Creation of excess electron and hole densities by photons.

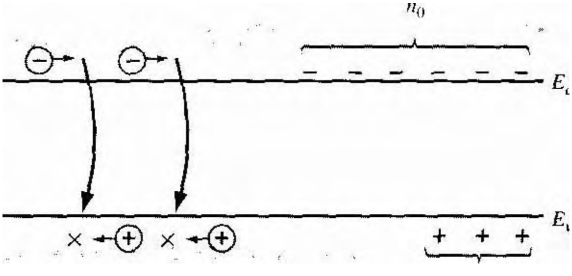

Figure 6.3 | Recombination of excess carriers reestablishing thermal equilibrium.

to the electron concentration and must also be proportional to the hole concentration. If there are no electrons or holes, there can be no recombination.

The net rate of change in the electron concentration can be written as

$$\frac{dn(t)}{dt} = \alpha_r\left[n_i^2 - n(t)p(t)\right] \tag{6.7}$$

where

$$n(t) = n_0 + \delta n(t) \tag{6.8a}$$

and

$$p(t) = p_0 + \delta p(t) \tag{6.8b}$$

The first term. $\alpha_r n_i^2$, in Equation (6.7) is the thermal-equilibrium generation rate. Since excess electrons and holes are created and recombine in pairs, we have that $\delta n(t) = \delta p(t)$. (Excess electron and hole concentrations are equal so we can simply use the phrase excess carriers to mean either.) The thermal-equilibrium parameters, n_0 and p_0, being independent of time, Equation (6.7) becomes

$$\begin{aligned}\frac{d(\delta n(t))}{dt} &= \alpha_r\left[n_i^2 - (n_0 + \delta n(t))(p_0 + \delta p(t))\right] \\ &= -\alpha_r \delta n(t)[(n_0 + p_0) + \delta n(t)]\end{aligned} \tag{6.9}$$

Equation (6.9) can easily be solved if we impose the condition of ***low-level injection.*** Low-level injection puts limits on the magnitude of the excess carrier concentration compared with the thermal equilibrium carrier concentrations. In an extrinsic n-type material, we generally have $n_0 \gg p_0$ and, in an extrinsic p-type material, we generally have $p_0 \gg n_0$. Low-level injection means that the excess carrier concentration is much less than the thermal equilibrium majority carrier concentration. Conversely. high-level injection occurs when the excess carrier concentration becomes comparable to or greater than the thermal equilibrium majority carrier concentrations.

If we consider a p-type material ($p_0 \gg n_0$) under low-level injection ($\delta n(t) \ll p_0$), then Equation (6.9) becomes

$$\frac{d(\delta n(t))}{dt} = -\alpha_r p_0 \delta n(t) \tag{6.10}$$

The solution to the equation is an exponential decay from the initial excess concentration, or

$$\delta n(t) = \delta n(0)e^{-\alpha_r p_0 t} = \delta n(0)e^{-t/\tau_{n0}} \tag{6.11}$$

where $\tau_{n0} = (\alpha_r p_0)^{-1}$ and is a constant for the low-level injection. Equation (6.11) describes the decay of excess minority carrier electrons so that τ_{n0} is often referred to as the ***excess*** *minority carrier lifetime.*[1]

---

[1] In Chapter 5 we defined τ as a mean time between collisions. We define τ here as the mean time before a recombination event occurs. The two parameters are not related.

The recombination rate—which is defined as a positive quantity--of excess minority carrier electrons can be written, using Equation (6.10). as

$$R'_n = \frac{-d(\delta n(t))}{dt} = +\alpha_r p_0 \delta n(t) = \frac{\delta n(t)}{\tau_{n0}} \tag{6.12}$$

For the direct hand-to-hand recombination, the excess majority carrier holes recombine at the same rate, so that for the p-type material

$$\boxed{R'_n = R'_p = \frac{\delta n(t)}{\tau_{n0}}} \tag{6.13}$$

In the case of an n-type material ($n_0 \gg p_0$) under low-level injection ($\delta n(t) \ll n_0$), the decay of minority carrier holes occurs with a time constant $\tau_{p0} = (\alpha_r n_0)^{-1}$, where τ_{p0} is also referred to as the excess minority carrier lifetime. The recombination rate of the majority carrier electrons will be the same as that of the minority carrier holes, so we have

$$\boxed{R'_n = R'_p = \frac{\delta n(t)}{\tau_{p0}}} \tag{6.14}$$

The generation rates of excess carriers are not functions of electron or hole concentrations. In general, the generation and recombination rates may be functions of the space coordinates and time.

TEST YOUR UNDERSTANDING

E6.1 Excess electrons have been generated in a semiconductor to a concentration of $\delta n(0) = 10^{15}$ cm^{-3}. The excess carrier lifetime is $\tau_{n0} = 10^{-6}$ s. The forcing function generating the excess carriers turns off at $t = 0$ so the semicdnductor is allowed to return to an equilibrium condition for $t > 0$. Calculate the excess electron concentration for (a) $t = 0$, (b) $t = 1$ μs, and (c) $t = 4$ μs.
[Ans. (a) 10^{15} cm^{-3}, (b) 3.68×10^{14} cm^{-3}, (c) 1.83×10^{13} cm^{-3}]

E6.2 Using the parameters given in E6.1, calculate the recombination rate of the excess electrons for (a) $t = 0$, (b) $t = 1$ μs, and (c) $t = 4$ μs.
[Ans. (a) 10^{21} cm^{-3} s^{-1}, (b) 3.68×10^{20} cm^{-3} s^{-1}, (c) 1.83×10^{19} cm^{-3} s^{-1}]

6.2 | CHARACTERISTICS OF EXCESS CARRIERS

The generation and recombination rates of excess carriers are important parameters, but how the excess carriers behave with time and in space in the presence of electric fields and density gradients is of equal importance. As mentioned in the preview section, the excess electrons and holes do not move independently of each other, but they diffuse and drift with the same effective diffusion coefficient and with the same effective mobility. This phenomenon is called amhipolar transport. The question that must be answered is what is the effective diffusion coefficient and what is the effective mobility that characterizes the behavior of these excess carriers? To answer these questions, we must develop the continuity equations for the carriers and then develop the ambipolar transport equations.

The final results show that. for an extrinsic semiconductor under low injection (this concept will be defined in the analysis). the effective diffusion coefficient and mobility parameters are those of the minority carrier. This result is thoroughly developed in the following derivations. **As** will he seen in the following chapters, the behavior of the excess carriers has a profound impact on the characteristics of semiconductor devices.

6.2.1 Continuity Equations

The continuity equations for electrons and holes are developed in this section. Figure 6.4 shows a differential volume element in which a one-dimensional hole-panicle flux is entering the differential element at x and is leaving the element at $x + dx$. The parameter F_{px}^+ is the hole-particle flux, or flow, and has units of number of holes/cm^2-s. For the x component of the particle current density shown, we may write

$$F_{px}^+(x + dx) = F_{px}^+(x) + \frac{\partial F_{px}^+}{\partial x} \cdot dx \tag{6.15}$$

This equation is a Taylor expansion of $F_{px}^+(x + dx)$, where the differential length dx is small, so that only the first two terms in the expansion are significant. The net increase in the number of holes per unit time within the differential volume element due to the x-component of hole flux is given by

$$\frac{\partial p}{\partial t} dx\,dy\,dz = [F_{px}^+(x) - F_{px}^+(x + dx)]\,dy\,dz = -\frac{\partial F_{px}^+}{\partial x} dx\,dy\,dz \tag{6.16}$$

If $F_{px}^+(x) > F_{px}^+(x + dx)$, for example, there will be a net increase in the number of holes in the differential volume element with time. If we generalize to a three-dimensional hole flux, then the right side of Equation (6.16) may be written as

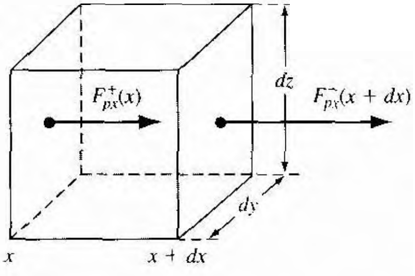

Figure 6.4 | Differential volume showing x component of the hole-particle flux.

$-\nabla \cdot F_p^+ \, dx\, dy\, dz$, where $\nabla \cdot F_p^+$ is the divergence of the flux vector. We will limit ourselves to a one-dimensional analysis.

The generation rate and recombination rate of holes will also affect the hole concentration in the differential volume. The net increase in the number of holes per unit time in the differential volume element is then given by

$$\frac{\partial p}{\partial t}\, dx\, dy\, dz = -\frac{\partial F_p^+}{\partial x}\, dx\, dy\, dz + g_p\, dx\, dy\, dz - \frac{p}{\tau_{pt}}\, dx\, dy\, dz \tag{6.17}$$

where p is the density of holes. The first term on the right side of Equation (6.17) is the increase in the number of holes per unit time due to the hole flux, the second term is the increase in the number of holes per unit time due to the generation of holes, and the last term is the decrease in the number of holes per unit time due to the recombination of holes. The recombination rate for holes is given by p/τ_{pt} where τ_{pt} includes the thermal equilibrium carrier lifetime and the excess carrier lifetime.

If we divide both sides of Equation (6.17) by the differential volume $dx\, dy\, dz$, the net increase in the hole concentration per unit time is

$$\frac{\partial p}{\partial t} = -\frac{\partial F_p^+}{\partial x} + g_p - \frac{p}{\tau_{pt}} \tag{6.18}$$

Equation (6.18) is known as the continuity equation for holes.

Similarly, the one-dimensional continuity equation for electrons is given by

$$\frac{\partial n}{\partial t} = -\frac{\partial F_n^-}{\partial x} + g_n - \frac{n}{\tau_{nt}} \tag{6.19}$$

where F_n^- is the electron-particle flow, or flux, also given in units of number of electrons/cm^2-s.

6.2.2 Time-Dependent Diffusion Equations

In Chapter 5, we derived the hole and electron current densities, which are given, in one dimension, by

$$J_p = e\mu_p p\mathrm{E} - eD_p\frac{\partial p}{\partial x} \tag{6.20}$$

and

$$J_n = e\mu_n n\mathrm{E} + eD_n\frac{\partial n}{\partial x} \tag{6.21}$$

If we divide the hole current density by $(+e)$ and the electron current density by $(-e)$, we obtain each particle flux. These equations become

$$\frac{J_p}{(+e)} = F_p^+ = \mu_p p\mathrm{E} - D_p\frac{\partial p}{\partial x} \tag{6.22}$$

and

$$\frac{J_n}{(-e)} = F_n^- = -\mu_n n\mathrm{E} - D_n\frac{\partial n}{\partial x} \tag{6.23}$$

Taking the divergence of Equations (6.22) and (6.23), and substituting back into the continuity equations of (6.18) and (6.19), we obtain

$$\frac{\partial p}{\partial t} = -\mu_p \frac{\partial (p\mathrm{E})}{\partial x} + D_p \frac{\partial^2 p}{\partial x^2} + g_p - \frac{p}{\tau_{pt}} \tag{6.24}$$

$$\frac{\partial n}{\partial t} = +\mu_n \frac{\partial (n\mathrm{E})}{\partial x} + D_n \frac{\partial^2 n}{\partial x^2} + g_n - \frac{n}{\tau_{nt}} \tag{6.25}$$

Keeping in mind that we are limiting ourselves to a one-dimensional analysis, we can expand the derivative of the product as

$$\frac{\partial (p\mathrm{E})}{\partial x} = \mathrm{E}\frac{\partial p}{\partial x} + p\frac{\partial \mathrm{E}}{\partial x} \tag{6.26}$$

In a more generalized three-dimensional analysis, Equation (6.26) would have to be replaced by a vector identity. Equations (6.24) and (6.25) can be written in the form

$$D_p \frac{\partial^2 p}{\partial x^2} - \mu_p\left(\mathrm{E}\frac{\partial p}{\partial x} + p\frac{\partial \mathrm{E}}{\partial x}\right) + g_p - \frac{p}{\tau_{pt}} = \frac{}{at} \tag{6.27}$$

and

$$D_n \frac{\partial^2 n}{\partial x^2} + \mu_n\left(\mathrm{E}\frac{\partial n}{\partial x} + n\frac{\partial \mathrm{E}}{\partial x}\right) + g_n - \frac{n}{\tau_{nt}} = \frac{\partial n}{\hat{a}t} \tag{6.28}$$

Equations (6.27) and (6.28) are the time-dependent diffusion equations for holes and electrons, respectively. Since both the hole concentration p and the electron concentration n contain the excess concentrations, Equations (6.27) and (6.28) describe the space and time behavior of the excess carriers.

The hole and electron concentrations are functions of both the thermal equilibrium and the excess values are given in Equations (6.5a) and (6.5b). The thermal-equilibrium concentrations, n_0 and p_0, are not functions of time. For the special case of a homogeneous semiconductor, n_0 and p_0 are also independent of the space coordinates. Equations (6.27) and (6.28) may then be written in the form

$$D_p \frac{\partial^2 (\delta p)}{\partial x^2} - \mu_p\left(\mathrm{E}\frac{\partial (\delta p)}{\partial x} + p\frac{\partial \mathrm{E}}{\partial x}\right) + g_p - \frac{p}{\tau_{pt}} = \frac{\partial (\delta p)}{\partial t} \tag{6.29}$$

$$D_n \frac{\partial^2 (\delta n)}{\partial x^2} + \mu_n\left(\mathrm{E}\frac{\partial (\delta n)}{\partial x} + n\frac{\partial \mathrm{E}}{\partial x}\right) + g_n - \frac{n}{\tau_{nt}} = \frac{\partial (\delta n)}{\partial t} \tag{6.30}$$

Note that the Equations (6.29) and (6.30) contain terms involving the total concentrations, p and n, and terms involving only the excess concentrations, δp and δn.

6.3 | AMBIPOLAR TRANSPORT

Originally, we assumed that the electric field in the current Equations (6.20) and (6.21) was an applied electric field. This electric field term appears in the time-dependent diffusion equations given by Equations (6.29) and (6.30). If a pulse of

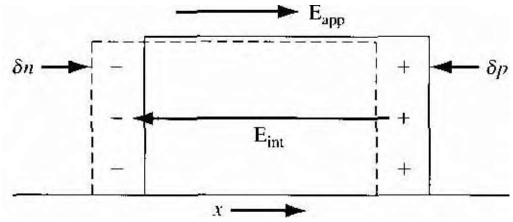

Figure 6.5 | The creation ot an internal electric field as excess electrons and holes rend to separate.

excess electrons and a pulse of excess holes are created at a particular point in a semiconductor with an applied electric field, the excess holes and electrons *will tend* to drift in opposite directions. However, because the electrons and holes are charged particles, any separation will induce an internal electric field between the two sets of particles. This internal electric field will create a force attracting the electrons and holes back toward each other. This effect is shown in Figure 6.5. The electric field term in Equations (6.29) and (6.30) is then composed of the externally applied field plus the induced internal field. This E-field may be written as

$$E = E_{app} + E_{int} \tag{6.31}$$

where E_{app} is the applied electric field and E_{int} is the induced internal electric field.

Since the internal E-field creates a force attracting the electrons and holes. this E-field will hold the pulses of excess electrons and excess holes together. The negatively charged electrons and positively charged holes then will drift or diffuse together with a single effective mobility or diffusion coefficient. This phenomenon is called *ambipolar diffusion* or *ambipolar transport.*

6.3.1 Derivation of the Ambipolar Transport Equation

The time-dependent diffusion Equations (6.29) and (6.30) describe the behavior of the excess carriers. However, a third equation is required to relate the excess electron and hole concentrations to the internal electric field. This relation is Poisson's equation, which may be written as

$$\nabla \cdot E_{int} = \frac{e(\delta p - \delta n)}{\epsilon_s} = \frac{\partial E_{int}}{\partial x} \tag{6.32}$$

where ϵ_s is the permittivity of the semiconductor material.

To make the solution of Equations (6.29), (6.30). and (6.32) more tractable, we need to make some approximations. We can show that only a relatively small internal electric field is sufficient to keep the excess electrons and holes drifting and diffusing together. Hence, we can assume that

$$|E_{int}| \ll |E_{app}| \tag{6.33}$$

However. the V . E_{int} term may not be negligible. We will impose the condition of charge neutrality: We will assume that the excess electron concentration is just balanced by an equal excess hole concentration at any point in space and time. If this assumption were exactly true, there would be no induced internal electric field to keep the two sets of panicles together. However, only a very small difference in the excess electron concentration and excess hole concentration will set up an internal E-field rufficient to keep the particles diffusing and drifting together. We can show that a I percent difference in δp and *Sn.* for example, will result in non-negligible values of the V . $E = V$. E_{int} term in Equations *(6.29)* and *(6.30).*

We can combine Equations *(6.29)* and *(6.30)* to eliminate the V . E term. Considering Equations (6.1) and (6.4), we can define

$$g_n = g_p \equiv g \tag{6.34}$$

and considering Equations *(6.2)* and (6.6), we can define

$$R_n = \frac{n}{\tau_{nt}} = R_p = \frac{p}{\tau_{pt}} \equiv R \tag{6.35}$$

The lifetimes in Equation *(6.35)* include the thermal-equilibrium carrier lifetimes and theexcess-carrier lifetimes. If we impose thecharge neutrality condition, then $\delta n \approx$ *Sp.* We will denote both the excess electron and excess hole concentrations in Equations *(6.29)* and *(6.30)* by δn. We may then rewrite Equations *(6.29)* and *(6.30)* as

$$D_p \frac{\partial^2(\delta n)}{\partial x^2} - \mu_p\left(\mathrm{E}\frac{\partial(\delta n)}{\partial x} + p\frac{\partial \mathrm{E}}{\partial x}\right) + g - R = \frac{\partial(\delta n)}{\partial t} \tag{6.36}$$

$$D_n \frac{\partial^2(\delta n)}{\partial x^2} + \mu_n\left(\mathrm{E}\frac{\partial(\delta n)}{\partial x} + n\frac{\partial \mathrm{E}}{\partial x}\right) + g - R = \frac{\partial(\delta n)}{\partial t} \tag{6.37}$$

If we multiply Equation *(6.36)* by $\mu_n n$, multiply Equation *(6.37)* by $\mu_p p$, and add the two equations, the V . E $= \partial \mathrm{E}/\partial x$ term will be eliminated. The result of this addition gives

$$\begin{aligned}(\mu_n n D_p + \mu_p p D_n)\frac{\partial^2(\delta n)}{\partial x^2} + (\mu_n \mu_p)(p - n)\mathrm{E}\frac{\partial(\delta n)}{\partial x} \\ + (\mu_n n + \mu_p p)(g - R) = (\mu_n n + \mu_p p)\frac{\partial(\delta n)}{\partial t}\end{aligned} \tag{6.38}$$

If we divide Equation *(6.38)* by the term $(\mu_n n + \mu_p p)$, this equation becomes

$$\boxed{D'\frac{\partial^2(\delta n)}{\partial x^2} + \mu' \mathrm{E}\frac{\partial(\delta n)}{\partial x} + g - R = \frac{\partial(\delta n)}{\partial t}} \tag{6.39}$$

where

$$D' = \frac{\mu_n n D_p + \mu_p p D_n}{\mu_n n + \mu_p p} \tag{6.40}$$

and

$$\boxed{\mu' = \frac{\mu_n \mu_p (p - n)}{\mu_n n + \mu_p p}} \tag{6.41}$$

Equation (6.39) is called the *ambipolar* transport *equation* and describes the behavior of the excess electrons and holes in time and space. The parameter D' is called the *ambipolar diffusion* coefficient and μ' is called the *ambipolar mobility*.

The Einstein relation relates the mobility and diffusion coefficient by

$$\frac{\mu_n}{D_n} = \frac{\mu_p}{D_p} = \frac{e}{kT} \tag{6.42}$$

Using these relations, the ambipolar diffusion coefficient may be written in the form

$$\boxed{D' = \frac{D_n D_p (n + p)}{D_n n + D_p p}} \tag{6.43}$$

The ambipolar diffusion coefficient, D', and the ambipolar mobility, μ', are functions of the electron and hole concentrations, n and p, respectively. Since both n and p contain the excess-carrier concentration δn, the coefficient in the ambipolar transport equation are not constants. The ambipolar transport equation, given by Equation (6.39), then, is a nonlinear differential equation.

6.3.2 Limits of Extrinsic Doping and Low Injection

The ambipolar transport equation may be simplified and linearized by considering an extrinsic semiconductor and by considering low-level injection. The ambipolar diffusion coefficient, from Equation (6.43), may be written as

$$D' = \frac{D_n D_p [(n_0 + \delta n) + (p_0 + \delta n)]}{D_n (n_0 + \delta n) + D_p (p_0 + \delta n)} \tag{6.44}$$

where n_0 and p_0 are the thermal-equilibrium electron and hole concentrations, respectively. and Sn is the excess carrier concentration. If we consider a p-type semiconductor, we can assume that $p_0 \gg n_0$. The condition of low-level injection, or just low injection, means that the excess carrier concentration is much smaller than the thermal-equilibrium majority carrier concentration. For the p-type semiconductor, then, low injection implies that $\delta n \ll p_0$. Assuming that $n_0 \ll p_0$ and $\delta n \ll p_0$, and assuming that D,, and D_p are on the same order of magnitude. the ambipolar diffusion coefficient from Equation (6.44) reduces to

$$D' = D_n \tag{6.45}$$

If we apply the conditions of an extrinsic p-type semiconductor and low injection to the ambipolar mobility, Equation (6.41) reduces to

It is important to *note that for* an *extrinsic p-type semiconductor* under low injection, the ambipolar *diffusion coefficient* and the *ambipolar* mobility *coefficient reduce* to *the* minority-carrier *electron parameter values, which* are constants. The ambipolar transport equation reduces to a linear differential equation with constant coefficients.

If we now consider an extrinsic n-type semiconductor under low injection, we may assume that $p_0 \ll n_0$ and $\delta n \ll n_0$. The ambipolar diffusion coefficient from Equation *(6.43)* reduces to

$$D' = D_p \tag{6.47}$$

and the ambipolar mobility from Equation *(6.41)* reduces to

$$\mu = -\mu_p \tag{6.48}$$

The ambipolar parameters *again* reduce to *the* minority-carrier *values,* which are constants. Note that, for the n-type semiconductor, the ambipolar mobility is a negative value. The ambipolar mobility term is associated with carrier drift; therefore. the sign of the drift term depends on the charge of the particle. The equivalent ambipolar particle is negatively charged, as one can see by comparing Equations (6.30) and *(6.39).* If the ambipolar mobility reduces to that of a positively charged hole, a negative sign is introduced as shown in Equation *(6.48).*

The remaining terms we need to consider in the ambipolar transport equation are the generation rate and the recombination rate. Recall that the electron and hole recombination rates are equal and were given by Equation (6.35) as $R_n = R_p = n/\tau_{nt} = p/\tau_{pt} \equiv R$. where τ_{nt} and τ_{pt} are the mean electron and hole lifetimes, respectively. If we consider the inverse lifetime functions, then $1/\tau_{nt}$ is the probability per unit time that an electron will encounter a hole and recombine. Likewise, $1/\tau_{pt}$ is the probability per unit time that a hole will encounter an electron and recombine. If we again consider an extrinsic p-type semiconductor under low injection, the concentration of majority carrier holes will be essentially constant, even when excess carriers are present. Then, the probability per unit time of a minority carrier electron encountering a majority carrier hole will be essentially constant. Hence $\tau_{nt} \equiv \tau_n$, the minority carrier electron lifetime, will remain a constant for the extrinsic p-type semiconductor under low injection.

Similarly, if we consider an extrinsic n-type semiconductor under low injection, the minority carrier hole lifetime, $\tau_{pt} \equiv \tau_p$, will remain constant. Even under the condition of low injection, the minority carrier hole concentration may increase by several orders of magnitude. The probability per unit time of a majority carrier electron encountering a hole may change drastically. The majority carrier lifetime, then, may change substantially when excess carriers are present.

Consider, again, the generation and recombination terms in the ambipolar transport equation. For electrons we may write

$$g - R = g_n - R_n = (G_{n0} + g'_n) - (R_{n0} + R'_n) \tag{6.49}$$

where G_{n0} and g'_n are the thermal-equilibrium electron and excess electron generation rates, respectively. The terms R_{n0} and R'_n are the thermal-equilibrium electron and excess electron recombination rates, respectively. For thermal equilibrium, we have that

$$G_{n0} = R_{n0} \tag{6.50}$$

so Equation (6.49) reduces to

$$g - R = g'_n - R'_n = g'_n - \frac{\delta n}{\tau_n} \tag{6.51}$$

where τ_n is the excess minority carrier electron lifetime.

For the case of holes, we may write

$$g - R = g_p - R_p = (G_{p0} + g'_p) - (R_{p0} + R'_p) \tag{6.52}$$

where G_{p0} and g'_p are the thermal-equilibrium hole and excess hole generation rates, respectively. The terms R_{p0} and R'_p are the thermal-equilibrium hole and excess hole recombination rates, respectively. Again, for thermal equilibrium, we have that

$$G_{p0} = R_{p0} \tag{6.53}$$

so that Equation *(6.52)* reduces to

$$g - R = g'_p - R'_p = g'_p - \frac{\delta p}{\tau_p} \tag{6.54}$$

where τ_p is the excess minority carrier hole lifetime.

The generation rate for excess electrons must equal the generation rate for excess holes. We may then define a generation rate for excess carriers as g', so that $g'_n = g'_p \equiv g'$. We also determined that the minority carrier lifetime is essentially a constant for low injection. Then the term $g - R$ in the ambipolar transport equation may he written in terms of the minority-carrier parameters.

The ambipolar transport equation, given by Equation (6.39), for a p-type semiconductor under low injection then becomes

$$\boxed{D_n \frac{\partial^2(\delta n)}{\partial x^2} + \mu_n \mathrm{E} \frac{\partial(\delta n)}{\partial x} + g' - \frac{\delta n}{\tau_{n0}} = \frac{\partial(\delta n)}{\partial t}} \tag{6.55}$$

The parameter δn is the excess minority carrier electron concentration, the parameter τ_{n0} is the minority carrier lifetime under low injection, and the other parameters are the usual minority carrier electron parameters.

Similarly, for an extrinsic n-type semiconductor under low injection, the ambipolar transport equation becomes

$$\boxed{D_p \frac{\partial^2(\delta p)}{\partial x^2} - \mu_p \mathrm{E} \frac{\partial(\delta p)}{\partial x} + g' - \frac{\delta p}{\tau_{p0}} = \frac{\partial(\delta p)}{\partial t}} \tag{6.56}$$

The parameter δp is the excess minority carrier hole concentration, the parameter τ_{p0} is the minority carrier hole lifetime under low injection, and the other parameters are the usual minority carrier hole parameters.

Table 6.2 | Common ambipolar transport equation simplifications

Specification	Effect
Steady state	$\frac{\partial(\delta n)}{\partial t} = 0, \quad \frac{\partial(\delta p)}{\partial t} = 0$
Uniform distribution of excess carriers (uniform generation rate)	$D_n \frac{\partial^2(\delta n)}{\partial x^2} = 0, \quad D_p \frac{\partial^2(\delta n)}{\partial x^2} = 0$
Zero electric field	$E\frac{\partial(\delta n)}{\partial x} = 0, \quad E\frac{\partial(\delta p)}{\partial x} = 0$
No excess carrier generation	$g' = 0$
No excess carrier recombination (infinite lifetime)	$\frac{\delta n}{\tau_{n0}} = 0, \quad \frac{\delta p}{\tau_{p0}} = 0$

It is extremely important to note that the transport and recombination parameters in Equations (6.55) and (6.56) are those of the minority carrier. *Equations (6.55) and (6.56) describe the drift, diffusion, and recombination of excess minority carriers as a function of spatial coordinates and as a function of time.* Recall that we had imposed the condition of charge neutrality; the excess minority carrier concentration is equal to the excess majority carrier concentration. The excess majority carriers, then, diffuse and drift with the excess minority carriers; thus, the behavior of the excess majority carrier is determined by the minority carrier parameters. This ambipolar phenomenon is extremely important in semiconductor physics, and is the basis for describing the characteristics and behavior of semiconductor devices.

6.3.3 Applications of the Ambipolar Transport Equation

We will solve the ambipolar transport equation for several problems. These examples will help illustrate the behavior of excess carriers in a semiconductor material, and the results will be used later in the discussion of the pn junction and the other semiconductor devices.

The following examples use several common simplifications in the solution of the ambipolar transport equation. Table 6.2 summarizes these simplifications and their effects.

Objective | **EXAMPLE 6.1**

To determine the time behavior of excess carriers as a semiconductor returns to thermal equilibrium.

Consider an infinitely large, homogeneous n-type semiconductor with zero applied electric field. Assume that at time $t = 0$, a uniform concentration of excess carriers exists in the crystal, but assume that $g' = 0$ for $t > 0$. If we assume that the concentration of excess carriers is much smaller than the thermal-equilibrium electron concentration, then the low-injection condition applies. Calculate the excess carrier concentration as a function of time for $t \geq 0$.

■ Solution

For the n-type semiconductor, we need to consider the ambipolar transport equation for the minority carrier holes, which was given by Equation (6.56). The equation is

$$D_p \frac{\partial^2 (\delta p)}{\partial x^2} - \mu_p \mathrm{E} \frac{\partial (\delta p)}{\partial x} + g' - \frac{\delta p}{\tau_{p0}} = \frac{\partial (\delta p)}{\partial t}$$

We are assuming a uniform concentration of excess holes so that $\partial^2 (\delta p)/\partial x^2 = \partial (\delta p)/\partial x = 0$. For $t > 0$, we are also assuming that $g' = 0$. Equation (6.56) reduces to

$$\frac{d(\delta p)}{dt} = -\frac{\delta p}{\tau_{p0}} \tag{6.57}$$

Since there is no spatial variation, the total time derivative may be used. At low injection, the minority carrier hole lifetime, τ_{p0}, is a constant. The solution to Equation *(6.57)* is

$$\boxed{\delta p(t) = \delta p(0) e^{-t/\tau_{p0}}} \tag{6.58}$$

where $\delta p(0)$ is the uniform concentration of excess carriers that exists at time $t = 0$. The concentration of excess holes decays exponentially with time, with a time constant equal to the minority carrier hole lifetime.

From the charge-neutrality condition, we have that $\delta n = \delta p$, so the excess electron concentration is given by

$$\delta n(t) = \delta p(0) e^{-t/\tau_{p0}} \tag{6.59}$$

■ Numerical Calculation

Consider n-type gallium arsenide doped at $N_d = 10^{16}$ cm^{-3}. Assume that 10^{14} electron-hole pairs per cm^3 have been created at $t = 0$, and assume the minority carrier hole lifetime is $\tau_{p0} = 10$ ns.

We may note that $\delta p(0) \ll n_0$, so low injection applies. Then from Equation (6.58) we can write

$$\delta p(t) = 10^{14} e^{-t/10^{-8}} \text{ cm}^{-3}$$

The excess hole and excess electron concentrations will decay to $1/e$ of their initial value in 10 ns.

■ Comment

The excess electrons and holes recombine at the rate determined by the excess minority carrier hole lifetime in the n-type semiconductor.

EXAMPLE 6.2

Objective

To determine the time dependence of excess carriers in reaching a steady-state condition.

Again consider an infinitely large, homogeneous n-type semiconductor with a zero applied electric field. Assume that, for $t < 0$, the semiconductor is in thermal equilibrium and that, for $t \ge 0$, a uniform generation rate exists in the crystal. Calculate the excess carrier concentration as a function of time assuming the condition of low injection.

Solution

The condition of a uniform generation rate and a homogeneous semiconductor again implies that $\partial^2(\delta p)/\partial x^2 = \partial(\delta p)/\partial x = 0$ in Equation *(6.56)*. The equation, for this case, reduces to

$$g' - \frac{\delta p}{\tau_{p0}} = \frac{d(\delta p)}{dt} \tag{6.60}$$

The solution to this differential equation is

$$\boxed{\delta p(t) = g'\tau_{p0}(1 - e^{-t/\tau_{p0}})} \tag{6.61}$$

■ **Numerical Calculation**

Consider n-type silicon at $T = 300$ K doped at $N_d = 2 \times 10^{16}$ cm^{-3}. Assume that $\tau_{p0} = 10^{-7}$ s and $g' = 5 \times 10^{21}$ cm^{-3} s^{-1}. From Equation *(6.61)* we can write

$$\delta p(t) = (5 \times 10^{21})(10^{-7})\left[1 - e^{-t/10^{-7}}\right] = 5 \times 10^{14}\left[1 - e^{-t/10^{-7}}\right] \text{ cm}^{-3}$$

■ **Comment**

We may note that for $t \to \infty$. we will create a steady-state excess hole and electron concentration of 5×10^{14} cm^{-3}. We may note that $\delta p \ll n_0$, so low injection is valid.

The excess minority carrier hole concentration increases with time with the same time constant τ_{p0}, which is the excess minority carrier lifetime. The excess carrier concentration reaches a steady-state value as time goes to infinity, even though a steady-state generation of excess electrons and holes exists. This steady-state effect can be seen from Equation (6.60) by setting $d(\delta p)/dt = 0$. The remaining terms simply state that, in steady state, the generation rate is equal to the recombination rate.

TEST YOUR UNDERSTANDING

E6.3 Silicon at $T = 300$ K has been doped with boron atoms to a concentration of $N_a = 5 \times 10^{16}$ cm^{-3}. Excess carriers have been generated in the uniformly doped material to a concentration of 10^{15} cm^{-3}. The minority carrier lifetime is 5 μs. (a) What carrier type is the minority carrier? *(b)* Assuming $g' = E = 0$ for $t > 0$, determine the minority carrier concentration for $t > 0$.
[Ans. (*a*) electrons, (*b*) $10^{15}e^{-t/5\times10^{-6}}$ cm^{-3}]

E6.4 Consider silicon with the same parameters as given in **E6.3.** The material is in thermal equilibrium for $t < 0$. At $t = 0$, a source generating excess carriers is turned on, producing a generation rate of $g' = 10^{20}$ cm^{-3}-s^{-1}. ***(a)*** What carrier type is the minority carrier? *(b)* Determine the minority carrier concentration for $t > 0$. ***(c)*** What is the minority carrier concentration as $t \to \infty$?
[Ans. (*a*) electrons, (*b*) $5 \times 10^{14}[1 - e^{-t/5\times10^{-6}}]$ cm^{-3}, (*c*) 5×10^{14} cm^{-3}]

EXAMPLE 6.3

Objective

To determine the steady-state spatial dependence of the excess carrier concentration.

Consider a p-type semiconductor that is homogeneous and infinite in extent. Assume a zero applied electric field. For a one-dimensional crystal, assume that excess carriers are being generated at $x = 0$ only, as indicated in Figure 6.6. The excess carriers being generated at $x = 0$ will begin diffusing in both the $+x$ and $-x$ directions. Calculate the steady-state excess carrier concentration as **a** function of x.

Solution

The ambipolar transport equation lor excess minority carrier electrons was given by Equation (6.55), and is written as

$$D_n \frac{\partial^2(\delta n)}{ax^2} + \mu_n \mathrm{E} \frac{\partial(\delta n)}{\partial x} + g' - \frac{\delta n}{\tau_{n0}} = \frac{\partial(\delta n)}{\text{ill}}$$

From our assumptions. we have E = 0, g' = 0 for $x \# 0$, and $\partial(\delta n)/\partial t = 0$ fur steady state. Assuming a one-dimensional crystal, Equation *(6.55)* reduces to

$$n_{,,}\frac{d^2(\delta n)}{dx'} - \frac{\delta n}{\tau_{n0}} = 0 \tag{6.62}$$

Dividing by the diffusion coefficient, Equation *(6.62)* may he written as

$$\frac{d^2(\delta n)}{dx^2} - \frac{\delta n}{D_n \tau_{n0}} = \frac{d^2(\delta n)}{dx^2} - \frac{\delta n}{L_n^2} = 0 \tag{6.63}$$

where we have defined $L_n^2 = D_n \tau_{n0}$. The parameter L_n has the unit of length and is called the minority carrier electron diffusion length. The general solution to Equation *(6.63) is*

$$\delta n(x) = Ae^{-x/L_n} + Be^{x/L_n} \tag{6.64}$$

As the minority carrier electrons diffuse away from x = 0. they will recombine with the majority carrier holes. The minority carrier electron concentration will then decay toward zero at both $x = +\infty$ and $x = -\infty$. These boundary conditions mean that $B \equiv 0$ for $x > 0$ and A ≡ 0 for $x < 0$. The solution to Equation (6.63) may then he written as

$$\boxed{\delta n(x) = \delta n(0)e^{-x/L_n} \qquad x \geq 0} \tag{6.65a}$$

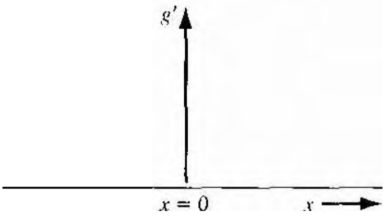

Figure 6.6 | Steady-state generation rate at x = 0.

$$\boxed{\delta n(x) = \delta n(0)e^{+x/L_n} \qquad x \le 0} \qquad (6.65b)$$

where $\delta n(0)$ is the value of the excess electron concentration at x = 0. The steady-state excess electron concentration decays exponentially with distance away from the source at $x = 0$.

■ Numerical Calculation

Consider p-type silicon at T = 300 K doped at N, = 5 × 10^{16} cm^{-3}. Assume that τ_{n0} = 5 x 10^{-7} s, D,, = 25 cm^2/s, and $\delta n(0) = 10^{15}$ cm^{-3}.

The minority carrier diffusion length is

$$L_{,,} = \sqrt{D_n\tau_{n0}} = \sqrt{(25)(5\times10^{-7})} = 35.4\ \mu\text{m}$$

Then for x $\geq$ 0, we have

$$\delta n(x) = 10^{15}e^{-x/35.4\times10^{-4}}\ \text{cm}^{-3}$$

■ Comment

We may note that the steady-state excess concentration decays to $1/e$ of its value at x = 35.4 μm.

As before, we will assume charge neutrality; thus, the steady-state excess majority carrier hole concentration also decays exponentially with distance with the same characteristic minority carrier electron diffusion length L,,. Figure 6.7 is a plot of the total electron and hole concentrations as a function of distance. We are assuming low injection, that is, $\delta n(0) \ll p_0$ in the p-type semiconductor. The total concentration of majority carrier holes barely changes. However, we may have $\delta n(0) \gg n_0$ and still satisfy the low-injection condition. The minority carrier concentration may change by many orders of magnitude.

TEST YOUR UNDERSTANDING

E6.5 Excess electrons and holes are generated at the end of a silicon bar ($x = 0$). The silicon is doped with phosphorus atoms to a concentration of $N_d = 10^{17}$ cm^{-3}. The minority carrier lifetime is 1 μs, the electron diffusion coefficient is D_n = 25 **cm^2/s,** and the hole diffusion coefficient is D_p = 10 cm^2/s. If $\delta n(0) = \delta p(0) = 10^{15}$ cm^{-3}, determine the steady-state electron and hole concentrations in the silicon for $x > 0$.
(Ans. $\delta n(x) = \delta p(x) = 10^{15}e^{-x/3.16\times10^{-3}}$ cm^{-3}, where x is in cm)

E6.6 Using the parameters given in E6.5, calculate the electron and hole diffusion current densities at x = 10 μm. (Ans. $J_p = +0.369$ A/cm^2, $J_n = -0.369$ A/cm^2)

The three previous examples, which applied the ambipolar transport equation to specific situations, assumed either a homogeneous or a steady-state condition; only the time variation or the spatial variation was considered. Now consider an example in which both the time and spatial dependence are considered in the same problem.

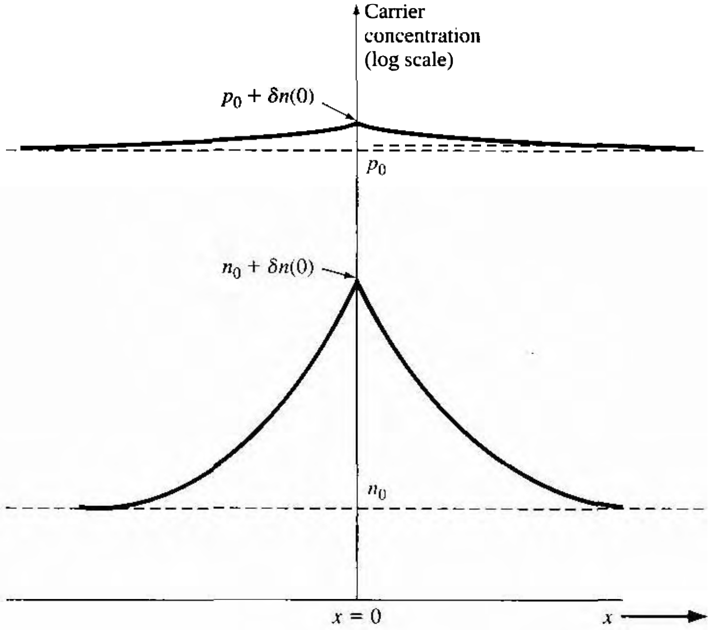

Figure 6.7 | Steady-state electron and hole concentrations for the case when excess electrons and holes are generated at $x = 0$.

EXAMPLE 6.4

Objective

To determine both the time dependence and spatial dependence of the excess carrier concentration.

Assume that a finite number of electron–hole pairs is generated instantaneously at time $t = 0$ and at $x = 0$, but assume $g' = 0$ for $t > 0$. Assume we have an n-type semiconductor with a constant applied electric field equal to E_0, which is applied in the $+x$ direction. Calculate the excess carrier concentration as a function of x and t.

Solution

The one-dimensional ambipolar transport equation for the minority carrier holes can be written from Equation (6.56) as

$$D_p \frac{\partial^2(\delta p)}{\partial x^2} - \mu_p \mathrm{E}_0 \frac{\partial(\delta p)}{\partial x} - \frac{\delta p}{\tau_{p0}} = \frac{\partial(\delta p)}{\partial t} \tag{6.66}$$

The solution to this partial differential equation is of the form

$$\delta p(x,t) = p'(x,t)e^{-t/\tau_{p0}} \tag{6.67}$$

By substituting Equation *(6.67)* into Equation (6.66), we are left with the partial differential equation

$$D_p \frac{\partial^2 p'(x,t)}{\partial x^2} - \mu_p \mathrm{E}_0 \frac{\partial p'(x,t)}{\partial x} = \frac{\partial p'(x,t)}{\partial t} \tag{6.68}$$

Equation (6.68) is normally solved using Laplace transform techniques. The solution, without going through the mathematical details, is

$$p'(x,t) = \frac{1}{(4\pi D_p t)^{1/2}} \exp\left[\frac{-(x-\mu_p \mathrm{E}_0 t)^2}{4D_p t}\right] \tag{6.69}$$

The total solution. from Equations (6.67) and (6.69). for the excess minority carrier hole concentration is

$$\boxed{\delta p(x,t) = \frac{e^{-t/\tau_{p0}}}{(4\pi D_p t)^{1/2}} \exp\left[\frac{-(x-\mu_p \mathrm{E}_0 t)^2}{4D_p t}\right]} \tag{6.70}$$

■ Comment

We could show that Equation (6.70) is a solution by direct substitution back into the partial differential equation. Equation (6.66).

Equation (6.70) can be plotted as a function of distance x, for various times. Figure 6.8 shows such a plot for the case when the applied electric field is zero. For $t > 0$, the excess minority carrier holes diffuse in both the $+x$ and $-x$ directions. During this time, the excess majority carrier electrons, which were generated, diffuse at exactly the same rate as the holes. **As** time proceeds, the excess holes recombine

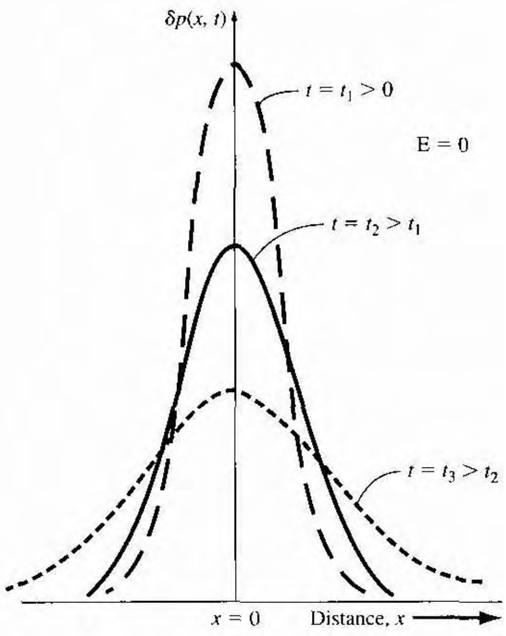

Figure 6.8 | Excess-hole concentration versus distance at various times for zero applied electric field.

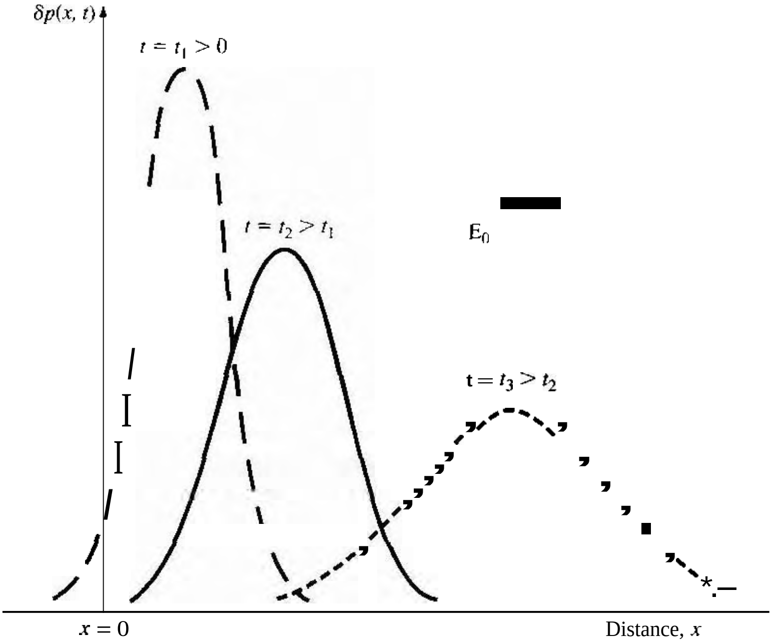

Figure **6.9** | Excess-hole concentration versus distance at various times for a constant applied electric field.

with the excess electrons so that at $t = \infty$ the excess hole concentration is zero. In this particular example, both diffusion and recombination processes are occurring at the same time.

Figure 6.9 shows a plot of Equation (6.70) as a function of distance x at various times for the case when the applied electric field is not zero. In this case, the pulse of excess minority carrier holes is drifting in the $+x$ direction, which is the direction of the electric field. We still have the same diffusion and recombination processes as we had before. An important point to consider is that, with charge neutrality, $\delta n = \delta p$ at any instant of time and at any point in space. The excess-electron concentration is equal to the excess-hole concentration. In this case, then, the excess-electron pulse is moving in the same direction as the applied electric field even though the electrons have a negative charge. In the ambipolar transport process, the excess carriers are characterized by the minority carrier parameters. In this example, the excess carriers behave according to the minority carrier hole parameters, which include D_p, μ_p, and τ_{p0}. The excess majority carrier electrons are being pulled along by the excess minority carrier holes.

TEST YOUR UNDERSTANDING

E6.7 As a good approximation, the peak value of a normalized excess carrier concentration, given by Equation (6.70), occurs at $x = \mu_p E_0 t$. Assume the following parameters:

$\tau_{p0} = 5\ \mu s$, $D_p = 10\ cm^2/s$, $\mu_p = 386\ cm^2/V\text{-}s$, and $E_0 = 10$ V/cm. Calculate the peak value at times of (a) $t = 1\ \mu s$, $(h) r = 5\ \mu s$, (c) $t = 15\ \mu s$, and **(d)** $t = 25\ \mu s$. What are the corresponding values of x for pans (a) to (d)? [Ans. (a) 73.0, $x = 38.6\ \mu m$; (b) 14.7, $x = 193\ \mu m$; (c) 1.15, $x = 579\ \mu m$; (d) 0.120, $x = 965\ \mu m$]

E6.8 The excess carrier concentration, given by Equation (6.70), is to be calculated at distances of one diffusion length away from the peak value. Using the parameters given in E6.7. calculate the values of δp for (a) $t = 1\ \mu s$ at (i) 1.093×10^{-2} cm and (ii) $x = -3.21 \times 10^{-3}$ cm; (b) $t = 5\ \mu s$ at (i) $x = 2.64 \times 10^{-2}$ cm and (ii) $x = 1.22 \times 10^{-2}$ cm; (c) $r = 15\ \mu s$ at (i) $x = 6.50 \times 10^{-2}$ cm and (ii) $x = 5.08 \times 10^{-2}$ cm.
[Ans. (a) (i) 20.9, (ii) 20.9; (b) (i) 11.4, (ii) 11.4; (c) (i) 1.05, (ii) 1.05]

Eh.9 Using the parameters given in E6.7, (a) plot $\delta p(x, t)$ from Equation (6.70) versus x for (i) $t = 1\ \mu s$, (ii) $t = 5\ \mu s$, and (iii) $t = 15\ \mu s$, a (b) pot $\delta p(x, t)$ versus time for (i) $x = 10^{-2}$ cm, (ii) $x = 3 \times 10^{-2}$ cm, and (iii) $x = 6 \times 10^{-2}$ cm.

6.3.4 Dielectric Relaxation Time Constant

We have assumed in the previous analysis that a quasi-neutrality conditions exists—that is, the concentration of excess holes is balanced by an equal concentration of excess electrons. Suppose that we have a situation as shown in Figure 6.10, in which a uniform concentration of holes δp is suddenly injected into a portion of the surface of a semiconductor. We will instantly have a concentration of excess holes and a net positive charge density that is not balanced by a concentration of excess electrons. How is charge neutrality achieved and how fast?

There are three defining equations to he considered. Poisson's equation is

$$\nabla \cdot E = \frac{\rho}{\epsilon} \tag{6.71}$$

The current equation, Ohm's law, is

$$J = \sigma E \tag{6.72}$$

The continuity equation, neglecting the effects of generation and recombination, is

$$\nabla \cdot J = -\frac{\partial \rho}{\partial t} \tag{6.73}$$

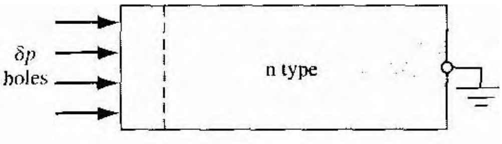

Figure 6.10 | The injection of a concentration of holes into a small region at the surface of an n-type semiconductor.

The parameter ρ is the net charge density and the initial value is given by $e(\delta p)$. We will assume that δp is uniform over a short distance at the surface. The parameter ϵ is the permittivity of the semiconductor.

Taking the divergence of Ohm's law and using Poisson's equation, we find

$$\nabla \cdot J = \sigma \nabla \cdot E = \frac{\sigma \rho}{\epsilon} \tag{6.74}$$

Substituting Equation (6.74) into the continuity equation, we have

$$\frac{\sigma \rho}{\epsilon} = -\frac{\partial \rho}{at} = -\frac{d\rho}{dr} \tag{6.75}$$

Since Equation (6.75) is a function of time only, we can write the equation as a total derivative. Equation (6.75) can be rearranged as

$$\frac{d\rho}{dt} + \left(\frac{\sigma}{\epsilon}\right)\rho = 0 \tag{6.76}$$

Equation (6.76) is a first-order differential equation whose solution is

$$\rho(t) = \rho(0)e^{-(t/\tau_d)} \tag{6.77}$$

where

$$\tau_d = \frac{\epsilon}{\sigma} \tag{6.78}$$

and is called the dielectric relaxation time constant.

EXAMPLE 6.5

Objective

Calculate the dielectric relaxation time constant for a particular semiconductor.

Assume an n-type semiconductor with a donor impurity concentration of $N_d = 10^{16}$ cm^{-3}.

■ Solution

The conductivity is found as

$$\sigma \approx e\mu_n N_d = (1.6 \times 10^{-19})(1200)(10^{16}) = 1.92\ (\Omega\text{-cm})^{-1}$$

where the value of mobility is the approximate value found from Figure 5.3. The permittivity of silicon is

$$\epsilon = \epsilon_r \epsilon_0 = (11.7)(8.85 \times 10^{-14})\ \text{F/cm}$$

The dielectric relaxation time constant is then

$$\tau_d = \frac{\epsilon}{\sigma} = \frac{(11.7)(8.85 \times 10^{-14})}{1.92} = 5.39 \times 10^{-13}\ \text{s}$$

Comment

Equation (6.77) then predicts that in approximately four time constants, or in approximately 2 ps, the net charge density is essentially zero; that is, quasi-neutrality has been achieved. Since the continuity equation, Equation (6.73), does not contain any generation or recombination terms, the initial positive charge is then neutralized by pulling in electrons from the bulk n-type material to create excess electrons. This process occurs very quickly compared to the normal excess carrier lifetimes of approximately 0.1 μs. The condition of quasi-charge-neutrality is then justified.

---

*6.3.5 Haynes–Shockley Experiment

We have derived the mathematics describing the behavior of excess carriers in a semiconductor. The Haynes–Shockley experiment was one of the first experiments to actually measure excess-carrier behavior.

Figure 6.11 shows the basic experimental arrangement. The voltage source V_1 establishes an applied electric field E_0 in the $+x$ direction in the n-type semiconductor sample. Excess carriers are effectively injected into the semiconductor at contact A. Contact B is a rectifying contact that is under reverse bias by the voltage source V_2. The contact B will collect a fraction of the excess carriers as they drift through the semiconductor. The collected carriers will generate an output voltage, V_0.

This experiment corresponds to the problem we discussed in Example 6.4. Figure 6.12 shows the excess-carrier concentrations at contacts A and B for two conditions. Figure 6.12a shows the idealized excess-carrier pulse at contact A at time $t = 0$. For a given electric field E_{01}, the excess carriers will drift along the semiconductor producing an output voltage as a function of time given in Figure 6.12b. The peak of the pulse will arrive at contact B at time t_0. If the applied electric field is reduced to a value E_{02}, $E_{02} < E_{01}$, the output voltage response at contact B will look approximately as shown in Figure 6.12c. For the smaller electric field, the drift velocity of the pulse of excess carriers is smaller, and so it will take a longer time for the

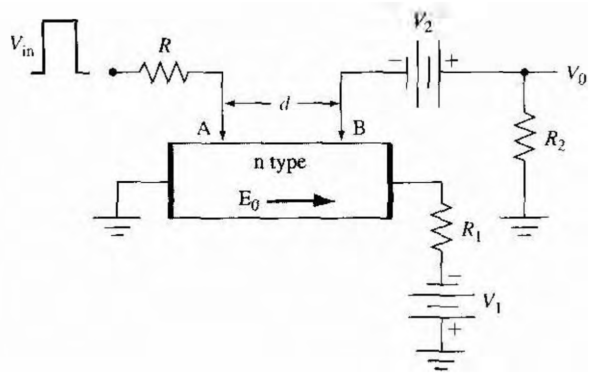

Figure 6.11 | The basic Haynes–Shockley experimental arrangement.

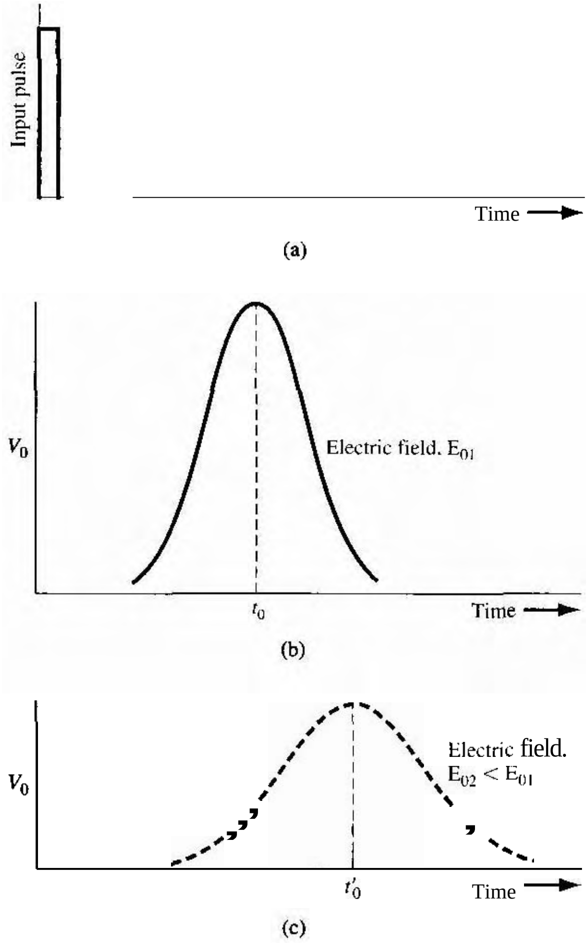

Figure 6.12 | (a) The idealized excess-carrier pulse at terminal **A** at $t = 0$. (**b**) The excess-carrier pulse versus time at terminal B for a given applied electric field. (c) The excess-carrier pulse versus time at terminal B for a smaller applied electric field.

pulse to reach the contact B. During this longer time period, there is more diffusion and more recombination. The excess-carrier pulse shapes shown in Figures 6.12b and 6.12c are different for the two electric field conditions.

The minority carrier mobility, lifetime, and diffusion coefficient can be determined from this single experiment. As a good first approximation, the peak of the minority carrier pulse will arrive at contact B when the exponent involving distance and time in Equation (6.70) is zero, or

In this case $x = d$, where d is the distance between contacts A and B, and $t = t_0$, where t_0 is the time at which the peak of the pulse reaches contact B. The mobility may be calculated as

$$\mu_p = \frac{d}{E_0 t_0} \tag{6.79b}$$

Figure 6.13 again shows the output response as a function of time. At times t_1 and t_2, the magnitude of the excess concentration is e^{-1} of its peak value. If the time difference between t_1 and t_2 is not too large, $e^{-t/\tau_{p0}}$ and $(4\pi D_p t)^{1/2}$ do not change appreciably during this time; then the equation

$$(d - \mu_p E_0 t)^2 = 4D_p t \tag{6.80}$$

is satisfied at both $t = t_1$ and $t = t_2$. If we set $t = t_1$ and $t = t_2$ in Equation (6.80) and add the two resulting equations, we may show that the diffusion coefficient is given by

$$D_p = \frac{(\mu_p E_0)^2 (\Delta t)^2}{16 t_0} \tag{6.81}$$

where

$$At = t_2 - t_1 \tag{6.82}$$

The area S under the curve shown in Figure 6.13 is proportional to the number of excess holes that have not recombined with majority carrier electrons. We may write

$$S = K \exp\left(\frac{-t_0}{\tau_{p0}}\right) = K \exp\left(\frac{-d}{\mu_p E_0 \tau_{p0}}\right) \tag{6.83}$$

where K is a constant. By varying the electric field, the area under the curve will change. A plot of $\ln(S)$ as a function of $(d/\mu_p E_0)$ will yield a straight line whose slope is $(1/\tau_{p0})$, so the minority carrier lifetime can also be determined from this experiment.

The Haynes–Shockley experiment is elegant in the sense that the three basic processes of drift, diffusion, and recombination are all observed in a single experiment.

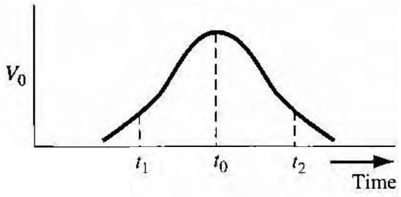

Figure 6.13 | The output excess-carrier pulse versus time to determine the diffusion coefficient.

The determination of mobility is straightforward and can yield accurate values. The determination of the diffusion coefficient and lifetime is more complicated and may lead to some inaccuracies.

6.4 | QUASI-FERMI ENERGY LEVELS

The thermal-equilibrium electron and hole concentrations are functions of the Fermi energy level. We can write

$$= n_i \exp\left(\frac{E_F - E_{Fi}}{kT}\right) \tag{6.84a}$$

and

$$p_0 = n_i \exp\left(\frac{E_{Fi} - E_F}{kT}\right) \tag{6.84b}$$

where E_F and E_{Fi} are the Fermi energy and intrinsic Fermi energy, respectively, and n_i is the intrinsic carrier concentration. Figure 6.14a shows the energy-band diagram for an n-type semiconductor in which $E_F > E_{Fi}$. For this case, we may note from Equations (6.84a) and (6.84b) that $n_0 > n_i$ and $p_0 < n_i$, as we would expect. Similarly, Figure 6.14b shows the energy-band diagram for a p-type semiconductor in which $E_F < E_{Fi}$. Again we may note from Equations (6.84a) and (6.84b) that $n_0 < n_i$ and $p_0 > n_i$, as we would expect for the p-type material. These results are for thermal equilibrium.

If excess carriers are created in a semiconductor, we are no longer in thermal equilibrium and the Fermi energy is strictly no longer defined. However, we may define a quasi-Fermi level for electrons and a quasi-Fermi level for holes that apply for nonequilibrium. If δn and δp are the excess electron and hole concentrations, respectively, we may write:

$$\boxed{n_0 + \delta n = n_i \exp\left(\frac{E_{Fn} - E_{Fi}}{kT}\right)} \tag{6.85a}$$

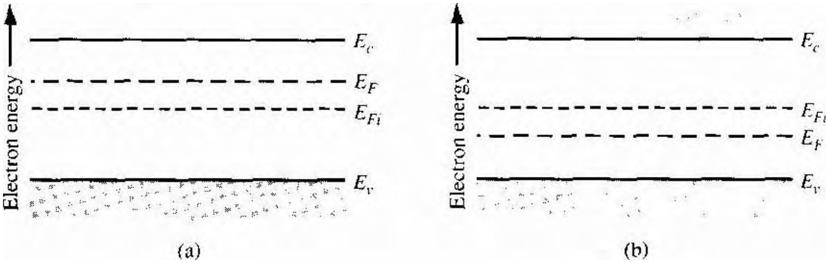

(a) (b)

Figure 6.14 | Thermal-equilibrium energy-band diagrams for *(a)* n-type semiconductor and *(b)* p-type semiconductor.

$$\boxed{p_0 + \delta p = n_i \exp\left(\frac{E_{Fi} - E_{Fp}}{kT}\right)} \tag{6.85b}$$

where E_{Fn} and E_{Fp} are the quasi-Fermi energy levels for electrons and holes, respectively. The total electron concentration and the total hole concentration are functions of the quasi-Fermi levels.

Objective **EXAMPLE 6.6**

To calculate the quasi-Fermi energy levels.

Consider an n-type semiconductor at T = 300 K with carrier concentrations of $n_0 = 10^{15}\ \text{cm}^{-3}$, $n_i = 10^{10}\ \text{cm}^{-3}$, and $p_0 = 10^5\ \text{cm}^{-3}$. In nonequilibrium, assume that the excess carrier concentrations are $\delta n = \delta p = 10^{13}\ \text{cm}^{-3}$.

■ **Solution**

The Fermi level for thermal equilibrium can be determined from Equation (6.84a). We have

$$E_F - E_{Fi} = kT \ln\left(\frac{n_0}{n_i}\right) = 0.2982\ \text{eV}$$

We can use Equation (6.85a) to determine the quasi-Fermi level for electrons in nonequilibrium. We can write

$$E_{Fn} - E_{Fi} = kT \ln\left(\frac{n_0 + \delta n}{n_i}\right) = 0.2984\ \text{eV}$$

Equation (6.85b) can be used to calculate the quasi-Fermi level for holes in nonequilibnum. We can write

$$E_{Fi} - E_{Fp} = kT \ln\left(\frac{p_0 + \delta p}{n_i}\right) = 0.179\ \text{eV}$$

Comment

We may note that the quasi-Fermi level for electrons is above E_{Fi} while the quasi-Fermi level for holes is below E_{Fi}

Figure 6.15a shows the energy-band diagram with the Fermi energy level corresponding to thermal equilibrium. Figure 6.15b now shows the energy-band diagram under the nonequilibrium condition. Since the majority carrier electron concentration does not change significantly for this low-injection condition, the quasi-Fermi level for electrons is not much different from the thermal-equilibrium Fermi level. The quasi-Fermi energy level for the minority carrier holes is significantly different from the Fermi level and illustrates the fact that we have deviated from thermal equilibrium significantly. Since the electron concentration has increased, the quad-Fermi level for electrons has moved slightly closer to the conduction band. The hole

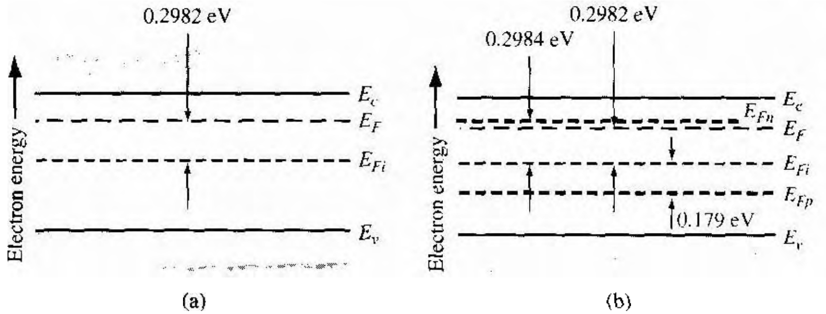

Figure 6.15 | (a) Thermal-equilibrium energy-band diagram for $N_d = 10^{15}$ cm^{-3} and $n_i = 10^{10}$ cm^{-3}. (b) Quasi-Fermi levels for electrons and holes if 10^{13} cm^{-3} excess carriers are present.

concentration has increased significantly so that the quasi-Fermi level for holes has moved much closer to the valence band. We will consider the quasi-Fermi energy levels again when we discuss forward-biased pn junctions.

TEST YOUR UNDERSTANDING

E6.10 Silicon at $T = 300$ K is doped at impurity concentrations of $N_d = 10^{16}$ cm^{-3} and $N_a = 0$. Excess carriers are generated such that the steady-state values are $\delta n = \delta p = 5 \times 10^{14}$ cm^{-3}. (*a*) Calculate the thermal equilibrium Fermi level with respect to E_{Fi}. **(*b*)**Determine E_{Fn} and E_{Fp} with respect to E_{Fi}.
[Ans. (*a*) $E_F - E_{Fi} = 0.3473$ eV;
(*b*) $E_{Fn} - E_{Fi} = 0.3486$ eV, $E_{Fi} - E_{Fp} = 0.2697$ eV]

E6.11 Impurity concentrations of $N_d = 10^{15}$ cm^{-3} and $N_a = 6 \times 10^{15}$ cm^{-3} are added to silicon at T = 300 K. Excess carriers are generated in the material such that the steady-state concentrations are $\delta n = \delta p = 2 \times 10^{14}$ cm^{-3}. **(*a*)** Find the thermal equilibrium Fermi level with respect to E_{Fi}. (b) Calculate E_{Fn} and E_{Fp} with respect to E_{Fi}.
[Ans. (*a*) $E_{Fi} - E_F = 0.3294$ eV;
(*b*) $E_{Fn} - E_{Fi} = 0.2460$ eV, $E_{Fi} - E_{Fp} = 0.3304$ eV]

*6.5 | EXCESS-CARRIER LIFETIME

The rate at which excess electrons and holes recombine is an important characteristic of the semiconductor and influences many of the device characteristics, as we will see in later chapters. We considered recombination briefly at the beginning of this chapter and argued that the recombination rate is inversely proportional to the mean carrier lifetime. We have assumed up to this point that the mean carrier lifetime is simply a parameter of the semiconductor material.

We have been considering an ideal semiconductor in which electronic energy states do not exist within the forbidden-energy bandgap. This ideal effect is present in a perfect single-crystal material with an ideal periodic-potential function. In a real semiconductor material, defects occur within the crystal and disrupt the perfect periodic-potential function. If the density of these defects is not too great, the defects will create discrete electronic energy states within the forbidden-energy band. These allowed energy states may be the dominant effect in determining the mean carrier lifetime. The mean carrier lifetime may be determined from the Shockley–Read–Hall theory of recombination.

6.5.1 Shockley–Read–Hall Theory of Recombination

An allowed energy state, also called a trap, within the forbidden bandgap may act as a *recombination center,* capturing both electrons and holes with almost equal probability. This equal probability of capture means that the capture cross sections for electrons and holes are approximately equal. The Shockley–Read–Hall theory of recombination assumes that a single recombination center, or trap, exists at an energy E_t within the bandgap. There are four basic processes, shown in Figure 6.16, that may occur at this single trap. We will assume that the trap is an acceptor-type trap; that is, it is negatively charged when it contains an electron and is neutral when it does not contain an electron.

The four basic processes are as follows:

Process 1: The capture of an electron from the conduction band by an initially neutral empty trap.

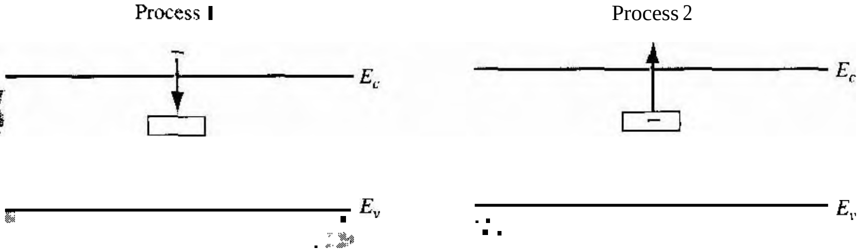
Process 1

Process 2

Electron capture

Electron emission

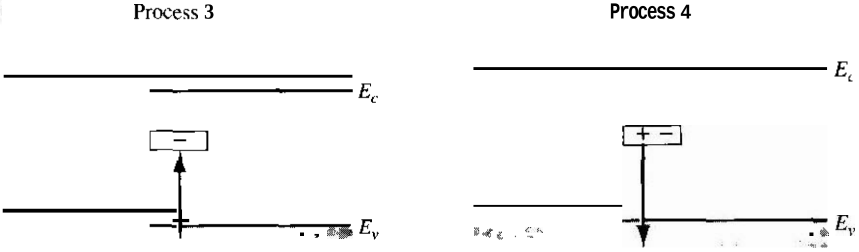
Process 3

Process 4

Hole capture

Hole emission

Figure 6.16 | The four basic trapping and emission processes for the case of an acceptor-type trap.

Process 2: The inverse of process 1—the emission of an electron that is initially occupying a trap level back into the conduction band.

Process **3:** The capture of a hole from the valence band by a trap containing an electron. (Or we may consider the process to be the emission of an electron from the trap into the valence band.)

Process 4: The inverse of process 3—the emission of a hole from a neutral trap into the valence band. (Or we may consider this process to be the capture of an electron from the valence band.)

In process 1, the rate at which electrons from the conduction band are captured by the traps is proportional to the density of electrons in the conduction band and proportional to the density of empty trap states. We can then write the electron capture rate as

$$R_{cn} = C_n N_t (1 - f_F(E_t))n \tag{6.86}$$

where

R_{cn} = capture rate (#/cm^3-s)
C_n = constant proportional to electron-capture cross section
N_t = total concentration of trapping centers
n = electron concentration in the conduction band
$f_F(E_t)$ = Fermi function at the trap energy

The Fermi function at the trap energy is given by

$$f_F(E_t) = \frac{1}{1 + \exp\left[\dfrac{E_t - E_F}{kT}\right]} \tag{6.87}$$

which is the probability that a trap will contain an electron. The function $(1 - f_F(E_t))$ is then the probability that the trap is empty. In Equation (6.87), we have assumed that the degeneracy factor is one, which is the usual approximation made in this analysis. However, if a degeneracy factor is included, it will eventually be absorbed in other constants later in the analysis.

For process 2, the rate at which electrons are emitted from filled traps back into the conduction band is proportional to the number of filled traps, so that

$$R_{en} = E_n N_t f_F(E_t) \tag{6.88}$$

where

R_{en} = emission rate (#/cm^3-s)
E_n = constant
$f_F(E_t)$ = probability that the trap is occupied

In thermal equilibrium, the rate of electron capture from the conduction band and the rate of electron emission back into the conduction band must be equal. Then

$$R_{en} = R_{cn} \tag{6.89}$$

so that

$$E_n N_t f_{F0}(E_t) = C_n N_t (1 - f_{F0}(E_t)) n_0 \tag{6.90}$$

where f_{F0} denotes the thermal-equilibrium Fermi function. Note that, in thermal equilibrium, the value of the electron concentration in the capture rate term is the equilibrium value n_0. Using the Boltrmann approximation for the Fermi function, we can find E_n in terms of C_n as

$$E_n = n' C_n \tag{6.91}$$

where n' is defined as

$$n' = N_c \exp\left[\frac{-(E_c - E_t)}{kT}\right] \tag{6.92}$$

The parameter n' is equivalent to an electron concentration that would exist in the conduction band if the trap energy E, coincided with the Fermi energy E_F.

In nonequilibrium, excess electrons exist, so that the net rate at which electrons are captured from the conduction band is given by

$$R_n = R_{,,,} - R_{en} \tag{6.93}$$

which is just the difference between the capture rate and the emission rate. Combining Equations (6.86) and (6.88) with (6.93) gives

$$R_n = [C_n N_t (1 - f_F(E_t)) n] - [E_n N_t f_F(E_t)] \tag{6.94}$$

We may note that, in this equation, the electron concentration n is the total concentration, which includes the excess electron concentration. The remaining constants and terms in Equation (6.94) are the same as defined previously and the Fermi energy in the Fermi probability function needs to be replaced by the quasi-Fermi energy for electrons. The constants E_n and C_n are related by Equation (6.91). so the net recombination rate can be written as

$$R_n = C_n N_t [n(1 - f_F(E_t)) - n' f_F(E_t)] \tag{6.95}$$

If we consider processes 3 and 4 in the recombination theory, the net rate at which holes are captured from the valence band is given by

$$R_p = C_p N_t [p f_F(E_t) - p'(1 - f_F(E_t))] \tag{6.96}$$

where C_p is a constant proportional to the hole capture rate, and p' is given by

$$p' = N_v \exp\left[\frac{-(E_t - E_v)}{kT}\right] \tag{6.97}$$

In a semiconductor in which the trap density is not too large, the excess electron and hole concentrations are equal and the recombination rates of electrons and holes are equal. If we set Equation (6.95) equal to Equation (6.96) and solve for the Fermi function, we obtain

$$f_F(E_t) = \frac{C_n n + C_p p'}{C_n(n + n') + C_p(p + p')} \tag{6.98}$$

We may note that $n'p' = n_i^2$. Then, substituting Equation (6.98) back into either Equation (6.95) or (6.96) gives

$$\boxed{R_n = R_p = \frac{C_n C_p N_t (np - n_i^2)}{C_n(n + n') + C_p(p + p')} \equiv R} \tag{6.99}$$

Equation (6.99) is the recombination rate of electrons and holes due to the recombination center at $E = E_t$. If we consider thermal equilibrium, then $np = n_0 p_0 = n_i^2$ so that $R_n = R_p = 0$. Equation (6.99). then, is the recombination rate of excess electrons and holes.

Since R in Equation (6.99) is the recombination rate of the excess carriers, w may write

$$R = \frac{\delta n}{\tau} \tag{6.100}$$

where δn is the excess-carrier concentration and τ is the lifetime of the excess carriers.

6.5.2 Limits of Extrinsic Doping and Low Injection

We simplified the ambipolar transport equation, Equation (6.39), from a nonlinear differential equation to a linear differential equation by applying limits of extrinsic doping and low injection. We may apply these same limits to the recombination rate equation.

Consider an n-type semiconductor under low injection. Then

$$n_0 \gg p_0, \quad n_0 \gg \delta p, \quad n_0 \gg n', \quad n_0 \gg p'$$

where δp is the excess minority carrier hole concentration. The assumptions of $n_0 \gg n'$ and $n_0 \gg p'$ imply that the trap level energy is near midgap so that n' and p' are not too different from the intrinsic carrier concentration. With these assumptions, Equation (6.99) reduces to

$$R = C_p N_t \delta p \tag{6.101}$$

The recombination rate of excess carriers in the n-type semiconductor is a function of the parameter C_p, which is related to the minority carrier hole capture cross section. The recombination rate, then, is a function of the minority carrier parameter in the same way that the ambipolar transport parameters reduced to their minority carrier values.

The recombination rate is related to the mean carrier lifetime. Comparing Equations (6.100) and (6.101), we may write

$$R = \frac{\delta n}{\tau} = C_p N_t \delta p \equiv \frac{\delta p}{\tau_{p0}} \tag{6.102}$$

where

$$\tau_{p0} = \frac{1}{C_p N_t} \tag{6.103}$$

and where τ_{p0} is defined as the excess minority carrier hole lifetime. If the trap concentration increases, the probability of excess carrier recombination increases; thus the excess minority carrier lifetime decreases.

Similarly, if we have a strongly extrinsic p-type material under low injection, we can assume that

$$p_0 \gg n_0, \quad p_0 \gg \delta n, \quad p_0 \gg n', \quad p_0 \gg p'$$

The lifetime then becomes that of the excess minority carrier electron lifetime, or

$$\tau_{n0} = \frac{1}{C_n N_t} \tag{6.104}$$

Again note that for the n-type material, the lifetime is a function of C_p, which is related to the capture rate of the minority carrier hole. And for the p-type material, the lifetime is a function of C_n, which is related to the capture rate of the minority carrier electron. The excess-carrier lifetime for an extrinsic material under low injection reduces to that of the minority carrier.

EXAMPLE 6.7

Objective

To determine the excess-carrier lifetime in an intrinsic semiconductor.

If we substitute the definitions of excess-carrier lifetimes from Equations (6.103) and (6.104) into Equation (6.99), the recombination rate can be written as

$$R = \frac{(np - n_i^2)}{\tau_{p0}(n + n') + \tau_{n0}(p + p')} \tag{6.105}$$

Consider an intrinsic semiconductor containing excess carriers. Then $n = n_i + \delta n$ and $p = n_i + \delta n$. Also assume that $n' = p' = n_i$.

■ Solution

Equation (6.105) now becomes

$$R = \frac{2n_i \delta n + (\delta n)^2}{(2n_i + \delta n)(\tau_{p0} + \tau_{n0})}$$

If we also assume very low injection, so that $\delta n \ll 2n_i$, then we can write

$$R = \frac{\delta n}{\tau_{p0} + \tau_{n0}} = \frac{\delta n}{\tau}$$

where τ is the excess carrier lifetime. We see that $\tau = \tau_{p0} + \tau_{n0}$ in the intrinsic material

■ Comment

The excess-carrier lifetime increases as we change from an extrinsic to an intrinsic semiconductor.

Intuitively, we can see that the number of majority carriers that are available for recombining with excess minority carriers decreases as the extrinsic semiconductor becomes intrinsic. Since there are fewer carriers available for recombining in the intrinsic material, the mean lifetime of an excess carrier increases.

TEST YOUR UNDERSTANDING

E6.12 Consider silicon at $T = 300$ K doped at concentrations of $N_d = 10^{15}$ cm^{-3} and $N_a = 0$. Assume that $n' = p' = n_i$ in the excess carrier recombination rate equation and assume parameter values of $\tau_{n0} = \tau_{p0} = 5 \times 10^{-7}$ s. Calculate the recombination rate of excess carriers if $\delta n = \delta p = 10^{14}$ cm^{-3}. (Ans. 1.83×10^{20} cm^{-3} s^{-1})

*6.6 | SURFACE EFFECTS

In all previous discussions. we have implicitly assumed the semiconductors were infinite in extent; thus, we were not concerned with any boundary conditions at a semiconductor surface. In any real application of semiconductors, the material is not infinitely large and therefore surfaces do exist between the semiconductor and an adjacent medium.

6.6.1 Surface States

When a semiconductor is abruptly terminated, the perfect periodic nature of the idealized single-crystal lattice ends abruptly at the surface. The disruption of the periodic-potential function results in allowed electronic energy states within the energy bandgap. In the previous section, we argued that simple defects in the semiconductor would create discrete energy states within the bandgap. The abrupt termination of the periodic potential at the surface results in a distribution of allowed energy states within the bandgap, shown schematically in Figure 6.17 along with the discrete energy states in the bulk semiconductor.

The Shockley–Read–Hall recombination theory shows that the excess minority carrier lifetime is inversely proportional to the density of trap states. We may argue

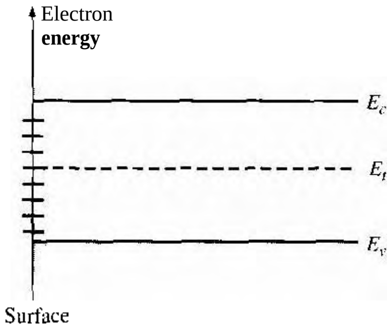

Figure 6.17 | Distribution of surface states within the forbidden bandgap.

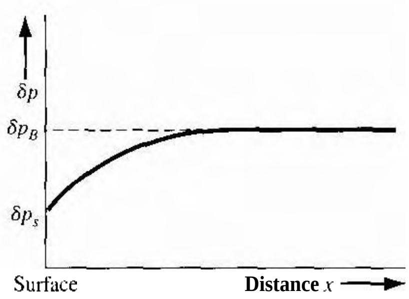

Figure 6.18 | Steady-state excess hole concentration versus distance from a semiconductor surface.

that, since the density of traps at the surface is larger than in the bulk, the excess minority carrier lifetime at the surface will he smaller than the corresponding lifetime in the bulk material. If we consider an extrinsic n-type semiconductor, for example, the recombination rate of excess carriers in the bulk. given by Equation (6.102), is

$$R = \frac{\delta p}{\tau_{p0}} \equiv \frac{\delta p_B}{\tau_{p0}} \tag{6.106}$$

where δp_B is the concentration of excess minority carrier holes in the bulk material. We may write a similar expression for the recombination rate of excess carriers at the surface as

$$R_s = \frac{\delta p_s}{\tau_{p0s}} \tag{6.107}$$

where δp_s is the excess minority carrier hole concentration at the surface and τ_{p0s} is the excess minority carrier hole lifetime at the surface.

Assume that excess carriers are being generated at a constant rate throughout the entire semiconductor material. We showed that, in steady state, the generation rate is equal to the recombination rate for the case of a homogeneous, infinite semiconductor. Using this argument, the recombination rates at the surface and in the hulk material must be equal. Since $\tau_{p0s} < \tau_{p0}$, then the excess minority carrierconcentration *at* the surface is smaller than the excess minority carrier concentration in the bulk region, or $\delta p_s < \delta p_B$. Figure 6.18 shows an example of the excess-carrier concentration plotted as a function of distance from the semiconductor surface.

EXAMPLE 6.8

Objective

To determine the steady-state excess-carrier concentration as a function of distance from the surface of a semiconductor.

Consider Figure 6.18, in which the surface is at $x = 0$. Assume that in the n-type semiconductor $\delta p_B = 10^{14}$ cm^{-3} and $\tau_{p0} = 10^{-6}$ s in the bulk, and $\tau_{p0s} = 10^{-7}$ s at the surface. Assume zero applied electric field and let $D_p = 10$ cm^2/s.

Solution

From Equations (6.106) and (6.107), we have

$$\frac{\delta p_B}{\tau_{p0}} = \frac{\delta p_s}{\tau_{p0s}}$$

so that

$$\delta p_s = \delta p_B \left(\frac{\tau_{p0s}}{\tau_{p0}}\right) = (10^{14})\left(\frac{10^{-7}}{10^{-6}}\right) = 10^{13} \text{ cm}^{-3}$$

From Equation (6.56), we can write

$$D_p \frac{d^2(\delta p)}{dx^2} + g' - \frac{\delta p}{\tau_{p0}} = 0 \tag{6.108}$$

The generation rate can be determined from the steady-state conditions in the bulk, or

$$g' = \frac{\delta p_B}{\tau_{p0}} = \frac{10^{14}}{10^{-6}} = 10^{20} \text{ cm}^{-3}\text{-s}^{-1}$$

The solution to Equation (6.107) is of the form

$$\delta p(x) = g'\tau_{p0} + Ae^{x/L_p} + Be^{-x/L_p} \tag{6.109}$$

As $x \rightarrow +\infty$, $\delta p(x) = \delta p_B = g'\tau_{p0} = 10^{14}$ cm^{-3}, which implies that $A = 0$. At $x = 0$, we have

$$\delta p(0) = \delta p_s = 10^{14} + B = 10^{13} \text{ cm}^{-3}$$

so that $B = -9 \times 10^{13}$. The entire solution for the minority carrier hole concentration as a function of distance from the surface is

$$\delta p(x) = 10^{14}(1 - 0.9e^{-x/L_p})$$

where

$$L_p = \sqrt{D_p\tau_{p0}} = \sqrt{(10)(10^{-6})} = 31.6\ \mu\text{m}$$

■ Comment

The excess carrier concentration is smaller at the surface than in the bulk.

6.6.2 Surface Recombination Velocity

A gradient in the excess-carrier concentration exists near the surface as shown in Figure 6.18; excess carriers from the bulk region diffuse toward the surface where they recombine. This diffusion toward the surface can be described by the equation

$$-D_p\left[\hat{n}\cdot\frac{d(\delta p)}{dx}\right]\bigg|_{\text{surf}} = s\delta p|_{\text{surf}} \tag{6.110}$$

where each side of the equation is evaluated at the surface. The parameter $\hat{n}$ is the unit outward vector normal to the surface. Using the geometry of Figure 6.18,

$d(\delta p)/dx$ is a positive quantity and $\hat{n}$ is negative, so that the parameters is a positive quantity.

Adimensional analysis of Equation (6.110) shows that the parameters has units of cm/sec, or velocity. The parameters is called the ***surface recombination velocity*** If the excess concentrations at the surface and in the bulk region were equal, then the gradient term would be zero and the surface recombination velocity would be zero. **As** the excess concentration at the surface becomes smaller, the gradient term becomes larger, and the surface recombination velocity increases. The surface recombination velocity gives some indication of the surface characteristics as compared with the bulk region.

Equation (6.110) may be used as a boundary condition to the general solution given by Equation (6.109) in Example 6.8. Using Figure 6.18, we have that $\hat{n} = -1$, and Equation (6.110) becomes

$$D_p \left.\frac{d(\delta p)}{dx}\right|_{\text{surf}} = s\delta p|_{\text{surf}} \tag{6.111}$$

We have argued that the coefficient A is zero in Equation (6.109). Then, from Equation (6.109), we can write that

$$\delta p_{\text{surf}} = \delta p(0) = g'\tau_{p0} + B \tag{6.112a}$$

and

$$\left.\frac{d(\delta p)}{dx}\right|_{\text{surf}} = \left.\frac{d(\delta p)}{dx}\right|_{x=0} = -\frac{B}{L_p} \tag{6.112b}$$

Substituting Equations (6.112a) and (6.112b) into Equation (6.111) and solving for the coefficient B, we obtain

$$B = \frac{-sg'\tau_{p0}}{(D_p/L_p) + s} \tag{6.113}$$

The excess minority carrier hole concentration can then be written as

$$\boxed{\delta p(x) = g'\tau_{p0}\left(1 - \frac{sL_p e^{-x/L_p}}{D_p + sL_p}\right)} \tag{6.114}$$

Objective **EXAMPLE 6.9**

To determine the steady-state excess concentration versus distance from the surface of a semiconductor as a function of surface recombination velocity.

Consider, initially, the case when the surface recombination velocity is zero, or $s = 0$.

Solution

Substituting $s = 0$ into Equation (6.114), we obtain

$$\delta p(x) = g'\tau_{p0}$$

Now consider the case when the surface recombination velocity is infinite, or $s = \infty$.

■ Solution

Substituting $s = \infty$ into Equation (6.114), we obtain

$$\delta p(x) = g'\tau_{p0}(1 - e^{-x/L_p})$$

Comment

For the case when $s = 0$, the surface has no effect and the excess minority carrier concentration at the surface is the same as in the bulk. In the other extreme when $s =$ no, the excess minority carrier hole concentration at the surface is zero.

An infinite surface recombination velocity implies that the excess minority carrier concentration and lifetime at the surface are zero.

EXAMPLE 6.10

Objective

To determine the value of surface recombinaion velocity corresponding to the parameten given in Example 6.8.

From Example 6.8, we have that $g'\tau_{p0} = 10^{14}$ cm^{-3}, $D_p = 10$ cm^2/s, $L_p = 31.6$ μm, and $\delta p(0) = 10^{13}$ cm^{-3}.

■ Solution

Writing Equation (6.114) at the surface, we have

$$\delta p(0) = g'\tau_{p0}\left[1 - \frac{s}{(D_p/L_p) + s}\right]$$

Solving for the surface recombination velocity, we find that

$$s = \frac{D_p}{L_p}\left(\frac{g'\tau_{p0}}{\delta p(0)} - 1\right)$$

which becomes

$$s = \frac{10}{31.6 \times 10^{-4}}\left[\frac{10^{14}}{10^{13}} - 1\right] = 2.85 \times 10^4 \text{ cm/s}$$

■ Comment

This example shows that a surface recombination velocity of approximately $s = 3$ x LO^4 cm/s could seriously degrade the performance of semiconductor devices, such as solar cells, since these devices tend to be fabricated close to a surface.

In the above example, the surface influences the excess-carrier concentration to the extent that, even at a distance of $L_p = 31.6$ μm from the surface, the excess-carrier concentration is only two-thirds of the value in the bulk. We will see in later chapters that device performance is dependent in large part on the properties of excess carriers.

6.7 | SUMMARY

- The processes of excess electron and hole generation and recombination were discussed. The excess carrier generation rate and recombination rate were defined.
- Excess electrons and holes do not move independently of each other, but move together. This common movement is called ambipolar transport.
- The ambipolar transport equation was derived and limits of low injection and extrinsic doping were applied to the coefficients. Under these conditions, the excess electrons and holes diffuse and drift together with the characteristics of the minority carrier, a result that is fundamental to the behavior of semiconductor devices
- The concept of excess carrier lifetime was developed.
- Examples of excess carrier behavior as a function of time, as a function of space, and as a function of both time and space were examined.
- The quasi-Fermi level for electrons and the quasi-Fermi level for holes were defined. These parameters characterize the total electron and hole concentrations in a semiconductor in nonequilibrium.
- The Shockley–Read–Hall theory of recombination was considered. Expressions for the excess minority carrier lifetime were developed.
- The effect of a semiconductor surface influences the behavior of excess electrons and holes. The surface recombination velocity was defined.

GLOSSARY OF IMPORTANT TERMS

ambipolar diffusion coefficient The effective diffusion coefficient of excess carriers.

ambipolar mobility The effective mobility of excess carriers.

ambipolar transport The process whereby excess electrons and holes diffuse, drift, and recombine with the same effective diffusion coefficient, mobility, and lifetime.

ambipolar transport equation The equation describing the behavior of excess carriers as a function of time and space coordinates.

carrier generation The process of elevating electrons from the valence band into the conduction band, creating an electron–hole pair.

carrier recombination The process whereby an electron "falls" into an empty state in the valence band (a hole) so that an electron-hole pair are annihilated.

excess carriers The term describing both excess electrons and excess holes.

excess electrons The concentration of electrons in the conduction band over and above the thermal-equilibrium concentration.

excess holes The concentration of holes in the valence band over and above the thermal-equilibrium concentration.

excess minority carrier lifetime The average time that an excess minority carrier exists before it recombines.

generation rate The rate ($\#/\text{cm}^3\text{-s}$) at which electron–hole pairs are created.

low-level injection The condition in which the excess-carrier concentration is much smaller than the thermal-equilibrium majority carrier concentration.

minority carrier diffusion length The average distance a minority carrier diffuses before recombining: a parameter equal to $\sqrt{D\tau}$ where D and τ are the minority carrier diffusion coefficient and lifetime, respectively.

quasi-Fermi level The quasi-Fermi level for electrons and the quasi-Fermi level for holes relate the nonequilibrium electron and hole concentrations, respectively, to the intrinsic carrier concentration and the intrinsic Fermi level.

recombination rate The rate (#/cm^3-s) at which electron–hole pairs recombine.

surface recombination velocity A parameter that relates the gradient of the excess carrier concentration at a surface to the surface concentration of excess carriers.

surface states The electronic energy states that exist within the bandgap at a semiconductor surface.

CHECKPOINT

After studying this chapter, the reader should have the ability to:

- Describe the concept of excess generation and recombination.
- Describe the concept of an excess carrier lifetime.
- Describe how the time-dependent diffusion equations for holes and electrons are derived.
- Describe how the ambipolar transport equation is derived.
- Understand the consequence of the coefficients in the ambipolar transport equation reducing to the minority carrier values under low injection and extrinsic semiconductors.
- Apply the ambipolar transport equation to various problems.
- Understand the conceot of the dielectric relaxation time constant.
- Calculate the quasi-Fermi levels lor electrons and holes.
- Calculate the excess carrier recombination rate for a given concentration of excess carriers.
- Understand the effect of a surface on the excess carrier concentrations.

REVIEW QUESTIONS

1. Why are the electron generation rate and recombination rate equal in thermal equilibrium?
2. Explain how the density of holes, for example, can change as a result of a change in the flux of particles.
3. Why is the general ambipolar transport equation nonlinear?
4. Explain qualitatively why a pulse of excess electrons and hales would move together in the presence of an applied electric field.
5. Explain qualitatively why the excess carrier lifetime reduces to that of the minority carrier under low injection.
6. What is the time dependence of the density of excess carriers when the generation rate becomes zero?
7. In the presence of an external force, why doesn't the density of excess carriers continue to increase with time?
8. When a concentration of one type of excess carrier is suddenly created in a semiconductor, what is the mechanism by which the net charge density quickly becomes zero?
9. State the definition of the quasi-Fermi level for electrons. Repeat for holes.
10. Why, in general. is the concentration of excess carriers less at the surface of a semiconductor than in the bulk?

PROBLEMS

(*Note:* Use the semiconductor parameters listed in Appendix B if they are not specifically given in a problem. Assume $T = 300$ K.)

Section 6.1 Carrier Generation and Recombination

6.1 Consider a semiconductor in which $n_0 = 10^{15}$ cm^{-3} and n, $= 10^{10}$ cm^{-3}. Assume that the excess-carrier lifetime is 10^{-6} s. Determine the electron–hole recombination rate if the excess-hole concentration is $\delta p = 5 \times 10^{13}$ cm^{-3}.

6.2 A semiconductor, in thermal equilibrium, has a hole concentration of $p_0 = 10^{16}$ cm^{-3} and an intrinsic concentration of n, $= 10^{10}$ cm^{-3}. The minority carrier lifetime is 2×10^{-7} s. ***(a)*** Determine the thermal-equilibrium recombination rate of electrons. (*b*) Determine the change in the recombination rate of electrons if an excess electron concentration of $\delta n = 10^{12}$ cm^{-3} exists.

6.3 An n-type silicon sample contains a donor concentration of $N_d = 10^{16}$ cm^{-3}. The minority carrier hole lifetime is found to be $\tau_{p0} = 20$ μs. ***(a)*** What is the lifetime of the majority carrier electrons? *(h)* Determine the thermal equilibrium generation rate for electrons and holes in this material. (*c*) Determine the thermal equilibrium recombination rate for electrons and holes in this material.

6.4 ***(a)*** A sample of semiconductor has a cross-sectional area of 1 cm^2 and a thickness of 0.1 cm. Determine the number of electron–hole pairs that are generated per unit volume per unit time by the uniform absorption of I watt of light at a wavelength of 6300 Å. Assume each photon creates one electron–hole pair. (b) If the excess minority carrier lifetime is 10 μs. what is the steady-state excess carrier concentration?

Section 6.2 Mathematical Analysis of Excess Carriers

6.5 Derive Equation (6.27) from Equations (6.18) and (6.20).

6.6 Consider a one-dimensional hole flux as shown in Figure 6.4. If the generation rate of holes in this differential volume is $g_p = 10^{20}$ cm^{-3}-s^{-1} and the recombination rate is 2×10^{19} cm^{-3}-s^{-1}, what must be the gradient in the particle current density to maintain a steady-state hole concentration?

6.7 Repeat Problem 6.6 if the generation rate becomes zero.

Section 6.3 Ambipolar Transport

6.8 Starting with the continuity equations given by Equations (6.29) and (6.30), derive the ambipolar transport equation given by Equation (6.39).

6.9 A sample of Ge at $T = 300$ K has a uniform donor concentration of 2×10^{13} cm^{-3}. The excess carrier lifetime is found to be $\tau_{p0} = 24$ μs. Determine the ambipolar diffusion coefficient and the ambipolar mobility. What are the electron and hole lifetimes?

6.10 Assume that an n-type semiconductor is uniformly illuminated, producing a uniform excess generation rate g'. Show that in steady state the change in the semiconductor conductivity is given by

6.11 Light is incident on a silicon sample starting at r = 0 and generating excess carriers uniformly throughout the silicon for $t > 0$. The generation rate is $g' = 5 \times 10''\ \text{cm}^{-3}\ \text{s}^{-1}$. The silicon ($T = 300$ K) is n type with $N_d = 5 \times 10^{16}$ cm ^{3} and $N_a = 0$. Letn, $= 1.5 \times 10^{10}$ cm^{-3}, $\tau_{n0} = 10\ ^{6}$ s, and $\tau_{p0} = 10^{-7}$ s. Also let $\mu_n = 1000$ cm^2/V-s and $\mu_p = 420$ cm^2/V-s. Determine the conductivity of the silicon as a function of time for $t \geq 0$.

6.12 An n-type gallium arsenide semiconductor is doped with $N_d = 10^{16}$ cm^{-3} and $N_a = 0$. The minority carrier lifetime is $\tau_{p0} = 2 \times 10^{-7}$ s. Calculate the steady-state increase in conductivity and the steady-state excess carrier recombination rate if a uniform generation rate, $g' = 2 \times 10^{21}$ cm^{-3}-s^{-1}, is incident on the semiconductor

6.13 A silicon sample at $T = 300$ K is n type with $N_d = 5 \times 10^{16}$ cm^{-3} and $N_a = 0$. The sample has a length of 0.I cm and a cross-sectional area of 10^{-4} cm^2. A voltage of 5 V is applied between the ends of the sample. Fort < 0. the sample has been illuminated with light. producing an excess-carrier generation rate of $g' = 5 \times 10''$ cm^{-3}-s^{-1} uniformly throughout the entire silicon. The minority carrier lifetime is $\tau_{p0} = 3 \times 10^{-7}$ s. At $t = 0$, the light is turned off. Derive the expression for the current in the sample as a function of time r ≥ 0. (Neglect surface effects.)

6.14 Consider a homogeneous gallium arsenide semiconductor at $T = 300$ K with $N_a = 10^{16}$ cm^{-3} and $N_d = 0$. A light source is turned on at $t = 0$ producing a uniform generation rate of $g' = 10^{20}$ cm^{-3}-s^{-1}. The electric field is zero. (*a*) Derive the expression for the excess-carrier concentration and excess carrier recombination rate as a function of time. (*b*) If the maximum, steady-state, excess-carrier concentration is to be 1×10^{14} cm^{-3}, determine the maximum value of the minority carrier lifetime. (*c*) Determine the times at which the excess minority carrier concentration will be equal to (i) three-fourths, (*ii*) one-half, and (*iii*) one-fourth of the steady-state value.

6.15 In a silicon semiconductor material at $T = 300$ K, the doping concentrations are $N_d = 10^{15}$ cm^{-3} and $N_a = 0$. The equilibrium recombination rate is $R_{p0} = 10^{11}$ cm^{-3}-s^{-1}. A uniform generation rate produces an excess-carrier concentration of $\delta n = \delta p = 10^{14}$ cm^{-3}. (*a*) By what factor does the total recombination rate increase? (*h*) What is the excess-carrier lifetime?

6.16 Consider a silicun material doped with 3×10^{16} cm^{-3} donor atoms. At $t = 0$, a light source is turned on, producing a uniform generation rate of $g' = 2 \times 10''$ cm^{-3}-s^{-1} At $t = 10^{-7}$ s, the light source is turned off. Determine the excess minority carrier concentration as a function of t for $0 \leq t \leq \infty$. Let $\tau_{p0} = 10^{-7}$ s. Plot the excess minority carrier concentration as a function of time.

6.17 A semiconductor has the following properties:

$$D_n = 25\ \text{cm}^2/\text{s} \qquad \tau_{n0} = 10^{-6}\ \text{s}$$
$$D_p = 10\ \text{cm}^2/\text{s} \qquad \tau_{p0} = 10^{-7}\ \text{s}$$

The semiconductor is a homogeneous. p-type ($N_a = 10^{17}$ cm^{-3}) material in thermal equilibrium for $t \leq 0$. At $t = 0$, an external source is turned on which produces excess carriers uniformly at the rate of $g' = 10^{20}$ cm^{-3}-s^{-1}. At r $= 2 \times 10^{-6}$ s, the external source is turned off. (*a*) Derive the expression for the excess-electron concentretion as a function of time for $0 \leq t \leq$ m. (*b*) Determine the value of the excess-electron concentration at (*i*) $t = 0$, (ii) r $= 2 \times 10\ ^{6}$ s, and (*iii*) $t = \infty$. (*c*) Plot the excess-electron concentration as a function of time.

6.18 Consider a bar of p-type silicon material that is homogeneously doped to a value of 3×10^{15} cm^{-3} at $T = 300$ K. The applied electric field is zero. A light source is

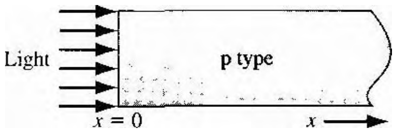

Figure 6.19 | Figure for Problems 6.18 and 6.20.

incident on the end of the semiconductor as shown in Figure 6.19. The excess-carrier concentration generated at $x = 0$ is $\delta p(0) = \delta n(0) = 10^{13}$ cm^{-3}. Assume the following parameters (neglect surface effects):

$$\mu_n = 1200 \text{ cm}^2/\text{V-s} \qquad \tau_{n0} = 5 \times 10^{-7} \text{ s}$$
$$\mu_p = 400 \text{ cm}^2/\text{V-s} \qquad \tau_{p0} = 1 \times 10^{-7} \text{ s}$$

*(a)*Calculate the steady-state excess electron and hole concentrations as **a** function of distance into the semiconductor. (*b*) Calculate the electron diffusion current density as a function of x.

6.19 The $x = 0$ end of an N,, = I x 10^{14} cm^{-3} doped semi-infinite ($x \geq 0$) bar of silicon maintained at T = 300 K is attached to **a** "minority carrier digester" which makes $n_p = 0$ at $x = 0$ (n_p is the minority carrier electron concentration in a p-type semiconductor). The electric field is zero. (*a*) Determine the thermal-equilibrium values of n_{p0} and p_{p0}. (*b*) What is the excess minority carrier concentration at $x = 0$? (*c*) Derive the expression for the steady-state excess minority carrier concentration as a function of x.

6.20 In a p-type silicon semiconductor, excess carriers are being generated at the end of the semiconductor bar at $x = 0$ as shown in Figure 6.19. The doping concentration is N, = 5 x 10^{16} cm^{-3} and $N_d = 0$. The steady-state excess-carrier concentration at $x = 0$ is 10^{15} cm^{-3}. (Neglect surface effects.) The applied electric field is zero. Assume that $\tau_{n0} = \tau_{p0} = 8 \times 10^{-7}$ s. (*a*) Calculate δn, and the electron and hole diffusion current densities at $x = 0$. (*b*) Repeat part (*a*) for $x =$ L,,

6.21 Consider an n-type silicon sample. Excess carriers are generated at $x = 0$ such as shown in Figure 6.6. A constant electric field E$_0$ is applied in the $+x$ direction. Show that the steady-state excess carrier concentration is given by

$$\delta p(x) = A \exp(s_- x) \qquad x > 0 \qquad \text{and} \qquad \delta p(x) = A \exp(s_+ x) \qquad x < 0$$

where

$$s_\mp = \frac{1}{L_p}\left[\beta \mp \sqrt{1 + \beta^2}\right]$$

and

$$\beta = \frac{\mu_p L_p \text{E}_0}{2D_p}$$

6.22 Plot the excess carrier concentration $\delta p(x)$ versus x from Problem 6.21 for *(a)*E$_0 = 0$ and *(h)*E$_0$ = 10 V/cm.

***6.23** Consider the semiconductor described in Problem 6.18. Assume a constant electric field E$_0$ is applied in the $+x$ direction. (*a*) Derive the expression for the steady-state excess-electron concentration. (Assume the solution is of the form $e^{-\alpha x}$.) (h) Plot δn

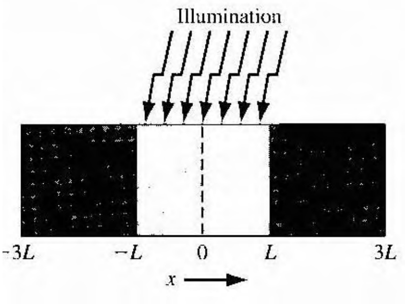

Figure 6.20 | Figure for Problem 6.25

versus x for (i) $E_0 = 0$ and (ii) $E_0 = 12$ V/cm. (c) Explain the general characteristics of the two curves plotted in part (b).

6.24 Assume that a p-type semiconductor is in thermal equilibrium for $t < 0$ and has an infinite minority carrier lifetime. Also assume that the semiconductor is uniformly illuminated, resulting in a uniform generation rate, $g'(t)$, which is given by

$$g'(t) = G'_0 \qquad \text{for } 0 < t < T$$
$$g'(t) = 0 \qquad \text{for } r < 0 \text{ and } t > T$$

where G'_0 is a constant. Find the excess minority carrier concentration as a function of time.

***6.25** Consider the n-type semiconductor shown in Figure h.20. Illumination produces a constant excess-carrier generation rate, G'_0, in the region L $< x < +L$. Assume that the minority carrier lifetime is infinite and assume that the excess minority carrier hole concentration is zero at $x = -3L$ and at $x = +3L$. Find the steady-state excess minority carrier concentration versus x, for the case of low injection and for zero applied electric field.

6.26 An n-type germanium sample is used in the Haynes–Shockley experiment. The length of the sample is 1 cm and the applied voltage is $V_1 = 2.5$ V The contacts A and B are separated by 0.75 cm. The peak of the pulse arrives at contact B 160 us after carrier injection at contact A. The width of the pulse is Ar $= 75.5$ μs. Determine the hole mobility and diffusion coefficient. Compare the results with the Einstein relation.

6.27 Consider the function $f(x, r) = (4\pi Dt)^{-1/2} \exp(-x^2/4Dt)$. (a) Show that this function is a solution to the differential equation $D(\partial^2 f/\partial x^2) = \partial f/\partial t$. (*b*) Show that the integral of the function f (x, t) over x from $-\infty$ to $+\infty$ is unity for all values of time. ***(r)***Show that this function approaches a δ function as t approaches zero.

6.28 The basic equation in the Haynes–Shockley experiment is given by Equation (6.70). (a) Plot $\delta p(x, r)$ versus x **for** various values of t and for $E_0 = 0$ as well as for $E_0 \neq 0$. ***(b)*** Plot $\delta p(x, r)$ versus r for various values of x and for $E_0 = 0$ as well as for $E_0 \neq 0$.

Section 6.4 Quasi-Fermi Energy Levels

6.29 An n-type silicon sample with $N_d = 10^{16}$ cm^{-3} is steadily illuminated such that $g' = 10^{21}$ cm^{-3}-s^{-1}. If $\tau_{n0} = \tau_{p0} = 10^{-6}$ s, calculate the position of the quasi-Fermi levels for electrons and holes with respect to the intrinsic level (assume that $n_i = 1.5 \times 10^{10}$ cm^{-3}). Plot these levels on an energy-band diagram.

6.30 Consider a p-type silicon semiconductor at $T = 300$ K doped at N,, $= 5 \times 10^{15}$ cm^{-3}. *(a)* Determine the position of the Fermi level with respect to the intrinsic Fermi level. (b) Excess carriers are generated such that the excess-carrier concentration is 10 percent of the thermal-equilibrium majority carrier concentration. Determine the quasi-Fermi levels with respect to the intrinsic Fermi level. (c) Plot the Fermi level and quasi-Fermi levels with respect to the intrinsic level.

6.31 Consider an n-type gallium arsenide semiconductor at T = 300 K doped at $N_d = 5 \times 10^{16}$ cm^{-3}. *(a)* Determine $E_{Fn} - E_F$ if the excess-carrier concentration is 0.1 N_d. (b) Determine $E_{Fi} - E_{Fp}$.

6.32 Ap-type gallium arsenide semiconductor at T = 300 K is doped at $N_a = 10^{16}$ cm^{-3}. The excess-carrier concentration varies linearly from 10^{14} cm^{-3} to rero over a distance of 50 μm. Plot the position of the quasi-Fermi levels with respect to the intrinsic Fermi level versus distance.

6.33 Consider p-type silicon at T = 300 K duped to $N_a = 5 \times 10^{14}$ cm^{-3}. Assume excess carriers arc present and assume that $E_F - E_{Fp} = (0.01)kT$. *(a)* Does this condition correspond to low injection? Why or why not? *(b)* Determine $E_{Fn} - E_{Fi}$

6.34 An n-type silicon sample is doped with donors at a concentration of $N_d = 10^{16}$ cm^{-3}. Excess carriers are generated such that the excess hole concentration is given by $\delta p(x) = 10^{14} \exp(-x/10^{-4})$ cm^{-3}. Plot the function $E_{Fi} - E_{Fp}$ versusx over the range $0 \le x \le 4 \times 10^{-4}$.

6.35 For a p-type silicon material doped at N,, $= 10^{16}$ cm^{-3}, plot $E_{Fn} - E_F$ versus δn over the range $0 \le \delta n \le 10^{14}$ cm^{-3}. Use a log scale for δn.

Section 6.5 Excess Carrier Lifetime

6.36 Consider Equation (6.99) and the definitions of τ_{p0} and τ_{n0} hy Equations (6.103) and (6.104). Let $n' = p' = n_i$. Assume that in a particular region of a semiconductor, $n = p = 0$. (a) Determine the recomhination rate R. (h) Explain what this result means physically.

6.37 Again consider Equation (6.99) and the definitions of τ_{p0} and τ_{n0} given by Equations (6.103) and (6.104). Let $\tau_{p0} = 10^{-7}$ s and $\tau_{n0} = 5 \times 10^{-7}$ s. Also let n' = p' = n; $= 10^{10}$ cm^{-3}. Assume very low injection so that $\delta n \ll n_i$. Calculate $R/\delta n$ for a semiconductor which is (o) n-type ($n_0 \gg p_0$), (h) intrinsic ($n_0 = p_0 = n_i$), and (c) p-type ($p_0 \gg n_0$).

Section 6.6 Surface Effects

***6.38** Consider an n-type semiconductor as shown in Figure 6.21. doped at $N_d = 10^{16}$ cm^{-3} and with a uniform excess-carrier generation rate equal to g' $= 10^{21}$ cm^{-3}-s^{-1}. Assume that $D_p = 10$ cm^2/s and $\tau_{p0} = 10^{-7}$ s. The electric field is rero.

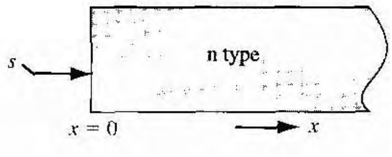

Figure 6.21 | Figure for Problem 6.38.

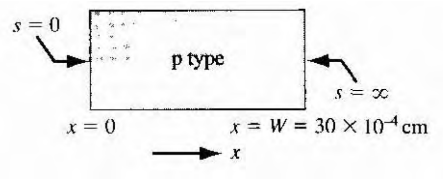

Figure 6.22 | Figure for Problem 6.39.

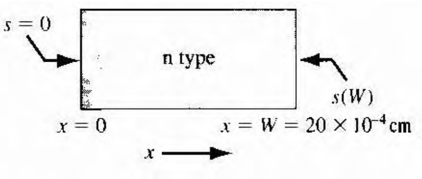

Figure 6.23 | Figure for Problem 6.40.

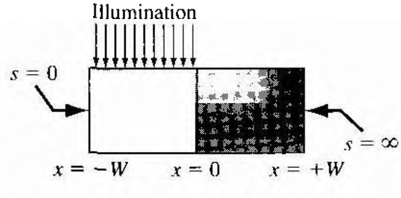

Figure 6.24 | Figure for Problem 6.41.

(a) Determine the steady-state excess minority carrier concentration versus x if the surface recombination velocity at $x = 0$ is (i) $s = 0$. (ii) $s = 2000$ cm/s, and (iii) $s = \infty$. (*b*) Calculate the excess minority carrier concentration at $x = 0$ for (*i*) $s = 0$, (*ii*) $s = 2000$ cm/s, and (iii) $s = \infty$.

***6.39** **(a)** Consider the p-type semiconductor shown in Figure 6.22 with the following parameters: $N_a = 5 \times 10^{16}$ cm^{-3}, $D_n = 25$ cm^2/s, and $\tau_{n0} = 5 \times 10^{\ 7}$ s. The surface recombination velocities at the two surfaces are shown. The electric field is zero. The semiconductor is illuminated at $x = 0$ with an excess-carrier generation rate equal to $g' = 2 \times 10''$ cm^{-3}-s^{-1}. Determine the excess minority carrier electron concentration versus x in steady state. (*b*) Repeat part (a) for $\tau_{n0} = \infty$.

***6.40** Consider the n-type semiconductor shown in Figure 6.23. Assume that $D_p = 10$ cm^2/s and $\tau_{p0} = \infty$. The electric field is zero. Assume that a flux of excess electrons and holes is incident at $x = 0$. Let the flux of each carrier type be 10^{19} carriers/cm^2-s. Determine the minority carrier hole current versus x if the surface recombination velocity is (a) $s(W) = \infty$ and (*b*) $s(W) = 2000$ cm/s.

***6.41** A p-type semiconductor is shown in Figure 6.24. The surface recombination velocities are shown. The semiconductor is uniformly illuminated for $-W < x < 0$ producing a constant excess-carrier generation rate G'_0. Determine the steady-state excess-carrier concentration versus x if the minority carrier lifetime is infinite and if the electric field is zero.

6.42 Plot $\delta p(x)$ versus x for various values of s using Equation (6.113). Choose reasonable parameter values.

Summary and Review

***6.43** Consider an n-type semiconductor as shown in Figure 6.21. The material is doped at $N_d = 3 \times 10^{16}$ cm^{-3} and $N_a = 0$. Assume that $D_p = 12$ cm^2/s and $\tau_{p0} = 2 \times 10^{-7}$ s. The electric field is zero. "Design" the surface recombination velocity so that the minority carrier diffusion current density at the surface is no greater than $J_p = -0.18$ A/cm^2 with a uniform excess-carrier generation rate equal to $g' = 3 \times 10^{21}$ cm^{-3}-s^{-1}.

6.44 Consider a semiconductor with excess carriers present. From the definition of carrier lifetimes and recombination rates, determine the average time that an electron stays in the conduction band and the average time that a hole stays in the valence band. Discuss these relations for (a) an intrinsic semiconductor and *(h)* an n-type semiconductor.

6.45 Design a gallium arsenide photoconductor that is 5 μm thick. Assume that $\tau_{n0} = \tau_{p0} = 10^{-7}$ s and $N_d = 5 \times 10^{15} cm^{-3}$. With an excitation of $g' = 10^{21} cm^{-3}$-s^{-1} a photocurrent of at least 1 μA is desired with an applied voltage of I V.

READING LIST

1. Bube, R. H. *Photoelectronic Properties **of** Semiconductors,* New York: Cambridge University Press, 1992.

2.** deCogan, D. ***Solid State Devices: A Quantum Physics Appmach. New York: Springer-Verlag, 1987.

3. Hall. R. H. "Electron-Hole Recombination." *Physical Review* 87, no. 2 (July 15, 1952), p. 387.

4. Haynes, J. R., and W. Shockley. "The Mobility and Life of Injected Holes and Electrons in Germanium." ***Physical Review*** 81, no. 5 (March 1, 1951), pp. 835–843.

5.** Hess, K. ***Advanced Theory of Semiconductor Devices. Englewood Cliffs, NJ: Prentice Hall, 1988.

6. Kano, K. ***Semiconducror Devices.*** Upper Saddle River, NJ: Prentice Hall, 1998.

7. Kingston, R. H. ***Semiconducror Surface Physics.*** Philadelphia: University of Pennsylvania Press, 1957.

8. McKelvey, J. P. ***Solid State Physics for Engineering and Materials Science.*** Malabar, FL.: Krieger Publishing, 1993.

9. Pierret, R. F. ***Semiconductor Device Fundamentals.*** Reading, MA: Addison-Wesley, 1996.

10. Shockley, W., and W. T. Read, Jr. "Statistics of the Recombinations of Holes and Electrons." ***Physical Review*** 87, no. 5 (September 1, 1952), pp. 835–842.

11. Singh, J. ***Semiconducror Devices: An Introduction.*** New York: McGraw-Hill, 1994.

12. Singh, J. ***Semiconducror Devices: Basic Principles.*** New York: John Wiley and Sons, 2001.

13. Streetman, B. G., and S. Banerjee. ***Solid State Electronic Devices.*** 5th ed. Upper Saddle River, NJ: Prentice Hall, 2000.

14.** Wang, S. ***Fundamentals of Semiconductor Theory and Device Physics. Englewood Cliffs. *NJ:* Prentice Hall, 1989.

CHAPTER 7

The pn Junction

PREVIEW

Up to this point in the text, we have been considering the properties of the semiconductor material. We calculated electron and hole concentrations in thermal equilibrium and determined the position of the Fermi level. We then considered the nonequilibrium condition in which excess electrons and holes are present in the semiconductor. We now wish to consider the situation in which a p-type and an n-type semiconductor are brought into contact with one another to form a pn junction.

Most semiconductor devices contain at least one junction between p-type and n-type semiconductor regions. Semiconductor device characteristics and operation are intimately connected to these pn junctions, so considerable attention is devoted initially to this basic device. The pn junction diode itself provides characteristics that are used in rectifiers and switching circuits. In addition, the analysis of the pn junction device establishes some basic terminology and concepts that are used in the discussion of other semiconductor devices. The fundamental analysis techniques used for the pnjunction will also be applied to other devices. Understanding the physics of the pn junction is, therefore, an important step in the study of semiconductor devices.

The electrostatics of the pn junction is considered in this chapter and the current–voltage characteristics of the pn junction diode are developed in the next chapter. ■

7.1 | BASIC STRUCTURE OF THE pn JUNCTION

Figure 7.1a schematically shows the pn junction. It is important to realize that the entire semiconductor is a single-crystal material in which one region is doped with acceptor impurity atoms to form the p region and the adjacent region is doped with donor atoms to form the n region. The interface separating the n and p regions is referred to as the *metallurgical junction.*

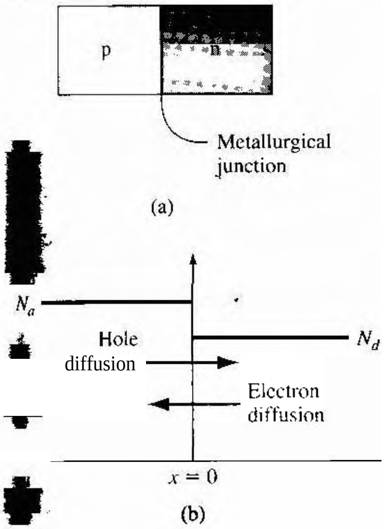
p
n
Metallurgical junction
(a)
N_a
Hole diffusion
N_d
Electron diffusion
$x = 0$
(b)

Figure 7.1 | (a) Simplified geometry of a pn junction; (b) doping profile of an ideal uniformly doped pn junction.

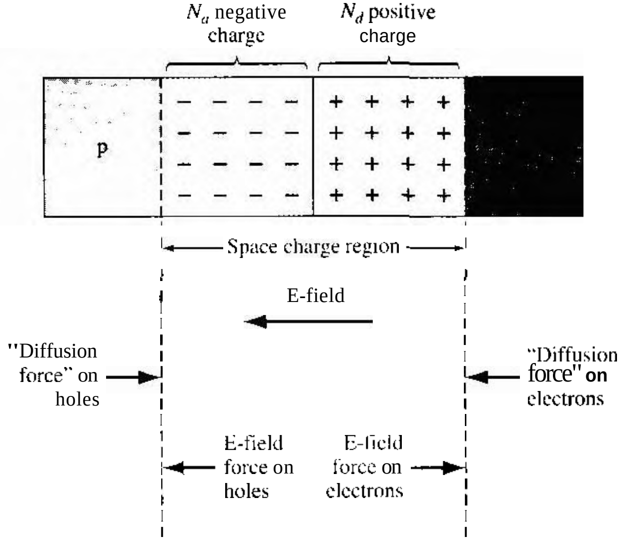
N_a negative charge
N_d positive charge
p
n
Space charge region
E-field
"Diffusion force" on holes
"Diffusion force" on electrons
E-field force on holes
E-field force on electrons

Figure 7.2 | The space charge region, the electric field, and the forces acting on the charged carriers.

The impurity doping concentrations in the p and n regions are shown in Figure 7.1b. For simplicity, we will consider a *step* junction in which the doping concentration is uniform in each region and there is an abrupt change in doping at the junction. Initially, at the metallurgical junction, there is a very large density gradient in both the electron and hole concentrations. Majority carrier electrons in the n region will begin diffusing into the p region and majority carrier holes in the p region will begin diffusing into the n region. If we assume there are no external connections to the semiconductor, then this diffusion process cannot continue indefinitely. As electrons diffuse from the n region, positively charged donor atoms are left behind. Similarly, as holes diffuse from the p region, they uncover negatively charged acceptor atoms. The net positive and negative charges in the n and p regions induce an electric field in the region near the metallurgical junction, in the direction from the positive to the negative charge, or from the n to the p region.

The net positively and negatively charged regions are shown in Figure 7.2. These two regions are referred to as the space charge region. Essentially all electrons and holes are swept out of the space charge region by the electric field. Since the space charge region is depleted of any mobile charge, this region is also referred to as the depletion region: these two terms will be used interchangeably. Density gradients still exist in the majority carrier concentrations at each edge of the space charge region. We can think of a density gradient as producing a "diffusion force" that acts on the majority carriers. These diffusion forces, acting on the electrons and holes at the edges of the space charge region, are shown in the figure. The electric field in the space charge region produces another force on the electrons and holes which is in the opposite direction to the diffusion force for each type of particle. In thermal equilibrium, the diffusion force and the E-field force exactly balance each other.

7.2 | ZERO APPLIED BIAS

We have considered the basic pn junction structure and discussed briefly how the space charge region is formed. In this section we will examine the properties of the step junction in thermal equilibrium, where no currents exist and no external excitation is applied. We will determine the space charge region width, electric field, and potential through the depletion region.

7.2.1 Built-in Potential Barrier

If we assume that no voltage is applied across the pn junction, then the junction is in thermal equilibrium—the Fermi energy level is constant throughout the entire system. Figure 7.3 shows the energy-band diagram for the pn junction in thermal equilibrium. The conduction and valance band energies must bend as we go through the space charge region, since the relative position of the conduction and valence hands with respect to the Fermi energy changes between p and n regions.

Electrons in the conduction band of the n region see a potential barrier in trying to move into the conduction hand of the p region. This potential barrier is referred to as the ***built-in potential harrier*** and is denoted by V_{bi}. The built-in potential barrier maintains equilibrium between majority carrier electrons in then region and minority carrier electrons in the p region, and also between majority carrier holes in the p region and minority carrier holes in then region. This potential difference across the junction cannot be measured with a voltmeter because new potential barriers will be formed between the probes and the semiconductor that will cancel V_{bi}. The potential V_{bi} maintains equilibrium, so no current is produced by this voltage.

The intrinsic Fermi level is equidistant from the conduction hand edge through the junction, thus the built-in potential barrier can be determined as the difference

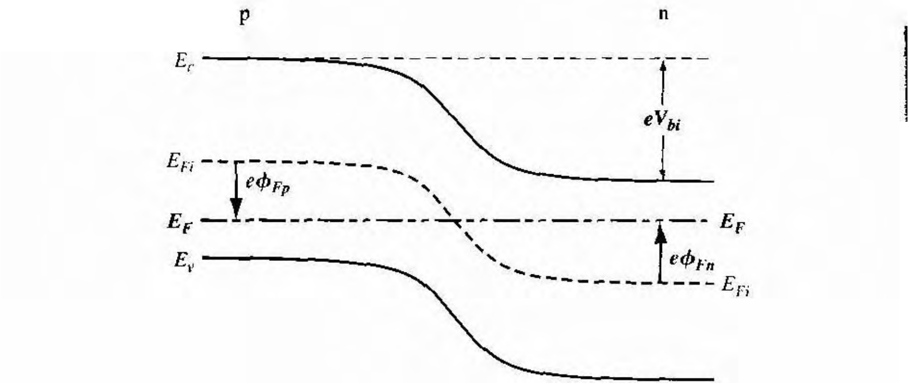

Figure **7.3** | Energy-band diagram of a pn junction in thermal equilibrium.

between the intrinsic Fermi levels in the p and n regions. We can define the potentials ϕ_{Fn} and ϕ_{Fp} as shown in Figure 7.3, so we have

$$V_{bi} = |\phi_{Fn}| + |\phi_{Fp}| \tag{7.1}$$

In the n region, the electron concentration in the conduction band is given by

$$n_0 = N_c \exp\left[\frac{-(E_c - E_F)}{kT}\right] \tag{7.2}$$

which can also be written in the form

$$n_0 = n_i \exp\left[\frac{E_F - E_{Fi}}{kT}\right] \tag{7.3}$$

where n_i and E_{Fi} are the intrinsic carrier concentration and the intrinsic Fermi energy, respectively. We may define the potential ϕ_{Fn} in the n region as

$$e\phi_{Fn} = E_{Fi} - E_F \tag{7.4}$$

Equation (7.3) may then be written as

$$n_0 = n_i \exp\left[\frac{-(e\phi_{Fn})}{kT}\right] \tag{7.5}$$

Taking the natural log of both sides of Equation (7.5), setting $n_0 = N_d$, and solving for the potential, we obtain

$$\phi_{Fn} = \frac{-kT}{e} \ln\left(\frac{N_d}{n_i}\right) \tag{7.6}$$

Similarly, in the p region, the hole concentration is given by

$$p_0 = N_a = n_i \exp\left[\frac{E_{Fi} - E_F}{kT}\right] \tag{7.7}$$

where N_a is the acceptor concentration. We can define the potential ϕ_{Fp} in the p region as

$$e\phi_{Fp} = E_{Fi} - E_F \tag{7.8}$$

Combining Equations (7.7) and (7.8), we find that

$$\phi_{Fp} = +\frac{kT}{e} \ln\left(\frac{N_a}{n_i}\right) \tag{7.9}$$

Finally, the built-in potential barrier for the step junction is found by substituting Equations (7.6) and (7.9) into Equation (7.1), which yields

$$\boxed{V_{bi} = \frac{kT}{e} \ln\left(\frac{N_a N_d}{n_i^2}\right) = V_t \ln\left(\frac{N_a N_d}{n_i^2}\right)} \tag{7.10}$$

where $V_t = kT/e$ and is defined as the thermal voltage.

At this time, we should note a subtle but important point concerning notation. Previously in the discussion of a semiconductor material, N_d and N_a denoted donor and acceptor impurity concentrations in the same region, thereby forming a compensated semiconductor. From this point on in the text, N_d and N_a will denote the net donor and acceptor concentrations in the individual n and p regions, respectively. If the p region, for example, is a compensated material, then N_a will represent the difference between the actual acceptor and donor impurity concentrations. The parameter N_d is defined in a similar manner for the n region.

EXAMPLE 7.1

Objective

To calculate the built-in potential barrier in a pn junction.

Consider a silicon pn junction at $T = 300$ K with doping densities $N_a = 1 \times 10^{18}$ cm^{-3} and $N_d = 1 \times 10^{15}$ cm^{-3}. Assume that $n_i = 1.5 \times 10^{10}$ cm^{-3}

■ Solution

The built-in potential barrier is determined from Equation (7.10) as

$$V_{bi} = (0.0259) \ln \left[\frac{(10^{18})(10^{15})}{(1.5 \times 10^{10})^2} \right] = 0.754 \text{ V}$$

If we change the acceptor doping from $N_a = 1 \times 10^{18}$ cm^{-3} to $N_a = 1 \times 10^{16}$ cm^{-3}, but keep all other parameter values constant, then the built-in potential barrier becomes $V_{bi} = 0.635$ V.

■ Comment

The built-in potential barrier changes only slightly as the doping concentrations change by orders of magnitude because of the logarithmic dependence.

TEST YOUR UNDERSTANDING

E7.1 Calculate the built-in potential barrier in a silicon pn junction at $T = 300$ K for (*a*) $N_a = 5 \times 10^{17}$ cm^{-3}, $N_d = 10^{16}$ cm^{-3} and (*b*) $N_a = 10^{15}$ cm^{-3}, $N_d = 2 \times 10^{16}$ cm^{-3}. [Ans. (*a*) 0.796 V, (*b*) 0.653 V]

E7.2 Repeat E7.1 for a GaAs pn junction. [Ans. (*a*) 1.26 V, (*b*) 1.12 V]

7.2.2 Electric Field

An electric field is created in the depletion region by the separation of positive and negative space charge densities. Figure 7.4 shows the volume charge density distribution in the pn junction assuming uniform doping and assuming an abrupt junction approximation. We will assume that the space charge region abruptly ends in the n region at $x = +x_n$ and abruptly ends in the p region at $x = -x_p$ (x_p is a positive quantity).

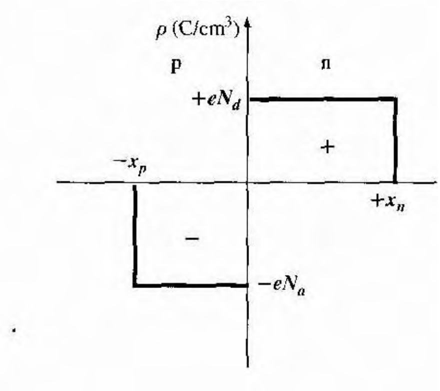

Figure 7.41 The space charge density in a uniformly doped pn junction assuming the abrupt junction approximation.

The electric field is determined from Poisson's equation which, for a one-dimensional analysis, is

$$\frac{d^2\phi(x)}{dx^2} = \frac{-\rho(x)}{\epsilon_s} = -\frac{dE(x)}{dx} \tag{7.11}$$

where $\phi(x)$ is the electric potential, $E(x)$ is the electric field, $\rho(x)$ is the volume charge density, and ϵ_s is the permittivity of the semiconductor. From Figure 7.4, the charge densities are

$$\rho(x) = -eN_a \qquad -x_p < x < 0 \tag{7.12a}$$

and

$\rho(x) = eN_d$ O c x c x , (7.12b)

The electric field in the p region is found by integrating Equation (7.11). We have that

$$E = \int \frac{\rho(x)}{\epsilon_s}\,dx = -\int \frac{eN_a}{\epsilon_s}\,dx = \frac{-eN_a}{\epsilon_s}x + C_1 \tag{7.13}$$

where C_1 is a constant of integration. The electric field is assumed to be zero in the neutral p region for $x < -x_p$ since the currents are zero in thermal equilibrium. As there are no surface charge densities within the pn junction structure. the electric field is a continuous function. The constant of integration is determined by setting $E = 0$ at $x = -x_p$. The electric field in the p region is then given by

$$E = \frac{-eN_a}{\epsilon_s}(x + x_p) \qquad -x_p \le x \le 0 \tag{7.14}$$

In the n region, the electric field is determined from

$$E = \int \frac{(eN_d)}{\epsilon_s}\,dx = \frac{eN_d}{\epsilon_s}x + C_2 \tag{7.15}$$

where C_2 is again a constant of integration. The constant C_2 is determined by setting E = 0 at x = x,,, since the E-field is assumed to be zero in then region and is a continuous function. Then

$$\mathrm{E} = \frac{-eN_d}{\epsilon_s}(x_n - x) \qquad 0 \le x \le x_n \tag{7.16}$$

The electric field is also continuous at the metallurgical junction, or at **x** = 0. Setting Equations (7.14) and (7.16) equal to each other at x = 0 gives

$$N_a x_p = N_d x_n \tag{7.17}$$

Equation (7.17) states that the number of negative charges per unit area in the p region is equal to the number of positive charges per unit area in the n region.

Figure 7.5 is a plot of the electric field in the depletion region. The electric field direction is from the n to the p region, or in the negative x direction for this geometry. For the uniformly doped pn junction, the E-field is a linear function of distance through the junction, and the maximum (magnitude) electric field occurs at the metallurgical junction. An electric field exists in the depletion region even when no voltage is applied between the p and n regions.

The potential in the junction is found by integrating the electric field. In the p region then, we have

$$\phi(x) = -\int \mathrm{E}(x)\,dx = \int \frac{eN_a}{\epsilon_s}(x + x_p)\,dx \tag{7.18}$$

or

$$\phi(x) = \frac{eN_a}{\epsilon_s}\left(\frac{x^2}{2} + x_p \cdot x\right) + C_1' \tag{7.19}$$

where C_1' is again a constant of integration. The potential difference through the pn junction is the important parameter, rather than the absolute potential, so we may arbitrarily set the potential equal to zero at **x** = $-x_p$. The constant of integration is

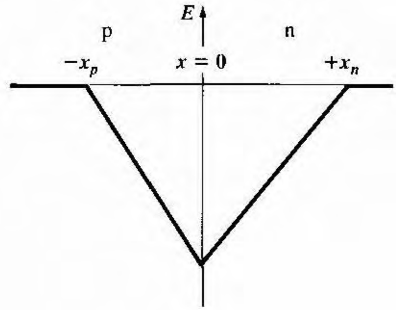

Figure 7.5 | Electric field in the **space** charge region of a uniformly doped pn junction.

then found as

$$C_1' = \frac{eN_a}{2\epsilon_s} x_p^2 \tag{7.20}$$

so that the potential in the p region can now be written as

$$\phi(x) = \frac{eN_a}{2\epsilon_s}(x + x_p)^2 \qquad (-x_p \le x \le 0) \tag{7.21}$$

The potential in the n region is determined by integrating the electric field in the n region, or

$$\phi(x) = \int \frac{eN_d}{\epsilon_s}(x_n - x)\,dx \tag{7.22}$$

Then

$$\phi(x) = \frac{eN_d}{\epsilon_s}\left(x_n \cdot x - \frac{x^2}{2}\right) + C_2' \tag{7.23}$$

where C_2' is another constant of integration. The potential is a continuous function, so setting Equation (7.21) equal to Equation (7.23) at the metallurgical junction, or at $x = 0$, gives

$$C_2' = \frac{eN_a}{2\epsilon_s} x_p^2 \tag{7.24}$$

The potential in the n region can thus be written as

$$\phi(x) = \frac{eN_d}{\epsilon_s}\left(x_n \cdot x - \frac{x^2}{2}\right) + \frac{eN_a}{2\epsilon_s} x_p^2 \qquad (0 \le x \le x_n) \tag{7.25}$$

Figure 7.6 is a plot of the potential through the junction and shows the quadratic dependence on distance. The magnitude of the potential at $x = x_n$ is equal to the

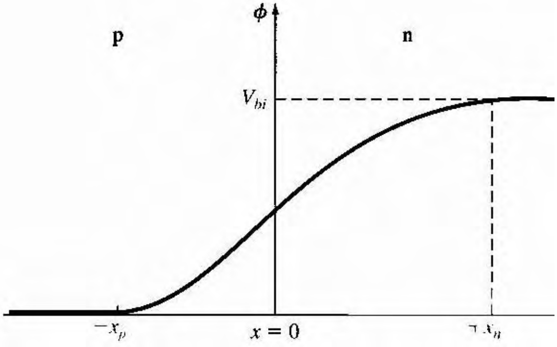

Figure 7.6 | Electric potential through the space charge region of a uniformly doped pn junction.

built-in potential barrier. Then from Equation (7.25), we have

$$V_{bi} = |\phi(x = x_n)| = \frac{e}{2\epsilon_s}\left(N_d x_n^2 + N_a x_p^2\right) \tag{7.26}$$

The potential energy of an electron is given by E = $-e\phi$, which means that the electron potential energy also varies as a quadratic function of distance through the space charge region. The quadratic dependence on distance was shown in the energy-band diagram of Figure 7.3, although we did not explicitly know the shape of the curve at that time.

7.2.3 Space Charge Width

We can determine the distance that the space charge region extends into the p and n regions from the metallurgical junction. This distance is known as the space charge width. From Equation (7.17). we may write, for example,

$$x_p = \frac{N_d x_n}{N_a} \tag{7.27}$$

Then, substituting Equation (7.27) into Equation (7.26) and solving for x_n, we obtain

$$\boxed{x_n = \left\{\frac{2\epsilon_s V_{bi}}{e}\left[\frac{N_a}{N_d}\right]\left[\frac{1}{N_a + N_d}\right]\right\}^{1/2}} \tag{7.28}$$

Equation (7.28) gives the space charge width, or the width of the depletion region, x_n extending into the n-type region for the case of zero applied voltage.

Similarly, if we solve for x_n from Equation (7.17) and substitute into Equation (7.26), we find

$$\boxed{x_p = \left\{\frac{2\epsilon_s V_{bi}}{e}\left[\frac{N_d}{N_a}\right]\left[\frac{1}{N_a + N_d}\right]\right\}^{1/2}} \tag{7.29}$$

where x_p is the width of the depletion region extending into the p region for the case of zero applied voltage.

The total depletion or space charge width W is the sum of the two components, or

$$W = x_n + x_p \tag{7.30}$$

Using Equations (7.28) and (7.29), we obtain

$$W = \left\{\frac{2\epsilon_s V_{bi}}{e}\left[\frac{N_a + N_d}{N_a N_d}\right]\right\}^{1/2} \tag{7.31}$$

The built-in potential barrier can be determined from Equation (7.10), and then the total space charge region width is obtained using Equation (7.31).

EXAMPLE 7.2

Objective

To calculate the space charge width and electric field in a pn junction.

Consider a silicon pn junction at T = 300 K with doping concentrations of $N_a = 10^{16}$ cm^{-3} and $N_d = 10^{15}$ cm^{-3}.

■ Solution

In Example 7.1. we determined the built-in potential barrier as $V_{bi} = 0.635$ V. From Equation (7.31), the space charge width is

$$W = \left\{ \frac{2\epsilon_s V_{bi}}{e} \left[\frac{N_a + N_d}{N_a N_d} \right] \right\}^{1/2}$$

$$= \left\{ \frac{2(11.7)(8.85 \times 10^{-14})(0.635)}{1.6 \times 10^{-19}} \left[\frac{10^{16} + 10^{15}}{(10^{16})(10^{15})} \right] \right\}^{1/2}$$

$$= 0.951 \times 10^{-4} \text{ cm} = 0.951\ \mu\text{m}$$

Using Equations (7.28) and (7.29). we can find **r,,** = 0.864 μm, and $x_p = 0.086\ \mu$m.

The peak electric field at the metallurgical junction, using Equation (7.16) for example. is

$$E_{max} = \frac{-eN_d x_n}{\epsilon_s} = \frac{-(1.6 \times 10^{-19})(10^{15})(0.864 \times 10^{-4})}{(11.7)(8.85 \times 10^{-14})} = 1.34 \times 10^4 \text{ V/cm}$$

■ Comment

The peak electric field in the space charge region of a pn junction is quite large. We must keep in mind. however, that there is no mobile charge in this region; hence there will be no drift current. We may also note, from this example, that the width of each space charge region is a reciprocal function of the doping concentration: The depletion region will extend further into the lower-doped region.

TEST YOUR UNDERSTANDING

E7.3 A silicon pn junction at T = 300 K with zero applied bias has doping concentrations of $N_d = 5 \times 10^{16}$ cm^{-3} and $N_a = 5 \times 10^{15}$ cm^{-3}. Determine x_n, x_p, W, and $|E_{max}|$.
(Ans. $x_n = 4.11 \times 10^{-6}$ cm, $x_p = 4.11 \times 10^{-5}$ cm, $W = 4.52 \times 10^{-5}$ cm, $|E_{max}| = 3.18 \times 10^4$ V/cm)

E7.4 Repeat E7.3 for a GaAs pn junction.
(Ans. $x_n = 5.60 \times 10^{-6}$ cm, $x_p = 5.60 \times 10^{-5}$ cm, $W = 6.16 \times 10^{-5}$ cm, $|E_{max}| = 3.86 \times 10^4$ V/cm)

7.3 | REVERSE APPLIED BIAS

If we apply a potential between the p and n regions, we will no longer be in an equilibrium condition — the Fermi energy level will no longer he constant through the system. Figure 7.7 shows the energy-band diagram of the pn junction for the case

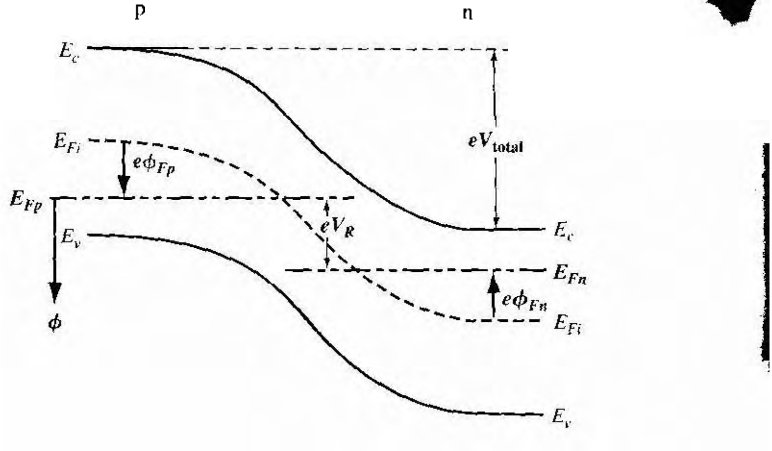

Figure 7.7 | Energy-band diagram of a pn junction under reverse bias.

when a positive voltage is applied to the n region with respect to the p region. As the positive potential is downward, the Fermi level on then side is below the Fermi level on the p side. The difference between the two is equal to the applied voltage in units of energy.

The total potential barrier, indicated by V_{total}, has increased. The applied potential is the reverse-bias condition. The total potential harrier is now given by

$$V_{total} = |\phi_{Fn}| + |\phi_{Fp}| + V_R \tag{7.32}$$

where V_R is the magnitude of the applied reverse-bias voltage. Equation (7.32) can he rewritten as

$$V_{total} = V_{bi} + V_R \tag{7.33}$$

where V_{bi} is the same built-in potential bamer we had defined in thermal equilibrium.

7.3.1 Space Charge Width and Electric Field

Figure 7.8 shows a pn junction with an applied reverse-bias voltage V_R. Also indicated in the figure are the electric field in the space charge region and the electric field E_{app}, induced by the applied voltage. The electric fields in the neutral p and n regions are essentially zero, or at least very small, which means that the magnitude of the electric field in the space charge region must increase above the thermal-equilibrium value due to the applied voltage. The electric field originates on positive charge and terminates on negative charge; this means that the number of positive and negative charges must increase if the electric field increases. For given impurity dopingconcentrations, the number of positive and negative charges in the depletion region can be increased only if the space charge width W increases. The space charge width W increases,

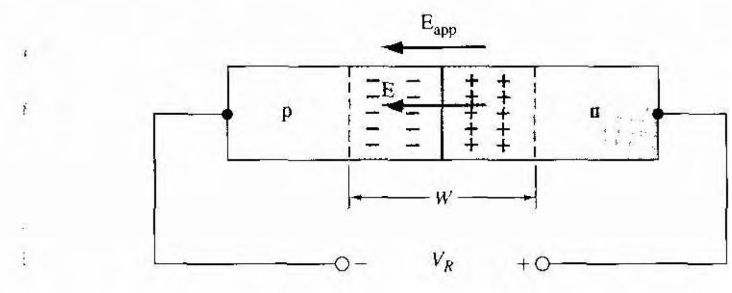

Figure 7.8 | A pn junction, with an applied reverse-bias voltage, showing the directions of the electric field induced by V_R and the space charge electric field.

therefore, with an increasing reverse-bias voltage V_R. We are assuming that the electric field in the bulk n and p regions is zero. This assumption will become clearer in the next chapter when we discuss the current-voltage characteristics.

In all of the previous equations, the built-in potential barrier can be replaced by the total potential barrier. The total space charge width can be written from Equation (7.31) as

$$\boxed{W = \left\{ \frac{2\epsilon_s (V_{bi} + V_R)}{e} \left[\frac{N_a + N_d}{N_a N_d} \right] \right\}^{1/2}} \tag{7.34}$$

showing that the total space charge width increases as we apply a reverse-bias voltage. By substituting the total potential barrier V_{total} into Equations **(7.28)** and (7.29), the space charge widths in the n and p regions, respectively, can be found as a function of applied reverse-bias voltage.

EXAMPLE 7.3

Objective

To calculate the width of the space charge region in a pn junction when a reverse-bias voltage is applied.

Again consider a silicon pn junction at $T = 300$ K with doping concentrations of $N_a = 10^{16}$ cm^{-3} and $N_d = 10^{15}$ cm^{-3}. Assume that $n_i = 1.5 \times 10^{10}$ cm^{-3} and let $V_R = 5$ V.

■ Solution

The built-in potential barrier was calculated in Example 7.1 for this case and is $V_{bi} = 0.635$ V. The space charge width is determined from Equation (7.34). We have

$$W = \left\{ \frac{2(11.7)(8.85 \times 10^{-14})(0.635 + 5)}{1.6 \times 10^{-19}} \left[\frac{10^{16} + 10^{15}}{(10^{16})(10^{15})} \right] \right\}^{1/2}$$

so that

$$W = 2.83 \times 10^{-4} \text{ cm} = 2.83\ \mu\text{m}$$

■ **Comment**

The space charge width has increased from 0.951 μm at zero bias to 2.83 μm at a reverse bias of 5 V.

The magnitude of the electric field in the depletion region increases with an applied reverse-bias voltage. The electric field is still given by Equations (7.14) and (7.16) and is still a linear function of distance through the space charge region. Since x_n and x_p increase with reverse-bias voltage. the magnitude of the electric field also increases. The maximum electric field still occurs at the metallurgical junction.

The maximum electric field at the metallurgical junction, from Equations (7.14 and (7.16), is

$$\mathrm{E}_{\max} = \frac{-eN_d x_n}{\epsilon_s} = \frac{-eN_a x_p}{\epsilon_s} \tag{7.35}$$

If we use either Equation (7.28) or (7.29) in conjunction with the total potential barrier, $V_{bi} + V_R$, then

$$\boxed{\mathrm{E}_{\max} = -\left\{\frac{2e(V_{bi}+V_R)}{\epsilon_s}\left(\frac{N_a N_d}{N_a+N_d}\right)\right\}^{1/2}} \tag{7.36}$$

We can show that the maximum electric field in the pn junction can also be written as

$$\boxed{\mathrm{E}_{\max} = \frac{-2(V_{bi}+V_R)}{W}} \tag{7.37}$$

where W is the total space charge width

DESIGN EXAMPLE 7.4

Objective

To design a pn junction to meet maximum electric field and voltage specifications.

Consider a silicon pn junction at T = 300 K with a p-type doping concentration of $N_a = 10^{18}$ cm^{-3}. Determine the n-type doping concentration such that the maximum electric field is $|\mathrm{E}_{\max}| = 3 \times 10^5$ V/cm at a reverse-bias voltage of $V_R = 25$ V.

■ **Solution**

The maximum electric field is given by Equation (7.36). Neglecting V_{bi} compared to V_R, we can write

$$|\mathrm{E}_{\max}| \approx \left\{\frac{2eV_R}{\epsilon_s}\left(\frac{N_a N_d}{N_a+N_d}\right)\right\}^{1/2}$$

or

$$3 \times 10^5 = \left\{\frac{2(1.6\times10^{-19})(25)}{(11.7)(8.85\times10^{-14})}\left(\frac{10^{18}\cdot N_d}{10^{18}+N_d}\right)\right\}^{1/2}$$

which yields

$$N_d = 1.18 \times 10^{16} \text{ cm}^{-3}$$

■ Conclusion

A smaller value of N_d results in a smaller value of $|E_{max}|$ for a given reverse-bias voltage. The value of N_d determined in this example, then, is the maximum value that will meet the specifications.

TEST YOUR UNDERSTANDING

E7.5 (*a*) A silicon pn junction at $T = 300$ K is reverse-biased at $V_R = 8$ V. The doping concentrations are $N_a = 5 \times 10^{16}$ cm^{-3} and $N_d = 5 \times 10^{15}$ cm^{-3}. Determine x_n, x_p, W, and $|E_{max}|$. (*b*) Repeat pan (a) for a reverse bias voltage of $V_R = 12$ V. [Ans. (*a*) $x_n = 1.43 \times 10^{-4}$ cm, $x_p = 1.43 \times 10^{-5}$ cm, $W = 1.57 \times 10^{-4}$ cm, $|E_{max}| = 1.11 \times 10^5$ V/cm; (*b*) $x_n = 1.73 \times 10^{-4}$ cm, $x_p = 1.73 \times 10^{-5}$ cm, $W = 1.90 \times 10^{-4}$ cm, $|E_{max}| = 1.34 \times 10^5$ V/cm]

E7.6 The maximum electric field in a reverse-biased GaAs pn junction at $T = 300$ K is to be $|E_{max}| = 2.5 \times 10^5$ V/cm. The doping concentrations are $N_d = 5 \times 10^{15}$ cm^{-3} and $N_a = 8 \times 10^{15}$ cm^{-3}. Determine the reverse-hias voltage that will produce this maximum electric field. (Ans. 72.5 V)

7.3.2 Junction Capacitance

Since we have a separation of positive and negative charges in the depletion region, a capacitance is associated with the pn junction. Figure 7.9 shows the charge densities in the depletion region for applied reverse-bias voltages of V_R and $V_R + dV_R$. An increase in the reverse-bias voltage dV_R will uncover additional positive charges in then region and additional negative charges in the p region. The junction capacitance is defined as

$$C' = \frac{dQ'}{dV_R} \tag{7.38}$$

where

$$dQ' = eN_d\,dx_n = eN_a\,dx_p \tag{7.39}$$

The differential charge dQ' is in units of C/cm^2 so that the capacitance C' is in units of farads per square centimeter (F/cm^2), or capacitance per unit area.

For the total potential barrier, Equation (7.28) may be written as

$$x_n = \left\{\frac{2\epsilon_s(V_{bi} + V_R)}{e}\left[\frac{N_a}{N_d}\right]\left[\frac{1}{N_a + N_d}\right]\right\}^{1/2} \tag{7.40}$$

The junction capacitance can be written as

$$C' = \frac{dQ'}{dV_R} = eN_d\frac{dx_n}{dV_R} \tag{7.41}$$

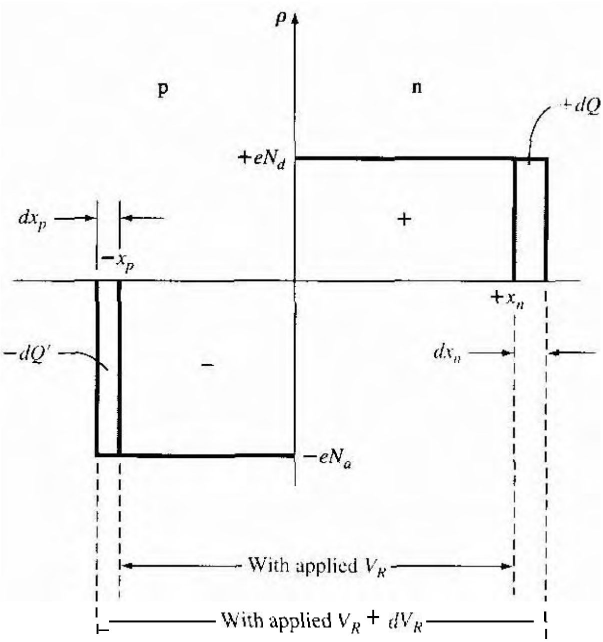

Figure 7.9 | Differential change in the space charge width with a differential change in reverse-bias voltage for a uniformly doped pn junction.

so that

$$\boxed{C' = \left\{\frac{e\epsilon_s N_a N_d}{2(V_{bi}+V_R)(N_a+N_d)}\right\}^{1/2}} \tag{7.42}$$

Exactly the same capacitance expression is obtained by considering the space charge region extending into the p region x_p. The junction capacitance is also referred to as the depletion *layer capacitance.*

EXAMPLE 7.5

Objective

To calculate the junction capacitance of a pn junction.

Consider the same pn junction as that in Example 7.3. Again assume that $V_R = 5$ **V.**

■ Solution

The junction capacitance is found from Equation (7.42) as

$$C' = \left\{\frac{(1.6\times10^{-19})(11.7)(8.85\times10^{-14})(10^{16})(10^{15})}{2(0.635+5)(10^{16}+10^{15})}\right\}^{1/2}$$

If the cross-sectional area of the pn junction is, for example, $A = 10^{-4}$ cm^2, then the total junction capacitance is

$$C = C' \cdot A = 0.366 \times 10^{-12} \text{ F} = 0.366 \text{ pF}$$

■ **Comment**

The value of junction capacitance is usually in the pF, or smaller, range.

If we compare Equation (7.34) for the total depletion width W of the space charge region under reverse bias and Equation (7.42) for the junction capacitance C', we find that we can write

$$C' = \frac{\epsilon_s}{W} \tag{7.43}$$

Equation (7.43) is the same as the capacitance per unit area of a parallel plate capacitor. Considering Figure 7.9, we may have come to this same conclusion earlier. Keep in mind that the space charge width is a function of the reverse bias voltage so that the junction capacitance is also a function of the reverse bias voltage applied to the pn junction.

73.3 One-Sided Junctions

Consider a special pn junction called the one-sided junction. If, for example, $N_a \gg N_d$, this junction is referred to as a p$^+$n junction. The total space charge width, from Equation (7.34), reduces to

$$W \approx \left\{ \frac{2\epsilon_s(V_{bi} + V_R)}{eN_d} \right\}^{1/2} \tag{7.44}$$

Considering the expressions for x_n and x,, we have for the p$^+$n junction

$$x_p \ll x_n \tag{7.45}$$

and

$$W \approx x_n \tag{7.46}$$

Almost the entire space charge layer extends into the low-doped region of the junction. This effect can be seen in Figure 7.10.

The junction capacitance of the p$^+$n junction reduces to

$$C' \approx \left\{ \frac{e\epsilon_s N_d}{2(V_{bi} + V_R)} \right\}^{1/2} \tag{7.47}$$

The depletion layer capacitance of a one-sided junction is a function of the doping concentration in the low-doped region. Equation (7.47) may be manipulated to give

$$\left(\frac{1}{C'}\right)^2 = \frac{2(V_{bi} + V_R)}{e\epsilon_s N_d} \tag{7.48}$$

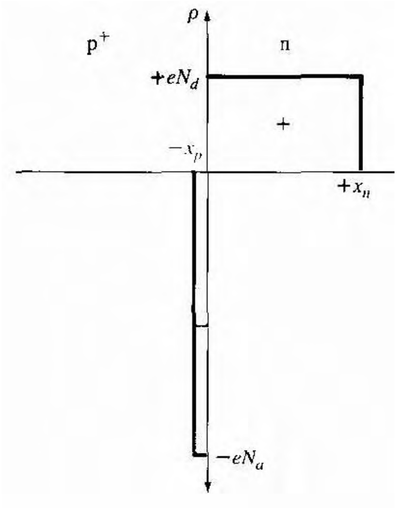

Figure 7.10 | Space charge density of a one-sided p^+n junction.

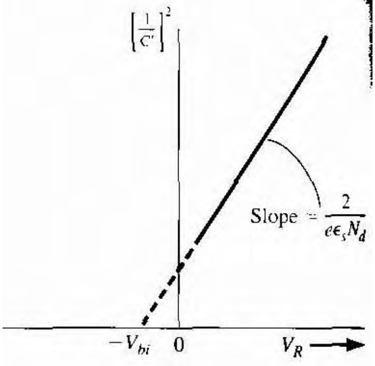

Figure 7.11 | $(1/C')^2$ versus V_R of a uniformly doped pn junction.

which shows that the inverse capacitance squared is a linear function of applied reverse-bias voltage.

Figure **7.11** shows a plot of Equation **(7.48).** The built-in potential of the junction can be determined by extrapolating the curve to the point where $(1/C')^2 = 0$. The slope of the curve is inversely proportional to the doping concentration of the low-doped region in the junction; thus, this doping concentration can be experimentally determined. The assumptions used in the derivation of this capacitance include uniform doping in both semiconductor regions, the abrupt junction approximation, and a planar junction.

EXAMPLE 7.6

Objective

To determine the impurity doping concentrations in a p^+n junction given the parameters from Figure 7.11.

Assume a silicon p+n junction at $T = 300$ K with $n_i = 1.5 \times 10^{10}$ cm^{-3}. Assume that the intercept of the curve in Figure 7.11 gives $V_{bi} = 0.855$ V and that the slope is 1.32×10^{15} (F/cm^2)$^{-2}$ (V)$^{-1}$.

■ Solution

The slope of the curve in Figure 7.11 is given by $2/e\epsilon_s N_d$, so we may write

$$N_d = \frac{2}{e\epsilon_s(\text{slope})} = \frac{2}{(1.6 \times 10^{-19})(11.7)(8.85 \times 10^{-14})(1.32 \times 10^{15})}$$

or

rom the expression for V_{bi}, which is

$$V_{bi} = V_t \ln\left(\frac{N_a N_d}{n_i^2}\right) = \frac{kT}{e}\ln\left(\frac{N_a N_d}{n_i^2}\right)$$

we can solve for N_a as

$$N_a = \frac{n_i^2}{N_d}\exp\left(\frac{eV_{bi}}{kT}\right) = \frac{(1.5 \times 10^{10})^2}{9.15 \times 10^{15}}\exp\left(\frac{0.855}{0.0259}\right)$$

ch yields

$$N_a = 5.34 \times 10^{18}\ \text{cm}^{-3}$$

Comment

The results of this example show that $N_a \gg N_d$; therefore the assumption of a one-sided junction was valid.

A one-sided pn junction is useful for experimentally determining the doping concentrations and built-in potential.

TEST YOUR UNDERSTANDING

E7.7 A silicon pn junction at T = 300 K has doping concentrations of $N_d = 3 \times 10^{16}\ \text{cm}^{-3}$ and $N_a = 8 \times 10^{15}\ \text{cm}^{-3}$, and has a cross-sectional area of $A = 5 \times 10^{-5}\ \text{cm}^2$. Determine the junction capacitance at (a) $V_R = 2$ V and (b) $V_R = 5$ V.
[Ans. (a) 0.694 pF, (b) 0.478 pF]

E7.8 The experimentally measured junction capacitance of a one-sided silicon n^+p junction biased at $V_R = 4$ V at T = 300 K is C = 1.10 pF. The built-in potential barrier is found to be $V_{bi} = 0.782$ V. The cross-sectional area is $A = 10^{-4}\ \text{cm}^2$. Find the doping concentrations. (Ans. $N_a = 7 \times 10^{15}\ \text{cm}^{-3}$, $N_d = 4.17 \times 10^{17}\ \text{cm}^{-3}$)

*7.4 | NONUNIFORMLY DOPED JUNCTIONS

In the pn junctions considered so far, we have assumed that each semiconductor region has been uniformly doped. In actual pn junction structures, this is not always true. In some electronic applications, specific nonuniform doping profiles are used to obtain special pn junction capacitance characteristics.

7.4.1 Linearly Graded Junctions

If we start with a uniformly doped n-type semiconductor, for example, and diffuse acceptor atoms through the surface, the impurity concentrations will tend to be like those shown in Figure 7.12. The point x = x' on the figure corresponds to the metallurgical junction. The depletion region extends into the p and n regions from the metallurgical junction as we have discussed previously. The net p-type doping

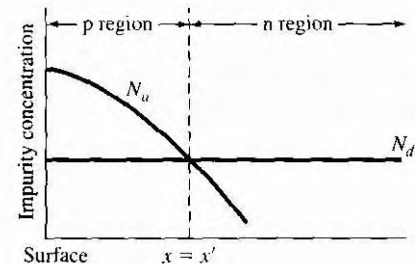

Figure **7.12** | Impurity concentrations of a pn junction with a nonuniformly doped p region.

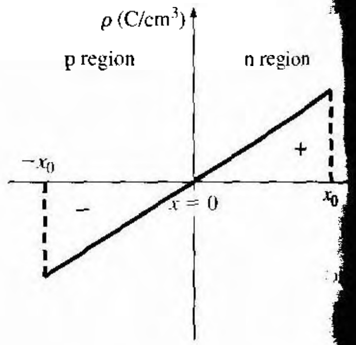

Figure 7.13 | Space charge density i linearly graded pn junction.

concentration near the metallurgical junction may be approximated as a linear fun tion of distance from the metallurgical junction. Likewise, as a first approximatio the net n-type doping concentration is also a linear function of distance extendi into the n region from the metallurgical junction. This effective doping profile referred to as a linearly graded junction.

Figure 7.13 shows the space charge density in the depletion region of the li early graded junction. For convenience, the metallurgical junction is placed at $x =$ The space charge density can he written as

$$\rho(x) = eax \qquad \text{(7.4}$$

where a is the gradient of the net impurity concentration.

The electric field and potential in the space charge region can be determine from Poisson's equation. We can write

$$\frac{d\mathrm{E}}{dx} = \frac{\rho(x)}{\epsilon_s} = \frac{eax}{\epsilon_s} \qquad \text{(7.}$$

so that the electric field can be found by integration as

$$\mathrm{E} = \int \frac{eax}{\epsilon_s}\, dx = \frac{ea}{2\epsilon_s}\left(x^2 - x_0^2\right) \qquad \text{(7.}$$

The electric field in the linearly graded junction is a quadratic function of distanc rather than the linear function found in the uniformly doped junction. The maximum electric field again occurs at the metallurgical junction. We may note that the electric field is zero at both $x = +x_0$ and at $x = -x_0$. The electric field in a nonuniformly doped semiconductor is not exactly zero, but the magnitude of this field is small, so setting $\mathrm{E} = 0$ in the bulk regions is still a good approximation.

The potential is again found by integrating the electric field as

$$\phi(x) = -\int \mathrm{E}\, dx \qquad (7.52)$$

If we arbitrarily set $\phi = 0$ at $x = -x_0$, then the potential through the junction is

$$\phi(x) = \frac{-ea}{2\epsilon_s}\left(\frac{x^3}{3} - x_0^2 x\right) + \frac{ea}{3\epsilon_s} x_0^3 \tag{7.53}$$

The magnitude of the potential at $x = +x_0$ will equal the built-in potential barrier for this function. We then have that

$$\phi(x_0) = \frac{2}{3} \cdot \frac{eax_0^3}{\epsilon_s} = V_{bi} \tag{7.54}$$

Another expression for the built-in potential harrier for a linearly graded junction can be approximated from the expression used for a uniformly doped junction. We can write

$$V_{bi} = V_t \ln\left[\frac{N_d(x_0)N_a(-x_0)}{n_i^2}\right] \tag{7.55}$$

where $N_d(x_0)$ and $N_a(-x_0)$ are the doping concentrations at the edges of the space charge region. We can relate these doping concentrations to the gradient, so that

$$N_d(x_0) = ax_0 \tag{7.56a}$$

and

$$N_a(-x_0) = ax_0 \tag{7.56b}$$

Then the built-in potential barrier for the linearly graded junction becomes

$$V_{bi} = V_t \ln\left(\frac{ax_0}{n_i}\right)^2 \tag{7.57}$$

There may be situations in which the doping gradient is not the same on either side of the junction, but we will not consider that condition here.

If a reverse-bias voltage is applied to the junction, the potential barrier increases. The built-in potential barrier V_{bi} in the above equations is then replaced by the total potential harrier $V_{bi} + V_R$. Solving for x_0 from Equation (7.54) and using the total potential bamer, we obtain

$$x_0 = \left\{\frac{3}{2} \cdot \frac{\epsilon_s}{ea}(V_{bi} + V_R)\right\}^{1/3} \tag{7.58}$$

The junction capacitance per unit area can be determined by the same method as we used for the uniformly doped junction. Figure 7.14 shows the differential charge dQ' which is uncovered as a differential voltage dV_R is applied. The junction capacitance is then

$$C' = \frac{dQ'}{dV_R} = (eax_0)\frac{dx_0}{dV_R} \tag{7.59}$$

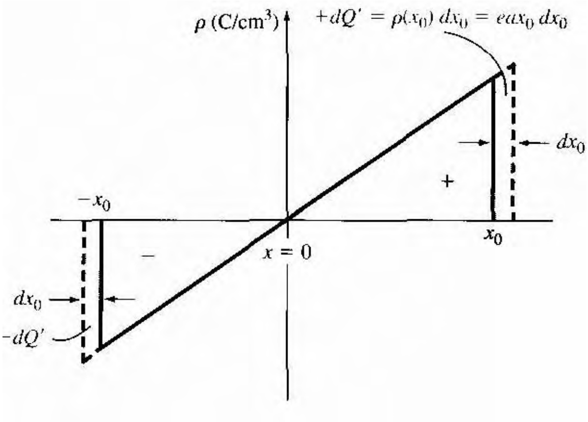

Figure 7.14 | Differential change in space charge width with a differential change in reverse-bias voltage for a linearly graded pn junction.

Using Equation (7.58), we obtain[1]

$$C' = \left\{\frac{ea\epsilon_s^2}{12(V_{bi} + V_R)}\right\}^{1/3} \tag{7.60}$$

We may note that C' is proportional to $(V_{bi} + V_R)^{-1/3}$ for the linearly graded junction as compared to $C' \alpha (V_{bi} + V_R)^{-1/2}$ for the uniformly doped junction. In the linearly graded junction, the capacitance is less dependent on reverse-bias voltage than in the uniformly doped junction.

7.4.2 Hyperabrupt Junctions

The uniformly doped junction and linearly graded junction are not the only possible doping profiles. Figure 7.15 shows a generalized one-sided p^+n junction where the generalized n-type doping concentration for $x > 0$ is given by

$$N = Bx^m \tag{7.61}$$

The case of $m = 0$ corresponds to the uniformly doped junction and $m = +1$ corresponds to the linearly graded junction just discussed. The cases of $m = +2$ and $m = +3$ shown would approximate a fairly low-doped epitaxial n-type layer grown on a much more heavily doped n^+ substrate layer. When the value of m is negative, we have what is referred to as a *hyperabrupt junction*. In this case, the n-type doping is larger near the metallurgical junction than in the bulk semiconductor. Equation (7.61) is used to approximate the n-type doping over a small region near $x = x_0$ and does not hold at $x = 0$ when m is negative.

---

[1] In a more exact analysis, V_{bi} in Equation (7.60) is replaced by a gradient voltage. However. this analysis is beyond the scope of this text.

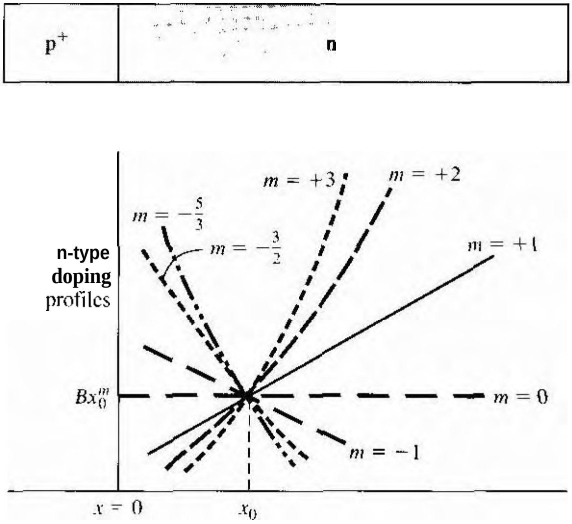

Figure 7.15 | Generalized doping profiles of a one-sided p+n junction.
(From Sze [14].)

The junction capacitance can be derived using the same analysis method as before and is given by

$$C' = \left\{ \frac{eB\epsilon_s^{(m+1)}}{(m+2)(V_{bi} + V_R)} \right\}^{1/(m+2)} \tag{7.62}$$

When m is negative, the capacitance becomes a very strong function of reverse-bias voltage, a desired characteristic in *varactor* ***diodes.*** The term *varactor* comes from the words *var*iable reactor and means a device whose reactance can be varied in a controlled manner with bias voltage.

If a varactor diode and an inductance are in parallel, the resonant frequency of the LC circuit is

$$f_r = \frac{1}{2\pi\sqrt{LC}} \tag{7.63}$$

The capacitance of the diode, from Equation (7.62). can be written in the form

$$C = C_0(V_{bi} + V_R)^{-1/(m+2)} \tag{7.64}$$

In a circuit application. we would, in general, like to have the resonant frequency be a linear function of reverse-bias voltage V_R, so we need

$$C \propto V^{-2} \tag{7.65}$$

From Equation (7.64). the parameter m required is found from

$$\frac{1}{m+2} = 2$$ (7.66a

or

$$m = -\frac{3}{2}$$ (7.66b

A specific doping profile will yield the desired capacitance characteristic.

7.5 | SUMMARY

- A uniformly doped pn junction was initially considered. in which one region *of* a semiconductor is uniformly duped with acceptor impurities and the adjacent region is uniformly doped with donor impurities. This type of junction is called a homojunction.
- A space charge region, or depletion region, is formed on either side of the metallurgical junction separating the n and p regions. This region is essentially depleted of any mobile electrons or holes. A net positive charge density, due to the positively charged donor impurity ions, exists in the n region and a net negative charge density, due to the negatively charged acceptor impurity ions, exists in the p region.
- An electric field exists in the depletion region due to the net space charge density. The direction of the electric field is from the n region to the p region.
- A potential difference exists across the space-charge region. Under zero applied bias, this potential difference. known as the built-in potential barrier, maintains thermal equilibrium and holds back majority carrier electrons in the n-region and majority carrier holes in the p region.
- An applied reverse bias voltage (n region positive with respect to the p region) increases the potential barrier. increases the space charge width, and increases the magnitude of the electric field.
- As the reverse bias voltage changes, the amount of charge in the depletion region changes. This change in charge with voltage defines the junction capacitance.
- The linearly graded junction represents a nonuniformly doped pn junction. Expressions for the electric field, built-in potential harrier, and junction capacitance were derived. The functional relationships differ from those of the uniformly doped junction.
- Specific doping profiles can be used to obtain specific capacitance characteristics. A hyperabrupt junction is one in which the doping decreases away from the metallurgical junction. This type ofjunction is advantageous in varactor diodes that are used in resonant circuits.

GLOSSARY OF IMPORTANT TERMS

abrupt junction approximation The assumption that there is an abrupt discontinuity in space charge density between the space charge region and neutral semiconductor region.

built-in potential harrier The electrostatic potential difference between the p and n regions of a pn junction in thermal equilibrium.

depletion layer capacitance Another term for junction capacitance.

depletion region Another term for space charge region.

hyperabrupt junction A pn junction in which the doping concentration on one side decreases away from the metallurgical junction to achieve a specific capacitance-voltage characteristic.

junction capacitance The capacitance of the pn junction under reverse bias.

linearly graded junction A pn junction in which the doping concentrations on either side of the metallurgical junction are approximated by a linear distribution.

metallurgical junction The interface between the p- and n-doped regions of a pn junction.

one-sided junction A pn junction in which one side of the junction is much more heavily doped than the adjacent side.

reverse bias The condition in which a positive voltage is applied to the n region with respect to the p region of a pn junction so that the potential barrier between the two regions increases above the thermal-equilibrium built-in potential barrier.

space charge region The region on either side of the metallurgical junction in which there is a net charge density due to ionized donors in the n-region and ionized acceptors in the p region.

space charge width The width of the space charge region, a function of doping concentrations and applied voltage.

varactor diode A diode whose reactance can be varied in a controlled manner with bias voltage.

CHECKPOINT

After studying this chapter, the reader should have the ability to:

- Describe why and how the space charge region is formed.
- Draw the energy band diagram of a zero-biased and reverse-biased pn junction.
- Define and derive the expression of the built-in potential barrier voltage.
- Derive the expression for the electric field in space charge region of the pn junction.
- Describe what happens to the parameters of the space charge region when a reverse bias voltage is applied.
- Define and explain the junction capacitance.
- Describe the characteristics and properties of a one-sided pn junction.
- Describe how a linearly graded junction is formed.
- Define a hyperabrupt junction.

REVIEW QUESTIONS

Define the built-in potential voltage and describe how it maintains thermal equilibrium.

Why is an electric field formed in the space charge region? Why is the electric field a linear function of distance in a uniformly doped pn junction?

3. Where does the maximum electric field occur in the space charge region?

4. Why is the space charge width larger in the lower doped side of a pn junction?

5. What is the functional dependence of the space charge width on reverse bias voltage?

6. Why does the space charge width increase with reverse bias voltage?

7. Why does a capacitance exist in a reverse-biased pn junction? Why does the capacitance decrease with increasing reverse bias voltage?

8. What is a one-sided pn junction? What parameters can be determined in a one-sided pn junction?
9. What is a linearly graded junction?
10. What is a hyperabrupt junction and what is one advantage or characteristic of such a junction'?

PROBLEMS

Section 7.2 Zero Applied Bias

7.1 (a) Calculate V_{bi} in a silicon pn junction at $T = 300$ K for (a) $N_d = 10^{15}$ cm^{-3} and $N_a =$ (i) 10^{15}, (ii) 10^{16}, (iii) 10^{17}, (iv) 10^{18} cm^{-3}. (b) Repeat part (a) for $N_d = 10^{18}$ cm^{-3}.

7.2 Calculate the built-in potential barrier, V_{bi}, for Si, Ge, and GaAs pn junctions if they each have the following dopant concentrations at $T = 300$ K:

(a) $N_d = 10^{14}$ cm^{-3} $\quad N_a = 10^{17}$ cm^{-3}

(b) $N_d = 5 \times 10^{16}$ $\quad N_a = 5 \times 10^{16}$

(c) N,, $= 10^{17}$ $\quad N_a = 10^{17}$

7.3 (a) Plot the built-in potential barrier for a symmetrical (N, $= N_d$) silicon pn junction at $T = 300$ K over the range $10^{14} \le N_a = N_d \le 10^{19}$ cm^{-3}. (b) Repeat part (a) for a GaAs pn junction.

7.4 Consider a uniformly doped GaAs pn junction with doping concentrations of $N_a = 5 \times 10^{18}$ cm^{-3} and $N_d = 5 \times 10^{16}$ cm^{-3}. Plot the built-in potential barrier voltage, V_{bi}, versus temperature for $200 \le T \le 500$ K.

7.5 An abrupt silicon pn junction at zero bias has dopant concentrations of $N_a = 10^{17}$ cm^{-3} and $N_d = 5 \times 10^{15}$ cm^{-3}. $T = 300$ K. (a) Calculate the Fermi level on each side of the junction with respect to the intrinsic Fermi level. (b) Sketch the equilibrium energy-band diagram for the junction and determine V_{bi} from the diagram and the results of part (a). (c) Calculate V_{bi} using Equation (7.10), and compare the results to part (b). (d) Determiner,,, r,,, and the peak electric field for this junction.

7.6 Repeat problem 7.5 for the case when the doping concentrations are N, $= N_d = 2 \times 10^{16}$ cm^{-3}.

7.7 A silicon abrupt junction in thermal equilibrium at $T = 300$K is doped such that E,. $- E_F = 0.21$ eV in the n region and $E_F -$ E, $= 0.18$ eV in the p region. (a) Draw the energy band diagram of the pn junction. (b) Determine the impurity doping concentrations in each region. (c) Determine V_{bi}.

7.8 Consider the uniformly doped GaAs junction at $T = 300$ K. At zero bias, only 20 percent of the total space charge region is to be in the p region. The built-in potential barrier is $V_{bi} = 1.20$ V. For zero bias, determine (a) N_a, (b) N_d, (c) x_n, (d) x_p, and (e) E_{max}.

7.9 Consider the impurity doping profile shown in Figure 7.16 in a silicon pn junction. For zero applied voltage, (a) determine V_{bi}, (b) calculate x,, and x_p, (c) sketch the thermal equilibrium energy band diagram, and (d) plot the electric field versus distance through the junction.

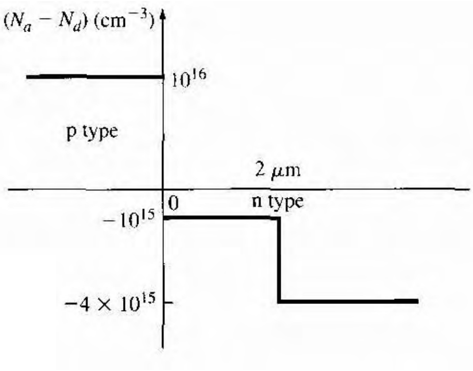

Figure 7.16 | Figure for Problem 7.9.

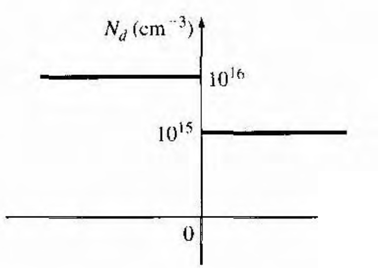

Figure 7.17 | Figure for Problem 7.12.

***7.10** A uniformly doped silicon pn junction is doped to levels of $N_d = 5 \times 10^{15}$ cm^{-3} and $N_a = 10^{16}$ cm^{-3}. The measured built-in potential barrier is $V_{bi} = 0.40$ V. Determine the temperature at which this result occurs. (You may have to use trial and error to solve this problem.)

7.11 Consider a uniformly doped silicon pn junction with doping concentrations N, = 5×10^{17} cm^{-3} and $N_d = 10^{17}$ cm^{-3}. (a) Calculate V_{bi} at T = 300 K. (*b*) Determine the temperature at which V_{bi} decreases by 1 percent.

7.12 An "isotype" step junction is one in which the same impurity type doping changes from one concentration value to another value. **An** n-n isotype doping profile is shown in Figure 7.17. (a) Sketch the thermal equilibrium energy band diagram of the isotype junction. *(b)* Using the energy band diagram. determine the built-in potential barrier. (c) Discuss the charge distribution through the junction.

7.13 A particular type of junction is an n region adjacent to an intrinsic region. This junction can be modeled as an n-type region to a lightly doped p-type region. Assume the doping concentrations in silicon at T = 300K are $N_d = 10^{16}$ cm^{-3} and $N_a = 10^{12}$ cm^{-3}. For zero applied bias. determine (*a*) V_{bi}, (b) **x,,**. (*c*) x_p, and (d) $\mathrm{E}_{\max}|$. Sketch the electric field versus distance through the junction.

7.14 We are assuming an abrupt depletion approximation for the space charge region. That is, no free carriers exist within the depletion region and the semiconductor abruptly changes to a neutral region outside the space charge region. This approximation is adequate for most applications. but the abrupt transition does not exist. The space charge region changes over a distance of a few Debye lengths, where the Debye length in the n region is given by

$$L_D = \left[\frac{\epsilon_s kT}{e^2 N_d}\right]^{1/2}$$

Calculate L_D and find the ratio of L_D/x_n for the following conditions. The p-type doping concentration is $N_a = 8 \times 10^{17}$ cm^{-3} and the n-type doping concentration is (*a*) $N_d = 8 \times 10^{14}$ cm^{-3}, (*b*) $N_d = 2.2 \times 10^{16}$ cm^{-3} and (*c*) $N_d = 8 \times 10^{17}$ cm^{-3}.

7.15 Examine how the electric field versus distance through a uniformly doped pn junction varies as the doping concentrations vary. For example, consider $N_d = 10^{18}$ cm^{-3} and let $10^{14} \le N_a \le 10^{18}$ cm^{-3}. then consider $N_d = 10^{14}$ cm^{-3} and let

$10^{14} \le N_a \le 10^{18}$ cm^{-3}. and finally consider $N_d = 10^{16}$ cm^{-3} and let $10^{14} \le N_a \le 10^{18}$ cm^{-3}. What can be said about the results for $N_a \ge 100N_d$ or $N_d \ge 100N_a$? Assume zero applied bias.

Section 7.3 Reverse Applied Bias

7.16 An abrupt silicon pnjunction has dopant concentrations of N„ = 2 *x* 10^{16} cm^{-3} and $N_d = 2 \times 10^{15}$ cm^{-3} at $T = 300$ K. Calculate *(a)* V_{bi}, *(h)* W at $V_R = 0$ and $V_R = 8$ V, and *(c)* the maximum electric field in the space charge region at $V_R = 0$ and $V_R = 8$ V.

7.17 Consider the junction described in Problem 7.11. The junction has a cross-sectional area of 10^{-4} cm^2 and has an applied reverse-bias voltage of $V_R = 5$ V. Calculate *(a)* V_{bi}, *(b)* x_n, x_p, W. *(c)* E_{max} . and *id)* the total junction capacitance.

7.18 An ideal one-sided silicon n^+p junction has uniform doping on both sides of the abrupt junction. The doping relation is $N_d = 50N_a$. The built-in potential barrier is $V_{bi} = 0.752$ V. The maximum electric field in the junction is $E_{max} = 1.14$ *x* 10' V/cm for a reverse-bias voltage of 10 V. $T = 300$ K. Determine *(a)* N_a, N_d *(b)* x_p for $V_R = 10$, and *(c)* C'_j for $V_R = 10$.

7.19 A silicon n^+p junction is biased at $V_R = 10$ V. Determine thc percent change in (a)junction capacitance and *(b)* built-in potential if the doping in the p region increases by a factor of 2.

7.20 Consider two p^+n silicon junctions at $T = 300$ K reverse biased at $V_R = 5$ V. The impurity doping concentrations in junction *A* are $N_a = 10^{18}$ cm^{-3} and $N_d = 10^{15}$ cm^{-3}, and those in junction B are N„ = 10^{18} cm^{-3} and $N_d = 10^{16}$ cm^{-3}. Calculate the ratio of the following parameters for junction ***A*** to junction *B*: *(a)* W. *(b)* $|E_{max}|$, and *(c)* C'_j.

7.21 *(a)*The peak electric field in a reverse-biased silicon pn junction is $|E_{max}| = 3 \times 10^5$ Vlcm. The doping concentrations are N, = 4 x 10^{15} cm^{-3} and $N_a = 4 \times 10^{17}$ cm^{-3}. Find the magnitude of the reverse-bias voltage. *(b)* Repeat pan *(a)* for $N_d = 4 \times 10^{16}$ cm^{-3} and N„ = 4 × 10^{17} c m . **(r)** Repeat part *(n)* for N_d = N, = 4 *x* 10^{17} cm^{-3}

7.22 Consider a uniformly doped GaAs pn junction at $T = 300$ K. The junction capacitance at zero bias is C, (0) and the junction capacitance with a 10-V reverse-bias voltage is $C_j(10)$. The ratio of the capacitances is

$$\frac{C_j(0)}{C_j(10)} = 3.13$$

Also under reverse bias, the space charge width into the p region is 0.2 of the total space charge width. Determine *(a)* V_{bi} and *(b)* N„, N_d.

7.23 GaAs pn junction at T = 300 K has impurity doping concentratians of $N_a = 10^{16}$ cm^{-3} and $N_d = 5 \times 10^{16}$ cm^{-3}. For a particular device application, the ratio ofjunction capacitances at two values of reverse bias voltage must he $C'_j(V_{R1})/C'_j(V_{R2}) = 3$ where the reverse bias voltage $V_{R1} = 1$ V. Determine V_{R2}.

7.24 An abrupt silicon pn junction at T = 300 K is uniformly doped with N„ = 10^{18} cm^{-3} and $N_d = 10^{15}$ cm^{-3}. The pn junction area is 6 *x* 10 ^{4} cm^2. An inductance of 2.2 millihenry is placed in parallel with the pn junction. Calculate the resonant frequency of the circuit for reverse-bias voltages of *(a)* $V_R = 1$ V and *(b)* $V_R = 10$ V.

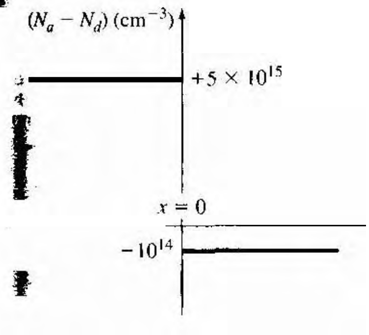

Figure 7.18 | Figure for Problem 7.27.

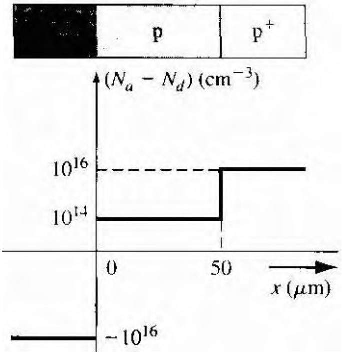

Figure 7.19 | Figure for Problem 7.28

7.25 A uniformly doped silicon p+n junction at $T = 300$ K is to be designed such that at a reverse-bias voltage of $V_R = 10$ V, the maximum electric field is limited to $E_{max} = 10^6$ V/cm. Determine the maximum doping concentration in the n region.

7.26 A silicon pn junction is to be designed which meets the following specifications at $T = 300$ K. At a reverse-bias voltage of 1.2 V, 10 percent of the total space charge region is to be in the n region and the total junction capacitance is to be 3.5 x 10^{-12} F with a cross-sectional area of 5.5 x 10^{-4} cm^2. Determine (*a*) N_a, (*b*) N_d, and (*c*) V_{bi}.

7.27 A silicon pn junction at $T = 300$ K has the doping profile shown in Figure 7.18. Calculate (a) V_{bi}, (*b*) x_n and x_p at zero bias, and (*c*) the applied bias required so that $x_n = 30$ μm.

7.28 Consider a silicon pn junction with the doping profile shown in Figure 7.19. $T = 300$ K. (*a*) Calculate the applied reverse-bias voltage required so that the space charge region extends entirely through the p region. (*b*) Determine the space charge width into the n$^+$-region with the reverse-bias voltage calculated in part (*a*). (*c*) Calculate the peak electric field for this applied voltage.

7.29 (a) A silicon p$^+$n junction has doping concentrations of $N_a = 10^{18}$ cm^{-3} and $N_d = 5$ x 10^{15} cm^{-3}. The cross-sectional area of the junction is $A = 5 \times 10^{-5}$ cm^2. Calculate the junction capacitance for (*i*) $V_R = 0$, (*ii*) $V_R = 3$ V, and (*iii*) $V_R = 6$ V. Plot $1/C^2$ versus V_R. Show that the slope of the curve can be used to find N_d and that the intersection with the voltage axis yields V_{bi}. (*b*) Repeat part (*a*) if the n-type doping concentration changes to $N_d = 6$ x 10^{16} cm^{-3}.

7.30 The total junction capacitance of a one-sided silicon pn junction at $T = 300$ K is measured at $V_R = 50$ mV and found to be 1.3 pF. The junction area is 10^{-5} cm^2 and $V_{bi} = 0.95$ V. (*a*) Find the impurity doping concentration of the low-doped side of the junction. (*b*) Find the impurity doping concentration of the higher-doped region.

7.31 Examine how the capacitance C' and the function $(1/C')^2$ vary with reverse-bias voltage V_R as the doping concentrations change. In particular, consider these plots versus N_a for $N_a \geq 100N_d$ and versus N_d for $N_d \geq 100N_a$

***7.32** A pn junction has the doping profile shown in Figure 7.20. Assume that $x_n > x_0$ for all reverse-bias voltages. (*a*) What is the built-in potential across the junction? (*b*) For

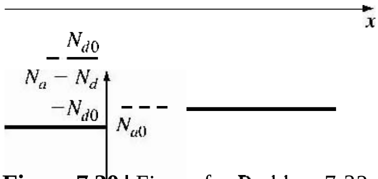

Figure 7.20 | Figure for Problem 7.32.

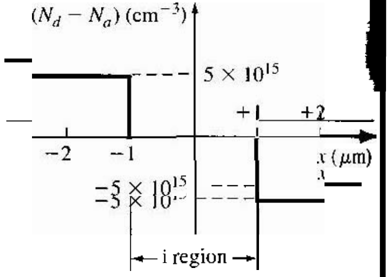

Figure 7.21 | Figure for Problem 7.33.

the abrupt junction approximation, cketch the charge density through the junction. (2) Derive the expression for the electric field through the space charge region.

***7.33** A silicon PIN junction has the doping profile shown in Figure 7.21. The "I" corresponds to an ideal intrinsic region in which there is no impurity doping concentration. A reverse-hias voltage is applied to the PIN junction so that the total depletion width extends from -2 μm to $+2$ μm. (a) Using Poisson's equation, calculate the magnitude of the electric field at $x = 0$. (*b*) Sketch the electric field through the PIN junction. (*c*) Calculate the reverse-bias voltage that must be applied.

Section 7.4 Nonuniformly Doped Junctions

7.34 Consider a linearly graded junction. (a) Starting with Equation (7.49), derive the expression for the electric field given in Equation (7.51). (*b*) Derive the expression for the potential through the space charge region given hy Equation (7.53).

7.35 The built-in potential barrier of a linearly graded silicon pn junction at T = 300 K is $V_{bi} = 0.70$ V The junction capacitance measured at $V_R = 3.5$ V is C' = 7.2 x F/cm^2. Find the gradient, a, of the net impurity concentration.

Summary and Review

7.36 Anne-sided p+n silicon diode at $T = 300$ K is doped at $N_a = 10^{18}$ cm^{-3}. Design the junction so that C, = 0.95 pF at $V_R = 3.5$ V. Calculate the junction capacitance when $V_R = 1.5$ V.

7.37 A one-sided p^+n junction with a cross-sectional **area** of 10^{-5} cm^2 has a measured built-in potential of $V_{bi} = 0.8$ V at T = 300 K. A plot of $(1/C_j)^2$ versus V_R is linear for $V_R <$ I V and is essentially constant for $V_R > 1$ V. The capacitance is C, = 0.082 pF at $V_R = 1$ V Determine the doping concentrations on either side of the metallurgical junction that will produce this capacitance characteristic.

***7.38** Silicon, at **T** = 300 K, is doped at $N_{d1} = 10^{15}$ cm^{-3} for $x < 0$ and $N_{d2} = 5 \times 10^{16}$ cm^{-3} for $x > 0$ to form an $n - n$ step junction. (*a*) Sketch the energy-band diagram. (*b*) Derive an expression for V_{bi}. (*c*) Sketch the charge density, electric held, and potential through the junction. (*d*) Explain where the charge density came from and is located.

***7.39** A diffused silicon pn junction has a linearly graded junction on the p side with $a = 2 \times 10^{19}$ cm^{-4}, and a uniform doping of 10^{15} cm^{-3} on the n side. (a) If the depletion width on the p side is 0.7 μm at zero bias, find the total depletion width, built-in potential, and maximum electric field at zero bias. *(b)* Plot the potential function through the junction.

READING LIST

1. Dimitrijev, S. *Understanding Semiconductor Devices.* New York: Oxford University Press, 2000.
2. Kano, K. *Semiconductor Devices.* Upper Saddle River, NJ: Prentice Hall, 1998.
*3. Li, S. S. *Semiconductor Physical Electronics.* New York: Plenum Press, 1993.
4. Muller, R. S., and T. I. Kamins. *Device Electronics for Integrated Circuits.* 2nd ed. New York: Wiley, 1986.
5. Navon, D. H. *Semiconductor Microdevices and Materials.* New York: Holt, Rinehart &Winston. 1986.
6. Neudeck, G. W. *The PN Junction Diode.* Vol. 2 of the *Modular Series* on *Solid State Devices.* 2nd ed. Reading, MA: Addison-Wesley, 1989.
*7. Ng, K. K. *Complete Guide to Semiconductor Devices.* New York: McGraw-Hill. 1995.
8. Pierret, R. F. *Semiconductor Device Fundamentals.* Reading, MA: Addison-Wesley. 1996.
*9. Roulston, D. J. *An Introduction to the Physics of Semiconductor Devices.* New York: Oxford University Press, 1999.
10. Shur, M. *Introduction to Electronic Devices.* New York: John Wiley and Sons, 1996.
*11. Shur, M. *Physics of Semiconductor Devices.* Englewood Cliffs, NJ: Prentice Hall, 1990.
12. Singh, J. *Semiconductor Devices; Basic Principles.* New York: John Wiley and Sons, 2001.
13. Streetman, B. G., and S. Banerjee. *Solid State Electronic Devices.* 5th ed. Upper Saddle River, NJ: Prentice-Hall, 2000.
14. Sze, S. M. *Physics of Semiconductor Devices.* 2nd ed. New York: Wiley, 1981.
15. Sze, S. M. *Semiconductor Devices: Physics and Technology,* 2nd ed. New York: John Wiley and Sons, Inc., 2001
*16. Wang, S. *Fundamentals of Semiconductor Theory and Device Physics.* Englewood Cliffs. NJ: Prentice Hall. 1989.
17. Yang, E. S. *Microelectronic Devices.* New York: McGraw-Hill, 1988.

CHAPTER 8

The pn Junction Diode

PREVIEW

In the last chapter, we discussed the electrostatics of the pn junction in thermal equilibrium and under reverse bias. We determined the built-in potential barrier at thermal equilibrium and calculated the electric field in the space charge region. We also considered the junction capacitance. In this chapter, we will consider the pn junction with a forward-bias voltage applied and will determine the current–voltage characteristics. The potential barrier of the pn junction is lowered when a forward-bias voltage is applied, allowing electrons and holes to flow across the space charge region. When holes flow from the p region across the space charge region into the n region, they become excess minority carrier holes and are subject to the excess minority carrier diffusion, drift, and recombination processes discussed in Chapter 6. Likewise, when electrons from the n region flow across the space charge region into the p region, they become excess minority carrier electrons and are subject to these same processes.

When semiconductor devices with pn junctions are used in linear amplifiers, for example, time-varying signals are superimposed on the dc currents and voltages. A small sinusoidal voltage superimposed on a dc voltage applied across a pn junction will generate a small-signal sinusoidal current. The ratio of the sinusoidal current to voltage yields the small-signal admittance of the pn junction. The admittance of a forward-biased pn junction contains both conductance and capacitance terms. The capacitance, called a diffusion capacitance, differs from the junction capacitance discussed in the last chapter. Using the admittance function, the small-signal equivalent circuit of the pn junction will be developed.

The last three topics considered in this chapter are junction breakdown, switching transients. and the tunnel diode. When a sufficiently large reverse-bias voltage is applied across a pn junction, breakdown can occur, producing a large reverse-bias current in the junction, which can cause heating effects and catastrophic failure of the diode. Zener diodes, however, are designed to operate in the breakdown region.

Breakdown puts limits on the amount of voltage that can be applied across a pn junction. When a pn junction is switched from one conducting state to the other, transients in the diode current and voltage occur. The switching time of the pn junction will be discussed here, and again in later chapters which deal with the switching of transistors..

8.1 | pn JUNCTION CURRENT

When a forward-bias voltage is applied to a pn junction, a current will be induced in the device. We initially consider a qualitative discussion of how charges flow in the pn junction and then consider the mathematical derivation of the current–voltage relationship.

8.1.1 Qualitative Description of Charge Flow in a pn Junction

We can qualitatively understand the mechanism of the current in a pn junction by again considering the energy band diagrams. Figure 8.1a shows the energy band diagram of a pn junction in thermal equilibrium that was developed in the last chapter. We argued that the potential barrier seen by the electrons, for example, holds back the large concentration of electrons in the n region and keeps them from flowing into the p region. Similarly, the potential barrier seen by the holes holds back the large

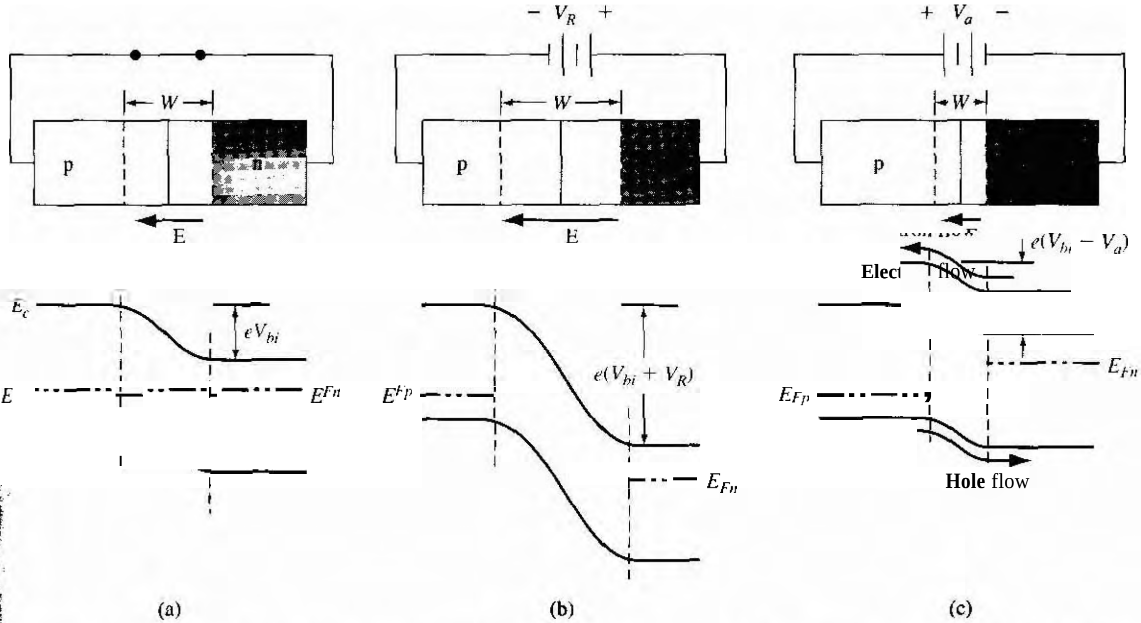

(a) (b) (c)

Figure 8.1 | A pn junction and its associated energy band diagram for (a) zero bias, (b) reverse bias, and (c) forward bias.

concentration of holes in the p region and keeps them from flowing into the n region. The potential barrier, then, maintains thermal equilibrium.

Figure 8.1b shows the energy band diagram of a reverse-biased pn junction. The potential of the n region is positive with respect to the p region so the Fermi energy in the n region is lower than that in the p region. The total potential harrier is now larger than for the zero-bias case. We argued in the last chapter that the incre potential barrier continues to hold back the electrons and holes so that there is still essentially no charge flow and hence essentially no current.

Figure 8.1c now shows the energy band diagram for the case when a positive voltage is applied to the p region with respect to the n region. The Fermi level in the p region is now lower than that in the n region. The total potential barrier is now reduced. The smaller potential barrier means that the electric field in the depletion region is also reduced. The smaller electric field means that the electrons and holes are no longer held hack in the n and p regions, respectively. There will be a diffusion of holes from the p region across the space-charge region where they now will How into the n region. Similarly, there will be a diffusion of electrons from the n region across the space-charge region where they will flow into the p region. The flow of charge generates a current through the pn junction.

The injection of holes into the n region means that these holes are minority carriers. Likewise, the injection of electrons into the p-region means thar these electrons are minority carriers. The behavior of these minority carriers is described by the ambipolar transport equations that were discussed in Chapter 6. There will be diffusion as well as recombination of excess carriers in these regions. The diffusion of carriers implies that there will be diffusion currents. The mathematical derivation of the pn junction current–voltage relationship is considered in the next section.

8.1.2 Ideal Current–Voltage Relationship

The ideal current–voltage relationship of a pn junction is derived on the basis of four assumptions. (The last assumption has three parts, but each part deals with current.) They are:

1. The abrupr depletion layer approximation applies. The space charge regions have abrupt boundaries and the semiconductor is neutral outside of the depletion region.
2. The Maxwell–Boltzmann approximation applies to carrier statistics.
3. The concept of low injection applies.
4a. The total current is a constant throughout the entire pn structure.
4b. The individual electron and hole currents are continuous functions through the pn structure.
4c. The individual electron and hole currents are constant throughout the depletion region.

Notation can sometimes appear to be overwhelming in the equations in this chapter. Table 8.1 lists some of the various electron and hole concentration terms that

Table 8.1 | Commonly used terms and notation for this chapter

Term	Meaning
N_a	Acceptor concentration in the p region of the pn junction
N_d	Donor concentration in the n region of the pn junction
$n_{n0} = N_d$	Thermal equilibrium majority carrier electron concentration in the n region
$p_{p0} = N_a$	Thermal equilibrium majority carrier hole concentration in the p region
$n_{p0} = n_i^2/N_a$	Thermal equilibrium minority carrier electron concentration in the p region
$p_{n0} = n_i^2/N_d$	Thermal equilibrium minority carrier hole concentration in the n region
n_p	Total minority carrier electron concentration in the p region
p_n	Total minority carrier hole concentration in the n region
$n_p(-x_p)$	Minority carrier electron concentration in the p region at the space-charge edge
$p_n(x_n)$	Minority carrier hole concentration in the n region at the space charge edge
$\delta n_p = n_p - n_{p0}$	Excess minority carrier electron concentration in the p region
$\delta p_n = p_n - p_{n0}$	Excess minority carrier hole concentration in the n region

appear. Many terms have already been used in previous chapters but are repeated here for convenience.

8.1.3 Boundary Conditions

Figure 8.2 shows the conduction-band energy through the pn junction in thermal equilibrium. The n region contains many more electrons in the conduction band than the p region; the built-in potential barrier prevents this large density of electrons from flowing into the p region. The built-in potential barrier maintains equilibrium between the carrier distributions on either side of the junction.

An expression for the built-in potential barrier was derived in the last chapter and was given by Equation (7.10) as

$$V_{bi} = V_t \ln\left(\frac{N_a N_d}{n_i^2}\right)$$

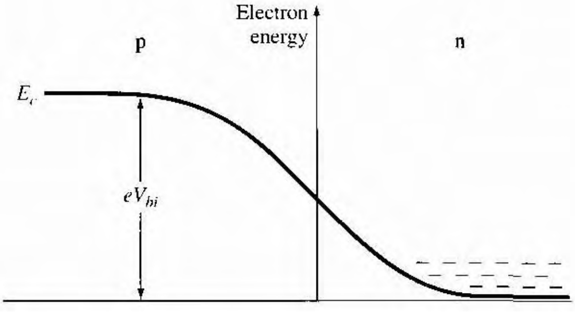

Figure 8.2 | Conduction-band energy through a pn junction.

If we divide the equation by $V_t = kT/e$, take the exponential of both sides, and then take the reciprocal, we obtain

$$\frac{n_i^2}{N_a N_d} = \exp\left(\frac{-eV_{bi}}{kT}\right) \tag{8}$$

If we assume complete ionization, we can write

$$n_{n0} \approx N_d \tag{8.2}$$

where n_{n0} is the thermal-equilibrium concentration of majority carrier electrons in the n region. In the p region, we can write

$$n_{p0} \approx \frac{n_i^2}{N_a} \tag{8.3}$$

where n_{p0} is the thermal-equilibrium concentration of minority carrier electrons. Substituting Equations (8.2) and (8.3) into Equation (8.1) yields

$$n_{p0} = n_{n0} \exp\left(\frac{-eV_{bi}}{kT}\right) \tag{8.4}$$

This equation relates the minority carrier electron concentration on the p side of the junction to the majority carrier electron concentration on the n side of the junction in thermal equilibrium.

If a positive voltage is applied to the p region with respect to the n region, the potential barrier is reduced. Figure 8.3a shows a pn junction with an applied voltage V_a. The electric field in the bulk p and n regions is normally very small. Essentially all of the applied voltage is across the junction region. The electric field E_{app} induced by the applied voltage is in the opposite direction to the thermal equilibrium space charge electric field, so the net electric field in the space charge region is reduced below the equilibrium value. The delicate balance between diffusion and the E-field force

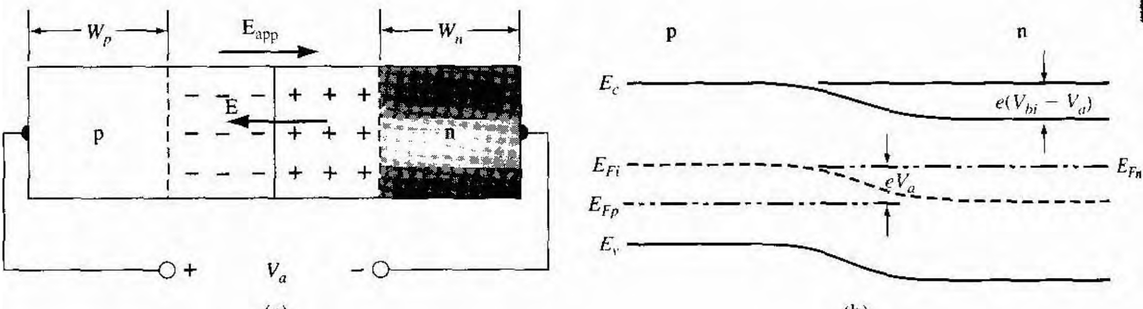

(a) (b)

Figure 8.3 | (a) A pn junction with an applied forward-bias voltage showing the directions of the electric field induced by V_a and the space charge electric field. (b) Energy-band diagram of the forward-biased pn junction.

achieved at thermal equilibrium is upset. The electric field force that prevented majority carriers from crossing the space charge region is reduced; majority carrier electrons from the n side are now injected across the depletion region into the p material, and majority carrier holes from the p side are injected across the depletion region into then material. As long as the bias V_a is applied, the injection of carriers across the space charge region continues and a current is created in the pn junction. This bias condition is known as forward bias; the energy-band diagram of the forward-biased pn junction is shown in Figure 8.3b.

The potential barrier V_{bi} in Equation (8.4) can be replaced by $(V_{bi} - V_a)$ when the junction is forward biased. Equation (8.4) becomes

$$n_p = n_{n0} \exp\left(\frac{-e(V_{bi} - V_a)}{kT}\right) = n_{n0} \exp\left(\frac{-eV_{bi}}{kT}\right) \exp\left(\frac{-eV_a}{kT}\right) \tag{8.5}$$

If we assume low injection, the majority carrier electron concentration n_{n0}, for example, does not change significantly. However, the minority carrier concentration, n_p, can deviate from its thermal-equilibrium value n_{p0} by orders of magnitude. Using Equation (8.4), we can write Equation (8.5) as

$$\boxed{n_p = n_{p0} \exp\left(\frac{eV_a}{kT}\right)} \tag{8.6}$$

When a forward-bias voltage is applied to the pn junction, the junction is no longer in thermal equilibrium. The left side of Equation (8.6) is the total minority carrier electron concentration in the p region, which is now greater than the thermal equilibrium value. The forward-bias voltage lowers the potential barrier so that majority carrier electrons from the n region are injected across the junction into the p region, thereby increasing the minority carrier electron concentration. We have produced excess minority carrier electrons in the p region.

When the electrons are injected into the p region, these excess carriers are subject to the diffusion and recombination processes we discussed in Chapter 6. Equation (8.6). then, is the expression for the minority carrier electron concentration at the edge of the space charge region in the p region.

Exactly the same process occurs for majority carrier holes in the p region which are injected across the space charge region into the n region under a forward-bias voltage. We can write that

$$\boxed{p_n = p_{n0} \exp\left(\frac{eV_a}{kT}\right)} \tag{8.7}$$

where p_n is the concentration of minority carrier holes at the edge of the space charge region in the n region. Figure 8.4 shows these results. By applying a forward-bias voltage, we create excess minority carriers in each region of the pn junction.

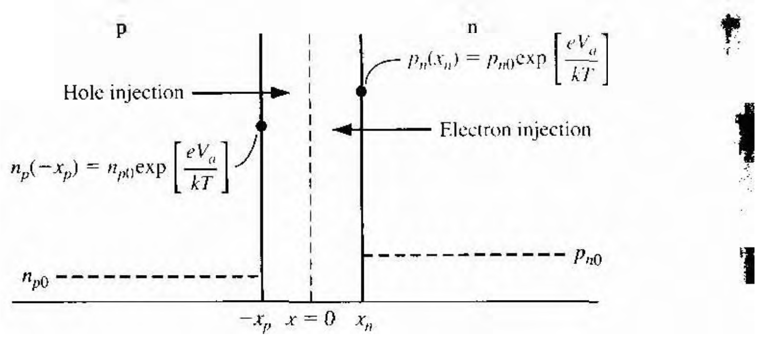
p
n
Hole injection
Electron injection
$p_n(x_n) = p_{n0}\exp\left[\frac{eV_a}{kT}\right]$
$n_p(-x_p) = n_{p0}\exp\left[\frac{eV_a}{kT}\right]$
n_{p0}
p_{n0}
$-x_p$
$x = 0$
x_n

Figure 8.4 | Excess minority carrier concentrations at the space charge edges generated by the forward-bias voltage.

EXAMPLE 8.1

Objective

To calculate the minority carrier hole concentration at the edge of the space charge region of a pn junction when a forward bias is applied.

Consider a silicon pn junction at T = 300 K so that $n_i = 1.5 \times 10^{10}$ cm^{-3}. Assume the n-type doping is 1×10^{16} cm^{-3} and assume that a forward bias of 0.60 V is applied to the pn junction. Calculate the minority carrier hole concentration at thr edge of the space charge region.

■ Solution

From Equation **(8.7)** we have

$$p_n = p_{n0}\exp\left(\frac{eV_a}{kT}\right)$$

The thermal-equilibrium minority carrier hole concentration is

$$p_{n0} = \frac{n_i^2}{N_d} = \frac{(1.5 \times 10^{10})^2}{10^{16}} = 2.25 \times 10^4 \text{ cm}^{-3}$$

We then have

$$p_n = 2.25 \times 10^4 \exp\left(\frac{0.60}{0.0259}\right) = 2.59 \times 10^{14} \text{ cm}^{-3}$$

■ Comment

The minority carrier concentration can increase by many orders of magnitude when a forward-bias voltage is applied. Low injection still applies. however, since the excess-electron concentration (equal to the excess-hole concentration in order to maintain charge neutrality) is much less than the thermal-equilibrium electron concentration.

TEST YOUR UNDERSTANDING

E8.1 A silicon pn junction at T = 300 K is doped with impurity concentrations of $N_d = 5 \times 10^{16}$ cm^{-3} and $N_a = 2 \times 10^{16}$ cm^{-3}. The junction is forward biasedat $V_a = 0.610$ V.

Determine the minority carrier concentrations at the space charge edges.
[Ans. $p_n(x_n) = 7.62 \times 10^{13}$ cm^{-3}, $n_p(-x_p) = 1.90 \times 10^{14}$ cm^{-3}]

E8.2 The impurity doping concentrations in a silicon pn junction at T = 300 K arc $N_d = 5 \times 10^{15}$ cm^{-3} and $N_a = 5 \times 10^{16}$ cm^{-3}. The minority carrier concentration at either space charge edge is to be no larger than 10 percent of the respective majority carrier concentration. Calculate the maximum forward bias voltage that can be applied to this junction and still meet the required specifications. [Ans. V_a(max) = 0.599 V]

E8.3 Repeat E8.2 for a GaAs pn junction with the same doping concentrations.
[Ans. V_a(max) = 1.067 V]

The minority carrier concentrations at the space charge edges, given by Equations (8.6) and (8.7), were derived assuming a forward-bias voltage ($V_a > 0$) was applied across the pn junction. However, nothing in the derivation prevents V_a from being negative (reverse bias). If a reverse-bias voltage greater than a few tenths of a volt is applied to the pn junction, then we see from Equations (8.6) and (8.7) that the minority carrier concentrations at the space charge edge are essentially zero. The minority carrier concentrations for the reverse-bias condition drop below the thermal-eauilibnum values.

8.1.4 Minority Carrier Distribution

We developed, in Chapter 6, the ambipolar transport equation for excess minority carrier holes in an n region. This equation, in one dimension, is

$$D_p \frac{\partial^2(\delta p_n)}{\partial x^2} - \mu_p \mathrm{E} \frac{\partial(\delta p_n)}{\partial x} + g' - \frac{\delta p_n}{\tau_{p0}} = \frac{\partial(\delta p_n)}{\partial t} \tag{8.8}$$

where $\delta p_n = p_n - p_{n0}$ is the excess minority carrier hole concentration and is the difference between the total and thermal equilibrium minority carrier concentrations. The ambipolar transport equation describes the behavior of excess carriers as a function of time and spatial coordinates.

In Chapter 5, we calculated drift current densities in a semiconductor. We determined that relatively large currents could bc created with fairly small electric fields. As a first approximation, we will assume that the electric field is zero in both the neutral p and n regions. In the n region for $x > x_n$, we have that E = 0 and g' = 0. If we alsoassume steady state so $\partial(\delta p_n)/\partial t = 0$, then Equation (8.8) reduces to

$$\frac{d^2(\delta p_n)}{dx^2} - \frac{\delta p_n}{L_p^2} = 0 \qquad (x > x_n) \tag{8.9}$$

where $L_p^2 = D_p \tau_{p0}$. For the same set of conditions, the excess minority carrier electron concentration in the p region is determined from

$$\frac{d^2(\delta n_p)}{dx^2} - \frac{\delta n_p}{L_n^2} = 0 \qquad (x < x_p) \tag{8.10}$$

The boundary conditions for the total minority carrier concentrations are

$$p_n(x_n) = p_{n0} \exp\left(\frac{eV_a}{kT}\right) \tag{8.11a}$$

$$n_p(-x_p) = n_{p0} \exp\left(\frac{eV_a}{kT}\right) \tag{8.11b}$$

$$p_n(x \to +\infty) = p_{n0} \tag{8.11c}$$

$$n_p(x \to -\infty) = n_{p0} \tag{8.11d}$$

As minority carriers diffuse from the space charge edge into the neutral semicondu tor regions, they will recombine with majority carriers. We will assume that th lengths W_n and W_p shown in Figure 8.3a are very long, meaning in particular tha $W_n \gg L_p$ and $W_p \gg L_n$. The excess minority carrier concentrations must approac zero at distances far from the space charge region. The structure is referred to as long pn junction.

The general solution to Equation (8.9) is

$$\delta p_n(x) = p_n(x) - p_{n0} = Ae^{x/L_p} + Be^{-x/L_p} \qquad (x \geq x_n) \tag{8.12}$$

and the general solution to Equation (8.10) is

$$\delta n_p(x) = n_p(x) - n_{p0} = Ce^{x/L_n} + De^{-x/L_n} \qquad (x \leq -x_p) \tag{8.13}$$

Applying the boundary conditions from Equations (8.11c) and (8.11d), the coefficients A and D must be zero. The coefficients B and C may be determined from the boundary conditions given by Equations (8.11a) and (8.11b). The excess carrier concentrations are then found to be, for $(x \geq x_n)$,

$$\delta p_n(x) = p_n(x) - p_{n0} = p_{n0}\left[\exp\Big) — \quad - 1\right] \exp (\text{"';}) — \tag{8.14}$$

and, for $(x \leq -x_p)$,

$$\delta n_p(x) = n_p(x) - n_{p0} = n_{p0}\left[\exp\left(\frac{eV_a}{kT}\right) - 1\right] \exp\left(\frac{x_p + x}{L_n}\right) \tag{8.15}$$

The minority carrier concentrations decay exponentially with distance away from the junction to their thermal-equilibrium values. Figure 8.5 shows these results. Again, we have assumed that both the n-region and the p-region lengths are long compared to the minority carrier diffusion lengths.

To review, a forward-bias voltage lowers the built-in potential barrier of a pn junction so that electrons from the n region are injected across the space charge region, creating excess minority carriers in the p region. These excess electrons begin diffusing into the bulk p region where they can recombine with majority carrier holes. The excess minority carrier electron concentration then decreases with distance from the junction. The same discussion applies to holes injected across the space charge region into the n region.

8.1.5 Ideal pn Junction Current

The approach we use to determine the current in a pn junction is based on the three parts of the fourth assumption stated earlier in this section. The total current in the junction is the sum of the individual electron and hole currents which are constant through the depletion region. Since the electron and hole currents are continuous functions through the pn junction, the total pn junction current will be the minority carrier hole diffusion current at $x = x_n$ plus the minority carrier electron diffusion current at $x = -x_p$. The gradients in the minority carrier concentrations, as shown in Figure 8.5, produce diffusion currents, and since we are assuming the electric field to be zero at the space charge edges, we can neglect any minority carrier drift current component. This approach in determining the pn junction current is shown in Figure 8.6.

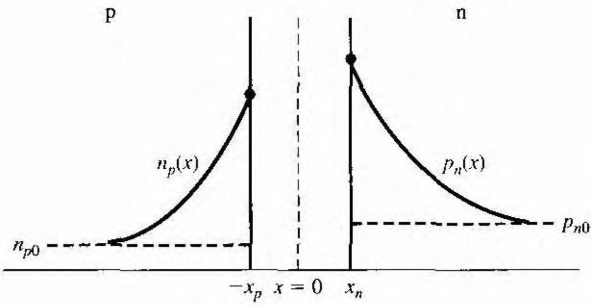

Figure 8.5 | Steady-state minority carrier concentrations in a pn junction under forward bias.

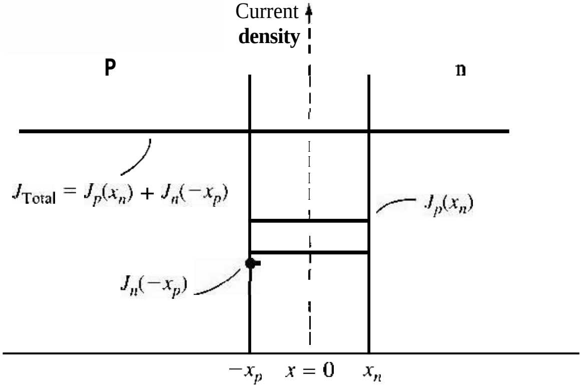

Figure 8.6 | Electron and hole current densities through the space charge region of a pn junction.

We can calculate the minority carrier hole diffusion current density at x = from the relation

$$J_p(x_n) = -eD_p \left.\frac{dp_n(x)}{dx}\right|_{x=x_n} \qquad \text{(8.1}$$

Since we are assuming uniformly doped regions, the thermal-equilibrium carr concentration is constant, so the hole diffusion current density may be written as

$$J_p(x_n) = -eD_p \left.\frac{d(\delta p_n(x))}{dx}\right|_{x=x_n} \qquad \text{(8.17}$$

Taking the derivative of Equation (8.14) and substituting into Equation (8.17). w obtain

$$\boxed{J_p(x_n) = \frac{eD_p p_{n0}}{L_p}\left[\exp\left(\frac{eV_a}{kT}\right) - 1\right]} \qquad \text{(8.}$$

The hole current density for this forward-bias condition is in the $+x$ direction, which is from the p to the n region.

Similarly, we may calculate the electron diffusion current density at $x = -x_p$ This may be written as

$$J_n(-x_p) = eD_n \left.\frac{d(\delta n_p(x))}{dx}\right|_{x=-x_p} \qquad \text{(8.19}$$

Using Equation (8.15). we obtain

$$\boxed{J_n(-x_p) = \frac{eD_n n_{p0}}{L_n}\left[\exp\left(\frac{eV_a}{kT}\right) - 1\right]} \qquad \text{(8 2}$$

The electron current density is also in the $+x$ direction.

An assumption we made at the beginning was that the individual electron and hole currents were continuous functions and constant through the space charge region The total current is the sum of the electron and hole currents and is constant throu the entire junction. Figure 8.6 again shows a plot of the magnitudes of these curren

The total current density in the pn junction is then

$$J = J_p(x_n) + J_n(-x_p) = \left[\frac{eD_p p_{n0}}{L_p} + \frac{eD_n n_{p0}}{L_n}\right]\left[\exp\left(\frac{eV_a}{kT}\right) - 1\right] \qquad \text{(8.21)}$$

Equation (8.21) is the ideal current–voltage relationship of a pn junction.

We may define a parameter J_s as

$$eD_p p_{n0} \qquad eD_n n_{p0} \qquad \text{(8.2}$$

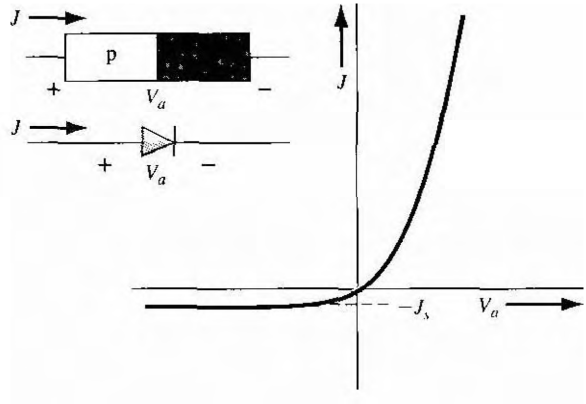

Figure 8.7 | Ideal I–V characteristic of a pn junction diode

so that Equadon (8.21) may he written as

$$\boxed{J = J_s\left[\exp\left(\frac{eV_a}{kT}\right) - 1\right]} \tag{8.23}$$

Equation (8.23), known as the ideal-diode equation, gives a good description of the current–voltage characteristics of the pn junction over a wide range of currents and voltages. Although Equation (8.23) was derived assuming a forward-bias voltage ($V_a > 0$), there is nothing to prevent V_a from being negative (reverse bias). Equation **(8.23)** is plotted in Figure 8.7 as a function of forward-bias voltage V_a. If the voltage V_a becomes negative (reverse bias) by a few kT/e V, then the reverse-bias current density becomes independent of the reverse-bias voltage. The parameter J_s is then referred to as the reverse saturation current density. The current–voltage characteristics of the pn junction diode are obviously not bilateral.

Objective | EXAMPLE 8.2

To determine the ideal reverse saturation current density in a silicon pn junction at T = 300 K.

Consider the following parameters in a silicon pn junction:

N„ $= N_d = 10^{16}$ cm^{-3} $\quad n_i = 1.5 \times 10^{10}$ cm^{-3}

$D_n = 25$ cm^2/s $\quad \tau_{p0} = \tau_{n0} = 5 \times 10^{-7}$ s

D„ $= 10$ cm^2/s $\quad \epsilon_r = 11.7$

■ Solution

The ideal reverse saturation current density is given by

$$J_s = \frac{eD_n n_{p0}}{L_n} + \frac{eD_p p_{n0}}{L_p}$$

which may be rewritten as

$$J_s = en_i^2\left[\frac{1}{N_a}\sqrt{\frac{D_n}{\tau_{n0}}} + \frac{1}{N_d}\sqrt{\frac{D_p}{\tau_{p0}}}\right]$$

Substituting the parameters, we obtain $J_s = 4.15 \times 10^{-11}$ Alcm^2

■ Comment

The ideal reverse-bias saturation current density is very small. If the pn junction cross-sectional area were $A = 10^{-4}$ cm^2, for example, then the ideal reverse-bias diode current would be $I_s = 4.15 \times 10^{-15}$ **A.**

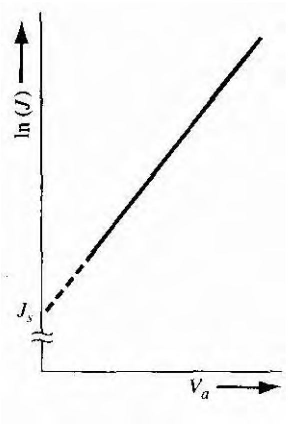

Figure 8.8 | Ideal *I–V* characteristic of *a* pn junction diode with the current plotted on a log scale.

If the forward-bias voltage in Equation (8.23) is positive by more than a few kT/e volts, then the (-1) term in Equation (8.23) becomes negligible. Figure 8.8 shows the forward-bias current–voltage characteristic when the current is plotted on a log scale. Ideally, this plot yields a straight line when V_a is greater than a few kT/e volts. The forward-bias current is an exponential function of the forward-bias voltage.

DESIGN EXAMPLE 8.3

Objective

To design a pn junction diode to produce particular electron and hole current densities at a given forward-bias voltage.

Consider a silicon pn junction diode at $T = 300$ K. Design the diode such that $J_n = 20$ A/cm^2 and $J_p = 5$ A/cm^2 at $V_a = 0.65$ *V*. Assume the remaining semiconductor parameters are as given in Example 8.2.

■ Solution

The electron diffusion current density is given by Equation (8.20) as

$$J_n = \frac{eD_n n_{p0}}{L_n}\left[\exp\left(\frac{eV_a}{kT}\right) - 1\right] = e\sqrt{\frac{D_n}{\tau_{n0}}}\cdot\frac{n_i^2}{N_a}\left[\exp\left(\frac{eV_a}{kT}\right) - 1\right]$$

Substituting the numbers, we have

$$20 = (1.6\times 10^{-19})\sqrt{\frac{25}{5\times 10^{-7}}}\cdot\frac{(1.5\times 10^{10})^2}{N_a}\left[\exp\left(\frac{0.65}{0.0259}\right) - 1\right]$$

which yields

$$N_a = 1.01\times 10^{15}\ \text{cm}^{-3}$$

The hole diffusion current density is given by Equation (8.18) as

$$J_p = \frac{eD_p p_{n0}}{L_p}\left[\exp\left(\frac{eV_a}{kT}\right) - 1\right] = e\sqrt{\frac{D_p}{\tau_{p0}}}\cdot\frac{n_i^2}{N_d}\left[\exp\left(\frac{eV_a}{kT}\right) - 1\right]$$

Substituting the numbers, we have

$$5 = (1.6\times 10^{-19})\sqrt{\frac{10}{5\times 10^{-7}}}\cdot\frac{(1.5\times 10^{10})^2}{N_d}\left[\exp\left(\frac{0.65}{0.0259}\right) - 1\right]$$

which yields

$$N_d = 2.55\times 10^{15}\ \text{cm}^{-3}$$

Comment

The relative magnitude of the electron and hole current densities through a diode can be varied by changing the doping concentrations in the device.

TEST YOUR UNDERSTANDING

E8.4 A silicon pn junction at T = 300 K has the following parameters: $N_a = 5\times 10^{16}\ \text{cm}^{-3}$, $N_d = 1\times 10^{16}\ \text{cm}^{-3}$, $D_n = 25\ \text{cm}^2/\text{s}$, $D_p = 10\ \text{cm}^2/\text{s}$, $\tau_{n0} = 5\times 10^{-7}$ s, and $\tau_{p0} = 1\times 10^{-7}$ s. The cross-sectional area is $A = 10^{-3}\ \text{cm}^2$ and the forward-bias voltage is $V_a = 0.625$ V. Calculate the (*a*) minority electron diffusion current at the space charge edge, (b) minority hole diffusion current at the space charge edge, and (*c*) total current in the pn junction diode. [Ans. (*a*) 0.154 mA, (*b*) 1.09 mA, (*c*) 1.24 mA]

E8.5 Repeat **E8.4** for a GaAs pn junction diode biased at $V_a = 1.10$ V. [Ans. (*a*) 0.204 mA, (*b*) 1.44 mA, (*c*) 1.65 mA]

8.1.6 Summary of Physics

We have been considering the case of a forward-bias voltage being applied to a pn junction. The forward-bias voltage lowers the potential barrier so that electrons and holes are injected across the space charge region. The injected carriers become minority carriers which then diffuse from the junction and recombine with majority carriers.

We calculated the minority carrier diffusion current densities at the edge of the space charge region. We can reconsider Equations (8.14) and (8.15) and determine the minority carrier diffusion current densities as a function of distance through the p- and n-regions. These results are

$$J_p(x) = \frac{eD_p p_{n0}}{L_p}\left[\exp\left(\frac{eV_a}{kT}\right) - 1\right]\exp\left(\frac{x_n - x}{L_p}\right) \qquad (x \ge x_n) \tag{8.24}$$

and

$$J_n(x) = \frac{eD_n n_{p0}}{L_n}\left[\exp\left(\frac{eV_a}{kT}\right) - 1\right]\exp\left(\frac{x_p + x}{L_n}\right) \qquad (x \le -x_p) \tag{8.25}$$

The minority carrier diffusion current densities decay exponentially in each region. However, the total current through the pn junction is constant. The difference between total current and minority carrier diffusion current is a majority carrier current. Figure 8.9 shows the various current components through the pn structure. The drift of majority carrier holes in the p region far from the junction, for example, is to supply holes that are being injected across the space charge region into the n region and also to supply holes that are lost by recombination with excess minority carrier electrons. The same discussion applies to the drift of electrons in the n region.

We have seen that excess carriers are created in a forward-biased pn junction. From the results of the ambipolar transport theory derived in Chapter 6, the behavior of the excess carriers is determined by the minority carrier parameters for low injection. In determining the current–voltage relationship of the pn junction, we consider the flow of minority carriers since we know the behavior and characteristics of these

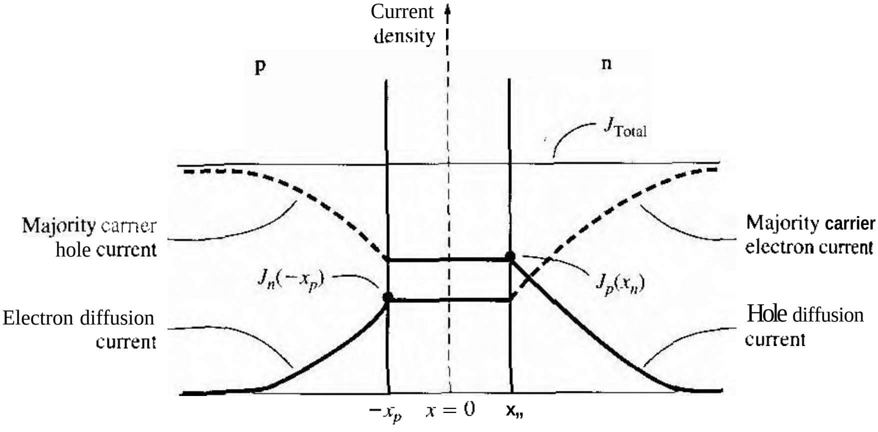

Figure 8.9 | Ideal electron and hole current components through a pn junction under forward bias.

particles. It may seem strange, at times, that we concern ourselves so much with minority carriers rather than with the vast number of majority carriers, but the reason for this can be found in the results derived from the ambipolar transport theory.

TEST YOUR UNDERSTANDING

E8.6 Consider the silicon pn junction diode described in E8.4. Calculate the electron and hole currents at (*a*) $x = x_n$, (*b*) $x = x_n + L_p$, and (*c*) $x = x_n + 10L_p$ (see Figure **8.9**).
[Ans. (*a*) $I_n = 0.154$ mA, $I_p = 1.09$ mA; (*b*) $I_n = 0.843$ mA, $I_p = 0.401$ mA; (*c*) $I_n = 1.244$ mA, $I_p \approx 0$]

The fact that we now have drift current densities in the p and n regions implies that the electric field in these regions is not zero as we had originally assumed. We can calculate the electric field in the neutral regions and determine the validity of our zero-field approximation.

Objective

EXAMPLE 8.4

To calculate the electric field required to produce a given majority carrier drift current.

Consider a silicon pn junction at T = 300 K with the parameters given in Example 8.2 and with an applied forward-bias voltage $V_a = 0.65$ V.

■ Solution

The total forward-bias current density is given by

$$J = J_s\left[\exp\left(\frac{eV}{kT}\right) - 1\right]$$

We determined the reverse saturation current density in Example 8.2, so we can write

$$J = (4.15 \times 10^{-11})\left[\exp\left(\frac{0.65}{0.0259}\right) - 1\right] = 3.29 \text{ A/cm}^2$$

The total current far from the junction in the n-region will be majority carrier electron drift current, so we can write

$$J = J_n \approx e\mu_n N_d \mathrm{E}$$

The doping concentration is $N_d = 10^{16}$ cm^{-3}, and, if we assume $\mu_n = 1350$ cm^2/V-s, then the electric field must be

$$\mathrm{E} = \frac{J_n}{e\mu_n N_d} = \frac{3.29}{(1.6 \times 10^{-19})(1350)(10^{16})} = 1.52 \text{ V/cm}$$

■ Comment

We assumed, in the derivation of the current–voltage equation, that the electric field in the neutral p and n regions was zero. Although the electric field is not zero, this example shows that the magnitude is very small—thus the approximation of zero electric field is **very** good.

8.1.7 Temperature Effects

The ideal reverse saturation current density J_s, given by Equation (8.22), is a functio of the thermal-equilibrium minority carrier concentrations n_{p0} and p_{n0}. These minority carrier concentrations are proportional to n_i^2, which is a very strong function of temperature. For a silicon pn junction, the ideal reverse saturation current density will increase by approximately a factor of four for every 10°C increase in temperature.

The forward-bias current-voltage relation was given by Equation (8.23). This relation includes J_s as well as the $\exp(eV_a/kT)$ factor, making the forward-bias current–voltage relation a function of temperature also. As temperature increases, less forward-bias voltage is required to obtain the same diode current. If the voltage is held constant, the diode current will increase as temperature increases. The change in forward-bias current with temperature is less sensitive than the reverse saturation current.

EXAMPLE 8.5

Objective

To determine the change in the forward-bias voltage on a pn junction with a change in temperature.

Consider a silicon pn junction initially biased at 0.60 V at T = 300 K. Assume the temperature increases to T = 310 K. Calculate the change in the forward-bias voltage required to maintain a constant current through the junction.

■ **Solution**

The forward-bias current can be written as follows:

$$J \propto \text{enp}\left(\frac{-E_g}{kT}\right)\exp\left(\frac{eV_a}{kT}\right)$$

If the temperature changes, we may take the ratio of the diode currents at the two temperatures. This ratio is

$$\frac{J_2}{J_1} = \frac{\exp(-E_g/kT_2)\exp(eV_{a2}/kT_2)}{\exp(-E_g/kT_1)\exp(eV_{a1}/kT_1)}$$

If current is to be held constant, then $J_1 = J_2$ and we must have

$$\frac{E_g - eV_{a2}}{kT_2} = \frac{E_g - eV_{a1}}{kT_1}$$

Let $T_1 = 300$ K, $T_2 = 310$ K, $E_g = 1.12$ eV, and $V_{a1} = 0.60$ V. Then, solving for V_{a2}, we obtain $V_{a2} = 0.5827$ V.

■ **Comment**

The change in the forward-bias voltage is −17.3 mV for a 10°C temperature change.

8.1.8 The "Short" Diode

We assumed in the previous analysis that both p and n regions were long compared with the minority carrier diffusion lengths. In many pn junction structures, one region

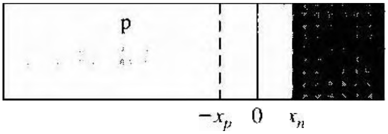

Figure 8.10 | Geometry of a "short" diode.

may, in fact, be short compared with the minority carrier diffusion length. Figure 8.10 shows one such example: the length W_n is assumed to be much smaller than the minority carrier hole diffusion length, L_p.

The steady-state excess minority carrier hole concentration in the n region is determined from Equation (8.9), which was given as

$$\frac{d^2(\delta p_n)}{dx^2} - \frac{\delta p_n}{L_p^2} = 0$$

The original boundary condition at $x = x_n$ still applies, given by Equation (8.11a) as

$$p_n(x_n) = p_{n0} \exp\left(\frac{eV_a}{kT}\right)$$

A second boundary condition needs to be determined. In many cases we will assume that an ohmic contact exists at $x = (x_n + W_n)$, implying an infinite surface-recombination velocity and therefore an excess minority carrier concentration of zero. The second boundary condition is then written as

$$p_n(x = x_n + W_n) = p_{n0} \tag{8.26}$$

The general solution to Equation (8.9) is again given by Equation (8.12), which was

$$\delta p_n(x) = p_n(x) - p_{n0} = Ae^{x/L_p} + Be^{-x/L_p} \qquad (x \geq x_n)$$

In this case, because of the finite length of the n region, both terms of the general solution must be retained. Applying the boundary conditions of Equations (8.11b) and (8.26), the excess minority carrier concentration is given by

$$\delta p_n(x) = p_{n0}\left[\exp\left(\frac{eV_a}{kT}\right) - 1\right] \frac{\sinh\left[(x_n + W_n - x)/L_p\right]}{\sinh\left[W_n/L_p\right]} \tag{8.27}$$

Equation (8.27) is the general solution for the excess minority carrier hole concentration in the n region of a forward-biased pn junction. If $W_n \gg L_p$ the assumption for the long diode, Equation (8.27) reduces to the previous result given by Equation (8.14). If $W_n \ll L_p$, we can approximate the hyperbolic sine terms by

$$\sinh\left(\frac{x_n + W_n - x}{L_p}\right) \approx \left(\frac{x_n + W_n - x}{L_p}\right) \tag{8.28a}$$

and

$$\sinh\left(\frac{W_n}{L_p}\right) \approx \left(\frac{W_n}{L_p}\right) \qquad (8.28b$$

Then Equation (8.27) becomes

$$\delta p_n(x) = p_{n0}\left[\exp(\%) - 1\right]\left(\frac{x_n + W_n - a}{W_n}\right) \qquad (8.29$$

The minority carrier concentration becomes a linear function of distance

The minority carrier hole diffusion current density is given by

$$J_p = -eD_p\frac{d(\delta p_n(x))}{dx}$$

so that in the short n region, we have

$$J_p(x) = \frac{eD_p p_{n0}}{W_n}\left[\exp\left(\frac{eV_a}{kT}\right) - 1\right] \qquad (8.30$$

The minority carrier hole diffusion current density now contains the length W„ in th denominator. rather than the diffusion length L,,. The diffusion current density is larger for a short diode than for a long diode since W„ $\ll L_p$. In addition, since the minority carrier concentration is approximately a linear function of distance through the n region, the minority carrier diffusion current density is a constant. This constant current implies that there is no recombination of minority carriers in the short region.

TEST YOUR UNDERSTANDING

E8.7 Consider the silicon pn junction diode described in ER.4. The p region is long and the n region is short with W„ $= 2\ \mu$m. *(a)* Calculate the electron and hole currents in the depletion region. *(b)* Why has the hole current increased compared to that found in E8.4?

[Ans. *(a)* $I_n = 0.154$ mA, $I_p = 5.44$ mA; *(b)* the hole density gradient has increased]

8.2 | SMALL-SIGNAL MODEL OF THE pn JUNCTION

We have been considering the dc characteristics of the pn junction diode. When semiconductor devices with pn junctions are used in linear amplifier circuits, for example, sinusoidal signals are superimposed on the dc currents and voltages, so that the small-signal characteristics of the pn junction become important.

8.2.1 Diffusion Resistance

The ideal current–voltage relationship of the pn junction diode was given by Equation (8.23), where J and J_s are current densities. If we multiply both sides of the

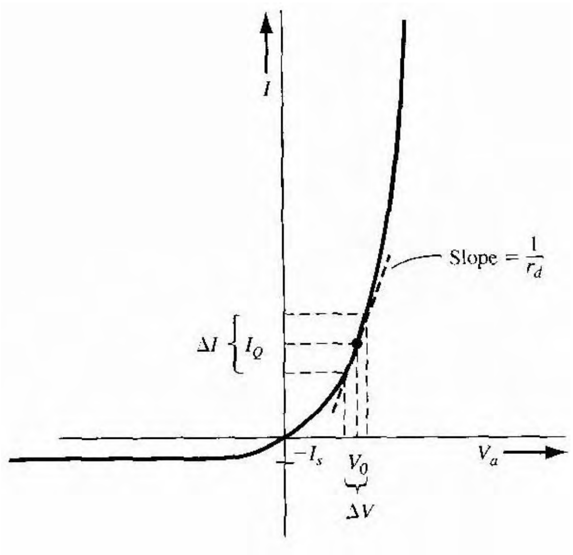

Figure 8.11 | Curve showing the concept of the small-signal diffusion resistance.

equation by the junction cross-sectional area, we have

$$I_D = I_s\left[\exp\left(\frac{eV_a}{kT}\right) - 1\right] \tag{8.31}$$

where I_D is the diode current and I_s is the diode reverse saturation current.

Assume that the diode is forward-biased with a dc voltage V_0 producing a dc diode current I_{DQ}. If we now superimposes small, low-frequency sinusoidal voltage as shown in Figure 8.11, then a small sinusoidal current will be produced, superimposed on the dc current. The ratio of sinusoidal current to sinusoidal voltage is called the incremental conductance. In the limit of a very small sinusoidal current and voltage, the small-signal incremental conductance is just the slope of the dc current-voltage curve, or

$$g_d = \left.\frac{dI_D}{dV_a}\right|_{V_a=V_0} \tag{8.32}$$

The reciprocal of the incremental conductance is the incremental resistance, defined as

$$r_d = \left.\frac{dV_a}{dI_D}\right|_{I_D=I_{DQ}} \tag{8.33}$$

where I_{DQ} is the dc quiescent diode current.

If we assume that the diode is biased sufficiently far in the forward-bias region, then the (-1) term can be neglected and the incremental conductance becomes

$$g_d = \left.\frac{dI_D}{dV_a}\right|_{V_a=V_0} = \left(\frac{e}{kT}\right) I_s \exp\left(\frac{eV_0}{kT}\right) \approx \frac{I_{DQ}}{V_t} \tag{8.34}$$

The small-signal incremental resistance is then the reciprocal function, or

$$\boxed{r_d = \frac{V_t}{I_{DQ}}} \tag{8.35}$$

The incremental resistance decreases as the bias current increases, and is inversely proportional to the slope of the I–V characteristic as shown in Figure 8.11. The incremental resistance is also known as the ***diffusion resistance.***

8.2.2 Small-Signal Admittance

In the last chapter, we considered the pn junction capacitance as a function of the reverse-bias voltage. When the pn junction diode is forward-hiased, another capacitance becomes a factor in the diode admittance. The small-signal admittance, or impedance, of the pn junction under forward bias is derived using the minority carrie diffusion current relations we have already considered.

Qualitative Analysis Before we delve into the mathematical analysis, we can qualitatively understand the physical processes that lead to a diffusion capacitance, whi is one component of the junction admittance. Figure 8.12a schematically shows pn junction forward biased with a dc voltage. A small ac voltage is also superimposed on the dc voltage so that the total forward-biased voltage can he written as $V_a = V_{dc} + \hat{v}\sin\omega t$.

As the voltage across the junction changes, the number of holes injected across the space charge region into the n region also changes. Figure 8.12b shows the hole concentration at the space charge edge as a function of time. At $t = t_0$, the ac voltage

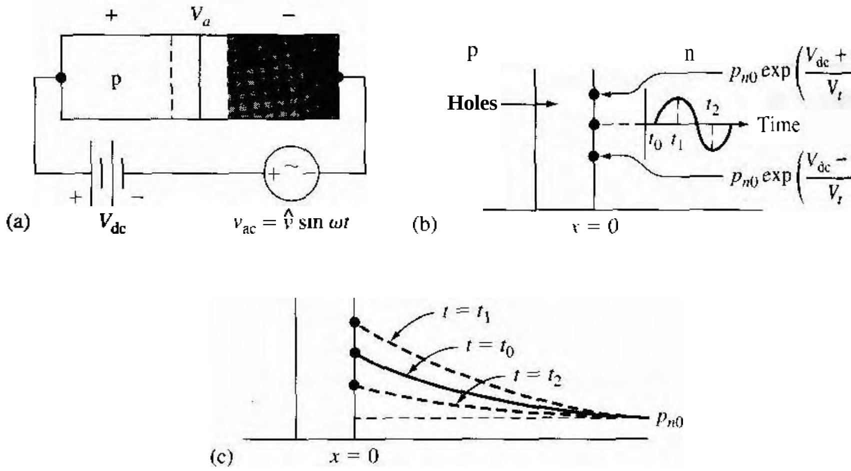

+
V_a
−
p
(a)
+
−
V_{dc}
$v_{ac} = \hat{v}\sin\omega t$
(b)
p
n
Holes
$p_{n0}\exp\left(\frac{V_{dc}+}{V_t}\right.$
t_2
Time
t_0 t_1
$p_{n0}\exp\left(\frac{V_{dc}-}{V_t}\right.$
$x = 0$
$t = t_1$
$t = t_0$
$t = t_2$
p_{n0}
(c)
$x = 0$

Figure 8.12 | (a) A pn junction with an ac voltage superimposed on a forward-biased dc value; (b) the hole concentration versus time at the space charge edge; (c) the hole concentration versus distance in then region at three different times.

is zero so that the concentration of holes at $x = 0$ is just given by $p_n(0) = p_{n0} \exp(V_{dc}/V_t)$, which is what we have seen previously.

Now, as the ac voltage increases during its positive half cycle, the concentration of holes at $x = 0$ will increase and reach a peak value at $t = t_1$, which corresponds to the peak value of the ac voltage. When the ac voltage is on its negative half cycle, the total voltage across the junction decreases so that the concentration of holes at $x = 0$ decreases. The concentration reaches a minimum value at $t = t_2$, which corresponds to the time that the ac voltage reaches its maximum negative value. The minority carrier hole concentration at $x = 0$, then, has an ac component superimposed on the dc value as indicated in Figure 8.12b.

As previously discussed, the holes at the space charge edge ($x = 0$) diffuse into the n region where they recombine with the majority carrier electrons. We will assume that the period of the ac voltage is large compared to the time it takes carriers to diffuse into the n region. The hole concentration as a function of distance into the n region can then be treated as a steady-state distribution. Figure 8.12c shows the steady-state hole concentrations at three different times. At $t = t_0$, the ac voltage is zero, so the $t = t_0$ curve corresponds to the hole distribution established by the dc voltage. The $t = t_1$ curve corresponds to the distribution established when the ac voltage has reached its peak positive value, and the $t = t_2$ curve corresponds to the distribution established when the ac voltage has reached its maximum negative value. The shaded areas represents the charge ΔQ that is alternately charged and discharged during the ac voltage cycle.

Exactly the same process is occurring in the p region with the electron concentration. The mechanism of charging and discharging of holes in the n region and electrons in the p region leads to a capacitance. This capacitance is called *diffusion capacitance*. The physical mechanism of this diffusion capacitance is different from that of the junction capacitance discussed in the last chapter. We will show that the magnitude of the diffusion capacitance in a forward-biased pn junction is usually substantially larger than the junction capacitance.

Mathematical Analysis The minority carrier distribution in the pn junction will be derived for the case when a small sinusoidal voltage is superimposed on the dc junction voltage. We can then determine small signal, or ac, diffusion currents from these minority carrier functions. Figure 8.13 shows the minority carrier distribution in a pn junction when a forward-biased dc voltage is applied. The origin, $x = 0$, is set at the edge of the space charge region on the n-side for convenience. The minority carrier hole concentration at $x = 0$ is given by Equation (8.7) as $p_n(0) = p_{n0} \exp(eV_a/kT)$, where V_a is the applied voltage across the junction.

Now let

$$V_a = V_0 + v_1(t) \tag{8.36}$$

where V_0 is the dc quiescent bias voltage and $v_1(t)$ is the ac signal voltage which is superimposed on this dc level. We may now write

$$p_n(x = 0) = p_{n0} \exp\left[\frac{e(V_0 + v_1(t))}{kT}\right] = p_n(0, t) \tag{8.37}$$

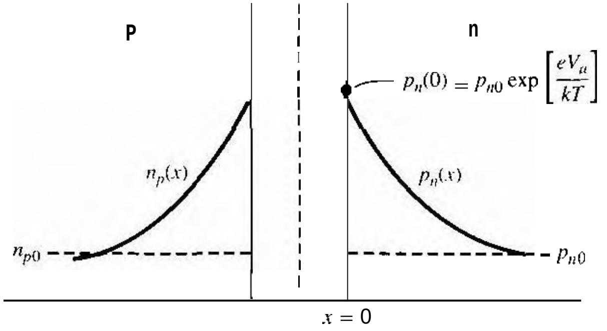

Figure 8.13 | The dc characteristics of a forward-biased pn junction used in the small-signal admittance calculations.

Equation (8.37) may be written as

$$p_n(0, t) = p_{\text{dc}} \exp\left(\frac{ev_1(t)}{kT}\right) \tag{8.38}$$

where

$$p_{\text{dc}} = p_{n0} \exp\left(\frac{eV_0}{kT}\right) \tag{8.39}$$

If we assume that $|v_1(t)| \ll (kT/e) = V_t$, then the exponential term in Equation (8.38) may be expanded into a Taylor series retaining only the linear terms, the minority carrier hole concentration at $x = 0$ can be written as

$$p_n(0, t) \approx p_{\text{dc}} \left(1 + \frac{v_1(t)}{V_t}\right) \tag{8.}$$

If we assume that the time-varying voltage $v_1(t)$ is a sinusoidal signal, we can write Equation (8.40) as

$$p_n(0, t) = p_{\text{dc}}\left(1 + \frac{\hat{V}_1}{V_t}\, e^{j\omega t}\right) \tag{8.4}$$

where $\hat{V}_1$ is the phasor of the applied sinusoidal voltage. Equation (8.41) will be used as the boundary condition in the solution of the time-dependent diffusion equation for the minority carrier holes in the n region.

In the neutral n region $(x > 0)$, the electric field is assumed to be zero, thus the behavior of the excess minority carrier holes is determined from the equation

$$D_p \frac{\partial^2(\delta p_n)}{\partial x^2} - \frac{\delta p_n}{\tau_{p0}} = \frac{\partial(\delta p_n)}{\partial t} \tag{8.42}$$

where δp_n is the excess hole concentration in the n region. We are assuming that the ac signal voltage $v_1(t)$ is sinusoidal. We then expect the steady-state solution for δp_n to be of the form of a sinusoidal solution superimposed on the dc solution, or

$$\delta p_n(x, t) = \delta p_0(x) + p_1(x) e^{j\omega t} \tag{8.43}$$

where $\delta p_0(x)$ is the dc excess carrier concentration and $p_1(x)$ is the magnitude of the ac component of the excess carrier concentration. The expression for $\delta p_0(x)$ is the same as that given in Equation (8.14).

Substituting Equation (8.43) into the differential Equation (8.42), we obtain

$$D_p\left[\frac{\partial^2(\delta p_0(x))}{\partial x^2} + \frac{\partial^2 p_1(x)}{\partial x^2}e^{j\omega t}\right] - \frac{\delta p_0(x) + p_1(x)\,e^{j\omega t}}{\tau_{p0}} = j\omega p_1(x)\,e^{j\omega t} \qquad (8.44)$$

We may rewrite this equation, combining the time-dependent and time-independent terms, as

$$\left[D_p\frac{\partial^2(\delta p_0(x))}{\partial x^2} - \frac{\delta p_0(x)}{\tau_{p0}}\right] + \left[D_p\frac{\partial^2 p_1(x)}{\partial x^2} - \frac{p_1(x)}{\tau_{p0}} - j\omega p_1(x)\right]e^{j\omega t} = 0 \qquad (8.45)$$

If the ac component, $p_1(x)$, is zero, then the first bracketed term is just the differential Equation (8.10). which is identically zero. Then we have. from the second bracketed term.

$$D_p\frac{d^2 p_1(x)}{dx^2} - \frac{p_1(x)}{\tau_{p0}} - j\omega p_1(x) = 0 \qquad (8.46)$$

Noting that L , = $D_p\tau_{p0}$. Equation (8.46) may be rewritten in the form

$$\frac{d^2 p_1(x)}{dx^2} - \frac{(1 + j\omega\tau_{p0})}{L_p^2}p_1(x) = 0 \qquad (8.47)$$

$$\frac{d^2 p_1(x)}{dx^2} - C_p^2 p_1(x) = 0 \qquad (8.48)$$

where

$$C_p^2 = \frac{(1 + j\omega\tau_{p0})}{L_p^2} \qquad (8.49)$$

The general solution to Equation (8.48) is

$$p_1(x) = K_1 e^{-C_p x} + K_2 e^{+C_p x} \qquad (8.50)$$

One boundary condition is that $p_1(x \to +\infty) = 0$, which implies that the coefficient K; $= 0$. Then

$$p_1(x) = K_1 e^{-C_p x} \qquad (8.51)$$

Applying the boundary condition at $x = 0$ from Equation (8.41) we obtain

$$p_1(0) = K_1 = p_{dc}\left(\frac{\hat{V}_1}{V_t}\right) \qquad (8.52)$$

The hole diffusion current density can he calculated at $x = 0$. This will be given by

$$J_p = -eD_p \frac{\partial p_n}{\partial x}\bigg|_{x=0} \tag{8.53}$$

If we consider a homogeneous semiconductor, the derivative of the hole concentration will be just the derivative of the excess hole concentration. Then

$$J_p = -eD_p \frac{\partial(\delta p_n)}{\partial x}\bigg|_{x=0} = -eD_p \frac{\partial(\delta p_0(x))}{\partial x}\bigg|_{x=0} - eD_p \frac{\partial p_1(x)}{\partial x}\bigg|_{x=0} e^{j\omega t} \tag{8.54}$$

We can write this equation in the form

$$J_p = J_{p0} + j_p(t) \tag{8.55}$$

where

$$J_{p0} = -eD_p \frac{\partial(\delta p_0(x))}{\partial x}\bigg|_{x=0} = \frac{eD_p p_{n0}}{L_p}\left[\exp\left(\frac{eV_0}{kT}\right) - 1\right] \tag{8.56}$$

Equation (8.56) is the dc component of the hole diffusion current density and is exactly the same as in the ideal *I–V* relation derived previously.

The sinusoidal component of the diffusion current density is then found from

$$j_p(t) = \hat{J}_p e^{j\omega t} = -eD_p \frac{\partial p_1(x)}{\partial x} e^{j\omega t}\bigg|_{x=0} \tag{8.57}$$

where $\hat{J}_p$ is the current density phasor. Combining Equations (8.57). (8.51), and (8.52), we have

$$\hat{J}_p = -eD_p(-C_p)\left[p_{dc}\left(\frac{\hat{V}_1}{V_t}\right)\right]e^{-C_p x}\bigg|_{x=0} \tag{8.58}$$

We can write the total ac hole current phasor as

$$\hat{I}_p = A\hat{J}_p = eAD_p C_p p_{dc}\left(\frac{\hat{V}_1}{V_t}\right) \tag{8.59}$$

where A is the cross-sectional area of the pn junction. Substituting the expression for C,,, we obtain

$$\hat{I}_p = \frac{eAD_p p_{dc}}{L_p}\sqrt{1 + j\omega\tau_{p0}}\left(\frac{\hat{V}_1}{V_t}\right) \tag{8.60}$$

If we define

$$I_{p0} = \frac{eAD_p p_{dc}}{L_p} = \frac{eAD_p p_{n0}}{L_p}\exp\left(\frac{eV_0}{kT}\right) \tag{8.61}$$

then Equation (8.60) becomes

$$\hat{I}_p = I_{p0}\sqrt{1 + j\omega\tau_{p0}}\left(\frac{\hat{V}_1}{V_t}\right) \tag{8.62}$$

We can go through the same type of analysis for the minority carrier electrons in the p region. We will obtain

$$\hat{I}_n = I_{n0}\sqrt{1 + j\omega\tau_{n0}}\left(\frac{\hat{V}_1}{V_t}\right) \tag{8.63}$$

where

$$I_{n0} = \frac{eAD_n n_{p0}}{L_n} \exp\left(\frac{eV_0}{kT}\right) \tag{8.64}$$

The total ac current phasor is the sum of $\hat{I}_p$ and $\hat{I}_n$. The pn junction admittance is the total ac current phasor divided by the ac voltage phasor, or

$$Y = \frac{\hat{I}}{\hat{V}_1} = \frac{\hat{I}_p + \hat{I}_n}{\hat{V}_1} = \left(\frac{1}{V_t}\right)\left[I_{p0}\sqrt{1 + j\omega\tau_{p0}} + I_{n0}\sqrt{1 + j\omega\tau_{n0}}\right] \tag{8.65}$$

There is not a linear, lumped, finite, passive, bilateral network that can be synthesized to give this admittance function. However, we may make the following approximations. Assume that

$$\omega\tau_{p0} \ll 1 \tag{8.66a}$$

and

$$\omega\tau_{n0} \ll 1 \tag{8.66b}$$

These two assumptions imply that the frequency of the ac signal is not too large. Then we may write

$$\sqrt{1 + j\omega\tau_{p0}} \approx 1 + \frac{j\omega\tau_{p0}}{2} \tag{8.67a}$$

and

$$\sqrt{1 + j\omega\tau_{n0}} \approx 1 + \frac{j\omega\tau_{n0}}{2} \tag{8.67b}$$

Substituting Equations (8.67a) and (8.67b) into the admittance Equation (8.65) yields

$$Y = \left(\frac{1}{V_t}\right)\left[I_{p0}\left(1 + \frac{j\omega\tau_{p0}}{2}\right) + I_{n0}\left(1 + \frac{j\omega\tau_{n0}}{2}\right)\right] \tag{8.68}$$

If we combine the real and imaginary portions, we get

$$Y = \left(\frac{1}{V_t}\right)(I_{p0} + I_{n0}) + j\omega\left\{\left(\frac{1}{2V_t}\right)[I_{p0}\tau_{p0} + I_{n0}\tau_{n0}]\right\} \tag{8.69}$$

Equation (8.69) may be written in the form

$$Y = g_d + j\omega C_d \tag{8.70}$$

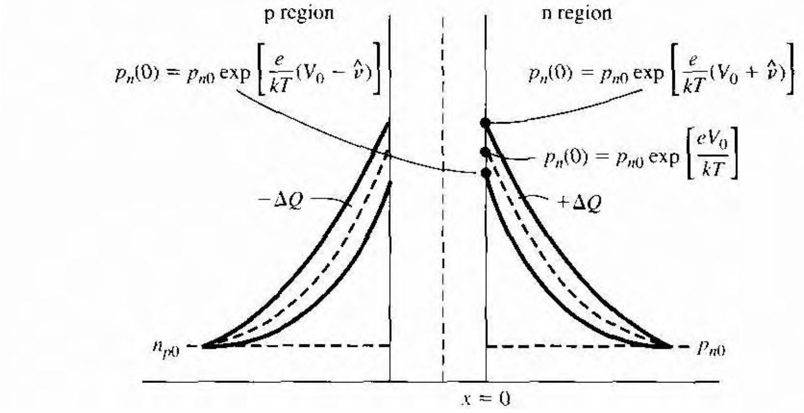
p region
n region
$p_n(0) = p_{n0} \exp\left[\frac{e}{kT}(V_0 - \hat{v})\right]$
$p_n(0) = p_{n0} \exp\left[\frac{e}{kT}(V_0 + \hat{v})\right]$
$p_n(0) = p_{n0} \exp\left[\frac{eV_0}{kT}\right]$
$-\Delta Q$
$+\Delta Q$
n_{p0}
p_{n0}
$x = 0$

Figure 8.14 | Minority carrier concentration changes with changing forward-bias voltage.

The parameter g_d is called the *diffusion conductance* and is given by

$$g_d = \left(\frac{1}{V_t}\right)(I_{p0} + I_{n0}) = \frac{I_{DQ}}{V_t} \tag{8.71}$$

where I_{DQ} is the dc bias current. Equation (8.71) is exactly the same conductance as we obtained previously in Equation (8.34). The parameter C_d is called the ***diffusion capacitance*** and is given by

$$\boxed{C_d = \left(\frac{1}{2V_t}\right)(I_{p0}\tau_{p0} + I_{n0}\tau_{n0})} \tag{8.72}$$

The physics of the diffusion capacitance may be seen in Figure 8.14. The dc values of the minority carrier concentrations are shown along with the changes due to the ac component of voltage. The A Q charge is alternately being charged and discharged through the junction as the voltage across the junction changes. The change in the stored minority carrier charge as a function of the change in voltage is the diffusion capacitance. One consequence of the approximations $\omega\tau_{p0} \ll$ I and $\omega\tau_{n0} \ll 1$ is that there are no "wiggles" in the minority carrier curves. The sinusoidal frequency is low enough so that the exponential curves are maintained at all times.

EXAMPLE 8.6

Objective

To calculate the small-signal admittance of a pn junction diode.

This example is intended to give an indication of the magnitude of the diffusion capacitance as compared with the junction capacitance considered in the last chapter. The diffusion resistance will also be calculated. Assume that $N_a \gg N_d$ so that $p_{n0} \gg n_{p0}$. This assumption implies that I,,,, $\gg I_{n0}$. Let $T = 300$ K, $\tau_{p0} = 10^{-7}$ s, and I,,,, $= I_{DQ} = 1$ mA.

Solution

The diffusion capacitance, with these assumptions, is given by

$$C_d \approx \left(\frac{1}{2V_t}\right)(I_{p0}\tau_{p0}) = \frac{1}{(2)(0.0259)}(10^{-3})(10^{-7}) = 1.93 \times 10^{-9} \text{ F}$$

The diffusion resistance is

$$r_d = \frac{V_t}{I_{DQ}} = \frac{0.0259 \text{ V}}{1 \text{ mA}} = 25.9 \ \Omega$$

Comment

The value of 1.93 nF for the diffusion capacitance of a forward-biased pn junction is 3 to 4 orders of magnitude larger than the junction capacitance of the reverse-biased pn junction, which we calculated in Example 7.5.

The diffusion capacitance tends to dominate the capacitance terms in a forward-biased pn junction. The small-signal diffusion resistance can be fairly small if the diode current is a fairly large value. As the diode current decreases, the diffusion resistance increases. We will consider the impedance of forward-biased pn junctions again when we discuss bipolar transistors.

TEST YOUR UNDERSTANDING

E8.8 A silicon pn junction diode at T = 300 K has the Following parameters: $N_d = 8 \times 10^{16}$ cm^{-3}, $N_a = 2 \times 10^{15}$ cm^{-3}, $D_n = 25$ cm^2/s, $D_p = 10$ cm^2/s, $\tau_{n0} = 5 \times 10^{-7}$ s, and $\tau_{p0} = 10^{-7}$ s. The cross-sectional area is $A = 10^{-3}$ cm^2. Determine the diffusion resistance and diffusion capacitance if the diode is forward biased at (*a*) $V_a = 0.550$ V and (*b*) $V_a = 0.610$ V.
[Ans. (*a*) $r_d = 118 \ \Omega$, $C_d = 2.07$ nF; (*b*) $r_d = 11.6 \ \Omega$, $C_d = 20.9$ nF]

E8.9 A GaAs pn junction diode at T = 300 K has the same parameters given in E8.8 except thet $D_n = 207$ cm^2/s and $D_p = 9.80$ cm^2/s. Determine the diffusion resistance and diffusion capacitance if the diode is forward biased at (*a*) $V_a = 0.970$ V and (b) $V_a = 1.045$ V. [Ans. (*a*) $r_d = 263 \ \Omega$, $C_d = 0.940$ nF; (*b*) $r_d = 14.6 \ \Omega$, $C_d = 17.0$ nF]

8.2.3 Equivalent Circuit

The small-signal equivalent circuit of the forward-biased pn junction is derived from Equation (8.70). This circuit is shown in Figure 8.15a. We need to add the junction capacitance, which will be in parallel with the diffusion resistance and diffusion capacitance. The last element we add, to complete the equivalent circuit, is a series resistance. The neutral n and p regions have finite resistances so the actual pn junction will include a series resistance. The complete equivalent circuit is given in Figure 8.15b.

The voltage across the actual junction is V_a and the total voltage applied to the pn diode is given by V_{app}. The junction voltage V_a is the voltage in the ideal

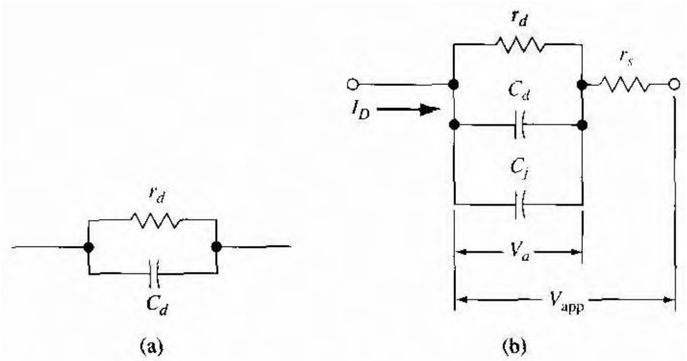

Figure 8.15 | (a) Small-signal equivalent circuit of ideal forward-biased pn junction diode; (b) Complete small-signal equivalent circuit of pn junction.

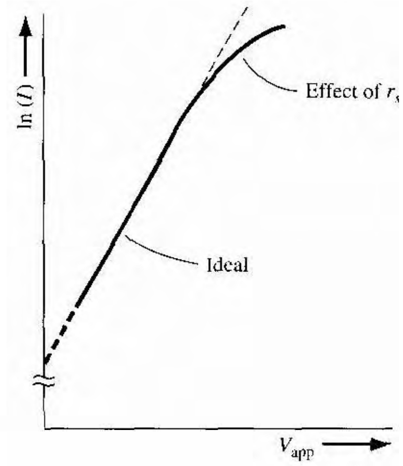

Figure 8.16 | Forward-biased I–V characteristics of a pn junction diode showing the effect of series resistance.

current–voltage expression. We can write the expression

$$V_{app} = V_a + Ir_s \tag{8.73}$$

Figure 8.16 is a plot of the current–voltage characteristic from Equation (8.73) showing the effect of the series resistance. A larger applied voltage is required to achieve the same current value when a series resistance is included. In most diodes, the series resistance will be negligible. In some semiconductor devices with pn junctions, however, the series resistance will be in a feedback loop: in these cases, the resistance is multiplied by a gain factor and becomes non-negligible.

TEST YOUR UNDERSTANDING

E8.10 A silicon pn junction diode at $T = 300$ K has the same parameters as those described in E8.8. The neutral n-region and neutral p-region lengths are 0.01 cm. Estimate the series resistance of the diode (neglect ohmic contacts). (Ans. $R = 66\ \Omega$)

8.3 | GENERATION–RECOMBINATION CURRENTS

In the derivation of the ideal current–voltage relationship, we neglected any effects occurring within the space charge region. Since other current components are generated within the space charge region, the actual *I–V* characteristics of a pn junction diode deviate from the ideal expression. The additional currents are generated from the recombination processes discussed in Chapter 6.

The recombination rate of excess electrons and holes, given by the Shockley–Read–Hall recombination theory, was written as

$$R = \frac{C_n C_p N_t (np - n_i^2)}{C_n(n + n') + C_p(p + p')} \tag{8.74}$$

The parameters n and p are, as usual. the concentrations of electrons and holes, respectively.

8.3.1 Reverse-Bias Generation Current

For a pn junction under reverse bias, we have argued that the mobile electrons and holes have essentially been swept out of the space charge region. Accordingly, within the space charge region, $n \approx p \approx 0$. The recombination rate from Equation (8.74) becomes

$$R = \frac{-C_n C_p N_t n_i^2}{C_n n' + C_p p'} \tag{8.75}$$

The negative sign implies a negative recombination rate; hence, we are really generating electron–hole pairs within the reverse-biased space charge region. The recombination of excess electrons and holes is the process whereby we are trying to reestablish thermal equilibrium. Since the concentration of electrons and holes is essentially zero within the reverse-biased space charge region. electrons and holes are being generated via the trap level to also try to reestablish thermal equilibrium. This generation process is schematically shown in Figure 8.17. As the electrons and holes are generated. they are swept out of the space charge region by the electric field. The flow of charge is in the direction of a reverse-bias current. This reverse-bias *generation current*, caused by the generation of electrons and holes in the space charge region. is in addition to the ideal reverse-bias saturation current.

We may calculate the density of the reverse-bias generation current by considering Equation (8.75). If we make a simplifying assumption and let the trap level be at the intrinsic Fermi level, then from Equations (6.92) and (6.97), we have that $n' = n_i$

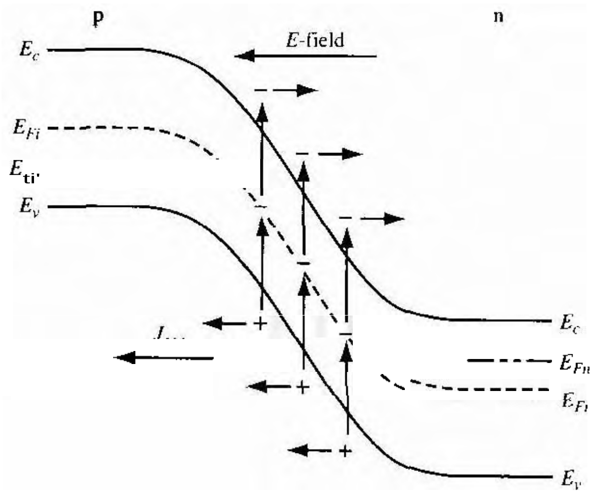

Figure 8.17 | Generation process in a reverse-biased pn junction.

and $p' = n_i$. Equation (8.75) now becomes

$$R = \frac{-n_i}{\dfrac{1}{N_t C_p} + \dfrac{1}{N_t C_n}} \tag{8.76}$$

Using the definitions of lifetimes from Equations (6.101) and (6.104), we may write Equation (8.76) as

$$R = \frac{-n_i}{\tau_{p0} + \tau_{n0}} \tag{8.77}$$

If we define a new lifetime as the average of τ_{p0} and τ_{n0}, or

$$\tau_0 = \frac{\tau_{p0} + \tau_{n0}}{2} \tag{8.78}$$

then the recombination rate can be written as

$$R = \frac{-n_i}{2\tau_0} \equiv -G \tag{8.79}$$

The negative recombination rate implies a generation rate, so G is the generation rate of electrons and holes in the space charge region.

The generation current density may be determined from

$$J_{\text{gen}} = \int_0^W eG\,dx \tag{8.80}$$

where the integral is over the space charge region. If we assume that the generation rate is constant throughout the space charge region, then we obtain

$$\boxed{J_{\text{gen}} = \frac{en_i W}{2\tau_0}} \tag{8.81}$$

The total reverse-bias current density is the sum of the ideal reverse saturation current density and the generation current density, or

$$J_R = J_s + J_{\text{gen}} \tag{8.82}$$

The ideal reverse saturation current density J_s is independent of the reverse-bias voltage. However, J_{gen} is a function of the depletion width W, which in turn is a function of the reverse-bias voltage. The actual reverse-bias current density, then, is no longer independent of the reverse-bias voltage.

EXAMPLE 8.7

Objective

To determine the relative magnitudes of the ideal reverse saturation current density and the generation current density in a silicon pn junction at T = 300 K.

Consider the silicon *pn* junction described in Example 8.2 and let $\tau_0 = \tau_{p0} = \tau_{n0} = 5 \times 10^{-7}$ s.

■ Solution

The ideal reverse saturation current density was calculated in Example 8.2 and was found to be $J_s = 4.15 \times 10^{-11}$ A/cm². The generation current density is again given by Equation (8.81) as

$$J_{\text{gen}} = \frac{en_i W}{2\tau_0}$$

and the depletion width is given by

$$W = \left\{\frac{2\epsilon_s}{e}\left(\frac{N_a + N_d}{N_a N_d}\right)(V_{bi} + V_R)\right\}^{1/2}$$

If we assume, for example, that $V_{bi} + V_R = 5$ V, then using the parameters given in Example 8.2 we find that $W = 1.14 \times 10^{-4}$ cm, and then calculate the generation current density to be

$$J_{\text{gen}} = 2.74 \times 10^{-7} \text{ A/cm}^2$$

■ Comment

Comparing the solutions for the two current densities, it is obvious that, for the silicon pn junction diode at room temperature, the generation current density is approximately four orders of magnitude larger than the ideal saturation current density. The generation current is the dominant reverse-bias current in a silicon pn junction diode.

TEST YOUR UNDERSTANDING

E8.11 **A GaAs** pn junction diode has the same parameters as described in E8.9. (a) Calculate the reverse-bias generation current if the diode is reverse biased at $V_R = 5$ V. ***(b)*** Determine the ratio of I_{gen} calculated in **part** (a) to the ideal reverse-saturation current I_S. [Ans. (a) $I_{gen} = 1.03 \times 10^{-13}$ A, (b) 1.93×10^7]

8.3.2 Forward-Bias Recombination Current

For the reverse-biased pn junction, electrons and holes are essentially completel swept out of the space charge region so that $n \approx p \approx 0$. Under forward bias, however, electrons and holes are injected across the space charge region, so we do, i fact, have some excess carriers in the space charge region. The possibility exists tha some of these electrons and holes will recombine within the space charge region an not become pan of the minority carrier distribution.

The recombination rate of electrons and holes is again given from Equation (8.74) as

$$R = \frac{C_n C_p N_t (np - n_i^2)}{C_n(n + n') + C_p(p + p')}$$

Dividing both numerator and denominator by $C_n C_p N_t$ and using the definitions o τ_{n0} and τ_{p0}, we may write the recombination rate as

$$R = \frac{np - n_i^2}{\tau_{p0}(n + n') + \tau_{n0}(p + p')} \tag{8.8}$$

Figure 8.18 shows the energy-band diagram of the forward-biased pn junction Shown in the figure are the intrinsic Fermi level and the quasi-Fermi levels fo

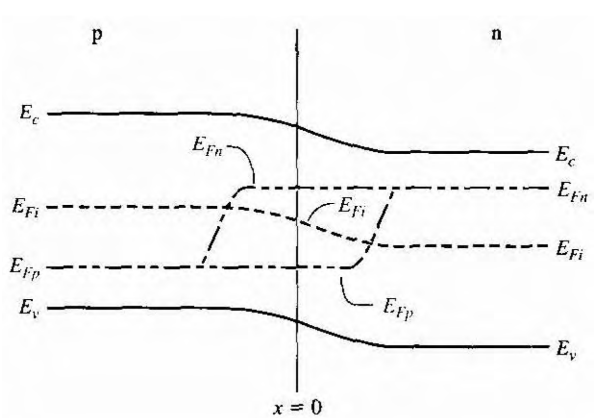

Figure 8.18 | Energy-band diagram of a forward-biased pn junction including quasi-Fermi levels.

electrons and holes. From the results of Chapter 6, we may write the electron concentration as

$$n = n_i \exp\left[\frac{E_{Fn} - E_{Fi}}{kT}\right] \tag{8.84}$$

and the hole concentration as

$$p = n_i \exp\left[\frac{E_{Fi} - E_{Fp}}{kT}\right] \tag{8.85}$$

where E_{Fn} and E_{Fp} are the quasi-Fermi levels for electrons and holes, respectively.

From Figure 8.18, we may note that

$$(E_{Fn} - E_{Fi}) + (E_{Fi} - E_{Fp}) = eV_a \tag{8.86}$$

where V_a is the applied forward-bias voltage. Again, if we assume that the trap level is at the intrinsic Fermi level, then $n' = p' = n_i$. Figure 8.19 shows a plot of the relative magnitude of the recombination rate as a function of distance through the space charge region. This plot was generated using Equations (8.83), (8.84). (8.85), and (8.86). A very sharp peak occurs at the metallurgical junction ($x = 0$).

At the center of the space charge region, we have

$$E_{Fn} - E_{Fi} = E_{Fi} - \quad {}_{Fp} = \frac{eV_a}{2} \tag{8.87}$$

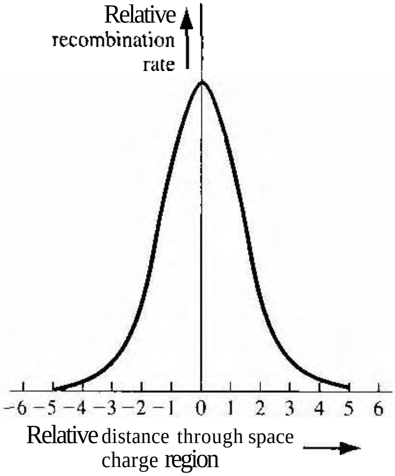

Figure 8.19 | Relative magnitude of the recombination rate through the space charge region of a forward-biased pn junction.

Equations (8.84) and (8.85) then become

$$n = n_i \exp\left(\frac{eV_a}{2kT}\right) \tag{8.88}$$

and

$$p = n_i \exp\left(\frac{eV_a}{2kT}\right) \tag{8.89}$$

If we assume that $n' = p' = n_i$, and that $\tau_{n0} = \tau_{p0} = \tau_0$, then Equation (8.83) becomes

$$R_{\max} = \frac{n_i\,[\exp(eV_a/kT) - 1]}{2\tau_0\,[\exp(eV_a/2kT) + 1]} \tag{8.90}$$

which is the maximum recombination rate for electrons and holes that occurs at the center of the forward-biased pn junction. If we assume that $V_a \gg kT/e$, we may neglect the (-1) term in the numerator and the $(+1)$ term in the denominator. Equation (8.90) then becomes

$$R_{\max} = \frac{n_i}{2\tau_0} \exp\left(\frac{eV_a}{2kT}\right) \tag{8.91}$$

The recombination current density may be calculated from

$$J_{\text{rec}} = \int_0^W eR\,dx \tag{8.92}$$

where again the integral is over the entire space charge region. In this case, however, the recombination rate is not a constant through the space charge region. We have calculated the maximum recombination rate at the center of the space charge region, so we may write

$$J_{\text{rec}} = ex'\frac{n_i}{2\tau_0} \exp\left(\frac{eV_a}{2kT}\right) \tag{8.93}$$

where x' is a length over which the maximum recombination rate is effective. However, since τ_0 may not be a well-defined or known parameter, it is customary to write

$$\boxed{J_{\text{rec}} = \frac{eWn_i}{2\tau_0} \exp\left(\frac{eV_a}{2kT}\right) = J_{r0} \exp\left(\frac{eV_a}{2kT}\right)} \tag{8.94}$$

where W is the space charge width.

TEST YOUR UNDERSTANDING

E8.12 Consider a silicon pn junction diode at $T = 300$ K with the same parameters given in E8.8. The diode is forward biased at $V_a = 0.50$ V. (*a*) Calculate the forward-biased recombination current. (*b*) Determine the ratio of I_{rec} calculated in part (*a*) to the ideal diffusion current. [Ans. (*a*) $I_{\text{rec}} = 2.30 \times 10^{6}$ A, (*b*) 7.21×10^{-2}]

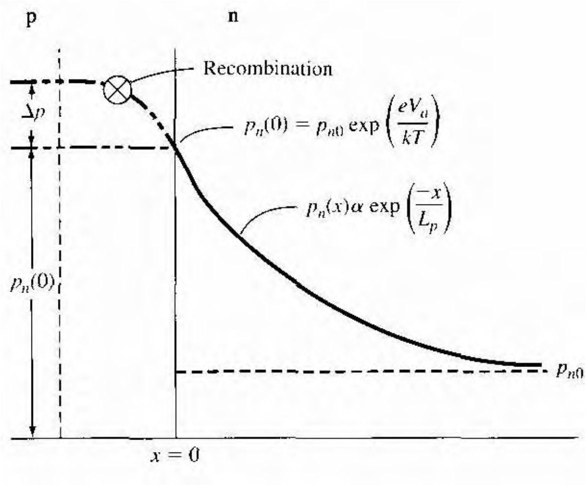
p
n
Recombination
Δp
$p_n(0) = p_{n0} \exp\left(\frac{eV_a}{kT}\right)$
$p_n(x) \alpha \exp\left(\frac{-x}{L_p}\right)$
$p_n(0)$
p_{n0}
$x = 0$

Figure 8.20 | Because of recombination, additional holes from the p region must be injected into the space charge region to establish the minority carrier hole concentration in the n region.

8.3.3 Total Forward-Bias Current

The total forward-bias current density in the pn junction is the sum of the recombination and the ideal diffusion current densities. Figure 8.20 shows a plot of the minority carrier hole concentration in the neutral n region. This distribution yields the ideal hole diffusion current density and is a function of the minority carrier hole diffusion length and the applied junction voltage. The distribution is established as a result of holes being injected across the space charge region. If, now, some of the injected holes in the space charge region are lost due to recombination, then additional holes must be injected from the p region to make up for this loss. The flow of these additional injected carriers, per unit time, results in the recombination current. This added component is schematically shown in the figure.

The total forward-bias current density is the sum of the recombination and the ideal diffusion current densities, so we can write

$$J = J_{\text{rec}} + J_D \tag{8.95}$$

where J_{rec} is given by Equation **(8.94)** and J_D is given by

$$J_D = J_s \exp\left(\frac{eV_a}{kT}\right) \tag{8.96}$$

The (-1) term in Equation **(8.23)** has been neglected. The parameter J_s is the ideal reverse saturation current density, and from previous discussion, the value of J_{r0} from the recombination current is larger than the value of J_s.

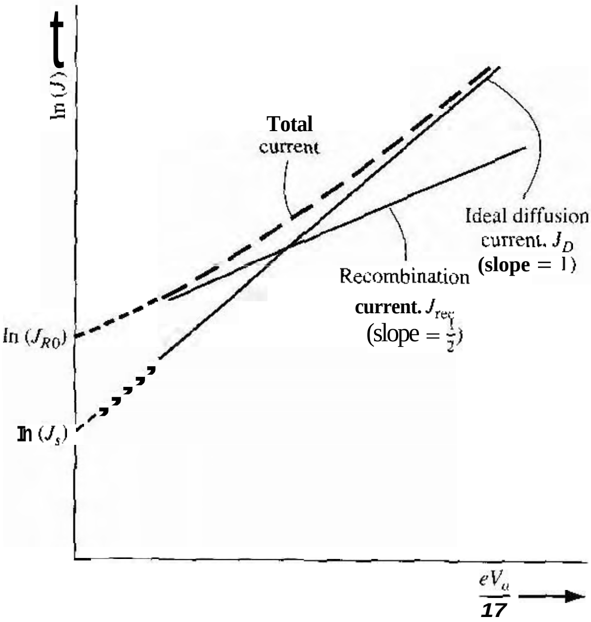

Figure 8.21 | Ideal diffusion, recombination, and total current in a forward-biased pn junction.

If we take the natural log of Equations (8.94) and (8.96), we obtain

$$\ln J_{\text{rec}} = \ln J_{r0} + \frac{eV_a}{2kT} = \ln J_{r0} + \frac{V_a}{2V_t} \tag{8.97a}$$

and

$$\ln J_D = \ln J_s + \frac{eV_a}{kT} = \ln J_s + \frac{V_a}{V_t} \tag{8.97b}$$

Figure 8.21 shows the recombination and diffusion current components plotted on a log current scale as a function of V_a/V_t. The slopes of the two curves are not the same. Also shown in the figure is the total current density—the sum of the two current components. We may notice that, at a low current density, the recombination current dominates, and at a higher current density, the ideal diffusion current dominates.

In general, the diode current-voltage relationship may be written as

$$\boxed{I = I_s\left[\exp\left(\frac{eV_a}{nkT}\right) - 1\right]} \tag{8.98}$$

where the parameter n is called the *ideality factor*. For a large forward-bias voltage, $n \approx 1$ when diffusion dominates, and for low forward-bias voltage, $n \approx 2$ when recombination dominates. There is a transition region where $1 < n < 2$.

8.4 | JUNCTION BREAKDOWN

In the ideal pn junction, a reverse-bias voltage will result in a small reverse-bias current through the device. However, the reverse-bias voltage may not increase without limit; at some particular voltage, the reverse-bias current will increase rapidly. The applied voltage at this point is called the *breakdown* ***voltage.***

Two physical mechanisms give rise to the reverse-bias breakdown in a pn junction: the ***Zener*** *effect* and the *avalanche effect.* Zener breakdown occurs in highly doped pn junctions through a tunneling mechanism. In a highly doped junction, the conduction and valence bands on opposite sides of the junction are sufficiently close during reverse bias that electrons may tunnel directly from the valence band on the p side into the conduction band on the n side. This tunneling process is schematically shown in Figure 8.22a.

The avalanche breakdown process occurs when electrons and/or holes, moving across the space charge region, acquire sufficient energy from the electric field to create electron–hole pairs by colliding with atomic electrons within the depletion region. The avalanche process is schematically shown in Figure 8.22b. The newly created electrons and holes move in opposite directions due to the electric field and thereby add to the existing reverse-bias current. In addition, the newly generated electrons and/or holes may acquire sufficient energy to ionize other atoms, leading to the avalanche process. For most pn junctions, the predominant breakdown mechanism will be the avalanche effect.

If we assume that a reverse-bias electron current I_{n0} enters the depletion region at $x = 0$ as shown in Figure 8.23, the electron current I_n will increase with distance through the depletion region due to the avalanche process. At $x =$ W, the electron

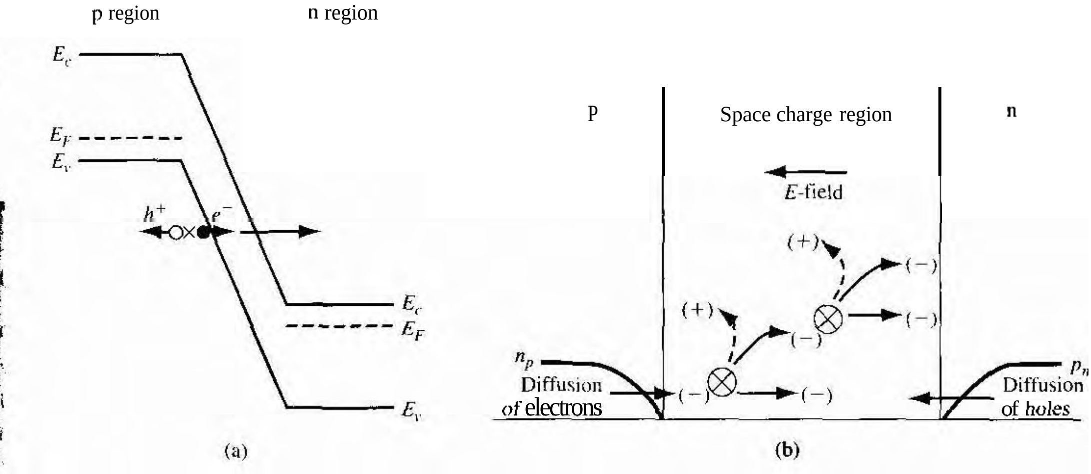

Figure 8.22 | **(a)** Zener breakdown mechanism in a reverse-biased pn junction; (b) avalanche breakdown process in a reverse-biascd pn junction.

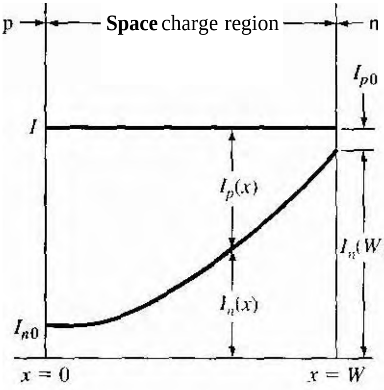

Figure **8.23** | Electron and hole current components through the space charge region during avalanche multiplication.

current may he written as

$$I_n(W) = M_n I_{n0} \tag{8.99}$$

where M_n is a multiplication factor. The hole current is increasing through the depletion region from the n to p region and reaches a maximum value at $x = 0$. The total current is constant through the pn junction in steady state.

We can write an expression for the incremental electron current at some point x as

$$dI_n(x) = I_n(x)\alpha_n\,dx + I_p(x)\alpha_p\,dx \tag{8.100}$$

where α_n and α_p are the electron and hole ionization rates, respectively. The ionization rates are the number of electron-hole pairs generated per unit length by an electron (α_n) or by a hole (α_p). Equation (8.100) may he written as

$$\frac{dI_n(x)}{dx} = I_n(x)\alpha_n + I_p(x)\alpha_p \tag{8.101}$$

The total current I is given by

$$I = I_n(x) + I_p(x) \tag{8.102}$$

which is a constant. Solving for $I_p(x)$ from Equation (8.102) and substituting into Equation (8.101), we obtain

$$\frac{dI_n(x)}{dx} + (\alpha_p - \alpha_n)I_n(x) = \alpha_p I \tag{8.103}$$

If we make the assumption that the electron and hole ionization rates are equal so then Equation (8.103) may be simplified and integrated through the space charge region. We will obtain

$$I_n(W) - I_n(0) = I\int_0^W \alpha\, dx \tag{8.105}$$

Using Equation (8.99), Equation (8.105) may be written as

$$\frac{M_n I_{n0} - I_n(0)}{I} = \int_0^W \alpha\, dx \tag{8.106}$$

Since $M_n I_{n0} \approx I$ and since $I_n(0) = I_{n0}$, Equation (8.106) becomes

$$1 - \frac{1}{M_n} = \int_0^W \alpha\, dx \tag{8.107}$$

The avalanche breakdown voltage is defined to be the voltage at which M_n approaches infinity. The avalanche breakdown condition is then given by

$$\int_0^W \alpha\, dx = 1 \tag{8.108}$$

The ionization rates are strong functions of electric field and, since the electric field is not constant through the space charge region. Equation (8.108) is not easy to evaluate.

If we consider, for example, a one-sided p+n junction, the maximum electric field is given by

$$\mathrm{E}_{\max} = \frac{eN_d x_n}{\epsilon_s} \tag{8.109}$$

The depletion width x_n is given approximately as

$$x_n \approx \left\{\frac{2\epsilon_s V_R}{e} \cdot \frac{1}{N_d}\right\}^{1/2} \tag{8.110}$$

where V_R is the magnitude of the applied reverse-bias voltage. We have neglected the built-in potential V_{bi}.

If we now define V_R to be the breakdown voltage V_B, the maximum electric field. $\mathrm{E}_{\max}$, will be defined as a critical electric field, E_{crit}, at breakdown. Combining Equations (8.109) and (8.110), we may write

$$\boxed{V_B = \frac{\epsilon_s \mathrm{E}_{\text{crit}}^2}{2eN_B}} \tag{8.111}$$

where N_B is the semiconductor doping in the low-doped region of the one-sided junction. The critical electric field, plotted in Figure 8.24, is a slight function of doping.

We have been considering a uniformly doped planar junction. The breakdown voltage will decrease for a linearly graded junction. Figure 8.25 shows a plot of the breakdown voltage for a one-sided abrupt junction and a linearly graded junction. If we take into account the curvature of a diffused junction as well, the breakdown voltage will be further degraded.

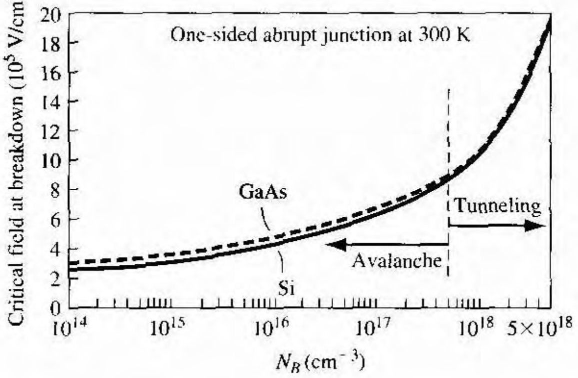

Figure 8.24 | Critical electric field at breakdown in a one sided junction as a function of impurity doping concentrations. *(From Sze [12].)*

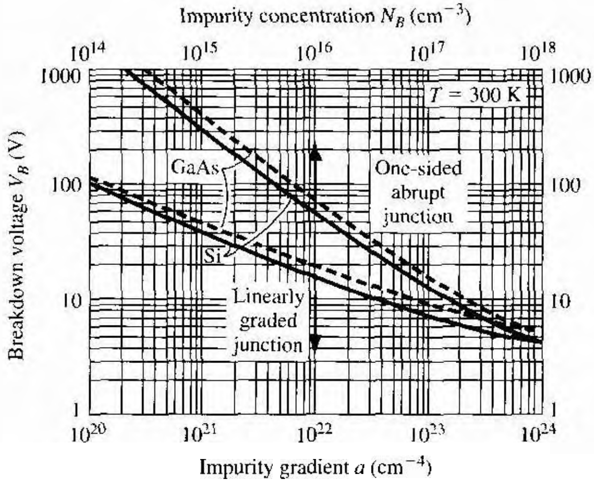

Figure 8.25 | Breakdown voltage versus impurity concentration in uniformly **doped** and linearly graded junctions. *(From Sze [12].)*

DESIGN EXAMPLE 8.8

Objective

To design an ideal one-sided n^+p junction diode to meet a breakdown voltage specification.

Consider a silicon pn junction diode at $T = 300$ K. Assume that $N_d = 3 \times 10^{18}$ cm^{-3}. Design the diode such that the breakdown voltage is $V_B = 100$ V.

■ Solution

From Figure 8.25, we find that the doping concentration in the low-doped side of a one-sided abrupt junction should be approximately 4×10^{15} cm^{-3} for a breakdown voltage of 100 V.

For a doping concentration of 4×10^{15} cm^{-3}, the critical electric field, from Figure 8.24, is approximately 3.7×10^5 V/cm. Then from Equation (8.111), the breakdown voltage is 110 V, which correlates quite well with the results from Figure 8.25.

Conclusion

As Figure 8.25 shows, the breakdown voltage increases as the doping concentration decreases in the low-doped region.

TEST YOUR UNDERSTANDING

E8.13 A one-sided, planar, uniformly doped silicon pn junction diode is required to have a reverse-bias breakdown voltage of $V_B = 60$ V. What is the maximum doping concentration in the low-doped region such that this specification is met! (Ans. $N_B \approx 8 \times 10^{15}$ cm^{-3})

E8.14 Repeat E8.13 for a GaAs diode. (Ans. $N_B \approx 1.5 \times 10^{16}$ cm^{-3})

*8.5 | CHARGE STORAGE AND DIODE TRANSIENTS

The pn junction is typically used as an electrical switch. In forward bias, referred to as the *on* state, a relatively large current can be produced by a small applied voltage; in reverse bias, referred to as the *off* state, only a very small current will exist. Of primary interest in circuit applications is the speed of the pn junction diode in switching states. We will qualitatively discuss the transients that occur and the charge storage effects. We will simply state the equations that describe the switching times without any mathematical derivations.

8.5.1 The Turn-off Transient

Suppose we want to switch a diode from the forward bias on state to the reverse-bias off state. Figure 8.26 shows a simple circuit that will switch the applied bias at $t = 0$. For $t < 0$, the forward-bias current is

$$I = I_F = \frac{V_F - V_a}{R_F} \tag{8.112}$$

The minority carrier concentrations in the device, for the applied forward voltage V_F, are shown in Figure 8.27a. There is excess minority carrier charge stored in both the p and n regions of the diode. The excess minority carrier concentrations at the space charge edges are supported by the forward-bias junction voltage V_a. When the voltage is switched from the forward- to the reverse-bias state, the excess minority carrier concentrations at the space charge edges can no longer be supported and they start to decrease, as shown in Figure 8.27b.

The collapse of the minority carrier concentrations at the edges of the space charge region leads to large concentration gradients and diffusion currents in the

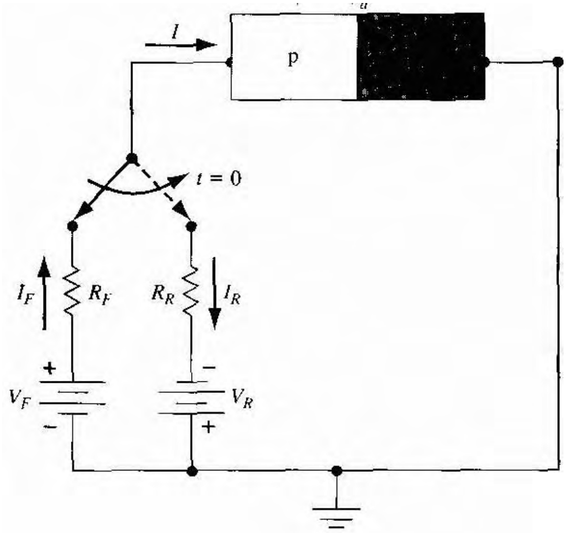

Figure **8.26** | Simple circuit for switching a diode from forward to reverse bias.

reverse-bias direction. If we assume, for the moment, that the voltage across the diode junction is small compared with V_R, then the reverse-bias current is limited to approximately

$$I = -I_R \approx \frac{-V_R}{R_R} \tag{8.113}$$

The junction capacitances do not allow the junction voltage to change instantaneously. If the current I_R were larger than this value, there would be a forward-bias voltage across the junction, which would violate our assumption of a reverse-bias current. If the current I_R were smaller than this value, there would be a reverse-bias voltage across the junction, which means that the junction voltage would have changed instantaneously. Since the reverse current is limited to the value given by Equation (8.113), the reverse-bias density gradient is constant; thus, the minority carrier concentrations at the space charge edge decrease with time as shown in Figure 8.27b.

This reverse current I_R will be approximately constant for $0^+ \le t \le t_s$, where t_s is called the ***storage time.*** The storage time is the length of time required for the minority carrier concentrations at the space charge edge to reach the thermal-equilibrium values. After this time, the voltage across the junction will begin to change. The current characteristic is shown in Figure 8.28. The reverse current is the flow of the stored minority carrier charge, which is the difference between the minority carrier concentrations at $t = 0^-$ and $t = \infty$, as was shown in Figure 8.27b.

The storage time t_s can be determined by solving the time-dependent continuity equation. If we consider a one-sided p^+n junction, the storage time is determined

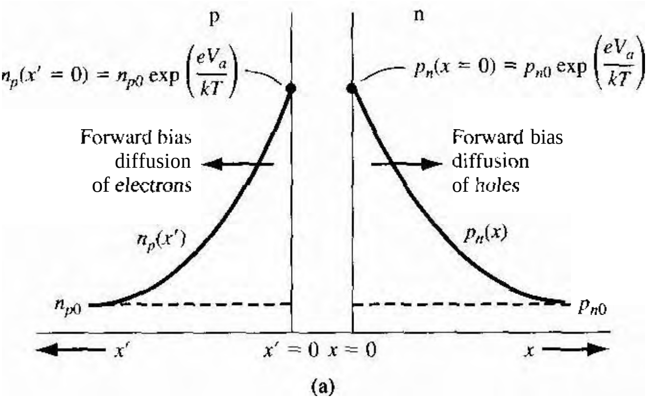
p
n
$n_p(x'=0) = n_{p0}\exp\left(\frac{eV_a}{kT}\right)$
$p_n(x=0) = p_{n0}\exp\left(\frac{eV_a}{kT}\right)$
Forward bias diffusion of electrons
Forward bias diffusion of holes
$n_p(x')$
$p_n(x)$
n_{p0}
p_{n0}
x'
$x' = 0$ $x = 0$
x
(a)

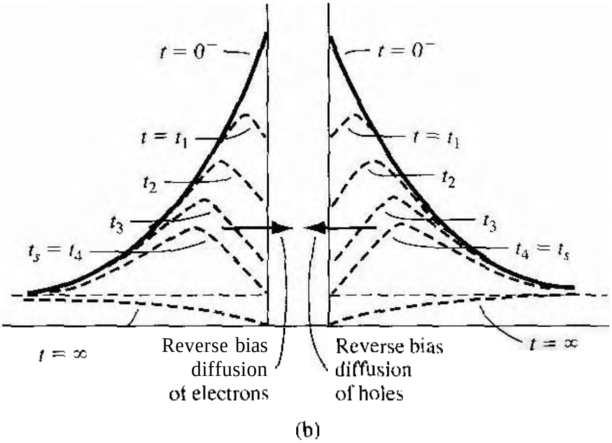
$t = 0^-$
$t = 0^-$
$t = t_1$
$t = t_1$
t_2
t_2
t_3
t_3
$t_s = t_4$
$t_4 = t_s$
$t = \infty$
$t = \infty$
Reverse bias diffusion of electrons
Reverse bias diffusion of holes
(b)

Figure **8.27 |** (a) Steady-state forward-bias minority carrier concentrations: (b) minority carrier concentrations at **various** times during switching.

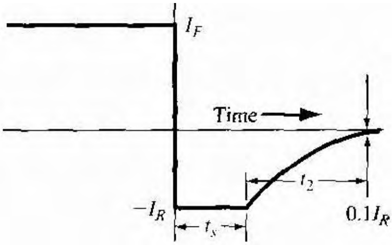

Figure 8.28 | Current characteristic versus time during diode switching.

from the equation

$$\operatorname{erf}\sqrt{\frac{t_s}{\tau_{p0}}} = \frac{I_F}{I_F + I_R} \quad (8.114)$$

where erf (x) is known as the error function. An approximate solution for the storag time can be obtained as

$$t_s \approx \tau_{p0} \ln\left[1 + \frac{I_F}{I_R}\right] \quad (8.115)$$

The recovery phase for $t > t_s$ is the time required for the junction to reach its steady-state reverse-bias condition. The remainder of the excess charge is bei removed and the space charge width is increasing to the reverse-bias value. The decay time t_2 is determined from

$$\operatorname{erf}\sqrt{\frac{t_2}{\tau_{p0}}} + \frac{\exp(-t_2/\tau_{p0})}{\sqrt{\pi t_2/\tau_{p0}}} = 1 + 0.1\left(\frac{I_R}{I_F}\right) \quad (8.116)$$

The total turn-off time is the sum of t_s and t_2.

To switch the diode quickly, we need to be able to produce a large reverse current as well as have a small minority carrier lifetime. In the design of diode circuits, then, the designer must provide a path for the transient reverse-bias current pulse in order to be able to switch the diode quickly. These same effects will be considered when we discuss the switching of bipolar transistors.

TEST YOUR UNDERSTANDING

E8.15 A one-sided p^+n silicon diode, that has a forward-bias current of $I_F = 1.75$ mA, is switched to reverse bias with an effective reverse-bias voltage of $V_R = 2$ V and an effective series resistance of $R_R = 4$ kΩ. The minority carrier hole lifetime is 10^{-7} s. (a) Determine the storage time t_s. (b) Calculate the decay time t_2. (c) What is the turn-off time of the diode?
[Ans. (a) 0.746×10^{-7} s, (b) 1.25×10^{-7} s, (c) $\approx 2 \times 10^{-7}$ s]

8.5.2 The Turn-on Transient

The turn-on transient occurs when the diode is switched from its "off" state into the forward-bias "on" state. The turn-on can be accomplished by applying a forward-bias current pulse. The first stage of turn-on occurs very quickly and is the length of time required to narrow the space charge width from the reverse-bias value to its thermal-equilibrium value when $V_a = 0$. During this time, ionized donors and acceptors are neutralized as the space charge width narrows.

The second stage of the turn-on process is the time required to establish the minority-carrier distributions. During this time the voltage across the junction is increasing toward its steady-state value. A small turn-on time is achieved if the minority carrier lifetime is small and if the forward-bias current is small.

*8.6 | THE TUNNEL DIODE

The *tunnel* diode is a pn junction in which both the n and p regions are degenerately doped. As we discuss the operation of this device, we will find a region that exhibits a negative differential resistance. The tunnel diode was used in oscillator circuits in the past, but other types of solid-state devices are now used as high-frequency oscillators: thus, the tunnel diode is really only of academic interest. Nevertheless, this device does demonstrate the phenomenon of tunneling we discussed in Chapter 2.

Recall the degenerately doped semiconductors we discussed in Chapter 4: the Fermi level is in the conduction band of a degenerately doped n-type material and in the valence band of a degenerately doped p-type material. Then, even at T = 0 K, electrons will exist in the conduction hand of the n-type material, and holes (empty states) will exist in the p-type material.

Figure 8.29 shows the energy-band diagram of a pn junction in thermal equilibrium for the case when both the n and p regions are degenerately doped. The depletion region width decreases as the doping increases and may be on the order of approximately 100 Å for the case shown in Figure 8.29. The potential barrier at the junction can be approximated by a triangular potential barrier, as is shown in Figure 8.30. This potential harrier is similar to the potential barrier used in Chapter 2 to illustrate the tunneling phenomenon. The barrier width is small and the electric field in the space charge region is quite large; thus, a finite probability exists that an electron may tunnel through the forbidden band from one side of the junction to the other.

We may qualitatively determine the current–voltage characteristics of the tunnel diode by considering the simplified energy-band diagrams in Figure 8.31.

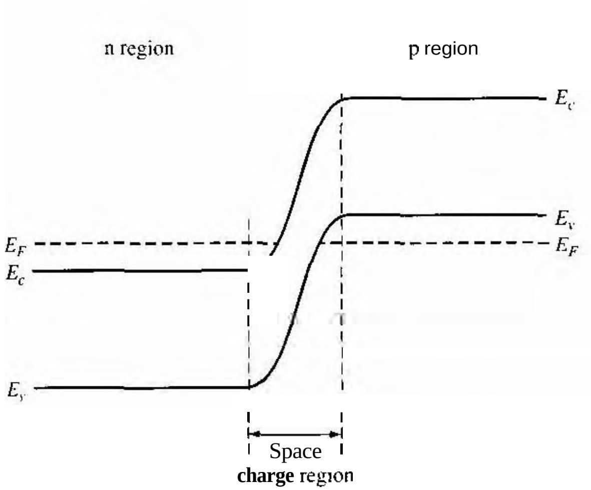

Figure 8.29 | Energy-hand diagram of a pn junction in thermal equilibrium in which both the **nand** p regions are degenerately doped.

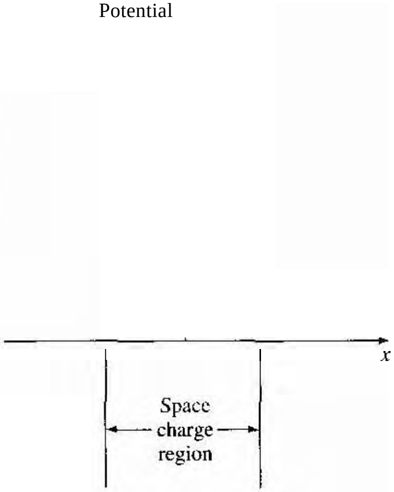

Figure 8.30 | Triangular potential harrier approximation of the potential harrier in the tunnel diode.

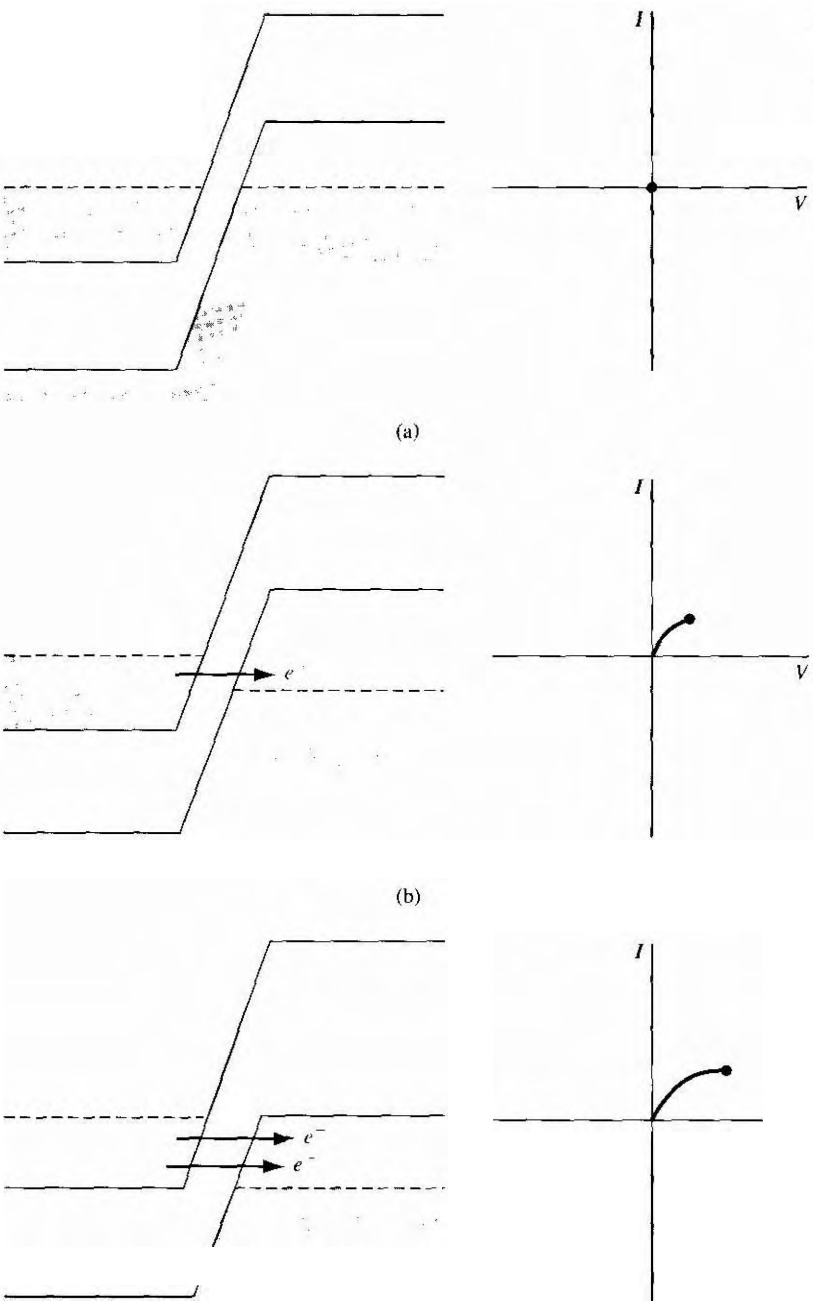

Figure 8.31 | Simplified energy-band diagrams and *I–V* characteristics of the tunnel diode at (a) zero bias; (b) a slight forward bias; (c) a forward bias producing maximum tunneling current.

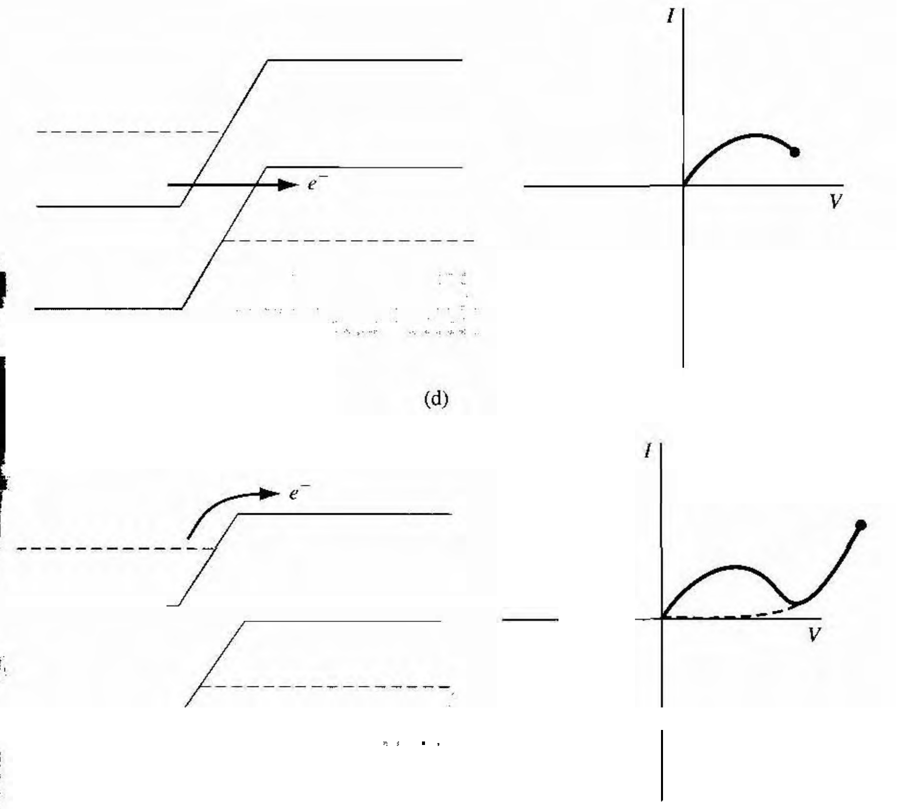

(d)

(e)

Figure 8.31 | *(concluded)* (d) A higher forward bias showing less tunneling current; (e) a forward bias for which the diffusion current dominates.

Figure 8.31a shows the energy-band diagram at zero bias, which produces zero current on the I–V diagram. If we assume, for simplicity, that we are near 0 K, then all energy states are filled below E_F on both sides of the junction.

Figure 8.31b shows the situation when a small forward-bias voltage is applied to the junction. Electrons in the conduction band of the n region are directly opposite to empty states in the valence band of the p region. There is a finite probability that some of these electrons will tunnel directly into the empty states, producing a forward-bias tunneling current as shown. With a slightly larger forward-bias voltage, as in Figure 8.31c, the maximum number of electrons in the n region will be opposite the maximum number of empty states in the p region; this will produce a maximum tunneling current.

As the forward-bias voltage continues to increase, the number of electrons on the n side directly opposite empty states on the p side decreases, as in Figure 8.31d, and the tunneling current will decrease. In Figure 8.31e, there are no electrons on the

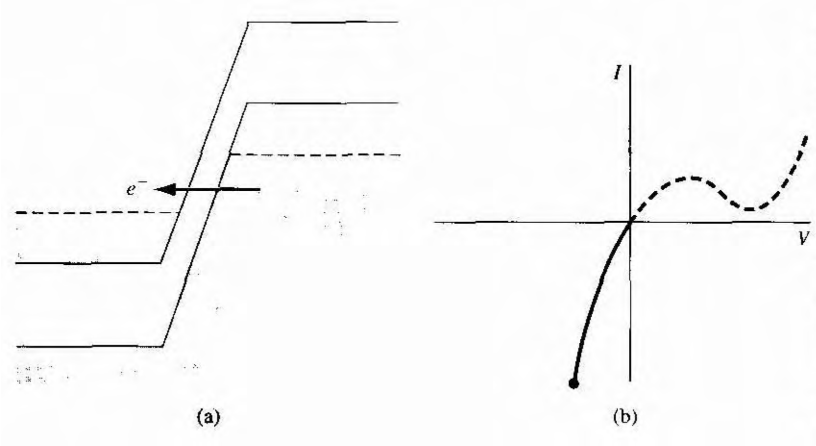

Figure 8.32 | (a) Simplified energy-band diagram of a tunnel diode with a reverse-bias voltage: (b) I–V characteristic of a tunnel diode with a reverse-bias voltage.

n side directly opposite available empty states on the p side. For this forward-bias voltage, the tunneling current will be zero and the normal ideal diffusion current will exist in the device as shown in the I–V characteristics.

The portion of the curve showing a decrease in current with an increase in voltage is the region of differential negative resistance. The range of voltage and current for this region is quite small; thus, any power generated from an oscillator using this negative resistance property would also be fairly small.

A simplified energy-band diagram of the tunnel diode with an applied reverse-bias voltage is shown in Figure 8.32a. Electrons in the valence band on the p side are directly opposite empty states in the conduction band on the n side, so electrons can now tunnel directly from the p region into the n region, resulting in a large reverse-bias tunneling current. This tunneling current will exist for any reverse-bias voltage. The reverse-bias current will increase monotonically and rapidly with reverse-bias voltage as shown in Figure 8.32b.

8.7 | SUMMARY

- When a forward-bias voltage is applied across a pn junction (p region positive with respect to the n region), the potential barrier is lowered so that holes from the p region and electrons from the n region can flow across the junction.
- The boundary conditions relating the minority carrier hole concentration in then region at the space charge edge and the minority carrier electron concentration in the p region at the space charge edge were derived.
- The holes that are injected into the n region and the electrons that are injected into the p region now become excess minority carriers. The behavior of the excess minority carrier is described by the ambipolar transoon equation developed and described in Chapter 6. Solving the ambipolar transpon equation and using the boundary conditions. the steady-state minority carrier hole and electron concentrations in the n region and p region, respectively, were derived.

- Gradients exist in the minority carrier hole and electron concentrations so that minority carrier diffusion currents exist in the pn junction. These diffusion currents yield the ideal current–voltage relationship of the pn junction diode.
- The small-signal equivalent circuit of the pn junction diode was developed. The two parameters of interest are the diffusion resistance and the diffusion capacitance.
- Excess carriers are generated in the space charge region of a reverse-biased pn junction. These carriers are swept out by the electric field and create the reverse-bias generation current that is another component of the reverse-bias diode current. Excess carriers recombine in the space charge region of a forward-biased pn junction. This recombination process creates the forward-bias recombination current that is another component of the forward-bias diode current.
- Avalanche breakdown occurs when a sufficiently large reverse-bias voltage is applied to the pn junction. A large reverse-bias current may then be induced in the pn junction. The breakdown voltage as a function of the doping levels in the pn junction was derived. In a one-sided pn junction, the breakdown voltage is a function of the doping concentration in the low-doped region.
- When a pn junction is switched from forward bias to reverse bias, the stored excess minority carrier charge must be removed from the junction. The time required to remove this charge is called the storage time and is a limiting factor in the switching speed of a diode.

GLOSSARY OF IMPORTANT TERMS

avalanche breakdown The process whereby a large reverse-bias pn junction current is created due to the generation of electron–hole pairs by the collision of electrons and/or holes with atomic electrons within the space charge region.

carrier injection The flow of carriers across the space charge region of a pn junction when a voltage is applied.

critical electric field The peak electric field in the space charge region at breakdown.

diffusion capacitance The capacitance of a forward-biased pn junction due to minority carrier storage effects.

diffusion conductance The ratio of a low-frequency, small-signal sinusoidal current to voltage in a forward-biased pn junction.

diffusion resistance The inverse of diffusion conductance.

forward bias The condition in which a positive voltage is applied to the p region with respect to the n region of a pn junction so that the potential barrier between the two regions is lowered below the thermal-equilibrium value.

generation current The reverse-bias pn junction current produced by the thermal generation of electron-hole pairs within the space charge region.

"long" diode A pn junction diode in which both the neutral p and n regions are long compared with the respective minority carrier diffusion lengths.

recombination current The forward-bias pn junction current produced as a result of the flow of electrons and holes that recombine within the space charge region.

reverse saturation current The ideal reverse-bias current in a pn junction.

"short" diode A pn junction diode in which at least one of the neutral p or n regions is short compared to the respective minority carrier diffusion length.

storage time The time required for the excess minority carrier concentrations at the space charge edge to go from their steady-state values to zero when the diode is switched forward to reverse bias.

CHECKPOINT

After studying this chapter, the reader should have the ability to:

- Describe the mechanism of charge flow across the space charge region of a pn junction when a forward-bias voltage is applied.
- State the boundary conditions for the minority carrier concentrations at the edge of the space charge region.
- Derive the expressions for the steady-state minority carrier concentrations in the pn junction.
- Derive the ideal current–voltage relationship for a pn junction diode.
- Describe the characteristics of a "short" diode.
- Describe what is meant by diffusion resistance and diffusion capacitance.
- Describe generation and recombination currents in a pn junction.
- Describe the avalanche breakdown mechanism in a pn junction.
- Describe the turn-off transient response in a pn junction.

REVIEW QUESTIONS

1. Why does the potential barrier decrease in a forward-biased pn junction?
2. Write the boundary conditions for the excess minority carriers in a pn junction (a) under forward bias and (b) under reverse bias.
3. Sketch the steady-state minority carrier concentrations in a forward-biased pn junction.
4. Explain the procedure that is used in deriving the ideal current–voltage relationship in a pn junction diode.
5. Sketch the electron and hole currents through a forward-biased pn junction diode.
6. What is meant by a "short" diode?
7. (a) Explain the physical mechanism of diffusion capacitance. (b) What is diffusion resistance?
8. Explain the physical mechanism of the (a) generation current and (b) recombination current.
9. Why does the breakdown voltage of a pn junction decrease as the doping concentration increases?
10. Explain what is meant by storage time.

PROBLEMS

Section 8.1 pn Junction Current

8.1 (*a*) Consider an ideal pn junction diode at $T = 300$ K operating in the forward-bias region. Calculate the change in diode voltage that will cause a factor of 10 increase in current. (*b*) Repeat part (*a*) for a factor of 100 increase in current.

8.2 Calculate the applied reverse-bias voltage at which the ideal reverse current in a pn junction diode at T = 300 K reaches 90 percent of its reverse saturation current value.

8.3 An ideal silicon pn junction at T = 300 K is under forward bias. The minority carrier lifetimes are $\tau_{n0} = 10^{-6}$ s and $\tau_{p0} = 10^{-7}$ s. The doping concentration in the n region is $N_d = 10^{16}$ cm^{-3}. Plot the ratio of hole current to the total current crossing the space charge region as the p-region doping concentration varies over the range $10^{15} \leq N_a \leq 10^{18}$ cm^{-3}. (Use a log scale for the doping concentrations.)

A silicon pn junction diode is to be designed to operate at T = 300 K such that the diode current is I = 10 mA at a diode voltage of $V_D = 0.65$ V. The ratio of electron current to total current is to be 0.10 and the maximum current density is to be no more than 20 A/cm^2. Use the semiconductor parameters given in Example 8.2.

8.5 For a silicon pn junction at T = 300 K, assume $\tau_{p0} = 0.1\tau_{n0}$ and $\mu_n = 2.4\,\mu_p$. The ratio of electron current crossing the depletion region to the total current is defined as the electron injection efficiency. Determine the expression for the electron injection efficiency as a function of (a) N_d/N_a and (b) the ratio of n-type conductivity to p-type conductivity.

8.6 Consider a p$^+$n silicon diode at T = 300 K with doping concentrations of $N_a = 10^{18}$ cm^{-3} and $N_d = 10^{16}$ cm^{-3}. The minority carrier hole diffusion coefficient is $D_p = 12$ cm^2/s and the minority carrier hole lifetime is $\tau_{p0} = 10^{-7}$ s. The cross-sectional area is $A = 10^{-4}$ cm^2. Calculate the reverse saturation current and the diode current at a forward-bias voltage of 0.50 V.

Consider an ideal silicon pn junction diode with the following parameters: $\tau_{n0} = \tau_{p0} = 0.1 \times 10^{-6}$ s, $D_n = 25$ cm^2/s, $D_p = 10$ cm^2/s. What must be the ratio of N_a/N_d so that 95 percent of the current in the depletion region is carried by electrons?

A silicon pn junction with a cross-sectional area of 10^{-4} cm^2 has the following properties at T = 300 K:

n region	p region
$N_d = 10^{17}$ cm^{-3}	$N_a = 5 \times 10^{15}$ cm^{-3}
$\tau_{p0} = 10^{-7}$ s	$\tau_{n0} = 10^{-6}$ s
$\mu_n = 850$ cm^2/V-s	$\mu_n = 1250$ cm^2/V-s
$\mu_p = 320$ cm^2/V-s	$\mu_p = 420$ cm^2/V-s

(*a*) Sketch the thermal equilibrium energy-band diagram of the pn junction, including the values of the Fermi level with respect to the intrinsic level on each side of the junction. (b) Calculate the reverse saturation current I_s and determine the forward-bias current I at a forward-bias voltage of 0.5 V. (c) Determine the ratio of hole current to total current at the space charge edge x_n.

A germanium p$^+$n diode at T = 300 K has the following parameters: $N_a = 10^{18}$ cm^{-3}, $N_d = 10^{16}$ cm^{-3}, $D_p = 49$ cm^2/s, $D_n = 100$ cm^2/s, $\tau_{p0} = \tau_{n0} = 5\ \mu$s, and $A = 10^{-4}$ cm^2. Determine the diode current for (*a*) a forward-bias voltage of 0.2 V and (b) a reverse-bias voltage of 0.2 V.

8.10 An n$^+$p silicon diode at T = 300 K has the following parameters: $N_d = 10^{18}$ cm^{-3}, $N_a = 10^{16}$ cm^{-3}, $D_n = 25$ cm^2/s, $D_p = 10$ cm^2/s, $\tau_{n0} = \tau_{p0} = 1\ \mu$s, and $A = 10^{-4}$ cm^2. Determine the diode current for (a) a forward-bias voltage of 0.5 V and (b) a reverse-bias voltage of 0.5 V.

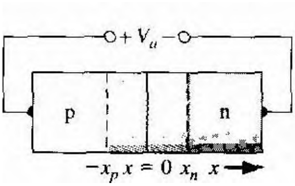

Figure 8.33 | Figure for Problem 8.11.

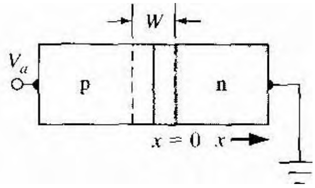

Figure 8.34 | Figure for Problem 8.12.

8.11 A silicon step junction has uniform impurity doping concentrations of $N_a = 5$ x 10^{15} cm^{-3} and $N_d = 1$ x 10^{15} c m ^{3}, and a cross-sectional area of $A = 10^{-4}$ cm^2. Let $\tau_{n0} = 0.4$ μs and $\tau_{p0} = 0.1$ μs. Consider the geometry in Figure 8.33. Calculate (a) the ideal reverse saturation current due to holes, (b) the ideal reverse saturation current due to electrons, (c) the hole concentration at x_n if $V_a = \frac{1}{2}V_{bi}$, and (d) the electron current at **x** = **x„** + $\frac{1}{2}L_p$ for $V_a = \frac{1}{2}V_{bi}$

8.12 Consider the ideal long silicon pn junction shown in Figure 8.34. $T = 300$ K. The n region is doped with 10'" donor atoms per cm' and the p region is doped with 5 x 10^{16} acceptor atoms per cm^3. The minority carrier lifetimes are $\tau_{n0} = 0.05$ μs a $\tau_{p0} = 0.01$ μs. The minority carrier diffusion coefficients are $D_n = 23$ cm^2/s and $D_p = 8$ cm^2/s. The forward-bias voltage is $V_a = 0.610$ V. Calculate (a) the excess hole concentration as a function of **x** for **x** ≥ 0, (b) the hole diffusion current density at $x = 3 \times 10^{-4}$ cm. and (r) the electron current density at $x = 3$ x 10^{-4} cm.

8.13 The limit of low injection is normally defined to he when the minority carrier concentration at the edge of the space charge region in the low-doped region becomes equal to one-tenth the majority carrier concentration in this region. Determine the value of the forward-bias voltage at which the limit of low injection is reached for the diode described in (a) Problem 8.9 and (b) Problem 8.10.

8.14 The cross-sectional area of a silicon pn junction is 10^{-3} cm^2. The temperature of the diode is $T = 300$ K, and the doping concentrations are $N_d = 10^{16}$ cm^{-3} and N„ = 8×10^{15} cm^{-3}. Assume minority carrier lifetimes of $\tau_{n0} = 10^{-6}$ s and $\tau_{p0} = 10^{-7}$ s. Calculate the total number of excess electrons in the p region and the total number of excess hales in the n region for (a) V„ = 0.3 V, ***(h)*** V, = 0.4 V, and (c) V„ = 0.5 V.

8.15 Consider two ideal pn junctions at $T = 300$ K. having exactly the same electrical and physical parameters except for the bandgap energy of the semiconductor materials. The tint pn junction has a bandgap energy **of** 0.525 eV and a forward-bias current of 10 mA with $V_a = 0.255$ V. For the second pn junction, "design" the bandgap energy so that a forward-bias voltage of $V_a = 0.32$ V will produce a current of I0 μA.

8.16 The reverse-bias saturation current is a function of temperature. (a) Assuming that I, varies with temperature only from the intrinsic carrier concentration, show that we can write I, = CT' exp $(-E_g/kT)$ where C is a constant and a function only of the diode parameters. (b) Determine the increase in I, as the temperature increases from $T = 300$ K to $T = 400$ K for a (i) germanium diode and (ii) silicon diode.

8.17 Assume that the mobilities, diffusion coefficients, and minority carrier lifetime parameters are independent of temperature (use the $T = 300$ K values). Assume that $\tau_{n0} = 10^{-6}$ s, $\tau_{p0} = 10^{-7}$ s, $N_d = 5 \times 10^{15}$ cm^{-3}, and N„ = 5 x 10^{16} cm^{-3}. Plot the ideal reverse saturation current density from $T =$ 2CU K to $T = 500$ K for (a) silicon, (*b*) germanium, and (*c*) gallium arsenide ideal pn junctions. (Use a log scale for the current density.)

.18 An ideal uniformly doped silicon pn junction diode has a cross-sectional area of 10^{-4} cm^2. The p region is doped with 5×10^{18} acceptor atoms per cm^3 and the n region is doped with 10^{15} donor atoms per cm^3. Assume that the following parameter values are independent of temperature: $E_g = 1.10$ eV, $\tau_{n0} = \tau_{p0} = 10^{-7}$ s, $D_n = 25$ cm^2/s, $D_p = 10$ cm^2/s, $N_c = 2.8 \times 10^{19}$ cm^{-3}, and $N_v = 1.04 \times 10^{19}$ cm^{-3}. The ratio of the forward to reverse current is to be no less than 10^4 with forward- and reverse-bias voltages of 0.50 V. Also, the reverse saturation current is to be no larger than 1 μA. What is the maximum temperature at which the diode will meet these specifications?

*8.19 A p$^+$n silicon diode is fabricated with a narrow n region as shown in Figure 8.10, in which $W_n < L_p$. Assume the boundary condition of $p_n = p_{n0}$ at $x = x_n + W_n$. (*a*) Derive the expression for the excess hole concentration $\delta p_n(x)$ as given by Equation (8.27). (*b*) Using the results of part (a), show that the current density in the diode is given by

$$J = \frac{eD_p p_{n0}}{L_p} \coth\left(\frac{W_n}{L_p}\right)\left[\exp\left(\frac{eV}{kT}\right) - 1\right]$$

8.20 A silicon diode can be used to measure temperature by operating the diode at a fixed forward-bias current. The forward-bias voltage is then a function of temperature. At T = 300 K, the diode voltage is found to be 0.60 V. Determine the diode voltage at (*a*) T = 310 K and (*b*) T = 320 K.

8.21 A forward-biased silicon diode is to be used as a temperature sensor. The diode is forward biased with a constant current source and V_a is measured as a function of temperature. (*a*) Derive an expression for $V_a(T)$ assuming that D/L for electrons and holes, and E_g are independent of temperature. (*b*) If the diode is biased at $I_D = 0.1$ mA and if $I_s = 10^{-15}$ A at $T = 300$ K, plot V_a versus T for 20°C < T < 200°C. (*c*) Repeat part (*b*) if $I_D = 1$ mA. (*d*) Determine any changes in the results of parts (*a*) through (*c*) if the change in bandgap energy with temperature is taken into account.

Section 8.2 Small-Signal Model of the pn Junction

8.22 Calculate the small-signal ac admittance of a pn junction biased at $V_a = 0.72$ V and $I_{DQ} = 2.0$ mA. Assume the minority carrier lifetime is 1 μs in both the n and p regions. T = 300 K.

8.23 Consider a p$^+$n silicon diode at $T = 300$ K. The diode is forward biased at a current of 1 mA. The hole lifetime in the n region is 10^{-7} s. Neglecting the depletion capacitance, calculate the diode impedance at frequencies of 10 **kHz,** 100 **kHz,** 1 **MHz,** and 10 **MHz.**

8.24 Consider a silicon pn junction with parameters as described in Problem 8.8. (*a*) Calculate and plot the depletion capacitance and diffusion capacitance over the voltage range $-10 \le V_a \le 0.75$ V. (*b*) Determine the voltage at which the two capacitances are equal.

8.25 Consider a p$^+$n silicon diode at $T = 300$ K. The slope of the diffusion capacitance versus forward-bias current is 2.5×10^{-6} F/A. Determine the hole lifetime and the diffusion capacitance at a forward-bias current of 1 mA.

8.26 A one-sided n$^+$p silicon diode at $T = 300$ K with a cross-sectional area of 10^{-3} cm^2 is operated under forward bias. The doping levels are $N_d = 10^{18}$ cm^{-3} and

$N_a = 10^{16}$ cm^{-3}, and the minority carrier parameters are $\tau_{p0} = 10^{-8}$ s. $\tau_{n0} =$ 10-' s, $D_p = 10$ cm^2/s, and $D_n = 25$ cm^2/s. The maximum diffusion capacitance is to be 1 n Determine (*a*) the maximum current through the diode, (*b*) the maximum forward-bias voltage, and (*c*) the diffusion resistance.

8.27 A silicon pn junction diode at T = 300 K has a cross-sectional area of 10^{-2} cm^2. length of the p region is 0.2 cm and the length of the n region is 0.1 cm. The dopin concentrations are $N_d = 10^{15}$ cm^{-3} and $N_a = 10^{16}$ cm^{-3}. Determine (*a*) approximately the series resistance of the diode and (b) the current through the diode that w produce a 0.1 V drop across this series resistance.

8.28 We want to consider the effect of a series resistance on the forward bias voltage required to achieve a particular diode current. (a) Assume the reverse saturation current in a diode is I, $= 10^{-10}$ A at $T = 300$ K. The resistivity of the n region is 0.2 Ω-cm and the resistivity of the p region is 0.1 R-cm. Assume the length of each neutral region is 10^{-2} cm and the cross-sectional area is 2 x 10^{-5} cm^2. Determine the required applied voltage to achieve a current of (i) 1 mA and (*ii*) 10 mA. (*h*) Repeat part **(a)** neglecting the series resistance.

8.29 The minimum mall-signal diffusion resistance of an ideal forward-biased silicon pn junction diode at $T = 300$ K is to be $r_d = 48$ Ω. The reverse saturation current is *I*, $= 2$ x 10^{-11} A. Calculate the maximum applied forward-bias voltage that can applied to meet this specification.

8.30 (*a*) An ideal silicon pn junction diode at $T = 300$ K is forward biased at V, = +20 mV. The reverse-saturation current is I, $= 10^{-13}$ A. Calculate the small-signal diffusion resistance. (*b*) Repeat pan (*a*) for an applied reverse-bias voltage of $V_a = -20$ mV.

Section 8.3 Generation-Recombination Currents

8.31 Consider a reverse-biased gallium arsenide pn junction at T = 300 K. Assume that a reverse-bias voltage, $V_R = 5$ V, is applied. Assume parameter values of: $N_a = N_d = 10^{16}$ cm^{-3}, Dp = 6 cm^2/s, D,, = 200 cm^2/s, and $\tau_{p0} = \tau_{n0} = \tau_0 = 10^{-8}$ s. Calculate the ideal reverse saturation current density and the reverse-biased generation current density. How does the relative value of these two currents compare to those of the silicon pn junction?

***8.32** (a) Consider Example 8.7. Assume that all parameters except n_i are independent of temperature. Determine the temperature at which J, and J_{gen} will be equal. What are the values of J_s and J_{gen} at this temperature? (*b*) Using the results of Example 8.7, calculate the forward-bias voltage at which the ideal diffusion current is equal to the recombination current.

8.33 Consider a GaAs pn diode at $T = 300$ K with N_a = N, $= 10^{17}$ cm^{-3} and with a cross-sectional area of 10^{-3} cm^2. The minority carrier mobilities are $\mu_n = 3000$ cm^2/V-s and $\mu_p = 200$ cm^2/V-s. The lifetimes are $\tau_{p0} = \tau_{n0} = \tau_0 = 10^{-8}$ s. As a first approximation, assume the electron-hole generation and recombination rates are constant across the space charge region. (*a*) Calculate the total diode current at a reverse-bias voltage of 5 V and at forward-bias voltages of 0.3 V and 0.5 V. (*h*) Compare the results of pan (*a*) to an ideal diode at the same applied voltages.

8.34 Consider the pn junction diode described in Problem 8.33. Plot the diode recombination current and the ideal diode current (on a log scale) versus forward bias voltage over the range 0.1 ≤ V, ≤ 1.0 V.

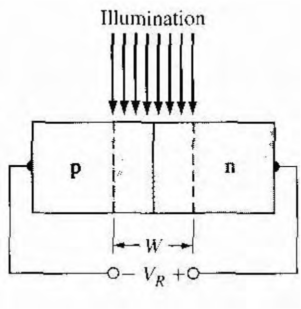

Figure 8.35 | Figure for Problem 8.38 and 8.39.

8.35 A silicon pn junction diode at T $= 300$ K has the following parameters: $N_a = N_d = 10^{16}$ cm^{-3}, $\tau_{p0} = T_{n0} = \tau_0 = 5 \times 10^{-7}$ s, $D_p = 10$ cm^2/s, $D_n = 25$ cm^2/s, and a cross-sectional area of 10^{-4} cm^2. Plot the diode recombination current and the ideal diode current (on a log scale) versus forward bias voltage over the range $0.1 \le V_a \le 0.6$ V.

8.36 Consider a GaAs pn diode at T $= 300$ K with N,, $= N_d = 10^{17}$ cm^{-3} and with a cross-sectional area of 5×10^{-3} cm^2. The minority carrier mobilities are $\mu_n = 3500$ cm^2/V-s and $\mu_p = 220$ cm^2/V-s. The electron-hole lifetimes are $\tau_{n0} = \tau_{p0} = \tau_0 = 10^{-8}$ s. Plot the diode forward-bias current including recombination current between diode voltages of $0.1 \le V_D \le 1.0$ V. Compare this plot to that for an ideal diode.

***8.37** Starting with Equation (8.83) and using the suitable approximations, show that the maximum recombination rate in a forward-biased pn junction is given by Equation (8.91i.

8.38 Consider. as shown in Figure 8.35, a uniformly doped silicon pn junction at $T = 300$ K with impurity doping concentrations of N, $= N_d = 5 \times 10^{15}$ cm^{-3} and minority carrier lifetimes of $\tau_{n0} = \tau_{p0} = \tau_0 = 10^{-7}$ s. A reverse-bias voltageof $V_R = 10$ V is applied. A light source is incident only on the space charge region. producing an excess carrier generation rate of $g' = 4 \times 10^{19}$ cm^{-3} s^{-1}. Calculate the generation current density.

8.39 Along silicon pn junction diode has the following parameters: $N_d = 10^{18}$ cm^{-3}, N,, $= 3 \times 10'''$ cm '. $\tau_{n0} = \tau_{p0} = \tau_0 = 10^{-7}$ s, $D_n = 18$ cm^2/s, and $D_p = 6$ cm^2/s. A light source is incident on the space charge region such as shown in Figure 8.35, producing a generation current density of $J_G = 25$ mA/cm^2. The diode is open circuited. The generation current density forward biases the junction, inducing a forward-bias current in the opposite direction to the generation current. A steady-state condition is reached when the generation current density and forward-bias current density are equal in magnitude. What is the induced forward-bias voltage at this steady-state condition?

Section 8.4 Junction Breakdown

8.40 The critical electric field for breakdown in silicon is approximately $E_{crit} = 4 \times 10^5$ V/cm. Determine the maximum n-type doping concentration in an abrupt p^+n junction such that the breakdown voltage is 30 V.

8.41 Design an abrupt silicon p^+n junction diode that has a reverse breakdown voltage o 120 V and has a forward-bias current of 2 mA at $V = 0.65$ V. Assume that $\tau_{p0} = 10^{-7}$ s, and find μ_p from Figure 5.3.

8.42 Consider an abrupt n^+p GaAs junction with a p-type doping concentration of $N_a = 10^{16}$ cm^{-3}. Determine the breakdown voltage.

8.43 A symmetrically doped silicon pn junction has doping concentrations of $N_a = N_d = 5 \times 10^{16}$ cm^{-3}. If the peak electric field in the junction at breakdown is $E = 4 \times 10^5$ V/cm, determine the breakdown voltage of this junction.

8.44 An abrupt silicon p^+n junction has an n-region doping concentration of $N_d = 5 \times 10^{15}$ cm^{-3}. What must be the minimum n-region width such that avalanche brea down occurs before the depletion region reaches an ohmic contact (punchthrough)?

8.45 A silicon pn junction diode is doped with $N_a = N_d = 10^{18}$ cm^{-3}. Zener breakdown occurs when the peak electric field reaches 10^6 V/cm. Determine the reverse-bias breakdown voltage.

8.46 A diode will very often have the doping profile shown in Figure 7.19, which is known as an n^+pp^+ diode. Under reverse bias, the depletion region must remain within the p region to avoid premature breakdown. Assume the p region doping is 10^{15} cm^{-3}. Determine the reverse-bias voltage such that the depletion region remains within the p region and does not reach breakdown if the p region width is (*a*) 75 μm and (*b*) 150 μm. For each case, state whether the maximum depletion width or the breakdown voltage is reached first.

8.47 Consider a silicon pn junction at $T = 300$ K whose doping profile varies linearly from $N_a = 10^{18}$ cm^{-3} to $N_d = 10^{18}$ cm^{-3} over a distance of 2 μm. Estimate the breakdown voltage.

Section 8.5 Charge Storage and Diode Transients

8.48 (*a*) In switching a pn junction from forward to reverse bias, assume that the ratio of reverse current, I_R, to forward current, I_F, is 0.2. Determine the ratio of storage time to minority carrier lifetime, t_s/τ_{p0}. (*b*) Repeat part (a) if the ratio of I_R to I_F is 1.0.

8.49 A pn junction is switched from forward to reverse bias. We want to specify that $t_s = 0.2\tau_{p0}$. Determine the required ratio of I_R to I_F to achieve this requirement. In this case, determine t_2/τ_{p0}.

8.50 Consider a diode with a junction capacitance of 18 pF at zero bias and 4.2 pF at a reverse bias voltage of $V_R = 10$ V. The minority carrier lifetimes are 10^{-7} s. The diode is switched from a forward bias with a current of 2 mA to a reverse bias voltage of 10 V applied through a 10 kΩ resistor. Estimate the turn-off time.

Section 8.7 The Tunnel Diode

8.51 Consider a silicon pn junction at $T = 300$ K with doping concentration of $N_d = N_a = 5 \times 10^{19}$ cm^{-3}. Assuming the abrupt junction approximation is valid, determine the space charge width at a forward-bias voltage of $V_a = 0.40$ V.

8.52 Sketch the energy-band diagram of an abrupt pn junction under zero bias in which the p region is degenerately doped and $E_C = E_F$ in the n region. Sketch the forward- and reverse-bias current–voltage characteristics. This diode is sometimes called a *back-*

Summary and Review

8.53 *(n)* Explain physically why the diffusion capacitance is not important in a reverse-biased pn junction. *(b)* Consider a silicon. a germanium, and gallium arsenide pn junction. If the total current density is the same in each diode under forward bids, discuss the expected relative values of electron and hole current densities.

***8.54** A silicon pn junction diode at $T = 300$ K is to be designed to have a reverse-bias breakdown voltage of at least 50 V and to handle a forward-bias current of $I_D = 100$ mA while still operating under low injection. The minority carrier diffusion coefficients and lifetimes are $D_n = 25$ cm^2/s, $D_p = 10$ cm^2/s, and $\tau_{n0} = \tau_{p0} = 5 \times 10^{-7}$ s. The diode is to be designed for minimum cross-sectional area.

***8.55** The donor and acceptor concentrations on either side of a silicon step junction are equal. *(a)* Derive an expression for the breakdown voltage in terms of the critical electric field and doping concentration. *(b)* If the breakdown voltage is to be $V_B =$ 50 V. specify the range of allowed doping concentrations.

READING LIST

1. Dimitrijev, S. *Understanding Semiconductor Devices.* New York: Oxford University Press, 2000.
2. Kano, K. *Semiconductor Devices.* Upper Saddle River, NJ: Prentice Hall, 1998.
3. Muller, R. S., and T. I. Kamins. *Device Electronics for Integrated Circuits.* 2nd ed. New York: Wiley. 1986.
4. Neudeck, G. W. *The PN Junction Diode.* Vol. 2 of the *Modular Series on Solid State Devices.* 2nd ed. Reading, MA: Addison-Wesley, 1989.

*5. Ng, K. K. *Complete Guide to Semiconductor Devices.* New York: McGraw-Hill, 1995.

6. Pierret, R. F. *Semiconductor Device Fundamentals.* Reading, MA: Addison-Wesley Publishing Co., 1996.
7. Roulston, D. J. *An Introduction to the Physics of Semiconductor Devices.* New York: Oxford University Press, 1999.
8. Shur, M. *Introduction to Electronic Devices.* New York: John Wiley and Sons, Inc., 1996.

*9. Shur, M. *Physics of Semiconductor Devices.* Englewood Cliffs, NJ: Prentice Hall, 1990.

10. Streetman, B. G., and S. Banerjee. *Solid State Electronic Devices.* 5th ed. Upper Saddle River, NJ: Prentice Hall, 2000.
11. Sze, S. M. *Physics of Semiconductor Devices.* 2nd ed. New York: John Wiley & Sons, 1981.
12. Sze, S. M. *Semiconductor Devices: Physics and Technology.* 2nd ed. New York: John Wiley and Sons, 2001.

*13. Wang. S. *Fundamentals of Semiconductor Theory and Device Physics.* Englewood Cliffs, NJ: Prentice Hall, 1989.

14. Yang, E. S. *Microelectronic Devices.* New York: McGraw-Hill, 1988.

CHAPTER 9

Metal–Semiconductor and Semiconductor Heterojunctions

PREVIEW

In the preceding two chapters, we considered the pn junction and assumed that the semiconductor material was the same throughout the entire structure. This type of junction is referred to as a *homojunction.* We developed the electrostatics of the junction and derived the current-voltage relationship. In this chapter, we will consider the metal-semiconductor junction and the semiconductor heterojunction, in which the material on each side of the junction is not the same. These junctions can also produce diodes.

Semiconductor devices, or integrated circuits, must make contact with the outside world. This contact is made through nonrectifying metal–semiconductor junctions, or *ohmic contacts*. An ohmic contact is a low-resistance junction providing current conduction in both directions. We will examine the conditions that yield metal–semiconductor ohmic contacts..

9.1 | THE SCHOTTKY BARRIER DIODE

One of the first practical semiconductor devices used in the early 1900s was the metal–semiconductor diode. This diode, also called a *point contact diode*, was made by touching a metallic whisker to an exposed semiconductor surface. These metal–semiconductor diodes were not easily reproduced or mechanically reliable and were replaced by the pn junction in the 1950s. However, semiconductor and vacuum technology is now used to fabricate reproducible and reliable metal–semiconductor contacts. In this section, we will consider the metal–semiconductor rectifying contact, or Schottky barrier diode. In most cases, the rectifying contacts are made on n-type semiconductors; for this reason we will concentrate on this type of diode.

9.1.1 Qualitative Characteristics

The ideal energy-band diagram for a particular metal and n-type semiconductor before making contact is shown in Figure 9.1a. The vacuum level is used as a reference level. The parameter ϕ_m is the metal work function (measured in volts), ϕ_s is the semiconductor work function, and χ is known as the ***electron affinity***. The work functions of various metals are given in Table 9.1 and the electron affinities of several semiconductors are given in Table 9.2. In Figure 9.1a, we have assumed that $\phi_m > \phi_s$. The ideal thermal-equilibrium metal–semiconductor energy-band diagram, for this situation, is shown in Figure 9.1b. Before contact, the Fermi level in the semiconductor was above that in the metal. In order for the Fermi level to become a constant through the system in thermal equilibrium, electrons from the semiconductor flow into the lower energy states in the metal. Positively charged donor atoms remain in the semiconductor, creating a space charge region.

The parameter ϕ_{B0} is the ideal barrier height of the semiconductor contact, the potential barrier seen by electrons in the metal trying to move into the semiconductor.

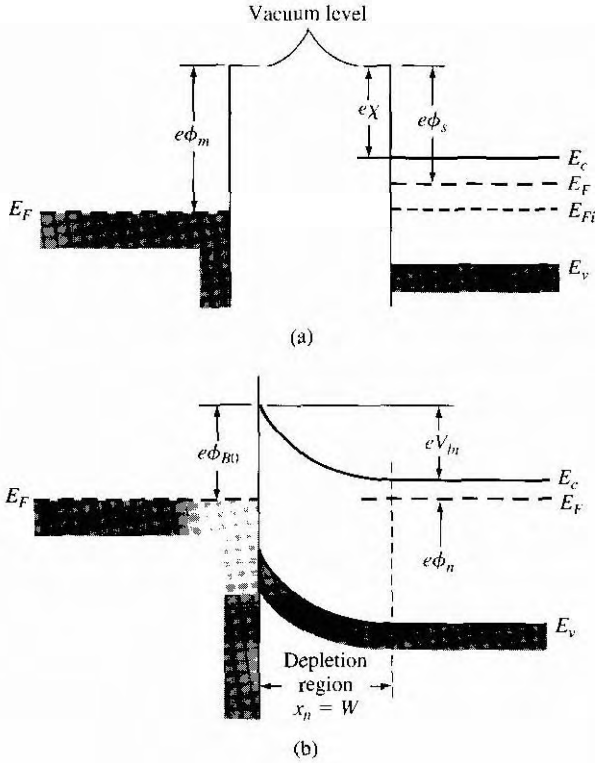

Figure 9.1 | (a) Energy-band diagram of a metal and semiconductor before contact; (b) ideal energy-band diagram of a metal-n-semiconductor junction for $\phi_m > \phi_s$.

Table **9.1** | Work functions of some elements

Element	Work function, ϕ_m
Ag, silver	4.26
Al, aluminum	4.28
Au, gold	5.1
Cr, chromium	4.5
Mo, molybdenum	4.6
Ni, nickel	5.15
Pd, palladium	5.12
Pt, platinum	5.65
Ti, titanium	4.33
W, tungsten	4.55

Table 9.2 | Electron affinity of some semiconductors

Element	Electron affinity, χ
Ge, germanium	4.13
Si, silicon	4.01
GaAs, gallium arsenide	4.07
AlAs, aluminum arsenide	3.5

This barrier is known as the *Schottky* barrier and is given, ideally, by

$$\boxed{\phi_{B0} = (\phi_m - \chi)} \qquad (9.1$$

On the semiconductor side, V_{bi} is the built-in potential barrier. This barrier, similar to the case of the pn junction, is the barrier seen by electrons in the conduction band trying to move into the metal. The built-in potential barrier is given by

$$\boxed{V_{bi} = \phi_{B0} - \phi_n} \qquad (9.2)$$

which makes V_{bi} a slight function of the semiconductor doping, as was the case in a pn junction.

If we apply a positive voltage to the semiconductor with respect to the metal, the semiconductor-to-metal barrier height increases, while ϕ_{B0} remains constant in this idealized case. This bias condition is the reverse bias. If a positive voltage is applied to the metal with respect to the semiconductor, the semiconductor-to-metal barrier V_{bi} is reduced while ϕ_{B0} again remains essentially constant. In this situation, electrons can more easily flow from the semiconductor into the metal since the barrier has been reduced. This bias condition is the forward bias. The energy-band diagrams for the reverse and forward bias are shown in Figures 9.2a and 9.2b, where V_R is the magnitude of the reverse-bias voltage and V_a is the magnitude of the forward-bias voltage.

The energy-band diagrams versus voltage for the metal-semiconductor junction shown in Figure 9.2 are very similar to those of the pn junction given in the last chapter. Because of the similarity, we expect the current–voltage characteristics of the Schottky barrier junction to be similar to the exponential behavior of the pn junction diode. The current mechanism here, however, is due to the flow of majority carrier electrons. In forward bias, the barrier seen by the electrons in the semiconductor is reduced, so majority carrier electrons flow more easily from the semiconductor into the metal. The forward-bias current is in the direction from metal to semiconductor; it is an exponential function of the forward-bias voltage V_a.

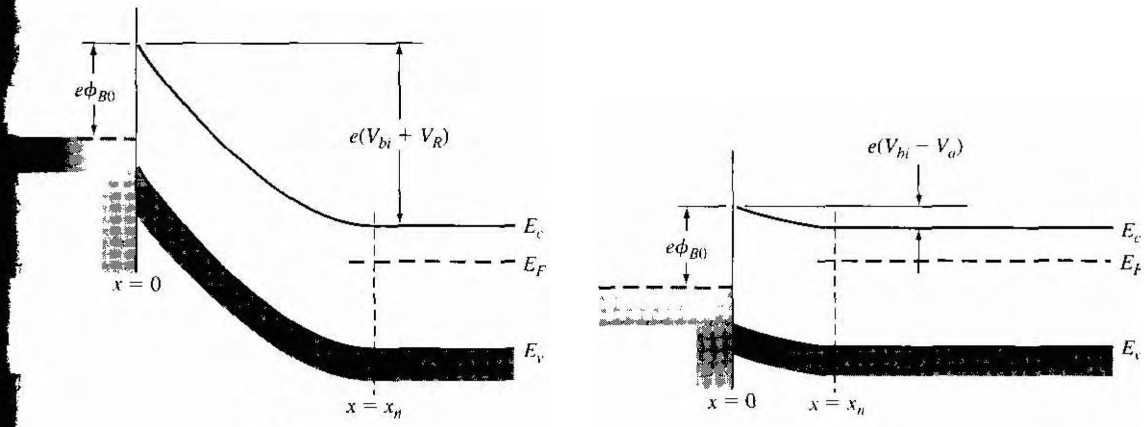

(a) (b)

Figure 9.2 | Ideal energy-band diagram of a metal–semiconductor junction (a) under reverse bias and (b) under forward bias.

9.1.2 Ideal Junction Properties

We can determine the electrostatic properties of the junction in the same way as we did for the pn junction. The electric field in the space charge region is determined from Poisson's equation. We have that

$$\frac{d\mathrm{E}}{dx} = \frac{\rho(x)}{\epsilon_s} \tag{9.3}$$

where $\rho(x)$ is the space charge volume density and ϵ_s is the permittivity of the semiconductor. If we assume that the semiconductor doping is uniform, then by integrating Equation (9.3), we obtain

$$\mathrm{E} = \int \frac{eN_d}{\epsilon_s}\,dx = \frac{eN_d x}{\epsilon_s} + C_1 \tag{9.4}$$

where C_1 is a constant of integration. The electric field is zero at the space charge edge in the semiconductor, so the constant of integration can he found as

$$C_1 = -\frac{eN_d x_n}{\epsilon_s} \tag{9.5}$$

The electric field can then be written as

$$\mathrm{E} = -\frac{eN_d}{\epsilon_s}(x_n - x) \tag{9.6}$$

which is a linear function of distance, for the uniformly doped semiconductor, and reaches a peak value at the metal-semiconductor interface. Since the E-held is zero inside the metal. a negative surface charge must exist in the metal at the metal-semiconductor junction.

The space charge region width, W, may be calculated as we did for the pn junction. The result is identical to that of a one-sided p^+n junction. For the uniformly doped semiconductor, we have

$$\boxed{W = x_n = \left[\frac{2\epsilon_s(V_{bi} + V_R)}{eN_d}\right]^{1/2}}$$

where V_R is the magnitude of the applied reverse-bias voltage. We are again assuming an abrupt junction approximation.

EXAMPLE 9.1

Objective

To calculate the theoretical barrier height, built-in potential barrier, and maximum electric field in a metal-semiconductor diode for zero applied bias.

Consider a contact between tungsten and n-type silicon doped to $N_d = 10^{16}$ cm^{-} at T = 300 K.

■ Solution

The metal work function for tungsten (W) from Table 9.1 is ϕ_m = 4.55 V and the electro affinity for silicon from Table 9.2 is χ = 4.01 V. The barrier height is then

$$= \phi_m - \chi = 4.55 - 4.01 = 0.54 \text{ V}$$

where ϕ_{B0} is the ideal Schottky barrier height. We can calculate ϕ_n as

$$\phi_n = \frac{kT}{e}\ln\left(\frac{N_c}{N_d}\right) = 0.0259 \ln\left(\frac{2.8 \times 10^{19}}{10^{16}}\right) = 0.206 \text{ V}$$

Then

$$V_{bi} = \phi_{B0} - \phi_n = 0.54 - 0.206 = 0.33 \text{ V}$$

The space charge width at zero bias is

$$x_n = \left[\frac{2\epsilon_s V_{bi}}{eN_d}\right]^{1/2} = \left[\frac{2(11.7)(8.85 \times 10^{-14})(0.33)}{(1.6 \times 10^{-19})(10^{16})}\right]^{1/2}$$

or

$$x_n = 0.207 \times 10^{-4} \text{ cm}$$

Then the maximum electric field is

$$|E_{\max}| = \frac{eN_d x_n}{\epsilon_s} = \frac{(1.6 \times 10^{-19})(10^{16})(0.207 \times 10^{-4})}{(11.7)(8.85 \times}$$

or finally

$$|E_{\max}| = 3.2 \times 10^4 \text{ V/cm}$$

■ Comment

The values of space charge width and electric field are very similar to those obtained for a pn junction.

A junction capacitance can also be determined in the same way as we did for the pn junction. We have that

$$C' = eN_d \frac{dx_n}{dV_R} = \left[\frac{e\epsilon_s N_d}{2(V_{bi} + V_R)}\right]^{1/2} \tag{9.8}$$

where C' is the capacitance per unit area. If we square the reciprocal of Equation (9.8), we obtain

$$\left(\frac{1}{C'}\right)^2 = \frac{2(V_{bi} + V_R)}{e\epsilon_s N_d} \tag{9.9}$$

We can use Equation (9.9) to obtain, to a first approximation, the built-in potential barrier V_{bi}, and the slope of the curve from Equation (9.9) to yield the semiconductor doping N_d. We can calculate the potential ϕ_n, and then determine the Schottky barrier ϕ_{B0} from Equation (9.2).

TEST YOUR UNDERSTANDING

E9.1 Consider an ideal chromium-to-n-type silicon Schottky diode at T = 300 K. Assume the semiconductor is doped at a concentration of $N_d = 3 \times 10^{16}$ cm^{-3}. Determine the *(a)* ideal Schottky barrier height, *(b)* built-in potential barrier, *(c)* peak electric field with an applied reverse-bias voltage of $V_R = 5$ V, and *(d)* junction capacitance per unit area for $V_R = 5$ V. [Ans. *(a)* $\phi_{B0} = 0.49$ V, *(b)* $V_{bi} = 0.253$ V, *(c)* $|E_{max}| = 7 \times 10^4$ V/cm, *(d)* $C' = 6.88 \times 10^{-9}$ F/cm^2]

E9.2 Repeat E9.1 for an ideal palladium-to-n-type GaAs Schottky diode with the same impurity concentration. [Ans. *(a)* $\phi_{B0} = 1.05$ V, *(b)* $V_{bi} = 0.919$ V, *(c)* $|E_{max}| = 7 \times 10^4$ V/cm, *(d)* $C' = 6.86 \times 10^{-9}$ F/cm^2]

EXAMPLE 9.2

Objective

To calculate the semiconductor doping and Schottky barrier height from the silicon diode experimental data shown in Figure 9.3. T = 300 K.

■ Solution

The intercept of the tungsten–silicon curve is approximately at $V_{bi} = 0.40$ V. From Equation (9.9), we can write

$$\frac{d(1/C')^2}{dV_R} \approx \frac{\Delta(1/C')^2}{\Delta V_R} = \frac{2}{e\epsilon_s N_d}$$

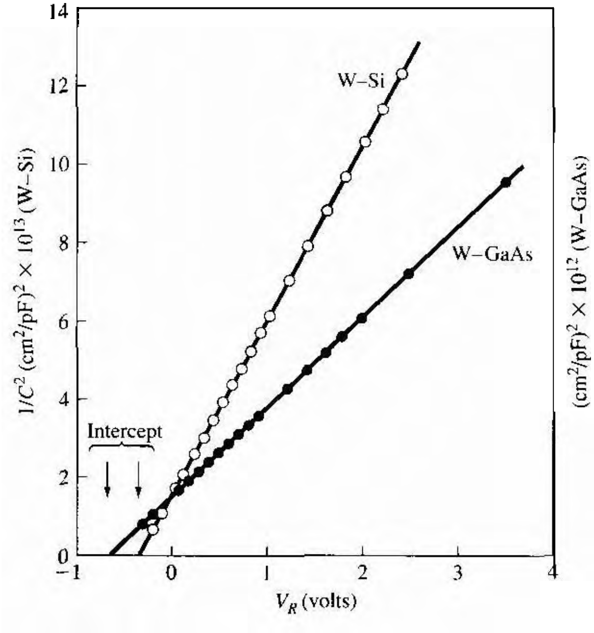

Figure 9.3 | $1/C^2$ versus V_R for W–Si and W–GaAs Schottky barrier diodes.
(From *Sze [14].)*

Then, from the figure, we have

$$\frac{\Delta(1/C')^2}{\Delta V_R} \approx 4.4 \times 10^{13}$$

so that

$$N_d = \frac{2}{(1.6 \times 10^{-19})(11.7)(8.85 \times 10^{-14})(4.4 \times 10^{13})} = 2.7 \times 10^{17} \text{ cm}^{-3}$$

We can calculate

$$\phi_n = \frac{kT}{e} \ln\left(\frac{N_c}{N_d}\right) = (0.0259) \ln\left(\frac{2.8 \times 10^{19}}{2.7 \times 10^{17}}\right) = 0.12 \text{ V}$$

so that

$$\phi_{Bn} = V_{bi} + \phi_n = 0.40 + 0.12 = 0.52 \text{ V}$$

where ϕ_{Bn} is the actual Schottky barrier height,

■ Comment

The experimental value of 0.52 V can be compared with the ideal barrier height of ϕ_{B0} = 0.54 V found in Example 9.1. These results agree fairly well. For other metals, the discrepancy between experiment and theory is larger.

We can see that the built-in potential barrier of the gallium arsenide Schottky diode is larger than that of the silicon diode. This experimental result is normally observed for all types of metal contacts.

9.1.3 Nonideal Effects on the Barrier Height

Several effects will alter the actual Schottky barrier height from the theoretical value given by Equation (9.1). The first effect we will consider is the ***Schottky*** effect, or image-force-induced lowering of the potential barrier.

An electron in a dielectric at a distance x from the metal will create an electric field. The field lines must be perpendicular to the metal surface and will be the same as if an image charge, $+e$, is located at the same distance from the metal surface, but inside the metal. This image effect is shown in Figure 9.4a. The force on the electron, due to the coulomb attraction with the image charge, is

$$F = \frac{-e^2}{4\pi\epsilon_s(2x)^2} = -e\mathrm{E} \tag{9.10}$$

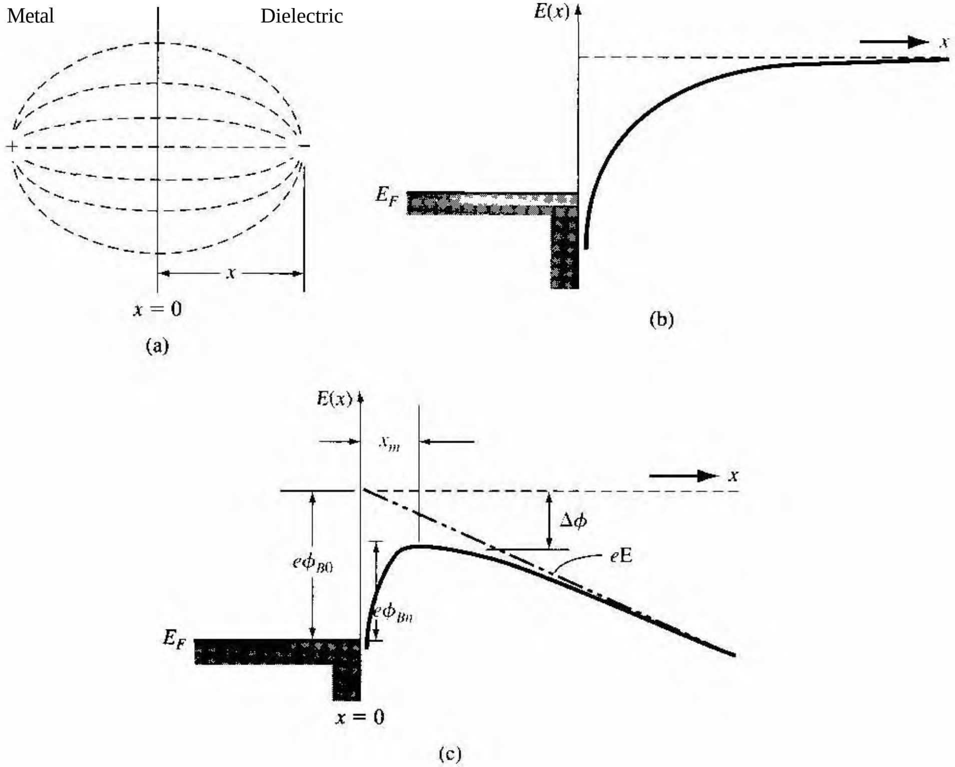

Figure 9.4 | (a) Image charge and electric field lines at a metal–dielectric interface. (b) Distortion of the potential barrier due to image forces with zero electric field and (c) with a constant electric field.

The potential can then be found as

$$-\phi(x) = +\int_x^\infty \mathrm{E}\,dx' = +\int_x^\infty \frac{e}{4\pi\epsilon_s \cdot 4(x')^2}\,dx' = \frac{-e}{16\pi\epsilon_s x} \tag{9.11}$$

where x' is the integration variable and where we have assumed that the potential is zero at $x = \infty$.

The potential energy of the electron is $-e\phi(x)$; Figure 9.4b is a plot of the potential energy assuming that **no** other electric fields exist. With an electric field present in the dielectric, the potential is modified and can be written as

$$-\phi(x) = \frac{-e}{16\pi\epsilon_s x} - \mathrm{E}x \tag{9.12}$$

The potential energy of the electron, including the effect of a constant electric field, is plotted in Figure 9.4c. The peak potential barrier is now lowered. This lowerinpof the potential barrier is the Schottky effect, or image-force-induced lowering.

We can find the Schottky barrier lowering, **A@,** and the position of the maximum barrier, x,,,, from the condition that

$$\frac{d(e\phi(x))}{dx} = 0 \tag{9.13}$$

We find that

$$x_m = \sqrt{\frac{e}{16\pi\epsilon_s \mathrm{E}}} \tag{9.14}$$

and

$$\boxed{\Delta\phi = \sqrt{\frac{e\mathrm{E}}{4\pi\epsilon_s}}} \tag{9.15}$$

EXAMPLE 9.3

Objective

To calculate the Schottky barrier lowering and the position of the maximum barrier height.

Consider a gallium arsenide metal-semiconductor contact in which the electric field in the semiconductoris assumed to be E = 6.8 x 10^4 V/cm.

Solution

The Schottky barrier lowering is given by Equation (9.15). which in this case yields

$$\Delta\phi = \sqrt{\frac{e\mathrm{E}}{4\pi\epsilon_s}} = \sqrt{\frac{(1.6 \times 10^{-19})(6.8 \times \text{lo"})}{4\pi(13.1)(8.85\times 10^{-14})}} = 0.0273\ \mathrm{V}$$

The position of the maximum barrier height is

$$x_m = \sqrt{\frac{e}{16\pi\epsilon_s \mathrm{E}}} = \sqrt{\frac{(1.6\times 10^{-19})}{16\pi(13.1)(8.85\times 10\ {}^{14})(6.8\times 10^4)}}$$

or

$$x_m = 2 \times 10^{-7} \text{ cm} = 20 \text{ Å}$$

■ Comment

Although the Schottky barrier lowering may seem like a small value, the barrier height and the barrier lowering will appear in exponential terms in the current-voltage relationship. A small change in the barrier height can thus have a significant effect on the current in a Schottky barrier diode.

TEST YOUR UNDERSTANDING

E9.3 Determine the Schottky barrier lowering and the position of the maximum barrier height for the junction described in E9.1. Use the value of the electric field found in this exercise. (Ans. $\Delta\phi = 0.0293$ eV, $x_m = 21$ Å)

E9.4 Repeat E9.3 for the junction described in E9.2. (Ans. $\Delta\phi = 0.0278$ V, $x_m = 19.8$ Å)

Figure 9.5 shows the measured barrier heights in gallium arsenide and silicon Schottky diodes as a function of metal work functions. There is a monotonic relation between the measured barrier height and the metal work function, but the curves do not fit the simple relation given in Equation (9.1). The barrier height of the

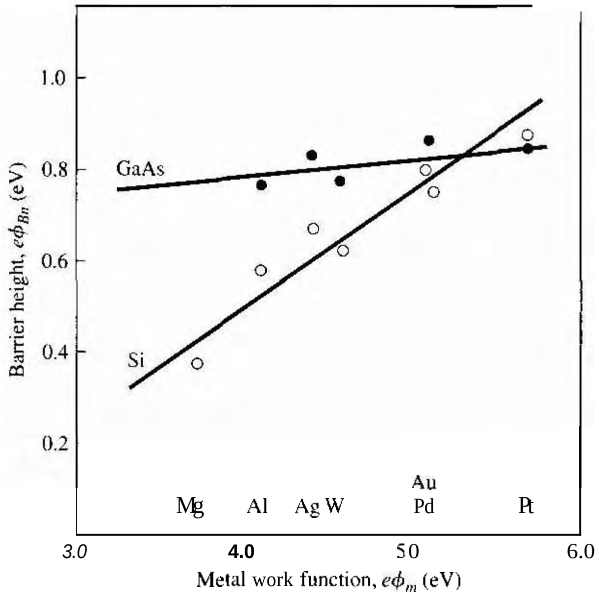

Figure 9.5 | Experimental barrier heights as a function of metal work functions for GaAs and Si.
(From *Crowley and Sze [2].*)

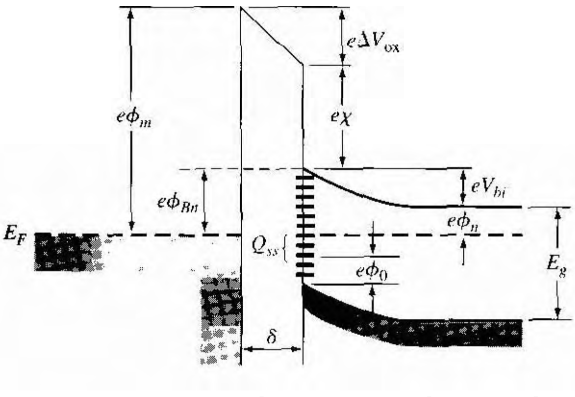

Figure 9.6 | Energy-band diagram of a metal–semiconductor junction with an interfacial layer and interface states.

metal–semiconductor junction is determined by both the metal work function and th semiconductor surface or interface states.

A more detailed energy-band diagram of a metal to n-type semiconductor contac in thermal equilibrium is shown in Figure 9.6. We will assume that a narrow interfaci layer of insulator exists between the metal and semiconductor. The interfacial layer ca support a potential difference, hut will be transparent to the flow of electrons betwee the metal and semiconductor. The semiconductor also shows a distribution of surfac states at the metal–semiconductor interface. We will assume that all states below th surface potential ϕ_0 are donor states, which will be neutral if the state contains an elec tron and positively charged if the slate does not contain an electron. We will also as sume that all states above ϕ_0 are acceptor states, which will be neutral if the state doe not contain an electron and negatively charged if the state contains an electron.

The diagram in Figure 9.6 shows some acceptor states above ϕ_0 and below E_F These states will tend to contain electrons and will be negatively charged. We may assume that the surface state density is constant and equal to D_{it} states/cm^2-eV. Th relation between the surface potential, surface state density, and other semiconducto parameters is found to be

$$(E_g - e\phi_0 - e\phi_{Bn}) = \frac{1}{eD_{it}}\sqrt{2e\epsilon_s N_d(\phi_{Bn} - \phi_n)} - \frac{\epsilon_i}{eD_{it}\delta}[\phi_m - (\chi + \phi_{Bn})] \tag{9.16}$$

We will consider two limiting cases

Case 1 Let $D_{it} \rightarrow \infty$. In this case, the right side of Equation (9.16) goes to zero. We then have

$$\phi_{Bn} = \frac{1}{e}(E_g - e\phi_0) \tag{9.17}$$

The barrier height is now fixed by the bandgap energy and the potential ϕ_0. The bar- rier height is totally independent of the metal work function and the semiconductor electron affinity. The Fermi level becomes "pinned" at the surface, at the surface potential ϕ_0.

Case 2 Let $D_{it}\delta \to 0$. Equation (9.16) reduces to

$$\phi_{Bn} = (\phi_m - \chi)$$

which is the original ideal expression.

The Schottky barrier height is a function of the electric field in the semiconductor through the barrier lowering effect. The barrier height is also a function of the surface states in the semiconductor. The barrier height, then, is modified from the ideal theoretical value. Since the surface state density is not predictable with any degree of certainty. the barrier height must be an experimentally determined parameter.

9.1.4 Current–Voltage Relationship

The current transport in a metal–semiconductor junction is due mainly to majority carriers as opposed to minority carriers in a pn junction. The basic process in the rectifying contact with an n-type semiconductor is by transport of electrons over the potential barrier. which can be described by the thermionic emission theory.

The thermionic emission characteristics arc derived by using the assumptions that the barrier height is much larger than kT, so that the Maxwell–Boltzmann approximation applies and that thermal equilibrium is not affected by this process. Figure 9.7 shows the one-dimensional barrier with an applied forward-bias voltage V_a and shows two electron current density components. The current $J_{s\to m}$ is the electron current density due to the flow of electrons from the semiconductor into the metal, and the current $J_{m\to s}$ is the electron current density due to the flow of electrons from the metal into the semiconductor. The subscripts of the currents indicate the direction of electron How. The conventional current direction is opposite to electron flow.

The current density $J_{s\to m}$ is a function of the concentration of electrons which have x-directed velocities sufficient to overcome the barrier. We may write

$$J_{s\to m} = e\int_{E'_c}^{\infty} v_x \, dn \tag{9.18}$$

where E'_c is the minimum energy required for thertnionic emission into the metal, v_x is the carrier velocity in the direction of transport, and e is the magnitude of the electronic charge. The incremental electron concentration is given by

$$dn = g_c(E) f_F(E)\, dE \tag{9.19}$$

where $g_c(E)$ is the density of states in the conduction band and $f_F(E)$ is the Fermi-Dirac probability function. Assuming that the Maxwell–Boltrmann approximation applies, we may write

$$dn = \frac{4\pi(2m_n^*)^{3/2}}{h^3}\sqrt{E - E_c}\, \exp\left[\frac{-(E - E_F)}{kT}\right] dE \tag{9.20}$$

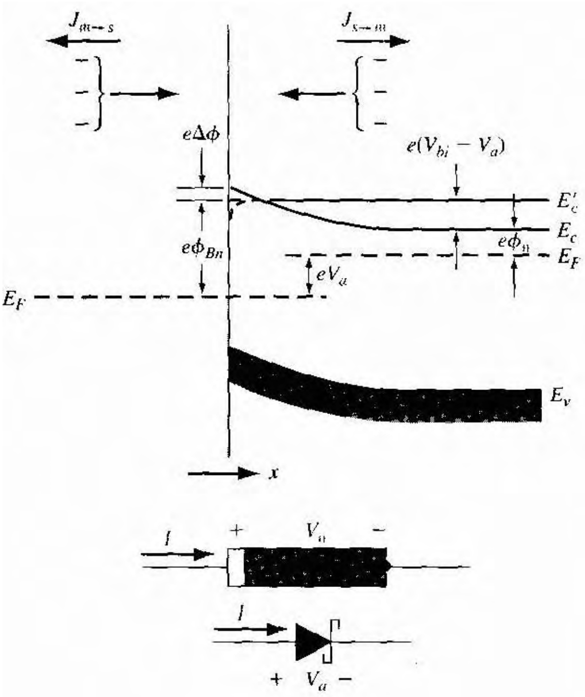

Figure 9.7 | Energy-band diagram of a forward-biased metal-semiconductor junction including the image lowering effect.

If all of the electron energy above E_c is assumed to be kinetic energy, then we hav

$$\frac{1}{2}m_n^* v^2 = E - E_c \qquad (9.21$$

The net current density in the metal-to-semiconductor junction can be written as

$$J = J_{s\to m} - J_{m\to s} \qquad (9.2$$

which is defined to be positive in the direction from the metal to the semiconductor. We find that

$$\boxed{J = \left[A^* T^2 \exp\left(\frac{-e\phi_{Bn}}{kT}\right)\right]\left[\exp\left(\frac{eV_a}{kT}\right) - 1\right]} \tag{9.23}$$

where

$$\boxed{A^* \equiv \frac{4\pi e m_n^* k^2}{h^3}} \tag{9.24}$$

The parameter A* is called the effective Richardson constant for thermionic emission.

Equation (9.23) can be written in the usual diode form as

$$\boxed{J = J_{sT}\left[\exp\left(\frac{eV_a}{kT}\right) - 1\right]} \tag{9.25}$$

where J_{sT} is the reverse-saturation current density and is given by

$$\boxed{J_{sT} = A^*T^2 \exp\left(\frac{-e\phi_{Bn}}{kT}\right)} \tag{9.26}$$

We may recall that the Schottky barrier height ϕ_{Bn} changes because of the image-force lowering. We have that $\phi_{Bn} = \phi_{B0} - \Delta\phi$. Then we can write Equation (9.26) as

$$J_{sT} = A^*T^2 \exp\left(\frac{-e\phi_{B0}}{kT}\right) \exp\left(\frac{e\Delta\phi}{kT}\right) \tag{9.27}$$

The change in barrier height, A@. will increase with an increase in the electric field, or with an increase in the applied reverse-bias voltage. Figure 9.8 shows a typical reverse-bias current-voltage characteristic of a Schottky barrier diode. The reverse-bias current increases with reverse-bias voltage because of the barrier lowering effect. This figure also shows the Schottky barrier diode going into breakdown.

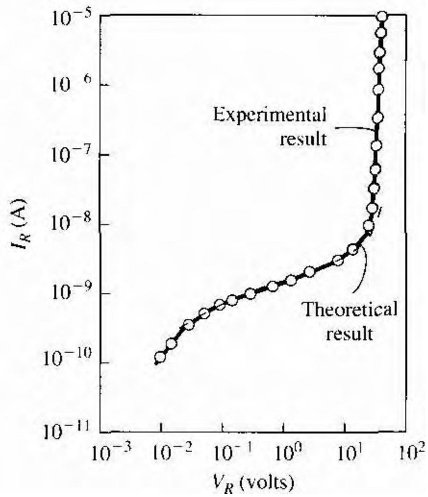

Figure 9.8 | Experimental and theoretical reverse-bias currents in a PtSi–Si diode. *(From Sip [14].)*

EXAMPLE 9.4

Objective

To calculate the effective Richardson constant from the *I–V* characteristics.

Consider the tungsten–silicon diode curve in Figure 9.9 and assume a barrier height of $\phi_{Bn} = 0.67$ V. From the figure, $J_{sT} \approx 6 \times 10^{-5}$ A/cm^2.

■ Solution

We have that

$$J_{sT} = A^* T^2 \exp\left(\frac{-e\phi_{Bn}}{kT}\right)$$

so that

$$A^* = \frac{J_{sT}}{T^2} \exp\left(\frac{+e\phi_{Bn}}{kT}\right)$$

Then

$$A^* = \frac{6 \times 10^{-5}}{(300)^2} \exp\left(\frac{0.67}{0.0259}\right) = 114 \text{ A/K}^2\text{-cm}^2$$

■ Comment

The experimentally determined value of A' is a very strong function of ϕ_{Bn} since ϕ_{Bn} is in the exponential term. A small change in ϕ_{Bn} will change the value of the Richardson constant substantially.

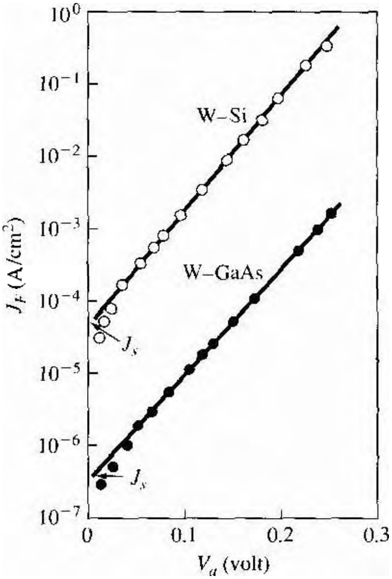

Figure 9.9 | Forward-bias current density J_F versus V„ for Wi–Si and W–GaAs diodes.
(From Sze [14].)

TEST YOUR UNDERSTANDING

E9.5 The Schottky barrier height of a silicon Schottky junction is $\phi_{Bn} = 0.59$ V, the effective Richardson constant is $A^* = 114$ A/K^2-cm^2, and the cross-sectional area is $A = 10^{-4}$ cm^2. For $T = 300$ K, calculate (*a*) the ideal reverse-saturation current and (*b*) the diode current for $V_a = 0.30$ V. [Ans. (*a*) $I_{sT} = 1.31 \times 10^{-7}$ A, (*b*) $I = 14.1$ mA]

We may note that the reverse-saturation current densities of the tungsten–silicon and tungsten–gallium arsenide diodes in Figure 9.9 differ by approximately 2 orders of magnitude. This 2 order of magnitude difference will be reflected in the effective Richardson constant, assuming the barrier heights in the two diodes are essentially the same. The definition of the effective Richardson constant, given by Equation (9.24), contains the electron effective mass, which differs substantially between silicon and gallium arsenide. The fact that the effective mass is in the expression for the Richardson constant is a direct result of using the effective density of states function in the thermionic emission theory. The net result is that A^* and J_{sT} will vary widely between silicon and gallium arsenide.

9.1.5 Comparison of the Schottky Barrier Diode and the pn Junction Diode

Although the ideal current-voltage relationship of the Schottky barrier diode given by Equation (9.25) is of the same form as that of the pn junction diode, there are two important differences between a Schottky diode and a pn junction diode: The first is in the magnitudes of the reverse-saturation current densities, and the second is in the switching characteristics.

The reverse-saturation current density of the Schottky barrier diode was given by Equation **(9.26)** and is

$$J_{sT} = A^* T^2 \exp\left(\frac{-e\phi_{Bn}}{kT}\right)$$

The ideal reverse-saturation current density of the pn junction diode can be written as

$$J_s = \frac{eD_n n_{po}}{L_n} + \frac{eD_p p_{no}}{L_p} \tag{9.28}$$

The form of the two equations is vastly different, and the current mechanism in the two devices is different. The current in a pn junction is determined by the diffusion of minority carriers while the current in a Schottky barrier diode is determined by thermionic emission of majority carriers over a potential barrier.

Objective

EXAMPLE 9.5

To calculate the reverse-saturation current densities of a Schottky barrier diode and a pn junction diode.

Consider a tungsten barrier on silicon with a measured barrier height of $e\phi_{Bn} = 0.67$ eV. The effective Richardson constant is $A^* = 114$ A/K^2-cm^2. Let $T = 300$ K.

Solution

If we neglect the barrier lowering effect, we have for the Schottky barrier diode

$$, \quad = A^*T^2 \exp\left(\frac{-e\phi_{Bn}}{kT}\right) = (114)(300)^2 \exp\left(\frac{-0.67}{0.0259}\right) = 5.98 \text{ x } 10^{-5} \text{ A/cm}^2$$

Consider a silicon pn junction with the following parameters at T = 300 K.

$N_a = 10^{18}$ cm^{-3} $\qquad N_d = 10^{16}$ cm^{-3}

D„ = 10 cm^2/s $\qquad$ D,, = 25 cm'ls

$\tau_{po} = 10^{-7}$ $\qquad \tau_{no} = 10^{-7}$

We can then calculate the following parameters:

$L_p = 1.0 \text{ x } 10^{-3}$ cm $\qquad$ L,, = 1.58 x 10^{-3} cm

$p_{no} = 2.25 \text{ x } 10^4$ cm^{-3} $\qquad$ n,,, = 2.25 x 10^2 cm^{-3}

The ideal reverse-saturation current density of the pn junction diode can be determined from Equation (9.28) as

$$J_s = \frac{(1.6\times10^{-19})(25)(2.25\times10^2)}{(1.58\times10^{-3})} + \frac{(1.6\times10^{-19})(10)(2.25\times10^4)}{(1.0\times10^{-3})}$$

$$= 5.7\times10^{-13} + 3.6\times10^{-11} = 3.66\times10^{-11} \text{ A/cm}^2$$

8 Comment

The ideal reverse-saturation current density of the Schottky barrier junction is orders of magnitude larger than that of the ideal pn junction diode.

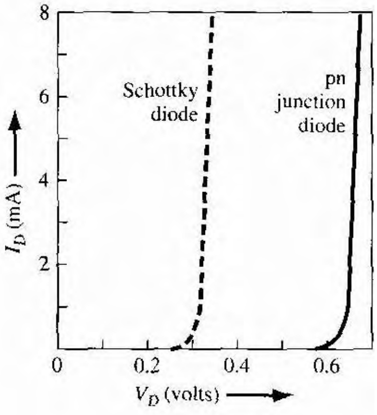

Figure 9.10 | Comparison of forward. bias *I–V* characteristics between a Schottky diode and a pn junction diode.

Recall that the reverse-bias current in a silicon pn junction diode is dominated by the generation current. A typical generation current density is approximately 10^{-7} A/cm^2. which is still 2 to 3 orders of magnitude less than the reverse-saturation current density of the Schottky barrier diode. A generation current also exists in the reverse-biased Schottky barrier diode; however, the generation current is negligible compared with the J_{sT} value.

Since $J_{sT} \gg J_s$, the forward-bias characteristics of the two types of diodes will also be different. Figure 9.10 shows typical I–V characteristics of a Schottky barrier diode and a pn junction diode. The effective turn-on voltage of the Schottky diode is less than that of the pn junction diode.

Objective

EXAMPLE 9.6

To calculate the forward-bias voltage required to generate a forward-bias current density of 10 A/cm^2 in a Schottky barrier diode and a pn junction diode.

Consider diodes with the parameters given in Example 9.5. We can assume that the pn junction diode will be sufficiently forward biased so that the ideal diffusion current will dominate. Let T = 300 K.

■ Solution

For the Schottky barrier diode, we have

$$J = J_{sT}\left[\exp\left(\frac{eV_a}{kT}\right) - 1\right]$$

Neglecting the (−1) term, we can solve for the forward-bias voltage. We find

$$V_a = \left(\frac{kT}{e}\right)\ln\left(\frac{J}{J_{sT}}\right) = V_t \ln\left(\frac{J}{J_{sT}}\right) = (0.0259)\ln\left(\frac{10}{5.98\times10^{-5}}\right) = 0.312\text{ V}$$

For the pn junction diode, we have

$$V_a = V_t \ln\left(\frac{J}{J_s}\right) = (0.0259)\ln\left(\frac{10}{3.66\times10^{-11}}\right) = 0.682\text{ V}$$

■ Comment

A comparison of the two forward-bias voltages shows that the Schottky barrier diode has a turn-on voltage that in this case, is approximately 0.37 V smaller than the turn-on voltage of the pn junction diode:

The actual difference between the turn-on voltages will be a function of the barrier height of the metal–semiconductor contact and the doping concentrations in the pn junction, but the relatively large difference will always be realized. We will consider one application that utilizes the difference in turn-on voltage in the next chapter, in what is referred to as a ***Schottky clamped transistor.***

TEST YOUR UNDERSTANDING

E9.6 (*a*) The reverse saturation currents of a pn junction and a Schottky diode are 10^{-14} A and 10^{-9} A, respectively. Determine the required forward-bias voltages in the pn junction diode and Schottky diode to produce a current of 100 μA in each diode (*b*) Repeat pan (a) for forward bias currents of 1 mA.
[Ans. (*a*) 0.596 V, 0.298 V, (*b*) 0.656 V, 0.358 V]

E9.7 A pn junction diode and a Schottky diode have equal cross-sectional areas and have forward-biased currents of 0.5 mA. The reverse-saturation current of the Schottky diode is 5×10^{-7} A. The difference in forward-bias voltage between the two diodes is 0.30 V Determine the reverse-saturation current of the pn junction diode.
(Ans. 4.66×10^{-12} A)

The second major difference between a Schottky barrier diode and a pn junctio diode is in the frequency response, or switching characteristics. In our discussion, w have considered the current in a Schottky diode as being due to the injection of majority carriers over a potential barrier. The energy-band diagram of Figure 9.1. for exam ple, showed that there can be electrons in the metal directly adjacent to empty states i the semiconductor. If an electron from the valence band of the semiconductor were t flow into the metal, this effect would be equivalent to holes being injected into th semiconductor. This injection of holes would create excess minority carrier holes i the n region. However, calculations as well as measurements have shown that the ratio of the minority carrier hole current to the total current is extremely low in most cases.

The Schottky barrier diode, then, is a majority carrier device. This fact means that there is no diffusion capacitance associated with a forward-biased Schottky diode. The elimination of the diffusion capacitance makes the Schottky diode a higher-frequency device than the pn junction diode. Also, when switching a Schottky diode from forward to reverse bias, there is no minority carrier stored charge to remove, as was the case in the pn junction diode. Since there is no minority carrier storage time, the Schottky diodes can be used in fast-switching applications. A typical switching time for a Schottky diode is in the picosecond range, while for a pn junction it is normally in the nanosecond range.

9.2 | METAL–SEMICONDUCTOR OHMIC CONTACTS

Contacts must be made between any semiconductor device, or integrated circuit, and the outside world. These contacts are made via ohmic *contacts*. Ohmic contacts are metal-to-semiconductor contacts, but in this case they are not rectifying contacts. An ohmic contact is a low-resistance junction providing conduction in both directions between the metal and the semiconductor. Ideally, the current through the ohmic contact is a linear function of applied voltage, and the applied voltage should be very small. Two general types of ohmic contacts are possible: The first type is the ideal nonrectifying barrier, and the second is the tunneling barrier. We will define a specific contact resistance that is used to characterize ohmic contacts.

9.2.1 Ideal Nonrectifying Barriers

We considered an ideal metal-to-n-type semiconductor contact in Figure 9.1 for the case when $\phi_m > \phi_s$. Figure 9.11 shows the same ideal contact for the opposite case of $\phi_m < \phi_s$. In Figure 9.11a we see the energy levels before contact and, in Figure 9.11b, the barrier after contact for thermal equilibrium. To achieve thermal equilibrium in this junction, electrons will flow from the metal into the lower energy states in the semiconductor, which makes the surface of the semiconductor more n type. The excess electron charge in the n-type semiconductor exists essentially as a surface charge density. If a positive voltage is applied to the metal, there is no barrier to electrons flowing from the semiconductor into the metal. If a positive voltage is applied to the semiconductor, the effective barrier height for electrons flowing from the metal into the semiconductor will be approximately $\phi_{Bn} = \phi_n$, which is fairly small for a moderately to heavily doped semiconductor. For this bias condition, electrons can easily flow from the metal into the semiconductor.

Figure 9.12a shows the energy-band diagram when a positive voltage is applied to the metal with respect to the semiconductor. Electrons can easily flow "downhill" from the semiconductor into the metal. Figure 9.12b shows the case when a positive voltage is applied to the semiconductor with respect to the metal. Electrons can easily flow over the barrier from the metal into the semiconductor. This junction, then, is an ohmic contact.

Figure 9.13 shows an ideal nonrectifying contact between a metal and a p-type semiconductor. Figure 9.13a shows the energy levels before contact for the case when $\phi_m > \phi_s$. When contact is made, electrons from the semiconductor will flow into the metal to achieve thermal equilibrium, leaving behind more empty states, or holes. The excess concentration of holes at the surface makes the surface of the semiconductor more p type. Electrons from the metal can readily move into the empty states in the semiconductor. This charge movement corresponds to holes flowing

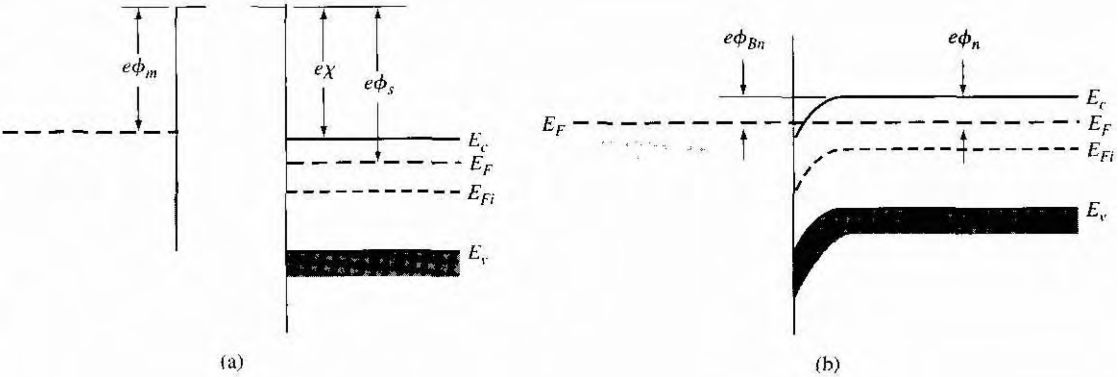

Figure 9.11 | Ideal energy-band diagram (a) before contact and (b) after contact for a metal–n-semiconductor junction for $\phi_m < \phi_s$

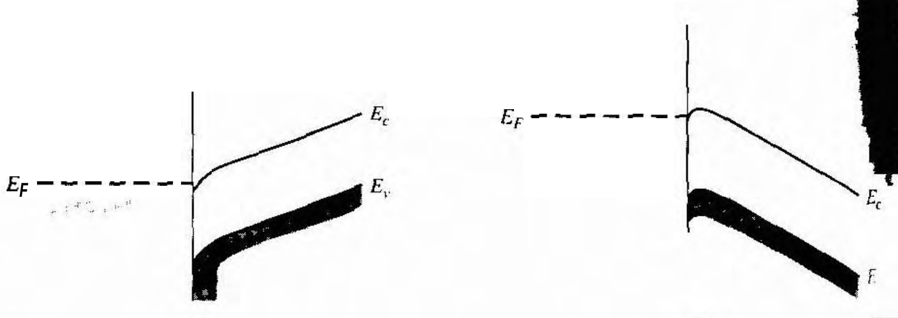

(a) (b)

Figure 9.12 | Ideal energy-band diagram of a metal–n-semiconductor ohmic contact (a) wit a positive voltage applied to the metal and (b) with a positive voltage applied to the semiconductor.

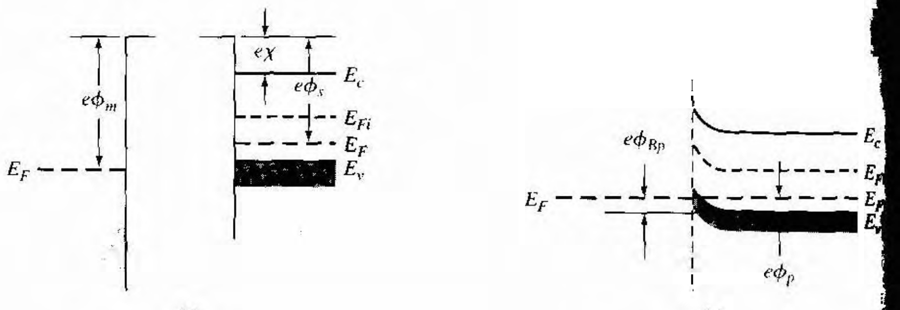

(a) (b)

Figure **9.13** | Ideal energy-band diagram (a) before contact and (b) after contact for a metal–p-semiconductor junction for $\phi_m > \phi_s$

from the semiconductor into the metal. We can also visualize holes in the metal flowing into the semiconductor. This junction is also an ohmic contact.

The ideal energy bands shown in Figures 9.11 and 9.13 do not take into account the effect of surface states. If we assume that acceptor surface states exist in the upper half of the semiconductor bandgap, then, since all the acceptor states are below E_F for the case shown in Figure 9.11b, these surface states will be negatively charged, and will alter the energy-band diagram. Similarly, if we assume that donor surface states exist in the lower half of the bandgap, then all of the donor states will be positively charged for the case shown in Figure 9.13b; the positively charged surface states will also alter this energy-band diagram. Therefore, if $\phi_m < \phi_s$ for the metal–n-type semiconductor contact, and if $\phi_m > \phi_s$ for the metal–p-type semiconductor contact. we may not necessarily form a good ohmic contact.

9.2.2 Tunneling Barrier

The space charge width in a rectifying metal–semiconductor contact is inversely proportional to the square root of the semiconductor doping. The width of the depletion

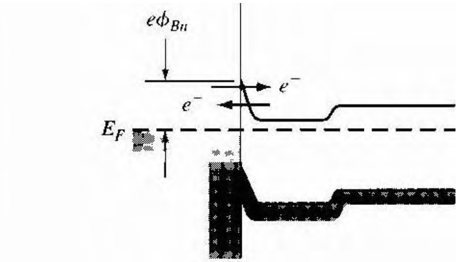

Figure 9.14 | Energy-band diagram of a heavily doped n-semiconductor-to-metal Junction.

region decreases as the doping concentration in the semiconductor increases; thus, as the doping concentration increases, the probability of tunneling through the barrier increases. Figure 9.14 shows a junction in which the metal is in contact with a heavily doped n-type epitaxial layer.

Objective **EXAMPLE 9.7**

calculate the space charge width for a Schottky barrier on a heavily doped semiconductor.

Consider silicon at T = 300K doped at $N_d = 7 \times 10^{18}$ cm^{-3}. Assume a Shottky barrier with $\phi_{Bn} = 0.67$ V. For this case. we can assume that $V_{bi} \approx \phi_{B0}$. Neglect the barrier lowering effect.

■ Solution

From Equation (9.7). we have for zero applied bias

$$x_n = \left[\frac{2\epsilon_s V_{bi}}{eN_d}\right]^{1/2} = \left[\frac{2(11.7)(8.85 \times 10^{-14})(0.67)}{(1.6 \times 10^{-19})(7 \times 10^{18})}\right]^{1/2}$$

$$x_n = 1.1 \times 10^{-6} \text{ cm} = 110 \text{ Å}$$

Comment

In a heavily doped semiconductor. the depletion width is on the order of angstroms, so that tunneling is now a distinct possibility. For these types of barrier widths, tunneling may become the dominant current mechanism.

The tunneling current has the form

$$J_t \propto \exp\left(\frac{-e\phi_{Bn}}{E_{oo}}\right) \tag{9.29}$$

where

$$E_{oo} = \frac{e\hbar}{2}\sqrt{\frac{N_d}{\epsilon_s m_n^*}} \tag{9.30}$$

The tunneling current increases exponentially with doping concentration

9.2.3 Specific Contact Resistance

A figure of merit of ohmic contacts is the specific contact resistance. R_c. This parameter is defined as the reciprocal of the derivative of current density with respect t voltage evaluated at zero bias. We may write

$$R_c = \left(\frac{\partial J}{\partial V}\right)^{-1}\Bigg|_{V=0} \qquad \Omega\text{-cm}^2 \tag{9.31}$$

We want R_c to be as small as possible for an ohmic contact.

For a rectifying contact with a low to moderate semiconductor doping concentration, the current–voltage relation was given by Equation (9.23) as

$$J_n = A^*T^2 \exp\left(\frac{-e\phi_{Bn}}{kT}\right)\left[\exp\left(\frac{eV}{kT}\right) - 1\right]$$

The thermionic emission current is dominant in this junction. The specific contact resistance for this case is then

$$R_c = \frac{\left(\dfrac{kT}{e}\right)\exp\left(\dfrac{+e\phi_{Bn}}{kT}\right)}{A^*T^2} \tag{9.32}$$

The specific contact resistance decreases rapidly as the barrier height decreases.

For a metal–semiconductor junction with a high impurity doping concentration, the tunneling process will dominate. From Equations (9.29) and (9.30), the specific contact resistance is found to be

$$R_c \propto \exp\left[\frac{+2\sqrt{\epsilon_s m_n^*}}{\hbar}\cdot\frac{\phi_{Bn}}{\sqrt{N_d}}\right] \tag{9.33}$$

which shows that the specific contact resistance is a very strong function of semiconductor doping.

Figure 9.15 shows a plot of the theoretical values of R_c as a function of semiconductor doping. For doping concentrations greater than approximately 10^{19} cm^{-3}, the tunneling process dominates and R_c shows the exponential dependence on N_d. For lower doping concentrations, the R_c values are dependent on the barrier heights and become almost independent of the doping. Also shown in the figure are experimental data for platinum silicide–silicon and aluminum–silicon junctions.

Equation (9.33) is the specific contact resistance of the tunneling junction, which corresponds to the metal-to-n$^+$ contact shown in Figure 9.14. However, the n$^+$n junction also has a specific contact resistance, since there is a barrier associated with this junction. For a fairly low doped n region, this contact resistance may actually dominate the total resistance of the junction.

The theory of forming ohmic contacts is straightforward. To form a good ohmic contact, we need to create a low barrier and use a highly doped semiconductor at the surface. However, the actual technology of fabricating good, reliable ohmic contacts is not as easy in practice as in theory. It is also more difficult to fabricate good ohmic

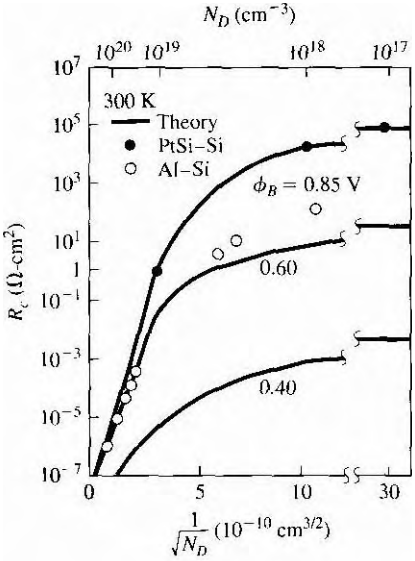

Figure 9.15 | Theoretical and experimental specific contact resistance as a function of doping.
(From Sze [14].)

contacts on wide-bandgap materials. In general, low barriers are not possible on these materials, so a heavily doped semiconductor at the surface must be used to form a tunneling contact. The formation of a tunneling junction requires diffusion, ion implantation, or perhaps epitaxial growth. The surface doping concentration in the semiconductor may be limited to the impurity solubility, which is approximately 5×10^{19} cm^{-3} for n-type GaAs. Nonuniformities in the surface doping concentration may also prevent the theoretical limit of the specific contact resistance from being reached. In practice, a good deal of empirical processing is usually required before a good ohmic contact is obtained.

9.3 | HETEROJUNCTIONS

In the discussion of pn junctions in the previous chapters, we assumed that the semiconductor material was homogeneous throughout the entire structure. This type of junction is called a ***homojunction.*** When two different semiconductor materials are used to form a junction, the junction is called a ***semiconductor heterojunction.***

As with many topics in this text, our goal is to provide the basic concepts concerning the heterojunction. The complete analysis of heterojunction structures involves quantum mechanics and detailed calculations that are beyond the scope of this text. The discussion of heterojunctions will, then, be limited to the introduction of some basic concepts.

9.3.1 Heterojunction Materials

Since the two materials used to form a heterojunction will have different energ bandgaps, the energy band will have a discontinuity at the junction interface. We ma have an abrupt junction in which the semiconductor changes abruptly from a narrow bandgap material to a wide-bandgap material. On the other hand, if we have GaAs–$Al_xGa_{1-x}As$ system, for example, the value of x may continuously vary ov distance of several nanometers to form a graded heterojunction. Changing the value of x in the $Al_xGa_{1-x}As$ system allows us to engineer, or design, the bandgap energy.

In order to have a useful heterojunction, the lattice constants of the two materials must be well matched. The lattice match is important because any lattice mismatch can introduce dislocations resulting in interface states. For example, germanium and gallium arsenide have lattice constants matched to within approximately 0.13 percent. Germanium–gallium arsenide heterojunctions have been studied quite extensively. More recently, gallium arsenide–aluminum gallium arsenide (GaAs–AlGaAs) junctions have been investigated quite thoroughly. since the lattice constants of GaAs and the AlGaAs system vary by no more than 0.14 percent.

9.3.2 Energy-Band Diagrams

In the formation of a heterojunction with a narrow-bandgap material and a wide-bandgap material. the alignment of the bandgap energies is important in determining the characteristics of the junction. Figure 9.16 shows three possible situations. In Figure 9.16a we see the case when the forbidden bandgap of the wide-gap material completely overlaps the bandgap of the narrow-gap material. This case, called *straddling*, applies to most heterojunctions. We will consider only this case here. The other possibilities are called ***staggered*** and *broken gap* and are shown in Figures 9.16b and 9.16c.

There are four basic types of heterojunction. Those in which the dopant type changes at the junction are called *anisotype*. We can form nP or Np junctions, where the capital letter indicates the larger-bandgap material. Heterojuncrions with the same dopant type on either side of the junction are called *isotype*. We can form nN and isotype heterojunctions.

Figure 9.17 shows the energy-band diagrams of isolated n-type and P-type materials, with the vacuum level used as a reference. The electron affinity of the

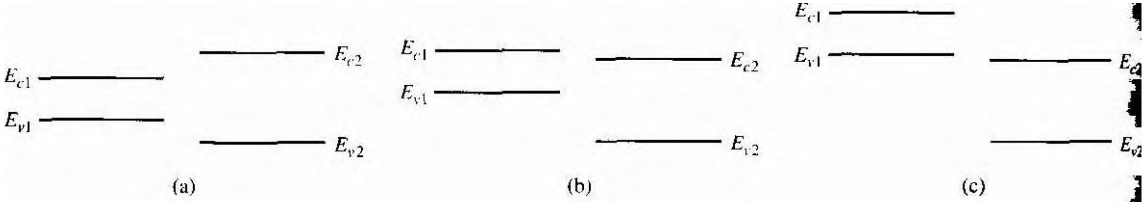

Figure 9.16 | Relation between narrow-bandgapand wide-bandgap energies: (a) straddling, (b) staggered, and (c) broken gap.

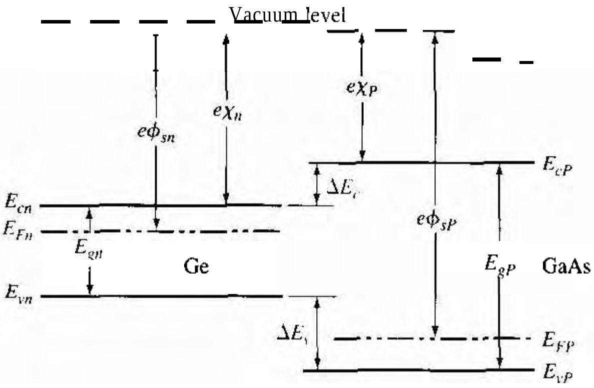

Figure 9.17 I Energy-band diagrams of a narrow-bandgep and a wide-bandgap material before contact.

wide-bandgap material is less than that of the narrow-bandgap material. The difference between the two conduction band energies is denoted by *AE,,* and the difference between the two valence band energies is denoted by AE,. From Figure 9.17. we can see that

$$\Delta E_c = e(\chi_n - \chi_P) \tag{9.34a}$$

$$\Delta E_c + \Delta E_v = E_{gP} - E_{gn} = \Delta E_g \tag{9.34b}$$

In the ideal abrupt heterojunction using nondegenerately doped semiconductors, the vacuum level is parallel to both conduction bands and valence bands. If the vacuum level is continuous, then the same *AE,* and *AE,* discontinuities will exist at the heterojunction interface. This ideal situation is known as the ***electron affinity rule.*** There is still some uncertainty about the applicability of this rule, but it provides a good starting point for the discussion of heterojunctions.

Figure 9.18 shows a general ideal nP heterojunction in thermal equilibrium. In order for the Fermi levels in the two materials to become aligned, electrons from the narrow-gap n region and holes from the wide-gap P region must flow across the junction. As in the case of a homojunction, this flow of charge creates a space charge region in the vicinity of the metallurgical junction. The space charge width into the n-type region is denoted by x,, and the space charge width into the P-type region is denoted by x_P. The discontinuities in the conduction and valence bands and the change in the vacuum level are shown in the figure.

9.3.3 Two-Dimensional Electron Gas

Before we consider the electrostatics of the heterojunction, we will discuss a unique characteristic of an isotype junction. Figure 9.19 shows the energy-band diagram of an nN GaAs–AlGaAs heterojunction in thermal equilibrium. The AlGaAs can he moderetely to heavily doped n type, while the GaAs can be more lightly doped or

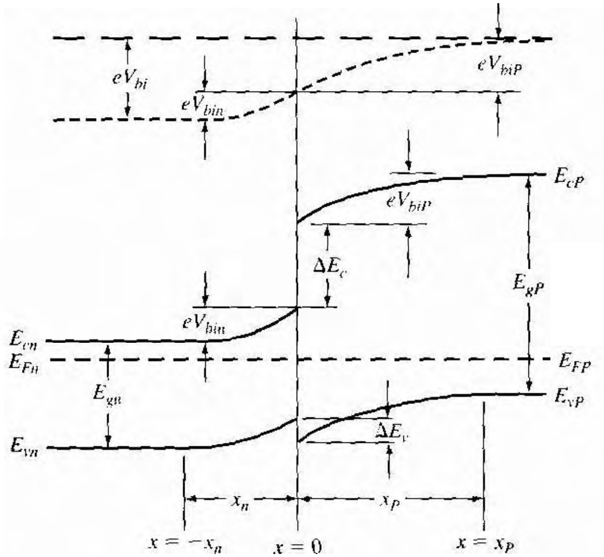
eV_{bi}
eV_{bin}
eV_{biP}
E_{cP}
eV_{biP}
ΔE_c
E_{gP}
eV_{bin}
E_{cn}
E_{Fn}
E_{FP}
E_{gn}
E_{vP}
ΔE_v
E_{vn}
x_n
x_p
$x = -x_n$
$x = 0$
$x = x_p$

Figure 9.18 | Ideal energy-band diagram of an nP heterojunction in thermal equilibrium.

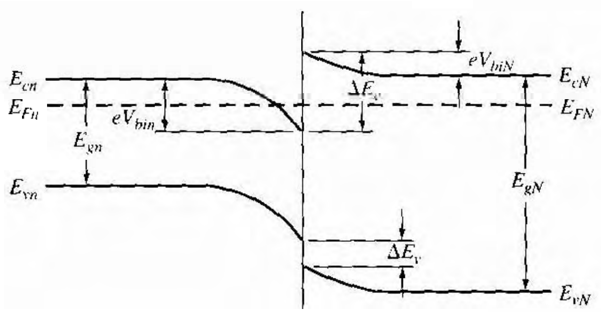
eV_{biN}
E_{cN}
E_{cn}
E_{Fn}
ΔE_c
E_{FN}
eV_{bin}
E_{gn}
E_{vn}
E_{gN}
ΔE_v
E_{vN}

Figure 9.19 | Ideal energy-hand diagram of an nN heterojunction in thermal equilibrium.

even intrinsic. As mentioned previously. to achieve thermal equilibrium, electron from the wide-bandgap AlGaAs flow into the GaAs. forming an accumulation laye of electrons in the potential well adjacent to the interface. One basic quantum-mechanical result that we have found previously is that the energy of an electron contained in a potential well is quantized. The phrase *two-dimensional electron gas* refers to the condition in which the electrons have quantized energy levels in one spatial direction (perpendicular to the interface), but are free to move in the other two spatial directions.

The potential function near the interface can be approximated by a triangular potential well. Figure 9.20a shows the conduction band edges near the abrupt junction

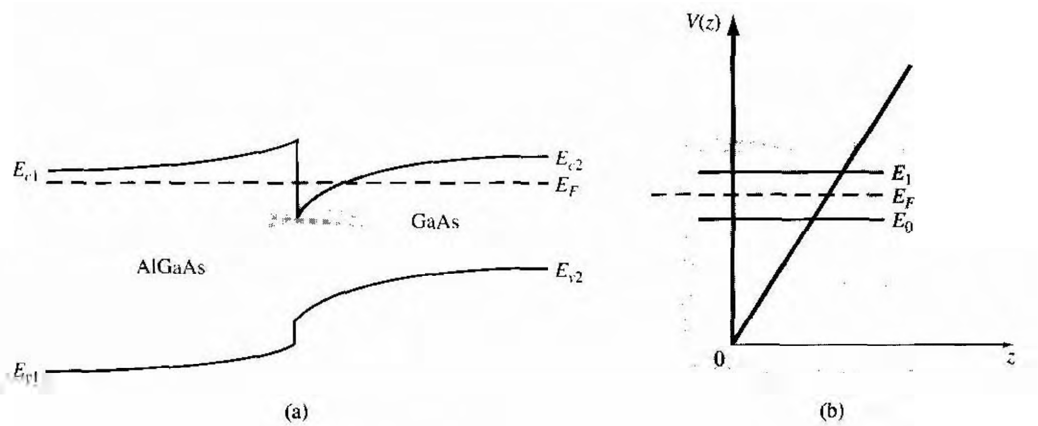

Figure 9.20 | (a) Conduction-band edge at N-AlGaAs, n-GaAs heterojunction; (b) triangular well approximation with discrete electron energies.

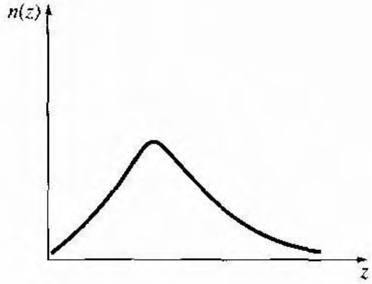

Figure 9.21 | Electron density in triangular potential well.

interface and Figure 9.20b shows the approximation of the triangular potential well. We can write

$$V(x) = e\mathrm{E}z \qquad z > 0 \tag{9.35a}$$

$$V(z) = \infty \qquad z < 0 \tag{9.35b}$$

Schrodinger's wave equation can be solved using this potential function. The quantized energy levels are shown in Figure 9.20b. Higher energy levels are usually not considered.

The qualitative distribution of electrons in the potential well is shown in Figure 9.21. A current parallel to the interface will be a function of this electron concentration and of the electron mobility. Since the GaAs can be lightly doped or intrinsic, the two-dimensional electron gas is in a region of low impurity doping so that impurity scattering effects are minimized. The electron mobility will be much larger than if the electrons were in the same region as the ionized donors.

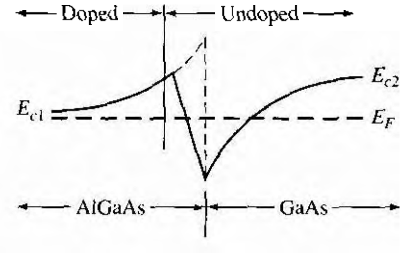

Figure 9.22 | Conduction-hand edge at a graded heterojunction.

The movement of the electrons parallel to the interface will still be influenced by the coulomb attraction of the ionized impurities in the AlGaAs. The effect of these forces can be further reduced by using a graded AlGaAs–GaAs heterojunction. The graded layer is $Al_xGa_{1-x}As$ in which the mole fraction x varies with distance. In this case, an intrinsic layer of graded AlGaAs can be sandwiched between the N-type AlGaAs and the intrinsic GaAs. Figure 9.22 shows the conduction-band edges across a graded AlGaAs–GaAs heterojunction in thermal equilibrium. The electrons in the potential well are further separated from the ionized impurities so that the electron mobility is increased above that in an abrupt heterojunction.

*9.3.4 Equilibrium Electrostatics

We will now consider the electrostatics of the nP heterojunction that was shown in Figure 9.18. As in the case of the homojunction, potential differences exist across the space charge regions in both the n region and the P region. These potential differences correspond to the built-in potential barriers on either side of the junction. The built-in potential barrier for this ideal case is defined as shown in Figure 9.18 to be the potential difference across the vacuum level. The built-in potential barrier is the sum of the potential differences across each of the space charge regions. The heterojunction built-in potential barrier, however, is not equal to the difference between the conduction bands across the junction or the difference between the valence bands across the junction, as we defined for the homojunction.

Ideally, the total built-in potential barrier V_{bi} can be found as the difference between the work functions, or

$$V_{bi} = \phi_{sP} - \phi_{sn} \tag{9.36}$$

Equation (9.36). from Figure 9.17, can be written as

$$eV_{bi} = [e\chi_P + E_{gP} - (E_{FP} - E_{vP})] - [e\chi_n + E_{gn} - (E_{Fn} - E_{vn})] \tag{9.37a}$$

or

$$eV_{bi} = e(\chi_P - \chi_n) + (E_{gP} - E_{gn}) + (E_{Fn} - E_{vn}) - (E_{FP} - E_{vP}) \tag{9.37b}$$

which can be expressed as

$$eV_{bi} = -\Delta E_c + \mathrm{AE}, + kT \ln\left(\frac{N_{vn}}{p_{no}}\right) - kT \ln\left(\frac{N_{vP}}{p_{po}}\right) \tag{9.38}$$

Finally, we can write Equation (9.38) as

$$eV_{bi} = \Delta E_v + kT \ln\left(\frac{p_{po}}{p_{no}} \cdot \frac{N_{vn}}{N_{vP}}\right) \tag{9.39}$$

where p_{po} and p,,, are the hole concentrations in the P and n materials, respectively, and N,,,and N_{vP} are the effective density of states functions in the n and P materials, respectively. We could also obtain an expression for the built-in potential barrier in terms of the conduction band shift as

$$eV_{bi} = -\Delta E_c + kT \ln\left(\frac{n_{no}}{n_{po}} \cdot \frac{N_{cP}}{N_{cn}}\right) \tag{9.40}$$

EXAMPLE 9.8

Objective

To determine **AE,. A t,.** and V_{bi} for an n–Ge to P–GaAs heterojunction using the electron affinity rule.

Consider n-type Ge doped with $N_d = 10^{16}$ cm^{-3} and P-type GaAs doped with N„ = 10^{16} cm^{-3}. Let $T = 300$ K so that $n_i = 2.4 \times 10^{13}$ cm^{-3} for Ce.

■ Solution

From Equation (9.34a), we have

$$\mathbf{AE,} = e(\chi_n - \chi_P) = e(4.13 - 4.07) = 0.06 \text{ eV}$$

and from Equation (9.34b), we have

$$\mathbf{AE,} = \Delta E_g - \mathbf{AE,} = (1.43 - 0.67) - 0.06 = 0.70 \text{ eV}$$

To determine V_{bi} using Equation (9.39), we need to determine p_{no} in Ge. or

$$p_{no} = \frac{}{N_d} = \frac{(2.4 \text{ x } 10'')'}{10^{16}} = 5.76 \times 10^{10} \text{ cm}^{-3}$$

$$eV_{bi} = 0.70 + (0.0259) \ln\left[\frac{(10^{16})(6 \times 10^{18})}{(5\,76 \times 10^{10})(7 \times 10^{18})}\right]$$

or, finally.

$$V_{bi} \approx 1.0 \text{ V}$$

■ Comment

There is a nonsymmetry in the AE, and **AE,** values that will tend to make the potential barriers seen by electrons and holes different. This nonsymmetry does not occur in homojunctions.

We can determine the electric field and potential in the junction from Poisson's equation in exactly the same way as we did for the homojunction. For homogeneous doping on each side of the junction, we have in the n region

$$\mathrm{E}_n = \frac{eN_{dn}}{\epsilon_n}(x_n + x) \qquad (-x_n \le x < 0) \tag{9.41}$$

and in the P region

$$Ep = \frac{eN_{aP}}{\epsilon_P}(x_P - x) \qquad (0 < x \le x_P) \tag{9.41b}$$

where ϵ_n and ϵ_P are the permittivities of the n and P materials, respectively. We may note that $\mathrm{E}_n = 0$ at $x = -x_n$ and $Ep = 0$ at $x = x_P$. The electric *flux* density D i continuous across the junction, so

$$\epsilon_n \mathrm{E}_n(x = 0) = \epsilon_P \mathrm{E}_P(x = 0) \tag{9.42a}$$

which gives

$$N_{dn}x_n = N_{aP}x_P \tag{9.42b}$$

Equation (9.42b) simply states that the net negative charge in the P region is equal to the net positive charge in the n region—the same condition we had in a pn homojunction. We are neglecting any interface states that may exist at the heterojunction.

The electric potential can be found by integrating the electric field through the space charge region so that the potential difference across each region can then be determined. We find that

$$V_{bin} = \frac{eN_{dn}x_n^2}{2\epsilon_n} \tag{9.43a}$$

and

$$V_{biP} = \frac{eN_{aP}x_P^2}{2\epsilon_P} \tag{9.43b}$$

Equation (9.42b) can be rewritten as

$$\frac{x_n}{x_P} = \frac{N_{aP}}{N_{dn}} \tag{9.44}$$

The ratio of the built-in potential baniers can then be determined as

$$\frac{V_{bin}}{V_{biP}} = \frac{\epsilon_P}{\epsilon_n} \cdot \frac{N_{dn}}{N_{aP}} \cdot \frac{x_n^2}{x_P^2} = \frac{\epsilon_P N_{aP}}{\epsilon_n N_{dn}} \tag{9.45}$$

Assuming that ϵ_n and cp are of the same order of magnitude, the larger potential difference is across the lower-doped region.

The total built-in potential barrier is

$$V_{bi} = V_{bin} + V_{biP} = \frac{eN_{dn}x_n^2}{2\epsilon_n} + \frac{eN_{aP}x_P^2}{2\epsilon_P} \tag{9.46}$$

If we solve for x_P, for example, from Equation (9.42b) and substitute into Equation (9.46), we can solve for **x,,** as

$$x_n = \left\{ \frac{2\epsilon_n \epsilon_P N_{aP} V_{bi}}{eN_{dn}(\epsilon_n N_{dn} + \epsilon_P N_{aP})} \right\}^{1/2} \tag{9.47a}$$

We can also find

$$x_P = \left\{ \frac{2\epsilon_n \epsilon_P N_{dn} V_{bi}}{eN_{aP}(\epsilon_n N_{dn} + \epsilon_P N_{aP})} \right\}^{1/2} \tag{9.47b}$$

The total depletion width is found to be

$$W = x_n + x_P = \left\{ \frac{2\epsilon_n \epsilon_P (N_{dn} + N_{aP})^2 V_{bi}}{eN_{dn} N_{aP}(\epsilon_n N_{dn} + \epsilon_P N_{aP})} \right\}^{1/2} \tag{9.48}$$

If a reverse-bias voltage is applied across the heterojunction, the same equations apply if V_{bi} is replaced by $V_{bi} + V_R$. Similarly, if a forward bias is applied, the same equations also apply if V_{bi} is replaced by $V_{bi} - V_a$. As before, V_R is the magnitude of the reverse-bias voltage and V_a is the magnitude of the forward-bias voltage.

As in the case of a homojunction, a change in depletion width with a change in junction voltage yields a junction capacitance. We can find for the nP junction

$$C'_j = \left\{ \frac{eN_{dn} N_{aP} \epsilon_n \epsilon_P}{2(\epsilon_n N_{dn} + \epsilon_P N_{aP})(V_{bi} + V_R)} \right\}^{1/2} \quad (\text{F/cm}^2) \tag{9.49}$$

A plot of $(1/C'_j)^2$ versus V_R again yields a straight line. The extrapolation of this plot of $(1/C'_j)^2 = 0$ is used to find the built-in potential barrier, V_{bi}.

Figure 9.18 showed the ideal energy-band diagram for the nP abrupt heterojunction. The experimentally determined values of ΔE_c and $AE,$ may differ from the ideal values determined using the electron affinity rule. One possible explanation for this difference is that most heterojunctions have interface states. If we assume that the electrostatic potential is continuous through the junction, then the electric flux density will be discontinuous at the heterojunction due to the surface charge trapped in the interface states. The interface states will then change the energy-band diagram of the semiconductor heterojunction just as they changed the energy-band diagram of the metal-semiconductor junction. Another possible explanation for the deviation from the ideal is that as the two materials are brought together to form the heterojunction, the electron orbitals of each material begin to interact with each other, resulting in a transition region of a few angstroms at the interface. The energy bandgap is then continuous through this transition region and not a characteristic of either material. However. we still have the relation that

$$\Delta E_c + \Delta E_v = AE, \tag{9.50}$$

for the straddling type of heterojunction, although the ΔE_c and $AE,$ values may differ from those determined from the electron affinity rule.

We may consider the general characteristics of the energy-band diagrams of the other types of heterojunction. Figure 9.23 shows the energy-band diagram of an Np

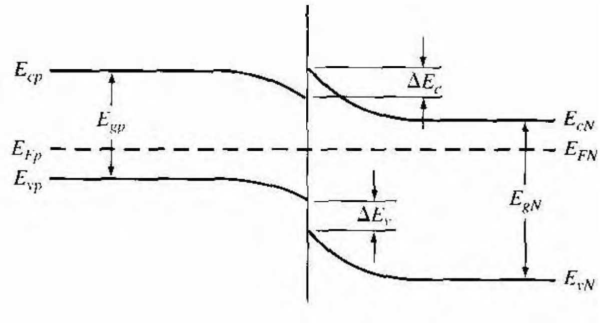

Figure 9.23 | Ideal energy-band diagram of an Np heterojunction in thermal equilibrium.

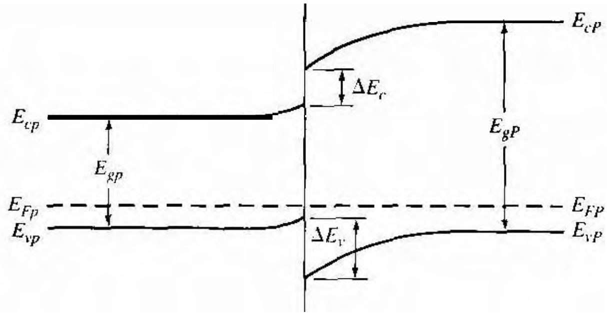

Figure 9.21 | Ideal energy-band diagram of a pP heterojunction in thermal equilibrium.

heterojunction. The same AE, and ΔE_v discontinuities exist, although the general shape of the conduction band, for example, is different in the nP and the Np junctions. This difference in energy bands will influence the I–V characteristics of the two junctions.

The other two types of heterojunctions are the nN and the pP isotype junctions. The energy-band diagram of the nN junction was shown in Figure 9.19. To achieve thermal equilibrium. electrons from the wide-bandgap material will flow into the narrow-bandgap material. A positive space charge region exists in the wide-gap material and an accumulation layer of electrons now exists at the interface in the narrow-gap material. Since there are a large number of allowed energy states in the conduction band, we expect the space charge width x_n and the built-in potential barrier V_{bin} to be small in the narrow-gap material. The energy-band diagram of the pP heterojunction in thermal equilibrium is shown in Figure 9.24. To achieve thermal equilibrium, holes from the wide-bandgap material will flow into the narrow-bandgap material, creating an accumulation layer of holes in the narrow-bandgap material at the interface. These types of isotype heterojunctions are obviously not possible in a homojunction.

*9.3.5 Current–Voltage Characteristics

The ideal current–voltage characteristics of a pn homojunction were developed in Chapter 8. Since the energy-band diagram of a heterojunction is more complicated than that of a homojunction, we would expect the I–V characteristics of the two junctions to differ.

One immediate difference between a homojunction and a heterojunction is in the barrier heights seen by the electrons and holes. Since the built-in potential barrier for electrons and holes in a homojunction is the same, the relative magnitude of the electron and hole currents is determined by the relative doping levels. In a heterojunction. the barrier heights seen by electrons and holes are not the same. The energy-band diagrams in Figures 9.18 and 9.23 demonstrated that the barrier heights for electrons and holes in a heterojunction can be significantly different. The barrier height for electrons in Figure 9.18 is larger than for holes, so we would expect the current due to electrons to be insignificant compared to the hole current. If the barrier height for electrons is 0.2 eV larger than for holes, the electron current will be approximately a factor of 10^4 smaller than the hole current, assuming all other parameters are equal. The opposite situation exists for the band diagram shown in Figure 9.23.

The conduction-band edge in Figure 9.23 and the valence-band edge in Figure 9.18 are somewhat similar to that of a rectifying metal–semiconductor contact. We derive the current–voltage characteristics of a heterojunction, in general. on the basis of thermionic emission of carriers over the barrier, as we did in the metal–semiconductor junction. We can then write

$$J = A^*T^2 \exp\left(\frac{-E_w}{kT}\right) \tag{9.51}$$

where E_w is an effective barrier height. The barrier height can be increased or reduced by an applied potential across the junction as in the case of a pn homojunction or a Schottky barrier junction. The heterojunction I–V characteristics, however, may need to be modified to include diffusion effects and tunneling effects. Another complicating factor is that the effective mass of a carrier changes from one side of the junction to the other. Although the actual derivation of the I–V relationship of the heterojunction is complex, the general form of the I–V equation is still similar to that of a Schottky barrier diode and is generally dominated by one type of carrier.

9.4 | SUMMARY

- A metal on a lightly doped semiconductor can produce a rectifying contact that is known as a Schottky barrier diode. The ideal barrier height between the metal and semiconductor is the difference between the metal work function and the semiconductor electron affinity.
- When a positive voltage is applied to an n-type semiconductor with respect to the metal (reverse bias), the barrier between the semiconductor and metal increases so that there is essentially no flow of charged carriers. When a positive voltage is applied to the metal

with respect to an n-type semiconductor (forward bias), the barrier between the semiconductor and metal is lowered so that electrons can easily flow from the semiconductor into the metal by a process called thennionic emission.

The ideal current–voltage relationship of the Schottky barrier diode is the same as that of the pn junction diode. However, since the current mechanism is different from that of the pn junction diode, the switching speed of the Schottky diode is faster. In addition, the reverse saturation current of the Schottky diode is larger than that of the pn junction diode, so a Schottky diode requires less forward bias voltage to achieve a given current compared to a pn junction diode.

Metal–semiconductor junctions can also form ohmic contacts, which are low-resistance junctions providing conduction in both directions with very little voltage drop across the junction.

Semiconductor heterojunctions are formed between two semiconductor materials with different bandgap encrgies One useful property of a heterojunction is the creation of a potential well at the interface. Electrons are confined to the potential well in the direction perpendicular to the interface, but are free to move in the other two directions.

GLOSSARY OF IMPORTANT TERMS

anisotype junction A heterojunction in which the type of dopant changes at the metallurgical junction.

electron affinity **rule** The rule stating that, in an ideal heterojunctian, the discontinuity the conduction band is the difference between the electron affinities in the two semiconductors.

heterojunction The junction formed by the contact between two different semiconducto materials.

image-force-induced lowering The lowering of the peak potential barrier at the metal–semiconductor junction due to an electric field.

isotype junction A heterojunction in which the type of dopant is the same on both sides the junction.

ohmic contact A low-resistance metal–semiconductor contact providing conduction in both directions between the metal and semiconductor.

Richardson constant The parameter A^* in the current–voltage relation of a Schottky diode.

Schottky harrier height The potential barrier ϕ_{Bn} from the metal to semiconductor in metal–semiconductor junction.

Schottky effect Another term for image-force-induced lowering.

specific contact resistance The inverse of the slope of the J versus V curve of a metal–semiconductor contact evaluated at $V = 0$.

thermionic emission The process by which charge flows over a potential barrier as a result of carriers with sufficient thermal energy.

tunneling harrier A thin potential barrier in which the current is dominated by the tunneling of carriers through the barrier.

two-dimensional electron gas (2-DEG) The accumulation layer of electrons contained ina potential well at a heterojunction interface that are free to move in the "other" two spatial directions.

CHECKPOINT

After studying this chapter, the reader should have the ability to:

- Sketch the energy band diagram of zero-biased. reverse-biased, and forward-biased Schottky barrier diodes.
- Describe the charge flow in a forward-biased Schottky barrier diode.
- Explain the Schottky barrier lowering and its effect on the reverse saturation current in a Schottky barrier diode.
- Explain the effect interface states on the characteristics of a Schottky barrier diode.
- Describe one effect of a larger reverse saturation current in a Schottky barrier diode compared to that of a pn junction diode.
- Describe what is meant by an ohmic contact.
- Draw the energy band diagram of an nN heterojunction.
- Explain what is meant by a two-dimensional electron gas.

REVIEW QUESTIONS

1. What is the ideal Schottky barrier height? Indicate the Schottky barrier height on an energy band diagram.
2. Using an energy band diagram, indicate the effect of the Schottky barrier lowering.
3. What is the mechanism of charge flow in a forward-biased Schottky barrier diode?
4. Compare the forward-biased current–voltage characteristic of a Schottky barrier diode to that of pn junction diode.
5. Sketch the ideal energy band diagram of a metal–semiconductor junction in which $\phi_m < \phi_s$. Explain why this is an ohmic contact.
6. Sketch the energy band diagram of a tunneling junction. Why is this an ohmic contact?
7. What is a heterojunction?
8. What is a 2-D electron gas?

PROBLEMS

(In the following problems, assume $A^* = 120$ A/K^2-cm^2 for silicon and $A^* = 1.12$ A/K^2-cm^2 for gallium arsenide Schottky diodes unless otherwise stated.)

Section 9.1 The Schottky Barrier Diode

9.1 Consider a contact between Al and n Si doped at $N_d = 10^{16}$ cm^{-3}. $T = 300$ K. (*a*) Draw the energy-band diagrams of the two materials before the junction is formed. (*b*) Draw the ideal energy band at zero bias after the junction is formed. (*c*) Calculate ϕ_{B0}, x_d, and E_{max} for part (*b*). (*d*) Repeat parts (*b*) and (*c*) using the data in Figure 9.5.

9.2 An ideal rectifying contact is formed by depositing gold on n-type silicon doped at 10^{15} cm^{-3}. At $T = 300$ K, determine (*a*) ϕ_{B0}, (*b*) V_{bi}, (*c*) W, and (*d*) E_{max}, all under equilibrium conditions.

9.3 Consider a gold Schottky diode at T = 300 K formed on n-type GaAs doped at $N_d = 5 \times 10^{16}$ cm^{-3}. Determine (*a*) the theoretical barrier height. ϕ_{B0}, (*b*) ϕ_n, (*c*) V_{bi},

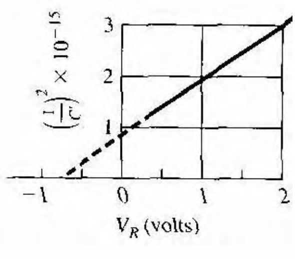

Figure 9.25 | Figure for Problem 9.6

(*d*) the space charge width, x_n, for $V_R = 5$ V. and (*e*) the electric field at the metal junction for $V_R = 5$ V.

9.4 Repeat problem 9.3, parts (b) through (*e*), if the experimentally determined barrier height is found to be $\phi_{Bn} = 0.86$ V.

9.5 An Au–n-Si junction with $N_d = 5 \times 10^{15}\ \text{cm}^{-3}$ has a cross-sectional area of $A = 5 \times 10^{-4}\ \text{cm}^2$. $T = 300$ K. Use the data in Figure 9.5. ***(a)*** Determine the junction capacitance when $V_R = 4$ V. ***(b)*** Repeat part (a) if the doping is increased to $N_d = 5 \times 10^{16}\ \text{cm}^{-3}$.

9.6 A Schottky diode with n-type GaAs at $T = 300$ K yields the $1/C'^2$ versus V_R plot shown in Figure 9.25, where C' is the capacitance per cm². Determine (a) V_{bi}, **(b)** N_d, (*c*) ϕ_n, and (*d*) ϕ_{B0}

9.7 Consider an Al–n-Si Schottky barrier at $T = 300$ K with $N_d = 10^{16}\ \text{cm}^{-3}$. Use the data in Figure 9.5 to determine the barrier height. (*a*) Determine V_{bi}, x_d, and E_{max} at zero bias. (*b*) Using the value of E_{max} from part (*a*), determine $\Delta\phi$ and x_m for the Schottky barrier lowering. (*c*) Repeat part (*b*) for the case when a reverse bias of $V_R = 4$ V is applied.

9.8 Starting with Equation (9.12), derive Equations (9.14) and (9.15).

9.9 An Au–n-GaAs Schottky diode is at $T = 300$ K with $N_d = 5 \times 10^{16}\ \text{cm}^{-3}$. Use the data in Figure 9.5 to determine the barrier height. (*a*) Determine V_{bi}, x_d, and E_{max} at zero bias. (b) Determine the reverse-bias voltage at which the Schottky barrier lowering, $\Delta\phi$, will be 7 percent of ϕ_{Bn}. (Use the value of E_{max} in the space charge region.)

9.10 Consider n-type silicon doped at $N_d = 10^{16}\ \text{cm}^{-3}$ with a gold contact to form a Schottky diode. Investigate the effect of Schottky barrier lowering. ***(a)*** Plot the Schottky barrier lowering $\Delta\phi$ versus reverse-bias voltage over the range $0 \le V_R \le 50$ V. (b) Plot the ratio $J_{sT}(V_R)/J_{sT}(V_R = 0)$ over the same range of reverse-bias voltage.

***9.11** The energy-band diagram of a Schottky diode is shown in Figure 9.6. Assume the following parameters:

$\phi_m = 5.2$ V	$\phi_n = 0.10$ V	$\phi_0 = 0.60$ V
$E_g = 1.43$ eV	$\delta = 25$ Å	$\epsilon_i = \epsilon_0$
$\epsilon_s = (13.1)\epsilon_0$	$\chi = 4.07$ V	$N_d = 10^{16}\ \text{cm}^{-3}$
		$D_{it} = 10^{13}\ \text{eV}^{-1}\ \text{cm}^{-2}$

(*a*) Determine the theoretical barrier height ϕ_{B0}, without interface states. (*b*) Determine the barrier height with interface states. (*c*) Repeat parts (a) and (*h*) if @ is changed to $\phi_m = 4.5$ V.

***9.12** A Schottky barrier diode contains interface states and an interfacial layer Assume the following parameters:

$\phi_m = 4.75$ V $\qquad \phi_n = 0.164$ V $\qquad \phi_0 = 0.230$ V

$E_g = 1.12$ eV $\qquad \delta = 20$ Å $\qquad \epsilon_i = \epsilon_0$

, $= (11.7)\epsilon_0$ $\qquad \chi = 4.01$ V $\qquad N_d = 5 \times 10^{16}$ cm^{-3}

$\phi_{B0} = 0.60$ V

Determine the interface state density, D_{it}, in units of eV^{-1} cm^{-2}.

9.13 A PtSi Schottky diode at T = 300 K is fabricated on n-type silicon with a doping of $N_d = 10^{16}$ cm^{-3}. From Figure 9.5, the barrier height is 0.89 V. Determine (*a*) ϕ_n, (b) V_{bi}, (*c*) J_{sT}, when the barrier lowering is neglected, and (*d*) V_a so that $J_n = 2$ A/cm^2.

9.14 (*a*) Consider a Schottky diode at $T = 300$ K formed with tungsten on n-type silicon. Let $N_d = 5 \times 10^{15}$ cm^{-3} and assume a cross-sectional area of $A = 5 \times 10^{-4}$ cm^2. Determine the forward-bias voltage required to obtain a current of 1 mA, 10 mA, and 100 mA. (*b*) Repeat part (*n*) if the temperature is increased to T = 400 K. (Neglect Schottky barrier lowering.)

9.15 A Schottky diode is formed by depositing Au on n-type GaAs doped at $N_d = 5 \times 10^{16}$ cm^{-3}. T = 300 K. (*a*) Determine the forward-bias voltage required to obtain $J_n = 5$ A/cm^2. (b) What is the change in forward-bias voltage necessary to double the current? (Neglect Schottky barrier lowering.)

9.16 (*a*) Consider an Au n-type GaAs Schottky diode with a cross-sectional area of $10\ ^{4}$ cm^2. Plot the forward-bias current–voltage characteristics over a voltage range of $0 \leq V_D \leq 0.5$ V. Plot the current on a log scale. (*b*) Repeat part (*a*) for an Au n-type silicon Schottky diode. (*c*) What conclusions can be drawn from these results?

9.17 A Schottky diode at T = 300 K is formed between tungsten and n-type silicon doped at $N_d = 10^{16}$ cm'. The cross-sectional area is $A = 10^{-4}$ cm^2. Determine the reverse-bias saturation current at (*a*) $V_R = 2$ V and (*b*) $V_R = 4$ V. (Take into account the Schottky barrier lowering.)

***9.18** Starting with the basic current equation given by Equation (9.18), derive the relation given by Equation (9.23).

9.19 A Schottky diode and a pn junction diode have cross-sectional areas of $A = 5 \times 10^{-4}$ cm^2. The reverse saturation current density of the Schottky diode is 3×10^{-8} A/cm^2 and the reverse saturation current density of the pn junction diode is 3×10^{-12} A/cm^2. The temperature is 300 K. Determine the forward-bias voltage in each diode required to yield diode currents of 1 mA.

9.20 The reverse saturation current densities in a pn junction diode and a Schottky diode are 5×10^{-12} A/cm^2 and 7×10^{-8} A/cm^2, respectively, at $T = 300$ K. The cross-sectional area of the pn junction diode is $A = 8 \times 10^{-4}$ cm^2. Determine the cross-sectional area of the Schottky diode so that the difference in forward-bias voltages to achieve 1.2 mA is 0.265 V.

9.21 (*a*) The reverse-saturation currents of a Schottky diode and a pn junction diode at T = 300 K are 5×10^{-8} A and 10^{-12} A, respectively. The diodes are connected in parallel and are driven by a constant current of 0.5 mA. (*i*) Determine the current in each diode. (ii) Determine the voltage across each diode. (*b*) Repeat part (*a*) if the diodes are connected in series.

9.22 A Schottky diode and a pn junction diode have cross-sectional areas of $A = 7 \times 10^{-4}$ cm^2. The reverse-saturation current densities at $T = 300$ K of the Schottky diode and pn junction are 4×10^{-8} A/cm^2 and 3×10^{-12} A/cm^2, respectively. A forward-bias current of 0.8 mA is required in each diode. (*a*) Determine the forward-bias voltage required across each diode. (*b*) If the voltage from part (a) is maintained across each diode, determine the current in each diode if the temperature is increased to 400 K. (Take into account the temperature dependence of the reverse-saturation currents. Assume E, = 1.12 eV for the pn junction diode and $\phi_{B0} = 0.82$ V. for the Schottky diode.)

9.23 Compare the current-voltage characteristics of a Schottky barrier diode and a pn junction diode. Use the results of Example 9.5, and assume diode areas of 5×10^{-4} cm^2. Plot the current–voltage characteristics on a linear scale over a current range of $0 \le I_D \le 10$ mA.

Section 9.2 Metal-Semiconductor Ohmic Contacts

9.24 It is possible, theoretically, to form an ohmic contact between a metal and silicon that has a very low barrier height. Considering the specific contact resistance, determine the value of ϕ_{Bn} that will give a value of $R_c = 10^{-5}$ Ω-cm^2 at T = 300 K.

9.25 A metal, with a work function $\phi_m = 4.2$ V, is deposited on an n-type silicon semiconductor with $\chi_s = 4.0$ V and $E_g = 1.12$ eV. Assume no interface states exist at the junction. Let T = 300 K. (*a*) Sketch the energy-band diagram for zero bias for the case when no space charge region exists at the junction. (*b*) Determine N_d so that the condition in part (*a*) is satisfied. (c) What is the potential barrier height seen by electrons in the metal moving into the semiconductor?

9.26 Consider the energy-band diagram of a silicon Schottky junction under zero bias shown in Figure 9.26. Let $\phi_{B0} = 0.7$ V and $T = 300$ K. Determine the doping required so that $x_d = 50$ Å at the point where the potential is $\phi_{B0}/2$ below the peak value. (Neglect the barrier lowering effect.)

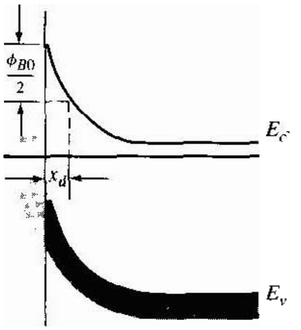

Figure 9.26 | Figure for Problem 9.26.

9.27 A metal–semiconductor junction is formed between a metal with a work function of 4.3 eV and p-type silicon with an electron affinity of 4.0 eV. The acceptor doping concentration in the silicon is $N_a = 5\ x\ 10^{16}\ \text{cm}^{-3}$. Assume T = 300 K. (a) Sketch the thermal equilibrium energy band diagram. *(h)* Determine the height of the Schottky barrier. (*c*) Sketch the energy band diagram with an applied reverse-bias voltage of $V_R = 3$ V. (*d*) Sketch the energy band diagram with an applied forward-bias voltage of $V_a = 0.25$ V.

9.28 (*a*) Consider a metal–semicanductor junction formed between a metal with a work function of 4.65 eV and Ge with an electron affinity of 4.13 eV. The dopingconcentration in the Ge material is $N_d = 6 \times 10^{13}\ \text{cm}^{-3}$ and $N_a = 3 \times 10^{13}\ \text{cm}^{-3}$. Assume T = 300 K. Sketch the zero bias energy-band diagram and determine the Schottky barrier height. (b) Repeat pan ***(a)*** if the metal work function is 4.35 eV.

Section 9.3 Heterojunctions

9.29 Sketch the energy-band diagrams of an abrupt $\text{Al}_{0\ 3}\text{Ga}_{0\ 7}\text{As}$–GaAs heterojunction for: (a) N^+–AlGaAs, intrinsic GaAs, (*b*) N^+–AlGaAs, p–GaAs, and (c) P^+–AlGaAs, n^+–GaAs. Assume $E_g = 1.85$ eV for $\text{Al}_{0\ 3}\text{Ga}_{0\ 7}\text{As}$ and assume $AE, = \frac{2}{3}\Delta E_g$.

9.30 Repeat Problem 9.29 assuming the ideal electron affinity rule. Determine ***AE,*** and ***AE,***

***9.31** Starting with Poisson's equation, derive Equation (9.48) for an abrupt heterojunction.

Summary and Review

***9.32** **(a)** Derive **an** expression for dV_a/dT as a function of current density in a Schottky diode. Assume the minority carrier current is negligible. (*b*) Compare dV_a/dT for a GaAs Schottky diode to that for a Si Schottky diode. (*c*) Compare dV_a/dT for a Si Schottky diode to that for a Si pn junction diode.

9.33 The $(1/C_j)^2$ versus V_R data are measured for two Schottky diodes with equal areas. One diode is fabricated with 1 Ω-cm silicon and the other diode with 5 Ω-cm silicon. The plots intersect the voltage axis as $V_R = -0.5$ V for diode A and at $V_R = -1.0$ V for diode B. The slope of the plot for diode A is $1.5\ x\ 10^{18}\ (\text{F}^2\text{-V})^{-1}$ and that for diode B is $1.5 \times 10^{17} (\text{F}^2\text{-V})^{-1}$. Determine which diode has the higher metal work function and which diode has the lower resistivity silicon.

***9.34** Both Schottky barrier diodes and ohmic contacts are to be fabricated by depositing a particular metal on a silicon integrated circuit. The work function of the metal is 4.5 V. Considering the ideal metal–semiconductor contact, determine the allowable range of doping concentrations for each type of contact. Consider both p- and n-type silicon regions.

9.30 Consider an n-GaAs–p-AlGaAs heterojunction in which the bandgap offsets are $AE, = 0.3$ eV and $\Delta E_v = 0.15$ eV. Discuss the difference in the expected electron and hole currents when the junction is forward biased.

READING LIST

1 Anderson, R. L. "Experimenls on Ge–GaAs Heterojunctions." *Solid-State* Electronics 5, no. 5 (September–October 1962), pp. 341–351

2. Crowley, A. M.. and S. M. Sre. "Surface States and Barrier Height of Metal Semiconductor Systems." *Journal of Applied Physics* 36 (1965), p. 3212.
3. MacMillan, H. F.; H. C. Hamaker; G. F. Virshup; and J. G. Werthrn. "Multijunction III-V Solar Cells: Recent and Projected Results." *Twentieth IEEE Photovoltaic Specialists Conference* (1988), pp. *48–54.*
4. Michaelson, H. B. "Relation between an Atomic Electronegativity Scale and the Work Function." *IBM Journal of Research and Development 22. no.* 1 (January 1978), pp. 72–80.
5. Pierret, R. F. *Semiconductor Device Fundamentals.* Reading, MA: Addison-Wesley, 1996.
6. Rideout, V. L. "A Review of the Theory, Technology and Applications of Metal-Semiconductor Rectifiers." *Thin Solid Films* 48, no. 3 (February 1, 1978), pp. 261–291.
7. Roulston, D. J. *Bipolar Semiconductor Devices.* New York: McGraw-Hill, 1990.
8. Shur, M. *Introduction to Electronic Devices. New* York: John Wiley and Sons, 1996.

*9. Shur, M. *GaAs Devices und Circuits.* New York: Plenum Press, 1987.

*10. ——. *Physics of Semiconductor Devices.* Englewood Cliffs. NJ: Prentice Hall. 1990.

*11. Singh. J. *Physics* of *Semiconductors and Their Heterostructures.* New York: McGraw-Hill, 1993.

12. Singh, J. *Semiconductor Devices: Basic Principles.* New York: John Wiley and Sons, 2001.
13. Streetman, B. G., and S. Banerjee. *Solid State Electronic Devices.* 5th cd. Upper Saddle River. NJ: Prentice Hall, 2000.
14. Sze, S. M. *Physics of Semiconductor Devices.* 2nd ed. New York: Wiley, 1981.

*15. Wang, S. *Fundamentals of Semiconductor Theory and Device* **Physics.** Englewood Cliffs, NJ: Prentice Hall. 1989.

*16. Wolfe, C. M., N. Holonyak, Jr., and G. E. Stillman. *Physical Properties* of *Semiconductors.* Englewood Cliffs, *NJ:* Prentice Hall, 1989.

17. Yang, E. S. *Microelectronic Devices.* New York: McGraw-Hill, 1988.

*18. Yuan. J. S. *SiGe, GaAs, and InP Heterojunction Bipolar Transistors.* New York: John Wiley and Sons. 1999.

CHAPTER

10

The Bipolar Transistor

PREVIEW

The single-junction devices we have considered, including the pn homojunction diode, can be used to obtain rectifying current–voltage characteristics, and to form electronic switching circuits. The transistor is a multifunction semiconductor device that, in conjunction with other circuit elements, is capable of current gain, voltage gain, and signal-power gain. The transistor is therefore referred to as an active device whereas the diode is passive. The basic transistor action is the control of current at one terminal by voltage applied across two other terminals of the device.

The three basic transistor types are the bipolar transistor, the metal-oxide-semiconductor field-effect transistor (MOSFET), and the junction field-effect transistor (JFET). The bipolar transistor is covered in this chapter, the MOSFET is treated in Chapters 11 and 12, and the JFET is discussed in Chapter 13. The chapters dealing with each of the transistor types are written to stand alone, so that each type of transistor may be covered in any order desired.

The bipolar transistor has three separately doped regions and two pn junctions, sufficiently close together so that interactions occur between the two junctions. We will use much of the theory developed for the pn junction in the analysis of the bipolar transistor. Since the flows of both electrons and holes are involved in this device, it is called a bipolar transistor.

We will first discuss the basic geometry and operation of the transistor. Since there is more than one pn junction in the bipolar transistor, several combinations of reverse- and forward-bias junction voltages are possible, leading to different operating modes in the device. As with the pn junction diode, minority carrier distributions in the bipolar transistor are an important part of the physics of the device—minority carrier gradients produce diffusion currents. We will determine the minority carrier distribution in each region of the transistor, and the corresponding currents.

The bipolar transistor is a voltage-controlled current source. We will consider the various factors that determine the current gain and derive its mathematical expression.

As with any semiconductor device. nonideal effects influence device characteristics: a few of these effects, such as breakdown voltage, will be described.

In order to analyze or design a transistor circuit. especially using computer simulations, one needs a mathematical model or equivalent circuit of the transistor. We will develop two equivalent circuits. The first equivalent circuit, the Ebers–Moll model, can be used for a transistor biased in any of its operating modes and is especially used for transistors in switching circuits. The second equivalent circuit, the hybrid-pi model, is applied when transistors are operated in a small signal linear amplifier and takes into account frequency effects within the transistor.

Various physical factors affect the frequency response of the bipolar transistor. There are several time-delay factors within the device that determine the limiting frequency response. We will define these time delays and develop expressions for each factor. The limiting frequency is given in terms of a cutoff frequency, a figure of merit for the transistor. The frequency response generally applies to the small signal, steady-state characteristics of the device. The switching characteristics, in contrast, determine the transient behavior of the transistor to large changes in the input signal..

10.1 | THE BIPOLAR TRANSISTOR ACTION

The bipolar transistor has three separately doped regions and two pn junctions. Figure 10.1 shows the basic structure of an npn bipolar transistor and a pnp bipolar transistor, along with the circuit symbols. The three terminal connections are called the emitter, base, and collector. The width of the base region is small compared to the minority carrier diffusion length. The (++)and (+) notation indicates the relative magnitudes of the impurity doping concentrations normally used in the bipolar transistor, with (++) meaning very heavily doped and (+) meaning moderately doped. The emitter region has the largest doping concentration: the collector region has the smallest. The reasons for using these relative impurity concentrations, and for the narrow base width. will become clear as we develop the theory of the bipolar transistor. The concepts developed for the pn junction apply directly to the bipolar transistor.

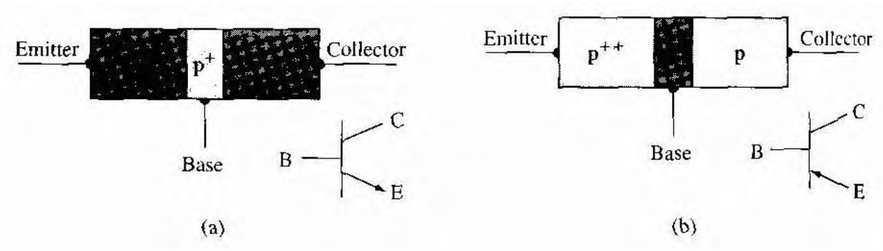

Figure 10.1 | Simplified block diagrams and circuit symbols **of** (a) npn and (b) pnp bipolar transistors.

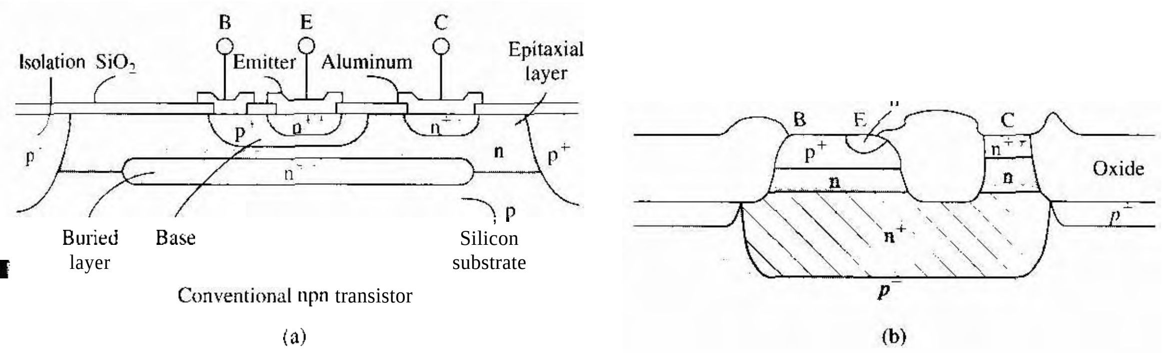

(a)

(b)

Figure 10.2 | Cross section of (a) a conventional integrated-circuit npn bipolar transistor and (b) an oxide-isolated npn bipolar transistor

(From Muller and Kamins [3].)

The block diagrams of Figure 10.1 show the basic structure of the transistor. but in very simplified sketches. Figure 10.2a shows a cross section of a classic npn bipolar transistor fabricated in an integrated circuit configuration, and Figure 10.2b shows the cross section of an npn bipolar transistor fabricated by a more modem technology. One can immediately observe that the actual structure of the bipolar transistor is not nearly as simple as the block diagrams of Figure 10.1 might suggest. A reason for the complexity is that terminal connections are made at the surface: in order to minimize semiconductor resistances, heavily doped n^+ buried layers must be included. Another reason for complexity arises out of the desire to fabricate more than one bipolar transistor on a single piece of semiconductor material. Individual transistors must be isolated from each other since all collectors, for example, will not be at the same potential. This isolation is accomplished by adding p^+ regions so that devices are separated by reverse-biased pn junctions as shown in Figure 10.2a, or they are isolated by large oxide regions as shown in Figure 10.2b.

An important point to note from the devices shown in Figure 10.2 is that the bipolar transistor is not a symmetrical device. Although the transistor may contain two n regions or two p regions, the impurity doping concentrations in the emitter and collector are different and the geometry of these regions can be vastly different. The block diagrams of Figure 10.1 are highly simplified, but useful, concepts in the development of the basic transistor theory.

10.1.1 The Basic Principle of Operation

The npn and pnp transistors are complementary devices. We will develop the bipolar transistor theory using the npn transistor, but the same basic principles and equations also apply to the pnp device. Figure 10.3 shows an idealized impurity doping profile in an npn bipolar transistor for the case when each region is uniformly doped. Typical impurity doping concentrations in the emitter, base, and collector may be on the order of 10^{19}, 10^{17}, and 10^{15} cm^{-3}, respectively.

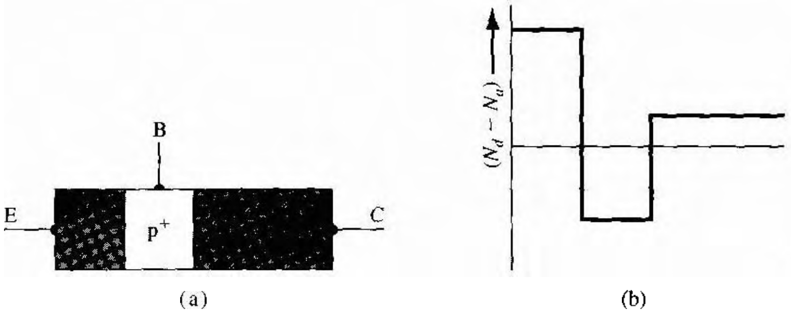

Figure 10.3 | Idealized doping profile of a uniformly doped npn bipolar transistor.

The base–emitter (B-E) pn junction is forward-biased, and the base–collector (B-C) pn junction is reverse-biased in the **normal bias** configuration as shown in Figure 10.4a. This configuration is called the *forward-active* operating mode: The B-E junction is forward-biased so electrons from the emitter are injected across the B-E junction into the base. These injected electrons create an excess concentration of minority carriers in the base. The B-C junction is reverse biased, so the minority carrier electron concentration at the edge of the B-C junction is ideally zero. We expect the electron concentration in the base to be like that shown in Figure 10.4b. The large gradient in the electron concentration means that electrons injected from the emitter will diffuse across the base region into the B-C space charge region. where the electric field will sweep the electrons into the collector. We want as many electrons as possible to reach the collector without recombining with any majority carrier holes in the base. For this reason, the width of the base needs to be small compared with the minority carrier diffusion length. If the base width is small, then the minority carrier electron concentration is a function of both the B-E and B-C junction voltages. The two junctions are close enough to be called *interacting* pn junctions.

Figure 10.5 shows a cross section of an npn transistor with the injection of electrons from the n-type emitter (hence the name emitter) and the collection of the electrons in the collector (hence the name collector).

10.1.2 Simplified Transistor Current Relations

We can gain a basic understanding of the operation of the transistor and the relations between the various currents and voltages by considering a simplified analysis. After this discussion, we will then delve into a more detailed analysis of the physics of the bipolar transistor.

The minority carrier concentrations are again shown in Figure 10.6 for an npn bipolar transistor biased in the forward active mode. Ideally. the minority carrier electron concentration in the base is a linear function of distance, which implies no recombination. The electrons diffuse across the base and are swept into the collector by the electric field in the B-C space charge region.

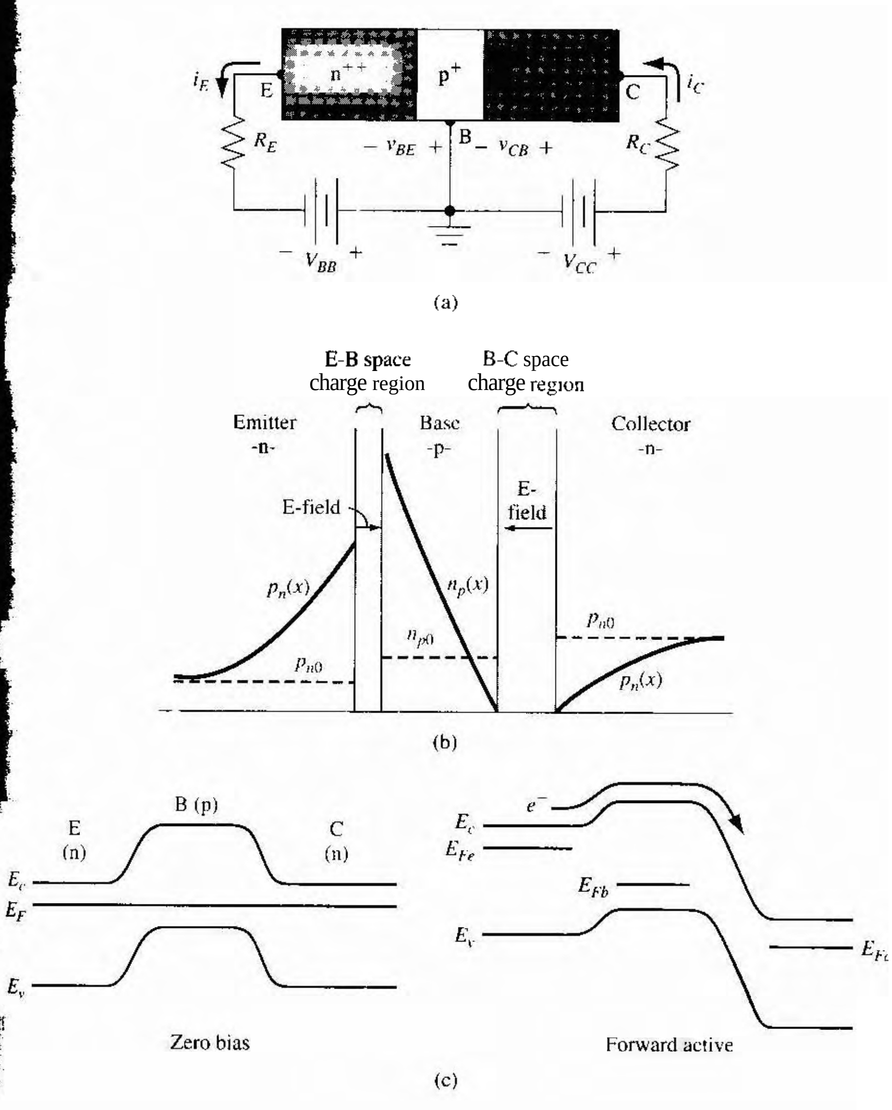
i_E
E
n++
p+
C
i_C
R_E
$-\ v_{BE}\ +$
B
$-\ v_{CB}\ +$
R_C
$-\ V_{BB}\ +$
$-\ V_{CC}\ +$
(a)
E-B space charge region
B-C space charge region
Emitter -n-
Base -p-
Collector -n-
E-field
E-field
$p_n(x)$
$n_p(x)$
n_{p0}
p_{n0}
p_{n0}
$p_n(x)$
(b)
B (p)
E (n)
C (n)
E_c
E_F
E_v
Zero bias
e^-
E_c
E_{Fe}
E_{Fb}
E_v
E_{Fc}
Forward active
(c)

Figure 10.4 | (a) Biasing of an npn bipolar transistor in the forwad-active mode, (b) minority carrier distribution in an npn bipolar transistor operating in the forward-active mode. and (c) energy band diagram of the npn bipolar transistor under zero bias **and** under a forward-active mode bias.

Collector Current Assuming the ideal linear electron distribution in the base, the collector current can be written as a diffusion current given by

$$i_C = eD_nA_{BE}\frac{dn(x)}{dx} = eD_nA_{BE}\left[\frac{n_B(0)-0}{0-x_B}\right] = \frac{-eD_nA_{BE}}{x_B}\cdot n_{B0}\exp\left(\frac{v_{BE}}{V_t}\right)$$

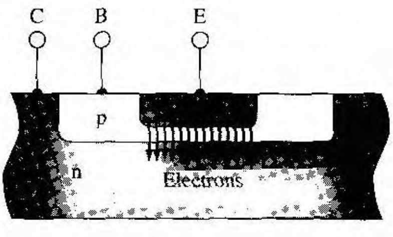
C
B
E
p
n
Electrons

Figure 10.5 | Cross section of an npn bipolar transistor showing the injection and collection of electrons in the forward-active mode.

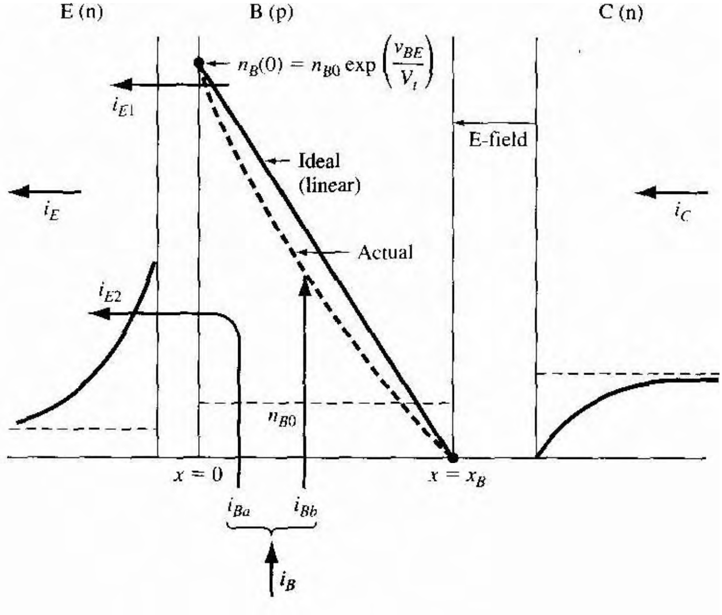
E (n)
B (p)
C (n)
$n_B(0) = n_{B0} \exp\left(\frac{v_{BE}}{V_t}\right)$
i_{E1}
Ideal (linear)
E-field
i_E
i_C
Actual
i_{E2}
n_{B0}
$x = 0$
$x = x_B$
i_{Ba}
i_{Bb}
i_B

Figure 10.6 | Minority carrier distributions and basic currents in a forward-biased npn bipolar transistor.

where A_{BE} is the cross-sectional area of the B-E junction, n_{B0} is the thermal equilibrium electron concentration in the base, and V_t is the thermal voltage. The diffusion of electrons is in the $+x$ direction so that the conventional current is in the $-x$ direction. Considering magnitudes only, Equation (10.1) can be written as

$$i_C = I_S \exp\left(\frac{v_{BE}}{V_t}\right) \tag{10.2}$$

The collector current is controlled by the base–emitter voltage; that is, the current at one terminal of the device is controlled by the voltage applied to the other two terminals of the device. As we have mentioned, this is the basic transistor action.

mitter Current One component of emitter current, i_{E1}, shown in Figure 10.6 is e to the flow of elections injected from the emitter into the hase. This current, then, equal to the collector current given by Equation (10.1).

Since the base–emitter junction is forward biased, majority canier holes in the se are injected across the B-E junction into the emitter. These injected holes proce a pn junction current i_{E2} as indicated in Figure 10.6. This current is only a B-E nction current so this component of emitter current is not part of the collector curnt. Since i_{E2} is a forward-biased pn junction current, we can write (considering agnitude only)

$$i_{E2} = I_{S2} \exp\left(\frac{v_{BE}}{V_t}\right) \tag{10.3}$$

where I_{S2} involves the minority carrier hole parameters in the emitter. The total emitter current is the sum of the two components, or

$$i_E = i_{E1} + i_{E2} = i_C + i_{E2} = I_{SE} \exp\left(\frac{v_{BE}}{V_t}\right) \tag{10.4}$$

Since all current components in Equation (10.4) are functions of exp $(v_{BE}/$ V,), the ratio of collector current to emitter current is a constant. We can write

$$\frac{i_C}{i_E} \equiv \alpha \tag{10.5}$$

where a is called the *common-base current gain*. By considering Equation (10.4), we see that $i_C < i_E$ or $\alpha < 1$. Since i_{E2} is not part of the basic transistor action, we would like this component of current to be as small as possible. We would then like the common base current gain to be as close to unity as possible.

Referring to Figure 10.4a and Equation (10.4), note that the emitter current is an exponential function of the base–emitter voltage and the collector current is $i_C = \alpha i_E$. To a first approximation, the collector current is independent of the hase–collector voltage as long as the B-C junction is reverse biased. We can sketch the common-base transistor characteristics as shown in Figure 10.7. The bipolar transistor acts like a constant current source.

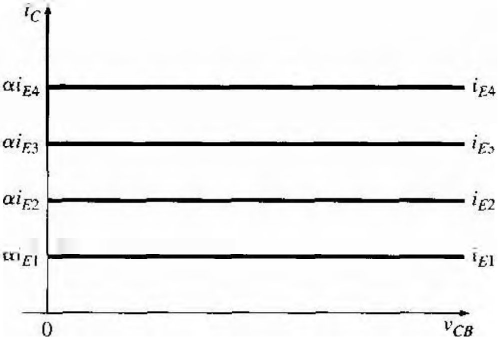

Figure 10.7 | Ideal bipolar transistor common-base current–voltage characteristics.

Base Current As shown in Figure 10.6, the component of emitter current i_{E2} is a B-E junction current so that this current is also a component of base current sh as i_{Ba}. This component of base current is proportional to $\exp(v_{BE}/V_t)$.

There is also a second component of base current. We have considered the ideal case in which there is no recombination of minority carrier electrons with ma carrier holes in the base. However, in reality, there will be some recombin Since majority carrier holes in the base are disappearing, they must be resuppli a flow of positive charge into the base terminal. This flow of charge is indicated as a current i_{Bb} in Figure 10.6. The number of holes per unit time recombining in the base is directly related to the number of minority carrier electrons in the base (see Equation (6.13)). Therefore, the current i_{Bb} is also proportional to $\exp(v_{BE}/V_t)$. The total base current is the sum of i_{Ba} and i_{Bb}, and is proportional to $\exp(v_{BE}/V_t)$.

The ratio of collector current to base current is a constant since both currents are directly proportional to $\exp(v_{BE}/V_t)$. We can then write

$$\frac{i_C}{i_B} \equiv \beta$$

(10

where β is called the common-emitter current **gain.** Normally. the base current will be relatively small so that, in general, the common-emitter current gain is much larger than unity (on the order of 100 or larger).

10.1.3 The Modes of Operation

Figure 10.8 shows the npn transistor in a simple circuit. In this configuration, the transistor may be biased in one of three modes of operation. If the B-E voltage is zero or reverse biased ($V_{BE} \le 0$), then majority carrier electrons from the emitter will not be injected into the base. The B-C junction is also reverse biased; thus. the emitter and collector currents will be zero for this case. This condition is referred to as *cutoff*—all currents in the transistor are zero.

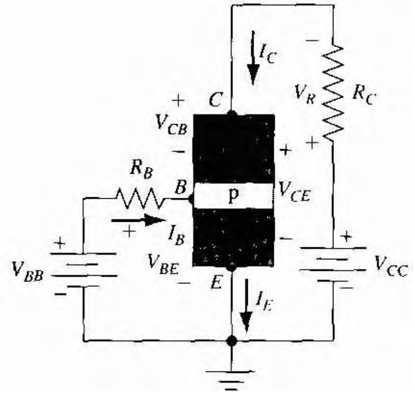

Figure 10.8 | An npn bipolar transistor in a common-emitter circuit configuration.

When the B-E junction becomes forward biased, an emitter current will be generated as we have discussed, and the injection of electrons into the base results in a collector current. We may write the KVL equations around the collector–emitter loop as

$$V_{CC} = I_C R_C + V_{CB} + V_{BE} = V_R + V_{CE} \tag{10.7}$$

If V_{CC} is large enough and if V_R is small enough, then $V_{CB} > 0$, which means that the B-C junction is reverse biased for this npn transistor. Again, this condition is the forward-active region of operation.

As the forward-biased B-E voltage increases, the collector current and hence V_R will also increase. The increase in V_R means that the reverse-biased C-B voltage decreases, or $|V_{CB}|$ decreases. At some point, the collector current may become large enough that the combination of V_R and V_{CC} produces zero voltage across the B-C junction. A slight increase in I_C beyond this point will cause a slight increase in V_R and the B-C junction will become forward biased ($V_{CB} < 0$). This condition is called saturation. In the saturation mode of operation, both B-E and B-C junctions are forward biased and the collector current is no longer controlled by the B-E voltage.

Figure 10.9 shows the transistor current characteristics, I_C versus V_{CE}, for constant base currents when the transistor is connected in the common-emitter configuration (Figure 10.8). When the collector–emitter voltage is large enough so that the base–collector junction is reverse biased, the collector current is a constant in this first-order theory. For small values of C-E voltage, the base–collector junction becomes forward biased and the collector current decreases to zero for a constant base current.

Writing a Kirchhoff's voltage equation around the C-E loop, we find

$$V_{CE} = V_{CC} - I_C R_C \tag{10.8}$$

Equation (10.8) shows a linear relation between collector current and collector–emitter voltage. This linear relation is called a ***load*** line and is plotted in Figure 10.9. The load line. superimposed on the transistor characteristics, can be used to visualize the bias condition and operating mode of the transistor. The cutoff mode occurs when

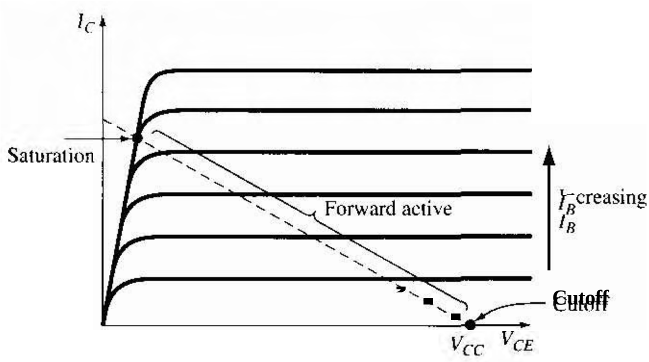

Figure 10.9 | Bipolar transistor common-emitter current–voltage characteristics with load line superimposed.

$I_C = 0$, saturation occurs when there is no longer a change in collector current for change in base current, and the forward-active mode occurs when the relatio $I_C = \beta I_B$ is valid. These three operating modes are indicated on the figure.

A fourth mode of operation for the bipolar transistor is possible, although n with the circuit configuration shown in Figure 10.8. This fourth mode, known as inverse *active*, occurs when the B-E junction is reverse biased and the B-C junction is forward biased. In this case the transistor is operating "upside down," and the roles of the emitter and collector are reversed. We have argued that the transistor is not a symmetrical device; therefore, the inverse-active characteristics will not be the same as the forward-active characteristics.

The junction voltage conditions for the four operating modes are shown in Figure 10.10.

10.1.4 Amplification with Bipolar Transistors

Voltages and currents can he amplified by bipolar transistors in conjunction wit other elements. We will demonstrate this amplification qualitatively in the followin discussion. Figure 10.11 shows an npn bipolar transistor in a common-emitter configuration. The dc voltage sources, V_{BB} and V_{CC}, are used to bias the transistor in the forward-active mode. The voltage source v_i represents a time-varying input voltage (such as a signal from a satellite) that needs to be amplified.

Figure 10.12 shows the various voltages and currents that are generated in the circuit assuming that v_i is a sinusoidal voltage. The sinusoidal voltage v_i induces a sinusoidal component of base current superimposed on a dc quiescent value. Since $i_C = \beta i_B$, then a relatively large sinusoidal collector current is superimposed on a dc value of collector current. The time-varying collector current induces a time-varying voltage across the R_C resistor which, by Kirchhoff's voltage law, means that a sinusoidal voltage, superimposed on a dc value, exists between the collector and emitter of the bipolar transistor The sinusoidal voltages in the collector-emitter

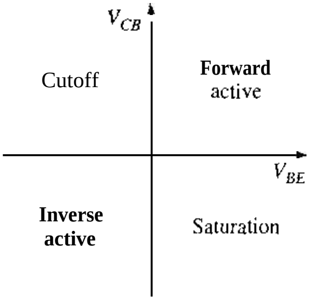

Figure 10.10 | Junction voltage conditions for the four operating modes of a bipolar transistor.

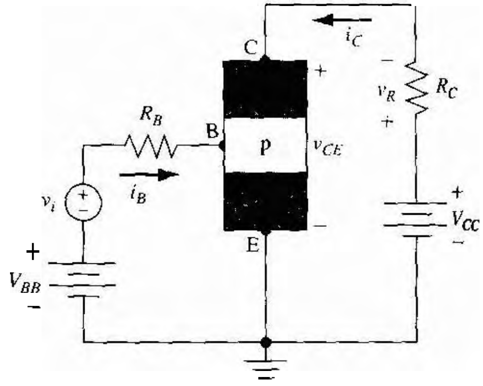

Figure 10.11 | Common-emitter npn bipolar circuit configuration with a time-varying signal voltage v_i included in the base-emitter loop.

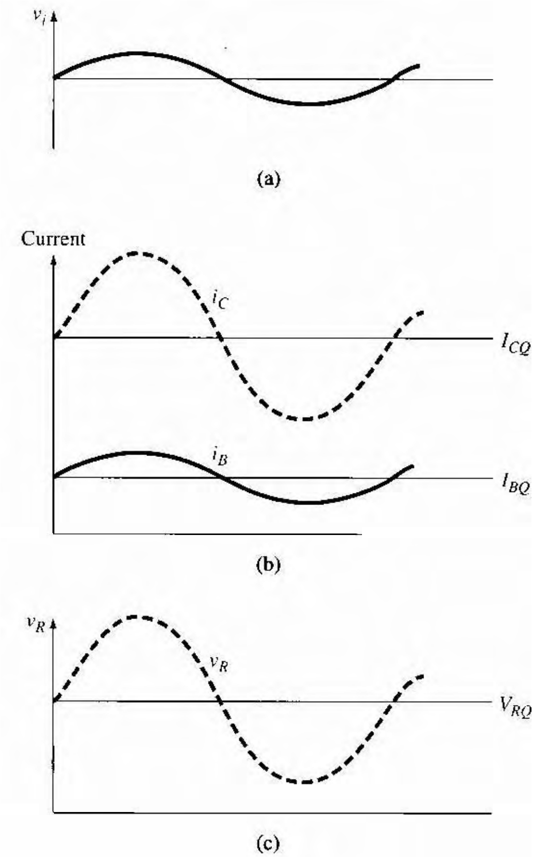

Figure 10.12 | Currents and voltages existing in the circuit shown in Figure 10.11. (a) Input sinusoidal signal voltage. (b) Sinusoidal base and collector currents superimposed on the quiescent dc values. (c) Sinusoidal voltage across the R_C resistor superimposed on the quiescent dc value.

portion of the circuit are larger than the signal input voltage v_i, so that the circuit has produced a ***voltage gain*** in the time-varying signals. Hence, the circuit is known as a ***voltage amplifier.***

In the remainder of the chapter, we will consider the operation and characteristics of the bipolar transistor in more detail.

10.2 | MINORITY CARRIER DISTRIBUTION

We are interested in calculating currents in the bipolar transistor which, as in the simple pn junction, are determined by minority carrier diffusion. Since diffusion currents are produced by minority carrier gradients, we must determine the steady-state

Table 10.1 | Notation used in the analysis of the bipolar transistor

Notation	Definition
For **both** the npn and pnp transistors	
N_E, N_B, N_C	Doping concentrations in the emitter, base, and collector
x_E, x_B, x_C	Widths of neutral emitter, base. and collector regions
D_E, D_B, D_C	***Minority carrier*** diffusion coefficients in emitter, base. and collector regions
L_E, L_B, L_C	***Minority carrier*** diffusion lengths in emitter, base, and collector regions
$\tau_{E0}, \tau_{B0}, \tau_{C0}$	***Minority carrier*** lifetimes in emitter, base, and collector regions
For the npn	
p_{E0}, n_{B0}, p_{C0}	Thermal equilibrium ***minority carrier*** hole, electron, and hole concentrations in the emitter, base, and collector
$p_E(x'), n_B(x), p_C(x'')$	Total ***minority carrier*** hole, electron. and hole concentrations in the emitter base, and collector
$\delta p_E(x'), \delta n_B(x), \delta p_C(x'')$	Excess ***minority carrier*** hole, electron. and hole concentrations in the emitter, base, and collector
For the pnp	
n_{E0}, p_{B0}, n_{C0}	Thermal equilibrium ***minority carrier*** electron, hole, and electron concentrations in the emitter, base. and collector
$n_E(x'), p_B(x), n_C(x'')$	Total ***minority carrier*** electron. hole, and electron concentrations in the emitter, base, and collector
$\delta n_E(x'), \delta p_B(x), \delta n_C(x'')$	Excess ***minority carrier*** electron, hole, and electron concentrations in the emitter, base, and collector

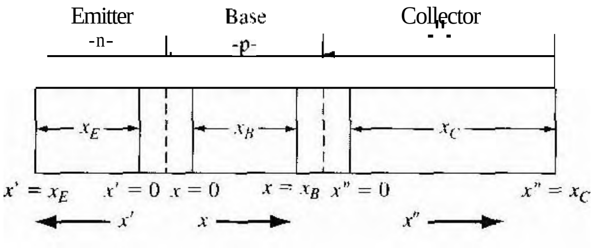

Figure 10.13 | Geometry of the npn bipolar transistor used to calculate the minority carrier distribution.

minority carrier distribution in each of the three transistor regions. Let us first consider the forward-active mode. and then the other modes of operation. Table 10.1 summarizes the notation used in the following analysis.

10.2.1 Forward-Active Mode

Consider a uniformly doped npn bipolar transistor with the geometry shown in Figure 10.13. When we consider the individual emitter, base, and collector regions, we

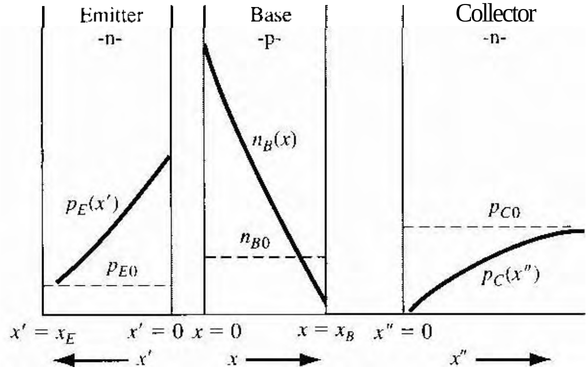

Figure 10.14 | Minority carrier distribution in an npn bipolar transistor operating in the forward-active mode.

will shift the origin to the edge of the space charge region and consider a positive x, x', or x'' coordinate as shown in the figure.

In the forward-active mode, the B-E junction is forward biased and the B-C is reverse biased. We expect the minority carrier distributions to look like those shown in Figure 10.14. As there are two n regions, we will have minority carrier holes in both emitter and collector. To distinguish between these two minority carrier hole distributions, we will use the notation shown in the figure. Keep in mind that we will be dealing only with minority carriers. The parameters p_{E0}, n_{B0}, and p_{C0} denote the thermal-equilibrium minority carrier concentrations in the emitter, base, and collector, respectively. The functions $p_E(x')$, $n_B(x)$, and $p_C(x'')$ denote the steady-state minority carrier concentrations in the emitter, base, and collector, respectively. We will assume that the neutral collector length x_C is long compared to the minority carrier diffusion length L_C in the collector, but we will take into account a finite emitter length x_E. If we assume that the surface recombination velocity at $x' = x_E$ is infinite, then the excess minority carrier concentration at $x' = x_E$ is zero, or $p_E(x' = x_E) = p_{E0}$. An infinite surface recombination velocity is a good approximation when an ohmic contact is fabricated at $x' = x_E$.

Base Region The steady-state excess minority carrier electron concentration is found from the ambipolar transport equation, which we discussed in detail in Chapter 6. For a zero electric field in the neutral base region, the ambipolar transport equation in steady state reduces to

$$D_B \frac{\partial^2(\delta n_B(x))}{\partial x^2} - \frac{\delta n_B(x)}{\tau_{B0}} = 0$$

where δn_B is the excess minority carrier electron concentration, and D_B and τ_{B0} are the minority carrier diffusion coefficient and lifetime in the base region, respectively. The excess electron concentration is defined as

$$\delta n_B(x) = n_B(x) - n_{B0} \tag{10.10}$$

The general solution to Equation (10.9) can be written as

$$\delta n_B(x) = A\exp\left(\frac{+x}{L_B}\right) + B\exp\left(\frac{-x}{L_B}\right) \tag{10.11}$$

where L_B is the minority carrier diffusion length in the base, given by $L_B = \sqrt{D_B\tau_{B0}}$. The base is of finite width so both exponential terms in Equation (10.11) must be retained.

The excess minority carrier electron concentrations at the two boundaries become

$$\delta n_B(x=0) \equiv \delta n_B(0) = A + B \tag{10.12a}$$

and

$$\delta n_B(x = x_B) \equiv \delta n_B(x_B) = A\exp\left(\frac{+x_B}{L_B}\right) + B\exp\left(\frac{-x_B}{L_B}\right) \tag{10.12b}$$

The B-E junction is forward biased, so the boundary condition at $x = 0$ is

$$\delta n_B(0) = n_B(x=0) - n_{B0} = n_{B0}\left[\exp\left(\frac{eV_{BE}}{kT}\right) - 1\right] \tag{10.13a}$$

The B-C junction is reverse biased, so the second boundary condition at $x = x_B$ is

$$\delta n_B(x_B) = n_B(x = x_B) - n_{B0} = 0 - n_{B0} = -n_{B0} \tag{10.13b}$$

From the boundary conditions given by Equations (10.13a) and (10.13b), the coefficients A and B from Equations (10.12a) and (10.12b) can be determined. The results are

$$A = \frac{-n_{B0} - n_{B0}\left[\exp\left(\frac{eV_{BE}}{kT}\right) - 1\right]\exp\left(\frac{-x_B}{L_B}\right)}{2\sinh\left(\frac{x_B}{L_B}\right)} \tag{10.14a}$$

and

$$B = \frac{n_{B0}\left[\exp\left(\frac{eV_{BE}}{kT}\right) - 1\right]\exp\left(\frac{x_B}{L_B}\right) + n_{B0}}{2\sinh\left(\frac{x_B}{L_B}\right)} \tag{10.14b}$$

Then, substituting Equations (10.14a) and (10.14b) into Equation (10.9), we can write the excess minority carrier electron concentration in the base region as

$$\boxed{\delta n_B(x) = \frac{n_{B0}\left\{\left[\exp\left(\frac{eV_{BE}}{kT}\right) - 1\right]\sinh\left(\frac{x_B - x}{L_B}\right) - \sinh\left(\frac{x}{L_B}\right)\right\}}{\sinh\left(\frac{x_B}{L_B}\right)}} \tag{10.15a}$$

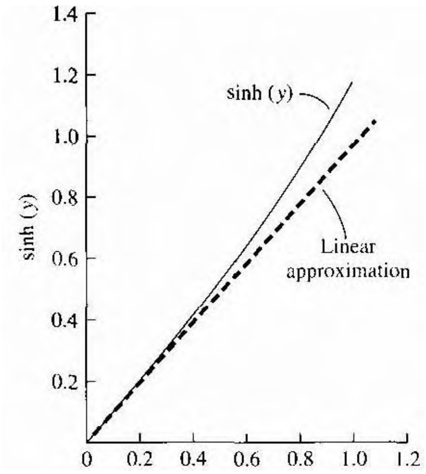

Figure 10.15 | Hyperbolic sine function **and** its linear approximation.

Equation (10.15a) may look formidable with the sinh functions. We have stressed that we want the base width x_B to be small compared to the minority carrier diffusion length L_B. This condition may seem somewhat arbitrary at this point, but the reason will become clear as we proceed through all of the calculations. Since we want $x_B < L_B$, the argument in the sinh functions is always less than unity and in most cases will be much less than unity. Figure 10.15 shows a plot of sinh (y) for $0 \le y \le 1$ and also shows the linear approximation for small values of y. If $y < 0.4$, the sinh (y) function differs from its linear approximation by less than 3 percent. All of this leads to the ***conclusion that the excess electron concentration δn_B in Equation (10.15a) is approximately a linear function of x through the neutral base region.*** Using the approximation that sinh $(x) \approx x$ for $x \ll 1$, the excess electron concentration in the base is given by

$$\boxed{\delta n_B(x) \approx \frac{n_{B0}}{x_B}\left\{\left[\exp\left(\frac{eV_{BE}}{kT}\right)-1\right](x_B-x)-x\right\}} \tag{10.15b}$$

We will use this linear approximation later in some of the example calculations. The difference in the excess carrier concentrations determined from Equations (10.15a) and (10.15b) is demonstrated in the following exercise.

TEST YOUR UNDERSTANDING

E10.1 The emitter and base of a silicon npn bipolar transistor are uniformly doped at impurity concentrations of 10^{18} cm^{-3} and 10^{16} cm^{-3}, respectively. A forward-bias B-E voltage of $V_{BE} = 0.610$ V is applied. The neutral base width is $x_B = 2\ \mu$m and the minority carrier diffusion length in the base is $L_B = 10\,\mu\text{m}$. Calculate the excess minority carrier concentration in the base at (*a*) $x = 0$ and (*b*) $x = x_B/2$. (*c*) Determine the ratio of the actual minority carrier concentration at $x = x_B/2$ (Equation (10.15a)) to that in the ideal case of a linear minority carrier distribution (Equation (10.15b)). [Ans. (*a*) $n_B(0) = 3.81 \times 10^{14}$ cm^{-3}, (*b*) $\delta n_B(x_B/2) \approx n_B(x_B/2) = 1.8947 \times 10^{14}$ cm^{-3}, (*c*) Ratio $= (1.8947 \times 10^{14}/1.9042 \times 10^{14}) = 0.9950$]

Table 10.2 shows the Taylor expansions of some of the hyperbolic functions tha will be encountered in this section of the chapter. In most cases. we will conside only the linear terms when expanding these functions.

Emitter Region Consider, now, the minority carrier hole concentration in the emitter. The steady-state excess hole concentration is determined from the equation

$$D_E \frac{\partial^2(\delta p_E(x'))}{\partial x'^2} - \frac{\delta p_E(x')}{\tau_{E0}} = 0 \tag{10.16}$$

where D_E and τ_{E0} are the minority carrier diffusion coefficient and minority carrier lifetime, respectively. in the emitter. The excess hole concentration is given by

$$\delta p_E(x') = p_E(x') - p_{E0} \tag{10.17}$$

The general solution to Equation (10.16) can be written as

$$\delta p_E(x') = C \exp\left(\frac{+x'}{L_E}\right) + D \exp\left(\frac{-x'}{L_E}\right) \tag{10.18}$$

where $L_E = \sqrt{D_E \tau_{E0}}$. If we assume the neutral emitter length x_E is not necessarily long compared to L_E. then both exponential terms in Equation (10.18) must be retained.

The excess minority carrier hole concentrations at the two boundaries are

$$\delta p_E(x' \geq 0) \equiv \delta p_E(0) = C + D \tag{10.19a}$$

and

$$\delta p_E(x' = x_E) \equiv \delta p_E(x_E) = C \exp\left(\frac{x_E}{L_E}\right) + D \exp\left(\frac{-x_E}{L_E}\right) \tag{10.19b}$$

Table 10.2 | Taylor expansions of hyperbolic functions

Function	Taylor expansion
$\sinh(x)$	$x + \frac{x^3}{3!} + \frac{x^5}{5!} + \cdots$
$\cosh(x)$	$1 + \frac{x^2}{2!} + \frac{x^4}{4!} + \cdots$
$\tanh(x)$	$x - \frac{x^3}{3} + \frac{2x^5}{15} + \cdots$

Again, the B-E junction is forward biased so

$$\delta p_E(0) = p_E(x' = 0) - p_{E0} = p_{E0}\left[\exp\left(\frac{eV_{BE}}{kT}\right) - 1\right] \qquad (10.20a)$$

An infinite surface recombination velocity at $x' = x_E$ implies that

$$\delta p_E(x_E) = 0 \qquad (10.20b)$$

Solving for C and D using Equations (10.19) and (10.20) yields the excess minority carrier hole concentration in Equation (10.18):

$$\boxed{\delta p_E(x') = \frac{p_{E0}\left[\exp\left(\frac{eV_{BE}}{kT}\right) - 1\right]\sinh\left(\frac{x_E - x'}{L_E}\right)}{\sinh\left(\frac{x_E}{L_E}\right)}} \qquad (10.21a)$$

This express *concentration* will also vary *approximately* linearly with distance *if* x_E is small. We find

$$\boxed{\delta p_E(x') \approx \frac{p_{E0}}{x_E}\left[\exp\left(\frac{eV_{BE}}{kT}\right) - 1\right](x_E - x')} \qquad (10.21b)$$

If x_E is comparable to L_E, then $\delta p_E(x')$ shows an exponential dependence on x_E

TEST YOUR UNDERSTANDING

E10.2 Consider a silicon npn bipolar transistor with emitter and base regions uniformly doped at concentrations of 10^{18} cm^{-3} and 10^{16} cm^{-3}, respectively. A forward bias B-E voltage of $V_{BE} = 0.610$ V is applied. The neutral emitter width is $x_E = 4\ \mu$m and the minority carrier diffusion length in the emitter is $L_E = 4\ \mu$m. Calculate the excess minority carrier concentration in the emitter at (a) $x' = 0$ and (b) $x' = x_E/2$
[Ans. (*a*) 3.808 × 10^{12} cm^{-3}; (*b*) 1.689 × 10^{12} cm^{-3}]

Collector **Region** The excess minority carrier hole concentration in the collector can be determined from the equation

$$D_C\frac{\partial^2(\delta p_C(x''))}{\partial x''^2} - \frac{\delta p_C(x'')}{\tau_{C0}} = 0 \qquad (10.22)$$

where D_C and τ_{C0} are the minority carrier diffusion coefficient and minority carrier lifetime, respectively, in the collector. We can express the excess minority carrier hole concentration in the collector as

$$\delta p_C(x'') = p_C(x'') - p_{C0} \qquad (10.23)$$

The general solution to Equation (10.22) can be written as

$$\delta p_C(x'') = G \exp\left(\frac{x''}{L_C}\right) + H \exp\left(\frac{-x''}{L_C}\right) \qquad (10.2$$

where $L_C = \sqrt{D_C \tau_{C0}}$. If we assume that the collector is long. then the coefficient must be zero since the excess concentration must remain finite. The second boundar condition gives

$$\delta p_C(x'' = 0) \equiv \delta p_C(0) = p_C(x'' = 0) - p_{C0} = 0 - p_{C0} = -p_{C0} \qquad (10.25$$

The excess minority carrier hole concentration in the collector is then given as

$$\boxed{\delta p_C(x'') = -p_{C0} \exp\left(\frac{-x''}{L_C}\right)} \qquad (10.26$$

This result is exactly what we expect from the results of a reverse-biased pn junctio

TEST YOUR UNDERSTANDING

E10.3 Consider the collector region of an npn bipolar transistor biased in the forward active region. At what value of x'', compared to L_C, does the magnitude of the minority carrier concentration reach 95 percent of the thermal equilibrium value.
(Ans. $x''/L_C \approx 3$)

10.2.2 Other Modes of Operation

The bipolar transistor can also operate in the cutoff, saturation, or inverse-active mode. We will qualitatively discuss the minority carrier distributions for these operating conditions and treat the actual calculations as problems at the end of the chapter.

Figure 10.16a shows the minority carrier distribution in an npn bipolar transistor in cutoff. In cutoff, both the B-E and B-C junctions are reverse biased: thus, the

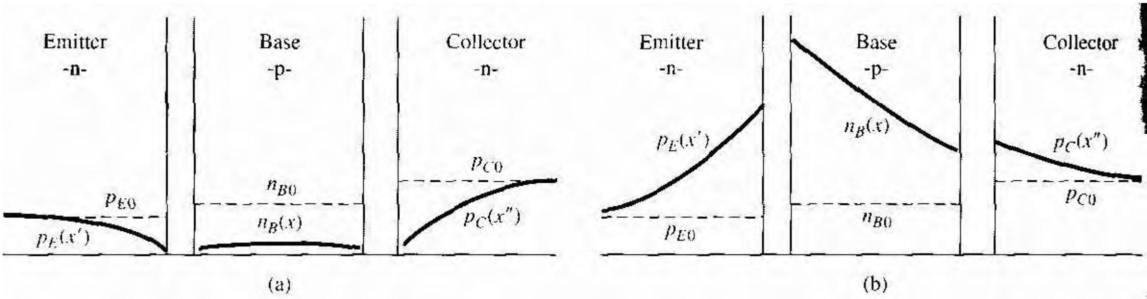

Figure 10.16 | Minority carrier distribution in an npn bipolar transistor operating in (a) cutoff and (b) saturation

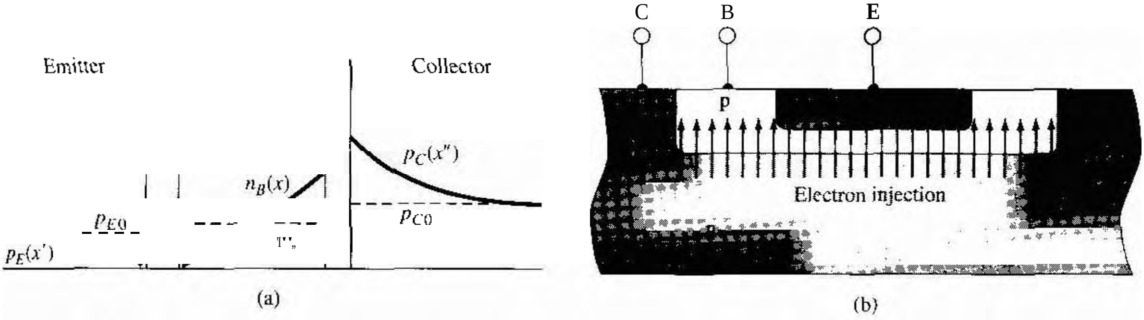

Figure 10.17 | (a) Minority carrier distribution in an npn bipolar transistor operating in the inverse-active mode. (b) Cross section of an npn bipolar transistor showing the injection and collection of electrons in the inverse-active mode.

minority carrier concentrations are zero at each space charge edge. The emitter and collector regions are assumed to be "long" in this figure, while the base is narrow compared with the minority carrier diffusion length. Since $x_B \ll L_B$, essentially all minority carriers are swept out of the base region.

Figure 10.16b shows the minority carrier distribution in the npn bipolar transistor operating in saturation. Both the B-E and B-C junctions are forward biased; thus, excess minority carriers exist at the edge of each space charge region. However, since a collector current still exists when the transistor is in saturation, a gradient will still exist in the minority carrier electron concentration in the base.

Finally, Figure 10.17a shows the minority carrier distribution in the npn transistor for the inverse-active mode. In this case, the B-E is reverse biased and the B-C is forward biased. Electrons from the collector are now injected into the base. The gradient in the minority carrier electron concentration in the base is in the opposite direction compared with the forward-active mode, so the emitter and collector currents will change direction. Figure 10.17b shows the injection of electrons from the collector into the base. Since the B-C area is normally much larger than the B-E area. not all of the injected electrons will be collected by the emitter. The relative doping concentrations in the base and collector are also different compared with those in the base and emitter; thus, we see that the transistor is not symmetrical. We then expect the characteristics to be significantly different between the forward-active and inverse-active modes of operation.

10.3 | LOW-FREQUENCY COMMON-BASE CURRENT GAIN

The basic principle of operation of the bipolar transistor is the control of the collector current by the B-E voltage. The collector current is a function of the number of majority carriers reaching the collector after being injected from the emitter across the B-E junction. The *common-base current gain* is defined as the ratio of collector current to emitter current. The flow of various charged carriers leads to definitions of particular currents in the device. We can use these definitions to define the current gain of the transistor in terms of several factors.

10.3.1 Contributing Factors

Figure 10.18 shows the various particle flux components in the npn bipolar transistor. We will define the various flux components and then consider the resulting currents. Although there seems to be a large number of flux components, we may help clarify the situation by correlating each factor with the minority carrier distributions shown in Figure 10.14.

The factor J_{nE}^- is the electron flux injected from the emitter into the base. As the electrons diffuse across the base, a few will recombine with majority carrier holes. The majority carrier holes that are lost by recombination must be replenished from the base terminal. This replacement hole flux is denoted by J_{RB}^+. The electron flux that reaches the collector is J_{nC}^-. The majority carrier holes from the base that are injected back into the emitter result in a hole flux denoted by J_{pE}^+. Some electrons and holes that are injected into the forward-biased B-E space charge region will recombine in this region. This recombination leads to the electron flux J_R^-. Generation of electrons and holes occurs in the reverse-biased B-C junction. This generation yields a hole flux J_G^+. Finally, the ideal reverse-saturation current in the B-C junction is denoted by the hole flux J_{pc0}^+.

The corresponding electric current density components in the npn transistor are shown in Figure 10.19 along with the minority carrier distributions for the forward-active mode. The curves are the same as in Figure 10.14. As in the pn junction, the currents in the bipolar transistor are defined in terms of minority carrier diffusion currents. The current densities are defined as follows:

J_{nE}: Due to the diffusion of minority carrier electrons in the base at $x = 0$.

J_{nC}: Due to the diffusion of minority carrier electrons in the base at $x = x_B$.

J_{RB}: The difference between J_{nE} and J_{nC}, which is due to the recombination of excess minority carrier electrons with majority carrier holes in the base. The J_{RB} current is the flow of holes into the base to replace the holes lost by recombination.

J_{pE}: Due to the diffusion of minority carrier holes in the emitter at $x' = 0$.

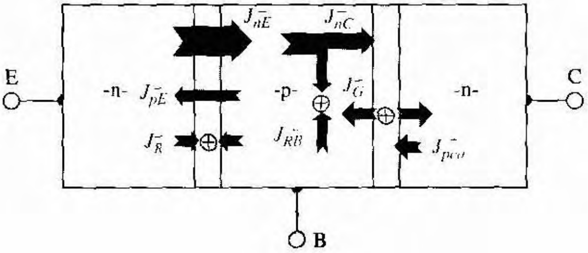

Figure 10.18 | Particle current density or flux components in an npn bipolar transistor operating in the forward-active mode

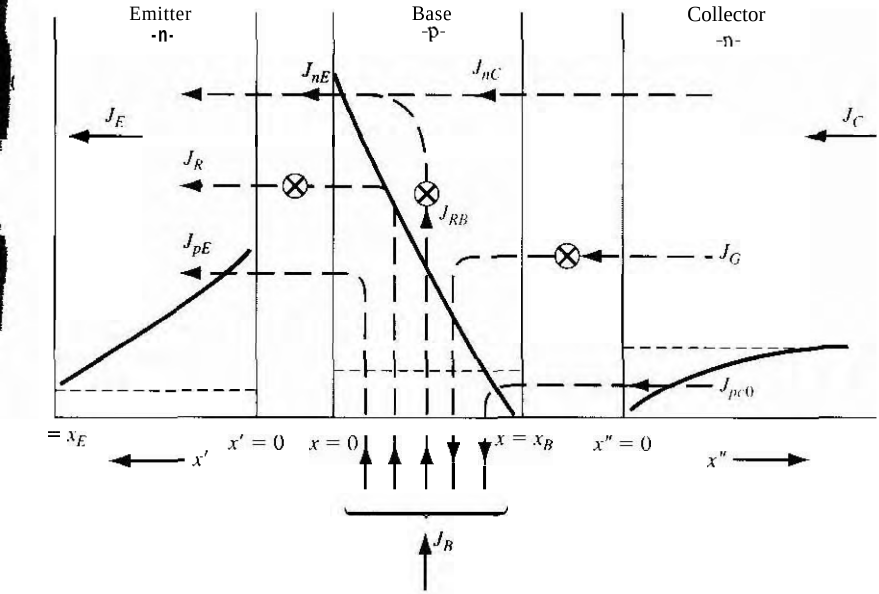

Figure 10.19 | Current density components in an npn bipolar transistor operating in the forward-active mode.

J_R: Due to the recombination of carriers in the forward-biased B-E junction.

J_{pc0}: Due to the diffusion of minority carrier holes in the collector at $x'' = 0$.

J_G: Due to the generation of carriers in the reverse-biased **B-C** junction.

The currents J_{RB}, J_{pE}, and J_R are B-E junction currents only and do not contribute to the collector current. The currents J_{pc0} and J_G are **B-C** junction currents only. These current components do not contribute to the transistor action or the current gain.

The dc common-base current gain is defined as

$$\alpha_0 = \frac{I_C}{I_E} \tag{10.27}$$

If we assume that the active cross-sectional area is the same for the collector and emitter, then we can write the current gain in terms of the current densities, or

$$\alpha_0 = \frac{J_C}{J_E} = \frac{J_{nC} + J_G + J_{pc0}}{J_{nE} + J_R + J_{pE}} \tag{10.28}$$

We are primarily interested in determining how the collector current will change with a change in emitter current. The small-signal, or sinusoidal, common-base current gain is defined as

$$\alpha = \frac{\partial J_C}{\partial J_E} = \frac{J_{nC}}{J_{nE} + J_R + J_{pE}} \tag{10.29}$$

The reverse-bias **B-C** currents, J_G and J_{pc0}, are not functions of the emitter current.

We can rewrite Equation (10.29) in the form

$$\alpha = \left(\frac{J_{nE}}{J_{nE} + J_{pE}}\right)\left(\frac{J_{nC}}{J_{nE}}\right)\left(\frac{J_{nE} + J_{pE}}{J_{nE} + J_R + J_{pE}}\right) \tag{10.30a}$$

or

$$a = \gamma \alpha_T \delta \tag{10.30b}$$

The factors in Equation (10.30b) are defined as:

$$\gamma = \left(\frac{J_{nE}}{J_{nE} + J_{pE}}\right) \qquad \equiv \text{emitter injection efficiency factor} \tag{10.31a}$$

$$\alpha_T = \left(\frac{J_{nC}}{J_{nE}}\right) \qquad \equiv \text{base transport factor} \tag{10.31b}$$

$$\delta = \frac{J_{nE} + J_{pE}}{J_{nE} + J_R + J_{pE}} \qquad \equiv \text{recombination factor} \tag{10.31c}$$

We would like to have the change in collector current be exactly the same as th change in emitter current or. ideally, to have $a = 1$. However, a consideration o Equation (10.29) shows that α will always be less than unity. The goal is to make as close to one as possible. To achieve this goal, we must make each term in Equ tion (10.30b) as close to one as possible, since each factor is less than unity.

The emitter injection *efficiency* factor γ takes into account the minority came hole diffusion current in the emitter. This current is part of the emitter current, bu does not contribute to the transistor action in that J_{pE} is not part of the collector current. The *base transport factor* α_T takes into account any recombination of exce minority carrier electrons in the base. Ideally, we want no recombination in the base The recombinution factor δ takes into account the recombination in the forward biased B-E junction. The current J_R contributes to the emitter current, but does no contribute to collector current.

10.3.2 Mathematical Derivation of Current Gain Factors

We now wish to determine each of the gain factors in terms of the electrical and geometrical parameters of the transistor. The results of these derivations will show how the various parameters in the transistor influence the electrical properties of the device and will point the way to the design of a "good bipolar transistor.

Emitter Injection Efficiency Factor Consider, initially, the emitter injection efficiency factor. We have from Equation (10.31a)

$$\gamma = \left(\frac{J_{nE}}{J_{nE} + J_{pE}}\right) = \frac{1}{\left(1 + \dfrac{J_{pE}}{J_{nE}}\right)} \tag{10.32}$$

We derived the minority carrier distribution functions for the forward-active mode in Section 10.2.1. Noting that J_{nE}, as defined in Figure 10.19, is in the negative

x direction, we can write the current densities as

$$J_{pE} = -eD_E \left. \frac{d(\delta p_E(x'))}{dx'} \right|_{x'=0} \tag{10.33a}$$

and

$$J_{nE} = (-)eD_B \left. \frac{d(\delta n_B(x))}{dx} \right|_{x=0} \tag{10.33b}$$

where $\delta p_E(x')$ and $\delta n_B(x)$ are given by Equations (10.21) and (10.15), respectively.

Taking the appropriate derivatives of $\delta p_E(x')$ and $\delta n_B(x)$, we obtain

$$J_{pE} = \frac{eD_E p_{E0}}{L_E} \left[\exp\left(\frac{eV_{BE}}{kT}\right) - 1 \right] \cdot \frac{1}{\tanh(x_E/L_E)} \tag{10.34a}$$

and

$$J_{nE} = \frac{eD_B n_{B0}}{L_B} \left\{ \frac{1}{\sinh(x_B/L_B)} + \frac{[\exp(eV_{BE}/kT) - 1]}{\tanh(x_B/L_B)} \right\}$$

Positive J_{pE} and J_{nE} values imply that the currents are in the directions shown in Figure 10.19. If we assume that the B-E junction is biased sufficiently far in the forward bias so that $V_{BE} \gg kT/e$, then

$$\exp\left(\frac{eV_{BE}}{kT}\right) \gg 1$$

and also

$$\frac{\exp(eV_{BE}/kT)}{\tanh(x_B/L_B)} \gg \frac{1}{\sinh(x_B/L_B)}$$

The emitter injection efficiency, from Equation (10.32), then becomes

$$\boxed{\gamma = \frac{1}{1 + \dfrac{p_{E0} D_E L_B}{n_{B0} D_B L_E} \cdot \dfrac{\tanh(x_B/L_B)}{\tanh(x_E/L_E)}}} \tag{10.35a}$$

If we assume that all the parameters in Equation (10.35a) except p_{E0} and n_{B0} are fixed, then in order for $\gamma \approx 1$, we must have $p_{E0} \ll n_{B0}$. We can write

$$p_{E0} = \frac{n_i^2}{N_E} \qquad \text{and} \qquad n_{B0} = \frac{n_i^2}{N_B}$$

where N_E and N_B are the impurity doping concentrations in the emitter and base, respectively. Then the condition that $p_{E0} \ll n_{B0}$ implies that $N_E \gg N_B$. For the emitter injection efficiency to be close to unity, the emitter doping must be large compared to the base doping. This condition means that many more electrons from the n-type emitter than holes from the p-type base will be injected across the B-E space charge region. If both $x_B \ll L_B$ and $x_E \ll L_E$, then the emitter injection efficiency can be written as

$$\boxed{\gamma \approx \frac{1}{1 + \dfrac{N_B}{N_E} \cdot \dfrac{D_E}{D_B} \cdot \dfrac{x_B}{x_E}}} \tag{10.35b}$$

Base Transport Factor The next term to consider is the base transport factor, given by Equation (10.31b) as $\alpha_T = J_{nC}/J_{nE}$. From the definitions of the current directions shown in Figure 10.19, we can write

$$J_{nC} = (-)eD_B \frac{d(\delta n_B(x))}{dx}\bigg|_{x=x_B} \tag{10.36a}$$

and

$$J_{nE} = (-)eD_B \frac{d(\delta n_B(x))}{dx}\bigg|_{x=0} \tag{10.36b}$$

Using the expression for $\delta n_B(x)$ given in Equation (10.15), we find that

$$J_{nC} = \frac{eD_B n_{B0}}{L_B}\left\{\frac{[\exp(eV_{BE}/kT) - 1]}{\sinh(x_B/L_B)} + \frac{1}{\tanh(x_B/L_B)}\right\} \tag{10.37}$$

The expression for J_{nE} was given in Equation (10.34a).

If we again assume that the B-E junction is biased sufficiently far in the forward bias so that $V_{BE} \gg kT/e$, then $\exp(eV_{BE}/kT) \gg 1$. Substituting Equations (10.37) and (10.34b) into Equation (10.31b), we have

$$\alpha_T = \frac{J_{nC}}{J_{nE}} \approx \frac{\exp(eV_{BE}/kT) + \cosh(x_B/L_B)}{1 + \exp(eV_{BE}/kT)\cosh(x_B/L_B)} \tag{10.38}$$

In order for α_T to be close to unity, the neutral base width x_B must be much smaller than the minority carrier diffusion length in the base L_B. If $x_B \ll L_B$, then $\cosh(x_B/L_B)$ will be just slightly greater than unity. In addition, if $\exp(eV_{BE}/kT) \gg 1$, then the base transport factor is approximately

$$\boxed{\alpha_T \approx \frac{1}{\cosh(x_B/L_B)}} \tag{10.39a}$$

For $x_B \ll L_B$, we may expand the cosh function in a Taylor series, so that

$$\boxed{\alpha_T = \frac{1}{\cosh(x_B/L_B)} \sim \frac{1}{1 + \frac{1}{2}(x_B/L_B)^2} \approx 1 - \frac{1}{2}(x_B/L_B)^2} \tag{10.39b}$$

The base transport factor α_T will be close to one if $x_B \ll L_B$. We can now see why we indicated earlier that the neutral base width x_B would be less than L_B.

Recombination Factor The recombination factor was given by Equation (10.31c). We can write

$$\delta = \frac{J_{nE} + J_{pE}}{J_{nE} + J_R + J_{pE}} \approx \frac{J_{nE}}{J_{nE} + J_R} = \frac{1}{1 + J_R/J_{nE}} \tag{10.40}$$

We have assumed in Equation (10.40) that $J_{pE} \ll J_{nE}$. The recombination current density, due to the recombination in a forward-biased pn junction, was discussed in Chapter 8 and can be written as

$$J_R = \frac{e x_{BE} n_i}{2\tau_0} \exp\left(\frac{eV_{BE}}{2kT}\right) = J_{r0} \exp\left(\frac{eV_{BE}}{2kT}\right) \tag{10.41}$$

where x_{BE} is the B-E space charge width.

The current J_{nE} from Equation (10 34b) can be approximated as

$$J_{nE} = J_{s0} \exp\left(\frac{eV_{BE}}{kT}\right) \tag{10.42}$$

where

$$J_{s0} = \frac{eD_B n_{B0}}{L_B \tanh\left(x_B/L_B\right)} \tag{10.41}$$

The recombination factor, from Equation (10.40), can then be written as

$$\boxed{\delta = \frac{1}{1 + \dfrac{J_{r0}}{J_{s0}} \exp\left(\dfrac{-eV_{BE}}{2kT}\right)}} \tag{10.44}$$

The recombination factor is a function of the B-E voltage. As V_{BE} increases, the recombination current becomes less dominant and the recombination factor approaches unity.

The recombination factor must also include surface effects. The surface effects can be described by the surface recombination velocity as we discussed in Chapter 6. Figure 10.20a shows the B-E junction of an npn transistor near the semiconductor surface. We will assume that the B-E junction is forward biased. Figure 10.20b shows the excess minority carrier electron concentration in the base along the cross section A-A'. This curve is the usual forward-biased junction minority carrier concentration. Figure 10.20c shows the excess minority carrier electron concentration along the cross section C-C' from the surface. We showed earlier that the excess concentration at a surface is smaller than the excess concentration in the bulk material. With this electron distribution, there is a diffusion of electrons from the bulk toward the surface where the electrons recombine with the majority carrier holes. Figure 10.20d shows the injection of electrons from the emitter into the base and the diffusion of electrons toward the surface. This diffusion generates another component of recombination current and this component of recombination current must be included in the recombination factor δ. Although the actual calculation is difficult because of the two-dimensional analysis required, the form of the recombination current is the same as that of Equation (10.41).

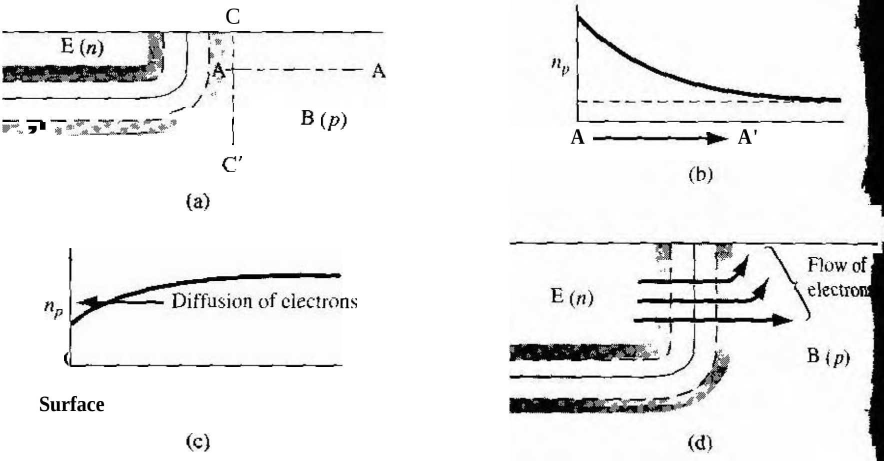

Figure 10.20 | The surface at the E-B junction showing the diffusion of carriers toward the surface.

10.3.3 Summary

Although we have considered an npn transistor in all of the derivations, exactly the same analysis applies to a pnp transistor; the same minority carrier distributions will be obtained except that the electron concentrations will become hole concentrations and vice versa. The current directions and voltage polarities will also change.

We have been considering the common-base current gain, defined in Equation (10.27) as $\alpha_0 = I_C/I_E$. The common-emitter current gain is defined as $\beta_0 = I_C/I_B$. From Figure 10.8 we see that $I_E = I_B + I_C$. We can determine the relation between common-emitter and common-base current gains from the KCL equation. We can write

$$\frac{I_E}{I_C} = \frac{I_B}{I_C} + 1$$

Substituting the definitions of current gains, we have

$$\frac{1}{\alpha_0} = \frac{1}{\beta_0} + 1$$

Since this relation actually holds for both dc and small-signal conditions, we can drop the subscript. The common-emitter current gain can now be written in terms of the common-base current gain as

$$\beta = \frac{\alpha}{1 - \alpha}$$

The common-base current gain, in terms of the common-emitter current gain, is found to be

$$\alpha = \frac{\beta}{1 + \beta}$$

Table 10.3 | Summary of limiting factors

Emitter injection efficiency

$$\gamma \approx \frac{1}{1 + \frac{N_B}{N_E} \cdot \frac{D_E}{D_B} \cdot \frac{x_B}{x_E}} \qquad (x_B \ll L_B),\ (x_E \ll L_E)$$

Base transport factor

$$\alpha_T \approx \frac{1}{1 + \frac{1}{2}\left(\frac{x_B}{L_B}\right)^2} \qquad (x_B \ll L_B)$$

Recombination factor

$$\delta = \frac{1}{1 + \frac{J_{r0}}{J_{s0}} \exp\left(\frac{-eV_{BE}}{2kT}\right)}$$

Common-base current gain

$$\alpha = \gamma\alpha_T\delta \approx \frac{1}{1 + \frac{N_B}{N_E} \cdot \frac{D_E}{D_B} \cdot \frac{x_B}{x_E} + \frac{1}{2}\left(\frac{x_B}{L_B}\right)^2 + \frac{J_{r0}}{J_{s0}} \exp\left(\frac{-eV_{BE}}{2kT}\right)}$$

Common-emitter current gain

$$\beta = \frac{\alpha}{1-\alpha} \approx \frac{1}{\frac{N_B}{N_E} \cdot \frac{D_E}{D_B} \cdot \frac{x_B}{x_E} + \frac{1}{2}\left(\frac{x_B}{L_B}\right)^2 + \frac{J_{r0}}{J_{s0}} \exp\left(\frac{-eV_{BE}}{2kT}\right)}$$

Table 10.3 summarizes the expressions for the limiting factors in the common base current gain assuming that $x_B \ll L_B$ and $x_E \ll L_E$. Also given are the approximate expressions for the common-base current gain and the common-emitter current gain.

10.3.4 Example Calculations of the Gain Factors

If we assume a typical value of β to be 100, then $\alpha = 0.99$. If we also assume that $\gamma = \alpha_T = \delta$, then each factor would have to be equal to 0.9967 in order that $\beta = 100$. This calculation gives an indication of how close to unity each factor must be in order to achieve a reasonable current gain.

DESIGN EXAMPLE 10.1

Objective

To design the ratio of emitter doping to base doping in order to achieve an emitter injection efficiency factor equal to $\gamma = 0.9967$.

Consider an npn bipolar transistor. Assume, for simplicity, that $D_E = D_B$, $L_E = L_B$, and

Solution

Equation (10.35a) reduces to

$$\gamma = \frac{1}{1 + \dfrac{p_{E0}}{n_{B0}}} = \frac{1}{1 + \dfrac{n_i^2/N_E}{n_i^2/N_B}}$$

so

$$y = \frac{I}{I + \dfrac{N_B}{N_E}} = 0.9967$$

Then

$$\frac{N_B}{N_E} = 0.00331 \qquad \text{or} \qquad \frac{N_E}{N_A} - 302$$

■ Comment

The emitter doping concentration must be much larger than the base doping concentration achieve a high emitter injection efficiency.

DESIGN EXAMPLE 10.2

Objective

To design the base width required to achieve a base transport factor equal to $\alpha_T = 0.99$

Consider a pnp bipolar transistor. Assume that $D_B = 10\ \text{cm}^2/\text{s}$ and $\tau_{B0} = 10^{-7}$ s.

Solution

The base transport factor applies to both pnp and npn transistors and is given by

$$\alpha_T = \frac{1}{\cosh(x_B/L_B)} = 0.9967$$

Then

$$x_B/L_B = 0.0814$$

We have

$$L_B = \sqrt{D_B \tau_{B0}} = \sqrt{(10)(10^{-7})} = 10^{-3}\ \text{cm}$$

so that the base width must then be

$$x_B = 0.814 \times 10^{-4}\ \text{cm} = 0.813\ \mu\text{m}$$

■ Comment

If the base width is less than approximately 0.8 μm, then the required base transport facto will be achieved. In most cases, the base transport factor will not be the limiting factor in th bipolar transistor current gain.

EXAMPLE 10.3

Objective

To calculate the forward-biased B-E voltage required to achieve a recombination factor equal to $\delta = 0.9967$.

Consider an npn bipolar transistor at $T = 300$ K. Assume that $J_{r0} = 10^{-8}$ A/cm^2 and that $J_{s0} = 10^{-11}$ A/cm^2.

■ Solution

The recombination factor, from Equation (10.44), is

$$\delta = \frac{1}{1 + \dfrac{J_{r0}}{J_{s0}} \exp\left(\dfrac{-eV_{BE}}{2kT}\right)}$$

We then have

$$0.9967 = \frac{1}{1 + \dfrac{10^{-8}}{10^{-11}} \exp\left(\dfrac{-eV_{BE}}{2kT}\right)}$$

We can rearrange this equation and write

$$\exp\left(\frac{+eV_{BE}}{2kT}\right) = \frac{0.9967 \times 10^3}{1 - 0.9967} = 3.02 \times 10^5$$

$$V_{BE} = 2(0.0259) \ln (3.02 \times 10^5) = 0.654 \text{ V}$$

■ Comment

This example demonstrates that the recombination factor may be an important limiting factor in the bipolar current gain. In this example, if V_{BE} is smaller than 0.654 V, then the recombination factor δ will fall below the desired 0.9967 value.

EXAMPLE 10.4

Objective

To calculate the common-emitter current gain of a silicon npn bipolar transistor at $T = 300$ K given a set of parameters.

Assume the following parameters:

$$\begin{array}{ll}
D_E = 10 \text{ cm}^2/\text{s} & x_B = 0.70\ \mu\text{m} \\
D_B = 25 \text{ cm}^2/\text{s} & x_E = 0.50\ \mu\text{m} \\
\tau_{E0} = 1 \times 10^{-7} \text{ s} & N_E = 1 \times 10^{18} \text{ cm}^{-3} \\
\tau_{B0} = 5 \times 10^{-7} \text{ s} & N_B = 1 \times 10^{16} \text{ cm}^{-3} \\
J_{r0} = 5 \times 10^{-8} \text{ A/cm}^2 & V_{BE} = 0.65 \text{ V}
\end{array}$$

The following parameters are calculated:

$$p_{E0} = \frac{(1.5 \times 10^{10})^2}{1 \times 10^{18}} = 2.25 \times 10^2 \text{ cm}^{-3}$$

$$n_{B0} = \frac{(1.5 \times 10^{10})^2}{1 \times 10^{16}} = 2.25 \times 10^4 \text{ cm}^{-3}$$

$$L_E = \sqrt{D_E \tau_{E0}} = 10^{-3} \text{ cm}$$

$$L_B = \sqrt{D_B \tau_{B0}} = 3.54 \times 10^{-3} \text{ cm}$$

■ Solution

The emitter injection efficiency factor, from Equation (10.35a), is

$$\gamma = \frac{1}{1 + \dfrac{(2.25 \times 10^2)(10)(3.54 \times 10^{-3})}{(2.25 \times 10^4)(25)(10^{-3})} \cdot \dfrac{\tanh(0.0198)}{\tanh(0.050)}} = 0.9944$$

The base transport factor, from Equation (10.39a) is

$$\alpha_T = \frac{1}{\cosh\left(\dfrac{0.70 \times 10^{-4}}{3.54 \times 10^{-3}}\right)} = 0.9998$$

The recombination factor, from Equation (10.44), is

$$\delta = \frac{1}{1 + \dfrac{5 \times 10^{-8}}{J_{s0}} \exp\left(\dfrac{-0.65}{2(0.0259)}\right)}$$

where

$$J_{s0} = \frac{eD_B n_{B0}}{L_B \tanh\left(\dfrac{x_B}{L_B}\right)} = \frac{(1.6 \times 10^{-19})(25)(2.25 \times 10^4)}{3.54 \times 10^{-3} \tanh(1.977 \times 10^{-2})} = 1.29 \times 10^{-9} \text{ A/cm}^2$$

We can now calculate $\delta = 0.99986$. The common-base current gain is then

$$\mathbf{a} = \gamma \alpha_T \delta = (0.9944)(0.9998)(0.99986) = 0.99406$$

which gives a common-emitter current gain of

$$\beta = \frac{\alpha}{1 - a} = \frac{0.99406}{1 - 0.99406} = 167$$

■ Comment

In this example, the emitter injection efficiency is the limiting factor in the current gain.

TEST YOUR UNDERSTANDING

NOTE: In Exercises E10.4 through E10.9, assume a silicon npn bipolar transistor at T = 300 K has the following minority carrier parameters: $D_E = 8 \text{ cm}^2/\text{s}$, $D_B = 20 \text{ cm}^2/\text{s}$, $D_C = 12 \text{ cm}^2/\text{s}$, $\tau_{E0} = 10^{-8}$ s, $\tau_{B0} = 10^{-7}$ s, $\tau_{C0} = 10^{-6}$ s.

E10.4 If the emitter doping concentration is $N_E = 5 \times 10^{18}$ cm^{-3}, find the base doping concentration such that the emitter injection efficiency is $\gamma = 0.9950$. Assume $x_E = 2x_B = 2\ \mu$m. (Ans. $N_B = 1.03 \times 10^{16}$ cm^{-3})

E10.5 Assume that $\alpha_T = \delta = 0.9967$, $x_B = x_E = 1\ \mu$m, $N_B = 5 \times 10^{16}$ cm^{-3}, and $N_E = 5 \times 10^{18}$ cm^{-3}. Determine the common emitter current gain β. (Ans. $\beta = 92.5$)

E10.6 Determine the minimum base width x_B such that the base transport factor is $\alpha_T = 0.9980$. (Ans. $x_B = 0.895\ \mu$m)

E10.7 Assume that $\gamma = \delta = 0.9967$ and $x_B = 0.80\ \mu$m. Determine the common-emitter current gain β. (Ans. $\beta = 121$)

E10.8 If $J_{r0} = 10^{-8}$ A/cm^2 and $J_{s0} = 10^{-11}$ A/cm^2, find the value of V_{BE} such that $\delta = 0.9960$. (Ans. $V_{BE} = 0.6436$ V)

E10.9 Assume that $\gamma = \alpha_T = 0.9967$, $J_{r0} = 5 \times 10^{-9}$ A/cm^2, $J_{s0} = 10^{-11}$ A/cm^2, and $V_{BE} = 0.585$ V. Determine the common-emitter current gain β. (Ans. $\beta = 77.4$)

10.4 | NONIDEAL EFFECTS

In all previous discussions, we have considered a transistor with uniformly doped regions, low injection, constant emitter and base widths, an ideal constant energy bandgap, uniform current densities, and junctions which are not in breakdown. If any of these ideal conditions are not present, then the transistor properties will deviate from the ideal characteristics we have derived.

10.4.1 Base Width Modulation

We have implicitly assumed that the neutral base width x_B was constant. This base width, however, is a function of the B-C voltage, since the width of the space charge region extending into the base region varies with B-C voltage. As the B-C reverse-bias voltage increases, the B-C space charge region width increases, which reduces x_B. A change in the neutral base width will change the collector current as can be observed in Figure 10.21. A reduction in base width will cause the gradient in the minority carrier concentration to increase, which in turn causes an increase in the diffusion current. This effect is known as ***base width modulation;*** it is also called the ***Early effect.***

The Early effect can be seen in the current-voltage characteristics shown in Figure 10.22. In most cases, a constant base current is equivalent to a constant B-E voltage. Ideally the collector current is independent of the B-C voltage so that the slope of the curves would be zero; thus the output conductance of the transistor would be zero. However, the base width modulation, or Early effect, produces a nonzero slope and gives rise to a finite output conductance. If the collector current characteristics are extrapolated to zero collector current, the curves intersect the voltage axis at a point that is defined as the Early voltage. The Early voltage is considered to be a positive value. It is a common parameter given in transistor specifications; typical values of Early voltage are in the 100- to 300-volt range.

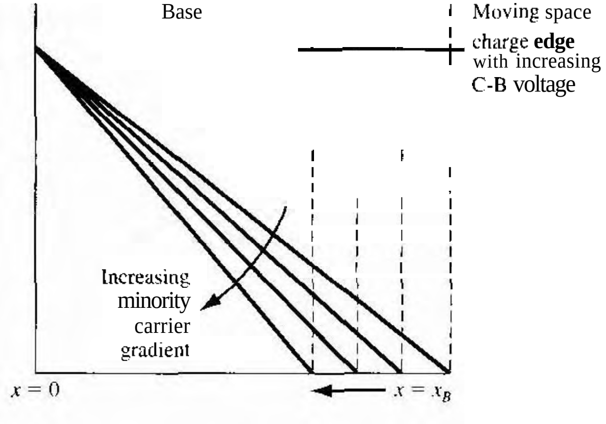
Base
Moving space charge edge with increasing C-B voltage
Increasing minority carrier gradient
$x = 0$
$x = x_B$

Figure 10.21 | The change in the base width and the change in the minority carrier gradient as the B-C space charge width changes.

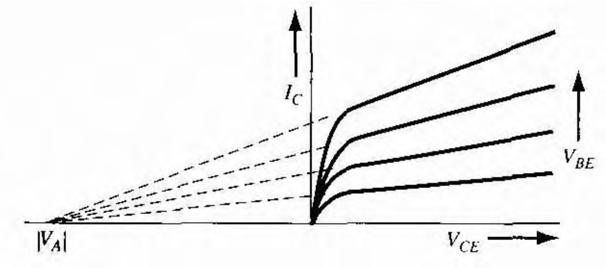

Figure 10.22 | The collector current versus collector–emitter voltage showing the Early effect and Early voltage.

From Figure 10.22, we can write that

$$\frac{dI_C}{dV_{CE}} \equiv g_0 = \frac{I_C}{V_{CE} + V_A} \tag{10.45a}$$

where V_A and V_{CE} are defined as positive quantities and g_0 is defined as the outpu conductance. Equation (10.45a) can be rewritten in the form

$$I_C = g_0(V_{CE} + V_A) \tag{10.45b}$$

showing explicitly that the collector current is now a function of the C-E voltage or the C-B voltage.

EXAMPLE 10.5

Objective

To calculate the change in the neutral base width with a change in C-B voltage.

Consider a uniformly doped silicon bipolar transistor at T = 300 K with a base doping of $N_B = 5 \times 10^{16}$ cm^{-3} and a collector doping of $N_C = 2 \times 10^{15}$ cm^{-3}. Assume the metallurgical base width is 0.70 μm. Calculate the change in the neutral base width as the C-B voltage changes from 2 to 10 V.

■ Solution

The space charge width extending into the base region can be written as

$$x_{dB} = \left\{ \frac{2\epsilon_s(V_{bi} + V_{CB})}{e} \left[\frac{N_C}{N_B} \cdot \frac{1}{(N_B + N_C)} \right] \right\}^{1/2}$$

$$x_{dB} = \left\{ \frac{2(11.7)(8.85 \times 10^{-14})(V_{bi} + V_{CB})}{1.6 \times 10^{-19}} \times \left[\frac{2 \times 10^{15}}{5 \times 10^{16}} \cdot \frac{1}{(5 \times 10^{16} + 2 \times 10^{15})} \right] \right\}^{1/2}$$

which becomes

$$x_{dB} = \{(9.96 \times 10^{-12})(V_{bi} + V_{CB})\}^{1/2}$$

The built-in potential is

$$V_{bi} = \frac{kT}{e} \ln\left[\frac{N_B N_C}{n_i^2} \right] = 0.718 \text{ V}$$

For $V_{CB} = 2$ V, we find $x_{dB} = 0.052$ μm, and for $V_{CB} = 10$ V, we find $x_{dB} = 0.103$ μm. If we neglect the B-E space charge region, which will be small because of the forward-biased junction, then we can calculate the neutral base width. For $V_{CB} = 2$ V.

$$x_B = 0.70 - 0.052 = 0.648 \ \mu\text{m}$$

and for $V_{CB} = 10$ V,

$$x_B = 0.70 - 0.103 = 0.597 \ \mu\text{m}$$

■ Comment

This example shows that the neutral base width can easily change by approximately 8 percent as the C-B voltage changes from 2 to 10 V.

Objective

EXAMPLE 10.6

To calculate the change in collector current with a change in neutral base width, and to estimate the Early voltage.

Consider a uniformly doped silicon npn bipolar transistor with parameters described in Example 10.5. Assume $D_B = 25$ cm^2/s, and $V_{BE} = 0.60$ V, and also assume that $x_B \ll L_B$.

■ Solution

The excess minority carrier electron concentration in the base is given by Equation (10.15) as

$$\delta n_B(x) = \frac{n_{B0}\left\{\left[\exp\left(\frac{eV_{BE}}{kT}\right) - 1\right] \sinh\left(\frac{x_B - x}{L_B}\right) - \sinh\left(\frac{x}{L_B}\right)\right\}}{\sinh\left(\frac{x_B}{L_B}\right)}$$

If $x_B \ll L_B$, then $(x_B - x) \ll L_B$ so we can write the approximations

$$\sinh\left(\frac{x_B}{L_B}\right) \quad \left(\frac{x_B}{L_B}\right) \qquad \text{and} \qquad \sinh\left(\frac{x_B - x}{L_B}\right) \approx \left(\frac{x_B - x}{L_B}\right)$$

The expression for $\delta n_B(x)$ can then be approximated as

$$\delta n_B(x) \approx \frac{n_{B0}}{x_B}\left\{\left[\exp\left(\frac{eV_{BE}}{kT}\right) - 1\right](x_B - x) - x\right\}$$

The collector current is now

$$|J_C| = eD_B \frac{d(\delta n_B(x))}{dx} \approx \frac{eD_B n_{B0}}{x_B} \exp\left(\frac{eV_{BE}}{kT}\right)$$

The value of n_{B0} is calculated as

$$n_{B0} = \frac{n_i^2}{N_B} = \frac{(1.5 \times 10^{10})^2}{5 \times 10^{16}} = 4.5 \times 10^3 \text{ cm}^{3}$$

If we let $x_B = 0.648\,\mu\text{m}$ when $V_{CB} = 2\text{ V}$ ($V_{CE} = 2.6\text{ V}$), then

$$|J_C| = \frac{(1.6 \times 10^{-19})(25)(4.5 \times 10^3)}{0.648 \times 10^{-4}} \exp\left(\frac{0.60}{0.0259}\right) = 3.20\text{ A/cm}^2$$

Now let $x_B = 0.597\,\mu\text{m}$ when $V_{CB} = 10\text{ V}$ ($V_{CE} = 10.6\text{ V}$). In this case we have $|J_C| = 3.47\text{ A/cm}^2$. From Equation (10.45a), we can write

$$\frac{dJ_C}{dV_{CE}} = \frac{J_C}{V_{CE} + V_A} = \frac{\Delta J_C}{\Delta V_{CE}}$$

Using the calculated values of current and voltage, we have

$$\frac{\Delta J_C}{\Delta V_{CE}} = \frac{3.47 - 3.20}{10.6 - 2.6} = \frac{J_C}{V_{CE} + V_A} \approx \frac{3.20}{2.6 + V_A}$$

The Early voltage is then determined to be

$$V_A \approx 92\text{ V}$$

■ Comment

This example indicates how much the collector current can change as the neutral base width changes with a change in the B-C space charge width. and it also indicates the magnitude of the Early voltage.

The example demonstrates, too, that we can expect variations in transistor properties due to tolerances in transistor-fabrication processes. There will be variations, in particular, in the base width of narrow-base transistors that will cause variations in the collector current characteristics simply due to the tolerances in processing.

TEST YOUR UNDERSTANDING

E10.10 A particular transistor has an output resistance of 200 kΩ and an Early voltage of $V_A = 125$ V. Determine the change in collector current when V_{CE} increases from 2 V to 8 V. (Ans. $\Delta I_C = 30\ \mu$A)

E10.11 (*a*) If, because of fabrication tolerances, the neutral base width for a set of transistors varies over the range of $0.800 \le x_B \le 1.00\ \mu$m, determine the variation in the base transport factor α_T. Assume $L_B = 1.414 \times 10^{-3}$ cm. (*b*) Using the results of part (*a*) and assuming $\gamma = \delta = 0.9967$, what is the variation in common emitter current gain. [Ans. (*a*) $0.9975 \le \alpha_T \le 0.9984$, (*b*) $109 \le \beta \le 121$]

10.4.2 High Injection

The ambipolar transport equation that we have used to determine the minority carrier distributions assumed low injection. As V_{BE} increases, the injected minority carrier concentration may approach, or even become larger than, the majority carrier concentration. If we assume quasi-charge neutrality, then the majority carrier hole concentration in the p-type base at $x = 0$ will increase as shown in Figure 10.23 because of the excess holes.

Two effects occur in the transistor at high injection. The first effect is a reduction in emitter injection efficiency. Since the majority carrier hole concentration at $x = 0$ increases with high injection, more holes are injected back into the emitter because of the forward-biased B-E voltage. An increase in the hole injection causes an increase in the J_{pE} current, and an increase in J_{pE} reduces the emitter injection efficiency. The common, emitter current gain decreases, then, with high injection. Figure 10.24 shows a typical common-emitter current gain versus collector current

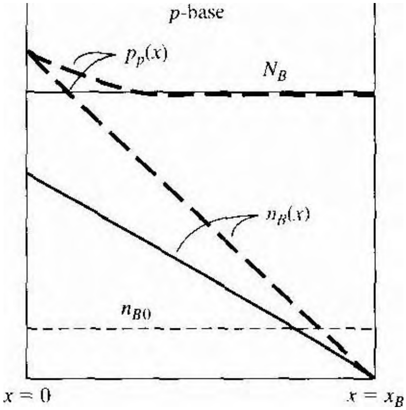

Figure 10.23 | Minority and majority carrier concentrations in the base under low and high injection (solid line: low injection: dashed line: high injection).

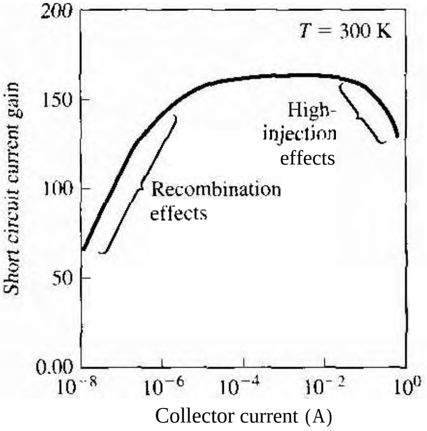

Figure 10.24 | Common-emitter current gain versus collector current. *(From Shur [13].)*

curve. The low gain at low currents is due to the small recombination factor and the drop-off at the high current is due to the high-injection effect.

We will now consider the second high-injection effect. At low injection, the majority carrier hole concentration at $x = 0$ for the npn transistor is

$$p_p(0) = p_{p0} = N_a \tag{10.46a}$$

and the minority carrier electron concentration is

$$n_p(0) = n_{p0} \exp\left(\frac{eV_{BE}}{kT}\right) \tag{10.46b}$$

The pn product is

$$p_p(0)n_p(0) = p_{p0}n_{p0} \exp\left(\frac{eV_{BE}}{kT}\right) \qquad (10.4$$

At high injection, Equation (10.46c) still applies. However, $p_p(0)$ will also increase, and for very high injection it will increase at nearly the same rate as $n_p(0)$. The increase in $n_p(0)$ will asymptotically approach the function

$$n_p(0) \approx n_{p0} \exp\left(\frac{eV_{BE}}{2kT}\right) \qquad (10.4$$

The excess minority carrier concentration in the base, and hence the collector current, will increase at a slower rate with B-E voltage in high injection than low injection. This effect is shown in Figure 10.25. The high-injection effect is very similar to the effect of a series resistance in a pn junction diode.

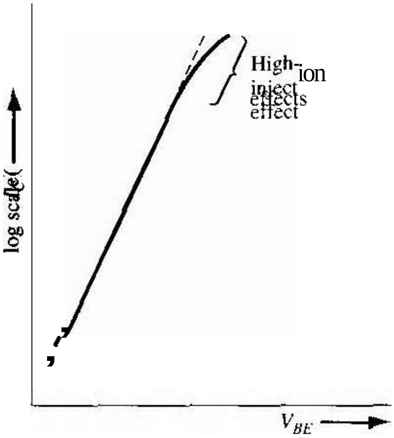

Figure 10.25 | Collector current versus base–emitter voltage showing high-injection effects.

10.4.3 Emitter Bandgap Narrowing

Another phenomenon affecting the emitter injection efficiency is bandgap narrowing. We implied from our previous discussion that the emitter injection efficiency factor would continue to increase and approach unity as the ratio of emitter doping to base doping continued to increase. As silicon becomes heavily doped, the discrete donor energy level in an n-type emitter splits into a band of energies. The distance between donor atoms decreases as the concentration of impurity donor atoms increases and the splitting of the donor level is caused by the interaction of donor atoms with each other. As the doping continues to increase, the donor band widens, becomes skewed, and moves up toward the conduction band, eventually merging with it. At this point, the effective bandgap energy has decreased. Figure 10.26 shows a plot of the change in the bandgap energy with impurity doping concentration.

A reduction in the bandgap energy increases the intrinsic carrier concentration. The intrinsic carrier concentration is given by

$$n_i^2 = N_c N_v \exp\left(\frac{-E_g}{kT}\right) \tag{10.48}$$

In a heavily doped emitter, the intrinsic carrier concentration can be written as

$$n_{iE}^2 = N_c N_v \exp\left[\frac{-(E_{g0} - \Delta E_g)}{kT}\right] = n_i^2 \exp\left(\frac{\Delta E_g}{kT}\right) \tag{10.49}$$

where E_{g0} is the bandgap energy at a low doping concentration and ΔE_g is the bandgap narrowing factor.

The emitter injection efficiency factor was given by Equation (10.35) as

$$\gamma = \frac{1}{1 + \dfrac{p_{E0} D_E L_B}{n_{B0} D_B L_E} \cdot \dfrac{\tanh(x_B/L_B)}{\tanh(x_E/L_E)}}$$

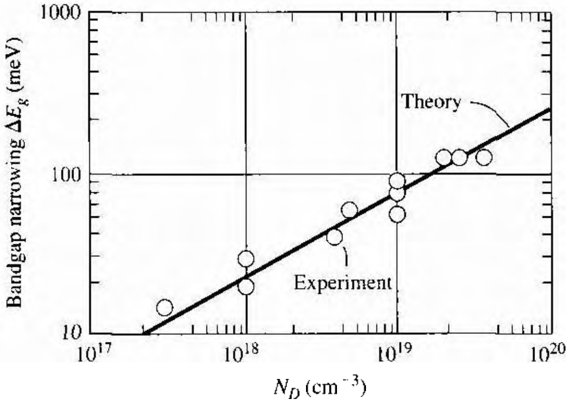

Figure 10.26 | Bandgap-narrowing factor versus donor impurity concentration in silicon.
(From Sze [18].)

The term p_{E0} is the thermal-equilibrium minority carrier concentration in the emitter and must be written as

$$p_{E0} = \frac{n_{iE}^2}{N_E} = \frac{n_i^2}{N_E}\exp\left(\frac{\Delta E_g}{kT}\right) \qquad \text{(10}$$

As the emitter doping increases, ΔE_g increases; thus, p_{E0} does not continue to decrease with increased emitter doping. If p_{E0} starts to increase because of the bandgap narrowing, the emitter injection efficiency begins to fall off instead of continuing increase with increased emitter doping.

EXAMPLE 10.7

Objective

To determine the increase in p_{E0} in the emitter due to bandgap narrowing.

Consider a silicon emitter at T = 300 K. Assume the emitter doping increases fr 10^{18} cm^{-3} to 10^{19} cm^{-3}. Calculate the change in the p_{E0} value.

Solution

For emitter dopings of $N_E = 10^{18}$ cm^{-3} and 10^{19} cm^{-3}, we have, neglecting bandgap narrowing,

$$p_{E0} = \frac{n_i^2}{N_E} = \frac{(1.5 \times 10^{10})^2}{10^{18}} = 2.25 \times 10^2 \text{ cm}^{-3}$$

and

$$p_{E0} = \frac{(1.5 \times 10^{10})^2}{10^{19}} = 2.25 \times 10^1 \text{ cm}^{-3}$$

Taking into account the bandgap narrowing, we obtain, respectively, for $N_E = 10^{18}$ cm^{-3} and $N_E = 10^{19}$ cm^{-3}

$$p_{E0} = \frac{(1.5 \times 10^{10})^2}{10^{18}}\exp\left(\frac{0.030}{0.0259}\right) = 7.16 \times 10^2 \text{ cm}^{-3}$$

and

$$p_{E0} = \frac{(1.5 \times 10^{10})^2}{10^{19}}\exp\left(\frac{0.1}{0.0259}\right) = 1.07 \times 10^3 \text{ cm}^{-3}$$

■ Comment

If the emitter doping increases from 10^{18} to 10^{19} cm^{-3}, the thermal-equilibrium minority carrier concentration actually increases by a factor of 1.5 instead of decreasing by the expected factor of 10. This effect is due to bandgap narrowing.

As the emitter doping increases, the **bandgap narrowing** factor, AE,, will increase; this can actually cause p_{E0} to increase. As p_{E0} increases, the emitter injection efficiency decreases; this then causes the transistor gain to decrease, as in Figure 10.24.

A very high emitter doping may result in a smaller current gain than we anticipate because of the bandgap-narrowing effect.

10.4.4 Current Crowding

It is tempting to minimize the effects of base current in a transistor since the base current is usually much smaller than either the collector or the emitter current. Figure 10.27 is a cross section of an npn transistor showing the lateral distribution of base current. The base region is typically less than a micrometer thick, so there can be a sizable base resistance. The nonzero base resistance results in a lateral potential difference under the emitter region. For the npn transistor, the potential decreases from the edge of the emitter toward the center. The emitter is highly doped, so as a first approximation the emitter can be considered an equipotential region.

The number of electrons from the emitter injected into the base is exponentially dependent on the B-E voltage. With the lateral voltage drop in the base between the edge and center of the emitter, more electrons will be injected near the emitter edges than in the center, causing the emitter current to be crowded toward the edges. This current-crowding effect is schematically shown in Figure 10.28. The larger current density near the emitter edge may cause localized heating effects as well as localized high-injection effects. The nonuniform emitter current also results in a nonuniform lateral base current under the emitter. A two-dimensional analysis would be required to calculate the actual potential drop versus distance because of the nonuniform base current. Another approach is to slice the transistor into a number of smaller parallel transistors and to lump the resistance of each base section into an equivalent external resistance.

Power transistors, designed to handle large currents, require large emitter areas to maintain reasonable current densities. To avoid the current-crowding effect, these transistors are usually designed with narrow emitter widths and fabricated with an interdigitated design. Figure 10.29 shows the basic geometry. In effect, many narrow emitters are connected in parallel to achieve the required emitter area.

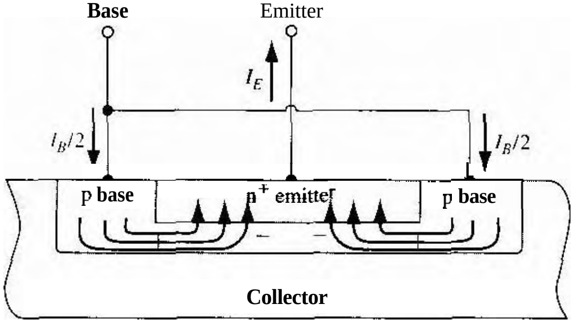

Figure 10.27 | Cross section of an npn bipolar transistor showing the base current distribution and the lateral potential drop in the base region.

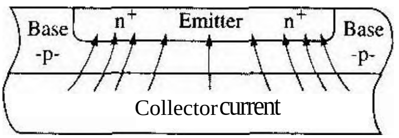

Figure 10.28 | Cross section of an npn bipolar transistor showing the emitter current-crowding effect.

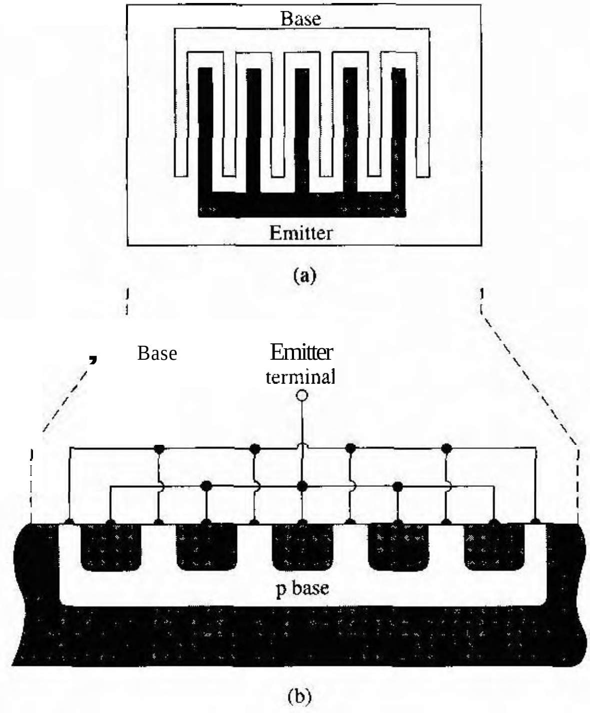

Figure 10.29 | (a) Top view and (b) cross section of an interdigitated npn bipolar transistor structure.

TEST YOUR UNDERSTANDING

E10.12 Consider the geometry shown in Figure 10.30. The base doping concentration is $N_B = 10^{16}$ cm^{-3}, the neutral base width is $x_B = 0.80$ μm, the emitter width is $S = 10$ μm, and the emitter length is $L = 10$ μm. (a) Determine the resistance of the base between $x = 0$ and $x = S/2$. Assume a hole mobility of $\mu_p = 400$ cm^2/V-s. (b) If the base current in this region is uniform and given by $I_B/2 = 5$ μA, determine the potential difference between $x = 0$ and $x = S/2$. (c) Using the results of part (b), what is the ratio of emitter current density at $x = 0$ to that at $x = S/2$?
[Ans. (a) 9.77 kΩ, (b) 48.85 mV, (c) 6.59]

*10.4.5 Nonuniform Base Doping

In the analysis of the bipolar transistor, we assumed uniformly doped regions. However, uniform doping rarely occurs. Figure 10.31 shows a doping profile in a doubly diffused npn transistor. We can start with a uniformly doped n-type substrate, diffuse acceptor atoms from the surface to form a compensated p-type base, and then diffuse donor atoms from the surface to form a doubly compensated n-type emitter. The diffusion process results in a nonuniform doping profile.

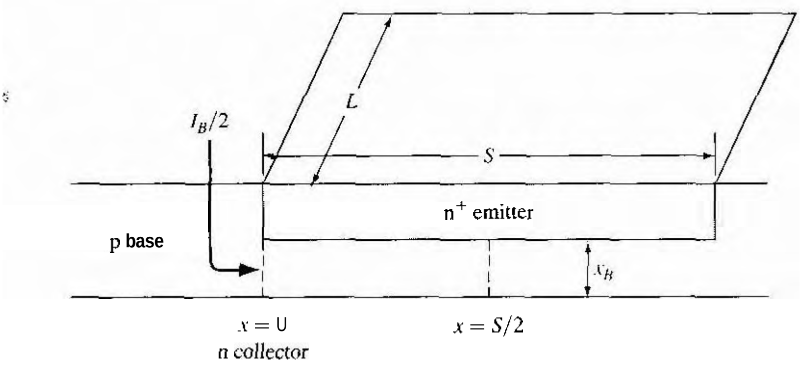

Figure 10.30 | Figure for E10.12.

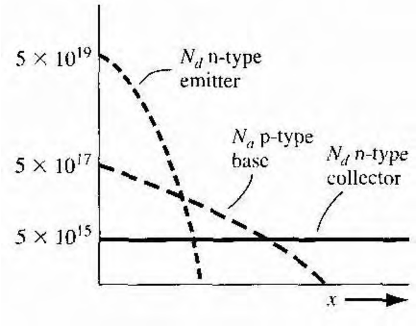

Figure 10.31 | Impurity concentration profiles of a double-diffused npn bipolar transistor.

We determined in Chapter 5 that a graded impurity concentration leads to an induced electric field. For the p-type base region in thermal equilibrium, we can write

$$J_p = e\mu_p N_a \mathrm{E} - eD_p \frac{dN_a}{dx} = 0 \tag{10.51}$$

Then

$$\mathrm{E} = +\left(\frac{kT}{e}\right)\frac{1}{N_a}\frac{dN_a}{dx} \tag{10.52}$$

According to the example of Figure 10.31, dN_a/dx is negative; hence, the induced electric field is in the negative x direction.

Electrons are injected from the n-type emitter into the base and the minority carrier base electrons begin diffusing toward the collector region. The induced electric field in the base, because of the nonuniform doping, produces a force on the electrons in the direction toward the collector. The induced electric field, then, aids the flow of minority carriers across the base region. This electric field is called an ***accelerating field.***

The accelerating field will produce a drift component of current that is in ad tion to the existing diffusion current. Since the minority carrier electron concent tion varies across the base, the drift current density will not he constant. The to current across the base, however, is nearly constant. The induced electric field in t base due to nonuniform base doping will alter the minority carrier distributi through the base so that the sum of drift current and diffusion current will be a co stant. Calculations have shown that the uniformly doped base theory is very useful for estimating the base characteristics.

10.4.6 Breakdown Voltage

There are two breakdown mechanisms to consider in a bipolar transistor. The first called punch-through. As the reverse-bias B-C voltage increases, the B-C space charge region widens and extends farther into the neutral base. It is possible for the B-C depletion region to penetrate completely through the base and reach the B-E space charge region, the effect called *punch-through.* Figure 10.32a shows the energy-band diagram of an npn bipolar transistor in thermal equilibrium and Figure 10.32b shows the energy-band diagram for two values of reverse-bias B-C junction voltag When a small C-B voltage, V_{R1}, is applied, the B-E potential barrier is not affecte thus, the transistor current is still essentially zero. When a large reverse-bias voltag V_{R2}, is applied, the depletion region extends through the base region and the B- potential barrier is lowered because of the C-B voltage. The lowering of the potentia barrier at the B-E junction produces a large increase in current with a very smal increase in C-B voltage. This effect is the punch-through breakdown phenomenon.

Figure 10.33 shows the geometry for calculating the punch-through voltage. Assume that N_B and N_C are the uniform impurity doping concentrations in the base an collector, respectively. Let W_B be the metallurgical width of the base and let x_{dB} be th space charge width extending into the base from the B-C junction. If we neglect th

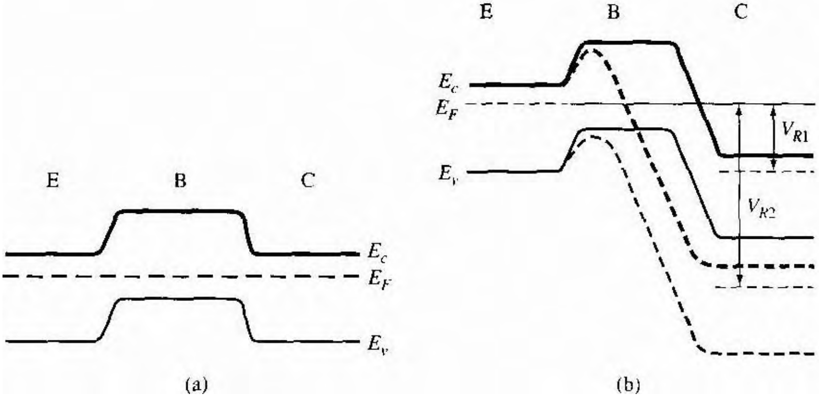

Figure 10.32 | Energy-band diagram of an npn bipolar transistor (a) in thermal equilibrium. and (b) with a reverse-bias B-C voltage before punch-through, V_{R1} and after punch-through, V_{R2}.

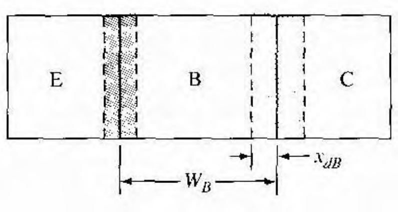

Figure 10.33 | Geometry of a bipolar transistor to calculate the punch-through voltage.

narrow space charge width of a zero-biased or forward-biased B-E junction, then punch-through, assuming the abrupt junction approximation, occurs when $x_{dB} = W_B$. We can write that

$$x_{dB} = W_B = \left\{ \frac{2\epsilon_s(V_{bi} + V_{pt})}{e} \cdot \frac{N_C}{N_B} \cdot \frac{1}{N_C + N_B} \right\}^{1/2} \tag{10.53}$$

where V_{pt} is the reverse-biased B-C voltage at punch-through. Neglecting V_{bi} compared to V_{pt}, we can solve for V_{pt} as

$$\boxed{V_{pt} = \frac{eW_B^2}{2\epsilon_s} \cdot \frac{N_B(N_C + N_B)}{N_C}} \tag{10.54}$$

DESIGN EXAMPLE 10.8

Objective

To design the collector doping and collector width to meet a punch-through voltage specification.

Consider a uniformly doped silicon bipolar transistor with a metallurgical base width of 0.5 μm and a base doping of $N_B = 10^{16}$ cm^{-3}. The punch-through voltage is to be $V_{pt} = 25$ V.

■ Solution

The maximum collector doping concentration can be determined from Equation (10.54) as

$$25 = \frac{(1.6 \times 10^{-19})(0.5 \times 10^{-4})^2(10^{16})(N_C + 10^{16})}{2(11.7)(8.85 \times 10^{-14})N_C}$$

or

$$12.94 = 1 + \frac{10^{16}}{N_C}$$

which yields

$$N_C = 8.38 \times 10^{14} \text{ cm}^{-3}$$

This n-type doping concentration in the collector must extend at least as far as the depletion width extends into the collector to avoid breakdown in the collector region. We have, using results from Chapter 7,

$$x_n = \left[\frac{2\epsilon_s(V_{bi} + V_R)}{e}\left(\frac{N_B}{N_C} \cdot \frac{1}{N_B + N_C}\right)\right]^{1/2}$$

Neglecting V_{bi} compared to $V_R = V_{pt}$, we obtain

$$x_n = \left[\frac{2(11.7)(8.85 \times 10^{-14})(25)}{1.6 \times 10^{-19}}\left(\frac{10^{16}}{8.38 \times 10^{14}}\right)\left(\frac{1}{10^{16} + 8.38 \times 10^{14}}\right)\right]^{1/2}$$

or

$$x_n = 5.97\ \mu\text{m}$$

■ Comment

From Figure 8.25, the expected avalanche breakdown voltage for this junction is greater than 300 volts. Obviously punch-through will occur before the normal breakdown voltage in this case. For a larger punch-through voltage, a larger metallurgical hase width will be required, since a lower collector doping concentration is becoming impractical. A larger punch-through voltage will also require a larger collector width in order to avoid premature breakdown in this region.

TEST YOUR UNDERSTANDING

E10.13 The metallurgical hase width of a silicon npn bipolar transistor is $W_B = 0.80\ \mu$m. The base and collector doping concentrations are $N_B = 2 \times 10^{16}$ cm^{-3} and $N_C = 10''$ cm^{-3}. Find the punch-through breakdown voltage. (Ans. 208 V)

E10.14 The base impurity doping concentration is $N_B = 3 \times 10^{16}$ cm^{-3} and the metallurgical base width is $W_B = 0.70\ \mu$m. The minimum required punch-through breakdown voltage is specified to be $V_{pt} = 70$ V. What is the maximum allowed collectordoping concentration? (Ans. $N_C = 5.81 \times 10^{15}$ cm^{-3})

The second breakdown mechanism to consider is avalanche breakdown, but taking into account the gain of the transistor.[1] Figure 10.34a is an npn transistor with a reverse-bias voltage applied to the B-C junction and with the emitter left open. The current I_{CBO} is the reverse-biased junction current. Figure 10.34b shows the transistor with an applied C-E voltage and with the base terminal left open. This bias condition also makes the B-C junction reverse biased. The current in the transistor for this bias configuration is denoted as I_{CEO}.

The current I_{CBO} shown in Figure 10.34b is the normal reverse-biased B-C junction current. Pan of this current is due to the flow of minority carrier holes from the collector across the B-C space charge region into the base. The Row of holes into the

---

[1] The doping concentrations in the base and collector of the transistor we assume to be small enough that Zener breakdown is not a factor to be considered.

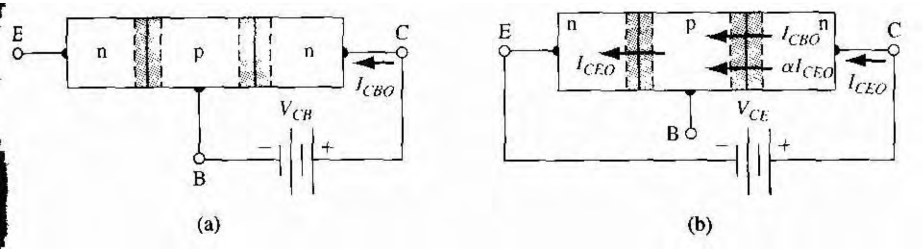

Figure 10.34 | (a) Open emitter configuration with saturation current I_{CBO}. (b) Open base configuration with saturation current I_{CEO}.

base makes the base positive with respect to the emitter, and the B-E junction becomes forward biased. The forward-biased B-E junction produces the current I_{CEO}, due primarily to the injection of electrons from the emitter into the base. The injected electrons diffuse across the base toward the B-C junction. These electrons are subject to all of the recombination processes in the bipolar transistor. When the electrons reach the B-C junction, this current component is αI_{CEO} where a is the common base current gain. We therefore have

$$I_{CEO} = \alpha I_{CEO} + I_{CBO} \tag{10.55a}$$

or

$$I_{CEO} = \frac{I_{CBO}}{1-\alpha} \approx \beta I_{CBO} \tag{10.55b}$$

where β is the common-emitter current pain. The reverse-biased junction current I_{CBO} is multiplied by the current gain β when the transistor is biased in the open-base configuration.

When the transistor is biased in the open-emitter configuration as in Figure 10.34a, thecurrent I_{CBO} at breakdown becomes $I_{CBO} \rightarrow M I_{CBO}$, where M is the multiplication factor. An empirical approximation for the multiplication factor is usually written as

$$M = \frac{1}{1 - (V_{CB}/BV_{CBO})^n} \tag{10.56}$$

where n is an empirical constant, usually between 3 and 6, and BV_{CBO} is the B-C breakdown voltage with the emitter left open.

When the transistor is biased with the base open circuited as shown in Figure 10.34b, the currents in the B-C junction at breakdown are multiplied, so that

$$I_{CEO} = M(\alpha I_{CEO} + I_{CBO}) \tag{10.57}$$

Solving for I_{CEO}, we obtain

$$I_{CEO} = \frac{M I_{CBO}}{1 - \alpha M} \tag{10.58}$$

The condition for breakdown corresponds to

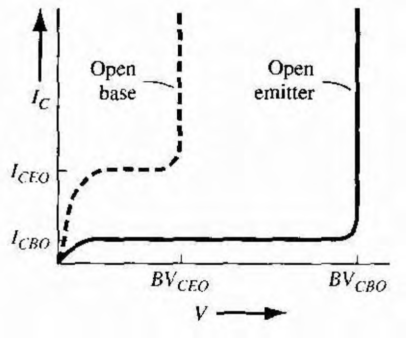

Figure 10.35 | Relative breakdown voltages and saturation currents of the open base and open emitter configurations

Using Equation (10.56) and assuming that $V_{CB} \approx V_{CE}$, Equation (10.59) becomes

$$\frac{\alpha}{1-(BV_{CEO}/BV_{CBO})^n} = 1 \tag{1}$$

where BV_{CEO} is the C-E voltage at breakdown in the open base configuration. Solving for BV_{CEO}, we find

$$BV_{CEO} = BV_{CBO}\sqrt[n]{1-\alpha} \tag{10.6}$$

where, again, α is the common-base current gain. The common-emitter and common-base current gains are related by

$$\beta = \frac{\alpha}{1-\alpha} \tag{10.62a}$$

Normally $\alpha \approx 1$, so that

$$1-\alpha \approx \frac{1}{\beta} \tag{10.62b}$$

Then Equation (10.61) can be written as

$$\boxed{BV_{CEO} = \frac{BV_{CBO}}{\sqrt[n]{\beta}}} \tag{10.63}$$

The breakdown voltage in the open-base configuration is smaller, by the factor $\sqrt[n]{\beta}$, than the actual avalanche junction breakdown voltage. This characteristic is shown in Figure 10.35.

DESIGN EXAMPLE 10.9

Objective

To design a bipolar transistor to meet a breakdown voltage specification.

Consider a silicon bipolar transistor with a common-emitter current gain of $\beta = 100$ and a base doping concentration of $N_B = 10^{17}$ cm^{-3}. The minimum open-base breakdown voltage is to be 15 volts.

■ Solution

From Equation (10.63), the minimum open-emitter junction breakdown voltage must be

$$BV_{CBO} = \sqrt[n]{\beta}\, BV_{CEO}$$

Assuming the empirical constant n is 3, we find

$$BV_{CBO} = \sqrt[3]{100}(15) = 69.6\ \text{V}$$

From Figure 8.25, the maximum collector doping concentration should be approximately $7 \times 10^{15}\ \text{cm}^{-3}$ to achieve this breakdown voltage.

■ Comment

In a transistor circuit, the transistor must be designed to operate under a worst-case situation. In this example, the transistor must be able to operate in an open-base configuration without going into breakdown. As we determined previously, an increase in breakdown voltage can be achieved by decreasing the collector doping concentration.

TEST YOUR UNDERSTANDING

E10.15 A uniformly doped silicon transistor has base and collector doping concentrations of $5 \times 10^{16}\ \text{cm}^{-3}$ and $5 \times 10^{15}\ \text{cm}^{-3}$, respectively. The common emitter current gain is $\beta = 85$. Assuming an empirical constant value of $n = 3$, determine BV_{CEO} (Ans. 21.6 V)

E10.16 The minimum required breakdown voltage of a uniformly doped silicon npn bipolar transistor is to be $BV_{CEO} = 70\ V$. The base impurity doping concentration is $N_B = 3 \times 10^{16}\ \text{cm}^{-3}$, the common-emitter current gain is $\beta = 85$, **and** the empirical constant value is $n = 3$. Determine the maximum collector impurity doping concentration. (Ans. $N_C \approx 1 \times 10^{15}\ \text{cm}^{-3}$)

10.5 | EQUIVALENT CIRCUIT MODELS

In order to analyze a transistor circuit either by hand calculations or using computer codes, one needs a mathematical model, or equivalent circuit, of the transistor. There are several possible models, each one having certain advantages and disadvantages. A detailed study of all possible models is beyond the scope of this text. However, we will consider three equivalent circuit models. Each of these follows directly from the work we have done on the pn junction diode and on the bipolar transistor. Computer analysis of electronic circuits is more commonly used than hand calculations, but it is instructive to consider the types of transistor model used in computer codes.

It is useful to divide bipolar transistors into two categories—switching and amplification—defined by their use in electronic circuits. Switching usually involves turning a transistor from its "off" state, or cutoff, to its "on" state, either forward-active or saturation, and then back to its "off" state. Amplification usually involves superimposing sinusoidal signals on dc values so that bias voltages and currents are only perturbed. The ***Ebers–Moll model*** is used in switching applications; the ***hybrid-pi model*** is used in amplification applications.

*10.5.1 Ebers–Moll Model

The Ebers–Moll model, or equivalent circuit, is one of the classic models of the bipolar transistor. This particular model is based on the interacting diode junctions and i applicable in any of the transistor operating modes. Figure 10.36 shows the current directions and voltage polarities used in the Ebers–Moll model. The currents are defined as all entering the terminals so that

$$I_E + I_B + I_C = 0 \qquad (10.6$$

The direction of the emitter current is opposite to what we have considered up to th point, but as long as we are consistent in the analysis, the defined direction does n matter.

The collector current can be written in general as

$$I_C = \alpha_F I_F - I_R \qquad (10.65$$

where α_F is the common base current gain in the forward-active mode. In this mode, Equation (10.65a) becomes

$$I_C = \alpha_F I_F + I_{CS} \qquad (10.65b)$$

where the current I_{CS} is the reverse-bias B-C junction current. The current I_F is given by

$$I_F = I_{ES}\left[\exp\left(\frac{eV_{BE}}{kT}\right) - 1\right] \qquad (10.66)$$

If the B-C junction becomes forward biased, such as in saturation, then we can write the current I_R as

$$I_R = I_{CS}\left[\exp\left(\frac{eV_{BC}}{kT}\right) - 1\right] \qquad (10.67)$$

Using Equations (10.66) and (10.67), the collector current from Equation (10.65a) can be written as

$$I_C = \alpha_F I_{ES}\left[\exp\left(\frac{eV_{BE}}{kT}\right) - 1\right] - I_{CS}\left[\exp\left(\frac{eV_{BC}}{kT}\right) - 1\right] \qquad (10.68)$$

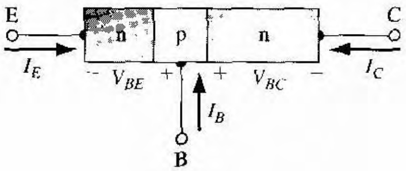

Figure 10.36 | Current direction and voltage polarity definitions lor the Ebers–Moll model.

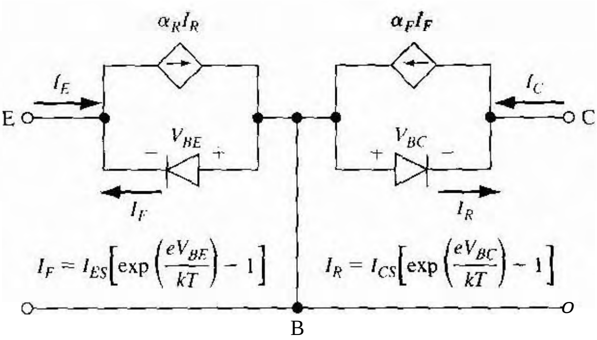
$\alpha_R I_R$
$\alpha_F I_F$
I_E
I_C
E
C
V_{BE}
V_{BC}
− +
+ −
I_F
I_R
$I_F = I_{ES}\left[\exp\left(\frac{eV_{BE}}{kT}\right) - 1\right]$
$I_R = I_{CS}\left[\exp\left(\frac{eV_{BC}}{kT}\right) - 1\right]$
B

Figure 10.37 | Basic Ebers–Moll equivalent circuit.

We can also write the emitter current as

$$I_E = \alpha_R I_R - I_F \tag{10.69}$$

or

$$I_E = \alpha_R I_{CS}\left[\exp\left(\frac{eV_{BC}}{kT}\right) - 1\right] - I_{ES}\left[\exp\left(\frac{eV_{BE}}{kT}\right) - 1\right] \tag{10.70}$$

The current I_{ES} is the reverse-bias B-E junction current and α_R is the common base current gain for the inverse-active mode. Equations (10.68) and (10.70) are the classic Ebers–Moll equations.

Figure 10.37 shows the equivalent circuit corresponding to Equations (10.68) and (10.70). The current sources in the equivalent circuit represent current components that depend on voltages across other junctions. The Ebers–Moll model has four parameters: α_F, α_R, I_{ES}, and I_{CS}. However, only three parameters are independent. The reciprocity relationship states that

$$\alpha_F I_{ES} = \alpha_R I_{CS} \tag{10.71}$$

Since the Ebers–Moll model is valid in each of the four operating modes, we can, for example, use the model for the transistor in saturation. In the saturation mode, both B-E and B-C junctions are forward biased, so that $V_{BE} > 0$ and $V_{BC} > 0$. The B-E voltage will be a known parameter since we will apply a voltage across this junction. The forward-biased B-C voltage is a result of driving the transistor into saturation and is the unknown to be determined from the Ebers–Moll equations. Normally in electronic circuit applications, the collector–emitter voltage at saturation is of interest. We can define the C-E saturation voltage as

$$V_{CE}(\text{sat}) = V_{BE} - V_{BC} \tag{10.72}$$

We will find an expression for $V_{CE}(\text{sat})$ by combining the Ebers–Moll equations. In the following example we see how the Ebers–Moll equations can be used in a hand calculation, and we may also see how a computer analysis would make the calculations easier.

Combining Equations (10.64) and (10.70), we have

$$-(I_B + I_C) = \alpha_R I_{CS}\left[\exp(f) \quad -1\right] - I_{ES}\left[\exp\left(\frac{eV_{BE}}{kT}\right) - 1\right] \qquad (10.7$$

If we solve for $[\exp(eV_{BC}/kT) - 1]$ from Equation (10.73). and substitute the re ing expression into Equation (10.68), we can then find V_{BE} as

$$V_{BE} = V_t \ln\left[\frac{I_C(1-\alpha_R) + I_B + I_{ES}(1-\alpha_F\alpha_R)}{I_{ES}(1-\alpha_F\alpha_R)}\right] \qquad (10.74)$$

where V_t is the thermal voltage. Similarly, if we solve for $[\exp(eV_{BE}/kT) - 1]$ from Equation (10.68), and substitute this expression into Equation (10.73), we can V_{BC} as

$$V_{BC} = V_t \ln\left[\frac{\alpha_F I_B - (1-\alpha_F)I_C + I_{CS}(1-\alpha_F\alpha_R)}{I_{CS}(1-\alpha_F\alpha_R)}\right] \qquad (10.75)$$

We may neglect the I_{ES} and I_{CS} terms in the numerators of Equations (10.74) and (10.75). Solving for $V_{CE}(\text{sat})$, we have

$$V_{CE}(\text{sat}) = V_{BE} - V_{CB} = V_t \ln\left[\frac{I_C(1-\alpha_R) + I_B}{\alpha_F I_B - (1-\alpha_F)I_C} \cdot \frac{I_{CS}}{I_{ES}}\right] \qquad (10.76)$$

The ratio of I_{CS} to I_{ES} can be written in terms of α_F and α_R from Equation (10.71). We can finally write

$$V_{CE}(\text{sat}) = V_t \ln\left[\frac{I_C(1-\alpha_R) + I_B}{\alpha_F I_B - (\mathrm{I}-\alpha_F)I_C} \cdot \frac{\alpha_F}{\alpha_R}\right] \qquad (10.77)$$

EXAMPLE 10.10

Objective

To calculate the collector–emitter saturation voltage of a bipolar transistor at T = 300 **K.**

Assume that ***a, .*** = 0.99. ***a,*** = 0.20. $I_C = 1$ mA, and $I_B = 50\ \mu$A.

■ Solution

Substituting the parameters into Equation (10.77). we have

$$V_{CE}(\text{sat}) = (0.0259)\ln\left[\frac{(1)(1-0.2) + (0.05)}{(0.99)(0.05) - (1-0.99)(1)}\left(\frac{0.99}{0.20}\right)\right] = 0.121 \text{ V}$$

■ Comment

This $V_{CE}(\text{sat})$ value is typical of collector-zmitter saturation voltages. Because of the log function, $V_{CE}(\text{sat})$ is not a strong function of I_C or I_B.

10.5.2 Gummel–Poon Model

The Gummel–Poon model of the BJT considers more physics of the transistor than the Ehers–Moll model. This model can he used if, for example, there is a nonunifom doping concentration in the base.

The electron current density in the base of an npn transistor can be written as

$$J_n = e\mu_n n(x)\mathrm{E} + eD_n \frac{dn(x)}{dx} \tag{10.78}$$

n electric field will occur in the base if nonuniform doping exists in the base. This was discussed in Section 10.4.5. The electric field, from Equation (10.52), can be written in the form

$$\mathrm{E} = \frac{kT}{e} \cdot \frac{1}{p(x)} \cdot \frac{dp(x)}{dx} \tag{10.79}$$

where $p(x)$ is the majority carrier hole concentration in the base. Under low injection, the hole concentration is just the acceptor impurity concentration. With the doping profile shown in Figure 10.31, the electric field is negative (from the collector to the emitter). The direction of this electric field aids the flow of electrons across the base.

Substituting Equation (10.79) into Equation (10.78), we obtain

$$J_n = e\mu_n n(x) \cdot \frac{kT}{e} \cdot \frac{1}{p(x)} \cdot \frac{dp(x)}{dx} + eD_n \frac{dn(x)}{dx} \tag{10.80}$$

Using Einstein's relation, we can write Equation (10.80) in the form

$$J_n = \frac{eD_n}{p(x)} \left(n(x)\frac{dp(x)}{dx} + p(x)\frac{dn(x)}{dx} \right) = \frac{eD_n}{p(x)} \cdot \frac{d(pn)}{dx} \tag{10.81}$$

, Equation (10.81) can be written in the form

$$\frac{J_n p(x)}{eD_n} = \frac{d(pn)}{dx} \tag{10.82}$$

Integrating Equation (10.82) through the base region while assuming that the electron current density is essentially a constant and the diffusion coefficient is a constant, we find

$$\frac{J_n}{eD_n} \int_0^{x_B} p(x)\,dx = \int_0^{x_B} \frac{dp(x)}{dx}\,dx = p(x_B)n(x_B) - p(0)n(0) \tag{10.83}$$

Assuming the B-E junction is forward biased and the B-C junction is reverse biased, we have $n(0) = n_{B0}\exp(V_{BE}/V_t)$ and $n(x_B) = 0$. We may note that $n_{B0}p = n_i^2$ so that Equation (10.83) can be written as

$$J_n = \frac{-eD_n n_i^2 \exp(V_{BE}/V_t)}{\int_0^{x_B} p(x)\,dx} \tag{10.84}$$

The integral in the denominator is the total majority carrier charge in the base and is known as the *base Gummel* number; defined as Q_B.

If we perform the same analysis in the emitter, we find that the hole current density in the emitter of an npn transistor can be expressed as

$$J_p = \frac{-eD_p n_i^2 \exp(V_{BE}/V_t)}{\int_0^{x_E} n(x')\,dx'} \tag{10.85}$$

The integral in the denominator is the total majority carrier charge in the emitter and is known as the emitter Gummel number, defined as Q_E

Since the currents in the Gummel–Poon model are functions of the total integrated charges in the base and emitter. these currents can easily be determined for nonuniformly doped transistors.

The Gummel–Poon model can also take into account nonideal effects, such as the Early effect and high-level injection. As the B-C voltage changes, the neutral base width changes so that the base Gummel number Q_B changes. The change in Q_B with B-C voltage then makes the electron current density given by Equation (10.84) a function of the B-C voltage. This is the base width modulation effect or Early effect as discussed previously in Section 10.4.1.

If the B-E voltage becomes too large. low injection no longer applies, which leads to high-level injection. In this case, the total hole concentration in the base increases because of the increased excess hole concentration. This means that the base Gummel number will increase. The change in base Gummel number implies, from Equation (10.84). that the electron current density will also change. High-level injection was also previously discussed in Section 10.4.2.

The Gummel–Poon model can then be used to describe the basic operation of the transistor as well as to describe nonideal effects.

10.5.3 Hybrid-Pi Model

Bipolar transistors are commonly used in circuits that amplify time-varying or sinusoidal signals. In these linear amplifier circuits, the transistor is biased in the forward-active region and small sinusoidal voltages and currents are superimposed on dc voltages and currents. In these applications, the sinusoidal parameters are of interest, so it is convenient to develop a small-signal equivalent circuit of the bipolar transistor using the small-signal admittance parameters of the pn junction developed in Chapter 8.

Figure 10.38a shows an npn bipolar transistor in a common emitter configuration with the small-signal terminal voltages and currents. Figure 10.38b shows the cross section of the npn transistor. The C, B, and E terminals are the external connections to the transistor, while the C', B', and E' points are the idealized internal collector, base, and emitter regions.

We can begin constructing the equivalent circuit of the transistor by considering the various terminals individually. Figure 10.39a shows the equivalent circuit between the external input base terminal and the external emitter terminal. The resistance r_b is the series resistance in the base between the external base terminal B and the internal base region B'. The B′-E′ junction is forward biased, so C_π is the junction diffusion capacitance and r_π is the junction diffusion resistance. The diffusion capacitance C_π is the same as the diffusion capacitance C_d given by Equation (8.72), and the diffusion resistance r_π is the same as the diffusion resistance r_d given by Equation (8.35). The values of both parameters are functions of the junction current. These two elements are in parallel with the junction capacitance, which is C_{je}. Finally, r_{ex} is the series resistance between the external emitter terminal and the

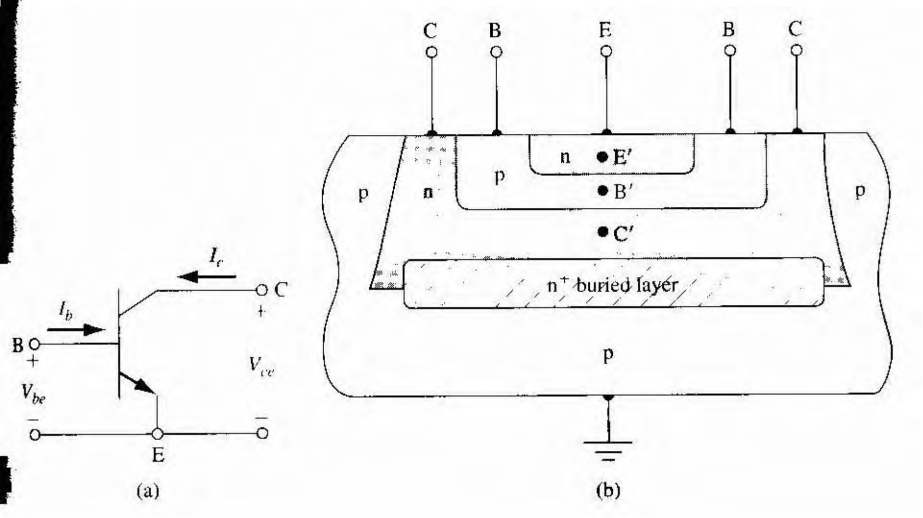
I_c
I_b
B
+
V_be
–
C
+
V_ce
–
E
(a)
C
B
E
B
C
n
E′
p
B′
p
n
p
C′
n⁺ buried layer
p
(b)

Figure 10.38 | **(a)** Common emitter npn bipolar transistor with small-signal current and voltages. (b) Cross section of an npn bipolar transistor for the hybrid-pi model.

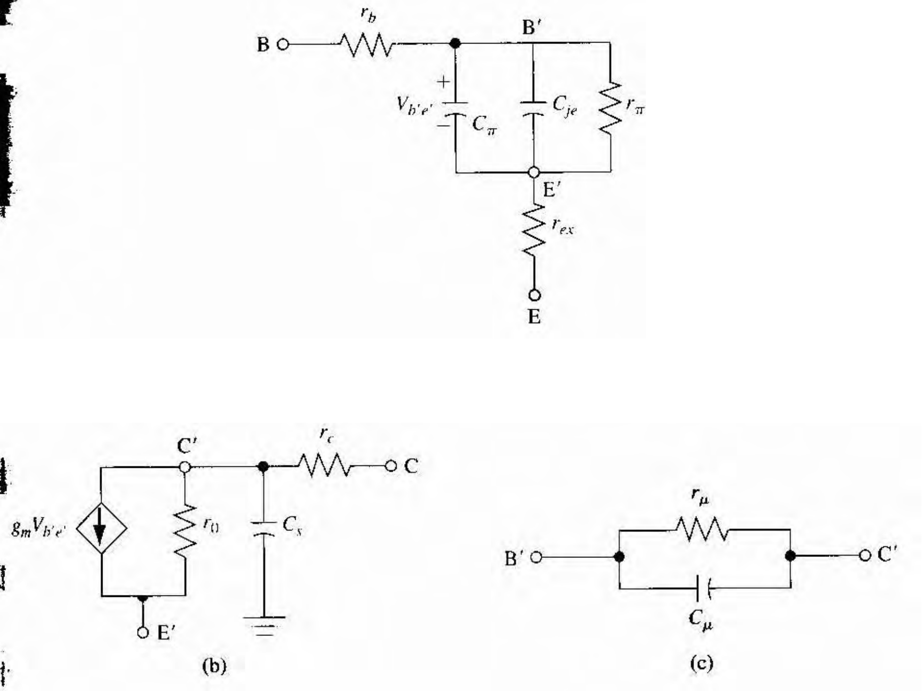
r_b
B
B′
+
V_b′e′
–
C_π
C_je
r_π
E′
r_ex
E
C′
r_c
C
g_m V_b′e′
r_0
C_s
E′
(b)
r_μ
B′
C′
C_μ
(c)

Figure 10.39 | Components of the hybrid-pi equivalent circuit between (a) the base and emitter, (h) the collector and emitter. and (c) the base and collector.

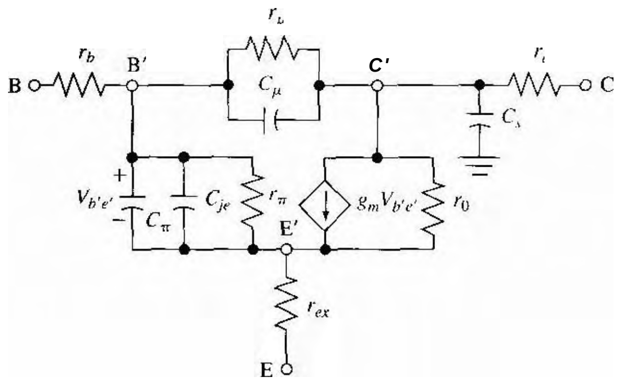

Figure 10.40 | Hybrid-pi equivalent circuit.

internal emitter region. This resistance is usually very small and may he on the ord of 1 to 2 Ω.

Figure 10.39b shows the equivalent circuit looking into the collector terminal. The r_c resistance is the series resistance between the external and internal collector connections and the capacitance C_s is the junction capacitance of the reverse-biased collector-substrate junction. The dependent current source. $g_m V_{b'e'}$, is the collector current in the transistor, which is controlled by the internal base-emitter voltage. The resistance r_0 is the inverse of the output conductance g_0 and is primarily due to the Early effect.

Finally, Figure 10.39c shows the equivalent circuit of the reverse-biased B'-C' junction. The **C,** parameter is the reverse-biased junction capacitance and r_μ is the reverse-biased diffusion resistance. Normally, r_μ is on the order of megohms and can be neglected. The value of C_μ is usually much smaller than C_π but, because of the feedback effect which leads to the Miller effect and Miller capacitance, C_μ cannot be ignored in most cases. The Miller capacitance is the equivalent capacitance between B' and E' due to C_μ and the feedback effect, which includes the gain of the transistor. The Miller effect also reflects C, between the C' and E' terminals at the output. However, the effect on the output characteristics can usually he ignored.

Figure 10.40 shows the complete hybrid-pi equivalent circuit. A computer simulation is usually required for this complete model because of the large number of elements. However, some simplifications can be made in order to gain an appreciation for the frequency effects of the bipolar transistor. The capacitances lead to frequency effects in the transistor, which means that the gain, for example, is a function of the input signal frequency.

EXAMPLE 10.11

Objective

To determine, to a first approximation, the frequency at which the small-signal current gain decreases to $1/\sqrt{2}$ of its low frequency value.

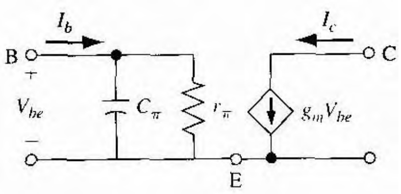

Figure 10.41 | Simplified hybrid-pi equivalent circuit.

Consider the simplified hybrid-pi circuit shown in Figure 10.41. We are ignoring C,,, C_s, r_μ, C,,, r_0, and the series resistances. We must emphasize that this is a first order calculation and that C_μ normally cannot be neglected.

■ Solution

At very low frequency, we may neglect C_π so that

$$V_{be} = I_b r_\pi \qquad \text{and} \qquad I_c = g_m V_{be} = g_m r_\pi I_t$$

We can then write

$$h_{fe0} = \frac{I_c}{I_b} = g_m r_\pi$$

where h_{fe0} is the low-frequency, small-signal common emitter current gain

Taking into account C_π, we have

$$V_{be} = I_b \left[\frac{r_\pi}{1 + j\omega r_\pi C_\pi} \right]$$

Then

$$I_c = g_m V_{be} = I_b \left[\frac{h_{fe0}}{1 + j\omega r_\pi C_\pi} \right]$$

or the small-signal current gain can be written as

$$A_i = \frac{I_c}{I_b} = \left[\frac{h_{fe0}}{1 + j\omega r_\pi C_\pi} \right]$$

The magnitude of the current gain drops to $1/\sqrt{2}$ of its low-frequency value at $f = 1/2\pi r_\pi C_\pi$.

If, for example, $r_\pi = 2.6\ \text{k}\Omega$ and $C_\pi = 4$ pF, then

$$f = 15.3 \text{ MHz}$$

■ Comment

High-frequency transistors must have small diffusion capacitances, implying the use of small devices.

10.6 | FREQUENCY LIMITATIONS

The hybrid-pi equivalent circuit, developed in the last section, introduces frequency effects through the capacitor-resistor circuits. We will now discuss the various physical factors in the bipolar transistor affecting the frequency limitations of the device, and then define the transistor cutoff frequency, which is a figure of merit for a transistor.

10.6.1 Time-Delay Factors

The bipolar transistor is a transit-time device. When the voltage across the B-E junction increases, for example, additional carriers from the emitter are injected into the base, diffuse across the base, and are collected in the collector region. As the frequency increases, this transit time can become comparable to the period of the input signal. At this point, the output response will no longer be in phase with the input and the magnitude of the current gain will decrease.

The total emitter-to-collector time constant or delay time is composed of four separate time constants. We can write

$$\tau_{ec} = \tau_e + \tau_b + \tau_d + \tau_c \tag{10.86}$$

where

τ_{ec} = emitter-to-collector time delay
τ_e = emitter–base junction capacitance charging time
τ_b = base transit time
τ_d = collector depletion region transit time
τ_c = collector capacitance charging time

The equivalent circuit of the forward-biased B-E junction was given in Figure 10.39a. The capacitance C_{je} is the junction capacitance. If we ignore the series resistance, then the emitter–base junction capacitance charging time is

$$\boxed{\tau_e = r'_e(C_{je} + C_p)} \tag{10.87}$$

where r'_e is the emitter junction or diffusion resistance. The capacitance C_p includes any parasitic capacitance between the base and emitter. The resistance r'_e is found as the inverse of the slope of the I_E versus V_{BE} curve. We obtain

$$r' = \frac{kT}{e} \cdot \frac{1}{I_E} \tag{10.88}$$

where I_E is the dc emitter current.

The second term, τ_b, is the base transit time, the time required for the minority carriers to diffuse across the neutral base region. The base transit time is related to the diffusion capacitance C_π of the B-E junction. For the npn transistor, the electron current density in the base can be written as

$$J_n = -en_B(x)v(x) \tag{10.89}$$

where $v(x)$ is an average velocity. We can write

$$v(x) = dx/dt \qquad \text{or} \qquad dt = dx/v(x) \tag{10.90}$$

The transit time can then be found by integrating, or

$$\tau_b = \int_0^{x_B} dt = \int_0^{x_B} \frac{dx}{v(x)} = \int_0^{x_B} \frac{en_B(x)\,dx}{(-J_n)} \tag{10.91}$$

The electron concentration in the base is approximately linear (see Example 10.6) so we can write

$$n_B(x) \approx n_{B0}\left[\exp\left(\frac{eV_{BE}}{kT}\right)\right]\left(1 - \frac{x}{x_B}\right) \tag{10.92}$$

and the electron current density is given by

$$J_n = eD_n\frac{dn_B(x)}{dx} \tag{10.93}$$

The base transit time is then found by combining Equations (10.92) and (10.93) with Equation (10.91). We find that

$$\boxed{\tau_b = \frac{x_B^2}{2D_n}} \tag{10.94}$$

The third time-delay factor is τ_d, the collector depletion region transit time. Assuming that the electrons in the npn device travel across the B-C space charge region at their saturation velocity, we have

$$\boxed{\tau_d = \frac{x_{dc}}{v_s}} \tag{10.95}$$

where x_{dc} is the B-C space charge width and u., is the electron saturation velocity.

The fourth time-delay factor, τ_c, is the collector capacitance charging time. The B-C is reverse biased so that the diffusion resistance in parallel with the junction capacitance is very large. The charging time constant is then a function of the collector series resistance r_c. We can write

$$\boxed{\tau_c = r_c(C_\mu + C_s)} \tag{10.96}$$

where C„ is the B-C junction capacitance and C_s is the collector-to-substrate capacitance. The series resistance in small epitaxial transistors is usually small; thus the time delay τ_c may be neglected in some cases.

Example calculations of the various time-delay factors will he given in the next section as part of the cutoff frequency discussion.

10.6.2 Transistor Cutoff Frequency

The current gain as a function of frequency was developed in Example 10.11 so that we can also write the common base current gain as

$$\alpha = \frac{\alpha_0}{1 + j\dfrac{f}{f_\alpha}} \tag{10.97}$$

where α_0 is the low-frequency common base current gain and f_α is defined as the *alpha cutoff frequency*. The frequency f_α is related to the emitter-to-collector time delay τ_{ec} as

$$f_\alpha = \frac{1}{2\pi\tau_{ec}} \tag{10.98}$$

When the frequency is equal to the alpha cutoff frequency, the magnitude of the common base current gain is $1/\sqrt{2}$ of its low-frequency value.

We can relate the alpha cutoff frequency to the common emitter current gain by considering

$$\beta = \frac{\alpha}{1 - \alpha} \tag*{(10.}$$

We may replace u in Equation (10.99) with the expression given by Equation (10.97). When the frequency f is of the same order of magnitude as f_α, then

$$|\beta| = \left|\frac{\alpha}{1 - \alpha}\right| \approx \frac{f_\alpha}{f} \tag{10.100}$$

where we have assumed that $\alpha_0 \approx 1$. When the signal frequency is equal to the alpha cutoff frequency. the magnitude of the common emitter current gain is equal to unity. The usual notation is to define this *cutoff frequency* as f_T, so we have

$$\boxed{f_T = \frac{1}{2\pi\tau_{ec}}} \tag{10.101}$$

From the analysis in Example 10.11, we may also write the common-emitter current gain as

$$\beta = \frac{\beta_0}{1 + j(f/f_\beta)} \tag{10.102}$$

where f_β is called the *beta cutoff frequency* and is the frequency at which the magnitude of the common-emitter current gain β drops to $1/\sqrt{2}$ of its low-frequency value

Combining Equations (10.99) and (10.97). we can write

$$\beta = \frac{\alpha}{1 - \alpha} = \frac{\dfrac{\alpha_0}{1 + j(f/f_T)}}{1 - \dfrac{\alpha_0}{1 + j(f/f_T)}} = \frac{\alpha_0}{1 - \alpha_0 + j(f/f_T)} \tag{10.103}$$

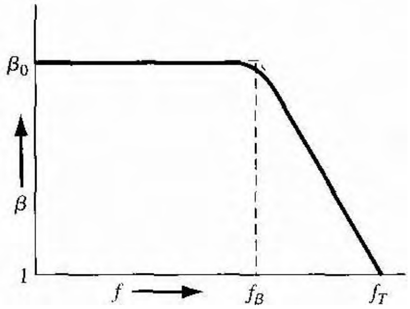

Figure 10.42 | Bode plot of common emitter current gain versus frequency.

$$\beta = \frac{\alpha_0}{(1-\alpha_0)\left[1 + j\dfrac{f}{(1-\alpha_0)f_T}\right]} \approx \frac{\beta_0}{1 + j\dfrac{\beta_0 f}{f_T}} \tag{10.104}$$

where

$$\beta_0 = \frac{\alpha_0}{1-\alpha_0} \approx \frac{1}{1-\alpha_0}$$

Comparing Equations (10.104) and (10.102), the beta cutoff frequency is related to the cutoff frequency by

$$\boxed{f_\beta \approx \frac{f_T}{\beta_0}} \tag{10.105}$$

Figure 10.42 shows a Bode plot of the common emitter current gain as a function of frequency and shows the relative values of the beta and cutoff frequencies. Keep in mind that the frequency is plotted on a log scale, so f_β and f_T usually have significantly different values.

EXAMPLE 10.12

Objective

To calculate the emitter-to-collector transit time and the cutoff frequency of a bipolar transistor, given the transistor parameters.

Consider a silicon npn transistor at T = 300 K. Assume the following parameters:

$$\begin{aligned} I_E &= 1 \text{ mA} & C_{je} &= 1 \text{ pF} \\ x_B &= 0.5\ \mu\text{m} & D_n &= 25 \text{ cm}^2/\text{s} \\ x_{dc} &= 2.4\ \mu\text{m} & r_c &= 20\ \Omega \\ C_\mu &= 0.1 \text{ pF} & C_s &= 0.1 \text{ pF} \end{aligned}$$

■ Solution

We will initially calculate the various time-delay factors. If we neglect the parasitic capacitance, the emitter-base junction charging time is

$$\tau_e = r'_e C_{je}$$

where

$$r'_e = \frac{kT}{e} \cdot \frac{1}{I_E} = \frac{0.0259}{1 \times 10^{-3}} = 25.9\ \Omega$$

Then

$$\tau_e = (25.9)(10^{-12}) = 25.9\ \text{ps}$$

The base transit time is

$$\tau_b = \frac{x_B^2}{2D_n} = \frac{(0.5 \times 10^{-4})^2}{2(25)} = 50\ \text{ps}$$

The collector depletion region transit time is

$$\tau_b = \frac{x_{dc}}{v_s} = \frac{2.4 \times 10^{-4}}{10^7} = 24\ \text{ps}$$

The collector capacitance charging time is

$$\tau_c = r_c(C_\mu + C_s) = (20)(0.2 \times 10^{-12}) = 4\ \text{ps}$$

The total emitter-to-collector time delay is then

$$\tau_{ec} = 25.9 + 50 + 24 + 4 = 103.9\ \text{ps}$$

so that the cutoff frequency is calculated as

$$f_T = \frac{1}{2\pi\tau_{ec}} = \frac{1}{2\pi(103.9 \times 10^{-12})} = 1.53\ \text{GHz}$$

If we assume a low-frequency common-emitter current gain of $\beta = 100$, then the beta cutoff frequency is

$$f_\beta = \frac{f_T}{\beta_0} = \frac{1.53 \times 10^9}{100} = 15.3\ \text{MHz}$$

■ Comment

The design of high-frequency transistors requires small device geometries in order to reduce capacitances, and narrow base widths in order to reduce the base transit time.

TEST YOUR UNDERSTANDING

E10.17 A silicon npn bipolar transistor is biased at $I_E = 0.5$ mA and has a junction capacitance of $C_{je} = 2$ pF. All other parameters are the same as listed in Example 10.12. Find the emitter-to-collector transit time, the cutoff frequency, and the beta cutoff frequency. (Ans. $\tau_{ec} = 181.6$ ps, $f_T = 1.14$ GHz, $f_\beta = 11.4$ MHz)

10.7 | LARGE-SIGNAL SWITCHING

Switching a transistor from one state to another is strongly related to the frequency characteristics just discussed. However, switching is considered to be a large-signal change whereas the frequency effects assumed only small changes in the magnitude of the signal.

10.7.1 Switching Characteristics

Consider an npn transistor in the circuit shown in Figure 10.43a switching from cutoff to saturation, and then switching back from saturation to cutoff. We will describe the physical processes taking place in the transistor during the switching cycle.

Consider, initially, the case of switching from cutoff to saturation. Assume that in cutoff $V_{BE} \approx V_{BB} < 0$, thus the B-E junction is reverse biased. At $t = 0$, assume that V_{BB} switches to a value of V_{BB0} as shown in Figure 10.43b. We will assume that V_{BB0} is sufficiently positive to eventually drive the transistor into saturation. For $0 \le t \le t_1$, the base current supplies charge to bring the B-E junction from reverse bias to a slight forward bias. The space charge width of the B-E junction is narrowing, and ionized donors and acceptors are being neutralized. A small amount of charge is also injected into the base during this time. The collector current increases from zero to 10 percent of its final value during this time period, referred to as the delay time.

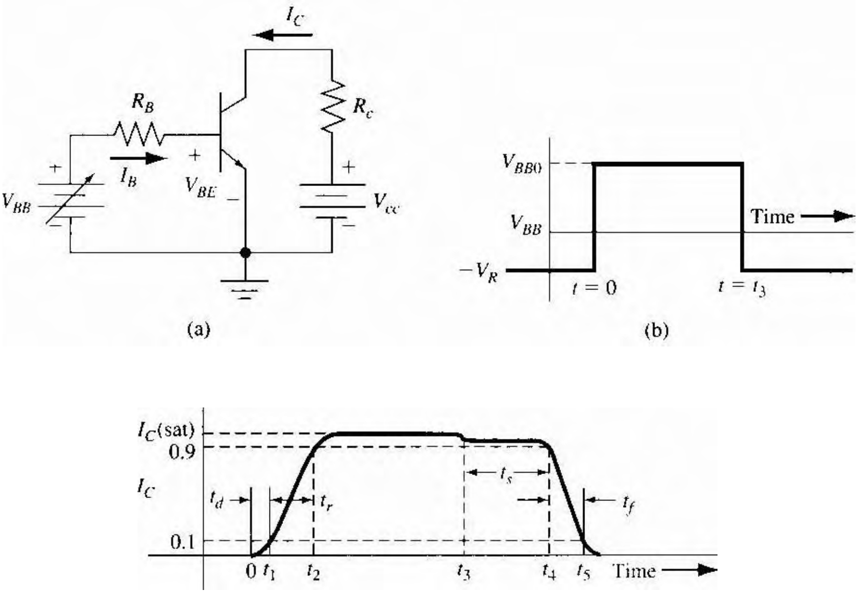

(a)

(b)

Figure 10.43 | (a) Circuit used for transistor switching. (b) Input base drive for transistor switching. *(c)* Collector current versus time during transistor switching.

During the next time period, $t_1 \le t \le t_2$, the base current is supplying charge which increases the B-E junction voltage from near cutoff to near saturation. Durin this time, additional carriers are being injected into the base so that the gradient of th minority carrier electron concentration in the base increases, causing the collecto current to increase. We refer to this time period as the rise time, during which the collector current increases from 10 percent to 90 percent of the final value. For $t > t_2$ the base drive continues to supply base current, driving the transistor into saturatio and establishing the final minority carrier distribution in the device.

The switching of the transistor from saturation to cutoff involves removing all o the excess minority carriers stored in the emitter, base, and collector regions. Figure 10.44 shows the charge storage in the base and collector when the transistor is in saturation. The charge Q_B is the excess charge stored in a forward-active transistor and Q_{BX} and Q_C are the extra charges stored when the transistor is biased in saturation. At $t = t_3$, the base voltage V_{BB} switches to a negative value of $(-V_R)$. The base current in the transistor reverses direction as was the case in switching a pn junction diode from forward to reverse bias. The reverse base current pulls the excess stored carriers from the emitter and base regions. Initially, the collector current does not change significantly, since the gradient of the minority carrier concentration in the base does not change instantaneously. Recall that when the transistor is biased in saturation, both the B-E and B-C junctions are forward biased. The charge Q_{BX} in the base must be removed to reduce the forward-biased B-C voltage to zero volts before the collector current can change. This time delay is called the *storage time* and is denoted by t_s. The storage time is the time between the point at which V_{BB} switches to the time when the collector current is reduced to 90 percent of its maximum saturation value. The storage time is usually the most important parameter in the switching speed of the bipolar transistor.

The final switching delay time is the fall time t_f during which the collector current decreases from the 90 percent to the 10 percent value. During this time, the B-C

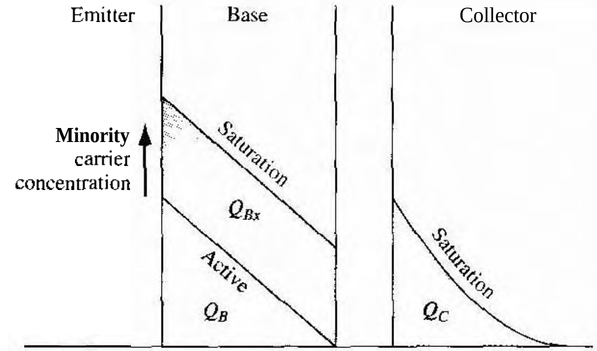

Figure 10.44 | Charge storage in the base and collector at saturation and in the active mode.

junction is reverse biased but excess carriers in the base are still being removed, and the **B-E** junction voltage is decreasing.

The switching-time response of the transistor can be determined by using the Ebers–Moll model. The frequency-dependent gain parameters must be used, and normally the Laplace transform technique is used to obtain the time response. The details of this analysis are quite tedious and will not be presented here.

10.7.2 The Schottky-Clamped Transistor

One method frequently employed to reduce the storage time and increase the switching speed is the use of a Schottky-clamped transistor. This is a normal npn bipolar device with a Schottky diode connected between base and collector, as shown in Figure 10.45a. The circuit symbol for the Schottky-clamped transistor is shown in Figure 10.45b. When the transistor is biased in the forward-active mode, the **B-C** junction is reverse biased; hence, the Schottky diode is reverse biased and effectively out of the circuit. The characteristics of the Schottky-clamped transistor—or simply the Schottky transistor — are those of the normal npn bipolar device.

When the transistor is driven into saturation, the **B-C** junction becomes forward biased; hence the Schottky diode also becomes forward biased. We may recall from our discussion in the previous chapter that the effective turn-on voltage of the Schottky diode is approximately half that of the pn junction. The difterence in turn-on voltage means that most of the excess base current will be shunted through the Schottky diode and away from the base so that the amount of excess stored charge in the base and collector is drastically reduced. The excess minority carrier concentration in the base and collector at the **B-C** junction is an exponential function of V_{BC}. If V_{BC} is reduced from 0.5 volt to 0.3 volt, for example, the excess minority carrier concentration is reduced by over 3 orders of magnitude. The reduced excess stored charge in the base of the Schottky transistor greatly reduces the storage time — storage times on the order of 1 ns or less are common in Schottky transistors.

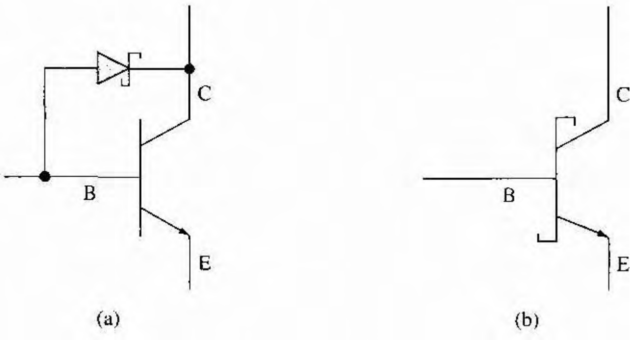

Figure 10.45 | (a) The Schottky-clamped transistor. (b) Circuit symbol of the Schottky-clamped transistor.

*10.8 | OTHER BIPOLAR TRANSISTOR STRUCTURES

This section is intended to briefly introduce three specialized bipolar transistor structures. The first structure is the polysilicon emitter bipolar junction transistor (BJT), the second is the SiGe-base transistor, and the third is the heterojunction bipolar transistor (HBT). The polysilicon emitter BJT is being used in some recent integrated circuits, and the SiGe-base transistor and HBT are intended for high-frequency/high-speed applications.

10.8.1 Polysilicon Emitter BJT

The emitter injection efficiency is degraded by the carriers injected from the base back into the emitter. The emitter width, in general, is thin, which increases speed and reduces parasitic resistance. However. a thin emitter increases the gradient in the minority carrier concentration, as indicated in Figure 10.19. The increase in the gradient increases the B-E junction current, which in turn decreases the emitter injection efficiency and decreases the common emitter current gain. This effect is also shown in the summary of Fable 10.3.

Figure 10.46 shows the idealized cross section of an npn bipolar transistor with a polysilicon emitter. As shown in the figure, there is a very thin n^+ single crystal silicon region between the p-type base and the n-type polysilicon. As a first approximation to the analysis, we may treat the polysilicon portion of the emitter as low-mobility silicon, which means that the corresponding diffusion coefficient is small.

Assuming that the neutral widths of both the polysilicon and single-crystal portions of the emitter are much smaller than the respective diffusion lengths, then the minority carrier distribution functions will be linear in each region. Both the minority carrier concentration and diffusion current must be continuous across the polysilicon/silicon interface. We can therefore write

$$eD_{E(\text{poly})}\frac{d\left(\delta p_{E(\text{poly})}\right)}{dx} = eD_{E(\text{n}^+)}\frac{d\left(\delta p_{E(\text{n}^+)}\right)}{dx} \tag{10.106}$$

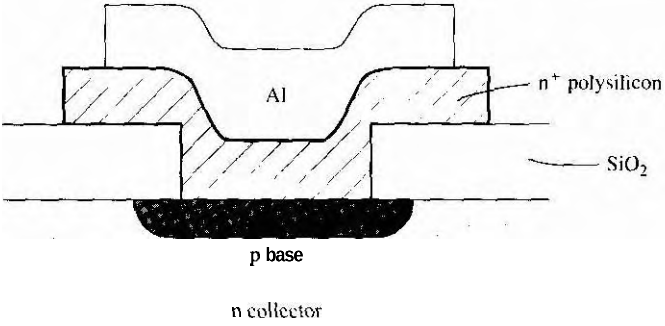

Figure 10.46 | Simplified cross section of an npn polysilicon emitter BJT.

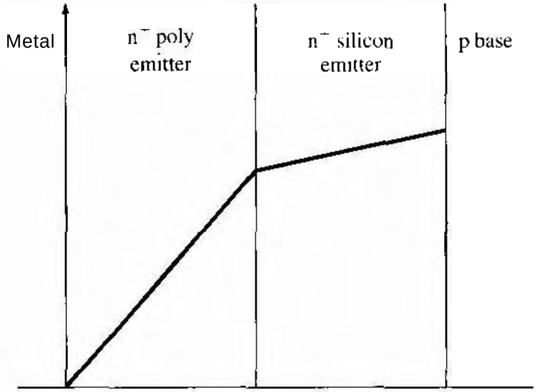

Figure 10.47 | Excess minority carrier hole concentrations in n^+ polysilicon and n^+ silicon emitter.

$$\frac{d\left(\delta p_{E(n^-)}\right)}{dx} = \frac{D_{E(\text{poly})}}{D_{E(n^+)}} \cdot \frac{d\left(\delta p_{E(\text{poly})}\right)}{dx} \tag{10.106b}$$

Since $D_{E(\text{poly})} < D_{E(n^+)}$, then the gradient of the minority carrier concentration at the emitter edge of the B-E depletion region in the n^+ region is reduced as Figure 10.47 shows. This implies that the current back-injected from the base into the emitter is reduced so that the common-emitter current gain is increased.

10.8.2 Silicon–Germanium Base Transistor

The bandgap energy of Ge (—0.67 eV) is significantly smaller than the bandgap energy of Si (—1.12 eV). By incorporating Ge into Si, the bandgap energy will decrease compared to pure Si. If Ge is incorporated into the base region of a Si bipolar transistor, the decrease in bandgap energy will influence the device characteristics. The desired Ge concentration profile is to have the largest amount of Ge near the base–collector junction and the least amount of Ge near the base–emitter junction. Figure 10.48a shows an ideal uniform boron doping concentration in the p-type base and a linear Ge concentration profile.

The energy bands of a SiGe-base npn transistor compared to a Si-base npn transistor, assuming the boron and Ge concentrations given in Figure 10.48a, are shown in Figure 10.48b. The emitter–base junctions of the two transistors are essentially identical, since the Ge concentration is very small in this region. However, the bandgap energy of the SiGe-base transistor near the base–collector junction is smaller than that of the Si-base transistor. The base current is determined by the base-emitter junction parameters and hence will be essentially the same in the two transistors. This change in bandgap energy will influence the collector current.

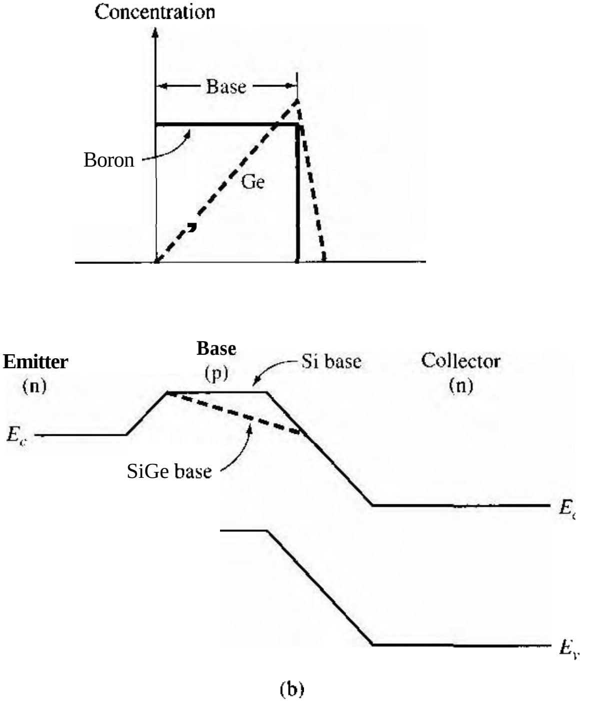

Figure 10.48 | (a) Assumed boron and germanium concentrations in the base of the SiGe-base transistor. (b) Energy band diagram of the Si- and SiGe-base transistors.

Collector Current and Current Gain Effects Figure 10.49 shows the thema equilibrium minority carrier electron concentration through the base region of th SiGe and Si transistors. This concentration is given by

$$n_{B0} = \frac{n_i^2}{N_B} \tag{10.107}$$

where N_B is assumed to be constant. The intrinsic concentration, however, is a function of the bandgap energy. We may write

$$\frac{n_i^2(\text{SiGe})}{n_i^2(\text{Si})} = \exp\left(\frac{\Delta E_g}{kT}\right) \tag{10.108}$$

where $n_i(\text{SiGe})$ is the intrinsic carrier concentration in the SiGe material, $n_i(\text{Si})$ is the intrinsic carrier concentration in the Si material, and AE, is the change in the bandgap energy of the SiGe material compared to that of Si

The collector current in a SiGe-base transistor will increase. As a first approximation, we can see this from the previous analysis. The collector current was found from Equation (10.36a), in which the derivative was evaluated at the base–collector

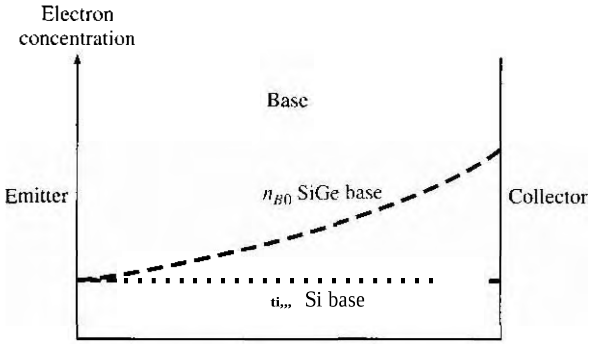

Figure **10.49** | Thermal equilibrium minority carrier electron concentration through the base of the Si- and SiGe-base transistors.

junction. This means that the value of n_{B0} in the collector current expression in Equation (10.37) is the value at the base–collector junction. Since this value is larger for the SiGe-base transistor (Figure 10.49), the collector current will be larger compared to the Si-base transistor. Since the base currents are the same in the two transistors, the increase in collector current then implies that the current gain in the SiGe-base transistor is larger. If the bandgap narrowing is 100 meV, then the increase in the collector current and current gain will be approximately a factor of four.

Early Voltage Effects The Early voltage in a SiGe-base transistor is larger than that of the Si-base transistor. The explanation for this effect is less obvious than the explanation for the increase in collector current and current gain. For a bandgap narrowing of 100 meV, the Early voltage is increased by approximately a factor of 12. Incorporating Ge into the base region can increase the Early voltage by a large factor.

Base Transit Time and Emitter–Base Charging Time Effects The decrease in bandgap energy from the base–emitter junction to the base–collector junction induces an electric field in the base that helps accelerate electrons across the p-type base region. For a bandgap narrowing of 100 meV, the induced electric field can be on the order of 10^3 to 10^4 V/cm. This electric field reduces the base-transit time by approximately a factor of *2.5*.

The emitter–base junction charging time constant, given by Equation (10.87), is directly proportional to the emitter diffusion resistance r'_e. This parameter is inversely proportional to the emitter current, as seen in Equation (10.88). For a given base current. the emitter current in the SiGe-base transistor is larger, since the current gain is larger. The emitter–base junction charging time is then smaller in a SiGe-base transistor than that in a Si-base transistor.

The reduction in both the base-transit time and the emitter–base charging time increases the cutoff frequency of the SiGe-base transistor. The cutoff frequency of these devices can be substantially higher than that of the Si-base device.

10.8.3 Heterojunction Bipolar Transistors

As mentioned previously, one of the basic limitations of the current gain in the bipolar transistor is the emitter injection efficiency. The emitter injection efficiency γ can be increased by reducing the value of the thermal-equilibrium minority carrier concentration p_{E0} in the emitter. However, as the emitter doping increases, the bandgap narrowing effect offsets any improvement in the emitter injection efficiency. One possible solution is to use a wide-bandgap material for the emitter, which will minimize the injection of carriers from the base back into the emitter.

Figure 10.50a shows a discrete aluminum gallium arsenide/gallium arsenide heterojunction bipolar transistor, and Figure 10.50b shows the band diagram of the

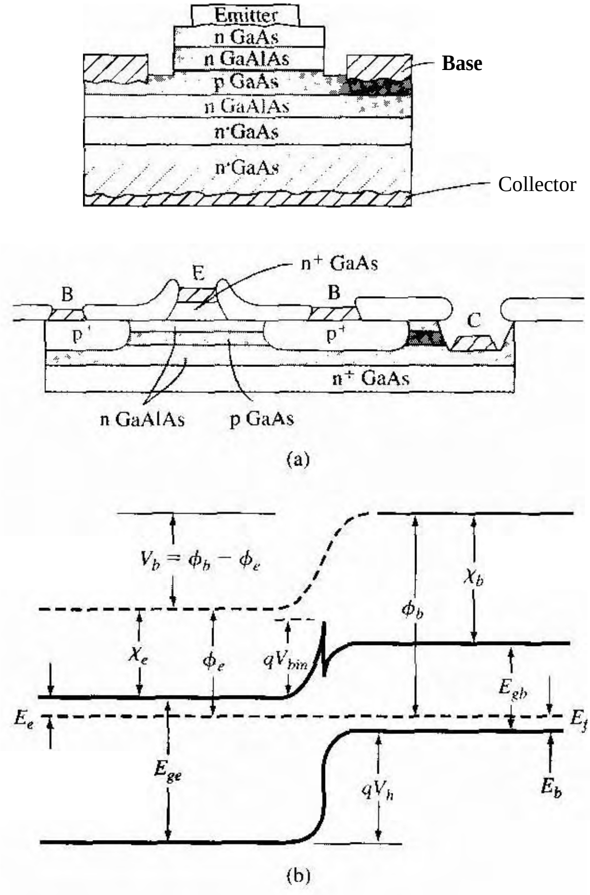
Emitter
n GaAs
n GaAlAs
p GaAs
n GaAlAs
n+GaAs
n+GaAs
Base
Collector
E
n+ GaAs
B
B
p+
p+
C
n+ GaAs
n GaAlAs
p GaAs
(a)
$V_b = \phi_b - \phi_e$
χ_b
ϕ_b
χ_e
ϕ_e
qV_{bin}
E_{gb}
E_e
E_f
E_{ge}
qV_h
E_b
(b)

Figure 10.50 | (a) Cross section of AlGaAs/GaAs heterojunction bipolar transistor showing a discrete and integrated structure. (b) Energy-band diagram of the n AlGaAs emitter and p GaAs base junction.
(From Tiwari et al. [19].)

n-AlGaAs emitter to p-GaAs base junction. The large potential barrier V_b limits the number of holes that will be injected back from the base into the emitter.

The intrinsic carrier concentration is a function of bandgap energy as

$$n_i^2 \propto \exp\left(\frac{-E_g}{kT}\right)$$

For a given emitter doping. the number of minority carrier holes injected into the emitter is reduced by a factor of

$$\exp\left(\frac{\Delta E_g}{kT}\right)$$

in changing from a narrow- to wide-bandgap emitter. If $\Delta E_g = 0.30$ eV, for example, n_i^2 would be reduced by approximately 10^5 at $T = 300$ K. The drastic reduction in n_i^2 for the wide-bandgap emitter means that the requirements of a very high emitter doping can be relaxed and a high emitter injection efficiency can still be obtained. A lower emitter doping reduces the bandgap-narrowing effect.

The heterojunction GaAs bipolar transistor has the potential of being a very high frequency device. A lower emitter doping in the wide-bandgap emitter leads to a smaller junction capacitance, increasing the speed of the device. Also, for the GaAs npn device. the minority carriers in the base are electrons with a high mobility. The electron mobility in GaAs is approximately 5 times that in silicon; thus, the base transit time in the GaAs base is very short. Experimental AlGaAs/GaAs heterojunction transistors with base widths on the order of 0.1 μm have shown cutoff frequencies on the order of 40 GHz.

One disadvantage of GaAs is the low minority carrier lifetime. The small lifetime is not a factor in the base of a narrow-base device, but results in a larger B-E recombination current. which decreases the recombination factor and reduces the current gain. A current gain of 150 has been reported.

10.9 | SUMMARY

- There are two complementary bipolar transistors—npn and pnp. Each transistor has three separately doped regions and two pn junctions. The center region (base) is very narrow. so the two pn junctions are said to be interacting junctions.
- In the forward-active mode. the B-E junction is forward biased and the B-C junction is reverse biased. Majority carriers from the emitter are injected into the base where they become minority carriers. These minority carriers diffuse across the base into the B-C space charge region where they are swept into the collector.
- When a transistor is biased in the forward-active mode of operation, the current at one terminal of the transistor (collector current) is controlled by the voltage applied across the other two terminals of the transistor (base–emitter voltage). This is the basic transistor action
- The minority carrier concentrations were determined in each region of the transistor. The principal currents in the device are determined by the diffusion of these minority carriers.

The common-base current gain, which leads to the common-emitter current gain, is a function of three factors—emitter injection efficiency, base transport factor, and recombination factor The emitter injection efficiency takes into account carriers from the base that are injected back into the emitter, the base transport factor takes into account recombination in the base region. and the recombination factor takes into account carriers that recombine within the forward-biased B-E junction.

- Several nonideal effects were considered:

  1. Base width modulation, or Early effect — the change in the neutral base width with a change in B-C voltage, producing a change in collector current with a change in B-C or C-E voltage.
  2. High-injection effects that cause the collector current to increase at a slower rate with base-emitter voltage.
  3. Emitter bandgap narrowing that produces a smaller emitter injection efficiency because of a very large emitter region doping concentration.
  4. Current crowding effects that produce a larger current density at the emitter edge than in the center of the emitter
  5. A nonuniform base doping concentration that induces an electric field in the base region, which aids the flow of minority carriers across the base.
  6. Two breakdown voltage mechanisms — punch-through and avalanche.

- Three equivalent circuits or mathematical models of the transistor were considered. The Ebers–Moll model and equivalent circuit are applicable in any of the transistor operating modes. The Gummel–Poon model is convenient to use when nonuniform doping exists in the transistor. The small-signal hybrid-pi model applies to transistors operating in the forward-active mode in linear amplifier circuits.

  The cutoff frequency of a transistor, a figure of merit for the transistor, is the frequency at which the magnitude of the common-emitter current gain becomes equal to unity. The frequency response is a function of the emitter–base junction capacitance charging time, the base transit time, the collector depletion region transit time, and the collector capacitance charging time.
- The switching characteristics are closely related to the frequency limitations although switching involves large changes in currents and voltages. An important parameter in switching is the charge storage time. which applies to a transistor switching from saturation to cutoff.

GLOSSARY OF IMPORTANT TERMS

alpha cutoff frequency The frequency at which the magnitude of the common base current is $1/\sqrt{2}$ of its low-frequency value; also equal to the cutoff frequency.

bandgap narrowing The reduction in the forbidden energy bandgap with high emitter doping concentration.

base transit time The time that it takes a minority carrier to cross the neutral base region.

base transport factor The factor in the common base current gain that accounts for recombination in the neutral base width.

base width modulation The change in the neutral base width with C-E or C-B voltage.

beta cutoff frequency The frequency at which the magnitude of the common emitter current gain is $1/\sqrt{2}$ of its low frequency value.

collector capacitance charging time The time constant that describes the time required for the **B-C** and collector–substrate space charge widths to change with a change in emitter current.

collector depletion region transit time The time that it takes a carrier to be swept across the B-C space charge region.

common-base current gain The ratio of collector current to emitter current.

common-emitter current gain The ratio of collector current to base current.

current crowding The nonuniform current density across the emitter junction area created by a lateral voltage drop in the base region due to a finite base current and base resistance.

cutoff The bias condition in which zero- or reverse-bias voltages are applied to both transistor junctions, resulting in zero transistor currents.

cutoff frequency The frequency at which the magnitude of the common emitter current gain is unity.

early effect Another term fur base width modulation.

early voltage The value of voltage (magnitude) at the intercept on the voltage axis obtained by extrapolating the I_C versus V_{CE} curves to zero current.

emitter–base junction capacitance charging time The time constant describing the time for the B-E space charge width to change with a change in emitter current.

emitter injection efficiency factor The factor in the common-base current gain that takes into account the injection of carriers from the base into the emitter.

forward active The bias condition in which the **B-E** junction is forward biased and ***the*** **B-C** junction is reverse biased.

inverse active The bias condition in which the **B-E** junction is reverse biased and the **B-C** junction is forward biased.

output conductance The ratio of a differential change in collector current to the corresponding differential change in C-E voltage.

CHECKPOINT

After studying this chapter, the reader should have the ability to:

- Describe the basic operation of the transistor.
- Sketch the energy bands of the transistor in thermal equilibrium and when biased in the various operating modes.
- Calculate, to a good first approximation, the collector current as a function of base–emitter voltage.
- Sketch the minority carrier concentrations throughout the transistor under the various operating modes.
- Define the various diffusion and other current components in the transistor from the minority carrier distribution curves.
- Explain the physical mechanisms of the current gain limiting factors.
  Define the current-limiting factors from the current components in the transistor.
- Describe the physical mechanism of base width modulation and its effect on the current–voltage characteristics of the transistor
- Describe the voltage breakdown mechanisms in **a** bipolar transistor
- Sketch the simplified small-signal hybrid-pi equivalent circuit of the transistor biased in the forward-active mode.

- Describe qualitatively the four time-delay or time-constant components in the frequen response of the bipolar transistor.

REVIEW QUESTIONS

1. Describe the charge flow in an npn bipolar transistor biased in the forward-active mode. Is the current by drift or diffusion?
2. Define the common-emitter current gain and explain why, to a first approximation, the current gain is a constant.
3. Explain the conditions of the cutoff, saturation, and inverse-active modes.
4. Sketch the minority carrier concentrations in a pnp bipolar transistor biased in the forward-active mode.
5. Define and describe the three limiting factors in the common-base current gain.
6. What is meant by base width modulation? What is another term used for this effect?
7. What is meant by high injection?
8. Explain emitter current crowding.
9. Define I_{CBO} and I_{CEO}, and explain why $I_{CEO} > I_{CBO}$
10. Sketch a simplified hybrid-pi model for an npn bipolar transistor and explain when thi equivalent circuit is used.
11. Describe the time-delay factors in the frequency limitation of the bipolar transistor.
12. What is the cutoff frequency of a bipolar transistor?
13. Describe the response of a bipolar transistor when it is switching between saturation and cutoff.

PROBLEMS

(Note: In the following problems, use the transistor geometry shown in Figure 10.13. Assum T = 300 K unless otherwise stated.)

Section 10.1 The Bipolar Transistor Action

10.1 Fur a uniformly doped $n^{++}p^{+}n$ bipolar transistor in thermal equilibrium, (a) sketch the energy-band diagram, (*b*) sketch the electric field through the device, and (c) repeat parts ***(a)*** and (h) for the transistor biased in the forward-active region.

10.2 Consider a $p^{++}n^{+}p$ bipolar transistor, uniformly doped in each region. Sketch the energy-band diagram for the case when the transistor is (a) in thermal equilibrium, (*b*) biased in the forward-active mode, (*c*) biased in the inverse-active region, and (*d*) biased in cutoff with both the B-E and B-C junctions **reverse** biased.

10.3 The parameters in the base region of an npn bipolar transistor are $D_n = 20\,\text{cm}^2/\text{s}$, $n_{B0} = 10^4\ \text{cm}^{-3}$, $x_B = 1\ \mu\text{m}$, and $A_{BE} = 10^{-4}\ \text{cm}^2$. (*a*) Comparing Equations (10.1) and (10.2), calculate the magnitude of 4. (*b*) Determine the collector current for (*i*) $v_{BE} = 0.5$ V, (*ii*) $v_{BE} = 0.6$ V, and (iii) $v_{BE} = 0.7$ V.

10.4 Assume the common-base current gain for the transistor described in Problem 10.3 is a $= 0.9920$. (*a*) What is the common-emitter current gain β? [Note that $\beta = \alpha/(1-\alpha)$.] (b) Determine the emitter and base currents corresponding to the collector currents determined in Problem 10.3b.

10.5 (a) In a bipolar transistor biased in the forward-active region, the base current is $i_B = 6.0\ \mu\text{A}$ and the collector current is $i_C = 510\ \mu\text{A}$. Determine β, α, and i_E. (Note that $i_E = i_C + i_B$.) (b) Repeat part (a) if $i_B = 50\ \mu\text{A}$ and $i_C = 2.65$ mA.

10.6 Assume that an npn bipolar transistor has a common-emitter current gain of $\beta = 100$. (a) Sketch the ideal current–voltage characteristics (i_C versus v_{CE}), like those in Figure 10.9, as i_B varies from zero to 0.1 mA in 0.01-mA increments. Let v_{CE} vary over the range $0 \le v_{CE} \le 10$ V. (b) Assuming $V_{CC} = 10$ V and $R_C = 1\ \text{k}\Omega$ in the circuit in Figure 10.8, superimpose the load line on the transistor characteristics in part (a). (c) Plot, on the resulting graph, the value of i_C and v_{CE} corresponding to $i_B = 0.05$ mA.

10.7 Consider Equation (10.7). Assume $V_{CC} = 10$ V, $R_C = 2\ \text{k}\Omega$, and $V_{BE} = 0.6\ V$. (a) Plot V_{CB} versus I_C over the range $0 \le I_C \le 5$ mA. (b) At what value of I_C does $V_{CB} = 0$?

Section 10.2 Minority Carrier Distribution

10.8 A uniformly doped silicon npn bipolar transistor is to be biased in the forward-active mode with the B-C junction reverse biased by 3 V The metallurgical base width is 1.10 μm. The transistor dopings are $N_E = 10^{17}\ \text{cm}^{-3}$, $N_B = 10^{16}\ \text{cm}^{-3}$, and $N_C = 10^{15}\ \text{cm}^{-3}$. (a) For T = 300 K, calculate the B-E voltage at which the minority carrier electron concentration at $x = 0$ is 10 percent of the majority carrier hole concentration. (b) At this bias, determine the minority carrier hole concentration at $x' = 0$. (c) Determine the neutral base width for this bias.

10.9 A silicon npn bipolar transistor is uniformly doped and biased in the forward-active region. The neutral base width is $x_B = 0.8\ \mu$m. The transistor doping concentrations are $N_E = 5 \times 10^{17}\ \text{cm}^{-3}$, $N_B = 10^{16}\ \text{cm}^{-3}$, and $N_C = 10^{15}\ \text{cm}^{-3}$. (a) Calculate the values of p_{E0}, n_{B0}, and p_{C0}. (b) For $V_{BE} = 0.625\ V$, determine n_B at $x = 0$ and p_E at $x' = 0$. (c) Sketch the minority carrier concentrations through the device and label each curve.

10.10 A uniformly doped silicon pnp transistor is biased in the forward-active mode. The doping concentrations are $N_E = 10^{18}\ \text{cm}^{-3}$, $N_B = 5 \times 10^{16}\ \text{cm}^{-3}$, and $N_C = 10^{15}\ \text{cm}^{-3}$. (a) Calculate the values of n_{E0}, p_{B0}, and n_{C0}. (b) For $V_{EB} = 0.650\ V$, determine p_B at $x = 0$ and n_E at $x' = 0$. (c) Sketch the minority carrier concentrations through the device and label each curve.

10.11 Consider the minority carrier electron concentration in the base of an npn bipolar transistor as given by Equation (10.15a). In this problem, we want to compare the gradient of the electron concentration evaluated at the B-C junction to that evaluated at the B-E junction. In particular, calculate the ratio of $d(\delta n_B)/dx$ at $x = x_B$ to $d(\delta n_B)/dx$ at $x = 0$ for (a) $x_B/L_B = 0.1$, (b) $x_B/L_B = 1.0$, and (c) $x_B/L_B = 10$.

10.12 Derive the expressions for the coefficients given by Equations (10.14a) and (10.14b).

***10.13** Derive the expression for the excess minority carrier hole concentration in the base region of a uniformly doped pnp bipolar transistor operating in the forward-active region.

10.14 The excess electron concentration in the base of an npn bipolar transistor is given by Equation (10.15a). The linear approximation is given by Equation (10.15b). If $\delta n_{B0}(x)$ is the linear approximation given by Equation (10.15b) and $\delta n_B(x)$ is the actual distribution given by Equation (10.15a), determine

$$\frac{\delta n_{B0}(x) - \delta n_B(x)}{\delta n_{B0}(x)} \times 100\%$$

at $x = x_B/2$ for (a) $x_B/L_B = 0.1$ and (b) $x_B/L_B = 1.0$. Assume $V_{BE} \gg kT/e$.

10.15 Consider a pnp bipolar transistor. Assume that the excess minority carrier hole concentrations at the edges of the B-E and B-C space charge regions are $\delta p_B(0) = 8 \times 10^{14}$ cm^{-3} and $\delta p_B(x_B) = -2.25 \times 10^4$ cm^{-3}, respectively. Plot, on the same graph, $\delta p_B(x)$ for (a) the ideal case when no recombination occurs in the base, and (b) the case when $x_B = L_B = 10$ μm. (c) Assuming $D_B = 10$ cm^2/s, calculate the diffusion current density at $x = 0$ and $x = x_B$ for the conditions in parts (a) and (b) Determine the ratio $J(x = x_B)/J(x = 0)$ for the two cases.

***10.16** (a) A uniformly doped npn bipolar transistor at $T = 300$ K is biased in saturation. Starting with the continuity equation for minority carriers, show that the excess electron concentration in the base region can be expressed as

$$\delta n_B(x) = n_{B0}\left\{\left[\exp\left(\frac{eV_{BE}}{kT}\right) - 1\right]\left[1 - \frac{x}{x_B}\right] + \left[\exp\left(\frac{eV_{BC}}{kT}\right) - 1\right]\left[\frac{x}{x_B}\right]\right\}$$

for $x_B/L_B \ll 1$ where x_B is the neutral base width. (b) Show that the minority carrier diffusion current in the base is then given by

$$J_n = -\frac{eD_B n_{B0}}{x_B}\left[\exp\left(\frac{eV_{BE}}{kT}\right) - \exp\left(\frac{eV_{BC}}{kT}\right)\right]$$

(c) Show that the total excess minority carrier charge (C/cm^2) in the base region is given by

$$\delta Q_{nB} = \frac{-en_{B0}x_B}{2}\left\{\left[\exp\left(\frac{eV_{BE}}{kT}\right) - 1\right] + \left[\exp\left(\frac{eV_{BC}}{kT}\right) - 1\right]\right\}$$

***10.17** Consider a silicon pnp bipolar transistor at $T = 300$ K with uniform dopings of $N_E = 5 \times 10^{18}$ cm^{-3}, $N_B = 10^{17}$ cm^{-3}, and $N_C = 5 \times 10^{15}$ cm^{-3}. Let $D_B = 10$ cm^2/s, $x_B = 0.7$ μm, and assume $x_B \ll L_B$. The transistor is operating in saturation with $J_p = 165$ A/cm^2 and $V_{EB} = 0.75$ V. Determine (a) V_{CB}, (b) V_{EC}(sat), (c) the #/cm^2 of excess minority carrier holes in the base, and (d) the #/cm^2 of excess minority carrier electrons in the long collector. Let $L_C = 35$ μm.

10.18 An npn silicon bipolar transistor at $T = 300$ K has uniform dopings of $N_E = 10^{19}$ cm^{-3}, $N_B = 10^{17}$ cm^{-3}, and $N_C = 7 \times 10^{15}$ cm^{-3}. The transistor is operating in the inverse-active mode with $V_{BE} = -2$ V and $V_{BC} = 0.565$ V. (a) Sketch the minority carrier distribution through the device. (b) Determine the minority carrier concentrations at $x = x_B$ and $x'' = 0$. (c) If the metallurgical base width is 1.2 μm, determine the neutral base width.

10.19 A uniformly doped silicon pnp bipolar transistor at $T = 300$ K with dopings of $N_E = 5 \times 10''$ cm^{-3}, $N_B = 10^{16}$ cm^{-3}, and $N_C = 5 \times 10^{14}$ cm^{-3} is biased in the inverse-active mode. What is the maximum B-C voltage so that the low-injection condition applies?

Section 10.3 Low-Frequency Common-Base Current Gain

10.20 The following currents are measured in a uniformly doped npn bipolar transistor:

I,,, $= 1.20$ mA   I,,, $= 0.10$ mA
$I_{nC} = 1.18$ mA $I_R = 0.20$ mA
$I_G = 0.001$ mA $I_{pc0} = 0.001$ mA

Determine (a) a. (b) γ, (c) α_T, (d) δ, and (e) β.

10.21 A silicon npn transistor at T $= 300$ K has an area of 10^{-3} cm^2, neutral base width of I μm, and doping concentrations of $N_E = 10^{18}$ cm^{-3}, $N_B = 10^{17}$ cm^{-3}, $N_C = 10^{16}$ cm^{-3}. Other semiconductorparameters are $D_B = 20$ cm^2/s, $\tau_{E0} = \tau_{B0} = 10^{-7}$ s, and $\tau_{C0} = 10^{-6}$ s. Assuming the transistor is biased in the active region and the recombination factor is unity, calculate the collector current for: (a) $V_{BE} = 0.5$ V, (b) $I_E = 1.5$ mA, and (c) $I_B = 2\ \mu$A.

10.22 Consider a uniformly doped npn bipolar transistor at $T = 300$ K with the following parameters:

$N_E = 10^{18}$ cm^{-3} $N_B = 5 \times 10^{16}$ cm^{-3} $N_C = 10^{15}$ cm^{-3}
$D_E = 8$ cm^2/s $D_B = 15$ cm^2/s $D_C = 12$ cm^2/s
$\tau_{E0} = 10^{-8}$ s $\tau_{B0} = 5 \times 10^{-8}$ s $\tau_{C0} = 10^{-7}$ s
$x_E = 0.8\ \mu$m $x_B = 0.7\ \mu$m $J_{r0} = 3 \times 10^{-8}$ A/cm^2

For $V_{BE} = 0.60$ V and $V_{CE} = 5$ V, calculate (a) the currents J_{nE}, J_{pE}, J_{nC}, and J_R and (b) the current gain factors γ, α_T, δ, a. and β.

10.23 Three npn bipolar transistors have identical parameters except for the bass doping concentrations and neutral base widths. The base parameters for the three devices are as follows:

Device	Base duping	Base width
A	$N_B = N_{B0}$	$x_B = x_{B0}$
B	$N_B = 2N_{B0}$	$x_B = x_{B0}$
C	$N_B = N_{B0}$	$x_B = x_{B0}/2$

(The base doping concentration for the B device is twice that of A and C, and the neutral base width for the C device is half that of A and B.)

(a) Determine the ratio of the emitter injection efficiency of (i) device B to device A and (ii) device C to device A.
(h) Repeat part (a) for the base lranspon factor.
(c) Repeat pan (a) for the recombination factor.
(d) Which device has the largest common-emitter current gain β?

10.24 Repeat Problem 10.23 for three devices in which the emitter paramelers **vary.** The emitter parameters for the three devices are as follows:

Device	Emitter doping	Emitter width
A	$N_E = N_{E0}$	$x_E = x_{E0}$
B	$N_E = 2N_{E0}$	$x_E = x_{E0}$
C	$N_E = N_{E0}$	$x_E = x_{E0}/2$

10.25 An npn silicon transistor is biased in the inverse active mode with $V_{BE} = -3$ V and $V_{BC} = 0.6$ V The doping concentrations are $N_E = 10^{18}$ cm^{-3}, $N_B = 10^{17}$ cm^{-3}, a $N_C = 10^{16}$ cm^{-3}. Other parameters are $x_B =$ I μm, $\tau_{E0} = \tau_{B0} = \tau_{C0} = 2$ x 10^{-7} $D_E = 10$ cm^2/s, $D_B = 20$ cm^2/s, D_C =15 cm^2/s, and $A = 10^{-3}$ cm'. (*a*) Calculate and plot the minority carrier distribution in the device. (*b*) Calculate the collector and emitter currents. (Neglect geometry factors and assume the recombination factor is unity.)

10.26 (a) Calculate the base transport factor, α_T, for $x_B/L_B = 0.01$, 0.10, 1.0, and 10. Assuming that γ and δ are unity, determine β for each case. (*b*) Calculate the emitter injection efficiency, γ, for $N_B/N_E = 0.01$, 0.10, 1.0, and 10. Assuming that α_T and δ are unity, determine β for each case. (*c*) Considering the results of pans (a) and (*b*), what conclusionr can be made concerning when the base transport factor or when the emitter injection efficiency are the limiting factors for the common-emitter current gain?

10.27 /a) Calculate the recombination factor for $V_{BE} = 0.2, 0.4$, and 0.6 V. Assume the following parameters:

$D_B = 25$ cm^2/s $D_E = 10$ cm^2/s

$N_E = 5$ x 10^{18} cm^{-3} $N_B = 1 \times 10^{17}$ cm^{-3}

$N_C = 5 \times 10^{15}$ cm^{-3} $x_B = 0.7$ μm

$\tau_{B0} = \tau_{E0} = 10^{-7}$ s $J_{r0} = 2$ x 10^{-9} A/cm^2

n, $= 1.5 \times 10^{10}$ cm^{-3}

(*b*) Assuming the base transport and emitter injection efficiency factors are unity, calculate the common-emitter current gain for the conditions in part (*a*). (*c*) Considering the results of part (*b*), what can be said about the recombination factor being the limiting factor in the common emitter current gain.

10.28 Consider an npn silicon bipolar transistor at T = 300 K with the following parameters:

$D_B = 25$ cm^{2}1s $D_E = 10$ cm^2/s

$\tau_{B0} =$ $\tau_{E0} = 5$ x

$N_B = 10^{16}$ cm^{-3} $x_E = 0.5$ μm

The recombination factor, δ, has been determined to he $\delta = 0.998$. We need a common-emitter current gain of $\beta = 120$. Assuming that $\alpha_T = \gamma$, determine the maximum base width, x_B, and the minimum emitter doping, N_E, to achieve this specification.

***10.29** (*a*) The recombination current density, J_{r0}, in an npn silicon bipolar transistor at $T = 300$ K is $J_{r0} = 5$ x 10^{-8} A/cm^2. The uniform dopings are $N_E = 10^{18}$ cm^{-3}, $N_B = 5$ x 10^{16} cm^{-3}, and $N_C = 10^{15}$ cm^{-3}. Other parameters are $D_E = 10$ cm^2/s, $D_B = 25$ cm^2/s. $\tau_{E0} = 10^{-8}$ s, and $\tau_{B0} = 10^{-7}$ s. Determine the neutral base width so that the recornbination factor is $\delta = 0.995$ when $V_{BE} = 0.55$ V (*b*) If J_{r0} remains constant with temperature, what is the value of δ when $V_{BE} = 0.55$ V for the case when the temperature is T = 400 K'? Use the value of x_B determined in pan (a).

10.30 (a) Plot, for a bipolar transistor, the base transport factor. α_T, as a function of (x_B/L_B) over the range $0.01 \le (x_B/L_B) \le 10$. (*Use* a log scale an the horizontal axis.)

(*b*) Assuming that the emitter injection efficiency and recombination factors are unity, plot the common emitter gain for the conditions in part (*a*). (*c*) Considering the results of pan (*b*), what can be said about the base transport factor being the limiting factor in the common emitter current gain?

1031 (a) Plot the emitter injection efficiency as a function of the doping ratio, N_B/N_E, over the range $0.01 \leq N_B/N_E \leq 10$. Assume that $D_E = D_B$, $L_B = L_E$, and $x_B = x_E$. (Use a log scale on the horizontal axis.) Neglect bandgap narrowing effects. (*b*) Assuming that the base transport factor and recombination factors are unity, plot the common emitter current gain for the conditions in part (a). (*c*) Considering the results of part (*b*), what can be said about the emitler injection efficiency being the limiting factor in the common emitter current gain.

10.32 **(a)** Plot the recombination factor as a function of the forward-bias B-E voltage for $0.1 \leq V_{BE} \leq 0.6$. Assume the following parameters:

$$\begin{aligned} D_B &= 25\ \text{cm}^2/\text{s} & D_E &= 10\ \text{cm}^2/\text{s} \\ N_E &= 5 \times 10^{18}\ \text{cm}^{-3} & N_B &= 1 \times 10^{17}\ \text{cm}^{-3} \\ N_C &= 5 \times 10^{15}\ \text{cm}^{-3} & x_B &= 0.7\ \mu\text{m} \\ \tau_{B0} = \tau_{E0} &= 10^{-7}\ \text{s} & J_{r0} &= 2 \times 10^{-9}\ \text{A/cm}^2 \\ n_i &= 1.5 \times 10^{10}\ \text{cm}^{-3} \end{aligned}$$

(*b*) Assuming the base transport and emitter injection efficiency factors are unity, plot the common emitter current gain for the conditions in part (*a*). (*c*) Considering the results of part (*b*), what can be said about the recombination factor being the limiting factor in the common emitter current gain.

10.33 The emitter in a BJT is often made very thin to achieve high operating speed. In this problem. we investigate the effect of emitter width an current gain. Consider the emitter injection efficiency given by Equation (10.35a). Assume that $N_E = 100N_B$, $D_E = D_B$, and $L_E = L_B$. Also let $x_B = 0.1L_B$. Plot the emitter injection efficiency for $0.01L_E \leq x_E \leq 10L_E$. From these results, discuss the effect of emitter width on the current gain.

Section 10.4 Nonideal Effects

10.34 A silicon pnp bipolar transistor at T = 300 K has uniform dopings of $N_E = 10^{18}\ \text{cm}^{-3}$, $N_B = 10^{16}\ \text{cm}^{-3}$, and $N_C = 10^{15}\ \text{cm}^{-3}$. The metallurgical hase width is 1.2 μm. Let $D_B = 10\ \text{cm}^2/\text{s}$ and $\tau_{B0} = 5 \times 10^{-7}$ s. Assume that the minority carrier hole concentration in the hase can be approximated by a linear distribution. Let $V_{EB} = 0.625$ V (*a*) Determine the hole diffusion current density in the base for $V_{BC} = 5$ V, $V_{BC} = 10$ V, and $V_{BC} = 15$ V (*b*) Estimate the Early voltage.

***10.35** The base width of a bipolar transistor is normally small to provide a large current gain and increased speed. The hase width also affects the Early voltage. In a silicon npn bipolar transistor at T = 300 K, the doping concentrations arc $N_E = 10^{18}\ \text{cm}^{-3}$, $N_B = 3 \times 10^{16}\ \text{cm}^{-3}$, and $N_C = 5 \times 10''\ \text{cm}^{-3}$. Assume $D_B = 20\ \text{cm}^2/\text{s}$ and $\tau_{B0} = 5 \times 10^{-7}$ s, and let $V_{BE} = 0.70$ V. Using voltages $V_{CB} = 5$ V and $V_{CB} = 10$ V as two data paints. estimate the Early voltage for metallurgical base widths of (a) 1.0 μm, (*b*) 0.80 μm, and (*c*) 0.60 μm.

10.36 An npn silicon bipolar **transistor** has a base doping concentration of $N_B = 10^{17}$ cm^{-} a collector doping concentration of $N_C = 10^{16}$ cm^{-3}, a metallurgical base width of 1.I μm, and a base minority carrier diffusion coefficient of $D_B = 20$ cm^2/s. The transistor is biased in the forward-active region with $V_{BE} = 0.60$ V. Determine *(a)* the change in the neutral base width as V_{CB} changes from I V to 5 V, and *(b)* the corresponding change in the collector current.

1037 Consider a uniformly doped silicon npn bipolar transistor in which $x_E = x_B$, $L_E = L_B$, and $D_E = D_B$. Assume that $\alpha_T = \delta = 0.995$ and let $N_B = 10^{17}$ cm^{-3}. Calculate and plot the common emitter current gain β for $N_E = 10^{17}, 10^{18}, 10^{19}$, and 10^{20} cm^{-3}, and for the case *(a)* when the bandgap narrowing effect is neglected. and (b) when the bandgap narrowing effect is taken into account.

10.38 A silicon pnp bipolar transistor at T = 300 K is to be designed so that the emitter injection efficiency is $\gamma = 0.996$. Assume that $x_E = x_B$, $L_E = L_B$, $D_E = D_B$, and let $N_E = 10^{19}$ cm^{-3}. *(a)* Determine the maximum base doping, taking into account bandgap narrowing. *(h)* If bandgap narrowing were neglected, what would be the maximum base doping required?

10.39 A first-approximation type calculation of the current crowding effect can be made using the geometry shown in Figure 10.5I. Assume that one-half of the base current enters from each side of the emitter strip and flows uniformly to the center of the emitter. Assume the base is p type with the following parameters:

$N_B = 10^{16}$ cm^{-3} $\quad$ $x_B = 0.70\ \mu$m

$\mu_p = 400$ cm^2/V-s $\quad$ $S = 8\ \mu$m

Emitter length $\quad$ L = 100 μm

(a) Calculate the resistance between $x = 0$ and $x = S/2$. *(b)* If $\frac{1}{2}\, I_B = 10\ \mu$A, calculate the voltage drop between $x = 0$ and $x = S/2$. *(c)* If $V_{BE} = 0.6$ V at $x = 0$ estimate in percent the number of electrons being injected into the base at $x = S/2$ compared to $x = 0$.

10.40 Consider the geometry shown in Figure 10.51 and the device parameters in Problem 10.39 except the emitter width S. The emitter width S is to be changed so that the number of electrons injected into the base at $x = Sf2$ is no more than 10 percent less than the number of electrons injected into the base at $x = 0$. Calculate S

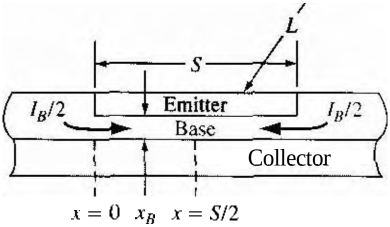

Figure 10.51 | Figure for Problems 10.39 and 10.40.

***10.41** The base doping in a diffused n$^+$pn bipolar transistor can be approximated by an exponential as

$$N_B = N_B(0)\exp\left(\frac{-ax}{x_B}\right)$$

where ***a*** is a constant and is given by

$$a = \ln\left(\frac{N_B(0)}{N_B(x_B)}\right)$$

(*a*) Show that, in thermal equilibrium, the electric field in the neutral base region is a constant. ***(b)*** Indicate the direction of the electric field. Does this electric field aid or retard the flow of minority carrier electrons across the base'? (*c*) Derive an expression for the steady-state minority carrier electron concentration in the base under forward bias. Assume no recombination occurs in the base. (Express the electron concentration in terms of the electron current density.)

10.42 Consider a silicon npn bipolar transistor with uniform dopings of $N_E = 5 \times 10^{18}$ cm^{-3}, $N_B = 10^{17}$ cm^{-3}, and $N_C = 5 \times 10^{15}$ cm^{-3}. Assume the common-base current gain is $\alpha = 0.9920$. Determine (*a*) BV_{CBO}, (*b*) BV_{CEO}, and (*c*) the base–emitter breakdown voltage. (Assume $n = 3$ for the empirical constant.)

10.43 A high-voltage silicon npn bipolar transistor is to be designed such that the uniform base doping is $N_B = 10^{16}$ cm^{-3} and the common-emitter current grain is $\beta = 50$. The breakdown voltage BV_{CEO} is to be at least 60 V. Determine the maximum collector doping and the minimum collector length to support this voltage. (Assume $n = 3$.)

10.44 **A** uniformly doped silicon epitaxial npn bipolar transistor is fabricated with a base doping of $N_B = 3 \times 10^{16}$ cm^{-3} and a heavily doped collector region with $N_C = 5 \times 10^{17}$ cm^{-3}. The neutral base width is $x_B = 0.70\ \mu m$ when $V_{BE} = V_{BC} = 0$. Determine V_{BC} at which punch-through occurs. Compare this value to the expected avalanche breakdown voltage of the junction.

10.45 A silicon npn bipolar transistor has a base doping concentration of $N_B = 10^{17}$ cm^{-3}, a collector doping concentration of $N_C = 7 \times 10^{15}$ cm^{-3}, and a metallurgical base width of 0.50 μm. Let $V_{BE} = 0.60$ V. (*a*) Determine V_{CE} at punch-through. (*b*) Determine the peak electric field in the B-C space charge region at punch-through.

10.46 A uniformly doped silicon pnp bipolar transistor is to be designed with $N_E = 10^{19}$ cm^{-3} and $N_C = 10^{16}$ cm^{-3}. The metallurgical base width is 0.75 μm. Determine the minimum base doping so that the punch-through voltage is no less than $V_{pt} = 25$ V.

Section 10.5 Equivalent Circuit Models

10.47 The $V_{CE}(\text{sat})$ voltage of an npn transistor in saturation continues to decrease slowly as the base current increases. In the Ehers–Moll model. assume $\alpha_F = 0.99$. $\alpha_R = 0.20$. and $I_C = 1$ mA. For $T = 300$ K, determine the base current, I_B, necessary to give (*a*) $V_{CE}(\text{sat}) = 0.30$ V, ***(b)*** $V_{CE}(\text{sat}) = 0.20$ V, and (*c*) $V_{CE}(\text{sat}) = 0.10$ V.

10.48 Consider an npn bipolar transistor biased in the active mode. Using the Ebers–Moll model, derive the equation for the base current, I_B, in terms of α_F, ***a*,,** I_{ES}, I_{CS}, and V_{BE}.

10.49 Consider the Ebers–Moll model and let the base terminal be open so $I_B = 0$. Sho that, when a collector-emitter voltage is applied, we have

$$I_C \equiv I_{CEO} = I_{CS}\frac{(1-\alpha_F\alpha_R)}{(1-\alpha_F)}$$

10.50 In the Ebers–Moll model, let $\alpha_F = 0.98$, $I_{ES} = 10^{-13}$ A, and $I_{CS} = 5 \times 10^{-13}$ A. $T = 300$ K. Plot I_C versus V_{CE} for $-V_{BE} < V_{CB} < 3$ V and for $V_{BE} = 0.2, 0.4$, and 0.6 V. (Note that $V_{CB} = -V_{BC}$.) What can be said about the base width modulation effect using this model?

10.51 The collector–emitter saturation voltage, from the Ebers–Moll model, is given by Equation (10.77). Consider a power BJT in which $\alpha_F = 0.98$, $\alpha_R = 0.20$, and 4 A. Plot $V_{CE}(\text{sat})$ versus I_B over the range $0.03 \le I_B \le 1.0$ A.

Section 10.6 Frequency Limitations

10.52 Consider a silicon npn transistor at $T = 300$ K. Assume the following parameters:

$I_E = 0.5$ mA
$x_B = 0.7\ \mu$m
$x_{dc} = 2.0\ \mu$m
$C_\mu = C_s = 0.08$ pF
$C_{je} = 0.8$ pF
$D_n = 25$ cm^2/s
$r_c = 30\ \Omega$
$\beta = 50$

(a) Calculate the transit time factors. *(b)* Calculate the cutoff and beta cutoff frequencies, f_T and f_β, respectively.

10.53 In a particular bipolar transistor, the base transit time is 20 percent of the total delay time. The base width is 0.5 μm and the base diffusion coefficient is $D_B = 20$ cm^2/s. Determine the cutoff frequency.

10.54 Assume the base transit time of a BJT is 100 ps and carriers cross the 1.2 μm B-C space charge region at a speed of 10^7 cm/s. The emitter–base junction charging time is 25 ps and the collector capacitance and resistance are 0.10 pF and 10 Ω, respectively. Determine the cutoff frequency.

Summary and Review

***10.55** *(a)* A silicon npn bipolar transistor at $T = 300$ K is to be designed with an Early voltage of at least 200 V and a current gain of at least $\beta = 80$. (b) Repeat part *(a)* for a pnp bipolar transistor.

***10.56** Design a uniformly doped silicon npn bipolar transistor so that $\beta = 100$ at $T = 300$ K. The maximum CE voltage is to be 15 V and any breakdown voltage is to be at least 3 times this value. Assume the recombination factor is constant at $\delta = 0.995$. The transistor is to be operated in low injection with a maximum collector current of $I_C = 5$ mA. Bandgap narrowing effects and base width modulation effects are to be minimized. Let $D_E = 6$ cm^2/s, $D_B = 25$ cm^2/s, $\tau_{E0} = 10^{-8}$ s, and $\tau_{B0} = 10^{-7}$ s. Determine doping concentrations, the metallurgical base width, the active area, and the maximum allowable V_{BE}.

***10.57** Design a pair of complementary npn and pnp bipolar transistors. The transistors are to have the same metallurgical base and emitter widths of $W_B = 0.75\ \mu$m and

$x_E = 0.5\ \mu\text{m}$. Assume that the following minority carrier parameters apply to each device.

$$D_n = 23\ \text{cm}^2/\text{s} \qquad \tau_{n0} = 10^{-7}\ \text{s}$$
$$D_p = 8\ \text{cm}^2/\text{s} \qquad \tau_{p0} = 5 \times 10^{-8}\ \text{s}$$

The collector doping concentration in each device is $5 \times 10^{15}\ \text{cm}^{-3}$ and the recombination factor in each device is constant at $\delta = 0.9950$. (*a*) Design, if possible, the devices so that $\beta = 100$ in each device. If this is not possible, how close a match can be obtained? (*b*) With equal forward-bias base–emitter voltages applied, the collector currents are to be $I_C = 5$ mA with each device operating in low-injection. Determine the active cross-sectional areas.

READING LIST

1. Dimitrijev, S. *Understanding Semiconductor Devices.* New York: Oxford University Press, 2000.
2. Kano, K. *Semiconductor Devices.* Upper Saddle River, NJ: Prentice Hall, 1998.
3. Muller, R. S., and T. I. Kamins. *Device Electronics for Integrated Circuits.* 2nd ed. New York: Wiley, 1986.
4. Navon, D. H. *Semiconductor Microdevices and Materials.* New York: Holt, Rinehart, & Winston, 1986.
5. Neudeck, G. W. *The Bipolar Junction Transistor.* Vol. 3 of the *Modular Series on Solid State Devices.* 2nd ed. Reading, MA: Addison-Wesley, 1989.
6. Ng, K. K. *Complete Guide to Semiconductor Devices.* New York: McGraw-Hill, 1995.
7. Ning, T. H., and R. D. Isaac. "Effect of Emitter Contact on Current Gain of Silicon Bipolar Devices." *Polysilicon Emitter Bipolar Transistors.* eds. A. K. Kapoor and D. J. Roulston. New York: IEEE Press, 1989.
8. Pierret, R. F. *Semiconductor Device Fundamentals.* Reading, MA: Addison-Wesley, 1996.
9. Roulston, D. J. *Bipolar Semiconductor Devices.* New York: McGraw-Hill, 1990.
10. Roulston, D. J. *An Introduction to the Physics of Semiconductor Devices.* New York Oxford University Press, 1999.

*11. Shur, M. *GaAs Devices and Circuits.* New York: Plenum Press. 1987.

12. Shur, M. *Introduction to Electronic Devices.* New York: John Wiley & Sons, Inc., 1996.

*13. Shur, M. *Physics of Semiconductor Devices.* Englewood Cliffs, NJ: Prentice Hall, 1990.

14. Singh, J. *Semiconductor Devices: An Introduction.* New York: McGraw-Hill, 1994.
15. Singh, J. *Semiconductor Devices: Basic Principles.* New York: John Wiley & Sons, Inc., 2001
16. Streetman, B. G., and S. Banerjee. *Solid State Electronic Devices,* 5th ed. Upper Saddle River, NJ: Prentice Hall, 2000.
17. Sze, S. M. *High-Speed Semiconductor Devices.* New York: Wiley, 1990.
18. Sze, S. M. *Physics of Semiconductor Devices.* 2nd ed. New York: Wiley, 1981.

19. Tiwari, S., S. L. Wright, and A. W. Kleinsasser. "Transport and Related Properties o (Ga. Al)As/GaAs Double Heterojunction Bipolar Junction Transistors." *IEEE Transactions on Electron Devices*, ED-34 (February 1987), pp. 185–87.

***20.** Taur, Y., and T. H. Ning. *Fundamentals of Modern VLSI Devices. New* York: Cambridge University Press, 1998.

***21.** Wang, S. *Fundamentals of Semiconductor Theory and Device Physics.* Englewood Cliff*, NJ: Prentice Hall, 1989.

***22.** Warner, R. M., Jr., and B. L. Grung. *Transistors: Fundamentals for the Integrated-Circuit Engineer.* New York: Wiley. 1983.

23. Yang. E. S. *Microelectronic Devices.* New York: McGraw-Hill, 1988.

***24.** Yuan, J. S. *SiGe, GaAs, and InP Heterojunction Bipolar Transistors.* New York: John Wiley & Sons, Inc., 1999.

CHAPTER 11

Fundamentals of the Metal–Oxide–Semiconductor Field-Effect Transistor

PREVIEW

The fundamental physics of the Metal–Oxide–Semiconductor Field-Effect Transistor (MOSFET) is developed in this chapter. Although the bipolar transistor was discussed in the last chapter, the material in this chapter presumes a knowledge only of the semiconductor material properties and characteristics of the pn junction.

The MOSFET, in conjunction with other circuit elements, is capable of voltage gain and signal-power gain. The MOSFET is also used extensively in digital circuit applications where, because of its relatively small size, thousands of devices can be fabricated in a single integrated circuit. The MOSFET is, without doubt. the core of integrated circuit design at the present lime.

The MOS designation is implicity used only for the metal–silicon dioxide (SiO_2)–silicon system. The more general terminology is metal–insulator–semiconductor (MIS), where the insulator is not necessarily silicon dioxide and the semiconductor is not necessarily silicon. We will use the MOS system throughout this chapter although the same basic physics applies to the MIS system.

The heart of the MOSFET is a metal–oxide–semiconductor structure known as an MOS capacitor. The energy bands in the semiconductor near the oxide–semiconductor interface bend as a voltage is applied across the MOS capacitor. The position of the conduction and valence bands relative to the Fermi level at the oxide–semiconductor interface is a function of the MOS capacitor voltage, so that the characteristics of the semiconductor surface can be inverted from p-type to n-type, or from n-type to p-type, by applying the proper voltage. The operation and characteristics of the MOSFET are dependent on this inversion and the creation of an inversion charge density at the semiconductor surface. The threshold voltage is defined as the applied gate voltage required to create the inversion layer charge and is one of the important parameters of the MOSFET.

The various types of MOSFETs are examined and a qualitative discussion of the current–voltage characteristics is initially presented. A mathematical derivation of the current–voltage relation is then covered in detail. The frequency response and limitations of the MOSFET are also considered.

Although we have not discussed fabrication processes in any detail in this text, there is an MOS technology that should be considered, since it directly influences the characteristics and properties of the MOS devices and circuits. We will consider the complementary MOS (CMOS) process. The discussion of this technology will be brief, but should provide a good base for further in-depth study. ■

11.1 | THE TWO-TERMINAL MOS STRUCTURE

The heart of the MOSFET is the metal–oxide–semiconductor capacitor shown in Figure 11.1. The metal may be aluminum or some other type of metal, although in many cases, it is actually a high-conductivity polycrystalline silicon that has been deposited on the oxide; however, the term metal is usually still used. The parameter t_{ox} in the figure is the thickness of the oxide and ϵ_{ox} is the permittivity of the oxide.

11.1.1 Energy-Band Diagrams

The physics of the MOS structure can be more easily explained with the aid of the simple parallel-plate capacitor. Figure 11.2a shows a parallel-plate capacitor with the top plate at a negative voltage with respect to the bottom plate. An insulator material separates the two plates. With this bias, a negative charge exists on the top plate, a positive charge exists on the bottom plate, and an electric field is induced between the two plates as shown. The capacitance per unit area for this geometry is

$$C' = \frac{\epsilon}{d} \tag{11.1}$$

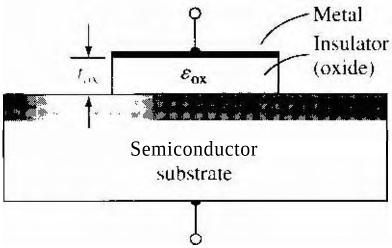

Figure 11.1 | The basic MOS capacitor structure.

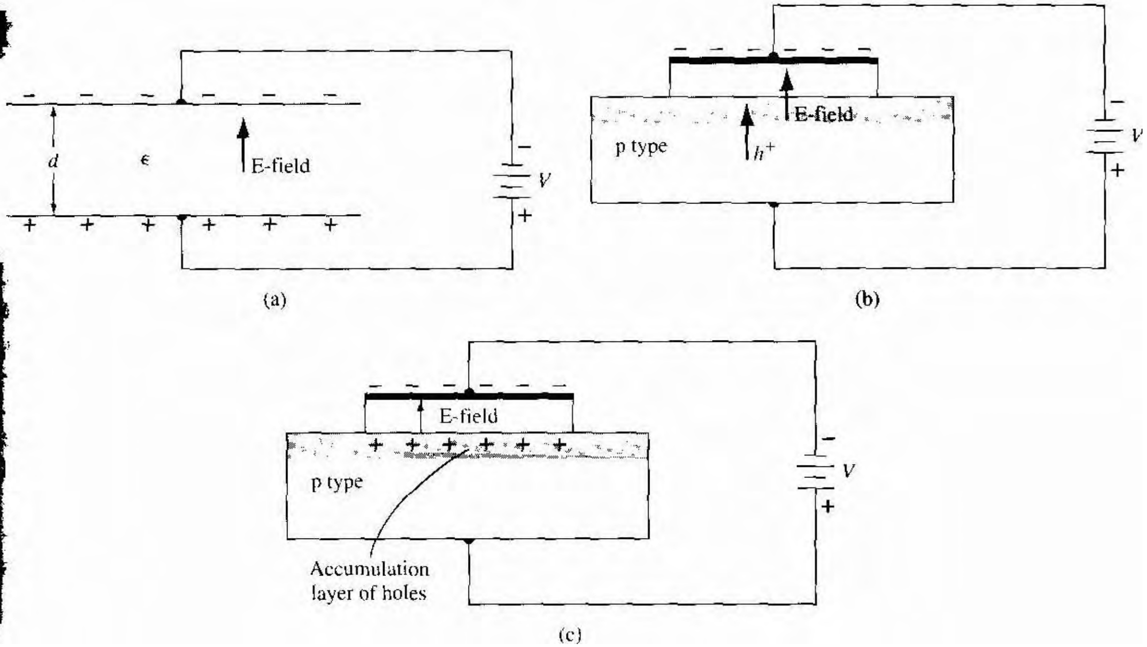

Figure 11.2 | (a) A parallel-plate capacitor showing the electric field and conductor charges. (b) A corresponding MOS capacitor with a negative gate bias showing the electric field and charge Row. (c) The MOS capacitor with an accumulation layer of holes.

where ϵ is the permittivity of the insulator and d is the distance between the two plates. The magnitude of the charge per unit area on either plate is

$$Q' = C'V \tag{11.2}$$

where the prime indicates charge or capacitance per unit area. The magnitude of the electric field is

$$E = \frac{V}{d} \tag{11.3}$$

Figure 11.2b shows an MOS capacitor with a p-type semiconductor substrate. The top metal gate is at a negative voltage with respect to the semiconductor substrate. From the example of the parallel-plate capacitor, we can see that a negative charge will exist on the top metal plate and an electric field will be induced with the direction shown in the figure. If the electric field were to penetrate into the semiconductor, the majority carrier holes would experience a force toward the oxide–semiconductor interface. Figure 11.2c shows the equilibrium distribution of charge in the MOS capacitor with this particular applied voltage. An *accumulation layer* of holes in the oxide–semiconductor junction corresponds to the positive charge on the bottom "plate" of the MOS capacitor.

Figure 11.3a shows the same MOS capacitor in which the polarity of the applie voltage is reversed. A positive charge now exists on the top metal plate and the induced electric field is in the opposite direction as shown. If the electric field penetrates the semiconductor in this case, majority carrier holes will experience a forc away from the oxide–semiconductor interface. As the holes are pushed away from the interface, a negative space charge region is created because of the fixed ionize acceptor atoms. The negative charge in the induced depletion region corresponds t the negative charge on the bottom "plate" of the MOS capacitor. Figure 11.3b show the equilibrium distribution of charge in the MOS capacitor with this applied voltage

The energy-hand diagram of the MOS capacitor with the p-type substrate, for the case when a negative voltage is applied to the top metal gate, is shown in Figure 11.4a The valence-band edge is closer to the Fermi level at the oxide–semiconductor interface than in the **bulk** material, which implies that there is an accumulation of holes The semiconductor surface appears to he more p-type than the bulk material. Th Fermi level is a constant in the semiconductor since the MOS system is in therma equilibrium and there is no current through the oxide.

Figure 11.4b shows the energy-band diagram of the MOS system when a positive voltage is applied to the gate. The conduction and valence band edges bend a

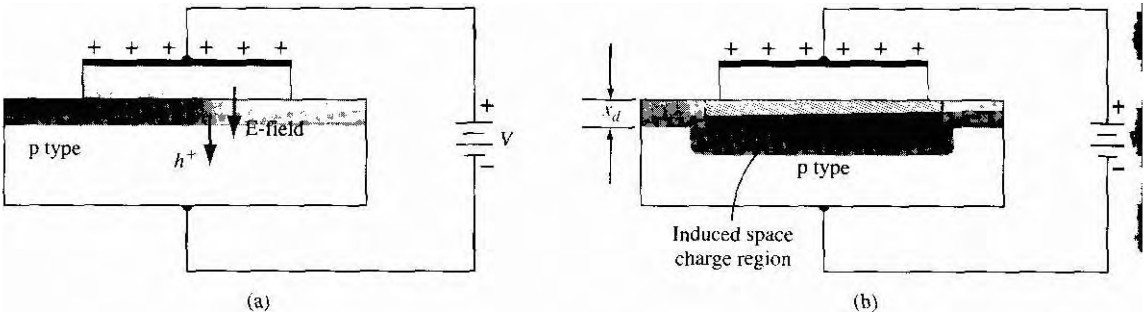
+ + + + + +
E-field
p type
h^+
+
V
−
(a)
x_d
+ + + + + +
p type
Induced space charge region
+
−
(b)

Figure **11.3** | The MOS capacitor with a moderate positive gate bias, showing (a) the electric field and charge flow and (b) the induced space charge region.

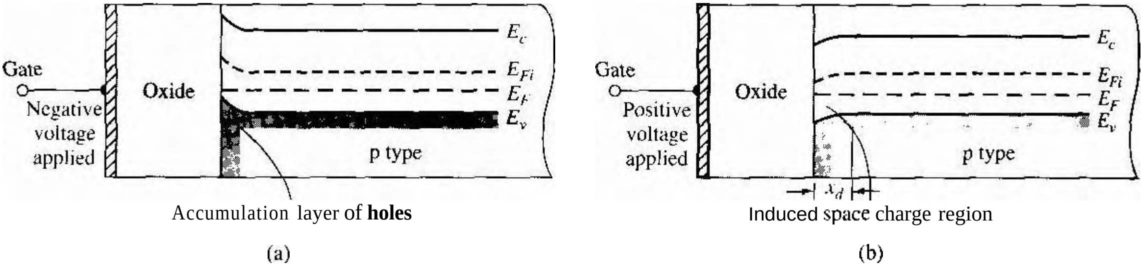
Gate
Negative voltage applied
Oxide
E_c
E_{Fi}
E_F
E_v
p type
Accumulation layer of holes
(a)
Gate
Positive voltage applied
Oxide
E_c
E_{Fi}
E_F
E_v
p type
x_d
Induced space charge region
(b)

Figure 11.4 | The energy-band diagram of an MOS capacitor with a p-type substrate for (a) a negative gate bias and (b) a moderate positive gate bias.

hown in the figure, indicating a space charge region similar to that in a pn junction. The conduction hand and intrinsic Fermi levels move closer to the Fermi level. The induced space charge width is x_d.

Now consider the case when a still larger positive voltage is applied to the top metal gate of the MOS capacitor. We expect the induced electric field to increase in magnitude and the corresponding positive and negative charges on the MOS capacitor to increase. Alarger negative charge in the MOS capacitor implies a larger induced space charge region and more band bending. Figure 11.5 shows such a condition. The intrinsic Fermi level at the surface is now below the Fermi level: thus, the conduction band is closer to the Fermi level than the valence band is. This result implies that the surface in the semiconductor adjacent to the oxide-semiconductor interface is n type. By applying a sufficiently large positive gate voltage, we have inverted the surface of the semiconductor from a p-type to an n-type semiconductor. We have created an *inversion layer* of electrons at the oxide-semiconductor interface.

In the MOS capacitor structure that we have just considered, we assumed a p-type semiconductor substrate. The same type of energy-band diagrams can be constructed for an MOS capacitor with an n-type semiconductor substrate. Figure 11.6a shows the MOS capacitor structure with a positive voltage applied to the top gate terminal. Apositive charge exists on the top gate and an electric field is induced with the direction shown in the figure. An accumulation layer of electrons will be induced in

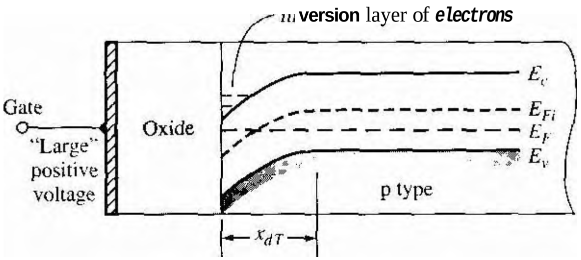

Figure 11.5 | The energy-band diagram of the MOS capacitor with a p-type substrate for a "large" positive gate bias.

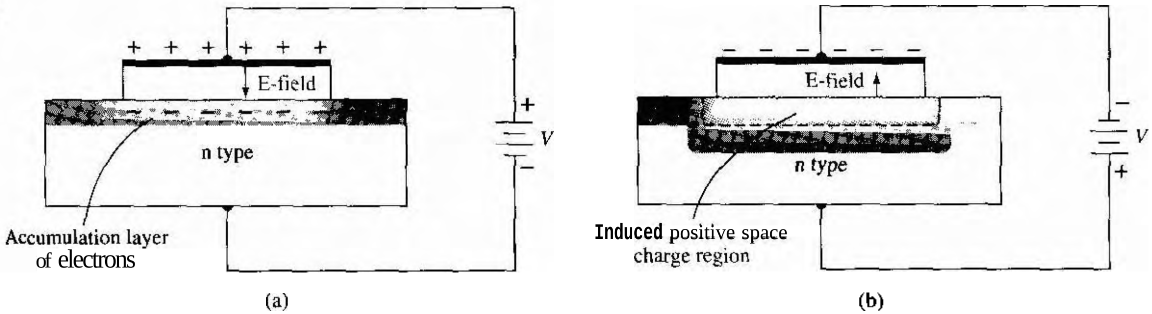
+ + + + + +
E-field
n type
+
V
−
Accumulation layer of electrons
(a)
− − − − − −
E-field
n type
−
V
+
Induced positive space charge region
(b)

Figure 11.6 | The MOS capacitor with an n-type substrate for (a) a positive gate bias and (b) a moderate negative gate bias.

the n-type substrate. The case when a negative voltage is applied to the top gate is shown in Figure 11.6b. A positive space charge region is induced in the n-type semiconductor in this situation.

The energy-band diagrams for this MOS capacitor with the n-type substrate ar shown in Figure 11.7. Figure 11.7a shows the case when a positive voltage is applied to the gate and an accumulation layer of electrons is formed. Figure 11.7 shows the positive space charge region induced by an applied negative gate voltage in it the conduction and valence band energies bend upward. Figure 11.7c shows the energy bands when a larger negative voltage is applied to the gate. The conduction and valence bands are bent even more and the intrinsic Fermi level has moved above the Fermi level so that the valence band is closer to the Fermi level than the

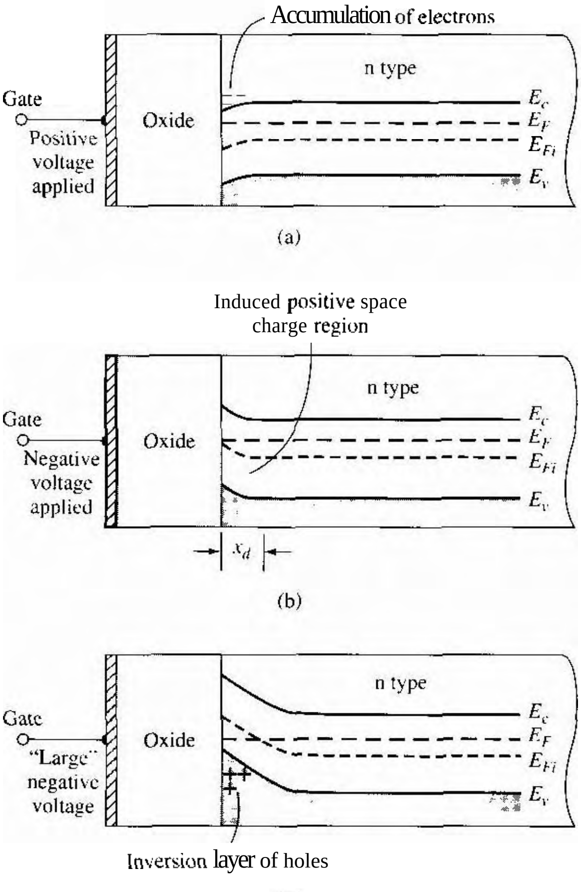
Accumulation of electrons
n type
Gate
Positive voltage applied
Oxide
E_c
E_F
E_{Fi}
E_v
Induced positive space charge region
n type
Gate
Negative voltage applied
Oxide
E_c
E_F
E_{Fi}
E_v
x_d
n type
Gate
"Large" negative voltage
Oxide
E_c
E_F
E_{Fi}
E_v
Inversion layer of holes

(a)

(b)

(c)

Figure 11.7 | The energy-band diagram of the MOS capacitor with an n-type substrate for (a) a positive gate bias, (b) a moderate negative bias, and (c) a "**large**" negative gate bias.

conduction band is. This result implies that the semiconductor surface adjacent to the oxide-semiconductor interface is p type. By applying a sufficiently large negative voltage to the gate of the MOS capacitor, the semiconductor surface has been inverted from n type to p type. An inversion layer of holes has been induced at the oxide-semiconductor interface.

11.1.2 Depletion Layer Thickness

We may calculate the width of the induced space charge region adjacent to the oxide-semiconductor interface. Figure 11.8 shows the space charge region in a p-type semiconductor substrate. The potential>@ is the difference (in volts) between E_{Fi} and E_F and is given by

$$\boxed{\phi_{fp} = V_t \ln\left(\frac{N_a}{n_i}\right)} \tag{11.4}$$

where N_a is the acceptor doping concentration and n_i is the intrinsic carrier concentration.

The potential ϕ_s is called the surface potential; it is the difference (in volts) between E_{Fi} measured in the bulk semiconductor and E_{Fi} measured at the surface. The surface potential is the potential difference across the space charge layer. The space charge width can now be written in a form similar to that of a one-sided pn junction. We can write that

$$x_d = \left(\frac{2\epsilon_s\phi_s}{eN_a}\right)^{1/2} \tag{11.5}$$

where ϵ_s is the permittivity of the semiconductor. Equation (11.5) assumes that the abrupt depletion approximation is valid.

Figure 11.9 shows the energy bands for the case in which $\phi_s = 2\phi_{fp}$. The Fermi level at the surface is as far above the intrinsic level as the Fermi level is below the

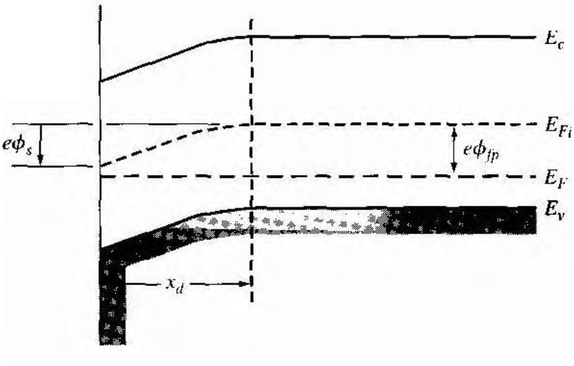

Figure 11.8 | The energy-band diagram in the p-type semiconductor, indicating surface potential.

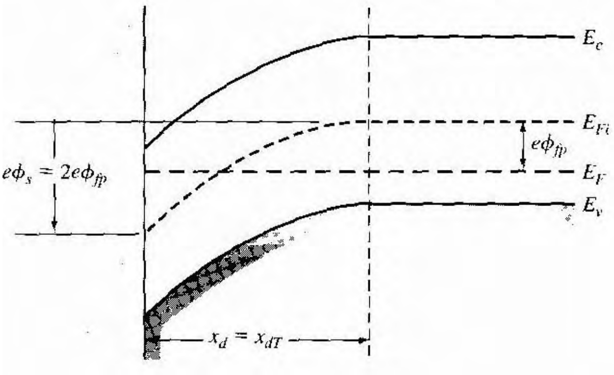

Figure 11.9 | The energy-band diagram in the p-type semiconductor at the threshold inversion point.

intrinsic level in the bulk semiconductor. The electron concentration at the surface is the same as the hole concentration in the bulk material. This condition is known as the *threshold inversion point.* The applied gate voltage creating this condition is known as the ***threshold voltage.*** If the gate voltage increases above this threshold value, the conduction bend will bend slightly closer to the Fermi level. but the change in the conduction band at the surface is now only a slight function of gate voltage. The electron concentration at the surface. however, is an exponential function of the surface potential. The surface potential may increase by a few (kT/e) volts, which will change the electron concentration by orders of magnitude, but the space charge width changes only slightly. In this case, then, the space charge region has essentially reached a maximum width.

The maximum space charge width, x_{dT}, at this inversion transition point can be calculated from Equation (11.5) by setting $\phi_s = 2\phi_{fp}$. Then

$$\boxed{x_{dT} = \left(\frac{4\epsilon_s\phi_{fp}}{eN_a}\right)^{1/2}} \qquad (11.6$$

EXAMPLE 11.1

Objective

To calculate the maximum space charge width given a particular semiconductor doping concentration.

Consider silicon at T = 300 K doped to $N_a = 10^{16}$ cm^{-3}. The intrinsic carrier concentration is $n_i = 1.5 \times 10^{10}$ cm^{-3}.

■ Solution

From Equation (11.4), we have

$$\phi_{fp} = V_t \ln\left(\frac{N_a}{n_i}\right) = (0.0259)\ln\left(\frac{10^{16}}{1.5\times10^{10}}\right) = 0.347 \text{ V}$$

Then the maximum space charge width is

$$x_{dT} = \left[\frac{4\epsilon_s \phi_{fp}}{eN_a}\right]^{1/2} = \left[\frac{4(11.7)(8.85 \times 10^{-14})(0.347)}{(1.6 \times 10^{-19})(10^{16})}\right]^{1/2}$$

or

$$x_{dT} = 0.30 \times 10^{-4} \text{ cm} = 0.30\,\mu\text{m}$$

■ Comment

The maximum induced space charge width is on the same order of magnitude as pn junction space charge widths.

We have been considering a p-type semiconductor substrate. The same maximum induced space charge region width occurs in an n-type substrate. Figure 11.10 is the energy-band diagram at the threshold voltage with an n-type substrate. We can write

$$\boxed{\phi_{fn} = V_t \ln\left(\frac{N_d}{n_i}\right)} \tag{11.7}$$

$$\boxed{x_{dT} = \left(\frac{4\epsilon_s \phi_{fn}}{eN_d}\right)^{1/2}} \tag{11.8}$$

Note that we are always assuming the parameters ϕ_{fp} and ϕ_{fn} to be positive quantities.

Figure 11.11 is a plot of x_{dT} at T = 300 K as a function of doping concentration in silicon. The semiconductor doping can be either n-type or p-type.

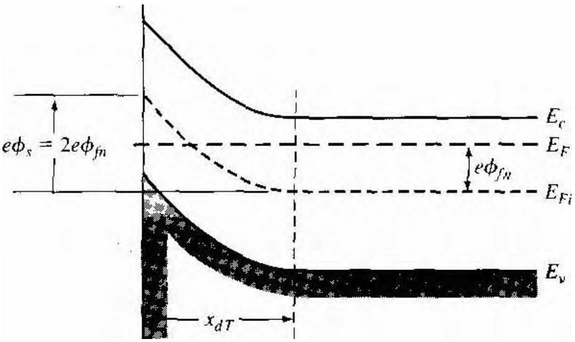

Figure 11.10 | The energy-band diagram in the n-type semiconductor at the threshold inversion point.

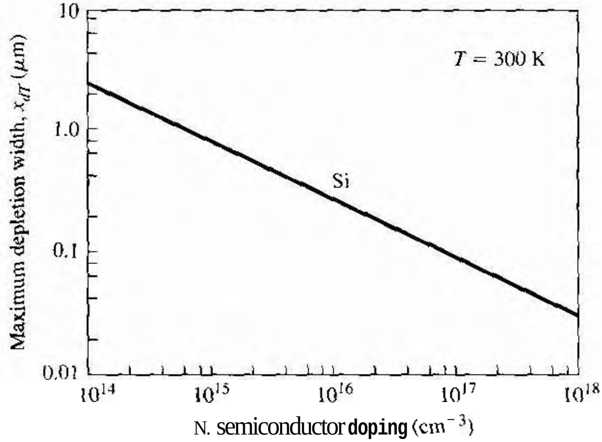

Figure 11.11 | Maximum induced space charge region width versus semiconductor doping.

TEST YOUR UNDERSTANDING

E11.1 (*a*) Consider as oxide-to-p-type silicon junction at $T = 300$ K. The impurity doping concentration in the silicon is $N_a = 3 \times 10^{16}$ cm^{-3}. Calculate the maximum space-charge width in the silicon. (*b*) Repeat part (*a*) for an impurity concentration of $N_a = 10^{15}$ cm^{-3}. [Ans. (*a*) 0.180 μm, (*b*) 0.863 μm]

E11.2 Consider an oxide-to-n-type silicon junction at $T = 300$ K. The impurity doping concentration in the silicon is $N_d = 8 \times 10^{15}$ cm^{-3}. Calculate the maximum space-charge width in the silicon. (Ans. 0.33 μm)

11.1.3 Work Function Differences

We have been concerned. so far. with the energy-band diagrams of the semiconductor material. Figure 11.12a shows the energy levels in the metal, silicon dioxide, and silicon relative to the vacuum level. The metal work function is ϕ_m and the electron affinity is χ. The parameter χ_i is the oxide electron affinity and, for silicon dioxide $\chi_i = 0.9$ V.

Figure 11.12b shows the energy-band diagram of the entire metal–oxide–semiconductor structure with zero gate voltage applied. The Fermi level is a constant through the entire system at thermal equilibrium. We may define ϕ'_m as a modified metal work function—the potential required to inject an electron from the metal into the conduction band of the oxide. Similarly, χ' is defined as a modified electron affinity. The voltage V_{ox0} is the potential drop across the oxide for zero applied gate voltage and is not necessarily zero because of the difference between ϕ_m and χ. The potential ϕ_{s0} is the surface potential for this case.

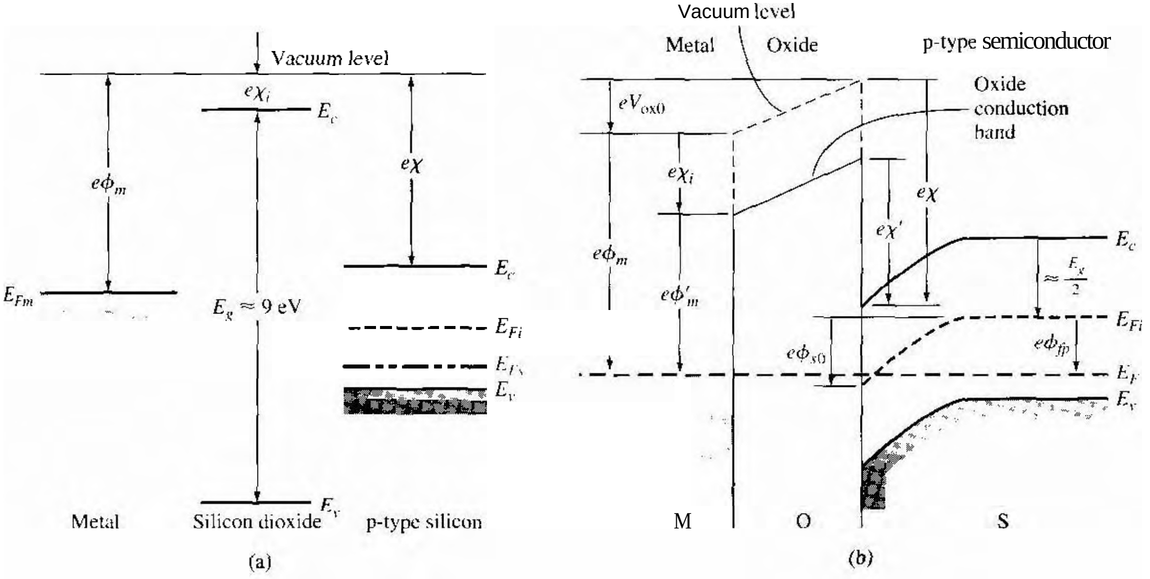
Vacuum level
$e\chi_i$
E_c
$e\phi_m$
$e\chi$
E_{Fm}
$E_g \approx 9$ eV
E_c
E_{Fi}
E_{Fs}
E_v
E_v
Metal
Silicon dioxide
p-type silicon
(a)
Vacuum level
Metal
Oxide
p-type semiconductor
Oxide conduction band
eV_{ox0}
$e\chi_i$
$e\phi_m$
$e\phi'_m$
$e\chi'$
$e\chi$
E_c
$\approx \frac{E_g}{2}$
E_{Fi}
$e\phi_{fp}$
$e\phi_{s0}$
E_F
E_v
M
O
S
(b)

Figure **11.12** | (a) Energy levels in an MOS system prior to contact and (b) energy-band diagram through the MOS structure in thermal equilibrium after contact.

If we sum the energies from the Fermi level on the metal side to the Fermi level on the semiconductor side, we have

$$e\phi'_m + eV_{ox0} = e\chi' + \frac{E_g}{2} - e\phi_{s0} + e\phi_{fp} \tag{11.9}$$

Equation (11.9) can be rewritten as

$$V_{ox0} + \phi_{s0} = -\left[\phi'_m - \left(\chi' + \frac{E_g}{2e} + \phi_{fp}\right)\right] \tag{11.10}$$

We can define a potential ϕ_{ms} as

$$\boxed{\phi_{ms} \equiv \left[\phi'_m - \left(\chi' + \frac{E_g}{2e} + \phi_{fp}\right)\right]} \tag{11.11}$$

which is known as the metal–semiconductor work function difference

Objective | **EXAMPLE 11.2**

To calculate the metal–semiconductor work function difference ϕ_{ms} for a given MOS system and semiconductor doping.

For an aluminium–silicon dioxide junction, $\phi'_m = 3.20$ V and for a silicon–silicon dioxide junction, $\chi' = 3.25$ V. We may assume that $E_g = 1.11$ eV. Let the p-type doping be $N_a = 10^{14}\ \text{cm}^{-3}$.

■ Solution

For silicon at $T = 300$ K, we may calculate ϕ_{fp} as

$$\phi_{fp} = V_t \ln\left(\frac{N_a}{n_i}\right) = (0.0259)\ln\left(\frac{10^{14}}{1.5\times 10^{10}}\right) = 0.228 \text{ V}$$

Then the work function difference is

$$\phi_{ms} = \phi'_m - \left(\chi' + \frac{E_g}{2e} + \phi_{fp}\right) = 3.20 - (3.25 + 0.555 + 0.228)$$

or

$$\phi_{ms} = -0.83 \text{ V}$$

■ Comment

The value of ϕ_{ms} will become more negative as the doping of the p-type substrate increases.

Degenerately doped polysilicon deposited on the oxide is also often used as the metal gate. Figure 11.13a shows the energy-band diagram of an MOS capacitor with an n^+ polysilicon gate and a p-type substrate. Figure 11.13b shows the energy-band diagram for the case of a p^+ polysilicon gate and the p-type silicon substrate. In the degenerately doped polysilicon, we will initially assume that $E_F = E_c$ for the n^+ case and $E_F = E_v$ for the p^+ case.

For the n^+ polysilicon gate, the metal-semiconductor work function difference can be written as

$$\boxed{\phi_{ms} = \left[\chi' - \left(\chi' + \frac{E_g}{2e} + \phi_{fp}\right)\right] = -\left(\frac{E_g}{2e} + \phi_{fp}\right)} \tag{11.12}$$

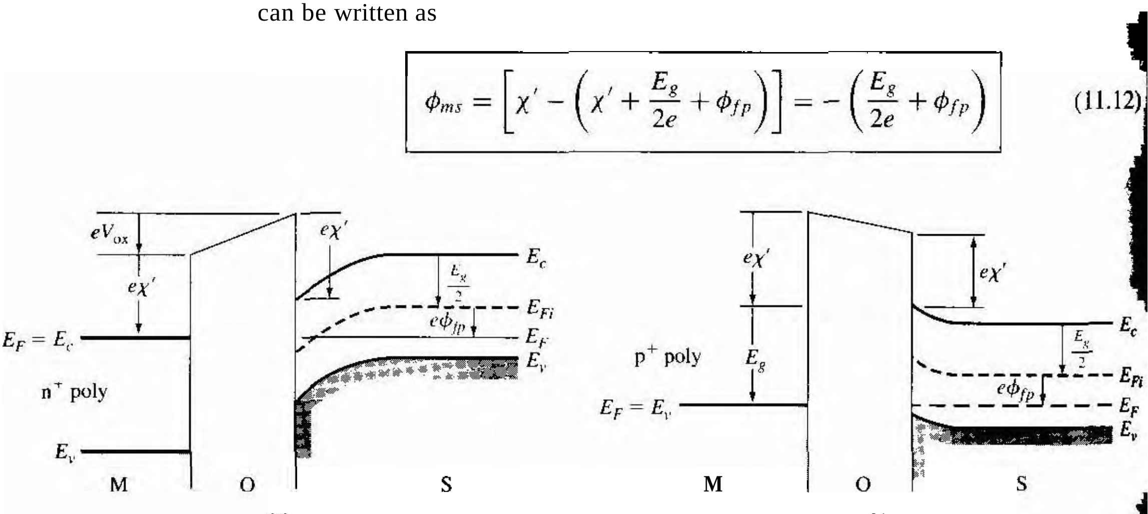

(a) (b)

Figure 11.13 | Energy-band diagram through the MOS structure with a p-type substrate at zero gate bias for (a) an n^+ polysilicon gate and (b) a p^+ polysilicon gate.

and for the p^+ polysilicon gate, we have

$$\boxed{\phi_{ms} = \left[\left(\chi' + \frac{E_g}{e}\right) - \left(\chi' + \frac{E_g}{2e} + \phi_{fp}\right)\right] = \left(\frac{E_g}{2e} - \phi_{fp}\right)} \tag{11.13}$$

However, for degenerately doped n^+ polysilicon and p^+ polysilicon, the Fermi level can be above E_c and below E_v, respectively, by 0.1 to 0.2 V. The experimental ϕ_{ms} values will then be slightly different from the values calculated by using Equations (11.12) and (11.13).

We have been considering a p-type semiconductor substrate. We may also have an n-type semiconductor substrate in an MOS capacitor. Figure 11.14 shows the energy-band diagram of the MOS capacitor with a metal gate and the n-type semiconductor substrate, for the case when a negative voltage is applied to the gate. The metal–semiconductor work function difference for this case is defined as

$$\boxed{\phi_{ms} = \phi'_m - \left(\chi' + \frac{E_g}{2e} - \phi_{fn}\right)} \tag{11.14}$$

where ϕ_{fn} is assumed to be a positive value. We will have similar expressions for n^+ and p^+ polysilicon gates.

Figure 11.15 shows the work function differences as a function of semiconductor doping for the various types of gates. We may note that the magnitude of ϕ_{ms} for the polysilicon gates are somewhat larger than Equations (11.12) and (11.13) predict. This difference again is because the Fermi level is not equal to the conduction band

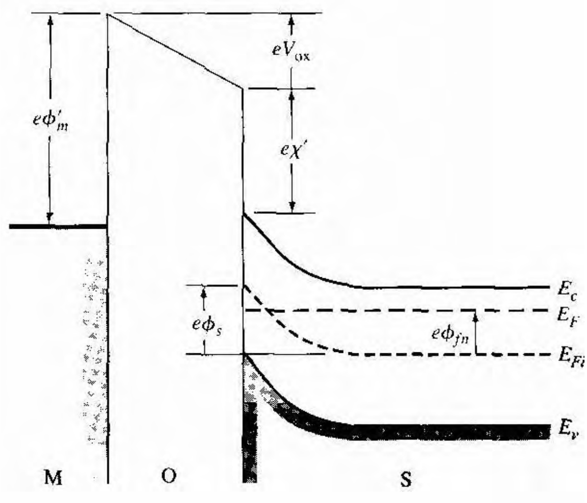

Figure 11.14 | Energy-band diagram through the MOS structure with an n-type substrate for a negative applied gate bias.

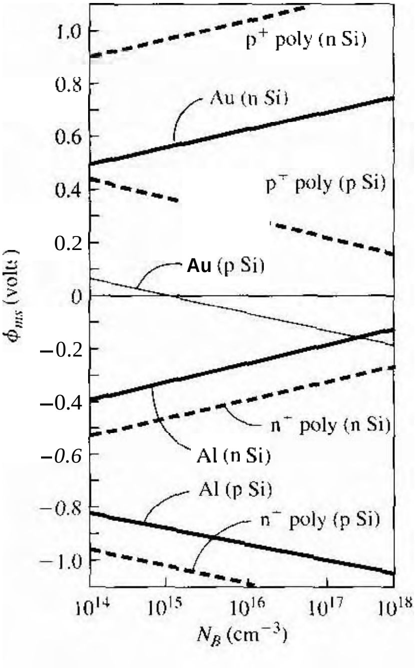

Figure **11.15** | Metal-semiconductor work function difference versus doping for aluminum, gold, and n^+ and p^+ polysilicon gates.
(From Sze [16] and Werner [19].)

energy for the n^+ gate and is not equal to the valence band energy for the p^+ gate. The metal-semiconductor work function difference becomes important in the flat-band and threshold voltage parameters discussed next.

TEST YOUR UNDERSTANDING

E11.3 The silicon impurity doping concentration in an aluminum–silicon dioxide–silicon MOS structure is $N_a = 3 \times 10^{16}$ cm^{-3}. Using the parameters in Example 11.2, determine the metal-semiconductor work function difference ϕ_{ms}. (Ans. $\phi_{ms} = -0.981$ V)

E11.4 Consider an n^+ polysilicon gate in an MOS structure with a p-type silicon substrate. The doping concentration of the silicon is $N_a = 3 \times 10^{16}$ cm^{-3}. Using Equation (11.12), find the value of ϕ_{ms}. (Ans. $\phi_{ms} = -0.931$ V)

E11.5 Repeat E11.4 for a p^+ polysilicon gate using Equation (11.13). (Ans. $\phi_{ms} = +0.179$ V)

11.1.4 Flat-Band Voltage

The *flat-band voltage* is defined as the applied gate voltage such that there is no band bending in the semiconductor and, as a result, zero net space charge in this region. Figure 11.16 shows this flat-band condition. Because of the work function difference

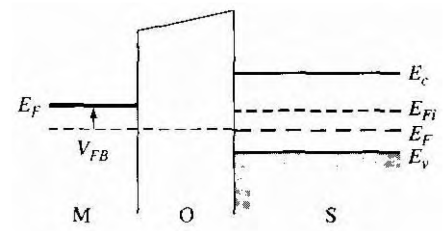

Figure 11.16 | Energy-band diagram of an MOS capacitor at flat band.

and possible trapped charge in the oxide, the voltage across the oxide for this case is not necessarily zero.

We have implicitly been assuming that there is zero net charge density in the oxide material. This assumption may not be valid—a net fixed charge density, usually positive, may exist in the insulator. The positive charge has been identified with broken or dangling covalent bonds near the oxide–semiconductor interface. During the thermal formation of SiO_2, oxygen diffuses through the oxide and reacts near the Si–SiO_2 interface to form the SiO_2. Silicon atoms may also break away from the silicon material just prior to reacting to form SiO_2. When the oxidation process is terminated, excess silicon may exist in the oxide near the interface, resulting in the dangling bonds. The magnitude of this oxide charge seems, in general, to be a strong function of the oxidizing conditions such as oxidizing ambient and temperature. The charge density can be altered to some degree by annealing the oxide in an argon or nitrogen atmosphere. However, the charge is rarely zero.

The net fixed charge in the oxide appears to be located fairly close to the oxide–semiconductor interface. We will assume in the analysis of the MOS structure that an equivalent trapped charge per unit area, Q'_{ss}, is located in the oxide directly adjacent to the oxide–semiconductor interface. For the moment, we will ignore any other oxide-type charges that may exist in the device. The parameter Q'_{ss} is usually given in terms of number of electronic charges per unit area.

Equation (11.10), for zero applied gate voltage, can be written as

$$V_{ox0} + \phi_{s0} = -\phi_{ms} \tag{11.15}$$

If a gate voltage is applied, the potential drop across the oxide and the surface potential will change. We can then write

$$V_G = \Delta V_{ox} + \Delta\phi_s = (V_{ox} - V_{ox0}) + (\phi_s - \phi_{s0}) \tag{11.16}$$

Using Equation (11.15), we have

$$V_G = V_{ox} + \phi_s + \phi_{ms} \tag{11.17}$$

Figure 11.17 shows the charge distribution in the MOS structure for the flat-band condition. There is zero net charge in the semiconductor and we can assume that an equivalent fixed surface charge density exists in the oxide. The charge density on the metal is Q'_m, and from charge neutrality we have

$$Q'_m + Q'_{ss} = 0 \tag{11.18}$$

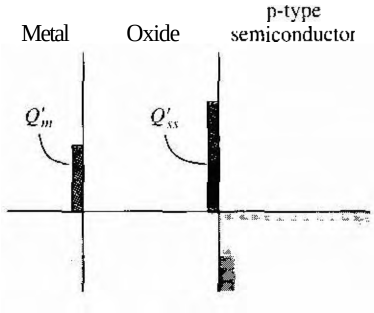

Figure **11.17** | Charge distribution in an **MOS** capacitor at flat band.

We can relate Q'_m to the voltage across the oxide by

$$V'; = \frac{Q'_m}{C_{\rm ox}} \tag{11.19}$$

where $C_{\rm ox}$ is the oxide capacitance per unit area.' Substituting Equation (11.18) int Equation (11.19), we have

$$V_{\rm ox} = \frac{-Q'_{ss}}{C_{\rm ox}} \tag{11.20}$$

In the flat-hand condition, the surface potential is zero, or $\phi_s = 0$. Then from Equation (11.17). we have

$$V_G = \boxed{V_{FB} = \phi_{ms} - \frac{Q'_{ss}}{C_{\rm ox}}} \tag{11.21}$$

Equation (11.21) is the flat-band voltage for this MOS device.

EXAMPLE 11.3

Objective

To calculate the flat-band voltage for **an** MOS capacitor with a p-type semiconductor substrate.

Consider an MOS structure with a p-type semiconductor substrate doped to $N_a = 10^{16}$ cm^{-3}, a silicon dioxide insulator with a thickness of $t_{\rm ox} = 500$ Å. and an n^+ polysilico gate. Assume that $Q'_{ss} = 10^{11}$ electronic charges percm'.

Solution

The work function difference, from Figure 11.15, is $\phi_{ms} = -1.1$ V. The oxide capacitance can be found as

$$C_{,,} = \frac{\epsilon_{\rm ox}}{t_{\rm ox}} = \frac{(3.9)(8.85 \times 10^{-14})}{500 \times} = 6.9 \times 10^{-8} \text{ F/cm}^2$$

---

[1] Although we will. in general, use the primed notation for capacitance per unit area or charge per unit area. we will omit, fur convenience, the prime on the oxide capacitance per unit area parameter

The equivalent oxide surface charge density is

$$Q'_{ss} = (10^{11})(1.6 \times 10^{-19}) = 1.6 \times 10^{-8}\ \text{C/cm}^2$$

The flat-band voltage is then calculated as

$$V_{FB} = \phi_{ms} - \frac{Q'_{ss}}{C_{ox}} = -1.1 - \left(\frac{1.6 \times 10^{-8}}{6.9 \times 10^{-8}}\right) = -1.33\ \text{V}$$

■ Comment

The applied gate voltage required to achieve the flat-band condition for this p-type substrate is negative. If the amount of fixed oxide charge increases, the flat-band voltage becomes even more negative.

TEST YOUR UNDERSTANDING

E11.6 Consider the MOS structure described in E11.3. For an oxide thickness of t_{ox} = 200 A and an oxide charge of $Q'_{ss} = 8 \times 10^{10}\ \text{cm}^{-2}$, calculate the flat-band voltage. (Ans. $V_{FB} = -1.06$ V)

E11.7 Repeat E11.6 for the MOS device described in E11.4. (Ans. $V_{FB} = -1.01$ V)

E11.8 Repeat E11.6 for the MOS device described in E11.5. (Ans. $V_{FB} = +0.105$ V)

11.1.5 Threshold Voltage

The threshold voltage was defined as the applied gate voltage required to achieve the threshold inversion point. The threshold inversion point, in turn, is defined as the condition when the surface potential is @, = ?@, for the p-type semiconductor and @, = $2\phi_{fn}$ for the n-type semiconductor. These conditions were shown in Figures 11.9a and 11.10. The threshold voltage will be derived in terms of the electrical and geometrical properties of the MOS capacitor.

Figure 11.18 shows the charge distribution through the MOS device at the threshold inversion point for a p-type semiconductor substrate. The space charge

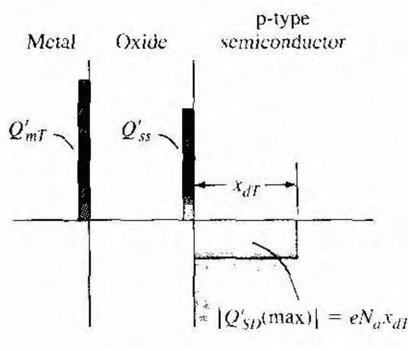

Figure 11.18 | Charge distribution in an MOS capacitor with a p-type substrate at the threshold inversion point.

width has reached its maximum value. We will assume that there is an equivalent oxide charge Q'_{ss} and the positive charge on the metal gate at threshold is Q'_{mT} .The prime on the charge terms indicates charge per unit area. Even though we are assuming that the surface has been inverted, we will neglect the inversion layer charge at this threshold inversion point. From conservation of charge, we can write

$$Q'_{mT} + Q'_{ss} = |Q'_{SD}(\max)| \tag{11.22}$$

where

$$\boxed{|Q'_{SD}(\max)| = eN_a x_{dT}} \tag{11.23}$$

and is the magnitude of the maximum space charge density per unit area of the depletion region.

The energy-band diagram of the MOS system with an applied positive gate voltage is shown in Figure 11.19. As we mentioned, an applied gate voltage will change the voltage across the oxide and will change the surface potential. We had from Equation (11.16) that

$$V_G = \Delta V_{ox} + \Delta\phi_s = V_{ox} + \phi_s + \phi_{ms}$$

At threshold, we can define $V_G = V_{TN}$, where V_{TN} is the threshold voltage that creates the electron inversion layer charge. The surface potential is $\phi_s = 2\phi_{fp}$ at threshold so Equation (11.16) can be written as

$$V_{TN} = V_{oxT} + 2\phi_{fp} + \phi_{ms} \tag{11.24}$$

where V_{oxT} is the voltage across the oxide at this threshold inversion point.

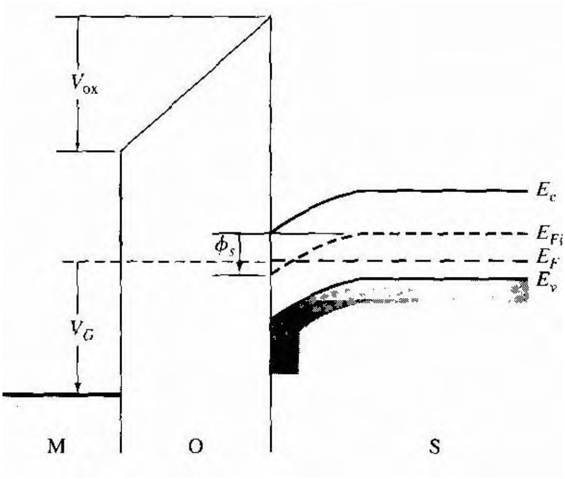

Figure 11.19 | Energy-band diagram through the MOS structure with apositive applied gate bias.

The voltage V_{oxT} can be related to the charge on the metal and to the oxide capacitance by

$$V_{oxT} = \frac{Q'_{mT}}{C_{ox}} \tag{11.25}$$

where again C_{ox} is the oxide capacitance per unit area. Using Equation (11.22), we can write

$$V_{oxT} = \frac{Q'_{mT}}{C_{ox}} = \frac{1}{C_{ox}}(|Q'_{SD}(\max)| - Q'_{ss}) \tag{11.26}$$

Finally, the threshold voltage can be written as

$$\boxed{V_{TN} = \frac{|Q'_{SD}(\max)|}{C_{ox}} - \frac{Q'_{ss}}{C_{ox}} + \phi_{ms} + 2\phi_{fp}} \tag{11.27a}$$

or

$$V_{TN} = (|Q'_{SD}(\max)| - Q'_{ss})\left(\frac{t_{ox}}{\epsilon_{ox}}\right) + \phi_{ms} + 2\phi_{fp} \tag{11.27b}$$

Using the definition of flat-band voltage from Equation (11.21), we can also express the threshold voltage as

$$V_{TN} = \frac{|Q'_{SD}(\max)|}{C_{ox}} + V_{FB} + 2\phi_{fp} \tag{11.27c}$$

For a given semiconductor material, oxide material, and gate metal, the threshold voltage is a function of semiconductor doping, oxide charge Q'_{ss}, and oxide thickness.

DESIGN EXAMPLE 11.4

Objective

To design the oxide thickness of an MOS system to yield a specified threshold voltage.

Consider an n^+ polysilicon gate and a p-type silicon substrate doped to $N_a = 3 \times 10^{16}$ cm^{-3}. Assume $Q'_{ss} = 10^{11}$ cm^{-2}. Determine the oxide thickness such that $V_{TN} = +0.65$ V.

■ **Solution**

From Figure 11.15, the work function difference is $\phi_{ms} = -1.13$ V. The various parameters can be calculated as

$$\phi_{fp} = V_t \ln\left(\frac{N_a}{n_i}\right) = (0.0259)\ln\left(\frac{3 \times 10^{16}}{1.5 \times 10^{10}}\right) = 0.376 \text{ V}$$

$$x_{dT} = \left\{\frac{4\epsilon_s\phi_{fp}}{eN_a}\right\}^{1/2} = \left\{\frac{4(11.7)(8.85 \times 10^{-14})(0.376)}{(1.6 \times 10^{-19})(3 \times 10^{16})}\right\}^{1/2} = 0.18\ \mu\text{m}$$

Then

$$|Q'_{SD}(\max)| = eN_a x_{dT} = (1.6 \times 10^{-19})(3 \times 10^{16})(0.18 \times 10^{-4})$$

or

$$|Q'_{SD}(\max)| = 8.64 \times 10^{-8}\ \text{C/cm}^2$$

The oxide thickness can be determined from the threshold voltage equation

$$V_{TN} = (|Q'_{SD}(\max)| - Q'_{ss})\left(\frac{t_{ox}}{\epsilon_{ox}}\right) + \phi_{ms} + 2\phi_{fp}$$

Then

$$0.65 = \frac{[(8.64 \times 10^{-8}) - (10^{11})(1.6 \times 10^{-19})]}{(3.9)(8.85 \times 10^{-14})} \cdot t_{ox} - 1.13 + 2(0.376)$$

or

$$0.65 = 2.0 \times 10^5 t_{ox} - 0.378$$

which yields

$$t_{ox} = 504\ \text{Å}$$

■ Comment

The threshold voltage for this case is a positive quantity, which means that the MOS device is an enhancement mode device: a gate voltage must be applied to create the inversion layer charge, which is zero for zero applied gate voltage.

The threshold voltage must be within the voltage range of a circuit design. Although we have not yet considered the current in an MOS transistor, the threshold voltage is the point at which the transistor turns on. If a circuit is to operate between 0 and 5 V and the threshold voltage of a MOSFET is 10 V, for example, the device and circuit cannot be turned "on" and "off." The threshold voltage, then, is one of the important parameters of the MOSFET.

EXAMPLE 11.5

Objective

To calculate the threshold voltage of an MOS system using the aluminum gate.

Consider a p-type silicon substrate at T = 300 K doped to $N_a = 10^{14}\ \text{cm}^{-3}$. Let $Q'_{ss} = 10^{10}\ \text{cm}^{-2}$, $t_{ox} = 500$ Å, and assume the oxide is silicon dioxide. From Figure 11.15, we have that $\phi_{ms} = -0.83$ V.

■ Solution

We can start calculating the various parameters as

$$\phi_{fp} = V_t \ln\left(\frac{N_a}{n_i}\right) = (0.0259)\ln\left(\frac{10^{14}}{1.5 \times 10^{10}}\right) = 0.228\ \text{V}$$

and

$$x_{dT} = \left\{\frac{4\epsilon_s\phi_{fp}}{eN_a}\right\}^{1/2} = \left\{\frac{4(11.7)(8.85 \times 10^{-14})(0.228)}{(1.6 \times 10^{-19})(10^{14})}\right\}^{1/2} = 2.43\ \mu\text{m}$$

Then

$$|Q'_{SD}(\max)| = eN_a x_{dT} = (1.6 \times 10^{-19})(10^{14})(2.43 \times 10^{-4}) = 3.89 \times 10^{-9}\ \text{C/cm}^2$$

We can now calculate the threshold voltage as

$$\begin{aligned} V_{TN} &= (|Q'_{SD}(\max)| - Q'_{ss})\left(\frac{t_{ox}}{\epsilon_{ox}}\right) + \phi_{ms} + 2\phi_{fp} \\ &= [(3.89 \times 10^{-9}) - (10^{10})(1.6 \times 10^{-19})]\left[\frac{500 \times 10^{-8}}{(3.9)(8.85 \times 10^{-14})}\right] \\ &\quad - 0.83 + 2(0.228) \\ &= -0.341\ \text{V} \end{aligned}$$

■ **Comment**

In this example, the semiconductor is very lightly doped which, in conjunction with the positive charge in the oxide and the work function potential difference, is sufficient to induce an electron inversion layer charge even with zero applied gate voltage. This condition makes the threshold voltage negative.

A negative threshold voltage for a p-type substrate implies a depletion mode device. A negative voltage must be applied to the gate in order to make the inversion layer charge equal to zero, whereas a positive gate voltage will induce a larger inversion layer charge.

Figure 11.20 is a plot of the threshold voltage V_{TN} as a function of the acceptor doping concentration for various positive oxide charge values. We may note that the p-type semiconductor must be somewhat heavily doped in order to obtain an enhancement mode device.

The previous derivation of the threshold voltage assumed a p-type semiconductor substrate. The same type of derivation can be done with an n-type semiconductor substrate, where a negative gate voltage can induce an inversion layer of holes at the oxide-semiconductor interface.

Figure 11.14 showed the energy-band diagram of the MOS structure with an n-type substrate and with an applied negative gate voltage. The threshold voltage for this case can be derived and is given by

$$\boxed{V_{TP} = (-|Q'_{SD}(\max)| - Q'_{ss})\left(\frac{t_{ox}}{\epsilon_{ox}}\right) + \phi_{ms} - 2\phi_{fn}} \tag{11.28}$$

where

$$\phi_{ms} = \phi'_m - \left(\chi' + \frac{E_g}{2e} - \phi_{fn}\right) \tag{11.29a}$$

$$|Q'_{SD}(\max)| = eN_d x_{dT} \tag{11.29b}$$

$$x_{dT} = \left\{\frac{4\epsilon_s \phi_{fn}}{eN_d}\right\}^{1/2} \tag{11.29c}$$

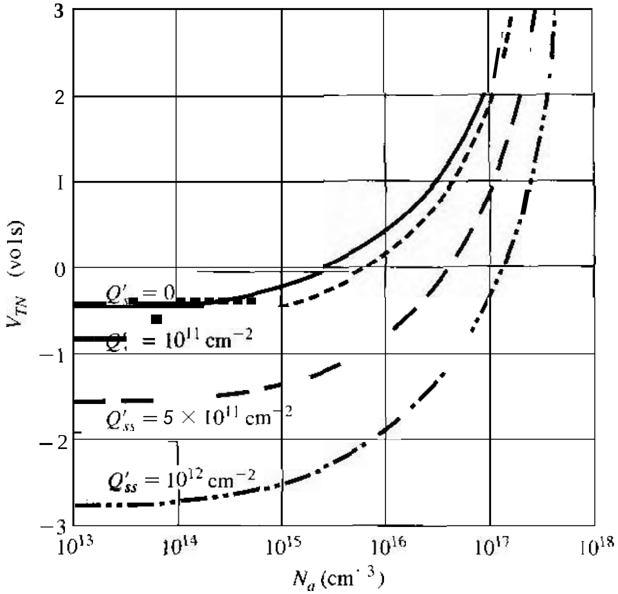

Figure 11.20 | Threshold voltage of an n-channel MOSFET versus the p-type substrate doping concentration for various values of oxide trapped charge ($t_{ox} = 500$ Å, aluminum gate).

and

$$\phi_{fn} = V_t \ln\left(\frac{N_d}{n_i}\right) \tag{11.29d}$$

We may note that x_{dT} and ϕ_{fn} are defined as positive quantities. We may also note that the notation of V_{TP} is the threshold voltage that will induce an inversion layer of holes. We will later drop the N and P subscript notation on the threshold voltage, but, for the moment, the notation may be useful for clarity.

DESIGN EXAMPLE 11.6

Objective

To design the semiconductor doping concentration to yield a specified threshold voltage.

Consider an aluminum–silicon dioxide–silicon MOS structure. The silicon is n type, the oxide thickness is $t_{ox} = 650$ Å, and the trapped charge density is $Q'_{ss} = 10^{10}$ cm^{-2}. Determine the doping concentration such that $V_{TP} = -1.0$ V.

■ Solution

The solution to this design problem is not straightforward, since the doping concentration appears in the terms ϕ_{fn}, x_{dT}, $Q'_{SD}(\max)$ and ϕ_{ms}. The threshold voltage, then, is a nonlinear function of N_d. Without a computer-generated solution, we resort to trial and error.

For $N_d = 2.5 \times 10^{14}\ \mathrm{cm}^{-3}$, we find

$$\phi_{fn} = V_t \ln\left(\frac{N_d}{n_i}\right) = 0.253\ \mathrm{V}$$

and

$$x_{dT} = \left\{\frac{4\epsilon_s \phi_{fn}}{eN_d}\right\}^{1/2} = 1.62\ \mu\mathrm{m}$$

Then

$$|Q'_{SD}(\max)| = eN_d x_{dT} = 6.48 \times 10^{-9}\ \mathrm{C/cm^2}$$

From Figure 11.15,

$$\phi_{ms} = -0.35\ \mathrm{V}$$

The threshold voltage is

$$V_{TP} = (-|Q'_{SD}(\max)| - Q'_{ss})\left(\frac{t_{ox}}{\epsilon_{ox}}\right) + \phi_{ms} - 2\phi_{fn}$$

$$= \frac{[-(6.48 \times 10^{-9}) - (10^{10})(1.6 \times 10^{-19})](650 \times 10^{-8})}{(3.9)(8.85 \times 10^{-14})} - 0.35 - 2(0.253)$$

which yields

$$V_{TP} = -1.008\ \mathrm{V}$$

and is essentially equal to the desired result.

■ Comment

The threshold voltage is negative, implying that this **MOS** capacitor, with the n-type substrate, is an enhancement mode device. The inversion layer charge is zero with zero gate voltage, and a negative gate voltage must be applied to induce the hole inversion layer.

Figure 11.21 is a plot of V_{TP} versus doping concentration for several values of Q'_{ss}. We may note that, for all values of positive oxide charge, this MOS capacitor is always an enhancement mode device. As the Q'_{ss} charge increases, the threshold voltage becomes more negative, which means that it takes a larger applied gate voltage to create the inversion layer of holes at the oxide-semiconductor interface.

11.1.6 Charge Distribution

We've discussed the various charges in the MOS structure. We may gain a better understanding by considering the following figures. The electron concentration in the inversion layer (p-type substrate) at the oxide interface is given by $n_s = (n_i^2/N_a)\exp(\phi_s/V_t)$. For silicon at T = 300 K with an impurity doping concentration of $N_a = 1 \times 10^{16}\ \mathrm{cm}^{-3}$, the surface potential at the threshold inversion point is $\phi_s = 2\phi_{fp} = 0.695$ V. The electron concentration at the oxide interface at this surface potential is just $n_s = 1 \times 10^{16}\ \mathrm{cm}^{-3}$ as we have discussed before. Figure 11.22

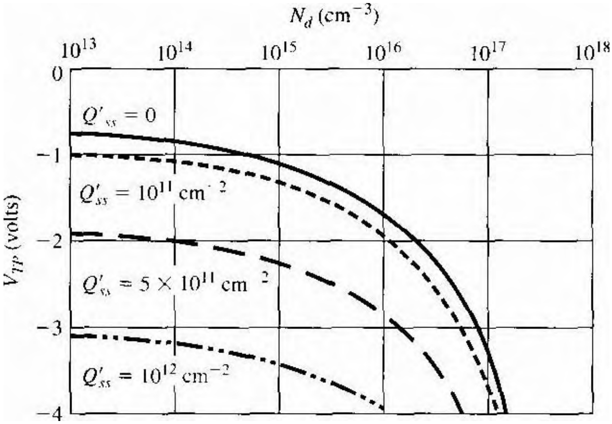

Figure 11.21 | Threshold voltage of a p-channel MOSFET versus the n-type substrate doping concentration for various values of oxide trapped charge ($t_{ox} = 500$ A. aluminum gate).

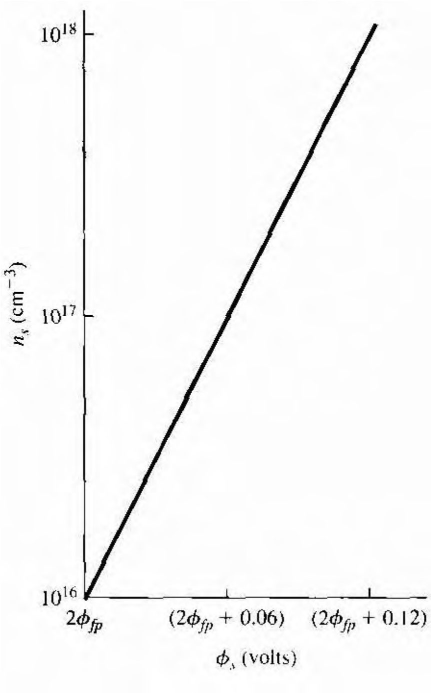

Figure 11.22 **|** Electron inversion charge density as a function of surface potential.

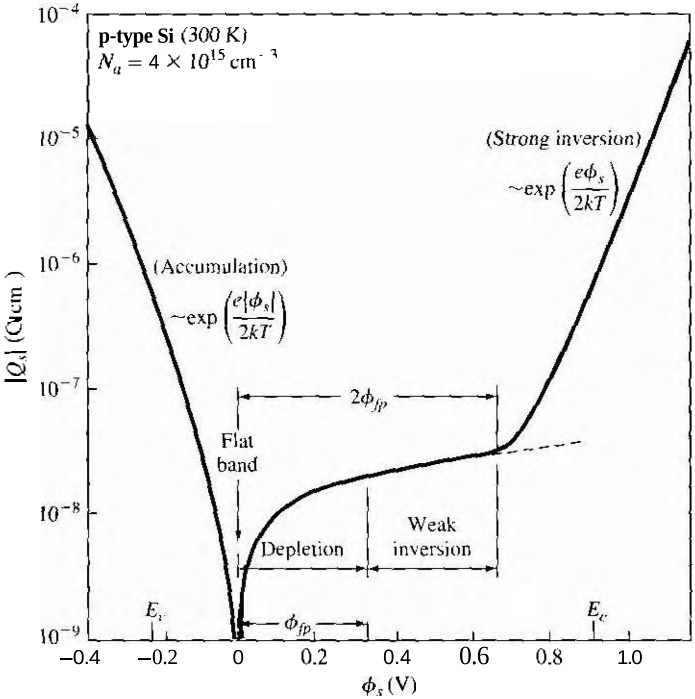

Figure 11.23 | Variation of surface charge density (accumulation charge and inversion charge) as a function of surfece potential.
(From Sze [16].)

shows the increase in electron concentration at the surface with an increase in surface potential. As discussed previously, since the electron concentration increases rapidly with very small changes in surface potential, the space charge width has essentially reached a maximum value.

Figure 11.23 shows the total charge density (C/cm^2) in the silicon as a function of the surface potential. At flat band. the total charge is zero. For $0 \le \phi_s \le \phi_{fp}$, we are operating in the depletion mode since the inversion charge has not yet been formed. For $\phi_{fp} \le \phi_s < 2\phi_{fp}$, the Fermi energy at the surface is in the upper half of the band diagram, which implies an n-type material, but we have not yet reached the threshold inversion point. This condition is referred to as weak inversion. The condition for $\phi_s > 2\phi_{fp}$ is called strong inversion, since the inversion charge density increases rapidly with an increase in surface potential. as we have seen.

TEST YOUR UNDERSTANDING

E11.9 An MOS device has the following parameters: aluminum gate, p-type substrate with $N_a = 3 \times 10^{16}$ cm^{-3}, $t_{ox} = 250$ A. and $Q'_{ss} = 10^{11}$ cm^{-2}. Determine **the** threshold voltage. (Ans. $V_{TN} = +0.281$ V)

E11.10 Consider an MOS device with the following parameters: p^+ polysilicon gate, n-type substrate with $N_d = 10^{15}$ cm^{-3}, $t_{ox} = 220$ Å, and $Q'_{ss} = 8 \times 10^{10}$ cm^{-2}. (Use Figure 11.15). Determine the threshold voltage. (Ans. $V_{TP} = +0.224$ V)

***E11.11** The device described in E11.10 is to be redesigned by changing the n-type doping concentration such that the threshold voltage is in the range $-0.50 \le V_{TP} \le -0.30$ V. (Ans. By trial and error, $V_{TP} = -0.405$ V for $N_d = 4 \times 10^{16}$ cm^{-3})

11.2 | CAPACITANCE–VOLTAGE CHARACTERISTICS

The MOS capacitor structure is the heart of the MOSFET. A great deal of information about the MOS device and the oxide–semiconductor interface can be obtained from the capacitance versus voltage or *C-V* characteristics of the device. The capacitance of a device is defined as

$$C = \frac{dQ}{dV} \tag{11.30}$$

where dQ is the magnitude of the differential change in charge on one plate as a function of the differential change in voltage dV across the capacitor. The capacitance is a small-signal or ac parameter and is measured by superimposing a small ac voltage on an applied dc gate voltage. The capacitance, then, is measured as a function of the applied dc gate voltage.

11.2.1 Ideal C-V Characteristics

First we will consider the ideal *C-V* characteristics of the MOS capacitor and then discuss some of the deviations that occur from these idealized results. We will initially assume that there is zero charge trapped in the oxide and also that there is no charge trapped at the oxide–semiconductor interface.

There are three operating conditions of interest in the MOS capacitor: accumulation, depletion, and inversion. Figure 11.24a shows the energy-band diagram of an MOS capacitor with a p-type substrate for the case when a negative voltage is applied to the gate, inducing an accumulation layer of holes in the semiconductor at the oxide-semiconductor interface. A small differential change in voltage across the MOS structure will cause a differential change in charge on the metal gate and also in the hole accumulation charge, as shown in Figure 11.24b. The differential changes in charge density occur at the edges of the oxide, as in a parallel-plate capacitor. The capacitance C' per unit area of the MOS capacitor for this accumulation mode is just the oxide capacitance, or

$$C'(\text{acc}) = C_{ox} = \frac{\epsilon_{ox}}{t_{ox}} \tag{11.31}$$

Figure 11.25a shows the energy-hand diagram of the MOS device when a small positive voltage is applied to the gate, inducing a space charge region in the semiconductor; Figure 11.25b shows the charge distribution through the device for

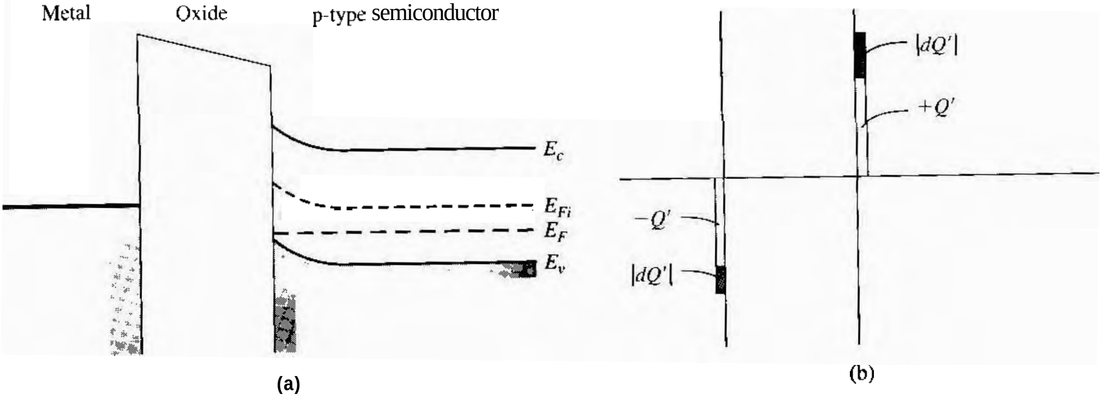
Metal
Oxide
p-type semiconductor
E_c
E_{Fi}
E_F
E_v
(a)
$|dQ'|$
$+Q'$
$-Q'$
$|dQ'|$
(b)

Figure 11.24 | (a) Energy-band diagram through an MOS capacitor for the accumulation mode. (b) Differential charge distribution at accumulation for a differential change in gate voltage.

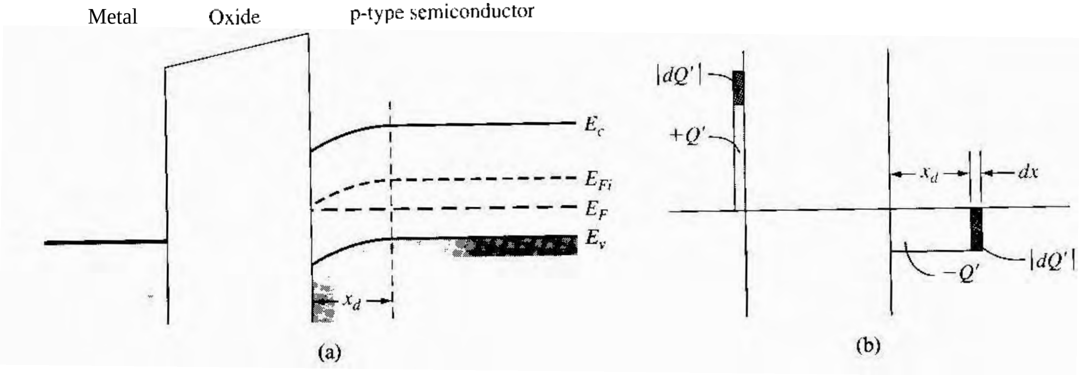
Metal
Oxide
p-type semiconductor
E_c
E_{Fi}
E_F
E_v
x_d
(a)
$|dQ'|$
$+Q'$
x_d
dx
$-Q'$
$|dQ'|$
(b)

Figure 11.25 | (a) Energy-band diagram through an MOS capacitor for the depletion mode. (b) Differential charge distribution at depletion for a differential change in gate voltage.

this condition. The oxide capacitance and the capacitance of the depletion region are in series. A small differential change in voltage across the capacitor will cause a differential change in the space charge width. The corresponding differential changes in charge densities are shown in the figure. The total capacitance of the series combination is

$$\frac{1}{C'(\text{depl})} = \frac{1}{C_{\text{ox}}} + \frac{1}{C'_{SD}} \tag{11.32a}$$

$$C'(\text{depl}) = \frac{C_{\text{ox}} C'_{SD}}{C_{\text{ox}} + C'_{SD}} \tag{11.32b}$$

Since $C_{ox} = \epsilon_{ox}/t_{ox}$ and $C'_{SD} = \epsilon_s/x_d$, Equation (11.32b) **can** be written as

$$C'(\text{depl}) = \frac{C_{ox}}{1 + \dfrac{C_{ox}}{C'_{SD}}} = \frac{\epsilon_{ox}}{t_{ox} + \left(\dfrac{\epsilon_{ox}}{\epsilon_s}\right) x_d} \tag{11.33}$$

As the space charge width increases, the total capacitance $C'(\text{depl})$ decreases.

We had defined the threshold inversion point to he the condition when the maximum depletion width is reached but there is essentially zero inversion charge density. This condition will yield a minimum capacitance $C'_{\min}$ which is given by

$$C'_{\min} = \frac{\epsilon_{ox}}{t_{ox} + \left(\dfrac{\epsilon_{ox}}{\epsilon_s}\right) x_{dT}} \tag{11.34}$$

Figure 11.26a shows the energy-band diagram of this MOS device for the inversion condition. In the ideal case, a small incremental change in the voltage across the MOS capacitor will cause a differential change in the inversion layer charge density The space charge width does not change. If the inversion charge can respond to the change in capacitor voltage as indicated in Figure 11.26b, then the capacitance is again just the oxide capacitance, or

$$C'(\text{inv}) = C_{ox} = \frac{\epsilon_{ox}}{t_{ox}}$$

(11.3

Figure 11.27 shows the ideal capacitance versus gate voltage, or C-V, characteristics of the MOS capacitor with a p-type substrate. The three dashed segments correspond to the three components C_{ox}, C'_{SD}, and $C'_{\min}$. The solid curve is the ideal net capacitance of the MOS capacitor. Moderate inversion, which is indicated in the figure, is the transition region between the point when only the space charge density

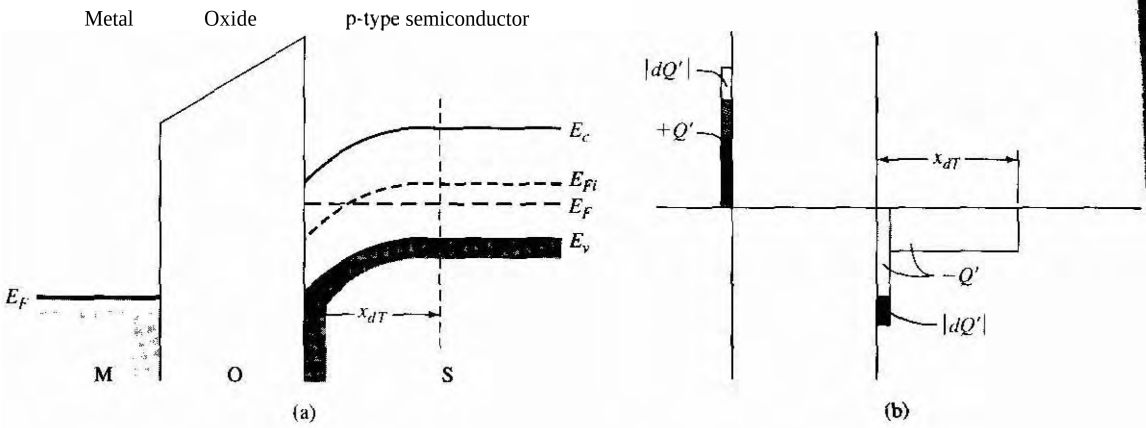

Figure 11.26 | (a) Energy-band diagram through an MOS capacitor for the inversion mode. (b) Differential charge distribution at inversion for a low-frequency differential change in gate voltage.

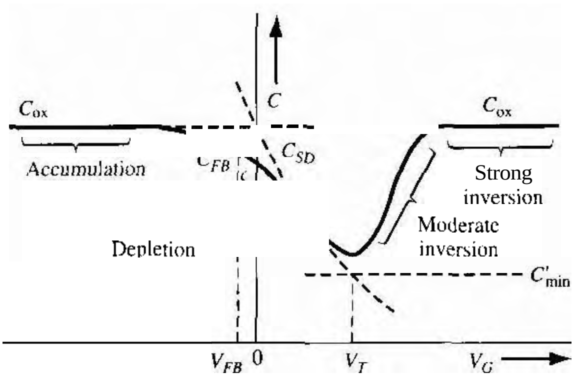

Figure 11.27 | Ideal low-frequency capacitance versus gate voltage of an MOS capacitor with a p-type substrate. Individual capacitance components are also shown.

changes with gate voltage and when only the inversion charge density changes with gate voltage.

The point on the curve that corresponds to the flat-band condition is of interest. The flat-band condition occurs between the accumulation and depletion conditions. The capacitance at flat band is given by

$$\boxed{C'_{FB} = \frac{\epsilon_{ox}}{t_{ox} + \left(\frac{\epsilon_{ox}}{\epsilon_s}\right)\sqrt{\left(\frac{kT}{e}\right)\left(\frac{\epsilon_s}{eN_a}\right)}}} \tag{11.36}$$

We may note that the flat-band capacitance is a function of oxide thickness as well as semiconductor doping. The general location of this point on the C-Vplot is shown in Figure 11.27.

Objective | **EXAMPLE 11.7**

To calculate C_{ox}, C'_{min}, and C'_{FB} for an MOS capacitor.

Consider a p-type silicon substrate at T = 300 K doped to $N_a = 10^{16}$ cm^{-3}. The oxide is silicon dioxide with a thickness of 550 Å and the gate is aluminum.

■ Solution

The oxide capacitance is

$$C_{ox} = \frac{\epsilon_{ox}}{t_{ox}} = \frac{(3.9)(8.85 \times 10^{-14})}{550 \times 10^{-8}} = 6.28 \times 10^{-8} \text{ F/cm}^2$$

To find the minimum capacitance, we need to calculate

$$\phi_{fp} = V_t \ln\left(\frac{N_a}{n_i}\right) = (0.0259) \ln\left(\frac{10^{16}}{1.5 \times 10^{10}}\right) = 0.347 \text{ V}$$

and

$$x_{dT} = \left\{\frac{4\epsilon_s \phi_{fp}}{eN_a}\right\}^{1/2} = \left\{\frac{4(11.7)(8.85 \times 10^{-14})(0.347)}{(1.6 \times 10^{-19})(10^{16})}\right\}^{1/2} = 0.30 \times 10^{-4} \text{ cm}$$

Then

$$C'_{\text{min}} = \frac{\epsilon_{ox}}{t_{ox} + \left(\dfrac{\epsilon_{ox}}{\epsilon_s}\right)x_{dT}} = \frac{(3.9)(8.85 \times 10^{-14})}{(550 \times 10^{-8}) + \left(\dfrac{3.9}{11.7}\right)(0.3 \times 10^{-4})} = 2.23 \times 10^{-8} \text{ F/cm}^2$$

We may note that

$$\frac{C'_{\text{min}}}{C_{ox}} = \frac{2.23 \times 10^{-8}}{6.28 \times 10^{-8}} = 0.355$$

The flat-band capacitance is

$$C'_{FB} = \frac{\epsilon_{ox}}{t_{ox} + \left(\dfrac{\epsilon_{ox}}{\epsilon_s}\right)\sqrt{\left(\dfrac{kT}{e}\right)\left(\dfrac{\epsilon_s}{eN_a}\right)}}$$

$$= \frac{(3.9)(8.85 \times 10^{-14})}{(550 \times 10^{-8}) + \left(\dfrac{3.9}{11.7}\right)\sqrt{(0.0259)\dfrac{(11.7)(8.85 \times 10^{-14})}{(1.6 \times 10^{-19})(10^{16})}}}$$

$$= 5.03 \times 10^{-8} \text{ F/cm}^2$$

We may also note that

$$\frac{C'_{FB}}{C_{ox}} = \frac{5.03 \times 10^{-8}}{6.28 \times 10^{-8}} = 0.80$$

■ Comment

The ratios of C'_{min} to C_{ox} and of C'_{FB} to C_{ox} are typical values obtained in C-V plots

---

TEST YOUR UNDERSTANDING

E11.12 For the device described in E11.9, determine C'_{min}/C_{ox} and C'_{FB}/C_{ox}. (Ans. $C'_{\text{min}}/C_{ox} = 0.294$, $C'_{FB}/C_{ox} = 0.736$)

Typical values of channel length and width are 2 μm and 20 μm, respectively. The total gate oxide capacitance for this example is then

$$C_{oxT} = (6.28 \times 10^{-8})(2 \times 10^{-4})(20 \times 10^{-4}) = 0.025 \times 10^{-12} \text{ F} = 0.025 \text{ pF}$$

The total oxide capacitance in a typical MOS device is quite small.

The same type of ideal C-V characteristics are obtained for an MOS capacitor with an n-type substrate by changing the sign of the voltage axis. The accumulation

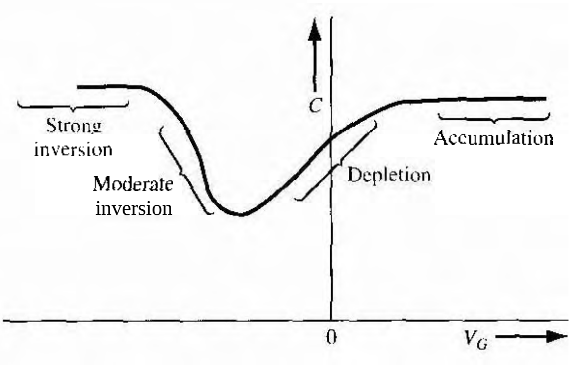

Figure 11.28 | Ideal low-frequency capacitance versus gate voltage of an MOS capacitor with an n-type substrate.

condition is obtained for a positive gate bias and the inversion condition is obtained for a negative gate bias. This ideal curve is shown in Figure 11.28.

11.2.2 Frequency Effects

Figure 11.26a showed the MOS capacitor with a p-type substrate and biased in the inversion condition. We have argued that a differential change in the capacitor voltage in the ideal case causes a differential change in the inversion layer charge density. However, we must consider the source of electrons that produces a change in the inversion charge density.

There are two sources of electrons that can change the charge density of the inversion layer. The first source is by diffusion of minority carrier electrons **from** the p-type substrate across the space charge region. This diffusion process is the same as that in a reverse-biased pn junction that generates the ideal reverse saturation current. The second source of electrons is by thermal generation of electron-hole pairs within the space charge region. This process is again the same as that in a reverse-biased pn junction generating the reverse-biased generation current. Both of these processes generate electrons at **a** particular rate. The electron concentration in the inversion layer. then, cannot change instantaneously. If the ac voltage across the MOS capacitor changes rapidly, the change in the inversion layer charge will not be able to respond. The C-V characteristics will then be a function of the frequency of the ac signal used to measure the capacitance.

In the limit of a very high frequency, the inversion layer charge will not respond to a differential change in capacitor voltage. Figure 11.29 shows the charge distribution in the MOS capacitor with ap-type substrate. At a high-signal frequency, the differential change in charge occurs at the metal and in the space charge width in the semiconductor. The capacitance of the MOS capacitor is then $C'_{\min}$, which we discussed earlier.

The high-frequency and low-frequency limits of the C-V characteristics are shown in Figure 11.30. In general, high frequency corresponds to a value on the order

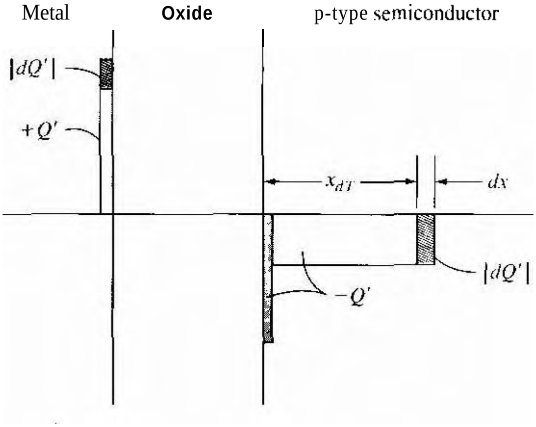

Figure 11.29 | Differential charge distribution at inversion for a high-frequency differential change in gate voltage.

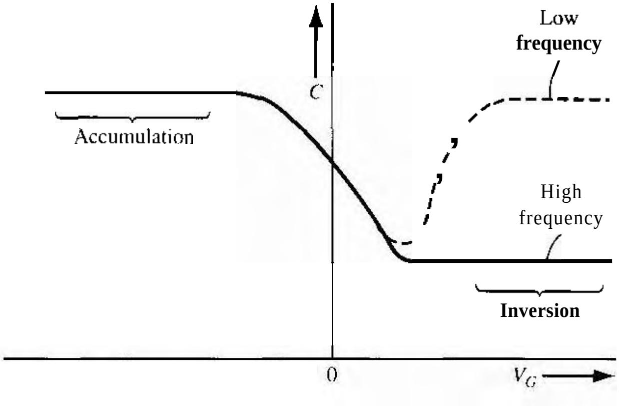

Figure **11.30** | Low-frequency and high-frequency capacitance versus gate voltage of an MOS capacitor with a p-type substrate.

of 1 MHz and low frequency corresponds to values in the range of 5 to 100 Hz. Typically, the high-frequency characteristics of the MOS capacitor are measured.

11.2.3 Fixed Oxide and Interface Charge Effects

In all of the discussion concerning C-V characteristics so far, we have assumed an ideal oxide in which there are no fixed oxide or oxide-semiconductor interface charges. These two types of charges will change the C-V characteristics.

We previously discussed how the fixed oxide charge affects the threshold voltage. This charge will also affect the flat-band voltage. The flat-band voltage from

Equation (11.21) was given by

$$V_{FB} = \phi_{ms} - \frac{Q'_{ss}}{C_{ox}}$$

where Q'_{ss} is the equivalent fixed oxide charge and ϕ_{ms} is the metal–semiconductor work function difference. The flat-band voltage shifts to more negative voltages for a positive fixed oxide charge. Since the oxide charge is not a function of gate voltage, the curves show a parallel shift with oxide charge. and the shape of the C-V curves remains the same as the ideal characteristics. Figure 11.31 shows the high-frequency characteristics of an MOS capacitor with a p-type substrate for several values of fixed positive oxide charge.

The C-V characteristics can be used to determine the equivalent fixed oxide charge. For a given MOS structure, ϕ_{ms} and C_{ox} are known, so the ideal flat-band voltage and flat-band capacitance can be calculated. The experimental value of flat-band voltage can be measured from the C-V curve and the value of fixed oxide charge can then be determined. The C-V measurements are a valuable diagnostic tool to characterize an MOS device. This characterization is especially useful in the study of radiation effects on MOS devices, for example, which we will discuss in the next chapter.

We first encountered oxide–semiconductor interface states in Chapter 9 in the discussion of Schottky barrier diodes. Figure 11.32 shows the energy-band diagram of a semiconductor at the oxide-semiconductor interface. The periodic nature of the semiconductor is abruptly terminated at the interface so that allowed electronic energy levels will exist within the forbidden bandgap. These allowed energy states are referred to as interface states. Charge can flow between the semiconductor and interface states, in contrast to the fixed oxide charge. The net charge in these interface states is a function of the position of the Fermi level in the bandgap.

In general, acceptor states exist in the upper half of the bandgap and donor states exist in the lower half of the bandgap. An acceptor state is neutral if the Fermi level

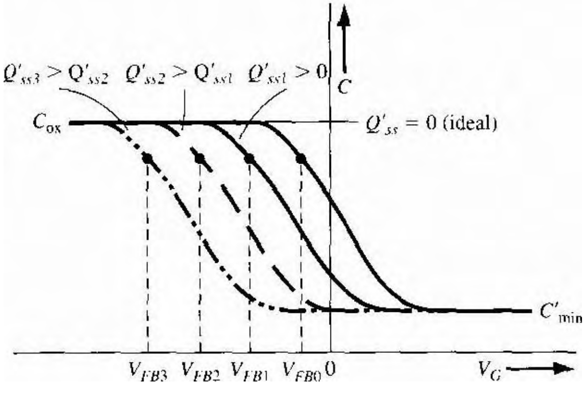

Figure 11.31 | High-frequency capacitance versus gate voltage of an MOS capacitor with a p-type substrate for several values of effective trapped oxide charge.

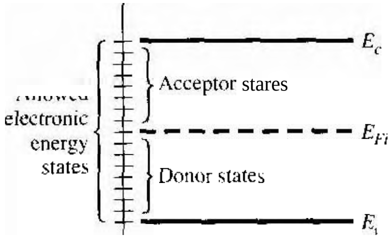

Figure 11.32 | Schematic diagram showing interface states at the oxide-semiconductor interface.

is below the state, and becomes negatively charged if the Fermi level is above the state. A donor state is neutral if the Fermi level is above the state and becomes positively charged if the Fermi level is below the state. The charge of the interface states is then a function of the gate voltage applied across the MOS capacitor.

Figure 11.33a shows the energy-band diagram in a p-type semiconductor of an MOS capacitor biased in the accumulation condition. In this case, there is a net positive charge trapped in the donor states. Now let the gate voltage change to produce the energy-band diagram shown in Figure 11.33b. The Fermi level corresponds to the intrinsic Fermi level at the surface; thus, all interface states are neutral. This

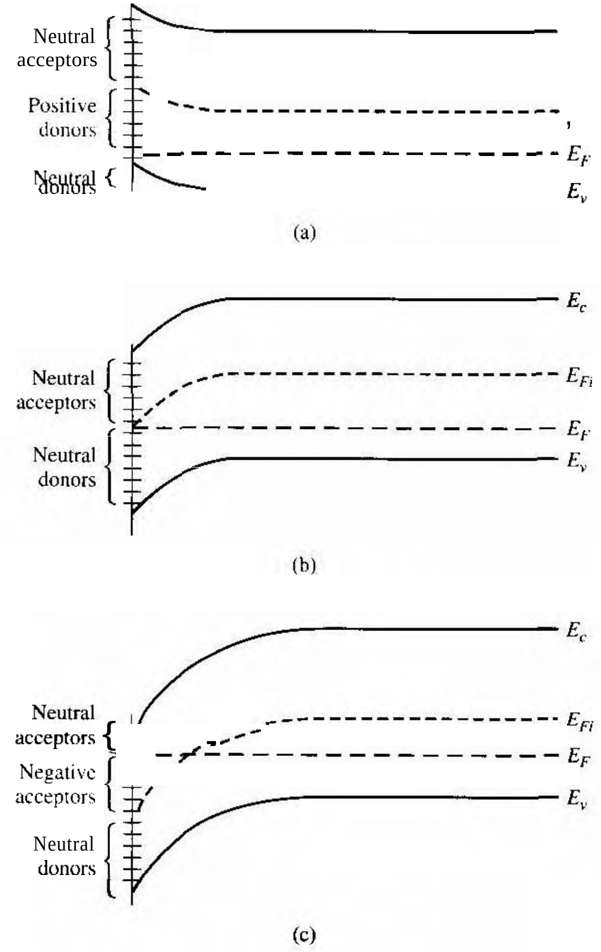
Neutral acceptors
Positive donors
Neutral donors
E_F
E_v
(a)
E_c
Neutral acceptors
E_{Fi}
E_F
Neutral donors
E_v
(b)
E_c
Neutral acceptors
E_{Fi}
E_F
Negative acceptors
E_v
Neutral donors
(c)

Figure **11.33** | Energy-band diagram in a p-type semiconductor showing the charge trapped in the interface states when the MOS capacitor is biased (a) in accumulation, (b) at midgap, and (c) at inversion.

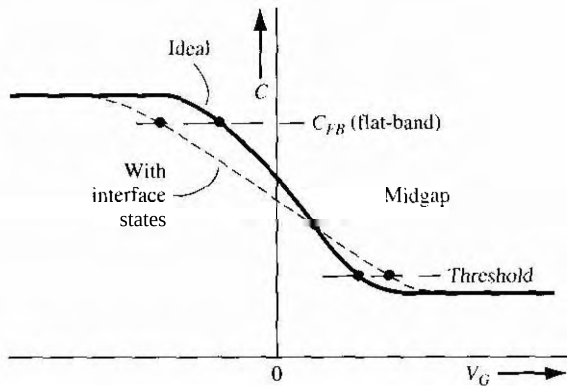

Figure 11.34 | High-frequency C-V characteristics of an MOS capacitor showing effects of interface states.

particular bias condition is known as *midgap*. Figure 11.33c shows the condition at inversion in which there is now a net negative charge in the acceptor states.

The net charge in the interface states changes from positive to negative as the gate voltage sweeps from the accumulation, depletion, to the inversion condition. We noted that the C-Vcurves shifted in the negative gate voltage direction due to positive fixed oxide charge. When interface states are present, the amount and direction of the shift changes as we sweep through the gate voltage, since the amount and sign of the interface trapped charge changes. The C-V curves now become "smeared out" as shown in Figure 11.34.

Again, the C-V measurements can be used as a diagnostic tool in semiconductor device process control. For a given MOS device, the ideal C-V curve can be determined. Any "smearing out" in the experimental curve indicates the presence of interface states and any parallel shift indicates the presence of fixed oxide charge. The amount of smearing out can be used to determine the density of interface states. These types of measurement are extremely useful in the study of radiation effects on MOS devices, which we will consider in the next chapter.

11.3 | THE BASIC MOSFET OPERATION

The current in an MOS field-effect transistor is due to the flow of charge in the inversion layer or channel region adjacent to the oxide-semiconductor interface. We have discussed the creation of the inversion layer charge in enhancement-type MOS capacitors. We may also have depletion-type devices in which a channel already exists at zero gate voltage.

11.3.1 MOSFET Structures

There are four basic MOSFET device types. Figure 11.35 shows an n-channel enhancement mode MOSFET. Implicit in the enhancement mode notation is the idea that the semiconductor substrate is not inverted directly under the oxide with zero gate voltage. A positive gate voltage induces the electron inversion layer, which then "connects" the n-type source and the n-type drain regions. The source terminal is the source of carriers that flow through the channel to the drain terminal. For this n-channel device, electrons flow from the source to the drain so the conventional current will enter the drain and leave the source. The conventional circuit symbol for this n-channel enhancement mode device is also shown in this figure.

Figure 11.36 shows an n-channel depletion mode MOSFET. An n-channel region exists under the oxide with zero volts applied to the gate. However, we have shown that the threshold voltage of an MOS device with a p-type substrate may be

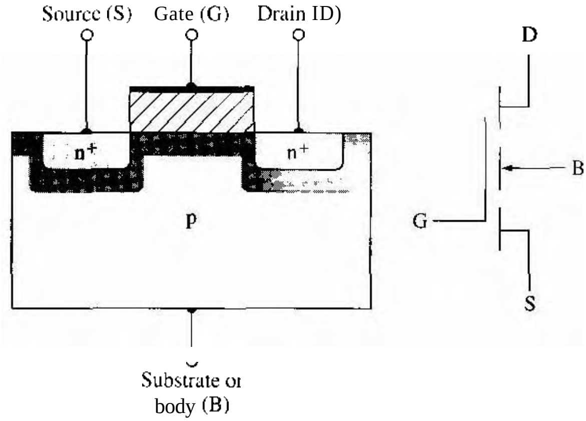

Figure 11.35 | Cross section and circuit symbol for an n-channel enhancement-mode MOSFET.

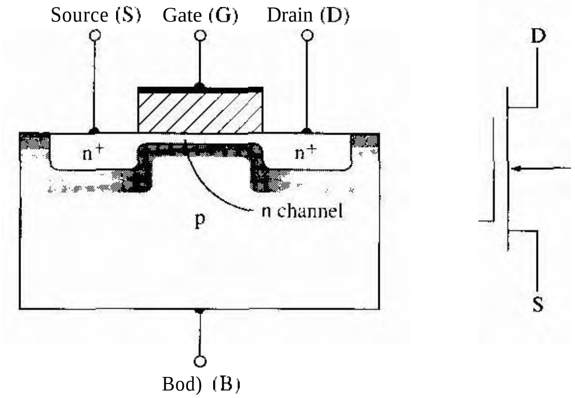

Figure 11.36 | Cross section and circuit symbol for an n-channel depletion-mode MOSFET.

negative; this means that an electron inversion layer already exists with zero gate voltage applied. Such a device is also considered to be a depletion mode device. The n-channel shown in this figure can be an electron inversion layer or an intentionally doped n-region. The conventional circuit symbol for the n-channel depletion mode MOSFET is also shown in the figure.

Figures 11.37a and 11.37b show a p-channel enhancement mode MOSFET and a p-channel depletion mode MOSFET. In the p-channel enhancement mode device, a negative gate voltage must be applied to create an inversion layer of holes that will "connect" the p-type source and drain regions. Holes flow from the source to the drain, so the conventional current will enter the source and leave the drain. A p-channel region exists in the depletion mode device even with zero gate voltage. The conventional circuit symbols are shown in the figure.

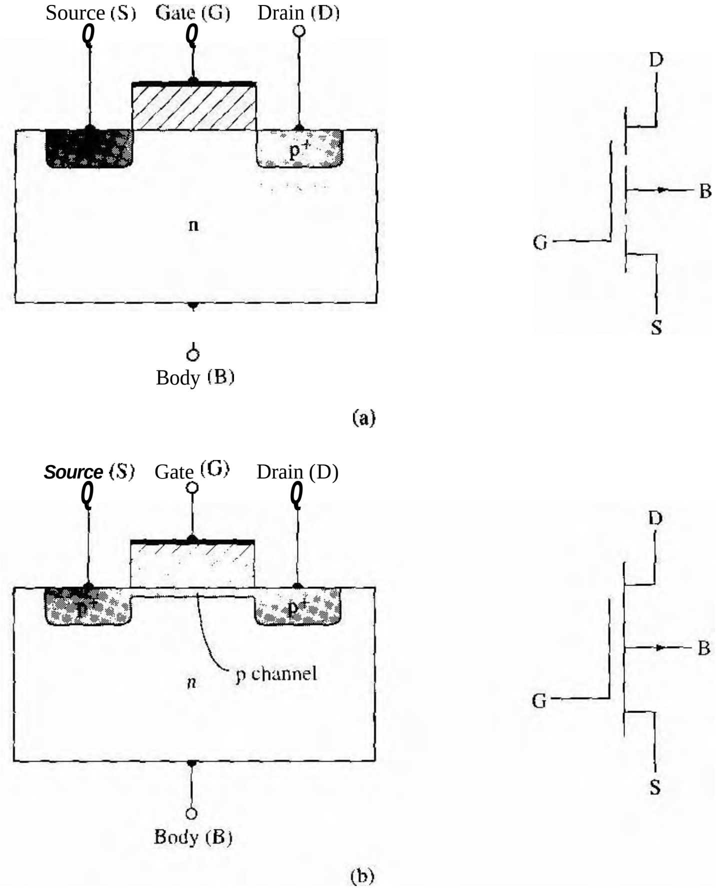

Figure 11.37 | Cross section and circuit symbol for (a) a p-channel enhancement mode MOSFET and (b) a p-channel depletion mode MOSFET

11.3.2 Current–Voltage Relationship—Concepts

Figure 11.38a shows **an** n-channel enhancement mode MOSFET with a gate-to source voltage that is less than the threshold voltage and with only a very smal drain-to-source voltage. The source and substrate, or body, terminals are held a ground potential. With this bias configuration, there is no electron inversion laye the drain-to-substrate pn junction is reverse biased, and the drain current is zero (disregarding pn junction leakage currents).

Figure 11.38b shows the same MOSFET with an applied gate voltage such tha $V_{GS} > V_T$. An electron inversion layer has been created so that, when a small drain voltage is applied, the electrons in the inversion layer will flow from the source to the positive drain terminal. The conventional current enters the drain terminal and leaves the source terminal. In this ideal case, there is no current through the oxide to the gate terminal.

For small V_{DS} values, the channel region has the characteristics of a resistor, so we can write

$$I_D = g_d V_{DS} \tag{11.37}$$

where g_d is defined as the channel conductance in the limit as $V_{DS} \rightarrow 0$. The channel conductance is given by

$$g_d = \frac{W}{L} \cdot \mu_n |Q'_n| \tag{11.38}$$

where μ_n is the mobility of the electrons in the inversion layer and $|Q'_n|$ is the magnitude of the inversion layer charge per unit area. The inversion layer charge is a function of the gate voltage; thus, the basic MOS transistor action is the modulation of the channel conductance by the gate voltage. The channel conductance, in turn determines the drain current. We will initially assume that the mobility is a constant; we will discuss mobility effects and variations in the next chapter.

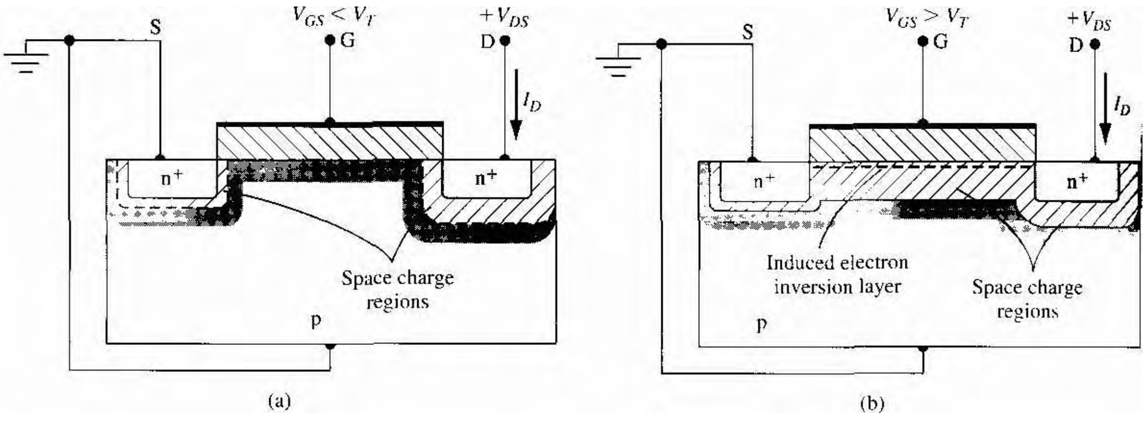

(a)

(b)

Figure 11.38 | The n-channel enhancement mode MOSFET (a) **with** an applied gate voltage $V_{GS} < V_T$, and (b) with an applied gate voltage $V_{GS} > V_T$.

The I_D versus V_{DS} characteristics, for small values of V_{DS}, are shown in Figure 11.39. When $V_{GS} < V_T$, the drain current is zero. As V_{GS} becomes larger than V_T, channel inversion charge density increases, which increases the channel conductance. A larger value of g_d produces a larger initial slope of the I_D versus V_{DS} characteristic as shown in the figure.

Figure 11.40a shows the basic MOS structure for the case when $V_{GS} > V_T$ and the applied V_{DS} voltage is small. The thickness of the inversion channel layer in the figure qualitatively indicates the relative charge density, which is essentially constant along the entire channel length for this case. The corresponding I_D versus V_{DS} curve is shown in the figure.

Figure 11.40b shows the situation when the V_{DS} value increases. As the drain voltage increases, the voltage drop across the oxide near the drain terminal decreases, which means that the induced inversion charge density near the drain also decreases. The incremental conductance of the channel at the drain decreases, which then means that the slope of the I_D versus V_{DS} curve will decrease. This effect is shown in the I_D versus V_{DS} curve in the figure.

When V_{DS} increases to the point where the potential drop across the oxide at the drain terminal is equal to V_T, the induced inversion charge density is zero at the drain terminal. This effect is schematically shown in Figure 11.40c. At this point, the incremental conductance at the drain is zero, which means that the slope of the I_D versus V_{DS} curve is zero. We can write

$$V_{GS} - V_{DS}(\text{sat}) = V_T \tag{11.39a}$$

or

$$\boxed{V_{DS}(\text{sat}) = V_{GS} - V_T} \tag{11.39b}$$

where $V_{DS}(\text{sat})$ is the drain-to-source voltage producing zero inversion charge density at the drain terminal.

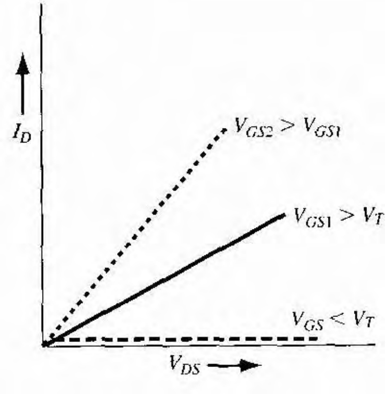

Figure 11.39 | I_D versus V_{DS} characteristics for small values of V_{DS} at three V_{GS} voltages.

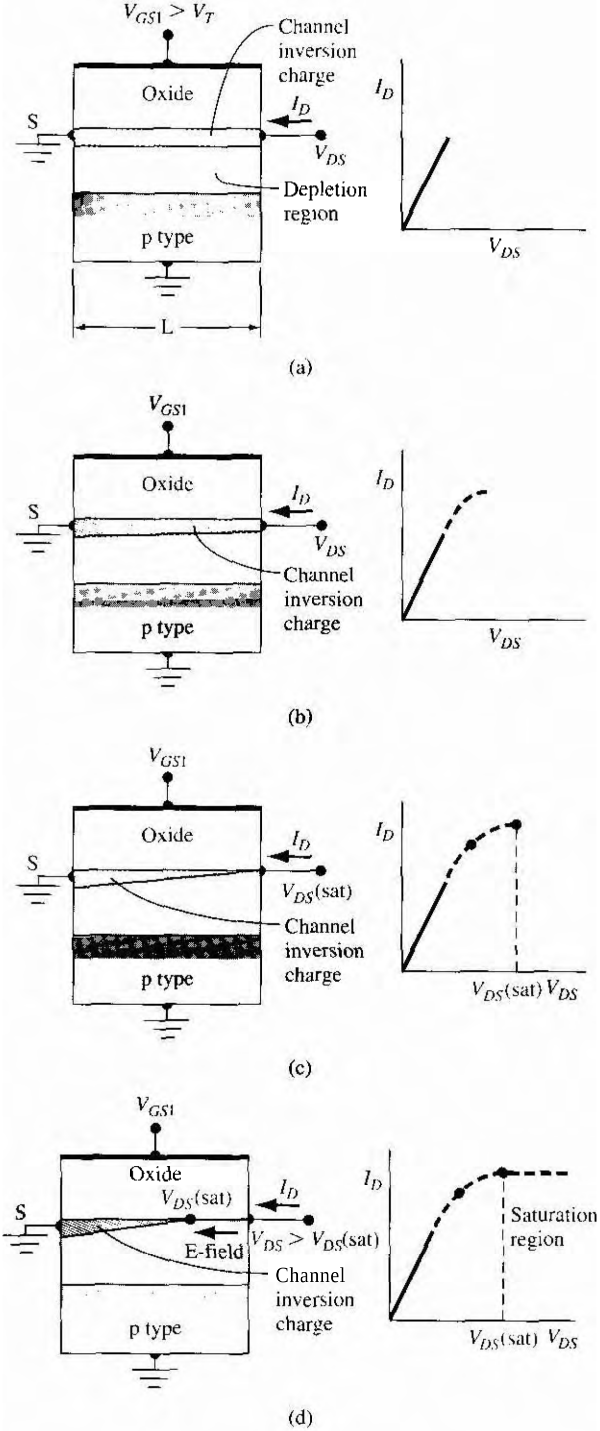
$V_{GS1} > V_T$
Channel inversion charge
Oxide
S
I_D
V_{DS}
Depletion region
p type
L
I_D
V_{DS}
(a)
V_{GS1}
Oxide
S
I_D
V_{DS}
Channel inversion charge
p type
I_D
V_{DS}
(b)
V_{GS1}
Oxide
S
I_D
V_{DS}(sat)
Channel inversion charge
p type
I_D
V_{DS}(sat) V_{DS}
(c)
V_{GS1}
Oxide
V_{DS}(sat)
S
I_D
E-field
$V_{DS} > V_{DS}$(sat)
Channel inversion charge
p type
I_D
Saturation region
V_{DS}(sat) V_{DS}
(d)

Figure 11.40 | Cross section and I_D versus V_{DS} curve when $V_{GS} < V_T$ for (a) a small V_{DS} value, (b) a larger V_{DS} value, (c) a value of $V_{DS} = V_{DS}(\text{sat})$, and (d) a value of $V_{DS} > V_{DS}(\text{sat})$.

When V_{DS} becomes larger than the $V_{DS}(\text{sat})$ value, the point in the channel at which the inversion charge is just zero moves toward the source terminal. In this case, electrons enter the channel at the source, travel through the channel toward the drain, and then, at the point where the charge goes to zero, the electrons are injected into the space charge region where they are swept by the E-field to the drain contact. If we assume that the change in channel length ΔL is small compared to the original length L, then the drain current will be a constant for $V_{DS} > V_{DS}(\text{sat})$. The region of the I_D versus V_{DS} characteristic is referred to as the ***saturation region.*** Figure 11.40d shows this region of operation.

When V_{GS} changes, the I_D versus V_{DS} curve will change. We saw that, if V_{GS} increases, the initial slope of I_D versus V_{DS} increases. We can also note from Equation (11.39b) that the value of $V_{DS}(\text{sat})$ is a function of V_{GS}. We can generate the family of curves for this n-channel enhancement mode MOSFET as shown in Figure 11.41.

Figure 11.42 shows an n-channel depletion mode MOSFET. If the n-channel region is actually an induced electron inversion layer created by the metal–semiconductor work function difference and fixed charge in the oxide, the current–voltage characteristics are exactly the same as we have discussed, except that V_T is a negative quantity. We may also consider the case when the n-channel region is actually an n-type semiconductor region. In this type of device, a negative gate voltage will induce a space charge region under the oxide, reducing the thickness of the n-channel region. The reduced thickness decreases the channel conductance, which reduces the drain current. A positive gate voltage will create an electron accumulation layer, which increases the drain current. One basic requirement for this device is that the channel thickness t_c must be less than the maximum induced space charge width in order to be able to turn the device off. The general I_D versus V_{DS} family of curves for an n-channel depletion mode MOSFET is shown in Figure 11.43.

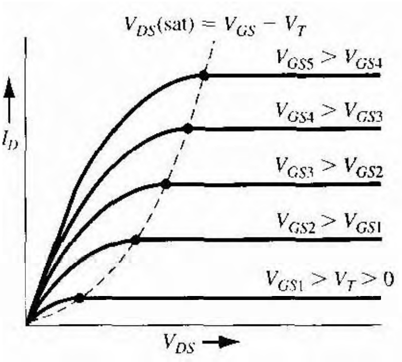

Figure 11.41 | Family of I_D versus V_{DS} curves for an n-channel enhancement-**mode** MOSFET.

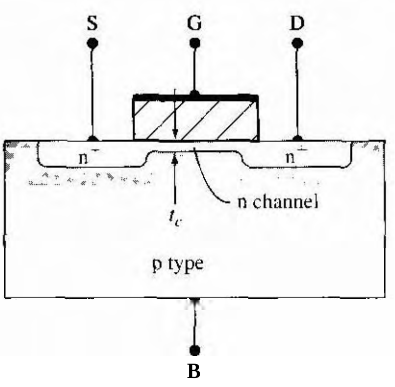

Figure 11.42 | Cross section of an n-channel depletion-mode MOSFET,

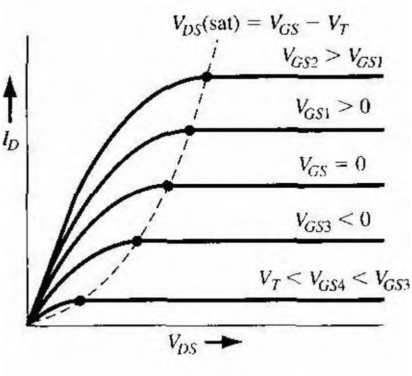

Figure 11.43 | Family of I_D versus V_{DS} curves for an n-channel depletion-mode MOSFET.

In the next section we will derive the ideal current–voltage relation for the n-channel MOSFET. In the nonsaturation region, we will obtain

$$\boxed{I_D = \frac{W\mu_n C_{\text{ox}}}{2L}\left[2(V_{GS} - V_T)V_{DS} - V_{DS}^2\right]} \tag{11.40}$$

and, in the saturation region, we will have

$$\boxed{I_D = \frac{W\mu_n C_{\text{ox}}}{2L}(V_{GS} - V_T)^2} \tag{11.41}$$

The operation of a p-channel device is the same as that of the n-channel device. except the charge carrier is the hole and the conventional current direction and voltage polarities are reversed.

*11.3.3 Current–Voltage Relationship—Mathematical Derivation

In the previous section, we qualitatively discussed the current–voltage characteristics. In this section, we will derive the mathematical relation between the drain current, the gate-to-source voltage, and the drain-to-source voltage. Figure 11.44 shows the geometry of the device that we will use in this derivation.

In this analysis, we will make the following assumptions:

1. The current in the channel is due to drift rather than diffusion.
2. There is no current through the gate oxide.
3. A gradual channel approximation is used in which $\partial E_y/\partial y \gg \partial E_x/\partial x$. This approximation means that E_x is essentially a constant.
4. Any fixed oxide charge is an equivalent charge density at the oxide-semiconductor interface.
5. The carrier mobility in the channel is constant.

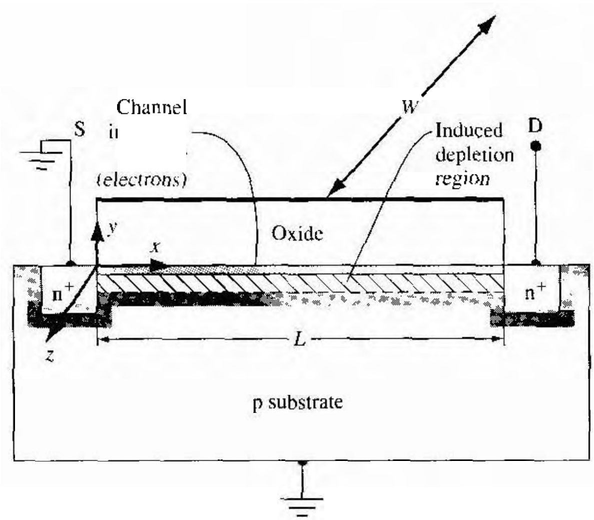

Figure 11.44 | Geometry of a MOSFET for I_D versus V_{DS} derivation.

We start the analysis with Ohm's law, which can be written as

$$J_x = \sigma E_x \tag{11.42}$$

where σ is the channel conductivity and E_x is the electric field along the channel created by the drain-to-source voltage. The channel conductivity is given by $\sigma = e\mu_n n(y)$ where μ_n is the electron mobility and $n(y)$ is the electron concentration in the inversion layer.

The total channel current is found by integrating J_x over the cross-sectional area in the y- and z-directions. Then

$$I_x = \int_y \int_z J_x \, dy \, dz \tag{11.43}$$

We may write that

$$Q'_n = -\int en(y) \, dy \tag{11.44}$$

where Q'_n is the inversion layer charge per unit area and is a negative quantity for this case.

Equation (11.43) then becomes

$$I_x = -W\mu_n Q'_n E_x \tag{11.45}$$

where W is the channel width, the result of integrating over z.

Two concepts we will use in the current-voltage derivation are charge neutrality and Gauss's law. Figure 11.45 shows the charge densities through the device for $V_{GS} > V_T$. The charges are all given in terms of charge per unit area. Using the

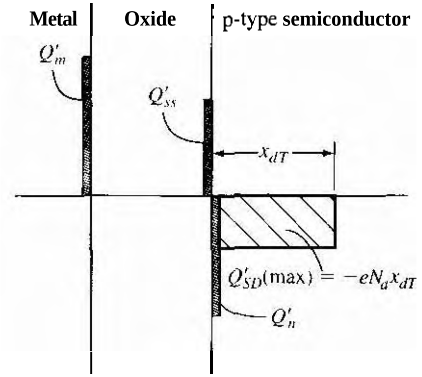
Metal
Oxide
p-type semiconductor
Q'_m
Q'_{ss}
x_{dT}
$Q'_{SD}(\text{max}) = -eN_a x_{dT}$
Q'_n

Figure 11.45 | Charge distribution in the n-channel enhancement mode MOSFET for $V_{GS} > V_T$.

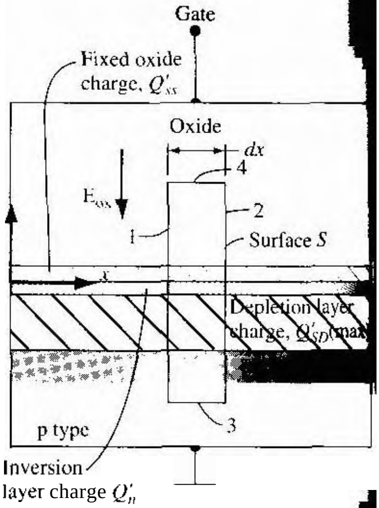
Gate
Fixed oxide charge, Q'_{ss}
Oxide
dx
4
E_{ox}
2
1
Surface S
x
Depletion layer charge, $Q'_{SD}(\text{max})$
p type
3
Inversion layer charge Q'_n

Figure 11.46 | Geometry for applying Gauss's law.

concept of charge neutrality, we can write

$$Q'_m + Q'_{ss} + Q'_n + Q'_{SD}(\text{max}) = 0 \tag{11.46}$$

The inversion layer charge and induced space charge will be negative for this n-channel device.

Gauss's law can be written as

$$\oint_S \epsilon \mathrm{E}_n \, dS = Q_T \tag{11.47}$$

where the integral is over a closed surface. Q_T is the total charge enclosed by the surface, and E_n is the outward directed normal component of the electric field crossing the surface S. Gauss's law will be applied to the surface defined in Figure 11.46. Since the surface must be enclosed, we must take into account the two end surfaces in the x-y plane. However, there is no z-component of the electric field so these two end surfaces do not contribute to the integral of Equation (11.47).

Now consider the surfaces labeled 1 and 2 in Figure 11.46. From the gradual channel approximation, we will assume that E_x is essentially a constant along the channel length. This assumption means that E_x into surface 2 is the same as E_x out of surface 1. Since the integral in Equation (11.47) involves the outward component of the E-field, the contributions of surfaces 1 and 2 cancel each other. Surface 3 is in the neutral p-region, so the electric field is zero at this surface.

Surface 4 is the only surface that contributes to Equation (11.47). Taking into account the direction of the electric field in the oxide, Equation (11.47) becomes

$$\oint_S \epsilon \mathrm{E}_n \, dS = -\epsilon_{ox} \mathrm{E}_{ox} W \, dx = Q_T \tag{11.48}$$

where ϵ_{ox} is the permittivity of the oxide. The total charge enclosed is

$$Q_T = (Q'_{ss} + Q'_n + Q'_{SD}(\max))W\,dx \tag{11.49}$$

Combining Equations (11.48) and (11.49), we have

$$-\epsilon_{ox}\mathrm{E}_{ox} = Q'_{ss} + Q'_n + Q'_{SD}(\max) \tag{11.50}$$

We now need an expression for E_{ox}. Figure 11.47a shows the oxide and channel. We will assume that the source is at ground potential. The voltage V_x is the potential in the channel at a point x along the channel length. The potential difference across the oxide at x is a function of V_{GS}, V_x, and the metal-semiconductor work function difference.

The energy-band diagram through the MOS structure at point x is shown in Figure 11.47b. The Fermi level in the p-type semiconductor is E_{Fp} and the Fermi level in the metal is E_{Fm}. We have

$$E_{Fp} - E_{Fm} = e(V_{GS} - V_x) \tag{11.51}$$

Considering the potential barriers, we can write

$$V_{GS} - V_x = (\phi'_m + V_{ox}) - \left(\chi' + \frac{E_g}{2e} - \phi_s + \phi_{fp}\right) \tag{11.52}$$

which can also be written as

$$V_{GS} - V_x = V_{ox} + 2\phi_{fp} + \phi_{ms} \tag{11.53}$$

where ϕ_{ms} is the metal–semiconductor work function difference, and $\phi_s = 2\phi_{fp}$ for the inversion condition.

The electric field in the oxide is

$$\mathrm{E}_{ox} = \frac{V_{ox}}{t_{ox}} \tag{11.54}$$

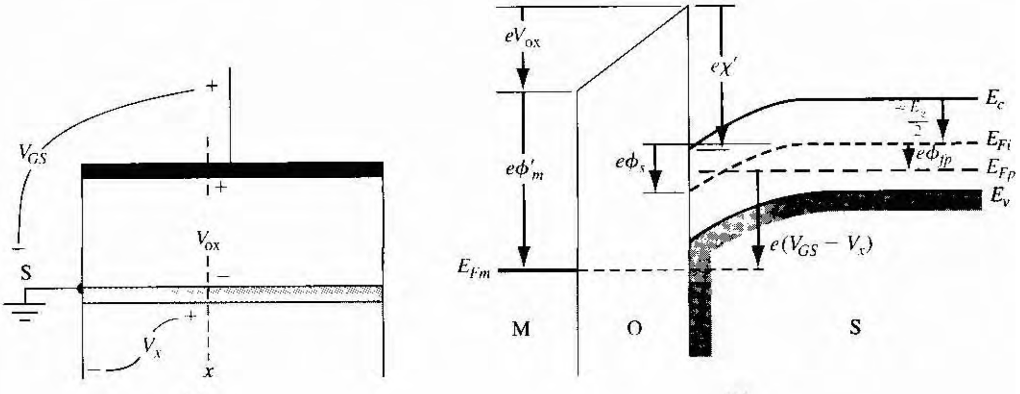

(a) (b)

Figure 11.47 | (a) Potentials at a point x along the channel. (b) Energy-band diagram through the MOS structure at the point x.

Combining Equations (11.50), (11.53). and (11.54), we find that

$$-\epsilon_{ox}E_{ox} = -\frac{\epsilon_{ox}}{t_{ox}}[(V_{GS} - V_x) - (\phi_{ms} + 2\phi_{fp})]$$

$$= Q'_{ss} + Q'_n + Q'_{SD}(\max) \tag{11.55}$$

The inversion charge density, Q'_n, from Equation (11.55) can he substituted into Equation (11.45) and we obtain

$$= -W\mu_n C_{ox}\frac{dV_x}{dx}[(V_{GS} \quad V_x) \quad V_T] \tag{11.56}$$

where $E_x = -dV_x/dx$ and V_T is the threshold voltage defined by Equation (11.27).

We can now integrate Equation (11.56) over the length of the channel. We have;

$$\int_0^L I_x\,dx = -W\mu_n C_{ox}\int_{V_x(0)}^{V_x(L)} [(V_{GS} - V_T) - V_x]\,dV_x \tag{11.57}$$

We are assuming a constant mobility μ_n. For the n-channel device, the drain current enters the drain terminal and is a constant along the entire channel length. Letting $I_D = -I_x$, Equation (11.57) becomes

$$I_D = \frac{W\mu_n C_{ox}}{2L}\left[2(V_{GS} - V_T)V_{DS} - V_{DS}^2\right] \tag{11.58}$$

Equation (11.58) is valid for $V_{GS} \geq V_T$ and for $0 \leq V_{DS} \leq V_{DS}(\text{sat})$.

Figure 11.48 shows plots of Equation (11.58) as a function of V_{DS} for several values of V_{GS}. We can find the value of V_{DS} at the peak current value from $\partial I_D/\partial V_{DS} = 0$. Then, using Equation (11.58), the peak current occurs when

$$V_{DS} = V_{GS} - V_T \tag{11.59}$$

This value of V_{DS} is just $V_{DS}(\text{sat})$, the point at which saturation occurs. For $V_{DS} > V_{DS}(\text{sat})$, the ideal drain current is a constant and is equal to

$$I_D(\text{sat}) = \frac{W\mu_n C_{ox}}{2L}\left[2(V_{GS} - V_T)V_{DS}(\text{sat}) - V_{DS}^2(\text{sat})\right] \tag{11.60}$$

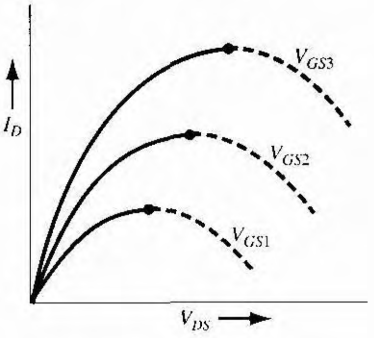

Figure 11.48 | Plots of I_D versus V_{DS} from Equation (11.58).

Using Equation (11.59) for $V_{DS}(\text{sat})$, Equation (11.60) becomes

$$I_D(\text{sat}) = \frac{W\mu_n C_{\text{ox}}}{2L}(V_{GS} - V_T)^2 \tag{11.61}$$

Equation (11.58) is the ideal current-voltage relationship of the n-channel MOSFET in the nonsaturation region for $0 \le V_{DS} \le V_{DS}(\text{sat})$, and Equation (11.61) is the ideal current-voltage relationship of the n-channel MOSFET in the saturation region for $V_{DS} \ge V_{DS}(\text{sat})$. These *I–V* expressions were explicitly derived for an n-channel enhancement mode device. However, these same equations apply to an n-channel depletion mode MOSFET in which the threshold voltage V_T is a negative quantity.

DESIGN EXAMPLE 11.8

Objective

To design the width of a MOSFET such that a specified current is induced for a given applied bias.

Consider an ideal n-channel MOSFET with parameters $L = 1.25\ \mu\text{m}$, $\mu_n = 650\ \text{cm}^2/\text{V-s}$, $C_{\text{ox}} = 6.9 \times 10^{-8}\ \text{F/cm}^2$, and $V_T = 0.65$ V Design the channel width ***W*** such that $I_D(\text{sat}) =$ 4 mA for $V_{GS} = 5$ V.

■ **Solution**

We have, from Equation (11.61),

$$I_D(\text{sat}) = \frac{W\mu_n C_{\text{ox}}}{2L}(V_{GS} - V_T)^2$$

$$4 \times 10^{-3} = \frac{W(650)(6.9 \times 10^{-8})}{2(1.25 \times 10^{-4})} \cdot (5 - 0.65)^2 = 3.39W$$

Then

$$W = 11.8\ \mu\text{m}$$

■ **Comment**

The current capability of a MOSFET is directly proportional to the channel width ***W***. The current handling capability can be increased by increasing ***W***.

TEST YOUR UNDERSTANDING

E11.13 The parameters of an n-channel MOSFET are $\mu_n = 650\ \text{cm}^2/\text{V-s}$, $t_{ox} = 200$ Å, $W/L = 50$, and $V_T = 0.40$ V. If the transistor is biased in the saturation region, find the drain current for $V_{GS} = 1$, 2, and 3 V. (Ans. I_D = 1.01, 7.19, and 19 mA)

E11.14 The n-channel MOSFET in E11.13 is to be redesigned by changing the W/L ratio such that $I_D = 100\ \mu\text{A}$ when the transistor is biased in the saturation region with $V_{GS} = 1.75$ V. (Ans. $W/L = 0.976$)

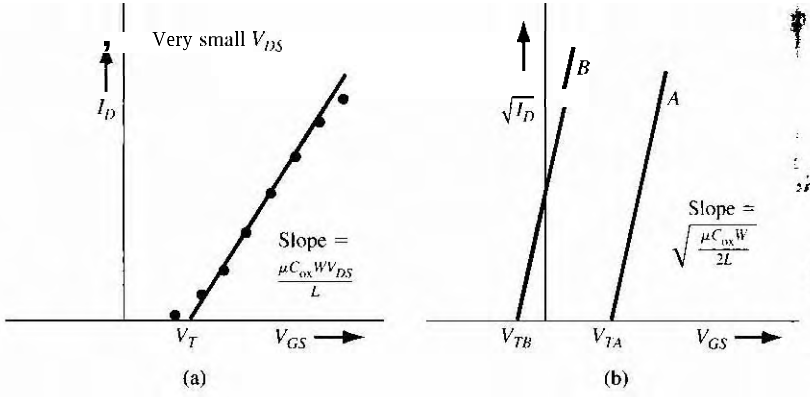

Figure 11.49 | (a) I_D versus V_{GS} (for small V_{DS}) for enhancement mode MOSFET. (b) Ideal $\sqrt{I_D}$ versus V_{GS} in saturation region for enhancement mode (curve A) and depletion mode (curve B) n-channel MOSFETs.

We can use the I–V relations to experimentally determine the mobility an threshold voltage parameters. From Equation (11.58), we can write, for very sma values of V_{DS},

$$I_D = \frac{W\mu_n C_{ox}}{L}(V_{GS} - V_T)V_{DS} \qquad (11.62$$

Figure 11.49a shows a plot of Equation (11.62a) as a function of V_{GS} for constant V_{D} A straight line is fitted through the points. The deviation from the straight line at lo values of V_{GS} is due to subthreshold conduction and the deviation at higher values o V_{GS} is due to mobility being a function of gate voltage. Both of these effects will be co sidered in the next chapter. The extrapolation of the straight line to zero current gives the threshold voltage and the slope is proportional to the inversion carrier mobility.

If we take the square root of Equation (11.61), we obtain

$$\sqrt{I_D(\text{sat})} = \sqrt{\frac{W\mu_n C_{ox}}{2L}}(V_{GS} - V_T) \qquad (11.62b$$

Figure 11.49b is a plot of Equation (11.62b). In the ideal case, we can obtain the same information from both curves. However, as we will see in the next chapter. the thresh- old voltage may be a function of V_{DS} in short-channel devices. Since Equation (11.62b) applies to devices biased in the saturation region. the V_T parameter in this equation may differ from the extrapolated value determined in Figure 11.49a. In general, the nonsaturation current–voltage characteristics will produce the more reliable data.

EXAMPLE 11.9

Objective

To determine the inversion carrier mobility from experimental results.

Consider an n-channel MOSFET with $W = 15$ μm, $L = 2$ μm, and $C_{ox} = 6.9 \times 10^{-8}$ F/cm^2. Assume that the drain current in the nonsaturation region for $V_{DS} = 0.10$ V is $I_D = 35$ μA at $V_{GS} = 1.5$ V and $I_D = 75$ μA at $V_{GS} = 2.5$ V.

■ Solution

From Equation (11.62a), we can write

$$I_{D2} - I_{D1} = \frac{W\mu_n C_{ox}}{L}(V_{GS2} - V_{GS1})V_{DS}$$

so that

$$75 \times 10^{-6} - 35 \times 10 = \left(\frac{15}{2}\right)\mu_n(6.9 \times 10^{-8})(2.5 - 1.5)(0.10)$$

which yields

$$\mu_n = 773 \text{ cm}^2/\text{V-s}$$

We can then determine

$$V_T = 0.625 \text{ V}$$

■ Comment

The mobility of carriers in the inversion layer is less than that in the bulk semiconductor due to the surface scattering effect. We will discuss this effect in the next chapter.

The current-voltage relationship of a p-channel device can be obtained by the same type of analysis. Figure 11.50 shows a p-channel enhancement mode MOSFET. The voltage polarities and current direction are the reverse of those in the n-channel device. We may note the change in the subscript notation for this device. For the current direction shown in the figure, the I–V relations for the p-channel MOSFET are

$$\boxed{I_D = \frac{W\mu_p C_{ox}}{2L}\left[2(V_{SG} + V_T)V_{SD} - V_{SD}^2\right]} \qquad (11.63)$$

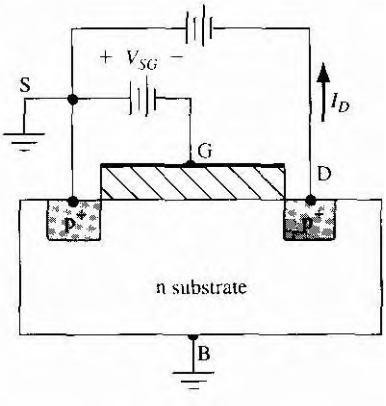

Figure 11.50 | Cross section and bias configuration for a p-channel enhancement-mode MOSFET.

for $0 \le V_{SD} \le V_{SD}(\text{sat})$, and

$$\boxed{I_D(\text{sat}) = \frac{W\mu_p C_{\text{ox}}}{2L}(V_{SG} + V_T)^2} \qquad (11$$

for $V_{SD} \ge V_{SD}(\text{sat})$, where

$$\boxed{V_{SD}(\text{sat}) = V_{SG} + V_T} \qquad (11.65)$$

Note the change in the sign in front of V_T and note that the mobility is now the mobility of the holes in the hole inversion layer charge. Keep in mind that V_T is negative for a p-channel enhancement mode MOSFET and positive for a depletion mode p-channel device.

TEST YOUR UNDERSTANDING

E11.15 The parameters of a p-channel MOSFET are $\mu_p = 310$ cm^2/V-s, $t_{\text{ox}} = 220$ Å, $W/L = 60$. and $V_T = -0.40$ V. If the transistor is biased in the saturation region, find the drain current for $V_{SG} = 1$, 1.5. and 2 V.
(Ans. $I_D = 0.526$, 1.77 and 3.74 mA)

E11.16 The p-channel MOSFET in E11.15 is to be redesigned by changing the (W/L) ratio such that $I_D = 200$ μA when the transistor is biased in the saturation region with $V_{SG} = 1.25$ V. (Ans. $W/L = 11.4$)

One assumption we made in the derivation of the current-voltage relationship was that the charge neutrality condition given by Equation (11.46) was valid over the entire length of the channel. We implicitly assumed that $Q'_{SD}(\max)$ was constant along the length of the channel. The space charge width, however, varies between source and drain due to the drain-to-source voltage; it is widest at the drain when $V_{DS} > 0$. A change in the space charge density along the channel length must be balanced by a corresponding change in the inversion layer charge. An increase in the space charge width means that the inversion layer charge is reduced, implying that the drain current and drain-to-source saturation voltage are less than the ideal values. The actual saturation drain current may be as much as 20 percent less than the predicted value due to this bulk charge effect.

11.3.4 Transconductance

The MOSFET transconductance is defined as the change in drain current with respect to the corresponding change in gate voltage, or

$$g_m = \frac{\partial I_D}{\partial V_{GS}} \qquad (11.66)$$

The transconductance is sometimes referred to as the transistor gain.

If we consider an n-channel MOSFET operating in the nonsaturation region, then, using Equation (11.58), we have

$$g_{mL} = \frac{\partial I_D}{\partial V_{GS}} = \frac{W\mu_n C_{ox}}{L} \cdot V_{DS} \tag{11.67}$$

The transconductance increases linearly with V_{DS} but is independent of V_{GS} in the nonsaturation region.

The I–V characteristics of an n-channel MOSFET in the saturation region were given by Equation (11.61). The transconductance in this region of operation is given by

$$g_{ms} = \frac{\partial I_D(\text{sat})}{\partial V_{GS}} = \frac{W\mu_n C_{ox}}{L}(V_{GS} - V_T) \tag{11.68}$$

In the saturation region, the transconductance is a linear function of V_{GS} and is independent of V_{DS}.

The transconductance is a function of the geometry of the device as well as of carrier mobility and threshold voltage. The transconductance increases as the width of the device increases, and it also increases as the channel length and oxide thickness decrease. In the design of MOSFET circuits, the size of the transistor, in particular the channel width W, is an important engineering design parameter.

11.3.5 Substrate Bias Effects

In all of our analyses so far, the substrate, or body, has been connected to the source and held at ground potential. In MOSFET circuits, the source and body may not be at the same potential. Figure 11.51a shows an n-channel MOSFET and the associated double-subscripted voltage variables. The source-to-substrate pn junction must always be zero or reverse biased, so V_{SB} must always be greater than or equal to zero.

If $V_{SB} = 0$, threshold is defined as the condition when $\phi_s = 2\phi_{fp}$ as we discussed previously and as shown in Figure 11.51b. When $V_{SB} > 0$ the surface will still try to invert when $\phi_s = 2\phi_{fp}$. However, these electrons are at a higher potential

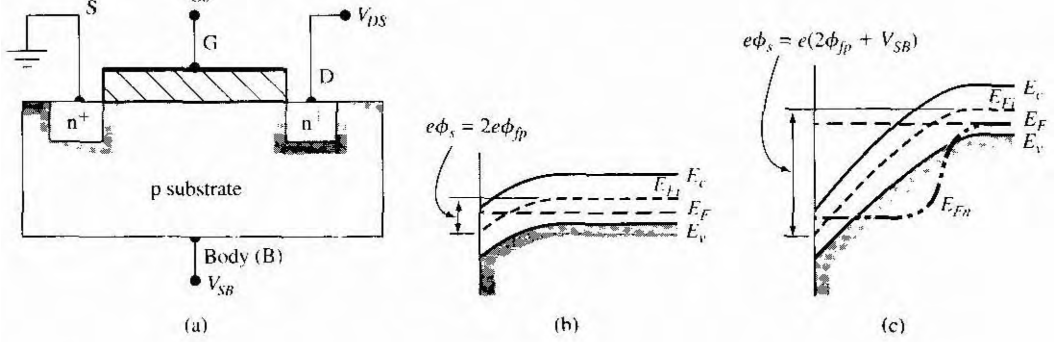

Figure 11.51 | (a) Applied voltages on an n-channel MOSFET (b) Energy-band diagram at inversion point when $V_{SB} = 0$. (c) Energy-band diagram at inversion point when $V_{SB} > 0$ is applied.

energy than are the electrons in the source. The newly created electrons will move laterally and flow out of the source terminal. When $\phi_s = 2\phi_{fp} + V_{SB}$, the surface reaches an equilibrium inversion condition. The energy-band diagram for this condition is shown in Figure 11.51c. The curve represented as E_{Fn} is the Fermi level from the p substrate through the reverse-biased source-substrate junction to the source contact.

The space charge region width under the oxide increases from the original x_{dT} value when a reverse-biased source-substrate junction voltage is applied. With an applied $V_{SB} > 0$, there is more charge associated with this region. Considering the charge neutrality condition through the MOS structure, the positive charge on the top metal gate must increase to compensate for the increased negative space charge in order to reach the threshold inversion point. So when $V_{SB} > 0$, the threshold voltage of the n-channel MOSFET increases.

When $V_{SB} = 0$, we had

$$Q'_{SD}(\max) = -eN_a x_{dT} = -\sqrt{2e\epsilon_s N_a(2\phi_{fp})} \tag{11.69}$$

When $V_{SB} > 0$, the space charge width increases and we now have

$$Q'_{SD} = -eN_a x_d = -\sqrt{2e\epsilon_s N_a(2\phi_{fp} + V_{SB})} \tag{11.70}$$

The change in the space charge density is then

$$\Delta Q'_{SD} = -\sqrt{2e\epsilon_s N_a}\left[\sqrt{2\phi_{fp} + V_{SB}} - \sqrt{2\phi_{fp}}\right] \tag{11.71}$$

To reach the threshold condition, the applied gate voltage must be increased. The change in threshold voltage can be written as

$$\boxed{\Delta V_T = -\frac{\Delta Q'_{SD}}{C_{\mathrm{ox}}} = \frac{\sqrt{2e\epsilon_s N_a}}{C_{\mathrm{ox}}}\left[\sqrt{2\phi_{fp} + V_{SB}} - \sqrt{2\phi_{fp}}\right]} \tag{11.72}$$

where $\Delta V_T = V_T(V_{SB} > 0) - V_T(V_{SB} = 0)$. We may note that V_{SB} must always be positive so that, for the n-channel device, ΔV_T is always positive. The threshold voltage of the n-channel MOSFET will increase as a function of the source-substrate junction voltage.

EXAMPLE 11.10

Objective

To calculate the change in the threshold voltage due to an applied source-to-body voltage.

Consider an n-channel silicon MOSFET at T = 300 K. Assume the substrate is doped to $N_a = 3 \times 10^{16}$ cm^{-3} and assume the oxide is silicon dioxide with a thickness of $t_{\mathrm{ox}} = 500$ Å. Let $V_{SB} = 1$ V.

■ Solution

We can calculate that

$$\phi_{fp} = V_t \ln\left(\frac{N_a}{n_i}\right) = (0.0259)\ln\left(\frac{3 \times 10^{16}}{1.5 \times 10^{10}}\right) = 0.376 \text{ V}$$

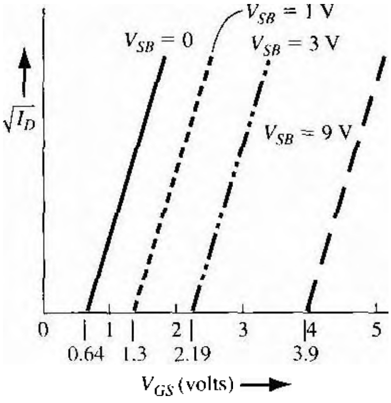

Figure 11.52 | Plots of $\sqrt{I_D}$ versus V_{GS} at several values of V_{SB} for an n-channel MOSFET.

We can also find

$$C_{ox} = \frac{\epsilon_{ox}}{t_{ox}} = \frac{(3.9)(8.85 \times 10^{-14})}{500 \times 10^{-8}} = 6.9 \times 10^{-8} \text{ F/cm}^2$$

Then from Equation (11.72), we can obtain

$$\Delta V_T = \frac{[2(1.6 \times 10^{-19})(11.7)(8.85 \times 10^{-14})(3 \times 10^{16})]^{1/2}}{6.9 \times 10^{-8}}$$

$$\times \{[2(0.376) + 1]^{1/2} - [2(0.376)]^{1/2}\}$$

or

$$\Delta V_T = 1.445(1.324 - 0.867) = 0.66 \text{ V}$$

Comment

Figure 11.52 shows plots of $\sqrt{I_D(\text{sat})}$ versus V_{GS} for various values of applied V_{SB}. The original threshold voltage, V_{T0}, is 0.64 V.

If a body or substrate bias is applied to a p-channel device, the threshold voltage is shifted to more negative values. Because the threshold voltage of a p-channel enhancement mode MOSFET is negative, a body voltage will increase the applied negative gate voltage required to create inversion. The same general observation was made for the n-channel MOSFET.

TEST YOUR UNDERSTANDING

E11.17 A silicon MOS device has the following parameters: $N_a = 10^{16}$ cm^{-3} and $t_{ox} = 200$ Å. Calculate (*a*) the body-effect coefficient and (*b*) the change in threshold voltage for (*i*) $V_{SB} = 1$ V and (ii) $V_{SB} = 2$ V.

[Ans. (*a*) $\gamma = 0.333$ V$^{1/2}$, (*b*) (*i*) $\Delta V_T = 0.156$ V, (*ii*) $\Delta V_T = 0.269$ V]

E11.18 Repeat exercise E11.17 for a substrate impurity doping concentration of $N_a = 10^{15}$ cm^{-3}. ns. (a) $\gamma = 0.105\ \text{V}^{1/2}$, (b) (i) $\Delta V_T = 0.052$ V, (ii) $\Delta V_T = 0.0888$ V

11.4 | FREQUENCY LIMITATIONS

In many applications, the MOSFET is used in a linear amplifier circuit. A small-signal equivalent circuit for the MOSFET is needed in order to mathematically analyze the electronic circuit. The equivalent circuit contains capacitances and resistances that introduce frequency effects. We will initially develop a small-signal equivalent circuit and then discuss the physical factors that limit the frequency response of the MOSFET. A transistor cutoff frequency, which is a figure of merit, will then be defined and an expression derived for this factor.

11.4.1 Small-Signal Equivalent Circuit

The small-signal equivalent circuit of the MOSFET is constructed from the basic MOSFET geometry. A model based on the inherent capacitances and resistances within the transistor structure, along with elements that represent the basic device equations, is shown in Figure 11.53. One simplifying assumption we will make in the equivalent circuit is that the source and substrate are both tied to ground potential.

Two of the capacitances connected to the gate are inherent in the device. These capacitances are C_{gs} and C_{gd}, which represent the interaction between the gate and the channel charge near the source and drain terminals, respectively. The remaining two gate capacitances, C_{gsp} and C_{gdp}, are parasitic or overlap capacitances. In real devices, the gate oxide will overlap the source and drain contacts because of tolerance or fabrication factors. As we will see, the drain overlap capacitance—C_{gdp}, in particular—will lower the frequency response of the device. The parameter C_{ds} is the

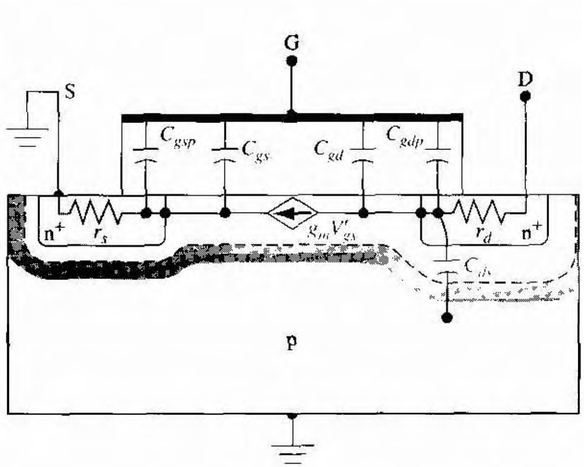

Figure 11.53 | Inherent resistances and capacitances in the n-channel MOSFET structure.

drain-to-substrate pn junction capacitance, and r_s and r_d are the series resistances associated with the source and drain terminals. The small-signal channel current is controlled by the internal gate-to-source voltage through the transconductance.

The small-signal equivalent circuit for the n-channel common-source MOSFET is shown in Figure 11.54. The voltage V'_{gs} is the internal gate-to-source voltage that controls the channel current. The parameters C_{gsT} and C_{gdT} are the total gate-to-source and total gate-to-drain capacitances. One parameter, r_{ds}, shown in Figure 11.54, is not shown in Figure 11.53. This resistance is associated with the slope I_D versus V_{DS}. In the ideal MOSFET biased in the saturation region, I_D is independent of V_{DS} so that r_{ds} would be infinite. In short-channel-length devices, in particular, r_{ds} is finite because of channel length modulation, which we will consider in the next chapter.

A simplified small-signal equivalent circuit valid at low frequency is shown in Figure 11.55. The series resistances, r_s and r_d, have been neglected, so the drain current is essentially only a function of the gate-to-source voltage through the transconductance. The input gate impedance is infinite in this simplified model.

The source resistance r_s can have a significant effect on the transistor characteristics. Figure 11.56 shows a simplified, low-frequency equivalent circuit including r_s but neglecting r_{ds}. The drain current is given by

$$I_d = g_m V'_{gs} \tag{11.73}$$

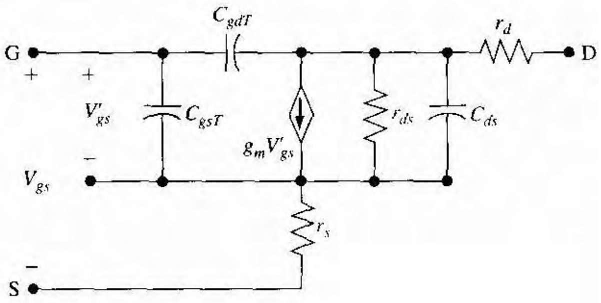

Figure 11.54 | Small-signal equivalent circuit of a common-source n-channel MOSFET.

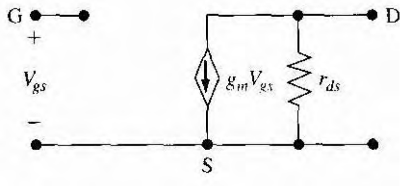

Figure 11.55 | Simplified, low-frequency small-signal equivalent circuit of a common-source n-channel MOSFET.

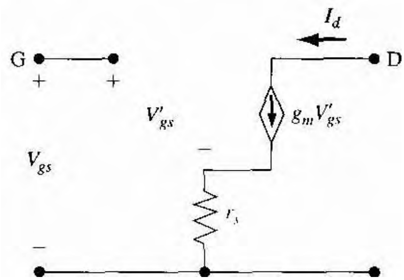

Figure 11.56 | Simplified, low-frequency small-signal equivalent circuit of common-source n-channel MOSFET including source resistance r_s

and the relation between V_{gs} and V'_{gs} can be found from

$$V_{gs} = V'_{gs} + (g_m V'_{gs}) r_s = (1 + g_m r_s) V'_{gs} \tag{11.74}$$

The drain current from Equation (11.73) can now be written as

$$I_d = \left(\frac{g_m}{1 + g_m r_s} \right) V_{gs} = g'_m V_{gs} \tag{11.75}$$

The source resistance reduces the effective transconductance or transistor gain.

The equivalent circuit of the p-channel MOSFET is exactly the same as that of the n-channel except that all voltage polarities and current directions are reversed. The same capacitances and resistances that are in the n-channel model apply to the p-channel model.

11.4.2 Frequency Limitation Factors and Cutoff Frequency

There are two basic frequency limitation factors in the MOSFET. The first factor is the channel transit time. If we assume that carriers are traveling at their saturation drift velocity v_{sat}, then the transit time is $\tau_t = L/v_{sat}$ where L is the channel length. If $v_{sat} = 10^7$ cm/s and L = 1 μm, then $\tau_t = 10$ ps, which translates into a maximum frequency of 100 GHz. This frequency is much larger than the typical maximum frequency response of a MOSFET. The transit time of carriers through the channel is usually not the limiting factor in the frequency responses of MOSFETs.

The second limiting factor is the gate or capacitance charging time. If we neglect r_s, r_d, r_{ds}, and C_{ds}, the resulting equivalent small-signal circuit is shown in Figure 11.57 where R_L is a load resistance.

The input gate impedance in this equivalent circuit is no longer infinite. Summing currents at the input gate node, we have

$$I_i = j\omega C_{gsT} V_{gs} + j\omega C_{gdT} (V_{gs} - V_d) \tag{11.76}$$

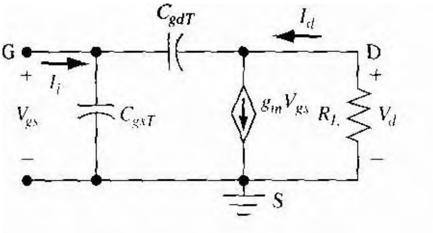

Figure 11.57 | High-frequency small-signal equivalent circuit of common-source n-channel MOSFET.

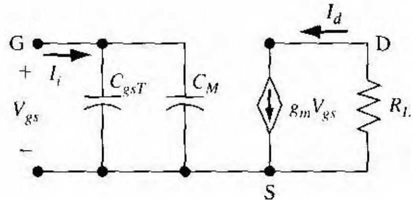

Figure 11.58 | Small-signal equivalent circuit including Miller capacitance.

where I, is the input current. Likewise, summing currents at the output drain node, we have

$$\frac{V_d}{R_L} + g_m V_{gs} + j\omega C_{gdT}(V_d - V_{gs}) = 0 \tag{11.77}$$

Combining Equations (11.76) and (11.77) to eliminate the voltage variable V_d, we can determine the input current as

$$I_i = j\omega\left[C_{gsT} + C_{gdT}\left(\frac{1 + g_m R_L}{1 + j\omega R_L C_{gdT}}\right)\right]V_{gs} \tag{11.78}$$

Normally, $\omega R_L C_{gdT}$ is much less than unity: therefore we may neglect the $(j\omega R_L C_{gdT})$ term in the denominator. Equation (11.78) then simplifies to

$$I_i = j\omega[C_{gsT} + C_{gdT}(1 + g_m R_L)]V_{gs} \tag{11.79}$$

Figure 11.58 shows the equivalent circuit with the equivalent input impedance described by Equation (11.79). The parameter C_M is the Miller capacitance and is given by

$$C_M = C_{gdT}(1 + g_m R_L) \tag{11.80}$$

The serious effect of the drain overlap capacitance now becomes apparent. When the transistor is operating in the saturation region, C_{gd} essentially becomes zero, but C_{gdp} is a constant. This parasitic capacitance is multiplied by the gain of the transistor and can become a significant factor in the input impedance.

The cutoff frequency f_T is defined to he the frequency at which the magnitude of the current gain of the device is unity, or when the magnitude of the input current I_i is equal to the ideal load current I_d. From Figure 11.58, we can see that

$$I_i = j\omega(C_{gsT} + C_M)V_{gs} \tag{11.81}$$

and the ideal load current is

$$I_d = g_m V_{gs} \tag{11.82}$$

The magnitude of the current gain is then

$$\left|\frac{I_d}{I_i}\right| = \frac{g_m}{2\pi f(C_{gsT} + C_M)} \tag{11.83}$$

Setting the magnitude of the current gain equal to unity at the cutoff frequency, we find

$$f_T = \frac{g_m}{2\pi(C_{gsT} + C_M)} = \frac{g_m}{2\pi C_G} \qquad (11.84$$

where C_G is the equivalent input gate capacitance.

In the ideal MOSFET, the overlap or parasitic capacitances, C_{gsp} and C_{gdp}, are zero. Also, when the transistor is biased in the saturation region, C_{gd} approaches zero and C_{gs} is approximately C_{ox} WL. The transconductance of the ideal MOSFET biased in the saturation region and assuming a constant mobility was given by Equation (11.68) as

$$g_{ms} = \frac{W\mu_n C_{ox}}{L}(V_{GS} - V_T)$$

Then, for this ideal case, the cutoff frequency is

$$f_T = \frac{}{2\pi C_G} = \frac{W\mu_n C_{ox}(V_{GS} - V_T)}{2\pi(C_{ox}WL)} = \frac{\mu_n(V_{GS} - V_T)}{2nL^2} \qquad (11.8$$

EXAMPLE 11.11

Objective

To calculate the cutoff frequency of an ideal MOSFET with a constant mobility.

Assume that the electron mobility in an n-channel device is $\mu_n = 400\ \text{cm}^2/\text{V-s}$ and that the channel length is $L = 4\ \mu\text{m}$. Also assume that $V_T = 1$ V and let $V_{GS} = 3$ V.

■ Solution

From Equation (11.85), the cutoff frequency is

$$f_T = \frac{\mu_n(V_{GS} - V_T)}{2\pi L^2} = \frac{400(3-1)}{2\pi(4\times10^{-4})^2} = 796\ \text{MHz}$$

Comment

In an actual MOSFET, the effect of the parasitic capacitance will substantially reduce the cutoff frequency from that calculated in this example.

TEST YOUR UNDERSTANDING

E11.19 An n-channel MOSFET has the following parameters: $\mu_n = 400\ \text{cm}^2/\text{V-s}$, $t_{ox} = 200$ Å, $W/L = 20$. and $V_T = 0.4$ V. The transistor is biased at $V_{GS} = 2.5$ V in the saturation region and is connected to an effective load of $R_L = 100\ \text{k}\Omega$. Calculate the ratio of Miller capacitance C_M to gate-to-drain capacitance C_{gdT}. (Ans. 292)

E11.20 An n-channel MOSFET has the same parameters as described in E11.19. The channel length is $L = 0.5\ \mu\text{m}$. Determine the cutoff frequency. (Ans. 53.5 GHz)

*11.5 | THE CMOS TECHNOLOGY

The primary objective of this text is topresent the basic physics of semiconductormaterials and devices without considering in detail the various fabrication processes; this important subject is left to other texts. However, there is one MOS technology that is usedextensively, for which the basic fabrication techniques must be considered in order tounderstand essential characteristics of these devices andcircuits. The one MOS technology we will consider briefly is the complementary MOS, or CMOS, process.

We have considered the physics of both n-channel and p-channel enhancement mode MOSFETs. Both devices are used in a CMOS inverter, which is the basis of CMOS digital logic circuits. The dc power dissipation in a digital circuit can he reduced to very low levels by using a complementary p-channel and n-channel pair.

It is necessary to form electrically isolated p- and n-substrate regions in an integrated circuit to accommodate the n- and p-channel transistors. The p-well process has been a commonly used technique for CMOS circuits. The process starts with a fairly low doped n-type silicon substrate in which the p-channel MOSFET will be fabricated. A diffused p-region, called a p well, is formed in which the n-channel MOSFET will be fabricated. In most cases. the p-type substrate doping level must be larger than the n-type substrate doping level to obtain the desired threshold voltages. The larger p doping can easily compensate the initial n doping to form the p well. A simplifiedcross section of the p-well CMOS structure is shown in Figure 11.59a. The

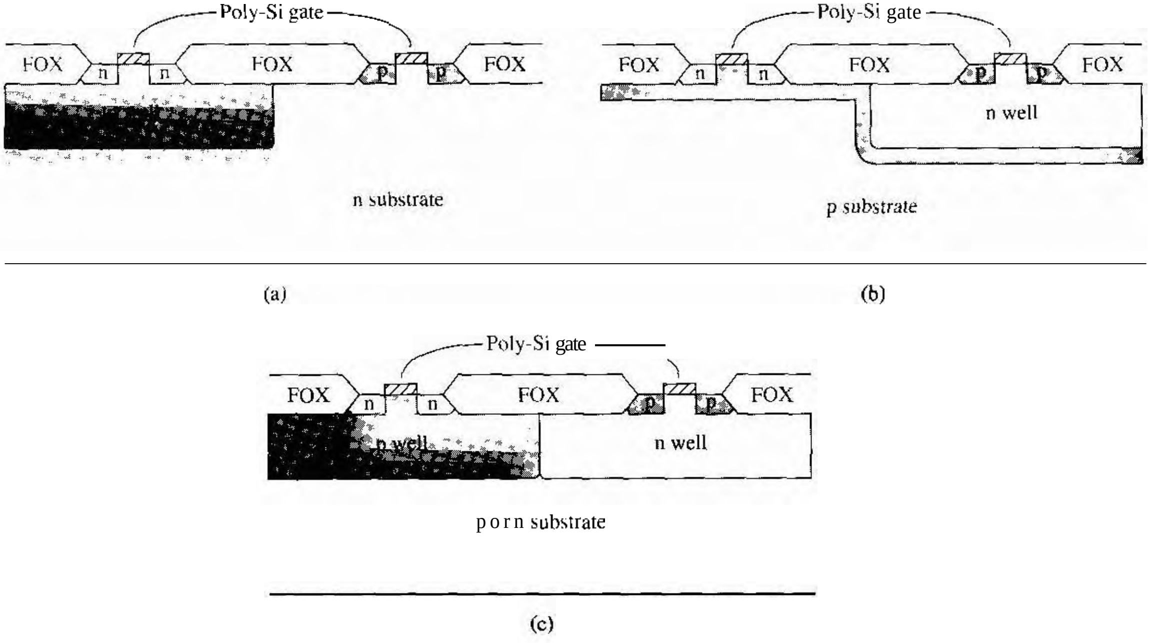

Figure 11.59 | CMOS structures: (a) p well, (b) n well, and (c) twin **well**
(From Yang [21])

notation FOX stands for field oxide, which is a relatively thick oxide separating the devices. The field oxide prevents either the n or p substrate from becoming inverted and helps maintain isolation between the two devices. In practice, additional processing steps must be included; for example, providing connections so that the p well and n substrate can be electrically connected to the appropriate voltages. The n substrate must always be at a higher potential than the p well; therefore, this pn junction will always be reverse biased.

With ion implantation now being extensively used for threshold voltage control, both the n-well CMOS process and twin-well CMOS process can be used. The n-well CMOS process, shown in Figure 11.59b, starts with an optimized p-type substrate that is used to form the n-channel MOSFETs. (The n-channel MOSFETs, in general, have superior characteristics, so this starting point should yield excellent n-channel devices.) The n well is then added, in which the p-channel devices are fabricated. The n-well doping can be controlled by ion implantation.

The twin-well CMOS process, shown in Figure 11.59c, allows both the p-well an n-well regions to be optimally doped to control the threshold voltage and transconductance of each transistor. The twin-well process allows a higher packing density because of self-aligned channel stops.

One major problem in CMOS circuits has been ***latch-up.*** Latch-up refers to a high-current, low-voltage condition that may occur in a four-layer pnpn structure. Figure 11.60a shows the circuit of a CMOS inverter and Figure 11.60b shows a simplified integrated circuit layout of the inverter circuit. In the CMOS layout, the p^+-source to n-substrate to p-well to n+-source forms such a four-layer structure.

The equivalent circuit of this four-layer structure is shown in Figure 11.61. The silicon controlled rectifier action involves the interaction of the parasitic pnp and npn transistors. The npn transistor corresponds to the vertical n^+ source to p well to n substrate structure and the pnp transistor corresponds to the lateral p-well to n-substrate to p^+-source structure. Under normal CMOS operation, both parasitic bipolar transistors are cut off. However, under certain conditions, avalanche breakdown may occur in the p-well to n-substrate junction, driving both bipolar transistors into saturation. This high-current, low-voltage condition—latch-up—can sustain itself by

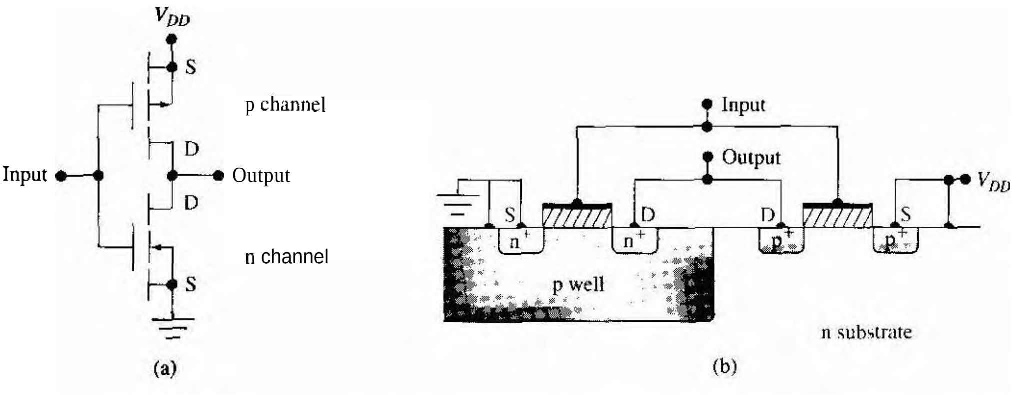

Figure 11.60 | (a) CMOS inverter circuit. (b) Simplified integrated circuit cross section of CMOS inverter.

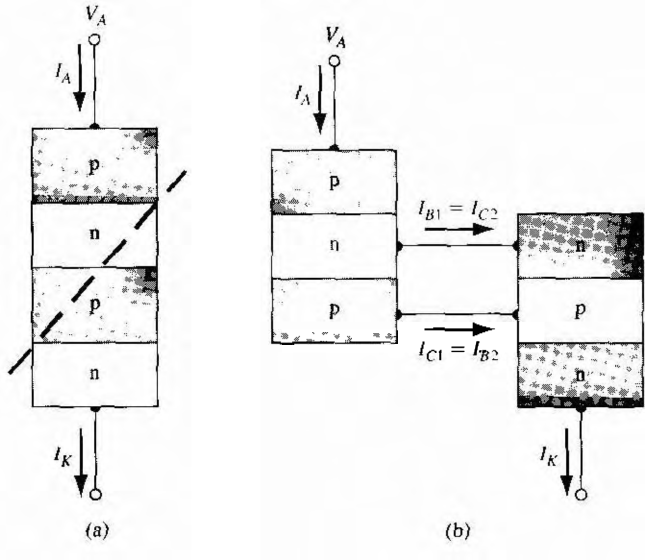

Figure 11.61 | (a) The splitting of the basic pnpn structure. (b) The two-transistor equivalent circuit of the four-layered pnpn device.

positive feedback. The condition can prevent the CMOS circuit from operating and can also cause permanent damage and burn-out of the circuit.

Latch-up can be prevented if the product $\beta_n\beta_p$ is less than unity at all times, where β_n and β_p are the common-emitter current gains of the npn and pnp parasitic bipolar transistors, respectively. One method of preventing latch-up is to "kill" the minority carrier lifetime. Minority carrier lifetime degradation can be accomplished by gold doping or neutron irradiation. either of which introduces deep traps within the semiconductor. The deep traps increase the excess minority carrier recombination rate and reduce current gain. A second method of preventing latch-up is by using proper circuit layout techniques. If the two bipolar transistors can he effectively decoupled, then latch-up can be minimized or prevented. The two parasitic bipolar transistors can also be decoupled by using a different fabrication technology. The silicon-on-insulator technology, for example, allows the n-channel and the p-channel MOSFETs to be isolated from each other by an insulator. This isolation decouples the parasitic bipolar transistors.

11.6 | SUMMARY

- The fundamental physics and characteristics of the metalkoxide–semiconductor field-effect transistor (MOSFET) have been considered in this chapter
- The heart of the MOSFET is the MOS capacitor. The energy hands in the semiconductor adjacent to the oxide–semiconductor interface bend, depending upon the voltage applied across the MOS capacitor. The position of the conduction and valence bands relative to the Fermi level at the surface is a function of the MOS capacitor voltage.
- The semiconductor surface at the oxide–semiconductor interface can be inverted from p type ton type by applying a positive gate voltage, or from n type top type by applying

a negative gate voltage. Thus, an *inversion* layer of *mobile* charge can be created adjacent to the oxide. The basic MOS field-effect action is the modulation of the inversion charge density, or channel conductance, by the gate voltage.

- The *C-V* characteristics of the MOS capacitor were considered. The amount of equivale oxide trapped charge and the density of interface states, for example, can be determined from the *C-V* measurements.
- Two basic types of MOSFETs are the n channel, in which current is due to the flow of electrons in the inversion layer, and the p channel, in which current is due to the flow of holes in the inversion layer. Each of these devices can be either enhancement mode, in which the device is normally "off" and is turned on by applying a gate voltage, or depletion mode, in which the device is normally "on" and is turned off by applying a gate voltage.
- The flat-band voltage is the gate voltage that must be applied to achieve the flat-band condition, in which the conduction and valence bands in the semiconductor do not ben and there is no space charge region in the semiconductor. The flat-band voltage is a function of the metal–oxide barrier height, the semiconductor–oxide barrier height, and the amount of fixed trapped oxide charge.
- The threshold voltage is the applied gate voltage required to reach the threshold inversion point, which is the condition at which the inversion charge density is equal in magnitude to the semiconductor doping concentration. The threshold voltage is a function of the flat-band voltage, semiconductor doping concentration, and oxide thickness.
- The current in a MOSFET is due to the flow of carriers in the inversion layer between the source and drain terminals. The inversion layer charge density and channel conductance are controlled by the gate voltage, which means that the channel current is also controlled by the gate voltage.
- When the transistor is biased in the nonsaturation region ($V_{DS} < V_{DS}(\text{sat})$), the inversion charge extends completely across the channel from the source to the drain terminals. The drain current is a function of both the gate-to-source and drain-to-source voltages. When the transistor is biased in the saturation region ($V_{DS} > V_{DS}(\text{sat})$), the inversion charge density is pinched off near the drain terminal, and the ideal drain current is only a function of the gate-to-source voltage.
- The MOSFET is actually a four-terminal device, with the substrate or body being the fourth terminal. As the magnitude of the reverse-bias source-to-substrate voltage increases, the magnitude of the threshold voltage increases. The substrate bias effect may become important in integrated circuits in which the source and substrate are not electrically tied together.
- A small-signal equivalent circuit, including capacitances, of the MOSFET was developed The various physical factors in the MOSFET that affect the frequency limitations were considered. In particular, the drain overlap capacitance may be a limiting factor in the frequency response of the MOSFET because of the Miller effect. The cutoff frequency, a figure of merit for the frequency response of the device, is inversely proportional to channel length; thus, a reduction in channel length results in an increased frequency capability of the MOSFET.
- The CMOS technology, in which both n-channel and p-channel devices are fabricated in the same semiconductor chip, was briefly considered. Electrically isolated p- and n-substrate regions are required to accommodate the two types of transistors. Various processes are used to fabricate this structure. One potential problem encountered in the CMOS structure is latch-up—the high-current, low-voltage condition that may occur in a four-layer pnpn structure.

GLOSSARY OF IMPORTANT TERMS

accumulation layer charge The induced charge directly under an oxide that is in excess of the thermal-equilibrium majority carrier concentration.

bulk charge effect The deviation in drain current from the ideal due to the space charge width variation along the channel length caused by a drain-to-source voltage.

channel conductance The ratio of drain current to drain-to-source voltage in the limit as $V_{DS} \to 0$.

channel conductance modulation The process whereby the channel conductance varies with gate-to-source voltage.

CMOS Complementary MOS; the technology that uses both p- and n-channel devices in an electronic circuit fabricated in a single semiconductor chip.

cutoff frequency The signal frequency at which the input ac gate current is equal to the output ac drain current.

depletion mode MOSFET The type of MOSFET in which a gate voltage must be applied to turn the device off.

enhancement mode MOSFET The type of MOSFET in which a gate voltage must be applied to turn the device on.

equivalent fixed oxide charge The effective fixed charge in the oxide, Q'_{ss}, directly adjacent to the oxide–semiconductor interface.

flat-band voltage The gate voltage that must be applied to create the flat-band condition in which there is no space charge region in the semiconductor under the oxide.

gate capacitance charging time The time during which the input gate capacitance is being charged or discharged because of a step change in the gate signal.

interface states The allowed electronic energy states within the bandgap energy at the oxide–semiconductor interface.

inversion layer charge The induced charge directly under the oxide, which is the opposite type compared with the semiconductor doping.

inversion layer mobility The mobility of carriers in the inversion layer.

latch-up The high-current, low-voltage condition that may occur in a four-layer pnpn structure such as in CMOS.

maximum induced space charge width The width of the induced space charge region under the oxide at the threshold inversion condition.

metal–semiconductor work function difference The parameter ϕ_{ms}, a function of the difference between the metal work function and semiconductor electron affinity.

moderate inversion The condition in which the induced space charge width is changing slightly when the gate voltage is at or near the threshold voltage and the inversion charge density is of the same magnitude as the semiconductor doping concentration.

oxide capacitance The ratio of oxide permittivity to oxide thickness, which is the capacitance per unit area, C_{ox}

saturation The condition in which the inversion charge density is zero at the drain and the drain current is no longer a function of the drain-to-source voltage.

strong inversion The condition in which the inversion charge density is larger than the magnitude of the semiconductor doping concentration.

threshold inversion point The condition in which the inversion charge density is equal in magnitude to the semiconductor doping concentration.

threshold voltage The gate voltage that must be applied to achieve the threshold inversion point.

transconductance The ratio of an incremental change in drain current to the corresponding incremental change in gate voltage.

weak inversion The condition in which the inversion charge density is less than the magnitude of the semiconductor doping concentration.

CHECKPOINT

After studying this chapter, the reader should have the ability to:

- Sketch the energy band diagrams in the semiconductor of the MOS capacitor under various bias conditions.
- Describe the process by which an inversion layer of charge is created in an MOS capacitor.
- Discuss the reason the space charge width reaches a maximum value once the inversion layer is formed.
- Discuss what is meant by the metal–semiconductor work function difference, and discuss why this value is different between aluminum. n^+ polysilicon, and p^+ polysilicon gates.
- Describe what is meant by flat-band voltage.
- Define threshold voltage.
- Sketch the C-Vcharacteristics of an MOS capacitor with p-type and n-type semiconductor substrates under high-frequency and low-frequency conditions.
- Discuss the effects of fixed trapped oxide charge and interface states on the C-V characteristics.
- Sketch the cross-sections of n-channel and p-channel MOSFET structures.
- Explain the basic operation of the MOSFET.
- Discuss the *I*–*V* characteristics of the MOSFET when biased in the nonsaturation and saturation regions.
- Describe the substrate bias effects on the threshold voltage.
- Sketch the small-signal equivalent circuit. including capacitances, of the MOSFET, and explain the physical origin of each capacitance.
- Discuss the condition that defines the cutoff frequency of a MOSFET.
- Sketch the cross section of a CMOS structure.
- Discuss what is meant by latch-up in a CMOS structure.

REVIEW QUESTIONS

1. Sketch the energy band diagrams in an MOS capacitor with an n-type substrate in accumulation, depletion, and inversion modes.
2. Describe what is meant by an inversion layer of charge. Describe haw an inversion layer of charge can be formed in an MOS capacitor with a p-type substrate.
3. Why does the space-charge region in the semicunductor of an MOS capacitor reach a maximum width once the inversion layer is formed?
4. Define electron affinity in the semiconductor of an MOS capacitor
5. Sketch the energy band diagram through an MOS structure with a p-type substrate and an n^+ polysilicon gate under zero bias.

6. Define the flat-band voltage.
7. Define the threshold voltage.
8. Sketch the *C-V* characteristics of an **MOS** capacitor with an n-type substrate under the low-frequency condition. How do the characteristics change for the high-frequency condition?
9. indicate the approximate capacitance at flat-band on the C-V characteristic of an MOS capacitor with a p-type substrate under the high-frequency condition.
10. What is the effect on the C-V characteristics of an **MOS** capacitor with a p-type substrate if the amount of positive trapped oxide charge increases?
11. Qualitatively sketch the inversion charge density in the channel region when the transistor is biased in the nonsaturation region. Repeat for the case when the transistor is biased in the saturation region.
12. Define $V_{DS}(\text{sat})$.
13. Define enhancement mode and depletion mode for both n-channel and p-channel devices.
14. Sketch the charge distribution through an MOS capacitor with a p-type substrate when biased in the inversion mode. Write the charge neutrality equation.
15. Discuss why the threshold voltage changes when a reverse-biased source-to-substrate voltage is applied to a **MOSFET.**

PROBLEMS

(*Note:* In the following problems, assume the semiconductor and oxide in the **MOS** system are silicon and silicon dioxide, respectively. and assume the temperature is $T = 300$ K unless otherwise stated. Use Figure 11.15 to determine the metal–semiconductor work function difference.)

Section 11.1 The Two-Terminal MOS Structure

11.1 The dc charge distributions of four ideal **MOS** capacitors are shown in Figure 11.62. For each case: (*a*) Is the semiconductor n- or p-type? (*b*) Is the device biased in the accumulation. depletion. or inversion mode'? (*c*) Draw the energy-band diagram in the semiconductor region.

11.2 (*a*) Calculate the maximum space charge width x_{dT} and the maximum space charge density $|Q'_{SD}(\text{max})|$ in p-type silicon. gallium arsenide, and germanium semiconductors of an MOS structure. Let $T = 300$ K and assume $N_a = 10^{16}$ cm^{-3}. (*b*) Repeat part (*a*) if $T = 200$ K.

11.3 (*a*) Consider n-type silicon in an **MOS** structure. Let $T = 300$ K. Determine the semiconductor doping so that $|Q'_{SD}(\text{max})| = 7.5 \times 10^{-9}$ C/cm^2. (*b*) Determine the surface potential that results in the maximum space charge width.

11.4 Determine the metal–semiconductor work function difference ϕ_{ms} in an **MOS** structure with p-type silicon for the case when the gate is (*a*) aluminum. (*b*) n$^+$ polysilicon, and (*c*) p$^+$ polysilicon. Let $N_a = 6 \times 10^{15}$ cm^{-3}

11.5 Consider an **MOS** structure with n-type silicon. A metal–semiconductor work function difference of $\phi_{ms} = -0.35$ V is required. Determine the silicon doping required to meet this specification when the gate is (*a*) n$^+$ polysilicon, (*b*) p$^+$ polysilicon, and (*c*) aluminum. If a particular gate cannot meet this requirement, explain why.

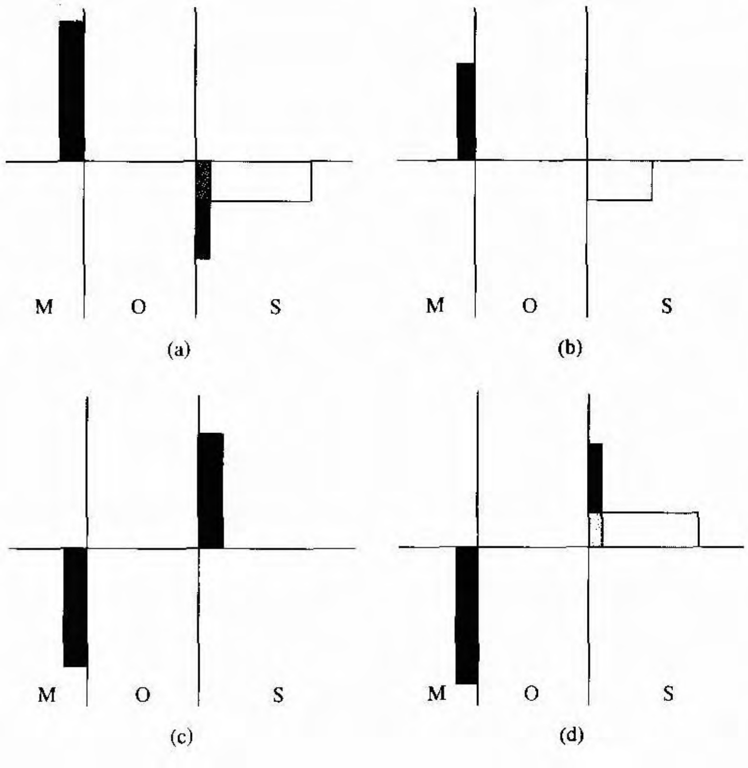

Figure 11.62 | Figure for Problem 11.1

11.6 Consider an n$^+$ polysilicon–silicon dioxide-n-type silicon MOS capacitor. Let $N_d = 10^{15}$ cm^{-3}. Calculate the flat-band voltage for (a) $t_{ox} = 500$ Å when Q'_{ss} is (*i*) 10^{10} cm^{-2}, (*ii*) 10^{11} cm^{-2}, and (*iii*) 5×10^{11} cm^{-2}. (*b*) Repeat pan (*a*) when $t_{ox} = 250$ Å.

11.7 Consider an aluminum gate–silicon dioxide–p-type silicon MOS structure with $t_{ox} = 450$ Å. The silicon doping is $N_a = 2 \times 10^{16}$ cm^{-3} and the flat-band voltage is $V_{FB} = -1.0$ V Determine the fixed oxide charge Q'_{ss}.

11.8 An MOS transistor is fabricated on a p-type silicon substrate with $N_a = 2 \times 10^{15}$ cm^{-3}. The oxide thickness is $t_{ox} = 450$ Å and the equivalent fixed oxide charge is $Q'_{ss} = 2 \times 10^{11}$ cm^{-2}. Calculate the threshold voltage for (*a*) an aluminum gate, (*b*) an n$^+$ polysilicon gate, and (*c*) a p$^+$ polysilicon gate.

11.9 Repeat Problem 11.8 for an n-type silicon substrate with $N_d = 10^{15}$ cm^{-3}.

11.10 A 400 Å oxide is grown on p-type silicon with $N_a = 5 \times 10^{15}$ cm^{-3}. The flat-band voltage is -0.9 V. Calculate the surface potential at the threshold inversion point as well as the threshold voltage assuming negligible oxide charge. Also find the maximum space charge width for this device.

***11.11** An MOS transistor with an aluminum gate is fabricated on a p-type silicon substrate. The oxide thickness is $t_{ox} = 750$ A, and the equivalent fixed oxide charge is $Q'_{ss} = 10^{11}$ cm^{-2}. The measured threshold voltage is $V_T = +0.80$ V. Determine the p-type doping concentration.

***11.12** Repeat Problem 11.11 for an n-type silicon substrate if the measured threshold voltage is $V_T = -1.50$ V. Determine the n-type doping concentration.

11.13 An Al–silicon dioxide–silicon MOS capacitor has an oxide thickness of 450 Å and a doping of $N_a = 10^{15}$ cm^{-3}. The oxide charge density is $Q'_{ss} = 3 \times 10^{11}$ cm^{-2}. Calculate (a) the flat-band voltage and (*b*) the threshold voltage. Sketch the electric field through the structure at the onset of inversion.

11.14 An n-channel depletion mode MOSFET with an n$^+$ polysilicon gate is shown in Figure 11.42. The n-channel doping is $N_d = 10^{15}$ cm^{-3}, and the oxide thickness is $t_{ox} = 500$ A. The equivalent fixed oxide charge is $Q'_{ss} = 10^{10}$ cm^{-2}. The n-channel thickness t_c is equal to the maximum induced space charge width. (Disregard the space charge region at the n-channel–p-substrate junction.) (a) Determine the channel thickness t_c, and (*b*) calculate the threshold voltage.

11.15 Consider an MOS capacitor with an n$^+$ polysilicon gate and n-type silicon substrate. Assume $N_a = 10^{16}$ cm^{-3} and let $E_F - E_c = 0.2$ eV in the n$^+$ polysilicon. Assume the oxide has a thickness of $t_{ox} = 300$ Å. Also assume that χ' (polysilicon) $= \chi'$ (single-crystal silicon). (a) Sketch the energy-band diagrams (*i*) for $V_G = 0$ and (ii) at flat band. (b) Calculate the metal–semiconductor work function difference. (c) Calculate the threshold voltage for the ideal case of zero fixed oxide charge and zero interface states.

11.16 The threshold voltage of an n-channel MOSFET is given by Equation (11.27). Plot V_T versus temperature over the range $200 \leq T \leq 450$ K. Consider both an aluminum gate and an n$^+$ polysilicon gate. Assume the work functions are independent of temperature and use device parameters similar to those in Example 11.4.

11.17 Plot the threshold voltage of an n-channel MOSFET versus p-type substrate doping concentration similar to Figure 11.20. Consider both n$^+$ and p$^+$ polysilicon gates. Use reasonable device parameters.

11.18 Plot the threshold voltage of a p-channel MOSFET versus n-type substrate doping concentration similar to Figure 11.21. Consider both n$^+$ and p$^+$ polysilicon gates. Use reasonable device parameters.

11.19 Consider an NMOS device with the parameters given in Problem 11.10. Plot V_T versus t_{ox} over the range $20 \leq t_{ox} \leq 500$ Å.

Section 11.2 Capacitance-Voltage Characteristics

11.20 An ideal MOS capacitor with an aluminum gate has a silicon dioxide thickness of $t_{ox} = 400$ Å on a p-type silicon substrate doped with an acceptor concentration of $N_a = 10^{16}$ cm^{-3}. Determine the capacitances C_{ox}, C'_{FB}, C'_{min}, and $C'(\text{inv})$ at (a) $f = 1$ Hz and (*b*) $f = 1$ MHz. (*c*) Determine V_{FB} and V_T. Sketch C'/C_{ox} versus V_G for parts (*a*) and (*b*).

11.21 Repeat Problem 11.20 for an n-type silicon substrate doped with a donor concentration of $N_d = 5 \times 10^{14}$ cm^{-3}.

***11.22** Using superposition, show that the shift in the flat-band voltage due to a fixed charge distribution $\rho(x)$ in the oxide is given by

$$\Delta V_{FB} = -\frac{1}{C_{ox}} \int_0^{t_{ox}} \frac{x\rho(x)}{t_{ox}}\, dx$$

***11.23** Using the results of Problem 11.22, calculate the shift in the flat-band voltage for the following oxide charge distributions: (*a*) $Q'_{ss} = 5 \times 10^{11}$ cm^{-2} is entirely located at the oxide-semiconductor interface. Let $t_{ox} = 750$ Å. (*b*) $Q'_{ss} = 5 \times 10^{11}$ cm^{-2} is uniformly distributed throughout the oxide. which has a thicknes of $t_{ox} = 750$ Å. (*c*) $Q'_{ss} = 5 \times 10^{11}$ cm^{-2} forms a triangular distribution with the peak at $x = t_{ox} = 750$ Å (the oxide–semiconductor interface) and which goes to zero at $x = 0$ (the metal–oxide interface).

11.24 An ideal MOS capacitor is fabricated by using intrinsic silicon and an n$^+$ polysilico gate. (a) Sketch the energy-band diagram through the MOS structure under flat-ban conditions. (b) Sketch the low-frequency *C-V* characteristics from negative to positive gate voltage.

11.25 Consider an MOS capacitor with a p-type substrate. Assume that donor-type interface traps exist only at midgap (i.e., at E_{Fi}). Sketch the high-frequency C-V curve from accumulation to inversion. Compare this sketch to the ideal C-Vplot.

11.26 Consider an SOS capacitor as shown in Figure 11.63. Assume the SiO$_2$ is ideal (no trapped charge) and has a thickness of $t_{ox} = 500$ Å. The doping concentrations are $N_d = 10^{16}$ cm^{-3} and $N_a = 10^{16}$ cm^{-3}, (*a*) Sketch the energy band diagram through the device for (*i*) flat-band, (ii) $V_G = +3$ V, and (*iii*) $V_G = -3$ V. (*b*) Calculate the flat-band voltage. (*c*) Estimate the voltage across the oxide for (*i*) $V_G = +3\,V$ and (*ii*) $V_G = -3\,V$. (d) Sketch the high-frequency *C-V* characteristic curve.

11.27 The high-frequency *C-V* characteristic curve of an MOS capacitor is shown in Figure 11.64. The area of the device is 2×10^{-3} cm'. The metal–semiconductor work function difference is $\phi_{ms} = -0.50$ V, the oxide is SiO$_2$, the semiconductor is silicon, and the semiconductor doping concentration is 2×10^{16} cm^{-3}. (a) Is the

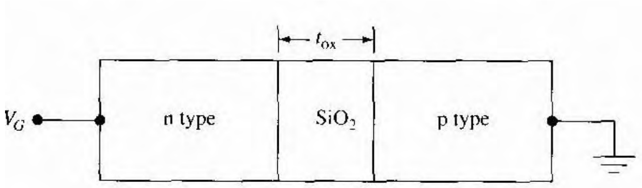

Figure 11.63 | Figure for Problem 11.26.

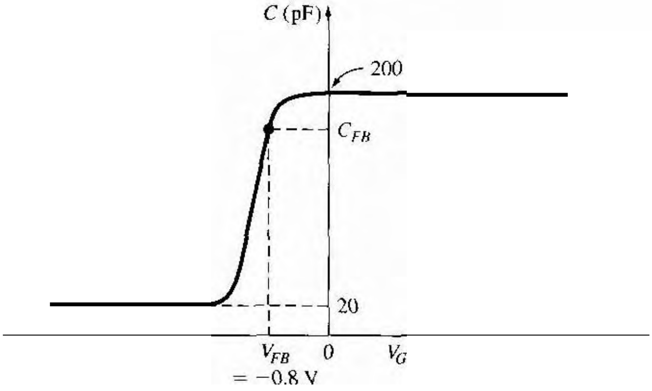

Figure **11.64** | Figure for Problem 112 7

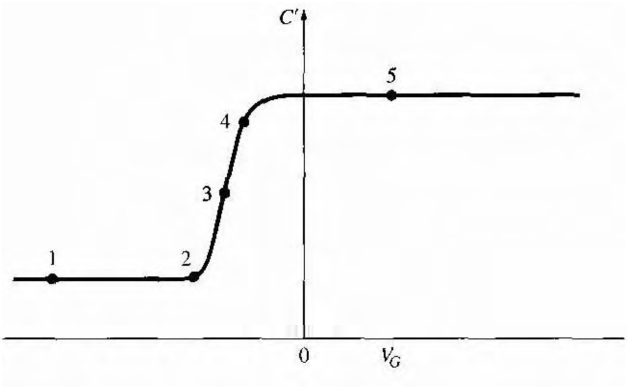

Figure 11.65 | Figure for Problem 11.28

semiconductor n or p type'?(*b*) What is the oxide thickness? ***(r)*** What is the equivalent trapped oxide charge density? (*d*) Determine the flat-hand capacitance.

11.28 Consider the high-frequency C-Vplot shown in Figure 11.65. (a) Indicate which points correspond to flat-band, inversion, accumulation, threshold, and depletion mode. (*b*) Sketch the energy band diagram in the semiconductor for each condition

Section 11.3 The Basic MOSFET Operation

11.29 An expression that includes the inversion charge density was given by Equation (11.55). Consider the definition of threshold voltage and show that the inversion charge density goes to zero at the drain terminal at saturation. (Hint: Let $V_x = V_{DS} = V_{DS}(\text{sat})$.)

11.30 An ideal n-channel MOSFET has the following parameters:

$$W = 30\ \mu\text{m} \qquad \mu_n = 450\ \text{cm}^2/\text{V-s}$$
$$L = 2\ \mu\text{m} \qquad t_{ox} = 350\ \text{A}$$
$$V_T = +0.80\ \text{V}$$

(*a*) Plot I_D versus V_{DS} for $0 \le V_{DS} \le 5$ V and for $V_{GS} = 0.\ 1, 2, 3.4,$ and 5 V. Indicate on each curve the $V_{DS}(\text{sat})$ point. (*b*) Plot $\sqrt{I_D(\text{sat})}$ versus V_{GS} for $0 \le V_{GS} \le 5$V. **(c)** Plot I_D versus V_{GS} for $V_{DS} = 0.1$ V and for $0 \le V_{GS} \le 5$V.

11.31 An ideal p-channel MOSFET has the following parameters:

$$W = 15\ \mu\text{m} \qquad \mu_p = 300\ \text{cm}^2/\text{V-s}$$
$$L = 1.5\ \mu\text{m} \qquad t_{ox} = 350\ \text{Å}$$
$$V_T = -0.80\ \text{V}$$

(a) Plot I_D versus V_{SD} for $0 \le V_{SD} \le 5$ V and for $V_{SG} = 0, 1, 2, 3, 4,$ and 5 V. Indicate on each curve the $V_{SD}(\text{sat})$ point. (*b*) Plot I_D versus V_{SG} for $V_{SD} = 0.1$ V and for $0 \le V_{SG} \le 5$ V.

11.32 Consider an n-channel MOSFET with the same parameters as given in Problem 11.30 except that $V_T = -2.0$V. (a) Plot I_D versus V_{DS} for $0 \le V_{DS} \le 5$ V and for $V_{GS} = -2, -1, 0, +1,$ and $+2$ V. (*b*) Plot $\sqrt{I_D(\text{sat})}$ versus V_{GS} for $-2\ 5\ V_{GS} \le +3$ V.

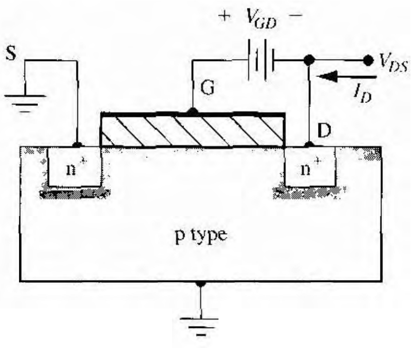

Figure **11.66** | Figure for Problem 11.33

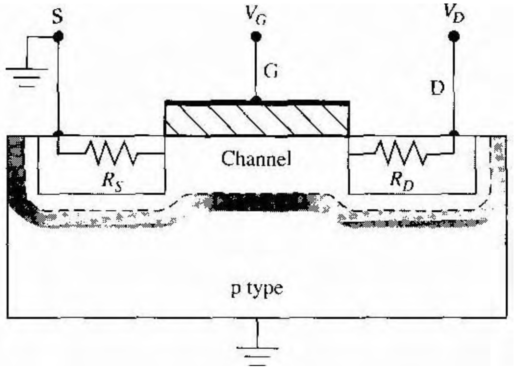

Figure **11.67** | Figure for Problem 11.34

11.33 Consider an n-channel enhancement mode MOSFET biased as shown in Figure 11.66. Sketch the current–voltage characteristics, I_D versus V_{DS}, for (*a*) $V_{GD} = 0$, (*b*) $V_{GD} = V_T/2$, and (*c*) $V_{GD} = 2V_T$.

11.34 Figure 11.67 shows the cross section of an NMOS device that includes source and drain resistances. These resistances take into account the bulk n^+ semiconductor resistance and the ohmic contact resistance. The current–voltage relations can be generated by replacing V_{GS} by $V_G - I_D R_S$ and V_{DS} by $V_D - I_D(R_S + R_D)$ in the ideal equations. Assume transistor parameters of $V_T = 1$ V and $K_n = 1$ mA/V^2 (a) Plot the following curves on the same graph: I_D versus V_D for $V_G = 2$ V and $V_G = 3$ V over the range $0 \le V_D \le 5$ V for (*i*) $R_S = R_D = 0$ and (*ii*) $R_S = R_D = 1$ kΩ. (b) Plot the following curves on the same graph: $\sqrt{I_D}$ versus V_G for $V_D = 0.1$ V and $V_D = 5$ V over the range $0 \le I_D \le 1$ mA for (*i*) $R_S = R_D = 0$ and (*ii*) $R_S = R_D = 1$ kΩ.

11.35 An n-channel MOSFET has the same parameters as given in Problem 11.30. The gate terminal is connected to the drain terminal. Plot I_D versus V_{DS} for $0 \le V_{DS} \le 5$ V. Determine the range of V_{DS} over which the transistor is biased in the nonsaturation and saturation regions.

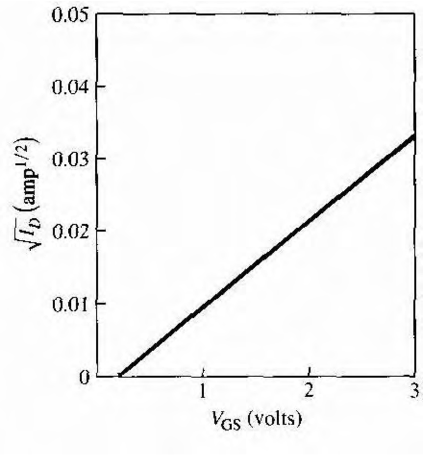

Figure 11.68 | Figure for Problem 11.37.

11.36 The channel conduclance for a p-channel MOSFET is defined as

$$g_d = \left.\frac{\partial I_D}{\partial V_{SD}}\right|_{V_{SD}\to 0}$$

Plot the channel conductance for the p-channel MOSFET in Problem 11.31 for $0 \le V_{SG} \le 5$ V.

1137 The experimental characteristics of an ideal n-channel MOSFET biased in the saturation region are shown in Figure 11.68. If $W/L = 10$ and $t_{ox} = 425$ Å, determine V_T and μ_n.

11.38 One curve of an n-channel MOSFET is characterized by the following parameters: $I_D(\text{sat}) = 2 \times 10^{-4}$ A, $V_{DS}(\text{sat}) = 4$ V, and $V_T = 0.8$ V.

(a) What is the gate voltage?
(*b*) What is the value of the conduction parameter?
(*c*) If $V_G = 2$ V and $V_{DS} = 2$ V, determine I_D.
(*d*) If $V_G = 3$ V and $V_{DS} = 1$ V, determine I_D
(e) For each of the conditions given in (c) and (d), sketch the inversion charge density and depletion region through the channel.

11.39 (*a*) An ideal n-channel MOSFET has an inversion carrier mobility $\mu_n = 525$ cm^2/V-s, a threshold voltage $V_T = +0.75$ V, and an oxide thickness $t_{ox} = 400$ Å. When biased in the saturation region, the required rated current is $I_D(\text{sat}) = 6$ mA when $V_{GS} = 5$ V. Determine the required W/L ratio. (*b*) A p-channel MOSFET has the same requirements when $V_{GS} = 5$ V and has the same parameters as part (*a*) except $\mu_p = 300$ cm^2/V-s and $V_T = -0.75$ V. Determine the W/L ratio.

11.40 Consider the transistor described in Problem 11.30. ***(a)*** Calculate g_{mL} for $V_{DS} = 0.5$ V. (*b*) Calculate g_{ms} for $V_{GS} = 4$ V.

11.41 Consider the transistor described in Problem 11.31. (a) Calculate g_{mL} for $V_{SD} = 0.5$ V. (*b*) Calculate g_{ms} for $V_{SG} = 4$ V.

11.42 An n-channel MOSFET has the following parameters:

$t_{ox} = 400$ A $\qquad N_a = 5 \times 10^{16}$ cm^{-3}

$V_{FB} = -0.5$ V $\qquad$ L = 2 μm

W = 10 μm $\qquad \mu_n = 450$ cm^2/V-s

Plot $\sqrt{I_D}$ versus V_{GS} over the range $0 \le I_D \le 1$ mA when the transistor is biased i the saturation region for the following values of source-to-body voltage: $V_{SB} = 0, 1, 2$ and 4 V.

11.43 Consider a p-channel MOSFET with $t_{ox} = 600$ Å and $N_d = 5 \times 10^{15}$ cm^{-3}. Determine the body-to-source voltage, V_{BS}, such that the shift in threshold voltage, ΔV_T, from the $V_{BS} = 0$ curve is $\Delta V_T = -1.5$ V.

11.44 An NMOS device has the following parameters: n$^+$ poly gate, $t_{ox} = 400$ A. N,, = 10^{15} cm^{-3}, and $Q'_{ss} = 5 \times 10^{10}$ cm^{-2}. (*a*) Determine V_T. (*b*) Is it possible to apply a V_{SB} voltage such that $V_T = 0$? If so, what is the value of V_{SB}?

11.45 Investigate the threshold voltage shift due to substrate bias. The threshold shift is given by Equation (11.72). Plat ΔV_I versus V_{SB} over the range $0 \le V_{SB} \le 5$ Vfor several values of N_a and I,,, . Determine the conditions for which AV_I is limited to a maximum value of 0.7 V over the range of V_{SB}

Section 11.4 Frequency Limitations

11.46 Consider an ideal n-channel MOSFET with a width-to-length ratio of $(W/L) = 10$, an electron mobility of $\mu_n = 400$ cm^2/V-s, an oxide thickness of $t_{ox} = 475$ Å, anda threshold voltage of $V_T = +0.65$ V. (a)Determine the maximum value of source resistance so that the saturation transconductance g_{ms} is reduced by no more than 20 percent from its ideal value when $V_{GS} = 5$ V. (*b*) Using the value of **r**, calculated in part (*a*), how much is g_{ms} reduced from its ideal value when $V_{GS} = 3$ V!

11.47 An n-channel MOSFET has the following parameters:

$\mu_n = 400$ cm^2/V-s $\qquad$ I,,, = 500 A

L = 2 μm $\qquad$ W = 20 μm

$V_I = +0.75$ V

Assume the transistor is biased in the saturation region at $V_{GS} = 4$ V. (*a*) Calculate the ideal cutoff frequency. (b) Assume that the gate oxide overlaps both the source and drain contacts by 0.75 μm. If a load resistance of $R_L = 10$ kΩ is connected to the output. calculate the cutoff frequency.

11.48 Repeat Problem 11.47 for the case when the electrons are traveling at a saturation velocity of $v_{sat} = 4 \times 10^6$ cm/s.

Summary and Review

***11.49** Design **an** ideal silicon n-channel MOSFET with a polysilicon gate to have a threshold voltage of $V_T = 0.65$ V Assume an oxide thickness of I,,, = 300 Å, a channel length of L = 1.25 μm, and a nominal value of $Q'_{ss} = 1.5 \times 10^{11}$ cm^{-2}. It is desired to have a drain current of $I_D = 50$ μA at $V_{GS} = 2.5$ V and $V_{DS} = 0.1$ V. Determine the substrate doping concentration, channel width. and type of gale required.

***11.50** Design an ideal silicon n-channel depletion mode MOSFET with a polysilicon gate to have a threshold voltage of $V_T = -0.65$ V. Assume an oxide thickness of $t_{ox} = 300$ Å, a channel length of L = 1.25 μm, and a nominal value of Q'_{ss} = 1.5 x 10^{11} cm^{-2}. It is desired to have a drain current of $I_D(\text{sat}) = 50\ \mu$A at $V_{GS} = 0$. Determine the type of gate, substrate doping concentration, and channel width required.

***11.51** Consider the CMOS inverter circuit shown in Figure 11.60a. Ideal n- and p-channel devices are to be designed with channel lengths of L = 2.5 μm and oxide thicknesses of t_{ox} = 450 Å. Assume the inversion channel mobilities are one-half the bulk values. The threshold voltages of the n and p-channel transistors are to be +0.5 V and −0.5 V, respectively. The drain current is to be $I_D = 0.256$ mA when the input voltage to the inverter is 1.5 V and 1.5 V with $V_{DD} = 5$ V. The gate material is to be the same in each device. Determine the type of gate, substrate doping concentrations, and channel widths.

***11.52** A complementary pair of ideal n-channel and p-channel MOSFETs are to be designed to produce the same *I–V* characteristics when they are equivalently biased. The devices are to have the same oxide thickness of 250 Å and the same channel length of L = 2 μm. Assume the SiO_2 layer is ideal. The n-channel device is to have a channel width of W = 20 μm. Assume constant inversion layer mobilities of μ_n = 600 cm^2/V-s and μ_p = 220 cm^2/V-s. (*a*) Determine p-type and n-type substrate doping concentrations. (*b*) What are the threshold voltages? (*c*) What is the width of the p-channel device?

READING LIST

1. Dimitrijev, S. *Understanding Semiconductor Devices.* New York: Oxford University Press, 2000.
2. Kano, K. *Semiconductor Devices.* Upper Saddle River, NJ: Prentice Hall, 1998.
3. Muller, R. S., and T. I. Kamins. *Device Electronics for Integrated Circuits.* 2nd ed. New York: Wiley, 1986.
4. Ng, K. K. *Complete Guide to Semiconductor Devices.* New York: McGraw-Hill, 1995.
5. Nicollian, E. H., and J. R. Brews. *MOS Physics and Technology.* New York: Wiley, 1982.
6. Ong, D. G. *Modern MOS Technology: Processes, Devices, and Design.* New York: McGraw-Hill, 1984.
7. Pirrret, R. F. *Semiconductor Device Fundamentals.* Reading, MA: Addison-Wesley, 1996.
8. Roulston, D. J. *An Introduction to the Physics of Semiconductor Devices.* New York: Oxford University Press, 1999.
9. Schroder, D. K. *Advanced MOS Devices, Modular Series on Solid State Devices.* Reading, MA: Addison-Wesley, 1987.
10. Shur, M. *Introduction to Electronic Devices.* New York: John Wiley & Sons, Inc., 1996.

*11. Shur, M. Physics *of Semiconductor Devices.* Englewood Cliffs, NJ: Prentice Hall, 1990.

12. Singh, J. *Semiconductor Devices: An Introduction.* New York: McGraw-Hill, 1994.
13. Singh, J. *Semiconductor Devices: Basic Principles.* New York: Wiley, 2001
14. Streetman, B. G., and S. Banerjee. *Solid State Electronic Devices.* 5th ed. Upper Saddle River, NJ: Prentice Hall, 2000.

15. Sze, S. M. ***High-speed Semiconductor Devices.*** New York: Wiley. 1990.

16. Sze, S. M. ***Physics of Semiconductor Devices.*** 2nd ed. New York: Wiley, 1981.

17.** Taur, Y., and T. H. Ning. ***Fundamentals of Modem VLSI Devices. New York: Cambridge University Press, 1998.

18.** Tsividis, Y. ***Operation and Modeling of the MOS Transistor. 2nd ed. Burr Ridge, IL.: McGraw-Hill, 1999.

19. Werner, W. M. "The Work Function Difference of the MOS System with Aluminum Field Plates and Polycrystalline Silicon Field Plates." *Solid State Electronics* 17 (1974), pp. 769–75.

20. Yamaguchi, T., S. Monmoto, G. H. Kawamoto, and J. C. DeLacy. "Process and Device Performance of 1 μm-Channel n-Well CMOS Technology." ***IEEE Transactions on Electron Devices*** ED-31 (February 1984), pp. 205–14.

21. Yang, E. S. ***Microelectronic Devices.*** New York: McGraw-Hill, 1988.

APPENDIX

A

Selected List of Symbols

This list does not include some symbols that are defined and used specifically in only one section. Some symbols have more than one meaning; however, the context in which the symbol is used should make the meaning unambiguous. The usual unit associated with each symbol is given.

	Unit cell dimension (Å), potential well width, acceleration, gradient of impurity concentration, channel thickness of a one-sided JFET (cm)
a_0	Bohr radius (Å)
c	Speed of light (cm/s)
d	Distance (cm)
e	Electronic charge (magnitude) (C), Napierian base
f	Frequency (Hz)
$f_F(E)$	Fermi–Dirac probability function
f_T	Cutoff frequency (Hz)
g	Generation rate (cm^{-3} s^{-1})
g'	Generation rate of excess carriers (cm^{-3} s^{-1})
$g(E)$	Density of states function (cm^{-3} eV^{-1})
g_c, g_v	Density of states function in the conduction band and valence band (cm^{-3} eV^{-1})
g_d	Channel conductance (S), small-signal diffusion conductance (S)
g_m	Transconductance (A/V)
g_n, g_p	Generation rate for electrons and holes (cm^{-3} s^{-1})
h	Planck's constant (J-s), induced space charge width in a JFET (cm)
$\hbar$	Modified Planck's constant ($h/2\pi$)

h_f	Small-signal common emitter current gain
j	Imaginary constant, $\sqrt{-1}$
k	Boltzmann's constant (J/K), wavenumber (cm^{-1})
k_n	Conduction parameter (A/V^2)
m	Mass (kg)
m_0	Rest mass of the electron (kg)
m^*	Effective mass (kg)
m_n^*, m_p^*	Effective mass of an electron and hole (kg)
n	Integer
n, l, m, s	Quantum numbers
n, p	Electron and hole concentration (cm^{-3})
$\bar{n}$	Index of refraction
n', p'	Constants related to the trap energy (cm^{-3})
n_{B0}, p_{E0}, p_{C0}	Thermal-equilibrium minority carrier electron concentration in the base and minority carrier hole concentration in the emitter and collector (cm^{-3})
n_d	Density of electrons in the donor energy level (cm^{-3})
n_i	Intrinsic concentration of electrons (cm^{-3})
n_0, p_0	Thermal-equilibrium concentration of electrons and holes (cm^{-3})
n_p, p_n	Minority carrier electron and minority carrier hole concentration (cm^{-3})
n_{p0}, p_{n0}	Thermal-equilibrium minority carrier electron and minority carrier hole concentration (cm^{-3})
n_s	Density of a two-dimensional electron gas (cm^{-2})
p	Momentum
p_a	Density of holes in the acceptor energy level (cm^{-3})
p_i	Intrinsic hole concentration ($= n_i$)(cm^{-3})
q	Charge (C)
r, θ, ϕ	Spherical coordinates
r_d, r_π	Small-signal diffusion resistance (Ω)
r_{ds}	Small-signal drain-to-source resistance (Ω)
s	Surface recombination velocity (cm/s)
t	Time (s)
t_d	Delay time (s)
t_{ox}	Gate oxide thickness (cm or A)
t_s	Storage time (s)
$u(x)$	Periodic wave function
v	Velocity (cm/s)
v_d	Carrier drift velocity (cm/s)

v_{ds}, v_s, v_{sat}	Carrier saturation drift velocity (cm/s)
x, y, z	Cartesian coordinates
x	Mole fraction in compound semiconductors
x_B, x_E, x_C	Neutral base, emitter, and collector region widths (cm)
x_d	Induced space charge width (cm)
x_{dT}	Maximum space charge width (cm)
x_n, x_p	Depletion width from the metallurgical junction into n-type and p-type semiconductor regions (cm)
A	Area (cm^2)
A^*	Effective Richardson constant ($\text{A/K}^2/\text{cm}^2$)
B	Magnetic flux density (Wb/m^2)
B, E, C	Base, emitter, and collector
BV_{CBO}	Breakdown voltage of collector-base junction with emitter open (volt)
BV_{CEO}	Breakdown voltage of collector-emitter with base open (volt)
C	Capacitance (F)
C'	Capacitance per unit area (F/cm^2)
C_d, C_π	Diffusion capacitance (F)
C_{FB}	Flat-band capacitance (F)
C_{gs}, C_{gd}, C_{ds}	Gate-source, gate-drain, and drain-source capacitance (F)
C'_j	Junction capacitance per unit area (F/cm^2)
C_M	Miller capacitance (F)
C_n, C_p	Constants related to capture rate of electrons and holes
C_{ox}	Gate oxide capacitance per unit area (F/cm^2)
C_μ	Reverse-biased B-C junction capacitance (F)
D, S, G	Drain, source, and gate of an FET
D'	Ambipolar diffusion coefficient ($\text{cm}^2\text{/s}$)
D_B, D_E, D_C	Base, emitter, and collector minority carrier diffusion coefficients ($\text{cm}^2\text{/s}$)
D_{it}	Density of interface states (#/eV-cm^3)
D_n, D_p	Minority carrier electron and minority carrier hole diffusion coefficient ($\text{cm}^2\text{/s}$)
E	Energy (joule or eV)
E_a	Acceptor energy level (eV)
E_c, E_v	Energy at the bottom edge of the conduction band and top edge of the valence band (eV)
AE,, AE,	Difference in conduction band energies and valence band energies at a heterojunction (eV)
	Donor energy level (eV)

E_F	Fermi energy (eV)
E_{Fi}	Intrinsic Fermi energy (eV)
E_{Fn}, E_{Fp}	Quasi-Fermi energy levels for electrons and holes (eV)
E_g	Bandgap energy (eV)
ΔE_g	Bandgap narrowing factor (eV), difference in bandgap energies at a heterojunction (eV)
E_t	Trap energy level (eV)
F	Force (N)
F_n^-, F_p^+	Electron and hole particle flux ($\text{cm}^{-2}\,\text{s}^{-1}$)
$F_{1/2}(\eta)$	Fermi–Dirac integral function
G	Generation rate of electron-hole pairs ($\text{cm}^{-3}\,\text{s}^{-1}$)
G_L	Excess carrier generation rate ($\text{cm}^{-3}\,\text{s}^{-1}$)
G_{n0}, G_{p0}	Thermal equilibrium generation rate for electrons and holes ($\text{cm}^{-3}\,\text{s}^{-1}$)
G_{01}	Conductance (S)
I	Current (A)
I_A	Anode current (A)
I_B, I_E, I_C	Base, emitter, and collector current (A)
I_{CBO}	Reverse-bias collector-base junction current with emitter open (A)
I_{CEO}	Reverse-bias collector–emitter current with base open (A)
I_D	Diode current (A), drain current (A)
$I_D(\text{sat})$	Saturation drain current (A)
I_L	Photocurrent (A)
I_{P1}	Pinchoff current (A)
I_S	Ideal reverse-bias saturation current (A)
I_{SC}	Short-circuit current (A)
I_ν	Photon intensity (energy/cm^2/s)
J	Electric current density (A/cm^2)
J_{gen}	Generation current density (A/cm^2)
J_L	Photocurrent density (A/cm^2)
J_n, J_p	Electron and hole electric current density (A/cm^2)
J_n^-, J_p^+	Electron and hole particle current density ($\text{cm}^{-2}\,\text{s}^{-1}$)
J_{rec}	Recombination current density (A/cm^2)
J_{r0}	Zero-bias recombination current density (A/cm^2)
J_R	Reverse-bias current density (A/cm^2)
J_S	Ideal reverse-bias saturation current density (A/cm^2)
J_{sT}	Ideal reverse saturation current density in a Schottky diode (A/cm^2)
L	Length (cm), inductance (H), channel length (cm)

ΔL	Channel length modulation factor (cm)
L_B, L_E, L_C	Minority carrier diffusion length in the base, emitter, and collector (cm)
L_D	Debye length (cm)
L_n, L_p	Minority carrier electron and hole diffusion length (cm)
M, M_n	Multiplication constant
N	Number density (cm^{-3})
N_a	Density of acceptor impurity atoms (cm^{-3})
N_B, N_E, N_C	Base, emitter, and collector doping concentrations (cm^{-3})
N_c, N_v	Effective density of states function in the conduction band and valence band (cm^{-3})
N_d	Density of donor impurity atoms (cm^{-3})
N_{it}	Interface state density (cm^{-2})
N_t	Trap density (cm^{-3})
P	Power (watt)
$P(r)$	Probability density function
Q	Charge (C)
Q'	Charge per unit area (C/cm^2)
Q_B	Gate controlled bulk charge (C)
Q'_n	Inversion channel charge density per unit area (C/cm^2)
Q'_{sig}	Signal charge density per unit area (C/cm^2)
$Q'_{SD}(\text{max})$	Maximum space charge density per unit area (C/cm^2)
Q'_{SS}	Equivalent trapped oxide charge per unit area (C/cm^2)
R	Reflection coefficient, recombination rate ($\text{cm}^{-3}\,\text{s}^{-1}$), resistance (52)
$R(r)$	Radial wave function
R_c	Specific contact resistance ($\Omega\text{-cm}^2$)
R_{cn}, R_{cp}	Capture rate for electrons and holes ($\text{cm}^{-3}\,\text{s}^{-1}$)
R_{en}, R_{ep}	Emission rate for electrons and holes ($\text{cm}^{-3}\,\text{s}^{-1}$)
R_n, R_p	Recombination rate for electrons and holes ($\text{cm}^{-3}\,\text{s}^{-1}$)
R_{n0}, R_{p0}	Thermal equilibrium recombination rate of electrons and holes ($\text{cm}^{-3}\,\text{s}^{-1}$)
	Temperature (K), kinetic energy (J or eV), transmission coefficient
V	Potential (volt), potential energy (J or eV)
V_a	Applied forward-bias voltage (volt)
V_A	Early voltage (volt), anode voltage (volt)
V_{bi}	Built-in potential barrier (volt)
V_B	Breakdown voltage (volt)
V_{BD}	Breakdown voltage at the drain (volt)

V_{BE}, V_{CB}, V_{CE}	Base-emitter, collector-base, and collector-emitter voltage (volt)
V_{DS}, V_{GS}	Drain-source and gate-source voltage (volt)
$V_{DS}(\text{sat})$	Drain-source saturation voltage (volt)
V_{FB}	Flat-band voltage (volt)
V_G	Gate voltage (volt)
V_H	Hall voltage (volt)
V_{oc}	Open-circuit voltage (volt)
V_{ox}	Potential difference across an oxide (volt)
V_{p0}	Pinchoff voltage (volt)
V_{pt}	Punch-through voltage (volt)
V_R	Applied reverse-bias voltage (volt)
V_{SB}	Source-body voltage (volt)
V_t	Thermal voltage (kT/e)
V_T	Threshold voltage (volt)
ΔV_T	Threshold voltage shift (volt)
W	Total space charge width (cm), channel width (cm)
W_B	Metallurgical base width (cm)
Y	Admittance
α	Photon absorption coefficient (cm^{-1}), ac common base current gain
α_n, α_p	Electron and hole ionization rates (cm^{-1})
α_0	dc common base current gain
α_T	Base transport factor
β	Common-emitter current gain
γ	Emitter injection efficiency factor
δ	Recombination factor
$\delta n, \delta p$	Excess electron and hole concentration (cm^{-3})
$\delta n_p, \delta p_n$	Excess minority carrier electron and excess minority carrier hole concentration (cm^{-3})
ϵ	Permittivity (F/cm^2)
ϵ_0	Permittivity of free space (F/cm^2)
ϵ_{ox}	Permittivity of an oxide (F/cm^2)
ϵ_r	Relative permittivity or dielectric constant
ϵ_s	Permittivity of a semiconductor (F/cm^2)
λ	Wavelength (cm or μm)
μ	Permeability (H/cm)
μ'	Ambipolar mobility ($\text{cm}^2/\text{V-s}$)
μ_n, μ_p	Electron and hole mobility ($\text{cm}^2/\text{V-s}$)

	Permeability of free space (H/cm)
	Frequency (Hz)
	Resistivity (R-cm), volume charge density (C/cm^3)
σ	Conductivity (Ω^{-1} cm^{-1})
$\Delta\sigma$	Photoconductivity (Ω^{-1} cm^{-1})
σ_i	Intrinsic conductivity (Ω^{-1} cm^{-1})
σ_n, σ_p	Conductivity of n-type and p-type semiconductor (Ω^{-1} cm^{-1})
τ	Lifetime (s)
τ_n, τ_p	Electron and hole lifetime (s)
τ_{n0}, τ_{p0}	Excess minority carrier electron and hole lifetime (s)
τ_0	Lifetime in space charge region (s)
ϕ	Potential (volt)
$\phi(t)$	Time-dependent wave function
$\Delta\phi$	Schottky barrier lowering potential (volt)
ϕ_{Bn}	Schottky barrier height (volt)
ϕ_{B0}	Ideal Schottky barrier height (volt)
ϕ_{fn}, ϕ_{fp}	Potential difference (magnitude) between E_{Fi} and E_F in n-type and p-type semiconductor (volt)
ϕ_{Fn}, ϕ_{Fp}	Potential difference (with sign) between E_{Fi} and E_F in n-type and p-type semiconductor (volt)
ϕ_m	Metal work function (volt)
ϕ'_m	Modified metal work function (volt)
ϕ_{ms}	Metal-semiconductor work function difference (volt)
ϕ_n, ϕ_p	Potential difference (magnitude) between E_c and E_F in n-type and between E_v and E_F in p-type semiconductor (volt)
ϕ_s	Semiconductor work function (volt). surface potential (volt)
χ	Electron affinity (volt)
χ'	Modified electron affinity (volt)
$\psi(x)$	Time-independent wave function
ω	Radian frequency (s^{-1})
Γ	Reflection coefficient
E	Electric field (V/cm)
E_H	Hall electric field (V/cm)
E_{crit}	Critical electric field at breakdown (V/cm)
$\Theta(\theta)$	Angular wave function
Φ	Photon flux (cm^{-2} s^{-1})
$\Phi(\phi)$	Angular wave function
$\Psi(x, t)$	Total wave function

APPENDIX

B

System of Units, Conversion Factors, and General Constants

Table B.1 | International system of units*

Quantity	Unit	Symbol	Dimension
Length	meter	m	
Mass	kilogram	kg	
Time	second	s or sec	
Temperature	kelvin	K	
Current	ampere	A	
Frequency	hertz	Hz	1/s
Force	newton	N	kg-m/s^2
Pressure	pascal	Pa	N/m^2
Energy	joule	J	N-m
Power	watt	W	J/s
Electric charge	coulomb	C	A-s
Potential	volt	V	J/C
Conductance	siemens	S	AN
Resistance	ohm	Ω	V/A
Capacitance	farad	F	C N
Magnetic flux	weber	Wb	V-s
Magnetic flux density	tesla	T	Wb/m^2
Inductance	henry	H	Wb/A

*The cm is the common unit of length and the electron-volt is the common unit of energy *(see* Appendix F) used in the study of semiconductors. However. the joule and in some cases the meter should be used in moat formulas.

Table B.2 | Conversion factors

1 Å (angstrom) = 10^{-8} cm = 10^{-10} m
1 μm (micron) = 10^{-4} cm
1 mil = 10^{-3} in. = 25.4 μm
2.54 cm = 1 in.
1 eV = 1.6 x 10^{-19} J
1 J = 10^{7} erg

Prefixes		
10^{-15}	femto-	= f
10^{-12}	pico-	= p
10^{-9}	nano-	= n
10^{-6}	micro-	= μ
10^{-3}	milli-	= m
10^{+3}	kilo-	= k
10^{+6}	mega-	= M
10^{+9}	giga-	= G
10^{+12}	tera	= T

Table B.3 | Physical constants

Avogadro's number	$N_A = 6.02 \times 10^{+23}$ atoms per gram molecular weight
Boltzmann's constant	$k = 1.38 \times 10^{-23}$ J/K $= 8.62 \times 10^{-5}$ eV/K
Electronic charge (magnitude)	$e = 1.60 \times 10^{-19}$ C
Free electron rest mass	$m_0 = 9.11 \times 10^{-31}$ kg
Permeability of free space	$\mu_0 = 4\pi \times 10^{-7}$ Wm
Permittivity of free space	$\epsilon_0 = 8.85 \times 10^{-14}$ F/cm $= 8.85 \times 10^{-12}$ F/m
Planck's constant	$h = 6.625 \times 10^{-34}$ J-s $= 4.135 \times 10^{-15}$ eV-s $\frac{h}{2\pi} = \hbar = 1.054 \times 10^{-34}$ J-s
Proton rest mass	$M = 1.67 \times 10^{-27}$ kg
Speed of light in vacuum	$c = 2.998 \times 10^{10}$ cm/s
Thermal voltage ($T = 300$ K)	$V_t = \frac{kT}{e} = 0.0259$ volt $kT = 0.0259$ eV

Table **B.4** | Silicon, gallium arsenide, and germanium properties ($T = 300$ K)

Property	**Si**	**GaAs**	**Ge**
Atoms (cm^{-3})	5.0×10^{22}	4.42×10^{22}	4.42×10^{22}
Atomic weight	28.09	144.63	72.60
Crystal structure	Diamond	Zincblende	Diamond
Density (g/cm^{-3})	2.33	5.32	5.33
Lattice constant (Å)	5.43	5.65	5.65
Melting point (°C)	1415	1238	937
Dielectric constant	11.7	13.1	16.0
Bandgap energy (eV)	1.12	1.42	0.66
Electron affinity. χ (volts)	4.01	4.07	4.13
Effective density of states in conduction band, N_c (cm^{-3})	2.8×10^{19}	4.7×10^{17}	1.04×10^{19}
Effective density of states in valence band. N_v (cm^{-3})	1.04×10^{19}	7.0×10^{18}	6.0×10^{18}
Intrinsic carrier concentration (cm^{-3})	1.5×10^{10}	1.8×10^{6}	2.4×10^{13}
Mobility ($\text{cm}^2/\text{V-s}$)			
Electron, μ_n	1350	8500	3900
Hole, μ_p	480	400	1900
Effective mass $\left(\dfrac{m^*}{m_0}\right)$			
Electrons	$m_l^* = 0.98$	0.067	1.64
	$m_t^* = 0.19$		0.082
Holes	$m_{lh}^* = 0.16$	0.082	0.044
	$m_{hh}^* = 0.49$	0.45	0.28
Effective mass (density of states)			
Electrons $\left(\dfrac{m_n^*}{m_0}\right)$	1.08	0.067	0.55
Holes $\left(\dfrac{m_p^*}{m_0}\right)$	0.56	0.48	0.37

Table **B.5** | Other semiconductor parameters

Material	E_g (eV)	a (Å)	ϵ_r	χ	n
Aluminum arsenide	2.16	5.66	12.0	3.5	2.97
Gallium phosphide	2.26	5.45	10	4.3	3.37
Aluminum phosphide	2.43	5.46	9.8		3.0
Indium phosphide	1.35	5.87	12.1	4.35	3.37

Table R.6 | Properties of SiO_2 and Si_3N_4 ($T = 300$ K)

Property	**SiO_2**	**Si_3N_4**
Crystal structure	[Amorphous for most integrated circuit applications]	
Atomic or molecular density (cm^{-3})	2.2×10^{22}	1.48×10^{22}
Density ($g\text{-}cm^{-3}$)	2.2	**3.4**
Energy gap	≈ 9 eV	4.7 eV
Dielectric constant	3.9	7.5
Melting point (°C)	≈ 1700	≈ 1900

APPENDIX C

The Periodic Table

	Group I		Group II		Group III		Group IV		Group V		Group VI		Group VII		Group VIII	
Period	a	b	a	b	a	b	a	b	a	b	a	b	a	b	a	b
I	1 H 1.0079															2 He 4.003
II	3 Li 6.94		4 Be 9.02			5 B 10.82		6 C 12.01		7 N 14.01		8 O 16.00		9 F 19.00		10 Ne 20.18
III	11 Na 22.99		12 Mg 24.32			13 Al 26.97		14 Si 28.06		15 P 30.98		16 S 32.06		17 Cl 35.45		18 Ar 39.94
IV	19 K 39.09	29 Cu 63.54	20 Ca 40.08	30 Zn 65.38	21 Sc 44.96	31 Ga 69.72	22 Ti 47.90	32 Ge 72.60	23 V 50.95	33 As 74.91	24 Cr 52.01	34 Se 78.96	25 Mn 54.93	35 Br 79.91	26 Fe 55.85 27 Co 58.94 28 Ni 58.69	36 Kr 83.7
V	37 Rb 85.48	47 Ag 107.88	38 Sr 87.63	48 Cd 112.41	39 Y 88.92	49 In 114.76	40 Zr 91.22	50 Sn 118.70	41 Nb 92.91	51 Sb 121.76	42 Mo 95.95	52 Te 127.61	43 Tc 99	53 I 126.92	44 Ru 101.7 45 Rh 102.91 46 Pd 106.4	54 Xe 131.3
VI	55 Cs 132.91	79 Au 197.2	56 Ba 137.36	80 Hg 200.61	57–71 *Rare earths*	81 Tl 204.39	72 Hf 178.6	82 Pb 207.21	73 Ta 180.88	83 Bi 209.00	74 W 183.92	84 Po 210	75 Re 186.31	85 At 211	76 Os 190.2 77 Ir 193.1 28 Pt 195.2	86 Rn 222
VII	87 Fr 223		88 Ra 226.05		89 Ac 227		90 Th 232.12		91 Pa 231		92 U 238.07 93 Np 237 94 Pu 239 95 Am 241 96 Cm 242 97 Bk 246 98 Ct 249 99 Es 254 100 Fm 256 101 Md 256					

Rare earths

VI	57La	58 Ce	59 R	60 Nd	61 Pm	62 Sm	63 Eu	M Gd	65 Tb	66 Dy	67 Ho	68 Er	69Tm	70 Yb	71 Lu
57-71	138.92	140.13	140.92	144.27	147	150.43	152.0	156.9	159.2	162.46	164.90	167.2	169.4	173.04	174.99

The numbers in front of the symbols of the elements denote the atomic numbers; the numbers underneath are the atomic weights.

APPENDIX

The Error Function

$$\mathrm{erf}(z) = \frac{2}{\sqrt{\pi}} \int_0^z e^{-t^2}\, dt$$

$$\mathrm{erf}(0) = 0 \qquad \mathrm{erf}(\infty) = 1$$

$$\mathrm{erfc}(z) = 1 - \mathrm{erf}(z)$$

z	**erf(z)**	z	**erf(z)**
0.00	0.00000	1.00	0.84270
0.05	0.05637	1.05	0.86244
0.10	0.11246	1.10	0.88021
0.15	0.16800	1.15	0.89612
0.20	0.22270	1.20	0.91031
0.25	0.27633	1.25	0.92290
0.30	0.32863	1.30	0.93401
0.35	0.37938	1.35	0.94376
0.40	0.42839	1.40	0.95229
0.45	0.47548	1.45	0.95970
0.50	0.52050	1.50	0.96611
0.55	0.56332	1.55	0.97162
0.60	0.60386	1.60	0.97635
0.65	0.64203	1.65	0.98038
0.70	0.67780	1.70	0.98379
0.75	0.71116	1.75	0.98667
0.80	0.74210	1.80	0.98909
0.85	0.77067	1.85	0.99111
0.90	0.79691	1.90	0.99279
0.95	0.82089	1.95	0.99418
1.00	0.84270	2.00	0.99532

APPENDIX E

"Derivation" of Schrodinger's Wave Equation

Schrodinger's wave equation was stated in Equation ***(2.6)*.**The time-independent form of Schrodinger's wave equation was then developed and given by Equation ***(2.13)*.**The time-independent Schrodinger's wave equation can also be developed from the classical wave equation. We may think of this development more in terms of a justification of the Schrodinger's time-independent wave equation rather than a strict derivation.

The time-independent classical wave equation, in terms of voltage, is given as

$$\frac{\partial^2 V(x)}{\partial x^2} + \left(\frac{\omega^2}{v_p^2}\right) V(x) = 0 \tag{E.1}$$

where ω is the radian frequency and v_p is the phase velocity.

If we make a change of variable and let $\psi(x) = V(x)$, then we have

$$\frac{\partial^2 \psi(x)}{\partial x^2} + \left(\frac{\omega^2}{v_p^2}\right) \psi(x) = 0 \tag{E.2}$$

We can write that

$$\frac{\omega^2}{v_p^2} = \left(\frac{2\pi\nu}{v_p}\right)^2 = \left(\frac{2\pi}{\lambda}\right)^2 \tag{E.3}$$

where v and A are the wave frequency and wavelength, respectively.

From the wave-particle duality principle, we can relate the wavelength and momentum as

$$\lambda = \frac{h}{p} \tag{E.4}$$

Then

$$\left(\frac{2\pi}{\lambda}\right)^2 = \left(\frac{2\pi}{h} \cdot p\right)^2 \tag{E.5}$$

and since $\hbar = \frac{h}{2\pi}$, we can write

$$\left(\frac{2\pi}{\lambda}\right)^2 = \left(\frac{p}{\hbar}\right)^2 = \frac{2m}{\hbar^2}\left(\frac{p^2}{2m}\right) \tag{E.6}$$

Now

$$\frac{p^2}{2m} = T = E - V \tag{E.7}$$

where T, E, and V are the kinetic energy, total energy, and potential energy terms. respectively.

We can then write

$$\frac{\omega^2}{v_p^2} = \left(\frac{2\pi}{\lambda}\right)^2 = \frac{2m}{\hbar^2}\left(\frac{p^2}{2m}\right) = \frac{2m}{\hbar^2}(E - V) \tag{E.8}$$

Substituting Equation (E.8) into Equation (E.2), we have

$$\frac{\partial^2 \psi(x)}{\partial x^2} + \frac{2m}{\hbar^2}(E - V)\psi(x) = 0 \tag{E.9}$$

which is the one-dimensional, time-independent Schrodinger's wave equation

APPENDIX F

Unit of Energy—The Electron-Volt

The electron-volt (eV) is a unit of energy that is used constantly in the study of semiconductor physics and devices. This short discussion may help in "getting a feel" for the electron-volt.

Consider a parallel plate capacitor with an applied voltage as shown in Figure F.1. Assume that an electron is released at $x = 0$ at time $t = 0$. We may write

$$F = m_0 a = m_0 \frac{d^2x}{dt^2} = eE \tag{F.1}$$

where e is the magnitude of the electronic charge and E is the magnitude of the electric field as shown. Upon integrating, the velocity and distance versus time are given by

$$v = \frac{eEt}{m_0} \tag{F.2}$$

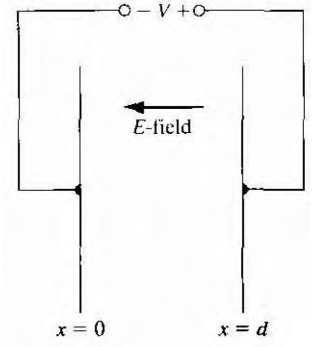

Figure F.1 | Parallel plate capacitor.

and

$$x = \frac{eEt^2}{2m_0} \tag{F.3}$$

where we have assumed that $v = 0$ at $t = 0$.

Assume that at $t = t_0$ the electron reaches the positive plate of the capacitor so that $x = d$. Then

$$d = \frac{eEt_0^2}{2m_0} \tag{F.4a}$$

or

$$t_0 = \sqrt{\frac{2m_0d}{eE}} \tag{F.4b}$$

The velocity of the electron when it reaches the positive plate of the capacitor is

$$v(t_0) = \frac{eEt_0}{m_0} = \sqrt{\frac{2eEd}{m_0}} \tag{F.5}$$

The kinetic energy of the electron at this time is

$$T = \frac{1}{2}m_0v(t_0)^2 = \frac{1}{2}m_0\left(\frac{2eEd}{m_0}\right) = eEd \tag{F.6}$$

The electric field is

$$E = \frac{V}{d} \tag{F.7}$$

so that the energy is

$$T = e \cdot V \tag{F.8}$$

If an electron is accelerated through a potential of 1 volt, then the energy is

$$T = e \cdot V = (1.6 \times 10^{-19})(1) = 1.6 \times 10^{-19} \text{ joule} \tag{F.9}$$

The electron-volt (eV) unit of energy is defined as

$$\text{Electron-volt} = \frac{\text{joule}}{e} \tag{F.10}$$

Then, the electron that is accelerated through a potential of 1 volt will have an energy of

$$T = 1.6 \times 10^{-19}\ J = \frac{1.6 \times 10^{-19}}{1.6 \times 10^{-19}}(\text{eV}) \tag{F.11}$$

or 1 eV.

We may note that the magnitude of the potential (1 volt) and the magnitude of the electron energy (1 eV) are the same. However, it is important to keep in mind that the unit associated with each number is different.

APPENDIX

J

ANSWERS TO SELECTED PROBLEMS

Chapter **1**

1.1 (*a*)4 atoms. (h) 2 atoms, (*c*) 8 atoms

1.3 (*a*) 52.4 percent, (h) 74 percent. (c) 68 percent, (*d*) 34 percent

1.5 (*a*) 2.36 Å. (*b*) 5×10^{22} atoms/cm^3

1.7 (b) $a = 2.8$ Å, **(*c*)**2.28×10^{22} cm^{-3} for both Na and Cl, (*d*) 2.21 gm/cm^3

1.9 (*a*) 3.31×10^{14} atoms/cm^2; Same for A atoms and B atoms. ***(b)*** Same as ***(a)***.(*c*) Same material.

1.13 (*a*) 5.63 Å, (*h*)3.98 Å. (*c*) 3.25 Å

1.15 (*a*) 6.78×10^{14} cm^{-2}. (b) 9.59×10^{14} cm^{-2}, (*c*) 7.83×10^{14} cm^{-2}

1.17 2×10^{23} cm^{-3}

1.19 (*a*) 4 x 10 ^{5} percent. (*b*) 2×10^{-6} percent

1.21 d = 7.94 x 10 ^{6} cm or $d/a_0 = 146$

Chapter **2**

2.5 $\lambda = 0.254\,\mu$m (gold). $\lambda = 0.654\,\mu$m (cesium)

2.7 $E_{av} = 0.01727$ eV, $P_{av} = 7.1 \times 10^{-26}$ kg-m/s. $\lambda = 93.3$ A

2.9 (*a*) $E = 1.14 \times 10$ ^{3} eV. $p = 1.82 \times 10^{-26}$ kg-m/s, A = 364 Å
(b) $p = 5.3 \times 10^{-26}$ kg-m/s, $v = 5.82 \times 10^{6}$ cm/s. $E = 9.64 \times 10^{-3}$ eV

2.11 ***(a)***Ap $= 1.054 \times 10^{-28}$ kg-m/s
(*b*) ***A E*** = 0.198 eV

2.13 (*a*)***Ap*** $= 8.78 \times 10^{-26}$ kg-m/s
(*b*) ***A E*** $= 4.82 \times 10^{-7}$ eV

2.15 (*a*) Ap $= 1.054 \times 10^{-24}$ kg-m/s
(*b*) ***Ar*** $= 6.6 \times 10^{-16}$ s

2.17 $|A|^2 = 1$, or $A = +1, -1, +j, -j$

2.19 (*a*) P = 0.393. (hi P = 0.239, (*c*) P = 0.865

2.21 $\Psi(x, t) = A \exp[-j(kx + \omega t)]$ where k $= 6.27 \times 10^{8}$ m ^{1} and $\omega = 2.28 \times 10^{13}$ rad/s

2.23 (*a*)$E_1 = 0.261$ eV, $E_2 = 1.04$ eV,
(*b*) A = 1.59 μm

2.25 $E_1 = 2.06 \times 10^{6}$ eV (neutron). $E_1 = 3.76 \times 10^{9}$ eV (electron)

2.29 (*b*) (*i*) A E $= 3.85 \times 10^{-3}$ eV,
(*ii*) ***A E*** $= 2.46 \times 10^{-17}$ eV

2.31 **(a) P** = 0.118 percent.
(*b*) P $= 1.9 \times 10^{-10}$ percent

2.33 **(*a*)T** = 0.138, (*b*) $T = 1.27 \times 10^{-5}$

2.38 $E_1 = -13.58$ eV, $E_2 = -3.395$ eV, $E_3 = -1.51$ eV, $E_4 = -0.849$ eV

Chapter **3**

3.9 **(*a*)*A E*** = 0.488 eV, (b) A E = 1.87 eV,
(*c*)*A E* = 3.83 eV. (*d*) ***A E*** = 6.27 eV

3.11 (*a*) ***A E*** = 0.638 eV. (*b*) $\Delta E = 2.36$ eV.
(c) ***A E*** = 4.73 eV, (d) ***A E*** = 7.39 eV

3.13 m* (A) < m^* (B)

3.15 A, B: velocity = −x; C, D: velocity = +x; B. C: positive mass; A, D: negative mass

3.17 A: $m/m_0 = 0.476$; B: $m/m_0 = 0.0953$

3.23 g $= 3.28 \times 10^{17}$ cm^{-3}

3.25 (*a*) At E_c, $g_c = 0$;
0.05 eV, $g_c = 1.71 \times 10^{21}$ cm^{-3} eV^{-1};
0.10 eV, $g_c = 2.41 \times 10^{21}$ cm^{-3} eV^{-1};

0.15 eV, $g_c = 2.96 \text{ x } 10^{21}\ \text{cm}^{-3}\ \text{eV}^{-1}$;
0.20 eV, $g_c = 3.41 \times 10''\ \text{cm}^{-3}\ \text{eV}^{-1}$,
(*b*) At E_v, $g_v = 0$,
-0.05 eV, $g_v = 0.637 \text{ x } 10''\ \text{cm}^{-3}\ \text{eV}^{-1}$;
-0.10 eV, $g_v = 0.901 \text{ x } 10^{21}\ \text{cm}^{-3}\ \text{eV}^{-1}$;
-0.15 eV, $g_v = 1.10 \text{ x } 10^{21}\ \text{cm}^{-3}\ \text{eV}^{-1}$;
-00.20 eV, $g_v = 1.27 \text{ x } 10^{21}\ \text{cm}^{-3}\ \text{eV}^{-1}$

3.29 (*a*) $f(E) = 0.269$, (*b*) $1 - f(E) = 0.269$

3.31 (*a*) $1 - f(E) = 0.269$,
(*b*) $1 - f(E) = 6.69 \text{ x } 10^{-3}$,
(*c*) $1 - f(E) = 4.54 \text{ x } 10^{-5}$

3.37 (*a*) $f(E) = 6.43 \text{ x } 10^{-3}$ percent,
(b) $f(E) = 4.53$ percent, (*c*) $T \approx 756$ K

3.39 (*a*) Far $E = E_1$, $f(E) = 9.3 \text{ x } 10^{-6}$;
For $E = E_2$, $1 - f(E) = 1.78 \times 10^{-14}$,
(b) For $E = E_1$, $f(E) = 8.45 \text{ x } 10^{-13}$;
For $E = E_2$, $1 - f(E) = 1.Y6 \text{ x } 10^{-7}$

3.43 T $\approx$ 461 K

Chapter 4

4.1 (*a*) $n_i = 7.68 \text{ x } 10^4\ \text{cm}^{-3}$; $2.38 \times 10^{12}\ \text{cm}^{-3}$;
$9.74 \times 10^{14}\ \text{cm}^{-3}$,
(*b*) $n_i = 2.16 \times 10^{10}\ \text{cm}^{-3}$; $8.60 \times 10^{14}\ \text{cm}^{-3}$;
$3.82 \times 10^{16}\ \text{cm}^{-3}$,
(*c*) $n_i = 1.38\ \text{cm}^{-3}$; $3.28 \text{ x } 10^9\ \text{cm}^{-3}$;
$5.72 \text{ x } 10^{12}\ \text{cm}^{-3}$

4.5 (*a*) $E = E_c + \frac{kT}{2}$ (*b*) $E = E_v - \frac{kT}{2}$

4.8 $\frac{n_i(A)}{n_i(B)} = 47.5$

4.10 $E_{Fi} - E_{\text{midgap}} = -0.0128$ eV (Si)
$E_{Fi} - E_{\text{midgap}} = -0.0077$ eV (Ge)
$E\quad - E_{\text{midgap}} = +0.038$ eV (GaAs)

4.12 $E_{Fi} - E_{\text{midgap}} = -8.51$ meV, -17.0 meV,
-25.5 meV

4.17 $r_1 = 104$ Å, E $= 0.0053$ eV

4.19 $p_0 = 2.13 \text{ x } 10^{15}\ \text{cm}^{-3}$, $n_0 = 2.27 \text{ x } 10^4\ \text{cm}^{-3}$

4.21 $E_c - E_F = 0.88$ eV, $n_0 = 4.9 \text{ x } 10^4\ \text{cm}^{-3}$

4.23 (a) $p_0 = 1.33 \text{ x } 10^{12}\ \text{cm}^{-3}$,
(*b*) $E_{Fi} - E_F = 0.207$ eV,
(c) For (a) $n_0 = 2.44\ \text{cm}^{-3}$;
For (*b*) $n_0 = 8.09 \text{ x } 10^6\ \text{cm}^{-3}$

4.25 $E_c - E_F = -0.034$ eV

4.27 (*a*) $n_0 = 2.45 \text{ x } 10''\ \text{cm}^{-3}$,
$p_0 = 9.12 \text{ x } 10^{16}\ \text{cm}^{-3}$,
(b) $n_0 = 1.87 \text{ x } 10^{16}\ \text{cm}^{-3}$,
$p_0 = 9.20 \text{ x } 10^{16}\ \text{cm}^{-3}$

4.29 (*a*) $p_0 = 2.95 \text{ x } 10''\ \text{cm}^{-3}$.
$n_0 = 1.95 \text{ x } 10^{13}\ \text{cm}^{-3}$, (h) $n_0 = 5 \text{ x } 10^{15}\ \text{cm}^{-3}$,
$p_0 = 1.15 \text{ x } 10^{11}\ \text{cm}^{\ 3}$

4.31 (*a*) $n_0 = 2 \times 10^{15}\ \text{cm}^{-3}$, $p_0 = 1.125 \times 10^5\ \text{cm}^{-3}$,
(b) $p_0 = 10^{16}\ \text{cm}^{-3}$, $n_0 = 2.25 \text{ x } 10^4\ \text{cm}^{-3}$,
(*c*) $n_0 = p_0 = n_i = 1.5 \text{ x } 10^{10}\ \text{cm}^{-3}$,
(*d*) $p_0 = 1.0 \text{ x } 10^{14}\ \text{cm}^{-3}$,
$n_0 = 5.66 \text{ x } 10^{10}\ \text{cm}^{-3}$,
(*e*) $n_0 = 1.49 \text{ x } 10^{14}\ \text{cm}^{-3}$,
$p_0 = 4.89 \text{ x } 10^{13}\ \text{cm}^{-3}$

4.33 (*a*) p type, (h) Si: $p_0 = 1.5 \text{ x } 10^{13}\ \text{cm}^{-3}$,
$n_0 = 1.5 \text{ x } 10^7\ \text{cm}^{-3}$,
Ge: $p_0 = 3.26 \text{ x } 10^{13}\ \text{cm}^{-3}$,
$n_0 = 1.77 \text{ x } 10^{13}\ \text{cm}^{-3}$, GaAs:
$p_0 = 1.5 \times 10^{13}\ \text{cm}^{-3}$, $n_0 = 0.216\ \text{cm}^{-3}$

4.35 $n_0 = 1.125 \text{ x } 10^{15}\ \text{cm}^{-3}$, n-type

4.41 (*a*) **n** type; $no = 10^{16}\ \text{cm}^{-3}$,
$p_{,,} = 2.25 \text{ x } 10^4\ \text{cm}^{-3}$. (*b*) p-type;
$p_0 = 2.8 \text{ x } 10^{16}\ \text{cm}^{-3}$, $n_0 = 8.04 \text{ x } 10^3\ \text{cm}^{-3}$

4.43 $T = 200\ \text{K} \Rightarrow E_{Fi} - E_F = 0.1855$ eV
T $= 400\ \text{K} \Rightarrow E_{Fi} - E_F = 0.01898$ eV
T $= 600\ \text{K} \Rightarrow E_{Fi} - E_F = 0.000674$ eV

4.45 $T \approx 762$ K

4.49 $N_d = 1.2 \text{ x } 10^{16}\ \text{cm}^{-3}$

4.51 (a) $E_F - E_{Fi} = 0.2877$ eV,
(b) $E_{Fi} - E_F = 0.2877$ eV. (*c*) For (*a*)
$n_0 = 10^{15}\ \text{cm}^{-3}$, For (*h*) $n_0 = 2.25 \text{ x } 10^5\ \text{cm}^{-3}$

4.53 (*a*) $E_F - E_{Fi} = 0.3056$ eV,
(*b*) $E_{Fi} - E_F = 0.3473$ eV,
(*c*) $E_F = E_{Fi}$. (*d*) $E_{Fi} - E_f = 0.1291$ eV,
(*e*) $E_{,.} - E_{Fi} = 0.0024$ eV

4.55 p type, $E_{Fi} - E_F = 0.3294$ eV

Chapter 5

5.1 (*a*) $n_0 = 10^{16}\ \text{cm}^{-3}$. $p_0 = 3.24 \times 10^{-4}\ \text{cm}^{-3}$
(b) $\mu_n \approx 7500\ \text{cm}^2/\text{V-s}$ so
$J = 120\ \text{A/cm}^2$, (*c*) (*i*) $p_0 = 10^{16}\ \text{cm}^{-3}$,
$n_0 = 3.24 \times 10^{-4}\ \text{cm}^{-3}$;
(ii) $\mu_p \approx 310\ \text{cm}^2/\text{V-s}$
so $J = 4.96\ \text{A/cm}^2$

5.3 (a) $I = 0.44$ mA, (*b*) I $= 4.4$ mA,
(*c*) For (*a*) $v_d = 5.5 \text{ x } 10'$ cm/s,
For (b) $v_d = 5.5 \times 10^5$ cm/s

5.5 (*a*) $\mu_n = 3333\ \text{cm}^2\text{N-s}$.
(*h*) $v_d = 2.4 \text{ x } 10'$ cm/s

5.7 (*a*) $\sigma_i = 4.39 \text{ x } 10^{-6}\ (\Omega\text{-cm})^{-1}$,
(b) $\sigma_i = 1.03 \text{ x } 10^{-6}\ (\Omega\text{-cm})^{-1}$

5.9 $n_i(300\text{ K}) = 3.91 \times 10^9\text{ cm}^{-3}$, $E_g = 1.122\text{ eV}$;
$n_i(500\text{ K}) = 2.27 \times 10^{13}\text{ cm}^{-3}$,
$\sigma(500\text{ K}) = 5.81 \times 10^{-3}\ (\Omega\text{-cm})^{-1}$

5.11 (a) $N_d = 9.26 \times 10^{14}\text{ cm}^{-3}$,
(*b*) $\rho(200\text{ K}) \approx 2.7\ \Omega\text{-cm}$,
p $\approx 9.64\ \Omega$-cm

5.13 (*a*) $T = 5.6 \times 10^{-8}$ eV, (b) T $= 5.6 \times 10^{-4}$ eV

5.17 $\mu = 316\text{ cm}^2/\text{V-s}$

5.19 $\mu = 167\text{ cm}^2/\text{V-s}$

5.23 1 = 18 mA

5.25 $J = 16\text{ A/cm}^2$

5.27 $J_n = 3.41 \exp\left(\frac{-x}{22.5}\right)\text{ A/cm}^2$

5.29 (*a*) $J_{h,diff} = 1.6 \exp\left(\frac{-x}{L}\right)\text{ A/cm}^2$,
(*b*) $J_{e,drf} = 4.8 - 1.6 \exp\left(\frac{-x}{L}\right)\text{ A/cm}^2$
(*c*) $E = \left[3 - 1 \cdot \exp\left(\frac{-x}{L}\right)\right]$ V/cm

5.31 (*a*) $n = n_i \exp\left[\frac{0.4 - 2.5 \times 10^2 x}{kT}\right]$,
(*b*) $J_n = -5.79 \times 10^{-4} \exp\left[\frac{0.4 - 2.5 \times 10^2 x}{0.0259}\right]$,
(*i*) $J_n(x = 0) = -2.95 \times 10^3\text{ A/cm}^2$,
(*ii*) $J_n(x = 5\ \mu\text{m}) = -23.7\text{ A/cm}^2$

5.33 (*a*) $E = \alpha\left(\frac{kT}{e}\right)$, (*b*) $V = -\left(\frac{kT}{e}\right)$

5.35 $N_d(x) = A\exp(-\alpha x)$ where
$\alpha = 3.86 \times 10^4\text{ cm}^{-1}$

5.39 (a) $V_H = 2.19$ mV, (*b*) $E_H = 0.219$ V/cm

5.41 (*a*) p type, (*b*) $p = 8.08 \times 10^{15}\text{ cm}^{-3}$,
(*b*) $\mu_p = 387\text{ cm}^2/\text{V-s}$

5.43 (*a*) n type, (b) $n = 8.68 \times 10^{14}\text{ cm}^{-3}$,
(*c*) $\mu_n = 8182\text{ cm}^2/\text{V-s}$,
(*d*) $\rho = 0.88\ \Omega$-cm

Chapter 6

6.1 $R' = 5 \times 10^{19}\text{ cm}^{-3}\text{ s}^{-1}$

6.3 (*a*) $\tau_{n0} = 8.89 \times 10^{+6}$ s,
(*b*) $G = 1.125 \times 10^9\text{ cm}^{-3}\text{ s}^{-1}$,
(*c*) $G = R = 1.125 \times 10^9\text{ cm}^{-3}\text{ s}^{-1}$

6.7 $\frac{\partial F_p^+}{\partial x} = -2 \times 10^{19}\text{ cm}^{-3}\text{ s}^{-1}$

6.9 $D' = 58.4\text{ cm}^2/\text{s}$, $\mu' = -868\text{ cm}^2/\text{V-s}$,
$\tau_{n0} = 54\ \mu\text{s}$, $\tau_{p0} = 24\ \mu\text{s}$

6.11 $a = 8 + 0.114(1 - e^{-t/\tau_{p0}})$, $\tau_{p0} = 10^{-7}$ s

6.13 $I = (54 + 2.20e^{-t/\tau_{p0}})$ mA, $\tau_{p0} = 3 \times 10^{-7}$ s

6.15 (*a*) $R'_p/R_{p0} = 4.44 \times 10^9$,
(b) $\tau_{p0} = 2.25 \times 10^{-7}$ s

6.17 (**a**) For $0 < t < 2 \times 10^{-6}$,
$\delta n = 10^{14}(1 - e^{-t/\tau_{n0}})$ where $\tau_{n0} = 10^{-6}$ s:
For $t > T = 2 \times 10^{-6}$,
$\delta n = 0.865 \times 10^{14} \exp\left[\frac{-(t -}{\tau_{n0}}\right]$

6.19 (*a*) $n_{p0} = 2.25 \times 10^6\text{ cm}^{-3}$,
(*b*) $\delta n(0) = -n_{p0} = -2.25 \times 10^6\text{ cm}^{-3}$,
(*c*) $\delta n = -n_{p0}e^{-x/L_n}$

6.25 For $-L < x < +L$, $\delta p = \frac{G'_0}{2D_p}(5L^2 - x^2)$;
For $L < x < 3L$, $\delta p = \frac{G'_0 L}{D_p}(3L - x)$;
For $-3L < x < -L$, $\delta p = \frac{G'_0 L}{D_p}(3L + x)$

6.29 $E_{Fn} - E_{Fi} = 0.3498$ eV,
$E_{Fi} - E_{Fp} = 0.2877$ eV

6.31 $\delta n = \delta p = 5 \times 10^{15}\text{ cm}^{-3}$,
(*a*) $E_{Fn} - E_F = 0.0025$ eV,
(*b*) $E_{Fi} - E_{Fp} = 0.5632$ eV

6.33 (*a*) $\delta p = 5 \times 10^{12}\text{ cm}^{-3}$,
(*b*) $E_{Fn} - E_{Fi} = 0.1505$ eV

6.37 (*a*) For n-type, $\frac{R}{\delta n} = \frac{1}{\tau_{p0}} = 10^{+7}\text{ s}^{-1}$,
(*b*) For intrinsic, $\frac{R}{\delta n} = \frac{1}{\tau_{p0} + \tau_{n0}}$
$= 1.67 \times 10^6\text{ s}^{-1}$,
(*c*) For p-type, $\frac{R}{\delta n} = \frac{1}{\tau_{n0}} = 2 \times 10^6\text{ s}^{-1}$

6.39 (*a*) $\delta n = \frac{\delta n_0 \sinh[(W - x)/L_n]}{\sinh[W/L_n]}$
$\delta n_0 = 10^{15}\text{ cm}^{-3}$ and $L_n = 35.4\ \mu$m.
(*b*) $\delta n = 10^{15}\left(1 - \frac{x}{W}\right)$

6.41 For $-W < x < 0$,
$\delta n = \frac{G'_0}{2D_n}(-x^2 - 2Wx + 2W^2)$;
For $0 < x < W$, $\delta n = \frac{G'_0 W}{D_n}(W - x)$

Chapter 7

7.1 (*a*) For $N_d = 10^{15}\text{ cm}^{-3}$; (*i*) $V_{bi} = 0.575$ V,
(ii) 0.635 V, (*iii*) 0.695 V, (*iv*) 0.754 V,
(b) For $N_d = 10^{18}\text{ cm}^{-3}$; (i) 0.754 V,
(*ii*) 0.814 V, (iii) 0.874 V, (*iv*) 0.933 V

.5 (*a*)n side. $E_F - E_{Fi} = 0.3294$ eV;
p side. $E_{Fi} - E_F = 0.4070$ eV
(*b*) $V_{bi} = 0.3294 + 0.4070 = 0.7364$ V
(*c*) $V_{bi} = 0.7363$ V
(*d*) $x_n = 0.426\ \mu$m, $x_p = 0.0213\ \mu$m,
$|E_{max}| = 3.29$ x 10^4 Vlcm

7.7 (*b*)(n region), $n_0 = N_d = 8.43$ x 10^{15} cm^{-3},
(p region), $p_0 = N_a = 9.97$ x 10^{15} cm^{-3},
(*c*) $V_{bi} = 0.690$ V

7.9 (*a*) $V_{bi} = 0.635$ V, (*b*) **x,,** $= 0.864\ \mu$m,
$x_p = 0.0864\ \mu$m,
(*d*) $|E_{max}| = 1.34$ x 10^4 Vlcm

7.11 (*a*) $V_{bi} = 0.8556$ V, (*b*) $T = 302.4$ K

7.13 (*a*) $V_{bi} = 0.456$ V, (*b*) x,, $= 2.43$ x 10^{-7} cm,
(*c*) $x_p = 2.43$ x 10^{-3} cm,
(*d*) $|E_{max}| = 3.75$ x 10' Vlcm

7.17 (*a*) $V_{bi} = 0.856$ V,
(*b*) W $= 0.301$ x 10^{-4} cm,
(*c*) $E_{max} = 3.89$ x 10^5 Vlcm,
(*d*) C $= 3.44$ pF

7.19 (*a*)Neglecting change in V_{bi}, 41.4 percent increase; (*b*) 17.95 mV increase

7.21 (*a*) $V_R = 73$ V, (*b*) $V_R = 7.18$ V,
(*c*) $V_R = 0.570$ V

7.23 $V_{R2} = 18.6$ V

7.25 $N_d = 3.24$ x 10^{17} cm^{-3}

7.27 (*a*) $V_{bi} = 0.557$ V, (*b*) x,, $= 5.32$ x 10^{-6} cm,
$x_n = 2.66 \times 10^{-4}$ cm, (*c*) $V_R = 70.3$ V

7.29 (*a*) (*i*) $C = 1.14$ pF, (*ii*) C $= 0.521$ pF,
(*iii*) $C = 0.389$ pF; (*b*) (*i*) $C = 3.69$ pF,
(*ii*) $C = 1.74$ pF, (*iii*) $C = 1.31$ pF

7.33 (*a*)E$(x = 0) = 7.73$ x 10^4 V/cm,
(*c*) $V_R = 23.2$ V

7.35 $a = 1\ 1 \times 10^{20}$ cm^{-4}

Chapter 8

8.1 (*a*) 60 mV, (*b*) 120 mV

8.5 (*a*) $\dfrac{J_n}{J_n + J_p} = \dfrac{1}{1 + (2.04)(N_a/N_d)}$

(*b*) $\dfrac{J_n}{J_n + J_n} = \dfrac{(\sigma_n/\sigma_p)}{(\sigma_n/\sigma_n) + 4.90}$

8.7 $N_a/N_d = 0.083$

8.9 $I_S = 2.91$ *x* 10^{-9} A, (*a*) $I = 6.55\ \mu$A,
(*b*) $I = -2.91$ nA

8.11 (*a*) $I_{p0} = 4.02$ *x* 10^{-14} A.
(*b*) $I_{n0} = 6.74$ x 10^{-15} A,
(*c*) p,, $= 3.42$ x 10^{10} cm^{-3},
(*d*) $I_n = 3.43 \times 10^{-9}$ A

8.13 **(a)** $V_a = 0.253$ V, (*b*) $V_a = 0.635$ V

8.15 $E_{g2} = 0.769$ eV

8.18 $T_{max} \approx 519$ K

8.20 For 300 **K,** $V_D = 0.60$ V; For 310 K,
$V_D = 0.5827$ V; For 320 K. $V_D = 0.5653$ V

8.23 For 10 **kHz,** $Z = 25.9 - j0.0814$;
For 100 kHz, $Z = 25.9 - j0.814$;
For 1 MHz, $Z = 23.6 -$ i7.41:
For 10 MHz, $Z = 2.38 -$ j7.49

8.25 $\tau_{p0} = 1.3$ x 10^{-7} s; $C_d = 2.5 \times 10^{-9}$ F

8.27 ***(a)***R $= 72.3\ \Omega$., $I = 1.38$ mA

8.29 $V_a = 0.443$ V

8.31 $J_S = 8.57$ x 10^{-18} A/cm^2.
$J_{gen} = 1.93 \times 10^{-9}$ A/cm^2

8.33 (*a*)For $V_a = 0.3$ V, $I = 7.96$ x 10^{-11} A;
For $V_a = 0.5$ V. $I = 3.36 \times 10^{-9}$ A

8.39 $V_D = 0.548$ V

8.41 $N_d \approx 3$ x 10^{15} cm^{-3}, A $= 1.99$ x 10^{-4} cm^2

8.43 $V_R = 19.9$ V

8.45 $V_R = 5.54$ V

8.47 $V_B \approx 15$ V

8.49 $I_R/I_F = 1.11$. $t_2/\tau_{p0} \approx 0.65$

8.51 $W = 61.9$ Å

Chapter 9

9.1 (*c*) $\phi_n = 0.206$ V, $\phi_{B0} = 0.27$ V,
$V_{bi} = 0.064$ V, $|E_{max}| = 1.41$ *x* 10^4 V/cm,
(*d*) $\phi_{Bn} = 0.55$ V, $|E_{max}| = 3.26 \times 10^4$ V/cm

9.3 (u) $\phi_{B0} = 1.03$ V, (*b*) $\phi_n = 0.058$ V,
(*c*) $V_{bi} = 0.972$ V, (*dl* $x_d = 0.416\ \mu$m,
(*e*) $|E_{max}| = 2.87$ x 10^5 Vlcm

9.5 (a) C $= 4.75$ pF, (*b*) C $= 15$ pF

9.7 (*a*) $V_{bi} = 0.334$ V, $x_d = 0.211\ \mu$m,
$|E_{max}| = 3.26$ *x* 10^4 Vlcm.
(*h*) **A@**$= 20$ mV, $x_m = 0.307 \times 10^{-6}$ cm,
(*c*) $|E_{max}| = 1.16$ x 10^5 Vlcm,
A@$= 37.8$ mV, $x_m = 0.163$ x 10^{-6} cm

9.9 (*a*) $V_{bi} = 0.812$ V, $x_d = 0.153\ \mu$m,
$|E_{max}| = 1.06$ x 10^5 V/cm,
(*b*) $V_R = 7.47$ V

9.11 (a) $\phi_{B0} = 1.13$ V, (*b*) $\phi_{Bn} = 0.858$ V.
(*c*) $\phi_{B0} = 0.43$ V. $\phi_{Bn} = 0.733$ V

9.13 (*a*) @,,$= 0.206$ V,
(*b*) $V_{bi} = 0.684$ V.

$(c)\ J_{ST} = 1.3 \times 10^{-8}$ A/cm^2,
(d) $V_a = 0.488$ V

9.15 *(a)* $V_a = 0.603$ V, $(b)\ \Delta V_a = 18$ mV

9.17 $V_{bi} = 0.474$ V, $(a)\ I_{R1} = 1.52 \times 10^{-8}$ A,
$(b)\ I_{R2} = 1.86 \times 10^{-8}$ A

9.19 For Schottky diode, $V_a = 0.467$ V; for pn diode. $V_a = 0.705$ V

9.21 (a) For Schottky diode, I $\approx 0.5 \times 10^{-3}$ A; for pn diode, I $= 1.02 \times 10^{-8}$ A; (b) for Schottky diode. $V_a = 0.239$ V; for pn diode, $V_a = 0.519$ V

9.25 *(b)* $N_d = 1.24 \times 10^{16}$ cm^{-3}, (c) 0.20 V

9.27 $(b)\ \phi_{B0} =$ @„= 0.138 V

Chapter 10

10.3 $(a)\ I_S = 3.2 \times 10^{-14}$ A; $(b)\ (i)\ i_C = 7.75\ \mu$A,
(ii) $i_C = 0.368$ mA, (iii) $i_C = 17.5$ mA

10.5 *(a)* $\beta = 85$, a $= 0.9884$. $i_E = 516\ \mu$A;
$(b)\ \beta = 53$. a $= 0.9815$, $i_E = 2.70$ mA

10.7 $(b)\ I_C = 4.7$ mA

10.9 (a) $p_{E0} = 4.5 \times 10'$ cm^{-3},
$n_{B0} = 2.25 \times 10^4$ cm^{-3},
$p_{C0} = 2.25 \times 10^5$ cm^{-3},
$(b)\ n_B(0) = 6.80 \times 10^{14}$ cm^{-3},
$p_E(0) = 1.36 \times 10^{13}$ cm^{-3}

10.11 Assume $\exp(V_{BE}/V_t) \gg \cosh(x_B/L_B)$,
(a) 0.9950, (b) 0.648, $(c)\ 9.08 \times 10^{-5}$

10.15 (c) For $x_B \ll L_B$, $J(x_B)/J(0) = 1$;
For $x_B = L_B = 10\ \mu$m,
$J(x_B)/J(0) = 0.648$

10.17 (a) $V_{CB} = 0.70$ V, $(b)\ V_{EC}(\text{sat}) = 0.05$ V,
(c) 3.41×10^{11} holes/cm^2,
$(d)\ 8.82 \times 10^{13}$ electrons/cm^2

10.19 $V_{CB} = 0.48$ V

10.21 *(o)* $I_C = 17.4\ \mu$A, (b) a $= 0.9067$.
$I_C = 1.36$ mA, $(c)\ I_C = 19.4\ \mu$A

10.23 $(a)\ (i)\ \dfrac{\gamma(B)}{\gamma(A)} \approx 1 - \dfrac{Nno}{N_C} \cdot \dfrac{D_E}{D_B} \cdot \dfrac{x_B}{x_E}$,

$(ii)\ \dfrac{\gamma(C)}{\gamma(A)} = \mathrm{I}$: $(b)\ (i)\ \dfrac{\alpha_T(B)}{\alpha_T(A)} = 1$,

$(ii)\ \dfrac{\alpha_T(C)}{\alpha_T(A)} \approx \mathrm{I} + \dfrac{1}{2} \cdot \dfrac{x_{B0}}{L_B}$; (c) neglect changes in space charge width,

$$\text{(i)}\ \frac{\delta(B)}{\delta(A)} \approx 1 - \frac{J_{r0} \exp\left(\dfrac{-V_{BE}}{V_t}\right)}{eD_B n_{B0}},$$

$$(ii)\ \frac{\delta(C)}{\delta(A)} \approx 1 + \frac{J_{r0} \exp\left(\dfrac{-V_{BE}}{V_t}\right)}{\dfrac{eD_B n_{B0}}{x_B}};$$

(d) Device C

10.25 $(b)\ I_C = 1.19$ mA, $I_E = 0.829$ mA

10.27 $$(a)\ \delta = \frac{1}{1 + 15.38 \exp\left(\dfrac{-V_{BE}}{0.0518}\right)},$$

$(b)\ \beta = \dfrac{S}{1 - \delta}$, (c) for $V_{BE} < 0.4$ V, recombination factor will be the limiting factor in current gain.

10.29 $(a)\ x_B = 0.742\ \mu$m, (b) S $= 0.9999994$

10.35 (a) $V_A = 47.8$ V, (b) V, $= 33.4$ V,
(c) $V_A = 19.0$ V

10.39 (a) $\boldsymbol{R} = 893\ \Omega$, $(b)\ V = 8.93$ mV,
(c) 70.8 percent

10.41 $$(a)\ \mathrm{E} = -\left(\frac{a}{x_B}\right)\left(\frac{kT}{e}\right),$$

(c) Total solution is

$$n = \frac{J_n}{e\mu_n \mathrm{E}} + n_H(0) \exp(-Ax)$$

where $\mathrm{A} = \dfrac{\mathrm{E}}{V_t}$ and

$$n_H(0) = \frac{n_i^2}{N_B(0)} \exp\left(\frac{V_{BE}}{V_t}\right) - \frac{J_n}{e\mu_n \mathrm{E}}$$

10.43 $BV_{CBO} = 221$ V, $N_C = 1.5 \times 10^{15}$ cm^{-3},
$x_C = 6.75\,\mu m$

10.45 $(a)\ V_{pt} = 295$ V: however, junction breakdown for these doping concentrations is $V_B \approx 70$ V, so punchthrough will not be reached.

10.47 $(a)\ I_B = 0.105$ mA. $(b)\ I_B = 11.9\ \mu$A,
(c) I'' $= 10.14\ \mu$A

10.53 $f_T = 509$ MHz

Chapter 11

11.1 *(a)* p type, inversion; (b) p type, depletion;
(c) p type. accumulation: (d) n type, inversion

11.3 *(a)* By trial and error,
$N_d = 3.27 \times 10^{14}$ cm^{-3},
$(b)\ \phi_s = -0.518$ V

11.5 (a) $N_d = 4.98 \times 10^{13}$ cm^{-3}, (b) cannot use p$^+$ poly gate, (c) $N_d = 3.43 \times 10^{14}$ cm^{-3}

11.7 $Q'_{ss}/e = 1.2 \times 10^{10}$ cm^{-2}

11.9 $V_{TP} = -1.44 + \phi_{ms}$, $(a)\ V_{TP} = -1.76$ V,
(b) $V_{TP} = -1.71$ V, $(c)\ V_{TP} = -0.592$ V

11.11 By trial and error, N,, = 1.71 x 10^{16} cm^{-3}

11.13 $(a)\ V_{FB} = -1.52$ V, $(b)\ V_T = -0.764$ V

11.15 $(b)\ \phi_{ms} = -1.11$ V, $(c)\ V_{TN} = +0.0012$ V

11.21 ***(a)***C,,,, $= 8.63$ x 10^{-8} F/cm^2,
$C'_{FB} = 3.42$ x 10^{-8} F/cm^2,
$C'_{\min} = 0.797$ x 10^{-8} F/cm^2,
$C'(\text{inv}) = C_{\text{ox}}$
(b) Same as (a) except $C'(\text{inv}) = C'_{\min}$
$(c)\ V_{TP} = -0.989$ V

11.23 (a) $\Delta V_{FB} = -1.74$ V,
$(b)\ \Delta V_{FB} = -0.869$ V,
$(c)\ \Delta V_{FB} = -1.16$ V

11.27 (a) n type, (b) $t_{\text{ox}} = 345$ Å,
$(c)\ Q'_{ss} = 1.875$ x 10^{11} cm^{-2},
$(d)\ C_{FB} = $ 15h pF

11.31 $V_{SG} = 1$ V, $I_D(\text{sat}) = 0.00592$ mA;
$V_{SG} = 3$ V, $I_D(\text{sat}) = 0.716$ mA;
$V_{SG} = 5$ V, $I_D(\text{sat}) = 2.61$ mA

11.37 $V_T \approx 0.2$ V, $\mu_n = 342$ cm^2/V-s

11.39 (a) $W/L = 14.7$, $(b)\ W/L = 25.7$

11.41 $(a)\ g_{mL} = 0.148$ mS, $(b)\ g_{ms} = 0.917$ mS

11.43 $V_{BS} = 7.92$ V

11.47 $(a)\ f_T = 5.17$ GHz, (b) $f_I = 1.0$ GHz

Chapter 12

12.1 $I_D = 10^{-15} \exp\left(\dfrac{V_{GS}}{(2.1)V_t}\right)$, $I_T = (10^6) I_D$,
P $= I_T \cdot V_{DD}$; for $V_{GS} = 0.5$ V,
$I_D = 9.83$ pA, IT $= 9.83$ μA,
P $= 49.2$ μW; for $V_{GS} = 0.7$ V,
$I_D = 0.388$ nA, $I_T = 0.388$ mA,
P $= 1.94$ mW; for $V_{GS} = 0.9$ V,
$I_D = 15.4$ nA, $I_T = 15.4$ mA, P $= 77$ mW

12.3 $(a)\ \Delta V_{DS} = 1$ V, AL $= 0.0451$ μm;
$\Delta V_{DS} = 3$ V, AL $= 0.122$ μm;
$\Delta V_{DS} = 5$ V, $\Delta L = 0.188$ μm;
(b) L $= 1.88$ μm

12.7 (a) Assume $V_{DS}(\text{sat}) =$ I V then
L $= 3$ μm $\Rightarrow$ E$_{\text{sat}} = 3.33$ x 10^3 Vlcm
L $=$ I μm $\Rightarrow$ E$_{\text{sat}} = 10^4$ V/cm
L $= 0.5$ μm $\Rightarrow$ E$_{\text{sat}} = 2$ x 10^4 V/cm
(b) Assume $\mu_n = 500$ cm^2/V-s,
$v = \mu_n$E$_{\text{sat}}$,
$L = 3$ μm $\Rightarrow v = 1.67 \times 10^6$ cm/s
$L = 1$ μm $\Rightarrow v = 5 \times 10^6$ cm/s
L ≤ 0.5 μm $\Rightarrow v \approx 10^7$ cm/s

12.13 (a) Both bias conditions. $I_D \approx kI_D$,
(b) P $\approx$ k^{2}P

12.15 (a) $(i)\ I_D = 1.764$ mA;
$(ii)\ I_D = 0.807$ mA;
(b) (i) $P = 8.82$ mW, (ii) P $= 2.42$ mW;
(c) current: 0.457; power: 0.274

12.17 **L** $= 1.59$ μm

12.23 $\Delta V_T = +0.118$ V

12.27 (a) $V_{BD} = 15$ V, $(b)\ V_G = 5$ V

12.31 L $= 0.844$ μm

12.33 $(a)\ V_T = -0.478$ V, (b) implant acceptors.
$D_I = 4.25$ x 10'' cm^{-2}

12.35 (a) $V_T = -0.624$ V, (b) implant acceptors,
$D_I = 4.37$ x 10^{11} cm^{-2}, $(c)\ V_T = 1.24$ V

12.37 $(a)\ V_T = -1.53$ V; enhancement PMOS,
(b) implant acceptors,
$D_I = 4.13 \times 10^{12}$ cm^{-2}

12.39 $\Delta V_I = -2.09$ V

Chapter 13

13.3 ***(a)***$V_P = 4.91$ V, (b) for $V_{GS} = 1$ V,
(i) a $- h = 0.215$ μm,
$(ii)\ a -$ h $= 0.0653$ μm,
(iii) $a - h = -0.045$ μm (zero depletion width)

13.5 (a) $V_{P0} = 15.5$ V, $(b)\ V_{GS} = -4.66$ V

13.7 (a) $V_{P0} = 1.863$ V, $V_P = 0.511$ V;
(b) (i) a $-$ h $= 4.45$ x 10^{-6} cm,
(ii) $a -$ h $= 1.70$ x 10^{-5} cm

13.9 (a) For $V_{DS} = 0$. $V_{GS} = -1.125$ V;
(b) For $V_{DS} = 1$ V. $V_{GS} = -0.125$ V

13.11 $V_{GS} = 0$, $g_d = 0.523$ x 10^{-3}; $V_{GS} = -0.53$ V,
$g_d = 0.236 \times 10^{-3}$; $V_{GS} = -1.06$ V, $g_d = 0$

13.13 $g_{ms}(\text{max}) = 1.31$ mS/mm

13.15 $(a)\ V_{P0} = 2.59$ V, $V_T = -17\ 8$ V,
(b) depletion mode

13.17 $V_{DS} = 0$, $\boldsymbol{a} - h = 0.716$ μm;
$V_{DS} = 2$ V, $a - h = 0.545$ μm;
$V_{DS} = 5$ V, $a -$ h $= 0.410$ μm

13.19 $N_d \approx 5.45$ x 10^{15} cm^{-3}

13.21 $(a)\ V_{bi} = 0.612$ V, $V_{P0} = 2.47$ V,
$V_T = -1.86$ V, $V_{DS}(\text{sat}) = 0.858$ V,
(b) add donors, $N_d = 1.64$ x 10^{16} cm^{-3};

$V_{bi} = 0.628$ V, $V_T = -3.87$ V,
$V_{DS}(\text{sat}) = 2.87$ V

13.23 (*a*) W = 2h.4 μm; (*b*) for $V_{GS} = 0.4$ V
$I_{D1} = 78.8$ μA; for $V_{GS} = 0.65$ V.
I_{D1}(sat) = 0.56 *m*A

13.29 (a) With velocity saturation.
I_{D1}(sat) = 4.86 mA; without velocity saturation, I_{D1}(sat) = 18.2 mA

13.31 (*a*) $t_d = 20$ ps, (b) $t_d = 20$ ps

13.33 (*a*) $g_{ms} = 2.82$ mS, (b) $r_s = 88.7\ \Omega$,
(*c*) L = 0.67 μm

13.35 (*a*) $f_t = 755$ GHz, (b) $f_T = 15.9$ GHz

13.37 (*a*) g_m/W = 502 mS/mm,
(*b*) I_{D1}(sat)/W = 537 mA/mm

Chapter 14

14.1 (*a*) $\lambda = 1.24/E$
(i) E = 0.66 ⇒ A = 1.88 μm
(*ii*) $E = 1.12$ ⇒ A = 1.11 μm
(*iii*) $E = 1.42$ ⇒ A = 0.873 μm
(*b*) (*i*) A = 570 nm ⇒ $E = 2.18$ eV
(*ii*) $\lambda = 700$ **nm** ⇒ $E = 1.77$ eV

14.3 $\delta n = g'\tau = 1.44 \times 10^{13}\ \text{cm}^{-3}$

14.5 (n) $x = 1.98$ μm, (b) $x = 0.41$ μm

14.11 $I_L = 500$ mA, $V_m = 0.577$ V,
$I_{,,} = 478.3$ mA, $P_m = 276$ mW

14.13 For $h\nu = 1.7$ eV, $x = 2.3$ μm;
For hv = 2.0 eV, $x = 0.23$ μm

14.15 (*a*) $\delta p = \delta n = 10^{13}\ \text{cm}^{-3}$,
(*b*) $\Delta\sigma = 1.32 \times 10^{-2}\ (\Omega\text{-cm})^{-1}$,
(*c*) $I_L = 0.66$ mA, (*d*) $\Gamma_{ph} = 4.13$

14.17 (*a*) $J_{L1} = 9.92$ mA/cm^2,
(*b*) $J_L = 0.528$ A/cm^2

14.19 W = I μm ⇒ $J_L = 4.15$ mA,
W = 10 μm ⇒ $J_L = 15.2$ mA,
W = 100 μm ⇒ $J_L = 16$ mA,

14.21 $0.625 \leq \lambda \leq 0.871$ μm

14.23 (*a*) 8.83 percent, (*b*) 5.95 percent

Chapter 15

15.1 $I_, = 5.33$ A

15.7 $V_{CC} = 25$ V

15.9 (*a*) $I_1 = 1.84$ A, $I_2 = 1.66$ A, $I_3 = 1.51$ A:
$P_1 = 6.09$ W, $P_2 = 5.48$ W, $P_3 = 4.98$ W
(b) $I_, = 2.16$ A, $I_2 = 1.08$ A, $I_3 = 1.77$ A;
$P_1 = 8.38$ W, $P_2 = 4.19$ W, $P_3 = 6.85$ W

15.11 (*b*)
(i) $V_{GS} = 5$ V, $I_D = 0.25$ A. $V_{DS} = 37.5$ V,
P = 9.38 W
(ii) $V_{GS} = 6$ V, $I_D = 1.0$ **A**, $V_{DS} = 30$ V,
$P = 30$ W
(iii) $V_{GS} = 7$ V, $I_D = 2.25$ A. $V_{DS} = 17.5$ V,
$P = 39.4$ W
(*iv*) $V_{GS} = 8$ V, $I_D = 4.0$ A, $V_{DS} = 2.92$ V,
$P = 11.7$ W
(*v*) $V_{GS} = 9$ V, $I_D = 6.25$ A, $V_{DS} = 1.88$ V,
$P = 11.7$ W

15.13 $P_D = \dfrac{125}{2.5 + \theta_{\text{case-amb}}}$

15.15 $\theta_{\text{case-amb}} = 4$°C/W